ORO-5194-T3

AREA OIL SHALE OFFICE
CENTRAL LIBRARY

AN ANALYSIS OF THE STRUCTURAL PARAMETERS THAT INFLUENCE GAS PRODUCTION FROM THE DEVONIAN SHALE

Annual Progress Report, 1978—1979

By
J. Negus-De Wys
Jeanette M. Dixon
Mark A. Evans
Kevin D. Lee
Robert C. Shumaker

Henry W. Rauch
James E. Ruotsala
Thomas H. Wilson
Richard T. Williams

Department of Geology and Geography
West Virginia University
Morgantown, West Virginia

U. S. DEPARTMENT OF ENERGY

4L QE.1

FOSSIL ENERGY

DISCLAIMER

AN ANALYSIS OF THE STRUCTURAL PARAMETERS

THAT INFLUENCE GAS PRODUCTION FROM THE DEVONIAN SHALE

1978 - 1979

ANNUAL PROGRESS REPORT

CONTRACT DE-AC21-76MC05194
Formerly EY-76-C-05-5194

SUBMITTED BY

DEPARTMENT OF GEOLOGY AND GEOGRAPHY
WEST VIRGINIA UNIVERSITY

ROBERT C. SHUMAKER, PROJECT DIRECTOR

CO-AUTHORED BY:

J. NEGUS-DE WYS, JEANETTE M. DIXON, MARK A. EVANS,
KEVIN D. LEE, HENRY W. RAUCH, JAMES E. RUOTSALA,
THOMAS H. WILSON AND RICHARD T. WILLIAMS

RESEARCH ASSOCIATES

AN ANALYSIS OF THE STRUCTURAL PARAMETERS

THAT INFLUENCE GAS PRODUCTION FROM THE DEVONIAN SHALE

1978 - 1979

ANNUAL PROGRESS REPORT
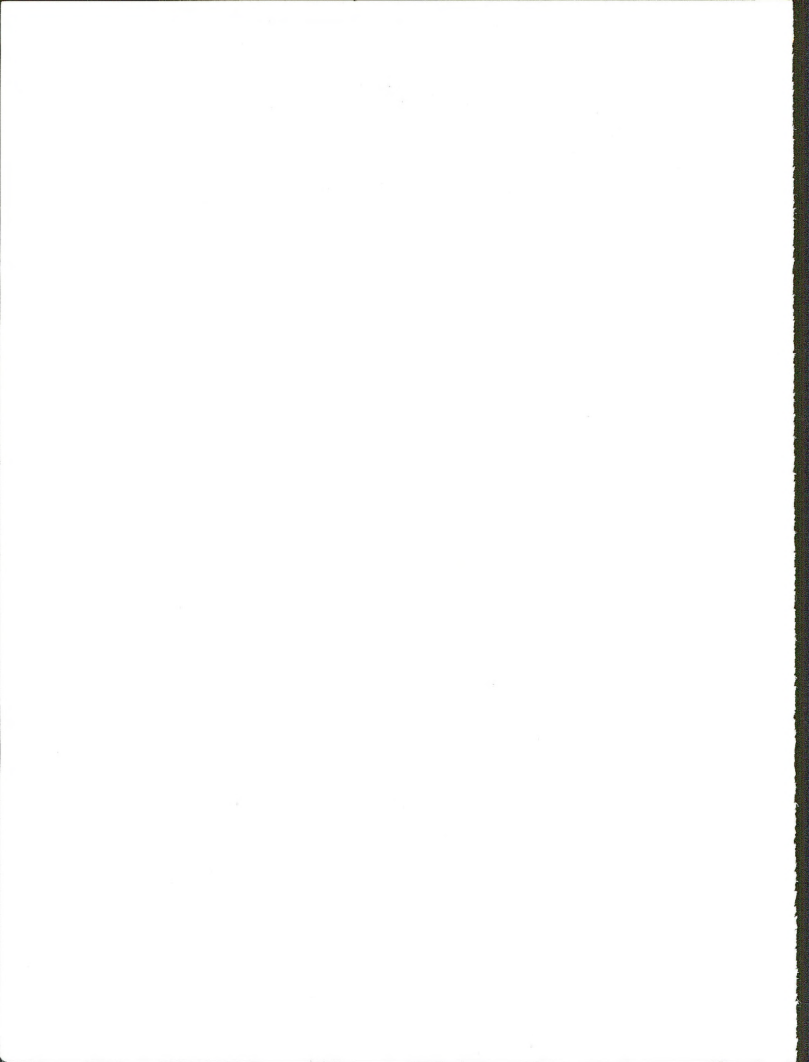

VOLUME II

DATA REPOSITORY

REPORTS PUBLISHED DURING FISCAL YEAR 1978 - 1979

iii

DATA AND FIGURES OF ALL APPENDICES

ARE AVAILABLE IN ORIGINAL SCALE AT REQUEST

APPENDIX A

Regional Structure Data

1978 - 1979

Robert C. Shumaker

PARAMETERS OF GEOLOGIC STRUCTURE WHICH AFFECT DEVONIAN GAS SHALE PRODUCTION

IN WEST VIRGINIA AND EASTERN KENTUCKY - A PROGRESS REPORT 1978-1979

by

R. C. Shumaker, Project Director
Devonian Shale Program

co-authored by

R. R. Beebe, J. Negus-de Wys, J. M. Dixon, M. A. Evans, K. G. Kirk,
K. D. Lee, B. R. Long, H. W. Rauch, J. E. Ruotsala, W. W. Schaefer,
R. L. Wheeler, R. T. Williams, T. H. Wilson

West Virginia University
Department of Geology and Geography
425 White Hall
Morgantown, West Virginia 26506

ABOUT THE AUTHORS

Dr. Shumaker is director of the West Virginia University - Department of Energy contract investigating the structural parameters that influence Devonian shale gas production. Drs. Wheeler, Williams, and Rauch direct the surface structure studies, geophysical, and ground water studies of this program respectively. Dr. Wheeler is presently with the U. S. Geological Survey, Denver, Colorado. All principal investigators were enrolled in the graduate studies program at West Virginia University during the 1978-79 academic year.

PRINCIPAL INVESTIGATORS

Robert R. Beebe, B.S. Northeastern University 1976, Boston, Massachusetts
- Hydrology (completed 2 years, M.S. candidate) presently with Exxon, Corpus Christi, Texas

Jane Negus-de Wys, A.B. Miami University 1946, Oxford, Ohio
- Production (2nd of 3 years, Ph.D. candidate)

Jeanette M. Dixon, A.B. Baylor University 1970, Waco, Texas; M.S. University of Akron 1976, Ohio
- Surface Structure (2nd of 3 years, Ph.D. candidate)

Mark A. Evans, B.S. West Virginia University 1978, Morgantown, West Virginia
- Subsurface Fractures (1st of 2 years, M.S. candidate)

Keith G. Kirk, B.S. Penn State University 1973; M.S. West Virginia University 1976
- Geophysics (completed 3 years, Ph.D. candidate) presently with U.S.G.S., Denver, Colorado

Kevin D. Lee, B.S. West Virginia University 1978
- Regional Structure (1st of 2 years, M.S. candidate)

Brian R. Long, A.B. Alfred University 1971, Alfred, NY; M.S. West Virginia University 1979
- Fractures - Eastern Kentucky (completed 2 years, M.S.) presently with W. Va. Department of Natural
  Resources, Charleston, W. Va.

James E. Ruotsala, B.S. Michigan Tech 1973; M.S. Michigan Tech 1975, Houghton,
   Michigan - Geophysics (1st year of 3 years, Ph.D. candidate)

William W. Schaefer, B.S. Campbell College 1971, Buies Creek, North Carolina;
   M.S. West Virginia University 1979 - Production, consulting geologist

Thomas H. Wilson, A.B. West Virginia University 1974; M.S. West Virginia
   University 1977 - Surface Structure (2nd of 3 years, Ph.D. candidate)

ABSTRACT

Major accomplishments during 1978-1979 include:

1. <u>Production studies</u>: A recognition that the best production (fracture
    porosity) occurs in synclines, off structure, in two West Virginia fields.
    Two exploration rationales developed from this study. Continued accumula-
    tion of basic geologic, geochemical, and production data for the large
    Eastern Kentucky Shale Gas Field is in preparation for an integrated
    analysis.

    Studies using XRF and XRD on well cuttings from 14 wells in eastern
    Kentucky yielded elemental data for 12 elements and mineralogical data
    for 16 minerals. A high correlation was found between contoured averages
    of seven elements and density contours of high producing wells (final
    open flow).

2. <u>Surface structure</u>: A technique was developed to estimate the fracture
    intensity in areas of limited rock exposure, and a study continues of
    Devonian shale deformation along a cross-strike structural discontinuity
    that intersects an Appalachian Valley and Ridge fold.

3. <u>Fracture studies</u>: Surface fractures of eastern Kentucky showed diverse
    trends dependent on lithology. Predicting the trends of subsurface
    fractured reservoirs from surface fracture trends is hazardous in areas
    of detached deformation. Natural fractures and induced fractures were
    logged and summarized for Devonian shale oriented cores taken in Mason
    County and Monongalia Counties, West Virginia. Gas shows in these two
    wells relate to partially mineralized fractures. Some 13 Appalachian
    Basin cores are described.

4. <u>Hydrology</u>: The comparison of shallow ground water productivity and
    quality with production from shale gas wells within the Midway-Extra
    field was completed, and there is a correlation of gas production with
    one low-altitude photo lineament trend.

5. <u>Geophysics</u>: Several seismic and resistivity techniques were tested to
    evaluate what method can best detect shallow fractures. These techniques
    are being applied to the Cottageville, West Virginia, field area to
    determine if shallow geophysical techniques are useful in determining
    fracture production trends.

INTRODUCTION

Most of the research tasks in our program, outlined below, reached or exceeded a two year level of effort this October, so that we are now beginning to reap benefits from our research efforts concerning the origin of fracture porosity in the Devonian shale of the study area (Figure 1). By the time of this third annual meeting of the Eastern Gas Shales Project and the publication of the Preprint volume, we will have completed five separate studies which relate fracture porosity and structural parameters; these include: two production studies which document the effect of geologic structure on production in specific West Virginia shale gas fields, the Cottageville and Midway-Extra fields, a third study which documents surface fractures in eastern Kentucky, a hydrologic study which compares shallow water well productivity and quality with shale gas production from the Midway-Extra field, and finally we completed a study on fracture porosity related to tectonic thinning and shale flowage as studied in selected folds of the Appalachian Plateau and Valley and Ridge physiographic-structural Provinces.

In the first part of this report we introduce the objectives and organization of our contract for those unfamiliar with its background. We then briefly summarize progress made toward attaining these objectives.

One important subject not covered in a referred paper includes work which the senior author considers to be a major breakthrough in understanding the origin of the fracture porosity in commercial shale gas wells that are located near the periphery of commercial production in West Virginia (Figure 1). This understanding is most significant to the Eastern Gas Shale Program; so we will place our emphasis in this text on a description of the examples and the data on which we base our conclusions. We believe that the results of our work on fracture porosity in shale also have application to other tight reservoirs, particularly in exploration for fractured tight reservoirs of the mid-continent region, an area where basement tectonics dominates. The senior author emphasizes this model developed through an integrated approach where the efforts of the following people have been essential: Mr. E. B. Nuckols III's effort in collecting the data at the Cottageville field (1976[1] and 1978),[2] Mr. William W. Schaefer's investigation and report on the Midway-Extra field (1979),[3] Mrs. Jane Negus-de Wys' analysis of production data from the Cottageville field (de Wys and Shumaker, 1978)[4] and Mr. Glenn R. Sundheimer's excellent seismic interpretation of the Cottageville field area (1978).[5] This integration of work and the extrapolation of ideas is the responsibility of the senior author.

OBJECTIVES

The general objective of our research funded under United States Department of Energy Contract number DE-AC21-76MC05194 (formerly EY-76-C-05-5194) is to study the structural parameters of the Devonian shales that affect gas production in eastern Kentucky and West Virginia (Figure 1).

To that end our program is specifically designed to:

1. Collect, compile, and analyze geologic data to construct regional structure maps of eastern Kentucky and West Virginia.

2. Determine if structural types and styles affect production and influence production characteristics.

3. Determine if shallow seismic surveys can detect near-surface faults and fracture zones, and if such structures can be detected, to further determine how fractures relate to both production from the shale and to lineations observed on remotely sensed data.

4. Determine if a relationship exists between ground water movement and shale gas productivity.

Through the integration of our work with others, it is our ultimate goal to discover if relationships exist between Devonian shale gas production and geologic structure. If such a relationship is established, we will attempt to develop a method or methods for selecting favorable sites to drill shale wells that have a greater potential for gas production than the norm for that region.

LEGEND

- Outcrop area of Devonian rocks
- Devonian Black Shale gas production
- Contract area
- Geophysical test site
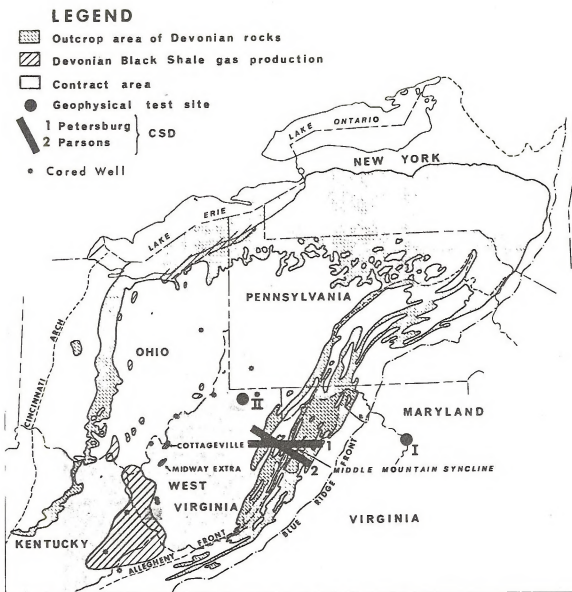- 1 Petersburg
- 2 Parsons } CSD
- Cored Well

Figure 1 Index Map - Structural Parameters that Affect Devonian Shale Gas Production

ORGANIZATION

In order to attain the stated objectives we have designed several tasks which have been organized into five study groups. Four of these groups: regional structure studies, fracture studies, structural type studies, and production studies, are carried under the U.S.D.O.E.'s Resource Inventory Tasks. One group, geophysical studies, is carried under Shale Characterization Tasks.

In essence, the first two tasks, that is the regional structure and fracture studies, are designed to provide a regional structure base for the study area. The structural type studies seek to document, by analytical field work, details of structures which are either similar to structures producing gas or which are similar to those which we feel could be prospective. The production studies will seek out and study gas fields where detailed well production records are available that permit thorough analysis and documentation of the geologic parameters that influence gas production from the shale. The geophysical studies are charged with the task of developing inexpensive geophysical techniques that can locate shallow fracture zones of high permeability.

PROGRESS AND PLANS 1978-1979

Regional Structure Studies

The emphasis of our effort here has shifted from compilation of areal structure maps to the construction of detailed structure maps for specific areas. A shift in emphasis was made because results of our production studies show that the shale gas production is related to structures that have very low structural relief at the Devonian level, and that such prospective structures frequently can be located only through the construction maps with a contour interval of ten or twenty feet. We are applying this technique to areas adjacent to the Cottageville and Midway-Extra fields in West Virginia, and we are accumulating data for analysis and characterization of the largest shale gas field, the Big Sandy Gas Field, of eastern Kentucky. The object of these investigations is to test our ideas concerning the relationships between production and geologic structure, characterize relationships in other productive areas of the basin, and to define prospective shale gas trends so that industry will be challenged to use our work or ideas in field well step outs and wildcat exploration.

Production Studies

Detailed investigation of the Midway-Extra field of Putnam County, West Virginia, by William W. Schaefer (1979)[3] established a direct relationship between production from the lower Huron Devonian shale and the structural trend of that field. Schaefer was able to confirm that initial and final open flows from wells at Midway-Extra are greatest along the northwestern limb of the Midway anticline, that is, in the adjacent syncline, off structure. He also found a lesser increase on the southeastern limb. The striking similarity of high flow rates with structural position along the fold is forcefully brought out by comparing Figures 2 and 3 taken directly from Schaefer's text (1979)[3]. Furthermore, he showed that the thickening of the lower Huron shale, the primary reservoir, into the adjacent syncline (Figure 4) suggests growth of the structure during sedimentation. He interpreted this to mean that basement deformation is important in the formation of the Midway anticline. From these data (Figures 2, 3, 4, and 5) at the Midway-Extra field one cannot be absolutely certain if it is the over-thickened lower Huron-organic shale or if it is fractures associated with the folding which contributes most to the noted increase of off-structure flow rates. One also might argue that even if fractures are present, they are not necessarily structural in origin. They could be caused by other lithologic factors or even as a result of differential compaction between thin shale and thick shale off structure. Regardless of the cause, an empirical exploration rationale was proposed based on Schaefer's study (1979).[3] Direct evidence for the exact underlying cause as well as the precise siting of wells expecting commercial production was still elusive even though Schaefer had made a major guiding breakthrough.

If, however, we combine what we learned at the Midway-Extra field with what we know of the Cottageville field, then additional insight is gained into the specific cause for shale gas production for that portion of West Virginia (Figure 1). At first glance, the similarity between Cottageville (Martin and Nuckols, 1976;[1] Nuckols, 1978;[2] and de Wys and Shumaker, 1978)[4] and the Midway-Extra field is not striking. Structurally, the Cottageville field appears to lie along a very low relief flexure on a southeast dipping regional slope. The cause for the flexure was inferred to be a basement fault (Martin and Nuckols, 1976[1] and Shumaker, unpublished maps).[7] Detailed interpretation of seismic data collected by Geophysical Services, Incorporated, by Glenn Sundheimer (1978[5]
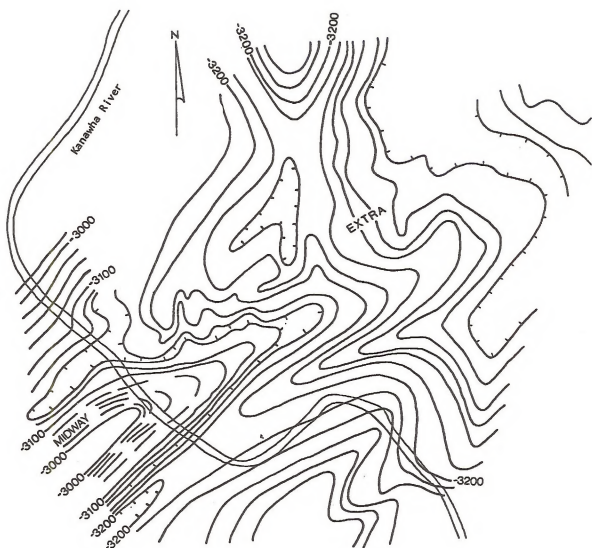
FIGURE 2
STRUCTURE-BASE OF BROWN SHALE (L.HURON)

Midway-Extra Field
Putnam County, W. Va.

C.I. = 20'
W. Schaefer, 1979

MIDWAY-EXTRA FIELD

Putnam County, W. Va.

Figure 3

BROWN SHALE ISOPOTENTIAL
OPEN FLOW AFTER STIMULATION

0   1   2
MILES
C.I. = 100
MCF/D
W. Schaefer 1979

MIDWAY-EXTRA FIELD
Putnam County, W. Va.

Figure 4

LOWER HURON ISOPACH MAP

W. Schaefer 1979

STRUCTURE AND ISOPOTENTIAL CROSS SECTIONS

Line Key

Berea ———
Brown Shale – – –
Prod. —·—·

MIDWAY-EXTRA FIELD

Putnam County, W. Va.
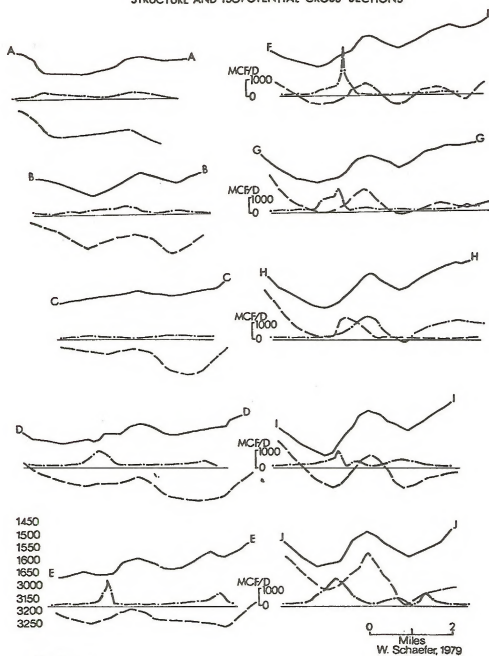
Figure 5

and 1979)[6] confirmed this interpretation, and his work further established that a basement fault directly underlies the trend of the most productive wells along the south flank of the Cottageville field (compare Figures 6 and 7). Please note the southeast regional dip, and also note that Sundheimer mapped a subdued flexure and syncline just updip from the fault (Figure 6), that is, northwest of the fault. These structures are similar to, although not identical to ones mapped by E. B. Nuckols III (Manuscript in preparation), from detailed subsurface geologic data. Nuckols has found that sedimentary patterns of the organic shales are complex around this structure. His unpublished maps also show that the best production does not uniquely follow the thickest lower Huron organic shale section. The best production lines up with the fault as mapped by Sundheimer. If one eliminates the regional dip from Sundheimer's isotime structure map (Figure 6), then the Cottageville field becomes a low fold with flanking synclines. It is only now that the Cottageville field appears similar to the Midway-Extra field, but Cottageville has far less relief. Keeping this in mind, compare the position of the fault, the fold crestal trace, and the trace of the flanking northern syncline with the production trends at Cottageville as mapped by de Wys and Shumaker (Figures 8, 9, and 10). There is a marked similarity of the final open flow map of the Midway-Extra field with production maps at Cottageville. This similarity is noted by lower productivity along the structural crest of both structures. In the case of Cottageville there is a near coincidence of productive trends shown on the summary trend map (Figure 11) above and parallel to the fault. The trends are not nearly as numerous for the northern syncline (Figures 6 and 11) which, incidentally, may be the southwest terminus of another buried fault. In the case of Cottageville, the comparison between structure and production seems far more conclusive than at Midway-Extra simply because of the greater quality and quantity of data. At Cottageville it is clear that better wells occur off-structure and that the best wells generally occur directly above the basement fault. De Wys and Shumaker (1978)[9] contoured the production data at Cottageville (Figures 7 thru 10) with a mechanical style, attempting to avoid bias in their contouring. Had they contoured the production data as Schaefer did, and if they had both Schaefer's results and Glenn Sundheimer's map, then the Cottageville production maps would be different, and the identity of structure with production trends would be more striking.

Using re-interpreted Cottageville as background, we can now go back to Midway-Extra and re-interpret the northwestern flank of the anticline suggesting that it is faulted at depth. The justification for this interpretation is that the high productivity wells at Cottageville are located along and above a fault.

Thus far we have pointed out the similarity between the fields, but there still is uniqueness to each field. This uniqueness is seen at Cottageville as we reimpose regional dip toward the southeast on that structure. We now have a logical reason for why the best producing wells occur near the western terminus of the fault and near the western terminus of the east plunging syncline on the north flank of the field. We interpret these areas as the updip end of fracture porosity associated with the structure. It is reasoned that the fracture porosity acts like a stratigraphic or diagenetic trap encased within the lower Huron shale (Shumaker 1978).[9] Shale gas has migrated up-plunge, westward, to the end of the fracture porosity. Furthermore this area appears to be along a change in the regional dip, a line of change or flexure from the broad flat Parkersburg syncline to the steeper slope leading toward the Cincinnati Arch. The significance of this observation remains unaccessed until we have more regional data, but it may be a key to why the Cottageville field produces compared with Devonian shale above other basement faults.

If we carefully study the Midway-Extra field we note a uniqueness there; the high flow wells align into minor north trending patterns (Figure 3) parallel to minor structural trends and an intersecting structural trend at the northeastern end of that field (Figure 2). We reason that these better wells occur at the intersection of the two fault trends. This, again, is a logical extension of the interpretation given above. We hypothesize that, if one fault yields good porosity, then the intersection of two should yield more porosity and therefore excellent production. This observation leads to a second substantive rationale for exploration; drill on the intersection of fault trends - on the low side.

There are a multitude of methods to develop fractures and thereby potential fracture permeability, that is, by: basement structure, detached structure, compaction, sedimentary diagene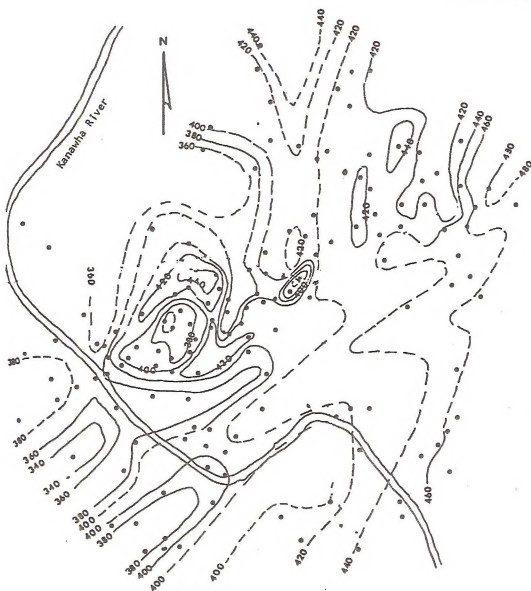sis, overburden removal, etc., it is the senior author's conclusion that basement growth structure is the most effective means of producing commercially effective porosity within this area of West Virginia. The importance of this understanding and the application of these exploration guidelines to southwestern West Virginia are heightened by a similar observation made by Don Neal (manuscript in preparation) of the West Virginia Geological and Economic Survey concerning the coincidence of higher initial flow from gas wells located on the flanks of geologic structures. This conclusion is based on his work in

ISOTIME STRUCTURAL MAP
TOP OF THE BASEMENT
CONTOUR INTERVAL =
0.010 SECONDS
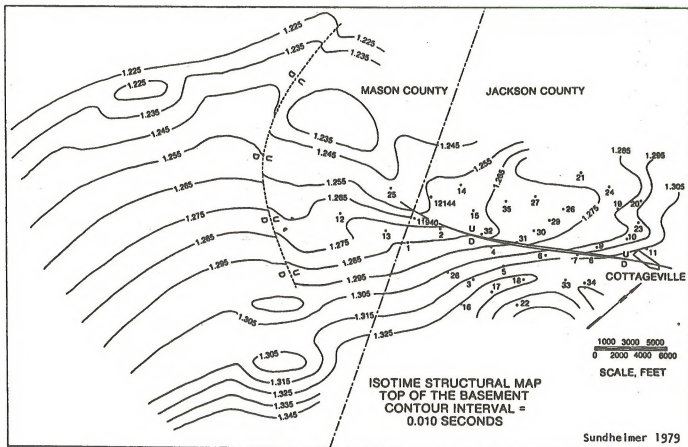
Sundheimer 1979
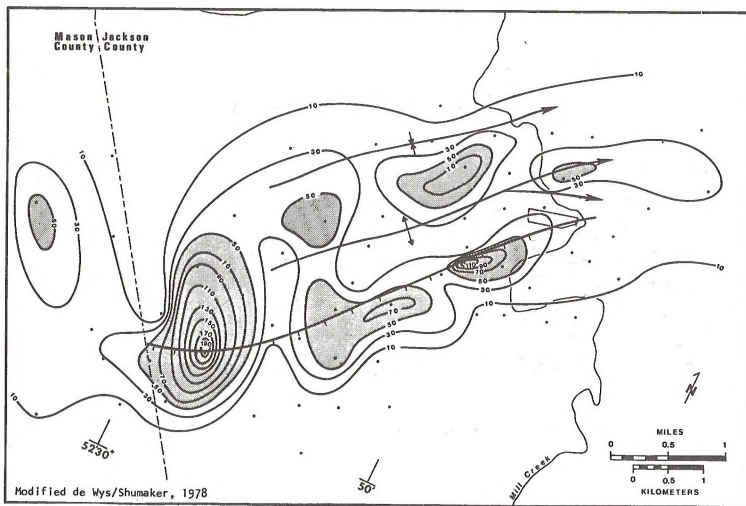
Figure 6

Figure 7 Isocontours of Highest Annual Production (1st or 2nd year production). Contour interval = 20MMcf/yr.

Fault and Fold Axes from Seismic - Sundheimer, 1978 (personal communication)

13.
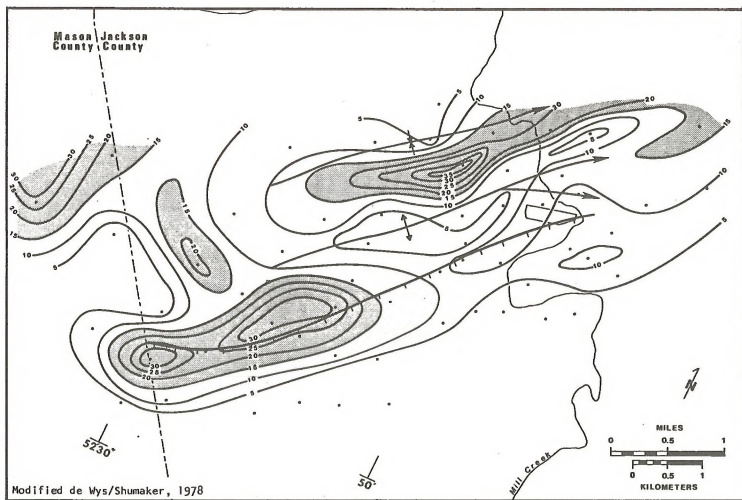
Figure 8 Isocontours of Mean Annual Gas Production. Contour Interval = 5MMcf

Fault and Fold Axes from Seismic - Sundheimer, 1978 (personal communication)

Modified de Wys/Shumaker, 1978

14.
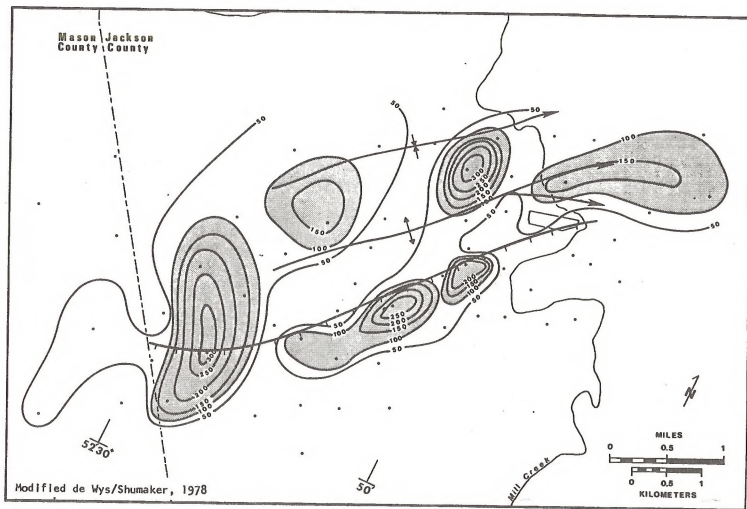
Figure 9 Isocontours of First Five Years Accumulated Gas Production. Contour Interval = 50MMcf/yr.

Fault and Fold Axes from Seismic - Sundheimer, 1978 (personal communication)

15.

Mason | Jackson
County | County
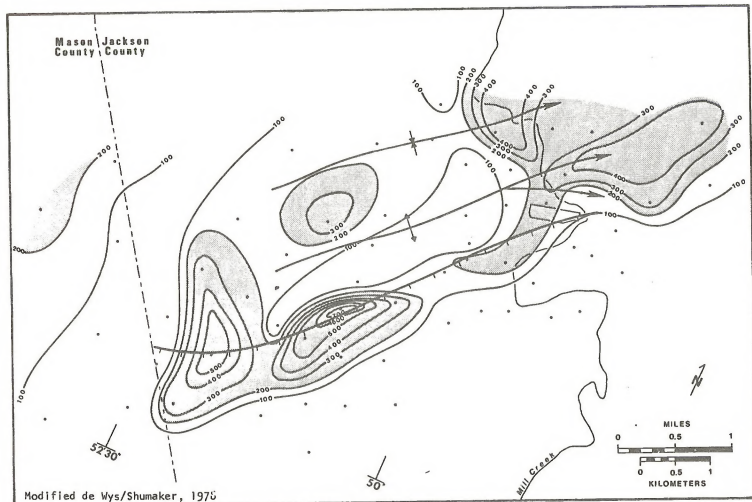
Modified de Wys/Shumaker, 1978

Figure 10   Isocontours of Total Accumulated Production.   Contour Interval = 100MMcf

Fault and Fold Axes from Seismic - Sundheimer, 1978 (personal communication)

16.

KEY
1 Drilling Completion Date
2 Highest Annual Production
3 First Five Years Cummulative Production
4 Total Cummulative Production
5 Mean Annual Production
6 Loss Ratio 1st Year
7 Loss Ratio 2nd Year
8 Loss Ratio 3rd Year
9 Loss Ratio 1st–5th Years
10 Structure Top Onondogo
11 Structure Bottom Huron Shales
12 Initial Well Pressure

Mason County | Jackson County

Mill Creek

MILES
0   0.5   1

0   0.5   1
KILOMETERS

5230°

50'

Modified de Wys/Shumaker, 1978

<u>Figure II</u> Axial Trends of Contours from Production Maps.

Shading on down side of fault.

17.

the adjacent area of West Virginia to the south. It therefore seems likely that these rationales can be extended southward into adjacent counties of southern West Virginia.

As to why the fractures select the lower Huron shale section as the host unit, one can only specu-late. The physical response of the lower Huron to deformation must be related to its lithology, but the exact nature and origin of the stress field creating the fractures still remains uncertain. Vertical basement tectonics seems to be an important source of that stress within the area described, but one cannot eliminate the importance of a horizontally directed stress field modifying and intens-ifying the local stress field (Advani 1978[9] and Shumaker 1978)[8]

A word of caution regarding the model and rationales described in this paper. The model was devel-oped as a result of our characterization of structural parameters that affect shale production in southwestern West Virginia, and therefore it should not be applied indiscriminately or universally as a unique solution to other areas. It clearly is not a unique solution for fracture porosity. Cer-tainly there are numerous ways to produce open fractures and therefore potentially productive shale gas areas in the multitude of tectonic environments and structural styles in the Appalachians. Our interpretations do not deny the existence or the influence of other fracture types on production even within these southwestern West Virginia shale gas fields, for we know that other genetic frac-ture types, which may be significant to production, are present within the Devonian shale (Shumaker 1978).[8]

The model described above obviously has its greatest application to southern West Virginia, but we believe it also has application to the mid-continent area. This area is largely undeformed. The prevailing structure is systematic, largely orthogonal, joints; but where the flat lying sediments are deformed, it is generally by basement deformation and often recurrent basement deformation (Shumaker).[10] We suggest for your consideration that a reason for lack of shale production within this immense mid-continent area may relate to the position of most wells on structural pro-spects. They clearly are not drilled on the flanks of structures, down-dip from the crest, unless there is a stratigraphic reason. We may have a reason for such exploration: structurally controlled fracture facies.

The Eastern Kentucky Gas Field is the third field selected for detailed analysis. We are presently in the midst of our work. Well cuttings (500+) in 14 wells in the Eastern Kentucky Gas Field have been examined and described. Cross sections are being constructed to study details of lithological changes in the Berea-Huron stratigraphic sequence.

Graphs, computer maps, and statistical analyses are in progress on a geochemical study of well cut-tings from 14 wells in the Eastern Kentucky Gas Field (same wells as lithology studies with one ex-ception). Fourteen elemental oxides (except Sulphur) and sixteen minerals are under examination. Certain maps show a high degree of correlation to density contours of high producing wells (based on 5000 wells).

Final stages of the study of the Eastern Kentucky Gas Field are commencing. Final open flow data are being compared to structural depths, shale thickness, lithological changes, evidence of fracture occurrence, high organic content, and geochemistry. Results of this phase of the field study will be presented at a later date.

Structural Type Studies

Analysis of the Parsons and Petersburg cross-strike structural lineaments (Figure 1) in the high plateau country of West Virginia have been conducted to determine: (1) joint intensity within and adjacent to the lineaments, (2) the nature of joint intensity with depth, and (3) the westward extent of the two lineaments. Rock is found to be more intensely jointed within the Parsons linea-ment in the Upper Devonian Chemung siltstones, mudstones, and shales of Tucker County, West Virginia, (Dixon, 1979a,[11] 1979b [12] Dixon and Wilson)[13] The lineament extends northwest and terminates in Taylor County. It is expressed in Lower and Middle Pennsylvanian sandstones as two zones of intense jointing (Dixon and Wilson)[13] The Petersburg lineament was stud-ied along the Allegheny Front to determine the effect of joint intensity with depth. Joints in Devonian shales, siltstones, and sandstones and Lower Mississippian sandstones were measured. The width of the zone of intense jointing does not vary with depth. However, intensity is significantly

greater in the Middle Devonian black shales than in other lithologies (Figure 12). The Petersburg lineament extends west-southwest to the Randolph-Upshur County line where it is disrupted or terminates. This lineament is manifest in Lower and Middle Pennsylvanian sandstones with intensities similar to those in Parsons lineament.

A three phase study of surface structures in Middle and Upper Devonian shales in Middle Mountain syncline (Figure 1) of the Valley and Ridge province, Pendleton County, West Virginia, has been completed. The study included the following: 1) detailed mapping of the Middle Mountain syncline, 2) an analysis of bedding orientation contours of the syncline (Wilson, 1979a[14] and 1979b),[15] and 3) a study of the orientations and spacings of systematic joints in the shales of the syncline. The studies were designed to characterize the Parsons cross-strike structural discontinuity (PCSD) in terms of faulting, folding and jointing in the exposed Devonian shale sequence. The PCSD is found to coincide with a zone in which structural shortening is taken up by smaller folds and more abundant thrust faults. In consequence, the shales within this zone are also more intensely jointed.

Fracture Studies

A regional survey of eastern Kentucky surface joints was completed to determine if surface fracture trends or domains, areas of similar trending joints, relate to high producing trends or high producing areas within the eastern Kentucky shale gas fields. Maps of joint strikes plotted as rose diagrams show that coal has the most consistent regional orientations of joints in the lithologies studied. Joints in black shale, brown shale, gray shale, and sandstone have varying angular relationships to regional coal cleat strikes. This dissimilarity between trends associated with each surface lithology makes prediction of subsurface fracture trends in the Devonian shale reservoir hazardous. Coal face cleats and coal structure form-lines change trend to become sub-parallel to the trace of the Pine Mountain thrust fault (Figure 13). Regardless of its origin, this gradual change in trend of face cleat trends is coincident with the most productive area in the eastern Kentucky shale gas field. The precise significance of this coincidence has not been determined as shale gas production extends into the areas of usual face cleat trend, that is, perpendicular to Appalachian fold axes.

Outcropping Devonian shales along the east flank of the Cincinnati Arch show consistent joint strikes of N25E, N45E and N65W. First-formed and second-formed joints strike northeast and northwest, respectively. This is opposed to the coal cleat trend over the eastern Kentucky gas field where face cleats (first-formed) strike northwest and change to become nearly E-W in the Pine Mountain thrust area.

Thirteen oriented Devonian shale cores from the Appalachian Plateau of West Virginia, Kentucky, Ohio, Virginia, and Pennsylvania have been examined for fractures (Figure 1). The orientation, type of mineralization (if any), and presence of fractographic features, i.e., plume, hackle, and arrest lines, were recorded for each fracture. Fractures were differentiated into three types: natural, core induced and slickenside. Frequency and orientation for each type of fracture have been plotted against core depth to determine the existence of possible fracture facies and decollement zones as well as changes in current in-situ stress and paleo stress as a function of depth or lithology. Regional subsurface fracture patterns are plotted and are being examined for comparison with the regional structure. Open file reports are available for two of the cores studied, Mason County #3 D/K core, West Virginia, and Monongalia County MERC #1 core, West Virginia. Reports on the other cores examined will be available in early 1980.

Ground Water

A hydrogeologic characterization study was done in the Midway-Extra Devonian shale gas field (Figure 1) of northern Putnam County, West Virginia. Lineaments were mapped and water wells were surveyed for physical and chemical parameters to compare with initial yield of nearby shale gas wells.

Northwest trending short straight photolineaments are significantly associated with water-well yield. Water wells located within 200 feet of a lineament's center line have significantly higher yields. Gas wells located near short photolineaments of the same trend had significantly higher initial open flows (both before and after stimulation) than wells located near other photolineaments. Gas wells also had significantly higher initial open flows when located in areas where photolineament density is high. Gas wells located near the most certain photolineaments had higher initial open flows than wells near less certain photolineaments. Landsat lineaments appear to be poor locations for gas

Joint Intensity of Petersburg Lineament
along Allegheny Front

Figure 12

FACE CLEATS WITH (B.Long)
COAL FORM LINES (Shumaker,1974)

```
10   0   10   20
[scale bar]
MILES
```
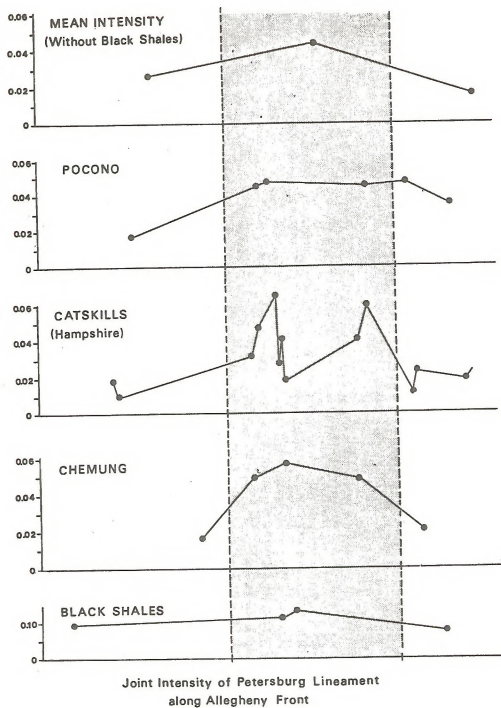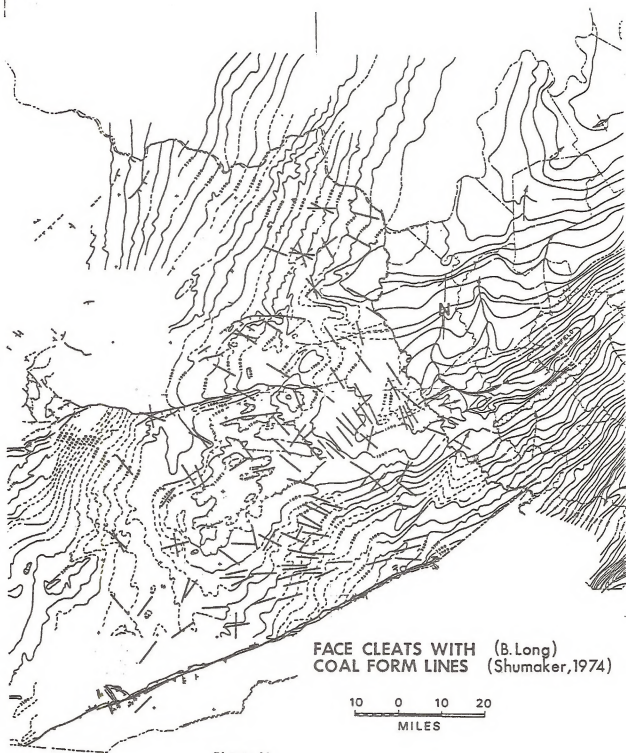
Figure 13

wells, and they do not overlap the high gas-producing areas.

Certain water-well parameters are also associated with initial gas well yield. Water wells located within high initial gas flow areas (over 100 MCF/day after stimulation) have significantly higher bicarbonate and nitrate concentrations than wells in low producing gas areas.

The results of our analyses here at Midway-Extra are similar to those found at Cottageville (Jones and Rauch, 1978)[16] except that at Cottageville the trend of gas associated short lineaments is west-northwest.

Geophysical Studies

The main thrust of the geophysical effort at West Virginia University is the characterization of some of the acoustic properties of both the fractured and unfractured zones. The hope, of course, is to determine which properties may serve as reliable exploration criteria.

Refraction seismic surveying will be used for shallow studies of lateral velocity changes. The nature of both the method and our equipment limits the depth of investigation to ± 800 feet. Since we will record waveforms (as well as travel times) attenuation anomalies may be observed.

High resolution reflection seismic surveying will provide data on small scale structures, attenuation anomalies, and acoustic velocity at depths greater than is possible with our refraction method. Our high resolution reflection seismic method uses an explosive source in a 7 foot deep shot hole. The geophones are in 4 foot deep holes. Since attenuation of high frequency acoustic energy is most severe in the weathered, near surface material, this procedure results in band width wider than that of more conventional techniques; and shot and geophone ground coupling are improved. Surface waves are eliminated from the records by burial of the geophones and high pass input filters. Burying the geophones also attenuates noise from other sources (e.g., wind, traffic, etc.). Signal to noise ratio is thus improved. Our signal band appears to be ± 300 hz to ± 1 khz resulting in vertical resolution of a few feet.

REFERENCES

1. Martin, P., and Nuckols, E. B., III, 1976, Geology and oil and gas occurrence in the Devonian shales, northern West Virginia, In Shumaker, R. C., and Overbey, W. K., eds., Devonian shale production and potential: USERDA - Morgantown Energy Research Center Special Report, MERC/SP-76/2, p. 20-40.

2. Nuckols, E. B., III, 1978, Exploration parameters derived from historical Devonian shale production in western West Virginia: Preprints 2nd Eastern Gas Shales Symposium, U. S. Department of Energy, METC/SP-78, v. 6, no. 1, p. 169-185.

3. Schaefer, William W., 1979, Geology and producing characteristics of certain Devonian brown shales in the Midway-Extra field, Putnam County, West Virginia: M.S. thesis, West Virginia University, 67 p.

4. de Wys, J. Negus, and Shumaker, R. C., 1978, Pilot study of gas production analysis methods applied to Cottageville field, Devonian Shale Program: Department of Geology and Geography, West Virginia University, under Contract EY-76-C-05-5194, U. S. Department of Energy, Morgantown Energy Research Center.

5. Sundheimer, Glenn R., 1978, Seismic analysis in the Cottageville field: Preprints 2nd Eastern Gas Shales Symposium, DOE/METC/SP-78/6, v. 1, p. 192-193.

6. Sundheimer, Glenn R., unpublished isotime structural map, top of the basement (Cottageville field, West Virginia).

7. Shumaker, Robert C., unpublished maps: structure on top of the basement, West Virginia and eastern Kentucky.

8. Shumaker, Robert C., 1978, Porous fracture facies in the Devonian shales of eastern Kentucky and West Virginia: Preprints 2nd Eastern Gas Shales Symposium, U. S. Department of Energy, METC/SP-78, v. 6, no. 1, p. 360-369.

9. Advani, S. H., Gangaroa, H. V. S., Chang, H. Y., Dean, C. S., and Overbey, W. K., 1977, Stress trajectory simulations across the Appalachian Plateau Province in West Virginia, in Schott, G. L., Overbey, W. K., Hunt, A. E., and Komar, C. A., eds., 1st Eastern Gas Shales Symposium, U. S. Department of Energy, Morgantown Energy Research Center, MERC/SP-77/5, p. 442-448.

10. Shumaker, Robert C., 1979, Paleozoic disruptive deformation in North American continent and its relationship to the formation and development of interior basins and deformation within the Orogenic core: oral presentation Eastern Section of Amer. Asso. of Pet. Geol., Oct. 1-4, 1979, Lakeview Country Club, Morgantown, WV.

11. Dixon, J. M., 1979a, A method to identify zones of intense jointing with application to the Parsons lineament, West Virginia: Morgantown Energy Technology Center Open-File Report, Morgantown, WV, 46 p.

12. Dixon, J. M., 1979b, A method to identify zones of intense jointing with application to the Parsons lineament, West Virginia (abs): Geol. Soc. Amer. Abs. with Programs, v. 7, p. 1286.

13. Dixon, J. M., and Wilson, T. H., 1979, The Parsons cross-strike structural discontinuity as an exploration area for fractured gas reservoirs: Preprints 3rd Eastern Gas Shales Symposium, Oct. 1-4, 1979, Lakeview Country Club, Morgantown, WV.

14. Wilson, T. H., 1979a, Bedding orientation contours of Middle Devonian shales in the Middle Mountain syncline, Valley and Ridge Province, West Virginia (abs): Geol. Soc. Amer. Abs. with Programs, Northeastern Sec. of the Geol. Soc. of Amer., 14th Annual Meeting, v. 11, no. 1, p. 60.

15. Wilson, T. H., 1979b, Bedding orientation contours of Middle Devonian shales exposed in the Middle Mountain syncline, Valley and Rodge Province, West Virginia: Morgantown Energy Technology Center Open-File Report, Morgantown, WV, 39 p.

16. Jones, D. S., and Rauch, H. W., 1978, Lineaments and ground water quality as exploration tools for ground water in the Cottageville area of western West Virginia: 2nd Eastern Gas Shales Symposium, U. S. Department of Energy, METC/SP-78, v. 6, no. 1, p. 196-206.

APPENDIX B

Surface Structure Studies

1978 - 1979

Jeanette M. Dixon

Thomas H. Wilson

Philip S. Berger

EXTENSION STRUCTURES

IN THE CENTRAL APPALACHIANS

by

Philip S. Berger
West Virginia University
Department of Geology and Geography
Morgantown, West Virginia 26506

1978

Table of Contents

LIST OF ILLUSTRATIONS

ABSTRACT

Late tectonic extension faults and extension fractures
may form abundantly in steep limbs of detached anticlines. The
Devonian Brallier formation of the central Appalachians
is the unit that has undergone the greatest amount of
extension faulting and fracturing, among Upper Ordovican to
Lower Mississippian units exposed and studied on the northwest
limb of the Wills Mountain anticline. Gravity data and analogy
with exposures on the northwest limb of the Wills Mountain
anticline indicate that the Blackwater and Glady
anticlines may also have thinned and fractured Brallier on
their northwest limbs in the subsurface. Given the
underlying dark shale source and updip thickened shales as
a seal, these volumes may contain gas in a fractured
reservoir.

INTRODUCTION

Fracture is defined by Dennis (1967) as a surface along which loss of cohesion has taken place. Therefore, unless the term is restricted by use of a modifier or used in conjunction with the term fault, fracture as used herein, will include faults, joints, and fissures. When used in conjunction with the term fault, fracture is defined as a surface along which little or no slip has occurred (joint or fissure). When used with a prefix, such as extension fracture, then the term is restricted to those fracture surfaces formed by bed-parallel extension, as defined and characterized in the main text of this thesis.

The purpose of the thesis is to investigate a particular class of bed-extending brittle structures known as extension faults and extension fractures. These formed late during the growth of anticlines in the detached tectonics characteristic of the central Appalachians. A specific goal of this investigation is to develop a predictive tool for the subsurface locations of unusually fractured rock in the Middle and Upper Devonian clastic sequence.

The field area investigated in this thesis was primarily the northwest limb of the Wills Mountain anticline, which extends through Pennsylvania, Maryland, West Virginia and Virginia. Other map-scale anticlines near the Wills Mountain anticline were examined, as well

as localities in Pennsylvania that expose outcrop-scale kink folds or kink-bands and which were suggested by Dr. R. T. Faill (written communication, 1978). Conclusions and speculations apply to these areas and to larger parts of the central Appalachians, chiefly in West Virginia.

The thesis is composed primarily of four short manuscripts, each having separate title, authors and abstract, and each building on or extending the last. The references and acknowledgements are a combined list from all four manuscripts. There is a separate section containing conclusions based on the work reported in the four manuscripts. Each manuscript has been or will be submitted for publication.

Each manuscript addresses the problem of predicting where the greatest amount of bed extension occurs. The first manuscript introduces the concept of fold-related brittle extension structures. It presents a relative time sequence for typical central Appalachian faulting and associated fracturing, and describes general field criteria for differentiating between earlier faults and the later extension faults. This manuscript refines a three stage model originally conceived by Dr. William J. Perry, Jr., of the U. S. Geological Survey, Reston, Virginia. Field work was done by all three authors, but most of the manuscript is based on a term paper written by

the senior author and his field work at Pinto, Maryland.

The second manuscript develops an approximate mathematical model using measured values of horizontal shortening to estimate the minimum bed dip at which extension structures will occur. This information places geographical constraints on areas which may be investigated for gas-bearing porosity or permeability produced as extension fractures or extension faults. The equations in this manuscript were developed by Dr. Russell. L. Wheeler.

The third manuscript concentrates on extension faults, as described and defined in the first manuscript, and represents the result of field investigations in the area delineated in the second manuscript. The third manuscript describes the stratigraphic distribution of extension faults in and near the Devonian clastic sequence and especially relates abundance of extension faults to structural position. It is also concerned with the relationship between the extension faults and large fold-related splay faults rising from deeper detachments. The manuscript estimates the contribution of extension faulting to anticlinal growth and estimates relative amounts of extension in fold limbs so that limbs may be selected which are most likely to contain gas in fractured reservoirs. The equations in the manuscript were derived by Dr. Russell L. Wheeler.

The fourth manuscript uses a kink-band model of fold development to estimate the amount of extension in the kink-band or in the more rotated limb of a kink fold. The extension can occur as porosity and permeability producing fractures or faults as described in the first and third manuscripts. The kink-band model of fold development is probably the best explanation for the observed geometric form of major folds in the central Appalachians. Field criteria are given for differentiating between folds of kink-band origin and those of buckling origin. The map distribution of gravity lows is used to explain the distribution of extension faulting from manuscript three in a kink fold model. Drilling areas are suggested for fractured reservoirs.

Three-Stage Model of Brittle Deformation in the Central Appalachians

Philip S. Berger[1], William J. Perry, Jr.[2], and Russell L. Wheeler[1]

ABSTRACT

Recent fieldwork in the central Appalachians shows the applicability of a three-stage model of brittle deformation. Distinct minor structures form at specific times during overall horizontal shortening and map-scale folding. Stage I contraction faults shorten horizontal or gently dipping beds and are closely associated with wedging. Stage II uplimb thrust faults shorten folded beds hingeward. Stage III extension faults and extension fractures lengthen steeply dipping to overturned beds. Opening or shearing directions of fractures and crosscutting relationships of faults, other fractures, and stylolites allow distinction of the three stages. Stage III may have produced fracture porosity and permeability on steep limbs of anticlines. We propose a three- stage model of outcrop-scale fault and other fracture development for steeply dipping to overturned beds in

----

[1]Department of Geology and Geography, West Virginia

   University, Morgantown, West Virginia 26506

[2]U.S. Geological Survey, Reston, Virginia 22092

eastern West Virginia and adjacent areas. Less rotated
beds may show at least two of the stages. Kinematic
analysis of faults and other fractures allows
differentiation of the three stages.

Structural Style

The central Appalachian foreland has many detached
anticlines but few outcropping major thrust faults. The
anticlines are interpreted as active features generated
mainly by duplication of strata by ramping of underlying
thrust faults, by splay faults, and by ductile flow of
shale-rich intervals into anticlinal crests (Perry and de
Witt, 1977, Perry, 1978, Wheeler, 1975). The synclines are
regarded as passive features resulting from anticlinal
growth in adjacent rocks, rather than from active
downbuckling (Gwinn, 1964).

We deal with the sequence of outcrop-scale structures
that formed at specific times during overall
southeast-northwest horizontal shortening and vertical
extension. We assume that each individual structure formed
in an orientation that allowed it to accommodate some of
that horizontal shortening, or vertical extension, or
both.

The first-order anticlines (Nickelsen, 1963, p. 16)
of the western Valley and Ridge and the Allegheny Plateau
provinces formed predominantly by flexural slip folding

(Faill, 1969), rather than by passive or flexural flow folding (Gair, 1950). Interlayering of shales and evaporites with sandstones, siltstones or limestones allows slip between units of low relative ductility. Stage I structures form before folding, or early during folding, when the angle between bedding and the maximum principal compressive stress is less than about 10 degrees. Experiments at room temperature and confining pressures to 2000 bars (equivalent to about 6 km in depth) suggest that slip parallel to bedding is possible when the angle between the maximum principal compressive stress and bedding ranges from 10 to 60 degrees (Price, 1967). Stage II structures form in this range of limb dips (see below). Stage III structures form in response to additional horizontal shortening, late in or after folding, when steep limb dips preclude further slip parallel to bedding. These structures form when the angle between bedding and the maximum principal compressive stress exceeds about 60 degrees. These conclusions are reinforced by the finite-element derived stress-history of folding (Dieterich and Carter, 1969).

Price (1967) described extension and contraction structures from the Canadian Rocky Mountains using the fault terminology of Norris (1958). We report the same types of structures from the central Appalachians, placing

them in a relative time sequence and describing simple
field criteria for differentiating among stages.

STAGE I STRUCTURES.--Cloos (1964) first recognized
and named the prefolding wedges common in the central
Appalachians. Wedges are the wedge-shaped ends of small
fault blocks in which the bounding contraction faults
(Norris, 1958) form angles of 30 degrees or less to
bedding. Examples provided by Cloos (1964, figs. 2, 3, 4
and 6) involve brittle layers (sandstone and limestone)
which have been "sheared, wedged, and telescoped together"
in a more ductile medium (shale). This process of
contraction faulting shortened the stratigraphic section
in a northwest-southeast direction and thickened it
perpendicular to bedding prior to or early during folding.
Such contraction faults can form dipping in either
direction (northwest or southeast).

Concerning the Canadian Rockies, Price (1967) writes
that if layering was planar and inclined at a low angle to
the maximum principal compressive stress, that stress'
trajectories would tend to parallel layering, and
subsequent failure would take the form of contraction
faults acting to shorten layers. The resulting geometry
of brittle beds in a more ductile matrix is that of Cloos'
wedges. Compound wedges involving a series of brittle beds
which have been telescoped together are shown by Cloos

(1964, fig. 7) and Perry and de Witt (1977, fig. 10).
Price (1967) used the term contraction faults to include
all faults that produce a shortening in the plane of the
bedding, thus including uplimb thrust faults (see below).

In wedged beds later rotated to vertical by folding,
the bounding contraction faults record normal-fault
separation at a low angle to bedding. In cratonward-facing
folds (asymmetric to the northwest in the Appalachians),
such stage I faults normally show a downlimb sense of
displacement (fig. 1). They did not form as normal faults
in their present orientation, because (1) the necessary
northwest-southeast horizontal extension is inconsistent
with central Appalachian structural style, and (2) their
formation in a contractional regime is indicated by drag
features and absence of associated extension features.

Prefolding fractures have been recognized in the
central Appalachians (Dean and Kulander, 1977). These
fractures may predate the contraction faults, because such
fractures are offset by these faults and by bed-parallel
compaction stylolites that are inferred to have formed
under overburden stress equal to maximum principal
compressive stress, when bedding was horizontal.

Prefolding calcite-filled fractures can be recognized
if orientations of calcite fibers record shearing on the
fractures. If the fractures are rotated to their original
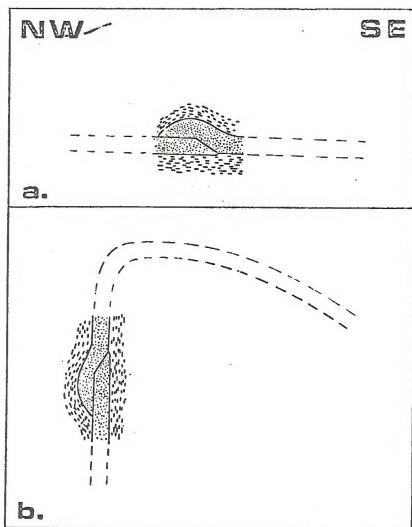
Figure 1. Contraction fault (stage I) formed wedges prior
to folding: (a) prefolding attitude, (b) postfolding
attitude on northwest limb of west-facing anticline,
The angles between the bedding and fault planes and the
size of the associated fold are variable.

(prefolding) orientations, the net growth direction of the
fibers should be about 30 degrees from the (horizontal)
maximum principal compressive stress.

STAGE II STRUCTURES.--Stage II structures formed
during folding. They record relative reverse movement
toward the anticlinal hinge as part of the Appalachian
fold's internal adjustments to southeast-northwest
horizontal shortening, and to fold growth by flexural
mechanisms. Perry and de Witt (1977) describe and define
uplimb thrust faults, the hanging walls of which move up
the limb of the anticline and away from the axis of the
adjacent syncline (figure 2). Similarly, Gair's (1950)
out-of-syncline thrusts, and Gwinn's (1964) symmetrical
thrust faults are northwest- and southeast-dipping reverse
faults that resolve space problems in cores of anticlines.
In concentric folding, upward and inward motion on
anticlines' flanks, and flexural slip above ductile rocks,
thrust strut-like brittle beds of the limbs over passive
anticlinal crests where flexural slip is inhibited. Perry
(1971) mapped southeast-dipping apparent normal faults at
a low angle to bedding in vertical beds on the northwest
limb of the Wills Mountain anticline in Pendleton County,
West Virginia. He interprets these as originally
northwest-dipping uplimb thrust faults (Perry, 1971,
1978), later rotated by continued growth and asymmetric
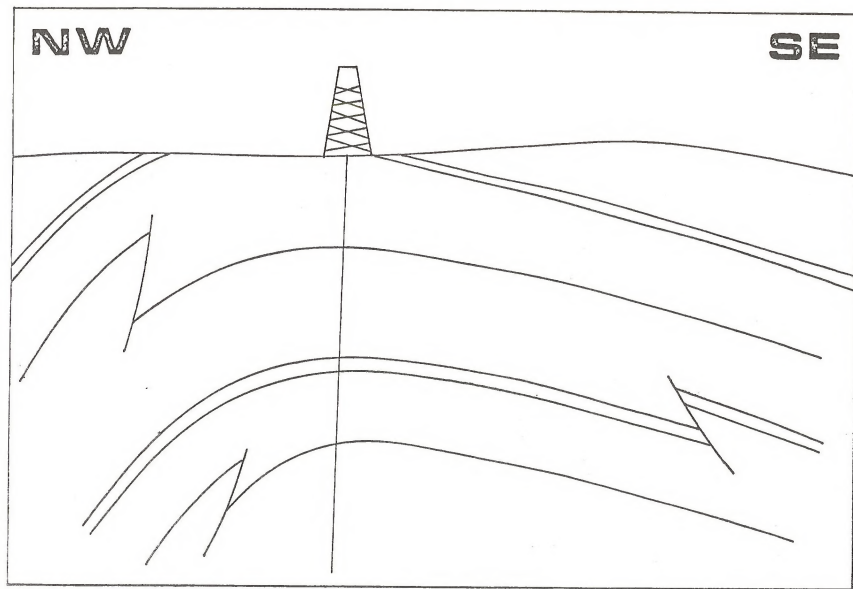
Figure 2. Southeast- and northwest-dipping uplimb thrust
faults (stage II).

development of the anticline. Rotated uplimb thrust faults are also present on the nearly vertical northwest limb of the Cacapon Mountain anticline in Maryland (Perry and de Witt, 1977. p. 32).

Stage II structures shorten beds and facilitate anticlinal growth. Both can occur contemporaneously in a planar, mechanically anisotropic medium if net transport is mostly toward the anticlinal hinge. Some rotation of stage II structures occurs if they form early, at low limb dips (Root, 1973). Uplimb thrusts also show a wedge-like geometry and may be difficult to distinguish from stage I wedges. Uplimb thrusts tend to cut many beds and die out in shale flowage (Gair, 1950), folds (Gwinn, 1964), or bed parallel slip (Price, 1964). Wedges tend to be small because they represent the adjustment to shortening of a single or a few strut-like beds. Wedges can show a downlimb sense of displacement on northwest limbs of anticlines. Uplimb thrusts tend to cut more beds because they represent adjustment to shortening of the entire fold. Uplimb thrusts always show hingeward displacement of the upper (or outer) fault block.

As uplimb thrust faults on limbs steepen during growth of the anticline, the normal stress across the thrust surface and the resulting friction increase until the fault locks (Gwinn, 1964). Further tightening of the

anticline can produce another fault or faults on the limbs. Continued growth of the anticline, beyond that which flexural slip is capable of relieving, causes onset of stage III.

STAGE III STRUCTURES.--Stage III structures begin to form when beds rotate so far towards the vertical that the effect of vertical extension exceeds that of horizontal shortening. Further growth of the anticline can then only occur by bed-parallel extension. Stages I and II both involve bed-parallel contraction, and so can overlap in time. Because the change from bed-parallel contraction to bed-parallel extension is a discrete event, stages II and III are unlikely to overlap, and their structures should be readily distinguishable. Stage III structures are most easily recognized on and are especially characteristic of steeply dipping to overturned beds.

Norris (1958, 1964) defined extension faults as those that result in elongation in the plane of the layering. He reported extension faulting in otherwise ductile beds (carbonaceous shales) dipping 10 to 25 degrees. Price (1964, 1967), Perry (1971, 1978) and this paper describe extension faults in brittle, steeply dipping beds. Norris and Price noted that if the layering rotated externally in the course of flexural-slip folding until it was at a high angle to the maximum principal compressive stress, then

the trajectories of that stress would tend to become perpendicular to the layering and subsequent brittle failure would take the form of extension faults. This rotation of the stress trajectories is shown by the finite-element modelling of Dieterich and Carter (1969). Price (1967) has found that extension faults tend to intersect bedding at about 70 degrees.

Extension faults show net bed-parallel lengthening unique in the kinematic history of a fold, thus allowing easy recognition. Characteristically, extension faults are low-angle, northwest- or southeast-dipping reverse faults on steep or overturned limbs (figure 3). Extension fractures which show bed-parallel lengthening and form normal to bedding are stage III structures. Extension faults have not undergone a significant amount of later rotation. If they formed prior to folding, they would have formed as high angle normal faults, which are inconsistent with Appalachian contractional deformation. Specifically, extension faults cut contraction faults of stages I and II (Perry, 1971, Perry and de Witt, 1977) and are therefore later features. In extreme cases, map-scale extension faults can lead to overthrust west limbs of anticlines (Dennison, written communication, 1978).

With the possible exception of some systematic joints, stage III structures are the latest recognizeable
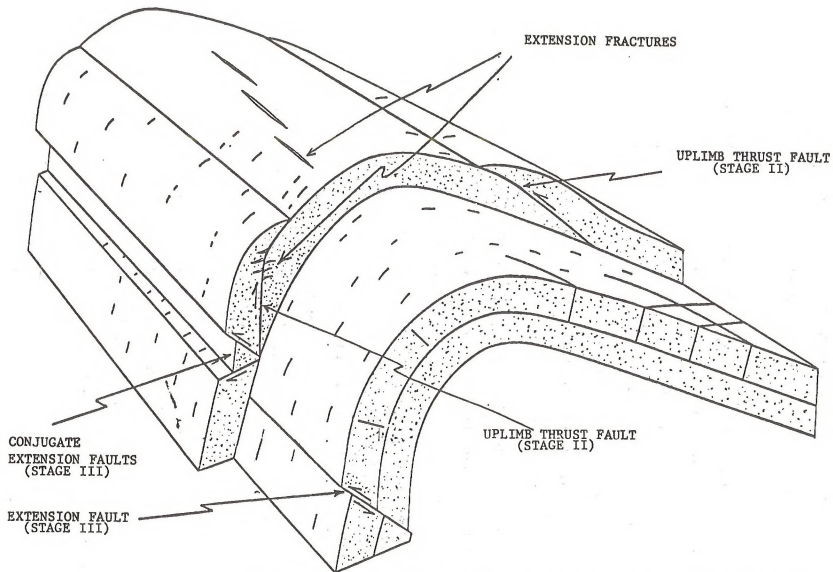
Figure 3. Relationships of stage II uplimb thrust faults to stage III extension faults on an asymmetric fold (modified from Perry and de Witt, 1977, after Price, 1967). Extension fracturing may be associated with both stages II and III.

effects of brittle, fold-related deformation in the central Appalachians. Because they are least likely to be filled by vein material or closed during later deformation, they are a possible target for gas exploration in fractured rock.

Field Applications

Recent fieldwork has shown the applicability of our three-stage model of brittle deformation in steeply dipping beds in the central Appalachians. Nine exposures of Ordovician through Mississippian limestones, sandstones, siltstones, and shales of West Virginia, Maryland and Virginia have been interpreted in terms of the model to yield a sequence of events consistent with Appalachian structural style. Slip-senses of minor faults are usually apparent and show either stage I contraction faulting, stage II crestward slip, or stage III bed parallel extension, depending on the angle between beds and horizontal shortening when failure occurred. Directions of fracture openings are ambiguous unless the fractures are filled with fibrous calcite, cut across compaction or tectonic stylolites, or are slickensided. Durney and Ramsay (1973) showed that crystal fibers in calcite fracture-fillings track the direction of opening of the fracture. If the fracture opened by simple dilatancy, then succesive orientations of incremental

extension during fiber growth can be determined. If the
direction of fracture opening is parallel or at a small
angle to bedding, then the fracture is unequivocally a
stage III feature. Fractures whose opening directions have
components of crestward shearing can be either stage I or
stage II.

An excellent exposure showing examples of all three
stages of brittle deformation is the cut in Silurian
limestones along the Baltimore and Ohio Railroad, on the
northwest flank of the Wills Mountain anticline at Pinto,
Allegany County, Maryland.

Acknowledgements

Western Limit of Extension Fracturing in West Virginia

Philip S. Berger and Russell L. Wheeler

Department of Geology and Geography

West Virginia University

Morgantown, West Virginia 26506

Abstract: Extension fractures can extend beds and create porosity, permeability or both where dips on anticlinal limbs are relatively steep (greater than 45 degrees if there is no strain parallel to hinge lines). Simple calculations and reasonable assumptions permit the conclusion that including the effect of hinge line parallel strain does not significantly alter the minimum bed dip at which extension fractures will open. Therefore the minimum conditions necessary for extension fracture formation are unlikely to occur west of Gwinn's (1964) high plateau, with the exception of the Burning Springs anticline, in Wood and Wirt Counties, West Virginia, where limb dips reach a maximum of 68 degrees.

INTRODUCTION

Detachment faults in ductile beds are the primary mechanism for map-scale deformation in the central Appalachian allochthon, and specifically for the Valley and Ridge and most of the Plateau provinces in West Virginia (Gwinn, 1964; Rodgers, 1963). The location of the

western limit of detachment in the central Appalachians is a matter of conjecture, although it may be significant in explaining the distribution or occurrence of gas production from the Middle and Upper Devonian clastic sequence (mostly shales). The purpose of this paper is to determine the western limit in West Virginia of detachment-related fracture porosity and permeability formed as folding rotates beds from low limb dips, where they are contracted, to high dips, where they are extended.

STRUCTURAL STYLE

The West Virginia allochthon has many detached anticlines but few outcropping major thrust faults. The major anticlines are interpreted as active features generated mainly by duplication of strata by ramping of underlying detachment faults, by splay faults, by kink band folding, and by ductile flow of shale rich intervals into anticlinal crests (Gwinn, 1964; Faill, 1969; Wheeler, 1975). The major synclines are regarded as passive features resulting from anticlinal growth in adjacent rocks, rather than from active downbuckling (Gwinn, 1964).

Location of the western limit of allochthonous anticlines involving the Devonian clastic sequence is ambiguous, because the folds generally become less distinctive towards the west. Limb dips and closure decrease westward. In some of the folds of central and

western West Virginia, such as the Arches Fork and Wolf Summit anticlines, closure is apparent below the Middle and Upper Devonian clastic sequence, on the Middle Devonian Onesquethaw Group (Cardwell, 1973), but not above the clastic sequence, on the Middle Mississippian Greenbrier Group (Haught, 1968). The limestones, sandstones, cherts, and thin shales of the Onesquethaw Group and the underlying Oriskany Sandstone, Helderberg Group, and Tonoloway Formation commonly form a single stiff unit about 600 to 1000 feet (180 to 300 meters) thick (Cardwell and others, 1968) in the mechanical stratigraphy of West Virginia. If the folds in the Onesquethaw are part of the allochthon, then a detachment below the Silurian Tonoloway and the thick Devonian clastic sequence (2600 to 7800 feet; 800 to 2400 meters) has absorbed the deformation by flow (Cardea, 1956) or upper detachment (Dahlstrom, 1969a). On the other hand, some folds show closure in the Mississippian Greenbrier Group but not in the Devonian Oriskany Sandstone, from which we infer that a detachment is above the Oriskany and probably in the ductile Middle Devonian black shales. Perry and Wilson (1977) describe an example of this on the Mann Mountain anticline.

We believe that extension fractures may form a significant part of gas-bearing fracture porosity and

permeability. Extension fractures that show bed-parallel extension are interpreted to be late tectonic, formed when folding beds rotated to such steep dips that the rocks were within the extensional, rather than contractional field of the strain ellipsoid (Berger, Perry and Wheeler, ms. in review). These extension fractures are unlikely to be filled by vein material or closed by later deformation and thus may produce gas. We attempt to locate the western limit of extension fracturing in the subsurface as part of a program to predict the location of more highly fractured rock for gas exploration.

In this paper we use the analytical and graphical techniques of Ramsay (1967) to determine the angle (θ) between the X strain axis (the direction of greatest lengthening: vertical) and the surface of no finite longitudinal strain. The surface of no finite longitudinal strain marks the boundary between the contractional and extensional fields in the strain ellipsoid and its dip increases with the horizontal contractional strain. Assuming that the maximum principal compressive stress and the Z strain axis (direction of greatest contraction) are horizontal and perpendicular to strike (Perry, 1971), then the minimum bed dip at which extension fractures can open is $90 - \theta$ degrees. Using published values of shortening or values measured on published cross-sections, we calculate

the critical (minimum) bed dip at which extension fracturing will begin. Comparison of predicted values of critical dips with observed or estimated values of limb dips or shortening in anticlines allows us to predict the distribution of extension fracturing and related fracture porosity and permeability in West Virginia.

METHODS

Ramsay (1967, p. 128) determined the equation for the angle (θ) between the surface of no finite longitudinal strain and the X strain axis, assuming constant volume and no hinge line parallel strain ($e_2 = 0$)

$$\theta = \pm \cos^{-1} \sqrt{\frac{\lambda_3' - 1}{\lambda_3' - \lambda_1'}} \qquad (1)$$

where $\lambda_i' = 1/\lambda_i$

and $\lambda_i = (1 + e_i)^2$, $i = 1, 2, 3$ $\qquad (2)$

Therefore to determine the minimum bed-dip at which extension fractures will begin to open for a given anticline and its estimated shortening value, we need values of λ_1 and λ_3.

λ_3 measures length change parallel to the X (contractional) strain axis. λ_2 measures length change parallel to the hinge line of the fold (intermediate strain axis: Y) and is assumed to be equal to 1. λ_1 measures strain parallel to the Z (extensional) strain axis. λ_3 is found by measuring the amount of shortening for a given anticline by the sinuous bed or equal area method,

after removal of synfolding or postfolding slip on faults
that changed bed length but did not rotate beds. We shall
regard folding of a stiff layer within a volume of softer
rock as grossly approximating overall homogenous
nonrotational strain. We assume that the volume of rock
containing the rotating stiff bed is not cut by through-
going detachments and thus has not been deformed by shear
on or near the detachment. That assumption is reasonable
within a single anticline (Kulander, oral communication,
1978). Then by the sinuous bed method after restoration of
fault slip, the shortening strain is

$$e_s = (l-l_o)/l_o \tag{3}$$

where l_o = the arc length of a stiff unit like the
Onesquethaw-Tonoloway sequence, and

l = the linear distance between the two inflection
points of the anticline (the distance into
which l_o has shortened).

The sinuous bed method is valid for stiff units that
have buckled, kinked, or faulted, but have not flowed
internally or pressure-dissolved. The values of
shortening in this paper are determined by the sinuous bed
method but are consistent with values determined by the
equal area method (Gwinn, 1970), which does not assume
that there has been no internal flowage or mass-removing

pressure solution.

Our values of shortening need not include shortening by layer parallel penetrative strain (Engelder and Engelder, 1977) or by formation of pressure solution cleavage (Geiser, 1977), because most of this shortening appears to have formed early, prior to folding (Geiser, 1970; Nickelsen, 1976, 1978; Berger, Perry and Wheeler, ms. in review).

λ_1 can be calculated as follows. For a unit sphere deforming at constant volume to a strain ellipsoid

$$V(\text{sphere}) = \frac{4}{3}\pi r^3 = \frac{4}{3}\pi$$

$$V(\text{ellipse}) = \frac{4}{3}\pi(1+e_1)(1+e_2)(1+e_3)$$

Substituting equation (2) and setting V(sphere) equal to V (ellipsoid)

$$\lambda_1 = \frac{1}{\lambda_2 \lambda_3} \qquad (4)$$

Therefore to determine λ_1 we need only λ_3, which we estimate from shortening, and λ_2, which we assume is equal to 1. Therefore

$$\theta = \pm \cos^{-1} \sqrt{\frac{\frac{1}{\left[\left(1 + \frac{\ell - \ell_0}{\ell_0}\right)^2 - 1\right]}}{\frac{1}{\left[\left(1 + \frac{\ell - \ell_0}{\ell_0}\right)^2 - \left(1 + \frac{\ell - \ell_0}{\ell_0}\right)^2\right]}}} \qquad (5)$$

If we take into account hinge line parallel strain, then λ_2 will be close to but not equal to 1. We assume that e_2 will be no more than ± 10 percent of e_3. This figure is arbitrary but is probably in excess of the true value in

most places, especially where large folds are straight in map view. There is no doubt that strain parallel to hinge lines occurs. The existence of cross joints in folded rocks demonstrates hinge line parallel extension, although hinge line parallel contraction may be equally likely in folded rocks. The arcuate trends in parts of the central Appalachians may help determine whether hinge line parallel contraction or extension has occurred. Where the Appalachians are convex toward the craton, as in central Pennsylvania, hinge line parallel extension may be more likely. Where the Appalachians are concave cratonward, as in southern West Virginia and western Virginia, hinge line parallel contraction is more likely.

Using our values of shortening, and reasonable estimates of λ_2, the angle (θ) between the vertical X strain axis and the surface of no finite longitudinal strain is determined graphically using a Mohr diagram for three-dimensional strain (Ramsay, 1967, p. 152). The points along the line $\lambda' = 1$ on the Mohr diagram yield values of points on the surface of no finite longitudinal strain, in degrees from the X and Y strain axes. These values can be plotted in equal area projection to determine the shape of the surface of no finite longitudinal strain: conical with hinge line-parallel strain, planar without (Ramsay, 1967, fig. 4-21). The

minimum bed dip at which extension fractures will open is
measured along the east-west axis of the projection.

RESULTS

Table 1 lists the predicted bed dips at which
extension fractures will begin to open for given values of
shortening and $\lambda_2 = 1$. These values were calculated using
equation (5) and are the complements of the angles (θ)
between the X strain axis and the surface of no finite
longitudinal strain. Some of the predicted dips were
checked by Mohr diagrams for three-dimensional strain.
With no change in length parallel to the hinge line, the
minimum bed dip at which extension fractures will begin to
open is 45 degrees. That finding is consistent with the
results of finite-element modeling of viscous layers
(Dieterich and Carter, 1969), and other work summarized
by Perry (1978, p. 524). Where there is $\pm.1(e_3)$ hinge line
parallel strain, the minimum bed dip at which extension
fractures will open does not differ significantly from the
values in Table 1.

Table 2 lists measurements of shortening for
anticlines in West Virginia, determined from
cross-sections by the sinuous bed method or from estimates
in the literature. With the exception of the Burning
Springs anticline, in Wood and Wirt Counties, West
Virginia, no anticlines west of Gwinn's (1964) high

TABLE 1

PERCENT SHORTENING	MINIMUM LIMB DIP
1%	45 degrees
2%	45 degrees
3%	46 degrees
4%	46 degrees
5%	46 degrees
10%	48 degrees
15%	50 degrees
20%	51 degrees
25%	53 degrees
30%	55 degrees
35%	57 degrees
40%	59 degrees
45%	61 degrees
50%	63 degrees

plateau, which have structural relief less than 300 feet
(90 meters), should show extension fracturing unless
faulting in the subsurface has created abnormally high
limb dips. Fault imbrication in the subsurface of the
Burning Springs anticline has caused dips as steep as 68
degrees (Shockey, 1954). The Arches Fork and Wolf Summit
anticlines may also show extension fracturing, since Gwinn
(1964) indicates that they have between 300 and 800 feet
(90 and 240 meters) of relief, intermediate between
anticlines of the high plateau and those of western West
Virginia.

ACKNOWLEDGEMENTS

Table 2.

Anticline	Location	Shortening	Maximum Limb Dip	Source
RELIEF GREATER THAN 800 FEET (240 METERS)				
Burning Spgs.	Wood/Wirt Co.	2%	68 degrees	Shockey (1954)
Briery Mtn.	Preston Co.	6%	45 degrees	Cardea (1959)
Chestnut Rdg.	Monongalia Co.	3%	12 degrees	Mitchell (1960)
Wills Mtn.	Pendleton Co.	20%	overturned	Perry (1971)
Browns Mtn.	Pocahontas Co.	16%	overturned	Kulander and Dean (1972)
RELIEF BETWEEN 300 and 800 FEET (90 and 240 METERS)				
Wolf Summit	Lewis Co.	<1%	5 degrees	Milner (1968)
Hiram	Harrison Co.	<1%	<1 degree	Cardwell (1973)
Arches Fork	Doddridge Co.	<1%	<1 degree	Cardwell (1973)
Warfield	Logan Co.	<1%	<1 degree	Cardwell (1973)
RELIEF LESS THAN 300 FEET (90 METERS)				
Mann Mtn.	Fayette Co.	<1%	<1 degree	Perry and Wilson (1977)

Late-Tectonic Extension Faulting in the Central Appalachians

Philip S. Berger and Russell L. Wheeler

Department of Geology and Geography

West Virginia University

Morgantown, West Virginia 26506

Abstract: Examination of outcrops in parts of the western
Valley and Ridge and eastern Allegheny Plateau provinces
of Maryland, Pennsylvania, Virginia and West Virginia
located 227 bed-extension faults of which 115 had
measurable separation at 24 stations. Previous work
showed the faults formed late during folding when beds
were steeply dipping, and not by early normal faulting
when beds were horizontal. The distribution and amount of
extension faulting have implications bearing on tectonic
development and gas potential. First, outcrop-size and
larger extension faults contribute significantly to
anticlinal growth in more brittle units when external
rotation steepens fold limbs. Second, stratigraphic
localization of extension faulting suggests that reported
thinning of brittle units on steep limbs of anticlines may
be partly due to late-tectonic extension faulting, rather
than wholly to splay faults rising from detachment
surfaces. Third, measured values of bed-parallel extension
for packets of especially brittle rocks indicate

significant amounts of fracture potentially suitable for gas reservoirs.

INTRODUCTION

The western Valley and Ridge and eastern Allegheny Plateau provinces of Maryland and West Virginia are characterized by anticlines with the greatest amounts of structural relief within their respective provinces. In the Valley and Ridge province, the Wills Mountain anticline (Fig. 4) has approximately 4000 m of structural relief (Perry, 1975). In the Plateau province, the Browns Mountain anticline may have structural relief as great as 2500 to 3000 m (Kulander and Dean, 1972). The Elkins Valley anticline also exposes vertical beds and may have structural relief of almost 3000 m (Rodgers, 1970). Northwest limbs of these folds are steeply dipping and locally overturned. Other eastern Plateau anticlines are characterized by more steeply dipping rocks in the subsurface than at the surface, at least to the level of the Lower Devonian (Rodgers, 1970), and may be asymmetric with more steeply dipping southeastern limbs at least to the level of the Oriskany (Gwinn, 1964).

The steeply dipping limbs of map-scale anticlines in the central Appalachians are due primarily to external rotation of stiff beds (mostly sandstones and limestones) during folding. The map-scale folding is caused by

stepwise westward rise (ramping) of detachment surfaces or by splay faulting from nearly horizontal detachment surfaces (Rodgers, 1963; Gwinn, 1964). In most places in the central Appalachians, the detachment surface or splay fault does not reach the surface. As bed rotation and accompanying horizontal shortening and vertical extension continued, anticlinal growth in stratigraphic units above the detachment involved flow of shaly sequences out of anticlinal limbs and into crests (Wheeler, 1975) and bed-parallel extension in steeply dipping to overturned beds (Perry, 1971).

This study is based on outcrop examination of bed-parallel extension structures, primarily faults, which begin to form when beds rotate sufficiently toward the vertical that the effect of vertical extension exceeds that of horizontal shortening. Extension faults can form at any bed orientation, depending on the attitude of the local maximum principal compressive stress (Norris, 1958, 1964). However in the central Appalachians, analysis of structural style and field investigation both indicate that extension faults form when the dip of beds exceeds 45 degrees (Berger and Wheeler, in review), and mostly as reverse faults, serving to thin the beds. Cloos and Broedel (1943) and Root and Wilshusen (1977) described faults with similar structural style in other parts of the

central Appalachians. Perry and de Witt (1977), Perry (1978), and Berger, Perry and Wheeler (in press) recognize these reverse faults as extension faults, analogous to those described from the Canadian Rockies by Norris (1958, 1964) and Price (1964, 1967).

With the possible exception of some systematic joints, these extension faults are the latest recognized effects of brittle but fold-related deformation in the central Appalachians (Berger, Perry and Wheeler, in press). Because they are formed late during deformation, they are least likely to be filled by vein material or closed during later deformation. If sufficiently numerous and extensive they are an excellent target for gas exploration assuming the presence of a gas-bearing source and reservoir seal. In particular, they may form permeable fractured reservoirs in the Middle and Upper Devonian clastic sequence. This paper attempts to evaluate that hypothesis.

FIELD METHODS

More than 100 large exposures of steeply dipping or overturned beds were examined in the western Valley and Ridge and eastern Allegheny Plateau provinces in parts of Maryland, Pennsylvania, Virginia and West Virginia (Fig. 4). Of these exposures, 24 were intersected by at least one measurable extension fault. Each fault was identified
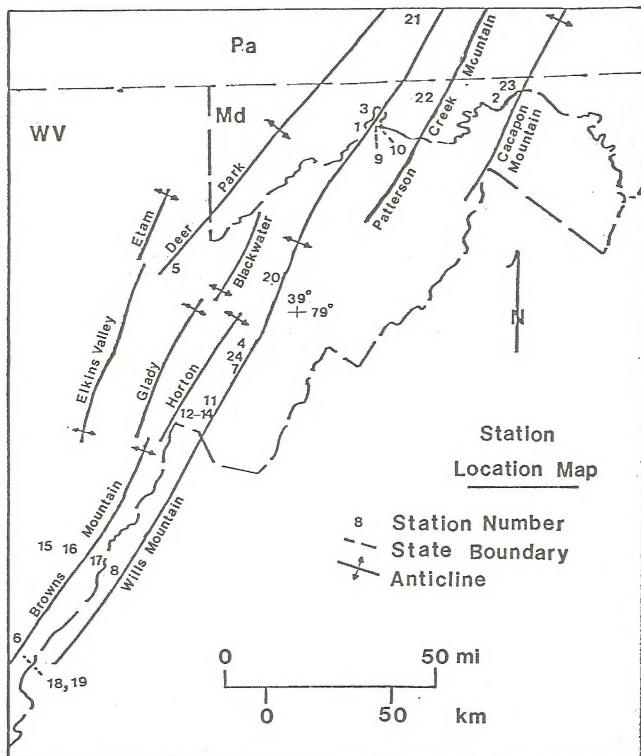
Figure 4. Map showing major anticlines in the study
area. Numbers show locations of stations
listed in Table 4.

either by the senses of asymmetry of associated drag folds
or by matching of beds across the fault. The following
were measured or calculated for each fault: vertical
separation, horizontal separation, dip separation,
bed-parallel extension (separation measured parallel to
the beds, not defined by Dennis, 1972), and the thickness
of the packet of beds affected by the fault. For each
station, the exposure length and thickness of each
stratigraphic unit present were measured. In exposures
with variable dip, only beds dipping more than 45 degrees
were included, because only there are extension faults
expected (Berger and Wheeler, in review).

At a few places in the exposures, zones of en echelon
filled feather fractures with sigmoidal habit were
presumed to mark incipient extension faults. The dip
separation was calculated as the sum of the zone-parallel
thicknesses of the fracture fillings and the other
separation values were calculated accordingly. Styles of
terminations of the fault surfaces were noted, as were
spatial relations to folds and to contraction faults
(faults that shortened beds: Norris, 1958, 1964).

STRUCTURAL STYLE

Perry (1971) recognized 31 extension faults on the
northwest limb of the Wills Mountain anticline in
Pendleton County, West Virginia. He (unpublished notes,

1965-1967) found extension faults in the Silurian
Tuscarora quartzite, Rose Hill formation, Keefer
sandstone, Williamsport sandstone and Tonoloway limestone
and the Devonian Oriskany sandstone. Table 3 details the
number of extension faults recognized in our study.
Extension faults were found in many of the same units in
the study area in which de Witt and Dennison (1972) noted
minor faulting and Perry (1971) noted minor extension
faults. Extension faults were found as well in other
units.

Outside the study area, Cloos and Broedel (1943,
their Plate 1) show 27 extension faults in 180 m of
outcrop in the Hamilton Group near Harrisburg,
Pennsylvania. Not all the reverse faults reported by
Cloos and Broedel (1943) are extension faults. Many are
fractures with unmeasurable amounts of offset or are
contraction faults. However, the number and distribution
of faults and other fractures (843 fractures in 12
stations) led Cloos and Broedel (1943) to conclude that
reverse faults in steeply dipping beds are widespread and
characteristic of Appalachian folding (p. 1388).

Some extension faults occur singly. Others are
conjugate pairs with associated synthetic and antithetic
extension faults. Numerous other fractures were observed,
especially in the shaly parts of the Brallier Formation,

Table 3.

STRATIGRAPHIC UNIT	NO. OF EXTENSION FAULTS	NO. OF MEASURABLE EXT. FAULTS	CUMULATIVE THICKNESS OF SECTION: OUTCROPS WITH MEAS. EXT. FAULTS	FAULTS PER M OF SECTION
Mississippian				
Pocono Formation	9	4	266 m	0.034
Devonian				
Hampshire Formation	1	0	--	--
Chemung Group	8	6	308 m	0.026
Brallier Formation	104	43	1251 m	0.063
Millboro Formation	1	1	75 m	0.01
Marcellus Formation	4	0	--	--
Silurian				
Tonoloway Formation	35	24	200 m	0.175
Wills Creek Formation	1	1	159 m	0.006
Bloomsburg Formation	7	2	94 m	0.074
McKenzie Formation	27	17	148 m	0.182
Rochester Shale	14	14	139 m	0.101
Keefer Sandstone	2	1	6 m	0.3
Rose Hill Formation	4	2	7 m	0.6
Tuscarora Formation	7	4	82 m	0.08
Ordovician				
Juniata Formation	3	2	40 m	0.08
Total	227	115		

many with slickenside, slickenline, or apparent dip
orientations similar to those of nearby extension faults
but not showing drag folding or matchable beds. The number
of extension faults recognized, as well as the numerous
undifferentiated fractures, indicates to us that extension
faults are an important and little recognized component
of, and are indeed characteristic of, certain
stratigraphic units where those units are rotated to steep
dips. Thus field observations indicate that in the
Devonian clastic sequence, the Brallier Formation may form
unusually many extension faults when bed dips increase
into the extensional field.

Field observations indicate that the extension faults
may terminate against each other, or against a thick bed
of siltstone or limestone. In some places the thick bed is
broken by a fracture zone along the continuation of the
extension fault, and the fractures may show small amounts
of slip. An extension fault may die out as a single fault
or by distributing its slip among several splays in
shales. At many places the extension faults curve upwards
or downwards into surfaces of bedding-plane slip (Price,
1964).

Extension faults may form and have been recognized
on limbs of folds ranging in size from typical
outcrop-scale to map-scale. Therefore they represent a

common response to the local maximum principal compressive
stress, which tends to be roughly parallel to beds until
dips reach 45 to 60 degrees, and then tends to be
perpendicular to the beds (Dieterich and Carter, 1969).
Previous workers have shown that most extension faults
form at high angles to beds, although they can form at
lower angle (Norris, 1958; Price, 1967; Perry, 1971).

Price (1964) writes that in less steeply dipping beds
in the Canadian Rockies, extension faults tend to show a
uniform dip direction and commonly begin and terminate in
a bedding-plane slip surface. With increased bed rotation,
he noted that extension faults form conjugate sets. We
have not found this to be generally true in the central
Appalachians. An extension fault that terminates in a
bedding-plane slip surface may be part of a conjugate set
of extension faults. Overturned beds in the central
Appalachians show both single faults and conjugate sets of
extension faults.

Because some extension faults are found to begin or
terminate in bedding planes, earlier flexural slip folding
may still have been active at the time of extension
faulting. We propose that extension faulting can occur
during flexural-slip folding if the contacts within a
packet of beds become locked, perhaps around small folds,
so that the shear strength at a bed contact exceeds the

tensile strength of the bed or beds. The slip surface may then cut across the locked beds, forming an extension fault. Some subsequent external rotation of those extension faults by further folding is likely (Price, 1964), especially where beds are now overturned.

Other extension structures found include boudinage of thin siltstone or limestone beds, abundant lenticular extension fractures oriented roughly perpendicular to bedding, and three normal faults of small displacement. There is a strong positive association between exposed fault length and amount of dip separation (for 119 observations, Spearman's correlation coefficint (Siegel, 1956) gives a significance level of .0001.

RESULTS

Table 4 summarizes the results of our field investigations for the 24 stations that showed measurable separation. Below, we suggest that useful conclusions of regional applicability can be reached by extrapolating our data into the subsurface. Inferences about fold growth and tectonic thinning of the limbs can be made from compilation of the vertical and horizontal separation data, respectively. Estimates of gas potential are based on the amount of bed parallel extension.

It must be emphasized that measurements reported here are minimum values. Only definite extension faults

Table 4.

STATION NO. AND NAME	E/R	T/R	F/R	LOCATION	STRATIGRAPHIC UNITS(S)
1 Pinto, Md	27.0%	1.6%	30.0%	NW limb, Wills Mt. ant.	Rose Hill/Keyser
2 Woodmont, Md	2.9%	0.4%	3.7%	NW limb, Cacapon Mt. ant.	Mahantango/Brallier
3 La Vale, Md	4.0%	0.5%	3.0%	NW limb, Wills Mt. ant.	Mahantango/Hampshire
4 Ketterman's Knob, WV	40.0%	0.1%	14.4%	NW limb, Wills Mt. ant.	Brallier
5 Parsons, WV	2.6%	3.5%	3.6%	axial region, Deer Park ant.	Chemung
6 White Sulfur Springs, WV	40.0%	0.1%	14.4%	NW limb, Browns Mt. ant.	Chemung/Pocono
7 Judy Gap-a, WV	<.1%	0.2%	-----	NW limb, Wills Mt. ant.	Tonoloway
8 Ryder Gap, VA	23.0%	3.7%	25.0%	NW limb, Wills Mt. ant.	Brallier/Chemung
9 Cedar Cliffs, Md	1.0%	0.6%	1.3%	SE limb, Wills Mt. ant.	Bloomsburg/McKenzie
10 Rose Hill, Md	0.5%	0.2%	0.2%	SE limb, Wills Mt. ant.	Rose Hill/McKenzie
11 Teeter Hollow, WV	<.1%	0.1%	<.1%	NW limb, Wills Mt. ant.	Rochester
12 Snowy Mt. Rd.-a, WV	2.0%	0.4%	2.4%	NW limb, Wills Mt. ant.	Rochester/Keefer
13 Snowy Mt. Rd.-b, WV	3.0%	2.9%	2.3%	NW limb, Wills Mt. ant.	Rochester/Keefer
14 Snowy Mt. Rd.-c, WV	1.0%	1.9%	2.3%	NW limb, Wills Mt. ant.	Rochester/Keefer
15 Huntersville, WV	0.1%	<.1%	0.6%	NW limb, Browns Mt. ant.	Bloomsburg
16 Rte. 39, WV	3.4%	<.1%	0.6%	axial region, Browns Mt. ant.	Tuscarora
17 Minnehaha Springs, WV	0.5%	0.8%	0.4%	SE limb, Browns Mt. ant.	Juniata/Tuscarora
18 I-64-a, WV	<.1%	0.1%	<.1%	SE limb, Browns Mt. ant.	Brallier
19 I-64-b, WV	<.1%	0.2%	<.1%	axial region, Browns Mt. ant.	Harrell/Brallier
20 North Fork Gap, Pa	0.2%	0.3%	<.1%	NW limb, Wills Mt. ant.	Tuscarora
21 Wolf Camp Run, Pa	<.1%	0.1%	<.1%	NW limb, Wills Mt. ant.	Mahantango/Brallier
22 Martin Mt., Md	<.1%	0.3%	<.1%	NW limb, Patterson Ck. Mt. ant.	Tonoloway
23 Hancock, Md	<.1%	0.1%	<.1%	SE limb, Cacapon Mt. ant.	Bloomsburg
24 Judy Gap-b, WV	31.0%	3.1%	34.8%	NW limb, Wills Mt. ant.	Brallier

E = anticlinal growth; T = tectonic thinning; F = amount of extension; R = structural relief

were measured. All measurements were taken in 2 to 3 m
high strips along the accessible basal segments of
exposures. The larger the displacement along the fault the
less the chance of matching beds across the fault. The
extrapolations into the subsurface could be maximum values
because they assume the same intensity of faulting
throughout the vertical extent of the fold limb as that
measured in our selected exposure. However, because it
seems unlikely that the present erosion level
preferentially exposes unusually extended rocks, the true
values may approach our extrapolated values. Thus the
results reported here are conservative (minimum) but
probably roughly accurate values for the amount of fold
growth by extension faulting.

FOLD GROWTH

The major anticlines of the central Appalachians are
active structures generated mainly by duplication of
strata by ramping of underlying detachment faults, by
splay faulting, and by ductile flow of shale or evaporite
sequences into anticlinal crests (Gwinn, 1964; Faill,
1969; Wheeler, 1975). The major synclines are passive
structures resulting from anticlinal growth in adjacent
rocks, rather than from active downbuckling (Gwinn, 1964).
We propose that extension faulting late during folding
provides an important contribution to anticlinal growth.

At Station 1, near Pinto, Maryland on the northwest limb of the Wills Mountain anticline (Fig. 4, Table 4), the amount of growth by bed-parallel extension may be as much as 27% of the entire structural relief of the fold. This value is based on data from a single exposure on the limb of the anticline and is extrapolated into the subsurface by

$$E = V(BPT/ET)(R/2.5) \qquad (1)$$

where E = the amount of anticline growth by extension, in meters,

V = the sum of the amounts of vertical separation of measured extension faults,

BPT = the sum of the thicknesses of the packets of beds containing the extension faults,

ET = the present (post-extension) length of the exposure measured perpendicular to beddinig,

R = the structural relief of the anticline, and

2.5 = the height of accessible exposure in meters.

Estimates of structural relief are: Wills Mountain anticline - 4000 m (Perry, 1971), Browns Mountain anticline - 3000 m (Kulander and Dean, 1972), Deer Park anticline, 3000 m (Gwinn, 1964), Cacapon Mountain

anticline - 4000 m (Perry and de Witt, 1977), and
Patterson Creek Mountain anticline - 2500 m (Cardwell,
1975). The amount of structural relief of the Wills
Mountain anticline in Maryland and Pennsylvania is equal
to or greater than the amount measured by Perry (1971) in
Pendleton County, West Virginia, because although the
anticline appears to lose structural relief northeastward
into Maryland (Cardwell and others, 1968), that is
compensated by increasing depths to basement from
southwest to northeast along the strike of the Wills
Mountain anticline (Kulander and Dean, 1978).

Using equation (1), values of E have been determined
for each station in which extension faulting was
measurable. Similar results have been obtained by Cloos
and Broedel (1943), using a similar method of
extrapolation. They estimated that the reverse faults
contribute 10% to the structural relief of the anticline
they studied. Table 4 lists our percentages of anticline
growth by extension. The contribution of extension to
fold growth is significant in many exposures, especially
considering that extension does not begin until late in
folding when the limbs are steeply dipping and the fold
may have already attained considerable relief. The
widespread stratigraphic and geographic distribution of
extension faults in steeply dipping beds (Tables 3 and 4,

Fig. 4) supports our suggestion that our results have
regional applicability.

TECTONIC THINNING

Tectonic thinning of measured stratigraphic sequences
has been reported in the study area (Dennison and Naegele,
1963; Dennison, Travis and Ferguson, 1966; de Witt and
Dennison, 1972; de Witt, 1974) and was used as a guide by
us in locating exposures that have undergone extension
faulting. We hoped to be able to recognize enough
extension faults to account for a large proportion of the
tectonic thinning. The amount of tectonic thinning (T) is
determined using equation (2)

$$T = H/ET \qquad\qquad (2)$$

where   H = the sum of the amounts of horizontal

separation of measured extension faults.

At Station 4, near Ketterman's Knob, Pendleton County,
West Virginia (Fig. 4, Table 4), Dennison and Naegele
(1963) report that approximately 60 m of the Brallier
formation is absent (about 25% tectonic thinning). Outcrop
examination at Station 4 indicates a minimum of .1%
tectonic thinning by extension faulting. Here Dennison and
Naegele (1963) write that tectonic thinning was probably
accomplished by minor faulting within a fault zone in the
Brallier Formation.

To the north along strike, Dennison, Travis and

Ferguson (1966) infer the presence of four major fault
zones in the Brallier Formation (Kittlelick, Dawson,
Cresaptown [station 3], and Hyndman [station 21] faults)
largely from geomorphic evidence of a narrow strike
valley, but also from measured stratigraphic sections.
Dennison, Travis and Ferguson (1966) infer that these
fault zones are splay faults rising from a deep
detachment, probably located in the Ordovician Reedsville
Formation. De Witt (1974 and written communication, 1978)
proposes on the basis of seismic data that the Hyndman
fault is a large splay fault with associated extension
faults in the fault zone, particularly in the vicinity of
the village of Hyndman.

We believe that the tectonic thinning reported by
Dennison and Naegele at our stations 3 (La Vale) and 4
(Ketterman's Knob) was accomplished more by small and
medium size late tectonic extension faults than by the
single splay faults envisioned by Dennison and Naegele
(1963) and de Witt and Dennison (1972) (Fig. 5). Our
arguments are three. First, all four inferred splay faults
crop out in and thin the Brallier Formation. This requires
a fortuitous coincidence of erosion level with the
intersection of the Brallier Formation and the fault
surface and must occur for all four faults. If a fault is
a splay and thus not confined to the Brallier, then it is
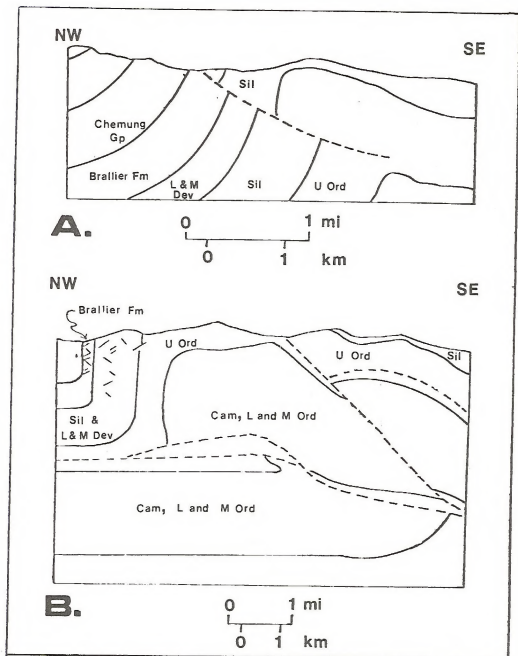
Figure 5. Contrasting models of tectonic thinning by
faulting on the northwest limb of the Wills
Mountain anticline. No vertical exaggeration. A.
Splay fault interpretation modified from Dennsion
and Naegele (1963), Dennison and others (1966) and
de Witt and Dennsion (1972). B. Extension fault
interpretation modified from Perry (1971). Dashed
lines are decollement or splay faults. Short
solid lines in upper left of section B are
extension faults. Cross-sections are not to the
same scale.

about equally likely to crop out stratigraphically above, within, or below that unit. Second, as shown in Table 3, the Brallier Formation shows more extension faults than does any other Devonian unit examined. Third, as noted above under "Field Methods", the Brallier contains more minor faults, many unclassifiable, than does any other unit examined. We suggest a simpler explanation that the Brallier Formation localizes extension faulting in our study area (Fig. 5). These small extension faults may not descend to the detachment in the Reedsville Formation, but could have considerable slip. Perry (1971) has recognized a map-scale extension-like fault on the Wills Mountain anticline (see also de Witt, 1974).

We suggest that the Dawson thrust of Dennison and Naegele (1963) and de Witt and Dennison (1972) is a large extension fault because we observed few minor extension faults in the outcrop belt of the fault zone (station 21 and in exposures near station 1).

The thinning in the Hyndman fault zone is more likely to be due to splay faulting than to the associated extension faults (de Witt, written communication, 1978) on the basis of confidential seismic data available to de Witt. However, the thinning mapped at the surface (de Witt, 1974) may not be clearly connected with the splay fault observed on the seismic section at depth because

poor reflections are usually received in such areas of steep dips.

The Kittlelick fault is thought to be a fault zone by Dennison, Travis and Ferguson (1966). We agree but suggest that the thinning along the Kittlelick fault is due to a zone of extension faulting similar to the zone of numerous extension faults observed along the Cresaptown fault and near Ketterman's Knob. We also suggest that thinning of stratigraphic units adjacent to the Kittlelick and Hyndman faults as reported by Dennison and others (1966) and de Witt and Dennison (1972) may also be due in part to extension faulting as well as to branches from splay faults.

PERCENT EXTENSION

Maximum possible amount of extension due to faulting (F) is estimated by

$$F = BPE(BPT/ET)(R/2.5) \qquad (3)$$

where   BPE = the sum of the amounts of bed-parallel extension of measured extension faults.

The value (F) is the amount of extension for a limb of a fold based on extrapolation of measured values of bed-parallel extension. The greater the (F) value the greater the possibility of a fold being suitable for gas in fractured reservoirs. This estimate is a maximum because the extension is generated as beds are faulted

apart in directions parallel to bedding but the resultant voids are simultaneously reduced by tectonic thinning.

As shown in Table 4, the (F) value due to bed-parallel extension on the Wills Mountain anticline can be locally almost 35% of total structural relief. We have noted that extension faults are always associated with extension fractures. We suggest that qualitative estimates of the relative amounts of fracture porosity and permeability in the subsurface can be made by comparison of bed-parallel extension values (F).

Murray (1968) obtained a value of .05 percent fracture porosity from a geometric analysis of bed curvature in a producing field with very low primary porosity. We believe there occur zones or patches of concentrated fracture porosity, or permeability, or both, depending on the response of a particular stratigraphic unit to the local maximum principal compressive stress. Where many small measurable faults extend the beds, rather than one or a few larger unmeasurable extension faults, then our data will show a higher percent extension. Along the Allegheny Front in southern Pennsylvania, Maryland and northern West Virginia (Dennison and Naegele, 1963), these faulted zones vary in intensity northeast and southwest along strike of the Brallier Formation. It is also possible that faulted zones vary vertically throughout the

limb in the subsurface. More detailed stratigraphic work is necessary before drilling targets can be selected. However, estimates of tectonic thinning by Dennison and Naegele (1962), Dennison and others (1966), and de Witt and Dennison (1972), values in our Table 3, and the abundant unclassified fractures observed in the shaly parts of the Brallier Formation all suggest to us that the Brallier may be the most highly extension-fractured and -faulted unit in the subsurface.

Extension faulting is usually restricted to a relatively brittle bed or beds bounded by more ductile shaly beds. Thick-bedded brittle units do not show well developed extension faults, nor do ductile black shales that we examined. Results consistent with these statements have been obtained in experimental work (Griggs and Handin, 1959). We suggest that the 0.3 to 0.7 m thick, shale-bounded siltstones near the base of the Brallier Formation would be the most likely candidates for production controlled by extension faults. They may be the equivalent of the Sycamore sandstone or siltstone (Patchen, 1977), a unit recognized only in the subsurface of central West Virginia and which produces small amounts of gas.

Any patchy distribution of tectonic thinning may be due to the presence or absence of lubrication between beds

(see Reches and Johnson, 1976). Where the bed packets are unlubricated, they may lock and fail by extension, as described above. Where they are lubricated, they may undergo flexural slip without extension. The type and distribution of lubrication is beyond the scope of this paper. Alternatively, there exists the possibility that the zones of intense extension fracturing and extension faulting may be due to the presence of a nearby large splay fault.

GAS POTENTIAL

Any potential fractured reservoir whose porosity and permeability are partly or wholly due to extension fracturing would be located in folds of the eastern or High Plateau (Gwinn, 1964) or Valley and Ridge province where dips greater than 45 degrees allow extension fracture formation (Berger and Wheeler, ms. in review). If the Brallier Formation is selected as the target gas bearing formation, then the Glady, Horton, Blackwater and Deer Park anticlines would be the best potential sites in the High Plateau because the Brallier is not exposed but is present at shallow depths and may contain steeply dipping beds. In the Valley and Ridge province the Broadtop synclinorium also offers steeply dipping Brallier Formation in subsurface anticlines (Jacobeen and Kanes, 1974). If the source of gas in the Brallier is the

underlying dark, kerogen-rich shales, then the prime
drilling targets would be off the crests of the anticlines
on the steep, extended limbs. Drilling targets on the
limbs have not been adequately tested in the past (R.
Shumaker, oral commuication, 1978). Here thinned, steeply
dipping, extended Brallier rocks may overlie dark shales
thinned by flowage toward cores of detached anticlines
that grew over imbricated stacks of Oriskany Sandstone and
older rocks. The presence of gravity lows near the crests
of anticlines indicates shale flowage (Kulander and Dean,
1978).

ACKNOWLEDGMENTS

Extension in Kink-Bands and on the Limbs of Kink Folds

Philip S. Berger and Russell L. Wheeler

Department of Geology and Geography

West Virginia University

Morgantown, West Virginia 26506

ABSTRACT: Beds in kink-bands can undergo bed-parallel extension when the angle between the kink surface and the kink-band is less than the angle between the kink surface and the enveloping beds. Field investigations in the Middle and Upper Devonian clastic sequence of the central Appalachians indicate that the kink-band undergoes more extension fracturing and jointing and shows more twist hackle than the enveloping beds. However, comparison of measured values of extension with predicted volume increases in kink-bands indicates that only about 10 percent of the volume change is translated into extension fractures.

The intersection of two inclined kink-bands produces a kink fold that is identical in gross form to a chevron fold formed by buckling, but can be distinguished by associated fold forms. The geometry of second order folds (Nickelsen, 1963) of the central Appalachians can best be accounted for by a kink fold model (Faill, 1969, 1973).

Gravity lows indicate thickened low density shale on

the northwest limbs of the Blackwater and Glady anticlines. We suggest that there exist thinned and extended units downdip from the thickened shale sections. Therefore, map-scale kink folds should have the most thinning by extension fracturing and faulting low on the steep limb in the subsurface. There, such folds are more likely to contain gas in fractured reservoirs.

INTRODUCTION

Dennis (1967) defines kink-band as a tabular zone along which foliation is deflected. A kink fold is formed from the intersection of two kink-bands. A kink fold may be in the form of a box fold or may have planar limbs and narrow hinges similarly to a chevron fold (Fig. 6B).

Recent work by Faill (1969, 1973) has shown that the typical map-scale folds of Pennsylvania have planar limbs and narrow hinges that can best be explained by kink-band deformation. The geometric and kinematic similarities between map- and outcrop-scale kink-bands suggest to Faill that the processes and mechanisms that gave rise to the large folds were identical to those that produced the small folds.

In this paper, we use outcrop-scale folds to provide information about relative amounts of bed extension on limbs in map-scale folds. Anticlines with large amounts of extension may contain suitable exploration targets for

gas in fractured reservoirs.

KINK-BANDS AND KINK FOLDS

Faill (1969, 1973) is able to explain most attributes of central Appalachian fold style by using the intersection of two kink-bands inclined toward each other with opposite senses of rotation and divergent kink axes. However, Johnson (1977) argued from elastic theory that folds with planar limbs and narrow hinges also can arise from another sequence of development (Fig. 6A). Johnson proposed that hinges can narrow and limbs straighten progressively during folding, thus transforming a concentric-like fold into a chevron fold. Conceivably, tension fractures may form due to initial bending and later straightening of the limb (B. Kulander, oral communication, 1978). These chevron folds can appear almost identical in outcrop to kink folds formed by the intersection of two inclined kink-bands. The kink-bands tend to form when the beds are lubricated (separated by very weak interbeds) and when the maximum principal compressive stress is at a small angle to beds (Johnson, 1977). Chevron folds formed from concentric-like folds are most likely to occur when the beds are not lubricated, when the surrounding medium is softer than the folded beds and when the maximum principal compressive stress parallels the beds. However, Chapple (1978) notes that
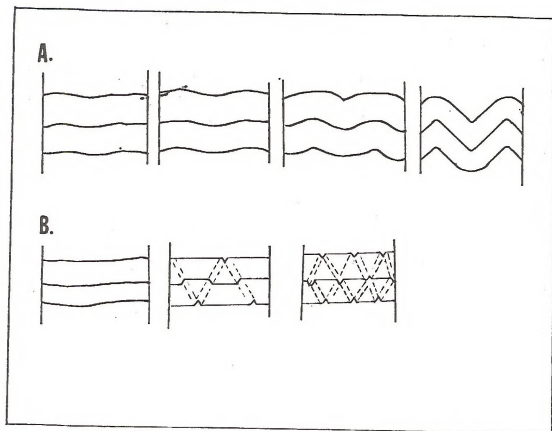
Figure 6. Contrasting models of formation of chevron and kink folds. Horizontal lines at left are selected beds. A. Sequence from sinusoidal to concentric-like to chevron forms. B. Sequence from low, sinusoidal forms to kink forms, with local chevron forms (after Johnson, 1977). Dashed lines denote kink surfaces.

the applicability of Johnson's elastic theory to folding
is not entirely clear.

We have tried to discriminate in the field between
chevron folds (Fig. 6A) and kink folds formed from the
intersection of two kink-bands (Fig. 6B). Johnson (1977)
suggests that chevron folds may have vestiges of their
earlier concentric-like form (Fig. 6A). The combination of
concentric-like and chevron forms causes no room problem
in the cores of folds. The folds are similar in style and
can extend indefinitely parallel to the axial surface. On
the other hand, Berger has observed that many kink-bands
and kink folds die out in either direction parallel to the
kink surface. If the fold is asymmetric, then it is
probably a kink fold formed by the intersection of two
kink-bands of unequal width (Faill, 1969). The chevron
folds of Johnson (1977) are usually symmetrical. Although
these diagnostic criteria are not infallible, they can
indicate the affinity of the fold.

Ramsay (1967, p. 450) concludes that less work is
expended to shorten a layer by the production of
kink-bands or paired conjugate kinks than by the formation
of symmetrical chevron folds. Thus it seems logical to
conclude that kink folds will be more prevalent in nature.
Planar-limbed folds of uncertain affinity are thus more
likely to be kink folds.

EXTENSION IN KINK-BANDS

Ramsay (1967, p. 449) uses a geometric model to predict the amount of dilation (Δ) in a kink-band (Fig. 7). The amount of dilation $\Delta = (\sin \beta_2 / \sin \beta_1) - 1$ (1) where β_1 is the angle between the axial surface and the enveloping beds, and β_2 is the angle between the axial surface and the kink-band. If $\beta_1 > \beta_2$, then $\Delta < 0$ and the layers thin and extend parallel to bedding. Kulander and Dean (in review) use this method to predict the amount of porosity in kink bands. They estimate that 10 percent porosity can occur when the beds separate ($\beta_1 < \beta_2$ and $\Delta > 0$). They determine that porosity can also occur as the beds separate in the hinges of kink-bands if $\beta_1 = \beta_2$, but that the amount of such hinge porosity depends on the thickness to length ratio of the beds composing the kink band.

In this study, we are interested in kink folds where $\Delta < 0$, so that one limb is extended. Generalizing this model to central Appalachian folds that have planar limbs and narrow hinges, β_1 is the angle between the axial surface and the shallow limb. β_2 is the angle between the axial surface and the steeper dipping limb. We have investigated several planar-limbed folds to try to observe more extension in the kink-band or in the steep limb. We compare the measured amount of extension with the amount of extension predicted by equation (1), and assume to
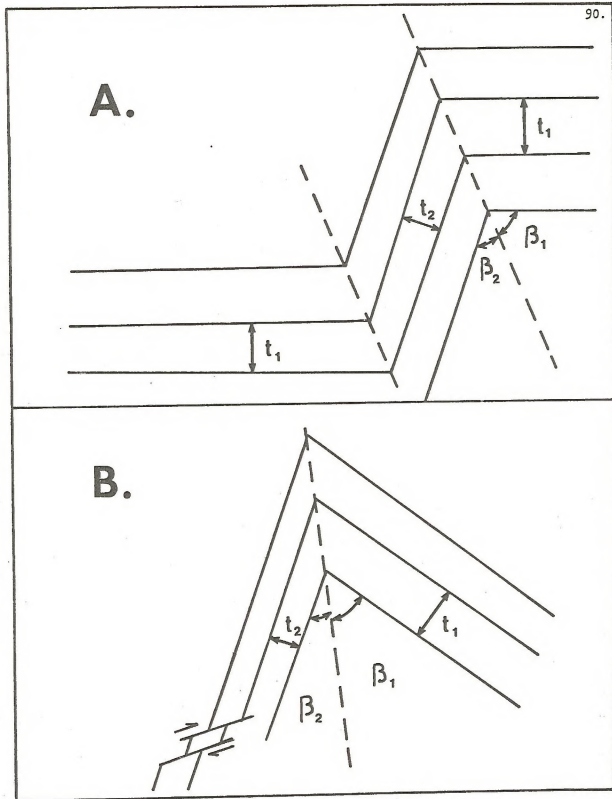
Figure 7. Kink-band model of fold development showing relationship of β_1 and β_2 to the kink surface and thinning and extension of beds in the kink-band (A) or steep limb of a kink fold (B). t_1 is original bed thickness, t_2 is thinned bed thickness.

start that the dilation is completely translated into extension fractures. As we shall see, that assumption is overly optimistic, but that will not change the validity of the following analysis.

FIELD INVESTIGATIONS

Tipton, Pennsylvania (Fig. 8, 9). This fold is a northeast-plunging kink-band in the steeply dipping Devonian Brallier Formation on the northwest limb of the Nittany Arch. The shallow limb is the kink-band. the steep limb is the enveloping bedding and $\Delta < 0$. As shown in Figure 9, there are more joints, unclassified fractures, extension fractures, and twist hackle (Kulander, Dean and Barton, 1977; Kulander, Barton and Dean, in review) in the kink-band than in the enveloping bedding. Berger measured 1.7 percent extension by fracturing in the kink-band. The amount of extension by fracturing is the sum of the amounts of separation of all fractures in a measured length of a single bed. Equation (1) predicts 19.5 percent extension in the kink-band.

Watts, Pennsylvania (Fig. 8). This kink-band in the Devonian Trimmers Rock Formation (Faill, written communication, 1978) dies upward in the exposure, parallel to the kink surface. In this case, the steep limb is the kink-band and $\Delta < 0$. Berger measured 3.0 percent extension by fracturing in the kink-band. Equation (1) predicts 35.8
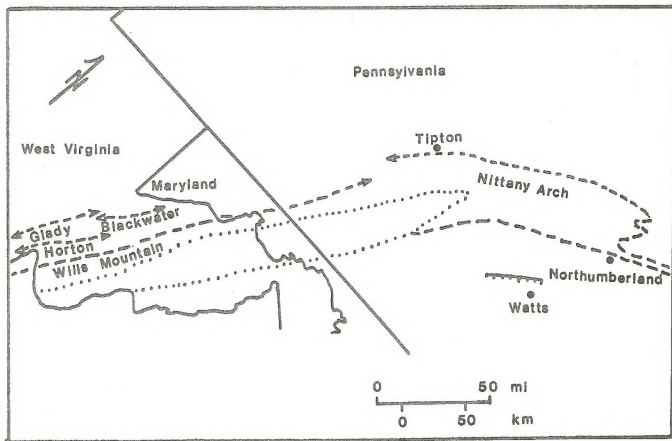
Figure 8. Location map showing exposures and significant
tectonic elements. Dashed lines are anticlines,
arrows denoting plunge. Dotted line marks boundary
of the Broadtop synclinorium. Hachured line is
a thrust fault. Circles are exposures.

Enveloping Bedding

Kink Surface
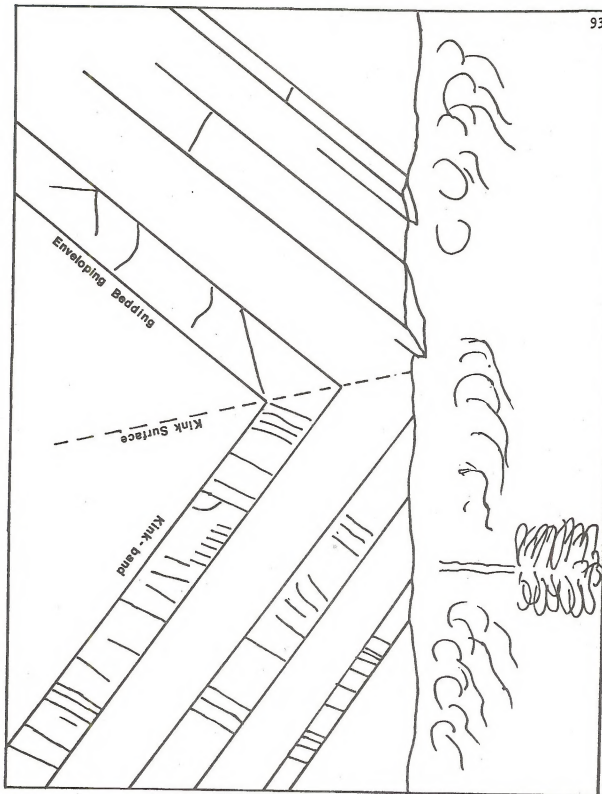
Kink-band

Figure 9. Outcrop at Tipton, Pennsylvania in the Devonian
Brallier Formation on the northwest limb of the
Nittany Arch. Siltstones show more fracturing in
the kink-band than in the enveloping bedding.
Schematic sketch from a photograph, looking
northeast. Outcrop width about 15 m.

percent extension.

Northumberland, Pennsylvania (Fig. 8). This large kink-band in nearly horizontal beds of the Devonian Catskill Formation (Faill, written communication, 1978) has $\Delta > 0$ so that we would expect shortening and separation of beds rather than extension. However, the kink-band showed excellent extension fractures (Berger and Wheeler, ms. in review) that produced 1.6 percent extension.

The results of our field investigations indicate that extension by fracturing amounting to approximately ten percent of the predicted value is likely in kink-bands. Berger noted as predicted that beds at Tipton, Pennsylvania are more extended in the kink-band than in the enveloping bedding. This is consistent with the Ramsay (1967) model of beds undergoing extension in the kink-band, if $\Delta < 0$. Results more consistent with predicted values might be found in thinner bedded units than we examined, because thicker units are extended a lesser amount, proportionally to their thickness (Ramsay, 1967, p. 451).

MAP-SCALE FOLDING

Anticlines in the central Appalachians can grow by crestward flowage of shale and mudstone units (Wheeler, 1975; Perry and de Witt, 1977; Kulander and Dean, 1978). For more brittle units, Berger and Wheeler (in preparation) show that extension faults can thin and

extend beds on the steep limbs of asymmetrical anticlines, providing a significant contribution to anticlinal growth. The presence of gravity lows on the northwest (steeper dipping) limbs of the Wills Mountain, Blackwater, Browns Mountain and Glady anticlines indicates to us one or both of (1) flowage of low density shale from low on the steep limbs to high on those limbs, or (2) thickened or repeated shale sections due to (a) detachment-related, pre-folding thrusting (Kulander and Dean, 1978; stage I of Berger and others, in press), or to (b) vertically dipping low density shales (B. Kulander, oral communication, 1978).

We would expect gravity lows that are detachment-related to extend parallel to the anticlinal axis until the detachment surface changes level along a transverse step. Thus the relatively long, linear gravity lows on the northwest limbs of the Wills Mountain and Browns Mountain anticlines (Kulander and Dean, 1978, plate 2) are probably more the result of fault repetition and thickening of the Ordovician Martinsburg Formation and Devonian shales than to lobate crestward flow of ductile rocks (B. Kulander, oral communication, 1978). In contrast, the circular lows on the northwest limbs of the Blackwater and Glady anticlines are more likely due to lobes of uplimb flowage in the ductile units of the Middle and Upper Devonian clastic sequence. On the northwest limb of the Wills

Mountain anticline, the discontinuous strike-parallel linear gravity lows terminate within a few kilometers along strike of the discontinuous strike-parallel linear belts of thinned Devonian Brallier Formation mapped by Dennison and Naegele (1963). The gravity lows are caused by thickening of Ordovician Martinsburg formation and the vertical beds of the Middle and Upper Devonian clastic sequence and the thinned outcrop belt is caused by extension and other tectonic thinning of the Devonian Brallier formation (Berger and Wheeler, in preparation; Dennison and Naegele, 1963). On the Blackwater and Glady anticlines the inferred thickened shale lobes suggest that there exists a thinned Brallier formation lower on the limb that is subjected to extension faulting (Berger, Perry and Wheeler, in press) in the brittle units and flowage in the ductile units. This thinning would be similar to that observed in outcrop in the Devonian Brallier Formation (Dennison and Naegle, 1963; Berger and Wheeler, in preparation) and could indicate gas potentially in a fractured reservoir. The source beds could be the Devonian black shales (the Marcellus and Harrell formations) and the flowed, thickened, perhaps heavily slickensided shale updip could seal the reservoir. We suggest further exploration for thinned and fractured shales down-dip of the buried, thickened shales that we

infer to lie beneath the observed gravity lows (Fig. 10).
For steep northwestward dips, the suggested exploration
target would lie roughly under the northwestern boundary
of a circular gravity low. Additional gravity
measurements and modeling of the gravity lows mapped by
Kulander and Dean (1978), guided by construction of
balanced cross sections (Dahlstrom, 1969b; Perry, 1971),
should define those targets more exactly.

The kink fold model of folding also implies that
thinning by extension can occur on the northwest (steep)
limb (Figure 2B). Folds thickened near the crest and
thinned lower on the limb can still have planar limbs and
narrow hinges consistent with a kink-fold model of
map-scale folds.

ACKNOWLEDGEMENTS
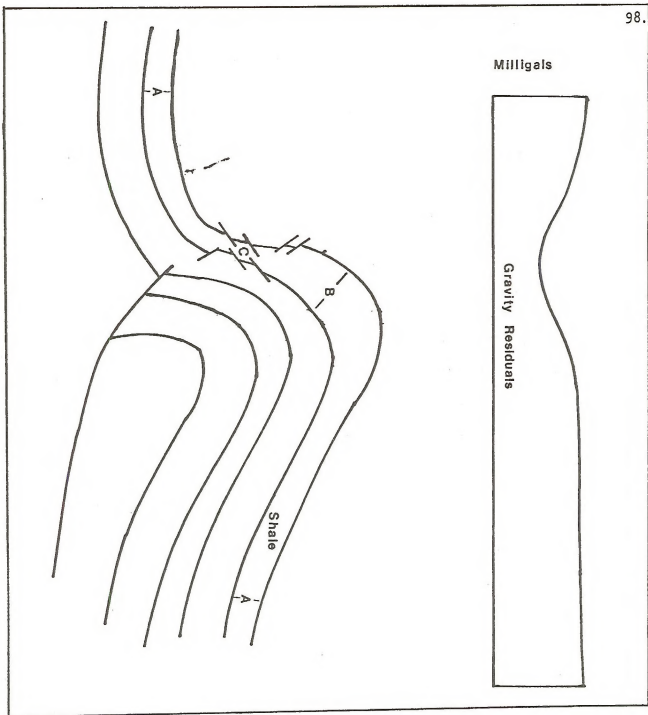
Figure 10. Relationship of gravity low to anticline.
A. Original thickness. B. Siltstone and shale
thickened by uplimb flow of shale. C. Siltstone
and shale thinned by uplimb flow of shale and
thinning by extension faulting of siltstones and
and shales.

CONCLUSIONS OF ENTIRE THESIS

1) Outcrop-scale and map-scale faults that formed during overall horizontal shortening and associated detached folding can be placed in a three-stage relative time sequence.

2) Wedge-shaped contraction faults form early (stage I) when beds are nearly horizontal. These faults may have associated anticlines and may be smaller versions of the detachment and ramp systems characteristic of allochthonous fold belts. In beds later rotated to steep dips by folding, contraction faults will show normal fault separation at a low angle to bedding. In cratonward-facing folds, contraction faults will show a downlimb sense of displacement.

3) Uplimb thrusts form during folding (stage II) and record relative reverse movement toward the anticlinal hinge. These faults serve to raise the limbs of anticlines to solve space problems.

4) Extension faults and extension fractures form late in folding (stage III) when beds rotate so far towards the vertical that the effect of vertical extension exceeds that of horizontal shortening. Extension faults are reverse faults formed at high angles to beds and rotated

little or not at all. Unequivocal extension fractures are lenticular and form normal to beds.

5) Extension fracturing will begin when bed dips reach 45 degrees assuming that there is no more than $\pm .1(e_3)$ hinge line parallel strain.

6) Extension faults and associated fractures provide a significant contribution to: a) anticlinal growth, b) unit thinning, and c) bed extension thus favoring formation of fractured gas reservoirs.

7) The Dawson, Cresaptown, and Kittlelick thrusts of Dennison and Naegle (1963) are more likely zones of extension faulting than single detachment-related splay faults. The Hyndman fault is more likely a splay fault but has associated extension faults.

8) The Brallier Formation is the Devonian unit most intensely deformed by extension faulting and extension fracturing. Given a gas source (the underlying Marcellus and Harrell Formations) and a seal, it may be a shallow gas exploration target on the northwest limbs of the Glady, Horton, Blackwater and Deer Park anticlines.

9) Limbs of kink folds and beds in kink bands can undergo extension parallel to the beds when the angle between the kink surface and the Kink-band is less than the angle between the kink surface and the enveloping beds.

10) Although kink-bands show evidence of more extension than do the enveloping beds, the amount of extension measured is less than the amount predicted. Only about 10 percent of the predicted volume change is translated into extension fractures.

11) Circular gravity lows on the northwest limbs of the Blackwater and Glady anticlines can be due to lobate thickening of shales high on the limbs and thinning low on the limbs. Thinning can occur in the Brallier formation similarly to that measured on the northwest limb of the Wills Mountain anticline by Dennison and Naegele (1963). We suggest exploration under the northwestern boundaries of the mapped gravity lows to intersect the inferred thinned shale sections, which may contain gas in fractured reservoirs.

SUGGESTIONS FOR FUTURE WORK

1) In many instances, contraction faults (stage I) have associated anticlines. These form over smaller versions of the ramps with which major detachment surfaces change stratigraphic level. I have identified many contraction fault localities. These are listed in Appendix IV. Study of these faults as well as those from other localities can give insights into relative ductilities of rocks involved in ramp formation, ratios of length of ramp to height of associated anticline, initiations and terminations of ramps, terminations of associated anticlines, problems of conservation of space, and the nature of the most energy efficient structures.

2) An outcrop study of uplimb thrust faults (stage II) would probably not be feasible because these faults are rarely exposed and are usually so large so as to be unidentifiable on outcrop scale. However, I found one uplimb thrust that is classic in form, but it may also be a shear zone associated with an igneous intrusion. Petrographic work in the fault zone to determine if the cataclastic material had igneous or sedimentary affinities would answer this question. The zone in question crops out in Ryder Gap, Bath County, Virginia (Station 8 of manuscript three, Appendix I).

3) Kink folds are formed by a different process than

are chevron folds (see Manuscript four). Kink folds are products of shearing and chevron folds, of buckling. Examination of strain markers such as burrows, fossils or oolites or analysis of quartz deformation lamellae and calcite twin lamellae can yield information on the origin of the fold.

REFERENCES

Berger, P. S. and Wheeler, R. L., ms, The western
limit of extension fracturing in West
Virginia: ms in review, 13 p.

Berger, P. S., Perry, W. J., and Wheeler, R. L.,
ms, Three stage model of brittle
deformation in the central Appalachians:
Southeastern Geology, in press, 17 p.

Cardea, Harry S., ms, 1959, A Geologic Study of the
Terra Alta Gas Field, Preston County, West
Virginia: M. S. thesis, W. Va. Univ., 220 p.

Cardwell, D., 1975, Geologic history of West
Virginia: W. Va. Geol. and Econ, Sur.,
Educational Series, 64 p.

Cardwell, D., 1973, Deep Well and Structural
Geologic Map of West Virginia: W. Va. Geol.
and Econ. Sur.

Cardwell, D., Erwin, R. and Woodward, H., 1968,
compilers, Geologic Map West Virginia:
Morgantown, W. Va., W. Va. Geol. and Econ. Sur.

Chapple, W., 1978, Styles of folding: Am. Geophys.
Union Trans., v. 59, p. 860-861.

Cloos, E., 1964, Wedging, bedding plane slips, and
gravity tectonics in the Appalachians: in
Tectonics of the Southern Appalachians,

Virginia Polytechnic Institute, Department
of Geological Sciences, Memoir 1, p. 63-70.

Cloos, E. and Broedel, C., 1943, Reverse faulting
north of Harrisburg, Pennsylvania: Geol.
Soc. Amer. Bull., v. 54, p. 1375-1398.

Dahlstrom, C., 1969a, The upper detachment in
concentric folding: Bull. Can. Petr.
Geol., v. 17, p. 326-346.

Dahlstrom, C., 1969b, Balanced cross sections:
Canadian jour. Earth Sci., v. 6, p.
743-757.

Dean, S., and Kulander, B., 1977, Kinematic
analysis of folding and pre-fold structures
on the southwestern flank of the
Williamsburg anticline, Greenbrier County,
West Virginia: Abstracts With Programs,
Geol. Soc. Amer., Vol. 9, n. 2, p. 132-133.

Dennis, J., 1967, International Tectonic Dictionary:
Am. Assoc. Petroleum Geol., Memoir 7, 196 p.

Dennis, J., 1972, Structural Geology: New York,
Ronald, 532 p.

Dennison, J. M. and Naegele, O. D., 1963, Structure
of Devonian strata along Allegheny Front
from Corriganville, Maryland, to Spruce
Knob, West Virginia: West Virginia Geol.

and Econ. Survey, Bulletin 24, 42 p.

Dennison, J. M., Travis, J. W., and Ferguson, J.
H., 1966, Kittlelick thrust: a new fault in
Mineral and Grant Counties, West Virginia:
Proceedings of the West Virginia Academy of
Science, 1966, v. 38, p. 177-185.

de Witt, W., 1974, Geologic Map of the Beans Cove
and Hyndman Quadrangles and part of the
Fairhope Quadrangle, Bedford County,
Pennsylvania: U.S.G.S. Map I-801.

de Witt, W. and Dennison, J. M., 1972, The
Allegheny Front from Bedford County,
Pennsylvania to Grant County, West Virginia
in Dennison, J. M., ed., Stratigraphy,
sedimentology, and structure of Silurian
and Devonian rocks along the Allegheny
Front in Bedford County, Pennsylvania,
Allegheny County, Maryland, and Mineral and
Grant Counties, West Virginia: Harrisburg,
Pa., Pennsylvania Bur. Topog. and Geol.
Survey, Guidebook for 37th Ann. Field Conf.
of Pennsylvania Geologists, p. 14-32.

Dieterich, J. H., and Carter, N. L., 1969,
Stress-history of folding: Am. Jour. Sci.,
v. 267, p. 129-154.

Durney, D. and Ramsay, J., 1973, Incremental
        strains measured by crystal growths: in
        Gravity and tectonics, ed. by De Jong, K.
        and Scholten, R., John Wiley and Sons, New
        York, p. 67-96.

Engelder, T. and Engelder, R., 1977, Fossil
        distortion and decollement tectonics of the
        Appalachian Plateau: Geology, v. 5, p.
        457-460.

Faill, R., 1969, Kink band structures in the Valley
        and Ridge province, central Pennsylvania:
        Geol. Soc. Amer. Bull., v. 61, p. 857-876.

Faill, R., 1973, Kink band folding, Valley and
        Ridge Province, central Pennsylvania: Geol.
        Soc. Amer. Bull., v. 84, p. 1289/1314.

Gair, J., 1950, Some effects of deformation in the
        central Appalachians: Geol. Soc. Amer.
        Bull., v. 61, p. 857-876.

Geiser, P., 1970, Deformation of the Bloomsburg
        Formation in the Cacapon Mountain
        anticline, Hancock, Maryland: Ph.D.
        dissert., The Johns Hopkins Univ., 150 p.
        [Ann Arbor, Mich., Univ. Microfilms]

Geiser, P., 1977, Early deformation structures in
        the central Appalachians: A model and its

implications (abs.): Geol. Soc. with
America, Abs. with Programs, v. 9, p.
267-268.

Griggs, D. T. and Handin, J., 1959, Observations on
fracture and a hypothesis of earthquakes,
in Griggs, D. and Handin, J., eds., Rock
deformation - a symposium: Geol. Soc.
America Mem. 79, p.347-373.

Gwinn, V., 1964, Thin-skinned tectonics in the
Plateau and northwestern Valley and Ridge
provinces of the central Appalachians:
Geol. Soc. Amer. Bull., v. 85, p. 863-900.

Gwinn, V., 1970, Kinematic patterns and estimates
of lateral shortening, Valley and Ridge and
Great Valley provinces, central
Appalachians, south-central Pennsylvania:
in Fisher, G., Pettijohn, F., Reed, J., and
Weaver, K., eds., Studies of Appalachian
Geology-Central and Southern: New York,
Interscience Pubs., p. 127-146.

Haught, O., 1968, Structural Contour Map Datum
Greenbrier Limestone in West Virginia:
Morgantown, W. Va., W. Va. Geol. and Econ.
Sur.

Jacobeen, F. and Kanes, W. H., 1974, Structure of

Broadtop synclinorium and its implications
for Appalachian structural style: Bull.
American Assoc. Petroleum Geologists, v.
58, p. 362-375.

Johnson, A., 1977, Styles of Folding: Amsterdam,
Elsevier, 406 p.

King, G., 1973, Geometric analysis of minor folds
in sedimentary rocks: M. S. thesis, W. Va. Univ.

Kulander, B. and Dean, S., 1972, Gravity and
structural reconnaissance across Browns
Mountain, Wills Mountain, and Warm Springs
anticlines - Gravity study of the folded
Plateau, West Virginia, Virginia, and
Maryland: in Appalachian Structures,
Origin, Evolution, and Possible Potential
for new Exploration Frontiers, Morgantown,
W. Va., W. Va. Geol. and Econ. Sur.

Kulander, B., Barton, C. and Dean, S., The application
of fractography to core and outcrop fracture
investigations: unpublished manuscript, in
review, 138 p.

Kulander, B. and Dean, S., 1978, Gravity,
Magnetics, and Structure, Allegheny
Plateau/Western Valley and Ridge in West
Virginia and Adjacent States: West Virginia

Geol. and Econ. Survey, Rept. of
Investigation RI-27, 61 p.

Kulander, B. and Dean, S., Rome trough relationship to
fracture domains, regional stress history and
decollement structures: unpublished manuscript,
in review, 17 p.

Kulander, B., Dean, S. and Barton, C., 1977, Fractographic
logging for determination of pre-core and
core-induced fractures--Nicholas Combs no.
7239 well, Hazard, Kentucky: MERC/CR-77/3,
Distribution Category UC-92, U. S. Dept.
of Energy, Morgantown Energy Research Center,
P. O. Box 880, Morgantown, West Virginia, 44 p.

Lundegard, P., Samuels, N. and Pryor, W., 1978, The Brallier
formation - Upper Devonian turbidite slope facies
of the central and southern Appalachians: in preprints
for: Second Eastern Gas Shales Symposium, vol. 1,
October, 1978, U. S. Department of Energy,
Morgantown Energy Technology Center METC/SP-78/6 vol. 1,
p. 4-17.

Milner, W., ms, 1968, Petrology, Stratigraphy, and
Structure of the Basal Section of the
Greenbrier Limestone in the Vadis Field in
Lewis and Gilmer Counties, West Virginia:
M. S. thesis, W. Va. Univ., 42 p.

Mitchell, F., ms, 1960, Geology of the Chestnut
        Ridge Gorge of Cheat River: M. S. thesis,
        W. Va. Univ., 84 p.

Murray, G., 1968, Quantitative fracture study-Sanish
        Pool, McKenzie County, North Dakota: Am.
        Assoc. Petroleum Geologists Bull., v. 52,
        p. 57-65.

Nickelsen, R., 1963, Fold patterns and continuous
        deformation mechanisms of the central
        Pennsylvania folded Appalachians: in Cate,
        A., ed., Guidebook: Tectonics and Cambro-
        Ordovician Stratigraphy, Central
        Appalachians of Pennsylvania, Pitt. Geol.
        Soc. with the Appal. Geol. Soc., p. 13-29.

Nickelsen, R., 1976, Sequence of structural phases,
        Allegheny orogeny, Pennsylvania (abs.):
        Geol. Soc. America Abs. with Programs, v.
        8, p. 235.

Nickelsen, R., 1978, Multistage deformation within
        an orogenic phase (abs.): Geol. Soc.
        America Abs. with Programs, v. 10, p. 23.

Norris, D. K., 1958, Structural conditions in
        Canadian coal mines: Canada Geol. Survey
        Bull. 44, 54 p.

Norris, D. K., 1964, Microtectonics of the Kootenay

Formation near Fernie, British Columbia:
Bull. Canadian Petroleum Geologists, v. 12,
p. 383-398.

Patchen, D. G., 1977, Terminology and correlation
of Middle and Upper Devonian clastic
formations: Mountain State Geology, West
Virginia Geol. and Econ. Survey, Dec. 1977,
p. 4-9.

Perry, W., Jr., 1971, Structural development of the
Nittany anticlinorium, Pendleton County,
West Virginia: New Haven, Conn., Yale
University., Ph. D. dissert., 227 p.

Perry, W., Jr., 1975, Tectonics of the western
Valley and Ridge Foldbelt, Pendleton
County, West Virginia - a summary report:
U. S. G. S. Jour. Research, v. 3, p.
583-588.

Perry, W., Jr., 1978, Sequential deformation in the
central Appalachians: Am. Jour. Sci., v.
278, p. 518-542.

Perry, W., Jr., and de Witt, W., 1977, A field
guide to thin-skinned tectonics in the
central Appalachians: Annual AAPG/SEPM
Convention, Washington, D. C., June 12-16,
1977, 54 p.

Price, R., 1964, Flexural-slip folds in the Rocky
        Mountains, southern Alberta and British
        Columbia: Seminars in tectonics-IV, Dept.
        Geol. Sciences, Queen's University,
        Kingston, Ont., p. 6-17.

Perry, W., Jr. and Wilson, N., 1977, Oil and gas
        data in New River Gorge Area, West
        Virginia: U.S.G.S. Open File Rept.
        OF-77-76-G, 2 sheets.

Price, R., 1964, Flexural-slip folds in the Rocky
        Mountains, southern Alberta and British
        Columbia: Seminars in tectonics-IV, Dept.
        Geol. Sciences, Queen's University,
        Kingston, Ont., p. 6-17.

Price, R., 1967, The tectonic significance of
        mesoscopic subfabrics in the southern Rocky
        Mountains of Alberta and British Columbia:
        Can. Jour. Earth Sciences, V. 4, p. 39-70.

Ramsay, J., 1967, Folding and Fracturing of Rocks:
        McGraw-Hill Book Co., New York, 568 p.

Reches, Z., and Johnson, A. M., 1976, A theory of
        concentric, kink and sinusoidal folding and
        of monoclinal flexing of compressible
        elastic multilayers. IV. assymetric
        folding and monoclinal kinking:

Tectonophysics, v. 35, p. 295-334.

Rodgers, J., 1963, Mechanics of Appalachian
foreland folding in Pennsylvania and West
Virginia: Am. Assoc. Petroleum Geologists
Bull., v. 47, p. 1527-1536.

Rodgers, J., 1970, The Tectonics of the
Appalachians: New York, Wiley, 271 p.

Root, S., 1973, Sequence of faulting, southern
Great Valley of Pennsylvania: Am. Jour.
Sci., v. 273, n. 1, p. 97-112.

Root, S. and Wilshusen, J., 1977, Structure and
engineering geology at the Rockville Cut:
Pennsylvania Geology, v. 8, no. 1, p. 2-6.

Shockey, P., ms, 1954, Some Aspects of the Surface
Geology of the Northern Portion of the
Burning Springs Anticline: M. S. thesis,
W. Va. Univ.

Siegel, S., 1956, Nonparametric Statistics for the
Behavioral Sciences: New York, McGraw-Hill,
312 p.

Sites, R., 1978, Structural analysis of the Petersburg
lineament, central Appalachians: Ann Arbor,
Mich., Univ. Microfilms.

Swartz, C., 1923, Silurian: Maryland Geologic
Survey, 794 p.

Wheeler, R. L., 1975, Geometric and kinematic analysis of folds in the Upper Devonian Chemung Group, and relationships to processes forming major structures of the eastern Plateau province (abs.): Abstracts with Programs, Geol. Soc. Amer., v. 7, n. 4, p. 548-549.

APPENDIX I

Location of field stations: "Late-tectonic
extension faulting in the central Appalachians"

Station 1 - West side of the railroad tracks, .1 km
north of Pinto, Allegany County, Maryland
(outcrop described in Swartz, 1923).

Station 2 - North side of the C & O Canal, 10 km
south of the intersection of U. S. 40 and
Woodmont Road, Woodmont, Allegany county,
Maryland. Outcrop is 1 km east of Woodmont
Road on Deneen Road and is described in
Perry and de Witt (1977), p. 33-39.

Station 3 - North side of U. S. 40 in La Vale,
Maryland. Outcrop is east of the La Vale
Plaza shopping center and is described by
de Witt and Dennison (1972) p. 63-68.

Station 4 - East side of U. S. 33, 4 km north of
Riverton, West Virginia. Outcrop is across
the road from the stream that drains the
south side of Ketterman's Knob and is
described in Dennison and Naegele (1963),
p. 37-39.

Station 5 - North side of Holly Meadows Road, 5 km
north of Parsons, West Virginia at bench
mark 1579.

Station 6 - Along the north side of I-64, 8 km west

of White Sulphur Springs, West Virginia.
First outcrop past west bound entrance to
I-64 from U. S. 60 at the bridge over Wolf
Creek.

Station 7 - In an abandoned quarry, .1 km east of
the intersection of U. S. 33 and W. Va.
28, Pendleton county, West Virginia.

Station 8 - Along Va. 39, Bath County, Virginia, .1
km east of the Virginia/West Virginia
border.

Station 9 - West side of the railroad tracks, 3 km
south of Cumberland, Maryland, .1 km north
of the Amcelle Corp. plant (outcrop
described in Swartz, 1923).

Station 10- West side of the railroad tracks, 3 km
south of Cumberland, Maryland, .3 km south
of the Allegany County Fairgrounds,
Allegany County, Maryland (outcrop
described by Swartz, 1923).

Station 11- North side of Teter Run, 3 km south of
Circleville, West Virginia and .5 km east,
up the dirt road into Teter Gap, .1 km east
of the first cattle guard.

Station 12 - East side of secondary W. Va. 17,
first exposure east (.8 km) of intersection

with secondary W. Va. 19, Pendleton County,
West Virginia.

Station 13- East side of secondary W. Va. 17,
second exposure east (1 km) of intersection
with secondary W. Va. 19, Pendleton County,
West Virginia.

Station 14- East side of secondary W. Va. 17, third
exposure east (1.1 km) of intersection with
secondary W. Va. 19, Pendleton County, West
Virginia.

Station 15- First outcrop on the south side of W.
Va. 39, 1 km east of Huntersville, West
Virginia at the spring.

Station 16- North side of W. Va. 39, 1.1 km west of
Minnehaha Springs, West Virginia. Outcrop
is .1 km east of the bridge over the stream
flowing through Buzzard Hollow and is
pictured on the cover of Cardwell (1975).

Station 17- North side of W. Va. 39, first outcrop
(.3 km) west of Minnehaha Springs, West Virginia.

Station 18- along the south side of I-64, 4 km
southeast of White Sulphur Springs, West
Virginia. Third outcrop east of the bridge

over the railroad tracks (outcrop described by King, 1973).

Station 19- Along the south side of I-64, 3.5 km east of White Sulphur Springs, West Virginia. Fourth outcrop east of the bridge over the railroad tracks.

Station 20- North side of W. Va. 28, 4 km north of Hopeville, West Virginia, .2 km east of Smoke Hole caverns (North Fork Gap). Outcrop figured in Sites (1978).

Station 21- South side of Wolf Camp Run, .3 km west of the intersection of Wolf Camp Run Road and Pa. 96. Outcrop described in de Witt and Dennison (1972), p.72-73. Outcrop is .5 km north of Madley, Pennsylvania.

Station 22- North side of U. S. 40, 1 km east of the crest of Martin Mountain, Allegheny County, Maryland.

Station 23- On the south side of the exit ramp, at the juncture of U. S. 40 and U. S. 522, on the exit ramp of U. S. 40 for eastbound traffic. Outcrop is 1 km west of Hancock, Maryland.

Station 24- West side of U. S. 33, first outcrop (1 km) north of the juncture of U. S. 33 and W. Va. 28, Pendleton County, West Virginia.

APPENDIX II

Location of field stations: 'Extension in kink-bands and on the limbs of kink folds'

Tipton, Pennsylvania - This outcrop is located on the north side of the Pennsylvania secondary road that extends from U. S. 220 northwest through Tipton, Pennsylvania. It is the first west of the town of Tipton.

Watts, Pennsylvania - This outcrop is located on the west side of U. S. 322, 3 km north of Amity Hall, Pennsylvania, .1 km north of the entrance ramp from the secondary road through Watts, Pennsylvania. this is the first entrance ramp north of Amity Hall.

Northumberland, Pennsylvania - This outcrop is located on the west side of U. S. 11, .1 km south of the bridge across the west branch of the Susquehanah River into Northumberland, Pennsylvania. The outcrop is overgrown but is identifiable by the words "Susan + Matt" spray painted on the outcrop.

Appendix III

A note on the size of extension faults.

Map-scale extension faults are large enough that body
forces (gravity) become significant relative to the
surface forces that form outcrop-scale extension faults.
Mechanics of faulting may differ between the two scales.
Accordingly, the term extension fault and its companion
term contraction fault may be limited to outcrop scale
structures (W. Perry, Jr., oral communication, 1978).
Although the size at which gravity becomes significant is
approximately 50 m (R. Wheeler, oral communication, 1978)
I do not restrict usage in this thesis because I am not
sure of the significance of this difference in mechanics
of faulting.

A note on the stratigraphy and sedimentology of the
    Brallier Formation

Lundegard and others (1978) characterize the
Brallier Formation as part of an overall thickening- and
coarsening-upward sequence, containing megasequences from
3 to 51 m thick. They recognize six facies of the Brallier,
of which three constitute 80 percent of the areal extent
of the formation and contain lithologies I observed to
contain extension faults and fractures. These three facies
are: A) Alternating beds of siltstone, shale or mudstone;
B) Bundles of siltstone and fine-grained sandstone with
minor interbeds of shale or mudstone; C) Olive-gray mudstone
or shale.

APPENDIX IV

Contraction Fault Localities

1) West side of the railroad tracks, .1 km north
   of Pinto, Allegany County, Maryland.

2) West side of the railroad tracks, 3 km south
   of Cumberland, Maryland, .3 km south of the
   Allegany County Fairgrounds, Allegany County,
   Maryland (two contraction faults).

3) North side of Holly Meadows Road, 5 km north of
   Parsons, West Virginia at bench mark 1579.

4) East side of secondary W. Va. 17, 1 km east of
   intersection with secondary W. Va. 19,
   Pendleton County, West Virginia (two contraction faults).

5) North side of W. Va. 39, first outcrop west of
   Minnehaha Springs, West Virginia.

6) North side of W. Va. 28, 4 km north of Hopeville,
   West Virginia, .5 km east of Smoke Hole Caverns
   (North Fork Gap).

7) West side of U. S. 33, 4 km north of Riverton, West
   Virginia. Outcrop is across the road from Station 4.

8) East and west sides of U. S. 322, 3 km north of Amity Hall,
   Watts, Pennsylvania.

BEDDING ORIENTATION CONTOURS OF MIDDLE DEVONIAN SHALES

EXPOSED IN THE MIDDLE MOUNTAIN SYNCLINE,

VALLEY AND RIDGE PROVINCE, WEST VIRGINIA

by

Thomas H. Wilson
West Virginia University
Department of Geology and Geography

July 1979

INDEX

LIST OF FIGURES

* Figure 11   Strike and dip values were drawn randomly from normally distri-
              buted populations having cell sample statistics for parameters.
              A) Absolute value of (random strike - 35 degrees) overlies their
              standard deviations, B) absolute value of dip overlies their
              standard deviations. CI = 10 degrees. Page 156

* An acetate overlay is included in the back of the report showing station
  location and the grid control points. The overlay is registered by match-
  ing the north arrows and PSL boundaries. Page 167

ABSTRACT

Bedding orientation contours have been used to estimate the effect of the Parsons structural lineament on exposed Middle Devonian shales in the Middle Mountain syncline of the Valley and Ridge province, Pendleton County, West Virginia. Models are developed which permit the interpretation of bedding orientation contours in terms of fold geometry and faulting. Patterns in the contours of bedding strike and dip have been related to: 1) the regional structure of the syncline, and 2) internal faulting and folding related to structure in the underlying Devonian Oriskany Sandstone (Wilson, 1979). The analysis shows that the strike line map and contours of standard deviations in bedding dip are most useful as a tool to locate structure.

Deformation domains defined as areas of high standard deviation in bedding dip have been used to locate and define the extent of faulting. Deformation domains are found to be larger and more numerous within the Parsons structural lineament where it intersects the exposed Middle Devonian shales of the syncline. These deformation domains contain more intensely jointed shale, and are directly related to faults and folds in the underlying Devonian Oriskany Sandstone. Deformation domains therefore represent a small scale analogue to Shumaker's (1978) fracture facies. Thus information on the Oriskany structure can be used to predict the location of intensely fractured reservoirs. Structural shortening in the Parsons structural lineament is taken up by more numerous faults and low amplitude folds, and thus more numerous

fractured reservoirs. Future exploration for fractured gas reservoirs can then be optimized by concentrating subsurface studies along cross-strike structural discontinuities (such as the Parsons structural lineament), and determining their westward extent into the Plateau.

BACKGROUND

The present paper is part of a study designed to characterize the structural effects of a cross-strike structural discontinuity (the Parsons structural lineament) on the exposed Middle Devonian shales of a Valley and Ridge structure, the Middle Mountain syncline. The difficulty faced in mapping these poorly exposed shales has been lessened through use of the techniques presented herein. It is hoped that some of the results of this study will be of use in the current exploration efforts to locate gas producing Devonian shales in the Appalachian Basin.

STUDY AREA

The regional locations of the Parsons and Petersburg structural lineaments are shown in Figures 1 and 2. The maps presented in this study are constructed from data collected in the Middle Mountain syncline of the Valley and Ridge province in Pendleton County, West Virginia (Figures 2 and 3). The Middle Mountain syncline exposes Middle and Upper Devonian formations (Figure 3). The geologic map (Figure 3) is modified from Tilton and others (1927). The area is of particular interest in that the less competent organic-rich Middle Devonian shales exposed in this syncline are intersected by the Parsons structural lineament (Figures 2 and 3). Only the northern boundary of the Parsons structural lineament is shown in Figure 3.

Figure 1 The locations of the Parsons (P) and Petersburg (P'bg) structural lineaments are shown on the West Virginia geologic map.

GEOLOGIC MAP OF WEST VIRGINIA

WEST VIRGINIA GEOLOGICAL AND ECONOMIC SURVEY

Robert B. Erwin, State Geologist

1969

LEGEND

PERMIAN OR PENNSYLVANIAN
(230+ mill. yrs. ago). Cyclic sequences of sandstone, red beds, shale, limestone and coal.
Coal.

PENNSYLVANIAN
(280-230 mill. yrs. ago). Cyclic sequences of sandstone, shale, clay, coal, and limestone.
Coal, gas, oil, brine.

MISSISSIPPIAN
(310-345 mill. yrs. ago). Limestone, red beds, shale, and sandstone.
Limestone, gas, oil, brine.

DEVONIAN
(345-405 mill. yrs. ago). Red beds, shale, sandstone, limestone, and chert.
Gas, silica sand, limestone.

SILURIAN
(405-425 mill. yrs. ago). Sandstone, shale, limestone, rock salt, and ferruginous beds.
Gas, limestone, artificial brine.

ORDOVICIAN
(425-500 mill. yrs. ago). Limestone, dolomite, sandstone, shale, and metamorphic rocks.
Limestone (particularly low silica), building stone, clay-shale.

CAMBRIAN
(500-600 mill. yrs. ago). Limestone and dolomite, some sandstone and shale.

PRECAMBRIAN
(More than 600 mill. yrs. ago). Greenstone. Present only in extreme eastern Jefferson County.

0 10 20 30 40 50
Miles

0 10 20 30 40 50 60
Kilometers

Figure 2   Alignments of noses, bends, and saddles defining the Parsons and Petersburg structural lineaments. The study area
along the Middle Mountain syncline is enclosed in the hachured rectangle. Abbreviations: EMA – Elkhorn Mountain
anticline, MMS – Middle Mountain syncline, CMA – Cave Mountain anticline, WMA – Wills Mountain anticline,
SRS – Stoney River syncline, JS – Job syncline, BA – Blackwater anticline, NPS – North Potomac syncline,
EVA – Elkins Valley anticline, HS – Hannahsville syncline, EA – Etam anticline.
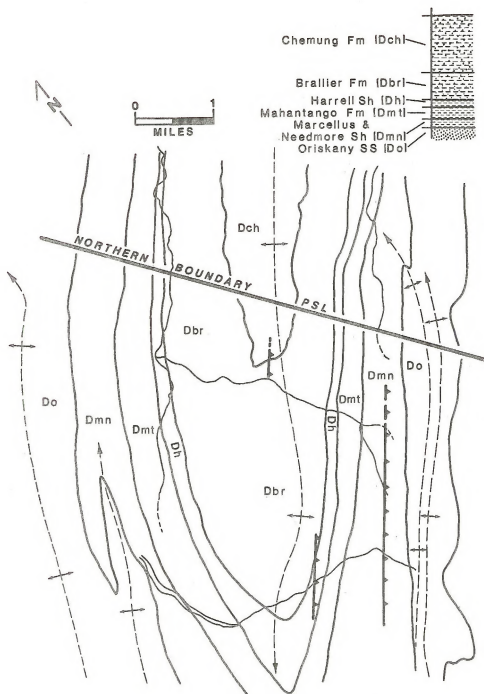
Figure 3. Geology and structure of the Middle Mountain syncline in the
Valley and Ridge Province in Pendleton County, West Virginia.
(taken from Tilton and others, 1927)

INTRODUCTION

The present work is stimulated by recent detailed mapping of structures in the Allegheny Plateau (Henderson, 1973; Mullennex, 1975; Trumbo, 1976; LaCaze, 1978) and Valley and Ridge Provinces (McColloch, 1976; Sites, 1978). These studies made use of bedding orientation contours in the structural analysis of the Parsons and Petersburg cross strike structural discontinuities (Figures 1 and 2) (Wheeler and others, 1979). Alignments of disruptions in bedding orientation contours often form zones colinear to these discontinuities. The widths of these zones are often cited as defining the widths of structural discontinuities (Wheeler and others, 1974; Sites and others, 1976; Wheeler and others, 1979).

During the present mapping and structural analysis of the Middle Mountain syncline (Valley and Ridge Province in the Central Appalachians of West Virginia) methods were developed which permit the interpretation of bedding orientation contours in terms of fold geometry and internal structure. The present study is similarly concerned with structural relationships between the Middle Mountain syncline and a structural discontinuity referred to locally as the Parsons structural lineament (PSL) (Figures 1, 2 and 3). The physical significance of zones of disruption in bedding orientation contours and their relationship to the PSL will be examined in detail.

MAP CONSTRUCTION

The bedding orientation contours are constructed from detailed measurements of bedding strike and dip. The map area is divided into a regularly spaced square grid. The contoured values of strike or dip are the mean of several measurements contained in each square grid division of the map area. The center of each square represents a control point. The control points and individual measurements are shown as large and small dots respectively on the enclosed acetate overlay.

Sampling

The effects of averaging and resolution should be considered in the interpretation of the actual data. Station spacing within the study area is determined by accessibility, the aims of the study, and the limitation of available time. The spacing of control points is ideally based on the structural variability of the area: a high rate of structural change requires a greater density of control points (Elliott, 1967). However, such an approach is infeasible in a study where contour maps are constructed specifically for the purpose of detecting unknown structure. A regular grid spacing then makes optimum use of the data. The choice of the grid spacing is determined by the sample density. A 0.38 mile grid spacing was chosen for use in constructing the contour maps from the Middle Mountain syncline.

Sample Distributions

Strike and dip values are members of directional distributions. Directional distributions have an angular period which repeats

any given attitude at cyclic intervals of 180 degrees (Elliott, 1965). Statistical treatment is thus complicated because there can be no unique origin or baseline to the distribution and the linear models of distribution such as the Gaussian (normal) are invalid (Elliott, 1965; Jizba, 1953; Chayes, 1954; Mardia, 1970). Normal statistics, however, can be applied to sample distributions of directional data having standard deviations less than 60 degrees (Chayes, 1954).

Sample distributions from each cell in the Middle Mountain area have standard deviations that are in all cases less than 60 degrees. The mean for the sample distribution in each cell was chosen as the mean value about which the standard deviation of the sample values was a minimum. This procedure is illustrated in Figure 4. In the example, north is chosen as the origin for the values of strike with east equal to 90 degrees and west equal to -90 degrees. It is customary to read values from the compass as so many degrees east or west of north. This confines the distributions to the northwest and northeast quadrants of the diagram. However, since the data is cyclical, the value 11 is the same as -179, 41 the same as -139, and so on. The mean of the distribution will be different depending on which value is chosen to represent the measurement. The distribution which minimizes the standard deviation is easily determined by inspection: the minimum standard deviation occurs for the most clustered grouping of values. The mean of the distribution in Figure 4A is 25 degrees, and its standard deviation is 57 degrees. The value A = -83 degrees in Figure 4A is clearly
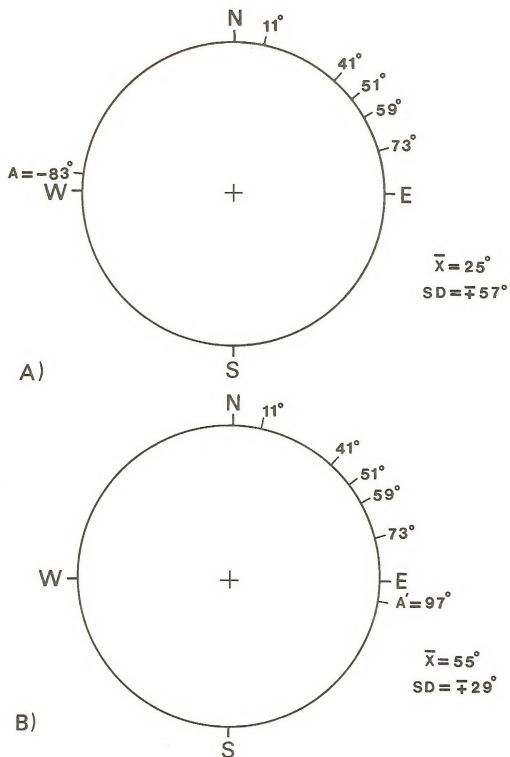
Figure 4 Sample distribution of strike illustrates the method for
determining the mean of a directional distribution by
minimizing the standard deviation.

an outlier. Choosing the supplement of this value A' = 97 degrees
clusters the distribution about a mean of 55 degrees and minimizes
the standard deviation at 29 degrees (Figure 4B).

The assumption that the distributions are normal is implicit
in the use of the mean and standard deviation to characterize these
distributions. Several of the sample distributions were tested for
normality using the Kolmogorov-Smirnov test for goodness of fit
(Siegel, 1959). The distributions were found in all cases to be
normally distributed. Some bimodal distributions are very likely
non-normal. However, the assumption of normality is in general valid.

MODELS (Figure 5)

Dip

The interpretation of dip contours is considerably simplified
if the magnitude of the dip is plotted and no distinction between dip
direction is made. This permits the dip values associated with a par-
ticular structure to be contoured as a continuous field. Contours drawn
through points having the same magnitude of dip outline structures much
the same as do structure contours. A series of confocal ellipses
(Figure 5-B) is suggested to represent the pattern formed by dip con-
tours of a symmetrical doubly plunging anticline or syncline. The trough
line of the fold is drawn as a line connecting points of greatest curva-
ture in the dip contours. Steeper limb dips show as more closely spaced
contours.
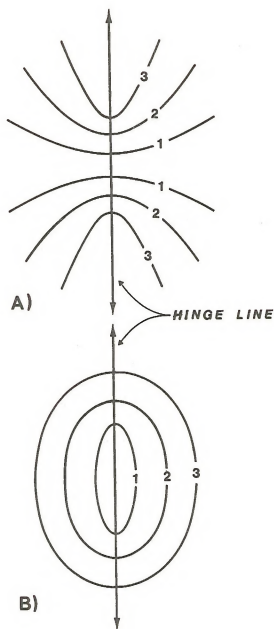
Figure 5   Theoretical bedding orientation contours for a doubly plunging
          symmetrical fold. A) Strike B) Dip. C1 = 10°

Strike

Choice of the mean trend of the fold hinge line or the regional trend of the structure under investigation as an origin for distributions of strike simplifies structural interpretation of strike contours. Modeling the contours of strike as a continuous field is possible only if the absolute value of the residuals from the regional trend is plotted. Contours of strike from a doubly plunging symmetrical anticline or syncline transformed in this manner will appear as a family of elliptic hyperbolae (Figure 5-A), with each hyperbola representing an isopleth of constant strike. The elliptic hyperbolae can be thought of as connecting points on the confocal ellipses, tangents to which make equal angles (strike) with the major axis of the ellipse. Assymmetry in the fold would be indicated by a closer spacing of contours on one limb. As with the dip contours, the crest line can be approximated by connecting points of greatest curvature in the contours. This model assumes that the hinge line of the fold has the regional trend to which all values of strike are reduced. Contours of strike associated with subsidiary folds whose hinge lines do not parallel that of the major fold will produce patterns that deviate from those of the model.

The models are based on an ideal conception of fold geometry. Since structures encountered in the field are never so simple, the patterns observed in contour maps of actual data should be considered with care. Although a pattern might appear quite similar to that suggested for a doubly plunging fold, it could be related to faulting,

statistical fluctuations in the data, to the resolution determined by cell spacing, or all three. The maps do permit the forming of preliminary hypotheses about the presence of subtle structures in a specific area, particularly if mappable marker units or distinct contacts are too few to outline structure.

Strike and Dip Standard Deviation Contours

The value of strike or dip plotted at a control point is a mean value calculated from samples collected in the cell containing that control point. The precision with which this value is representative of the parent population within a cell can be estimated as the standard deviation of values in the cell sample.

The standard deviations can also be thought of as a measure of the reliability of the contours drawn on the basis of those values. Perhaps a more reliable contouring method would be to use a contour interval equal to the 95% confidence interval of the values within a certain area (Elliott, 1967). However, since there is considerable variation in the standard deviations of samples over the entire map area, the standard deviations of each cell sample are contoured.

The contours of standard deviation not only provide a measure of the reliability of the strike and dip contours but are directly related to internal structure of the cell mass. A band of high standard deviations in strike will parallel the fold hinge line, fanning outward in the plunging nose. The high standard deviations near the crest line or trough line reflect the large errors present in the measurement of strike of low-dipping beds (Woodcock, 1976). The noseward

fanning of the high standard deviation band results from increased bedding curvature in the nose as well as from the measurement error. Disruption near faults will also produce high standard deviations in strike.

Dip values are not affected by the large measurement errors associated with strike. The standard deviations of bedding dip within a certain area are thus a measure of the intensity of deformation of that area. High standard deviation areas (referred to below as deformation domains) result from faulting and folding of the bedding in those areas.

BEDDING ORIENTATION CONTOURS OF THE MIDDLE MOUNTAIN SYNCLINE

Strike Contours (Figures 6A and 7A)

Contours of strike used by previous workers have been constructed with north or east as an origin for values of strike (see Sites, 1978). There are two shortcomings in this method: 1) the contours cannot be modelled as a continuous field; and 2) although the values of strike can be contoured as a continuous field, the resultant patterns are confusing to interpret structurally. However, such contours do permit general statements about relative amounts of structurally related disruption in an area. This leads to the question of the validity and the nature of associations between disrupted contours and actual structure.

The strike contours in Figure 6A have north as an origin (north = 0°, east = 90°, and west = -90°). Quite pronounced changes in
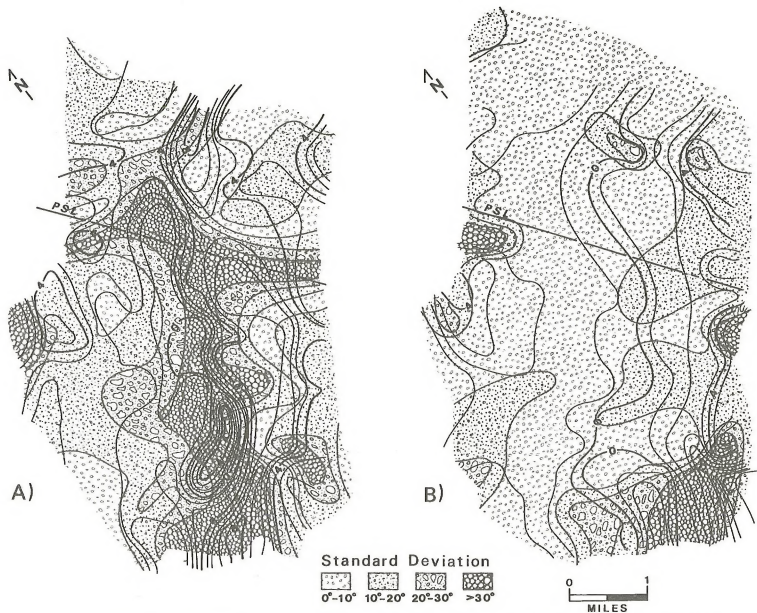
Figure 6   A) Average strike from samples taken in 0.38 mile square divisions of the map area overlies standard deviations of sample strike from each division, B) average dip overlies standard deviation of dip. C1 =10°

Figure 7 A) Absolute value of (strike -35°) overlies standard deviation of strike, B) absolute value of dip overlies standard deviation of dip. C1 = 10°

Standard Deviation

0°-10°   10°-20°   20°-30°   >30°

the orientation of strike are associated with the bullseye in the lower central portion of this figure. Changes in strike are also seen to the left and right of this bullseye. Contours of the absolute values of the residuals of bedding strike from the regional structural trend (Figure 7A) considerably simplify the appearance of the contours from this area. Comparison of these contours with the model (Figure 5A) suggests that most of the changes in strike occurring in the map area are associated with the swing in bedding strike across the fold axis.

If two models of strike contours (Figure 5A) are placed nose to nose, a region of closed contours centers over the saddle formed by the plunging noses. The values of strike increase toward the center of this bullseye. This closed pattern is apparent in the contours of strike in the Middle Mountain syncline (Figures 6A and 7A) and locates the area across which there is a northeastward plunge.

The compressed appearance of the contours toward the trough line indicates that the Middle Mountain syncline is more elongate or eccentric than the model fold. Changes in the orientation of the crest line observed in these contours may be the result of increased measurement error in the values of strike of these low-dipping beds. The changes may result from sampling older and softer units to the southwest, where the syncline may have a different orientation.

The nose of contours on the central northwest border of the map area (Figures 6A and 7A) occurs on the northeast plunging nose of an anticline (Figure 3). Structural interpretation of the contours from an area this small is restricted since the pattern is drawn from

only three or four control points. Resolution limits imposed by grid spacing require field verification of interpretations of small disruptions.

The analysis illustrates that many of the irregularities, bullseyes, and offsets observed in Figure 6A are purely an artifact of the north justified assignment of strike values. It further illustrates that shifting zero to the regional trend and contouring only the absolute values of the residuals of strike from this value produce patterns which can be interpreted in terms of actual structure.

Dip Contours (Figures 6B and 7B)

Contours of the absolute value of dip (Figure 7B) are considerably simplified in comparison to those for dip (Figure 6B). As discussed earlier, contours of absolute value of dip associated with a given structure can be modeled as a continuous field thus facilitating structural interpretation of the contours.

The trough line of the Middle Mountain syncline lies within the band of low dipping beds shown in Figure 7B. There is good agreement between the position of the trough line defined by strike contours (Figure 7A) with the position defined by contours of dip. The absence of closure in the contours in the southwest of the map area indicates that the change in structural level is gradual and at no point dips more steeply than 10°. The lack of closure at either end also implies that the Middle Mountain syncline is more elongate than the model fold in agreement with the strike contours and field observations.

The nose-like pattern in the southern corner of the map area
(Figure 7B) is similar to that suggested for the plunging nose of a fold
(see dip model, Figure 5A). An anticline in the Devonian Oriskany
Sandstone plunges out beneath the Middle Devonian shales just to the
southwest of this area and may in part explain this pattern. However,
field investigation reveals that the area is thrust faulted with steep-
ly dipping to overturned bedding present in the hanging wall. This
fault splays off a major ramp beneath the Elkhorn Mountain anticline
east of the map area (Figure 2) and dies out in the Middle Devonian
shales of the Middle Mountain syncline. The pattern in dips is then
related in part to both these structures. Other dip disruptions north-
east of this area are related primarily to the faulting.

The disturbance in dip on the central northwest border of
the map area just southwest of the PSL (Figure 7B) is in part related
to the plunge-out of an anticline in this area. It is not understood
why this pattern extends further to the northeast than that for strikes
(Figure 7A). Examination of this area revealed faulting to the southwest,
and it is expected that this faulting continues further to the northeast.

As with the contours of strike, the interpretation of con-
tours of absolute value of dip must consider the effects of resolution
and statistical error in the data.

STRIKE LINE MAP   (Figure 8)

The strike line map is easily constructed by plotting the mean
value of strike from each cell as a vector and approximating the contin-
uous outline of the structure by drawing lines tangent to these vectors.
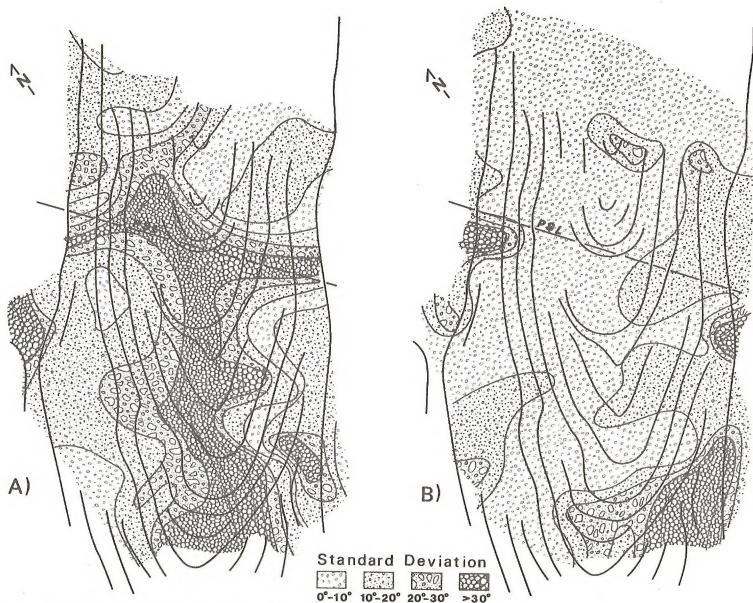
Figure 8   Strike line map overlies A) standard deviation of strike, B) standard deviation of dip.

Standard Deviation

0°-10°   10°-20°   20°-30°   >30°

0   1
MILES

147.

The strike line map (Figures 8A and 8B) is easily interpreted and clearly illustrates the basic structural elements of the Middle Mountain syncline discussed in the previous sections. Elliott (1965) has examined the interpretation and use of lineation isogonic maps in structural interpretation of various metamorphic fabrics, and similarly finds that the strike line map is "probably the clearest way of showing the structural geometry of the lineation surface." This map is combined with the contours of standard deviations of strike and dip (Figures 8A and 8B) to provide a structural reference and to illustrate structural correlation with these contours.

STANDARD DEVIATION CONTOURS

Resolution and the effects of resolution on data interpretation are predetermined by the choice of cell spacing. However, statistical errors of various origins need to be broken down, and their effects on interpretation considered in detail. This problem has been approached in several ways, one of which was to examine the continuous field of statistical error associated with the data sets, by contouring the standard deviations of the cell samples (see patterned contours in Figures 7A, 7B, 8A, and 8B).

Standard Deviations of Strike Contours (Figures 6A, 7A, and 8A)

One of the obvious characteristics in the contours of standard deviations in strike is the high s. d. (standard deviation) zone following the crest line of the Middle Mountain syncline.(Figures 7A and 8A). Association of this zone with low dipping and curved bedding

(see dip contours Figure 7B, and strike line map Figures 8A and 8B) indicates that the large standard deviations are due, respectively, to increased measurement error of strikes in low dipping beds (Woodcock, 1976) and to actual structural variation within each cell. The significance of structural variation in the area is obscured by the much larger measurement errors (see subsection on Strike Contours above).

The arm-like high s.d. appendages extending to the borders across the north central part of the map area and along the northern boundary of the PSL are largely related to measurement error in low dipping beds (Figure 7A and 8A) although there may be some faulting to the northwest.

Dispersion related to map scale structures is found in high s.d. areas on the west central border and south corner of the map area. The high s.d. area on the west central border is in part due to measurement error in the low dipping bedding (Figure 7B) but also coincides with the plunging nose of an anticline discussed earlier (Figure 3). The strike line map clearly illustrates this structural involvement (Figures 8A and 8B). The high s.d. area in the south corner of the map results from thrust faulting.

Standard Deviation of Dip Contours (Figures 6B, 7B, and 8B)

The measurement error in dip is a constant for all values of dip. Systematic errors, such as errors in calibration, personal errors, experimental conditions, or technique (Beers, 1953) can be disregarded since discrepancy with other determinations of dip is of no concern here. Random errors such as errors in judgement probably

contribute no more than ± 5° in error. Standard deviations in dip
greater than five or ten degrees are therefore structural in origin.

The high s.d. zone in the south corner of the map area
(Figures 7B and 8B) coincides with the nose-like pattern of dips
(Figure 7B) and the disrupted area on the strike line map (Figures
8A and 8B). With standard deviations in dip due primarily to struc-
ture, high s.d. areas provide reliable evidence of the existance and
extent of structural disruption. Northeast of this zone the s.d.'s
decrease and then increase (Figures 7B and 8B). Additional field
work in this area along with records of cuttings from water wells
support an extension of the faulting into this area at least to the
northern boundary of the PSL (Figure 3). The high s.d. area in the
south corner extends across the axis of the syncline. This area is
also faulted, and represents branches of the major splay rising from
the southeast as it dies out in the Middle Devonian shales. The
northern border of this high s.d. area (>20 degrees) coincides roughly
with the contact between the siltstone-rich Braillier Formation and
the Harrell shales, illustrating the pronounced differences in the
mechanical strengths of the Middle and Upper Devonian lithologies.

The small area in the west corner of the map area with
standard deviations between 20 and 30 degrees is not associated with
any mapped structures; however, the South Branch of the North Fork of
the Potomac River bends sharply across strike in this area before
turning along strike into the faulted core of the Cave Mountain anti-
cline (Sites, 1970) and may represent the effect of a transverse fault.

Contours of standard deviation in dip locate areas of bedding disruption, defined as deformation domains, that are the result of faulting and folding. As a field tool these contours were found to be the most useful and reliable for locating internal structures of the Middle Mountain syncline. Although these contours do not define structures, they define areas of deformation associated with the structures.

CONTOURS OF RANDOM NUMBERS AND REPRESENTATIVE SAMPLING

It has been suggested that the patterns observed in the contours of strike and dip are similar to the patterns observed in the contours of random numbers, and that consequently structural interpretations of these maps are of questionable significance. This criticism is no longer valid in view of the correlation of contour patterns with the models and observable structure. However, useful information concerning the question of representative sampling, and the characteristics of the underlying population distribution(s) can be gained by contouring random numbers generated from a population(s) having a specified distribution(s).

In a non-plunging cylindrical fold, for instance, the bedding strike will equal the fold trend. If the fold is not complicated by internal structures, measured values of strike differing from the regional trend will be due to measurement error and surface irregularities resulting from sedimentary structures.

As a simple case, in a low amplitude fold, standard deviations in observed strike could be roughly 30 degrees over the entire structure. The regional trend of the Middle Mountain syncline is N35E.
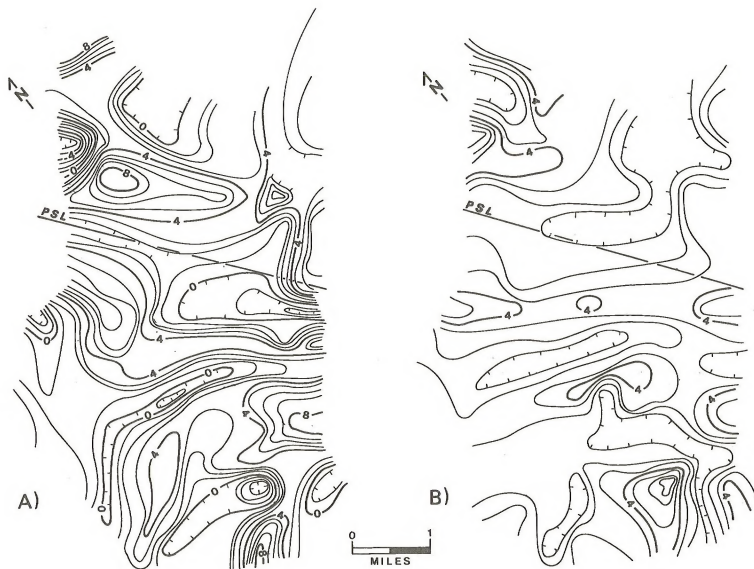
Figure 9   A) Strike values of 82 control points are drawn randomly from a population with mean ≈35 degrees (the regional structural trend) and standard deviation = 30°, B) absolute value of (random strike -35°). C1 = 10°

It would be instructive to examine the patterns in contours of strikes drawn randomly from a population having these parameters (i.e., mean = 35 degrees, and standard deviation = 30 degrees). To do this a number for each of the 82 control points was drawn randomly from a normally distributed population with the above parameters. Contours of north justified strikes are shown in Figure 9A. The absolute value of the residuals from regional strike are contoured in Figure 9B. The resultant patterns are not those expected for a cylindrical non-plunging fold, and further, they do not suggest the presence of structures that are in any way consistent with known regional structure. The presence of such a large standard deviation (30 degrees) of non-structural error would thus require that the values assigned to each control point be an average of several measurements from the surrounding area.

Additional numbers were generated from this population to match the sample density associated with each control point in the Middle Mountain syncline. Contours of the absolute values of the residuals and the standard deviations of the samples from the control areas are shown in Figures 10A and 10B. Again, it is not apparent from the contours that this is a cylindrical non-plunging fold. However, it is apparent that if non-structural error in the measured values of bedding strike from the Middle Mountain area is comparable to that in the random example, then structural interpretation of those data is meaningless.

The large non-structural error requires that an even greater number of measurements be made to yield a value that is representative of the population mean. The required number of measurements will
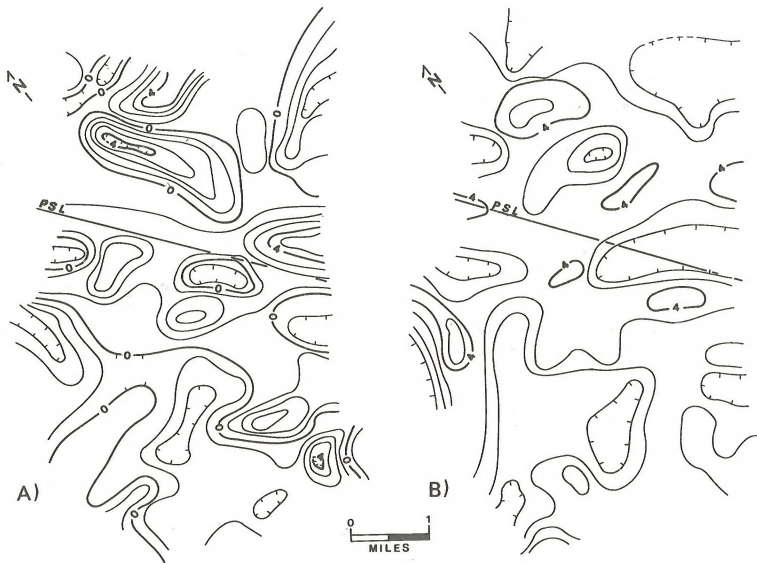
Figure 10 Stations within each cell division of the map area were assigned values drawn randomly from a population having a mean of 0 degrees and standard deviation of 30 degrees. A) Average value of the samples within each cell division, B) their standard deviation. C1 = 10°

depend on the desired precision of the sample average. For instance, to produce a value that is within 5 degrees of the population mean 95% of the time, can be determined by setting the expression for the 95% confidence interval equal to 5 degrees and then solve for the required number of samples. To reach this desired precision requires the measurement of 138 values of strike for each control point, and an extreme waste of field time.

It is particularly apparent from this discussion that structural interpretation of strike contours is least reliable since measurement error in a value of strike often exceeds 30 degrees (Woodcock, 1976).

The representativeness of the sampling in the Middle Mountain area has been examined more specifically by drawing values randomly from normally distributed populations having cell sample statistics as the population parameters for each cell in the map area. Contours of the means and standard deviations of these random numbers are shown in Figures 11A and 11B. The control values from the original data were averaged from two to eleven samples. The standard deviations of the samples in each control division are quite variable from cell to cell (see Figures 7 and 8). Structural and non-structural errors in the measured values of strike and dip were discussed earlier (see STANDARD DEVIATION CONTOURS). The presence of high standard deviation areas raises the doubt that, particularly in these areas, the means and thus the contours may not be representative of the parent populations of bedding orientations. However, the structural elements observed in
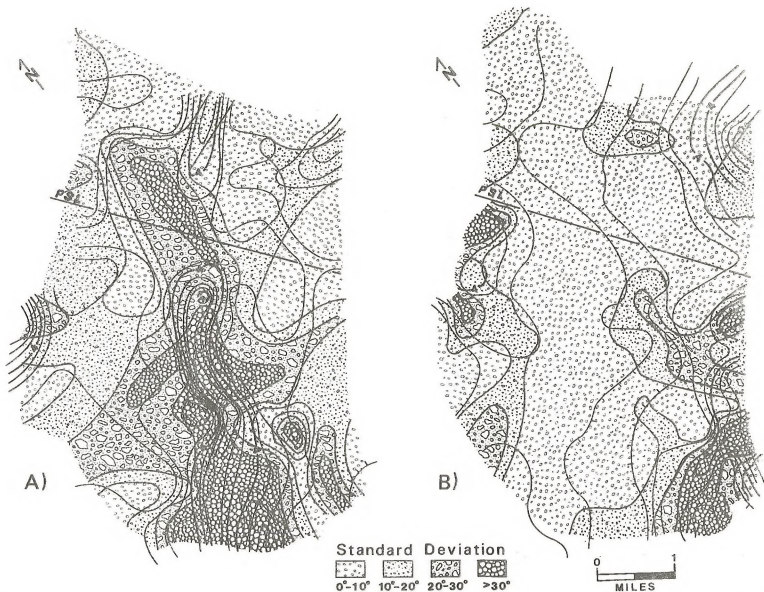
Standard Deviation

0°-10° 10°-20° 20°-30° >30°

0   1
MILES

Figure 11 Strike and dip values were drawn randomly from normally distributed populations having cell sample statistics for parameters. A) Absolute value of (random strike -35 degrees) overlies their standard deviations, B) absolute value of random dip overlies their standard deviations. C1 = 10°

the contours of the Middle Mountain data (see BEDDING ORIENTATION CON-
TOURS OF THE MIDDLE MOUNTAIN SYNCLINE and STANDARD DEVIATION CONTOURS
above) are also present in the random contours (Figures 11A and 11B).
The differences in the patterns are quite apparent but do not signifi-
cantly alter the interpretation. More pronounced differences result
in areas of poor control, such as the disappearance of the arm-like
appendages in the contours of standard deviations of strike discussed
earlier (see Figures 7A, 8A and 11A).

The deformation domains defined by areas of high standard
deviation in bedding dip retain the greatest similarity to the original
contours (Figures 7B and 8B). With the exception of the 20 to 30
degree high standard deviation area present in the northeast quadrant
of the original contours, every high standard deviation area present
in the original contours is also present in the random contours.

The small non-structural errors in measurement of bedding dip
and the reproducibility of the contours again support the usefullness
of contours of standard deviations in bedding dip in detecting struc-
tural disruption.

The assumption of normality (see SAMPLE DISTRIBUTIONS above)
is further supported by the similarity of the contours of the original
data to those generated from normally distributed populations.

DEFORMATION DOMAINS AND FRACTURED GAS RESERVOIRS

Much of the current research in the D.O.E.'s Eastern Gas
Shales project is directed toward predicting the locations of fractured

reservoirs in the gas producing Devonian shales. The Middle Devonian shales that crop out in the Valley and Ridge province belt are the mechanical equivalent of the Upper Devonian Brown Shale beneath the Allegheny Plateau province. The current work in the Middle Mountain syncline is aimed at determining the effects of cross-strike structural discontinuities (in this case the Parsons structural lineament) on the organic-rich Middle Devonian shales exposed in this area, and to suggest an exploration rationale for locating fractured gas reservoirs associated with structural discontinuities in the Allegheny Plateau.

The effects of structural lineaments on the characteristics of jointing have been examined previously (Wheeler, 1979a; LaCaze, 1978; Dixon, 1979a & b; Wheeler, 1978a; Wheeler and Holland, 1977). A method for estimating fracture intensity (Vialon and others, 1976) has been used to determine the effects on systematic joint intensity of the Parsons and Petersburg structural lineaments in the Plateau (Wheeler and Dixon, 1979; Dixon, 1979a and b). The results show that the Parsons and Petersburg structural lineaments represent zones of increased joint intensity.

The Parsons structural lineament is expressed on a regional scale as a cross-strike alignment of noses, bends and saddles of major folds in the Valley and Ridge and Plateau provinces (Wheeler and others, 1974) (see Figure 2). Structural shortening within the Parsons structural lineament in the Middle Mountain syncline is in general taken up by smaller folds and more abundant thrust faults than outside this structural lineament. The increase in minor folding and

particularly the increased number of thrust faults in the Middle
Devonian shales of the Middle Mountain syncline result in the increase
in size and number of deformation domains. Preliminary results
(Wilson and Wheeler, in prep.) show that the intensity of systematic
jointing is greater within the deformation domains. Thus the Parsons
structural lineament in the Middle Mountain syncline is a zone of
greater fracture intensity because it is also a zone of larger and
more numerous deformation domains.

A thrust fault is more likely to flatten out as it propagates
into a weak layer, although higher angle faulting is possible (Rodgers
and Rizer, 1979a and b). As the fault propagates into the weak layer,
secondary structures and fractures will remain in the region initially
near the fault tip, after the fault tip has propagated out of that
region (Rodgers and Rizer, 1979a and b; Rodgers, oral communication,
1979). Relic secondary faults observed in the Upper Devonian Lower
Huron Shale member of the Ohio Shale Formation were used to identify
the interval of detachment in the Pine Mountain thrust sheet (Wilson
and others, 1978). An increased intensity of jointing was also
observed in the interval of detachment (Wilson and others, 1978).
Secondary faulting will also deform the area in advance of the leading
edge of a thrust fault (Anderson, 1951; Hafner, 1951; Chinnery, 1966;
Rodgers and Rizer, 1979). Northwest trending slickenlines observed
in the Brown Shales of the Nicholas Combs #7239 core (Kulander, Dean
and Barton, 1977) and slickenlines observed in the Martin County core
were explained in this way (Wilson and others, 1978) and were suggested
to represent the porous fracture facies discussed by Shumaker (1978).

Bedding-transverse thrust faults cut across the Devonian Oriskany Sandstone on the northwest limb of the Elkhorn Mountain anticline and probably represent secondary splay thrusts off a major splay that rises from a decollement in the Ordovician Reedsville Formation and above which the Elkhorn Mountain anticline is formed. The deformation domains on both limbs of the Middle Mountain syncline are interpreted as a direct result of the thrust faults and associated folding in the underlying Devonian Oriskany Sandstone. The association of deformation domains with mapped faults and more intensely jointed shales suggests that the deformation domain is a small analogue of the fracture facies. Although the presence of shear surfaces may act to decrease the porosity of these shales (Bagnell and Ryan, 1976) the documented presence of more intense jointing in these shales may increase the porosity and the permeability producing a fractured gas reservoir.

RECOMMENDATIONS FOR FUTURE EXPLORATION EFFORTS

The increased abundance of deformation domains in the Parsons structural lineament and their relationship to Oriskany structure suggest an exploration rationale:

I.   Concentrate subsurface studies in the Appalachian Plateau on Oriskany-Onondaga structures.

II. Exploration efforts should be most productive if subsurface studies of Oriskany-Onondaga structure are concentrated in cross-strike structural discontinuities (for example the Parsons structural lineament).

Work currently under way will recommend sites as primary exploration targets.

CONCLUSIONS

The strike line map and contours of standard deviations in bedding dip are of considerable value in mapping structures in poorly exposed, mechanically incompetent shales, where exposure is often limited and structural interpretation highly speculative.

Deformation domains are more intensely fractured and represent small analoques of Shumaker's (1978) fracture facies.

The relationship of deformation domains to Oriskany structure, and the presence of more numerous larger deformation domains in cross strike structural discontinuities are important factors to consider in developing an exploration rationale to locate fractured gas reservoirs.

ACKNOWLEDGEMENTS

REFERENCES

Anderson, E. M., 1951, The dynamics of faulting: Oliver and Boyd, Ltd.

Bagnall, W. D., and Ryan, M., 1976, The geology and production character-
istics of the Devonian shale in southwestern West Virginia, in
Shumaker, R. C., and Overbey, W. K., Jr., eds., 1976, Devonian Shale
Production and Potential: Seventh Appalachian Petroleum Geology
Symposium Proc.: U. S. Energy Research and Development Administra-
tion, Morgantown Energy Research Center, MERC/SP-76/2, pp. 41-53;
Springfield, Virginia, National Tech. Inf. Service.

Beers, Y., 1953, Introduction to the theory of error, Addison-Wesley
Publishing Co., Inc., 65 pp.

Chayes, F., 1954, Effect of change of origin on mean and variance of two
dimensional fabric: A. J. S. v. 253, pp. 567-570.

Chinnery, M. A., 1966, Secondary Faulting: Canadian Journal of Earth
Science, v. 3, pp. 163-190.

Dixon, J. M., 1979a, A method to identify zones of intense jointing with
applications to the Parsons lineament, Morgantown Energy Technology
Center Open-File Report, Morgantown, West Virginia, 46 pp.

Dixon, J. M., 1979b, A method to identify zones of intense jointing with
application to the Parsons lineament, West Virginia (abs): Geol.
Soc. Amer. Abs. with Programs, v. 7, p. 1286.

Elliott, D., 1965, Quantitative mapping of directional minor structures,
Jour. Geol., v. 73, pp. 865-880.

Elliott, D., 1967, Interpretation of fold geometry from lineation isogonic
maps, Jour. Geol., v. 76, pp. 171-190.

Hafner, W., 1951, Stress distributions and faulting: Geol. Soc. Amer.
Bull., v. 62, pp. 373-398.

Henderson, C. D., ms, 1973, Minor structures of the high plateau, north-
eastern Tucker County, West Virginia: M. S. thesis, West Virginia
Univ., 43 pp.

Holland, S., and Wheeler, R. L., 1977, Parsons structural lineament: a
cross-strike zone of more intense jointing in West Virginia (abs):
Geol. Soc. America Abs. with Programs, v. 9, pp. 147-148.

Jizba, Z. V., 1953, Mean and standard deviation of certain geological
data, a discussion: A. J. S. v. 251, pp. 899-906.

Kulander, B. R., Dean, S. L., Barton, C. C., 1977, Fractographic logging for determination of pre-core and core-induced fractures . . . Nicholas Combs No. 7239 Well, Hazzard, Kentucky, U. S. Energy Research and Development Administration, Morgantown Energy Research Center, MERC/CR-77/3, 44 pp.

LaCaze, J. A., ms, 1978, Structural analysis of the Petersburg structural lineament in the eastern Appalachian Plateau province, Tucker County, West Virginia: M.S. thesis, West Virginia Univ., 69 pp.

Mardia, K. V., 1972, Statistics of directional data: Academic Press, New York.

McColloch, G. H., Jr., ms, 1976, Structural analysis in the central Appalachian Valley and Ridge, Grant and Hardy Counties, West Virginia Univ., 111 pp.

Mullennex, R. H., ms, 1976 Surface expression of the Parsons lineament, southwestern Tucker County, West Virginia: M. S. thesis, West Virginia Univ., 62 pp.

Rodgers, D. A., Rizer, S. D., 1979a, Deformation and secondary faulting near the leading edge of a thrust fault (abs), Thrust and Nappes Symposium, Imperial College, London, Abstracts Volume, p. 6.

Rodgers, D. A., Rizer, W. D., 1979b, Deformation and secondary faulting near the leading edge of a thrust fault (preprint), Proceedings Volume, Thrust and Nappes Tectonics Symposium, Imperial College, London.

Shumaker, R. C., 1978, Porous fracture facies in the Devonian Shales of West Virginia and Eastern Kentucky: Second Eastern Gas Shales Symposium, MArgantown Energy Technology Center, Morgantown, West Virginia, v. 1, METC/SP-78/6, pp. 360-369.

Siegel, S., 1956, Nonparametric statistics for the behavioral sciences, McGraw-Hill Book Company, 312 pp.

Sites, R. S., 1971, Geology of the Smoke Hole region on Grant and Pendleton Counties, West Virginia: M. S. thesis, West Virginia Univ., 2 vols., 106 pp.

Sites, R. S., 1978, Structural analysis of the Petersburg lineament, Central Appalachians: Ph.D. Dissert., West Virginia Univ., 274 pp. (Ann Arbor, Michigan, Univ. Microfilms).

Sites, R. S., McColloch, G. H., Wheeler, R. L., and Wilson, T. H., The Petersburg discontinuity of the central Appalachians in eastern West Virginia (abs): Geol. Soc. America Abstracts with Programs, v. 8, no. 2, p. 268.

Tilton, J. L., Prouty, W. F., and Price, P. H., 1927, Pendleton County: West Virginia Geol. and Econ. Survey County Geologic Report, 384 pp.

Trumbo, D. B., ms, 1976, The Parsons lineament, Tucker County, West Virginia: M. S. thesis, West Virginia Univ., 81 pp.

Vialon, P., Ruland, M., and Grolier, J., 1976, Elements de tectonique analytique: Paris, Masson, 118 pp.

Wheeler, R. L., 1979a, A numerical estimate of joint intensity, confidence limits on it, and applications to large structural lineaments (abs), Geol. Soc. America, Abstracts with Programs, Northeastern Section of the Geological Society of America 14th Annual Meeting, v. 11, no. 1, pp. 58-59.

Wheeler, R. L., 1979b, A robust statistical comparison of jacknifed pseudovalues, applications to joint intensity, (in press).

Wheeler, R. L., Mullennex, R. H., Henderson, C. D., and Wilson, T. H., 1974, Cross-strike structural discontinuities: possible exploration tool in detached forelands (abs): Geol. Soc. America Abstracts with Programs, v. 10, p. 201.

Wheeler, R. L., Winslow, M., Horne, R. R., Dean, S., Kulander, B., Drahovzal, J. A., Gold, D. P., Gilbert, O. E., Jr., Werner, E., Sites, R. S., Perry, W. J., Jr., 1979, Cross-strike structural discontinuities in thrust belt, mostly Appalachians, Southeastern Geology, in press.

Wheeler, R. L., and Dixon, J. M., ms, Intensity of systematic joints (in review).

Wilson, T. H., 1979, Bedding orientation contours of Middle Devonian shales in the Middle Mountain syncline, Valley and Ridge Province, West Virginia (abs), Geol. Soc. America, Abstracts with Programs, Northeastern Section of the Geological Society of America, 14th Annual Meeting, v. 11, no. 1, p. 60.

Wilson, T. H., Dixon, J. M., Shumaker, R. C., Wheeler, R. L., 1978, Fracture patterns observed in cores from the Appalachian Basin: ms submitted for the proceedings of the Southeastern Section Geological Society of America Symposium on Western Limits of Detachment and Related Structures in the Appalachian Foreland.

Wilson, T. H., and Wheeler, R. L., 1979, The characteristics of systematic jointing of the Middle Devonian shales in the Middle Mountain syncline, Valley and Ridge, West Virginia, in preparation.

Woodcock, N. H., 1976, Accuracy of structural field measurements, Jour. of Geol., v. 84, pp. 350-355.

- • Station Location
- • Grid Control Point
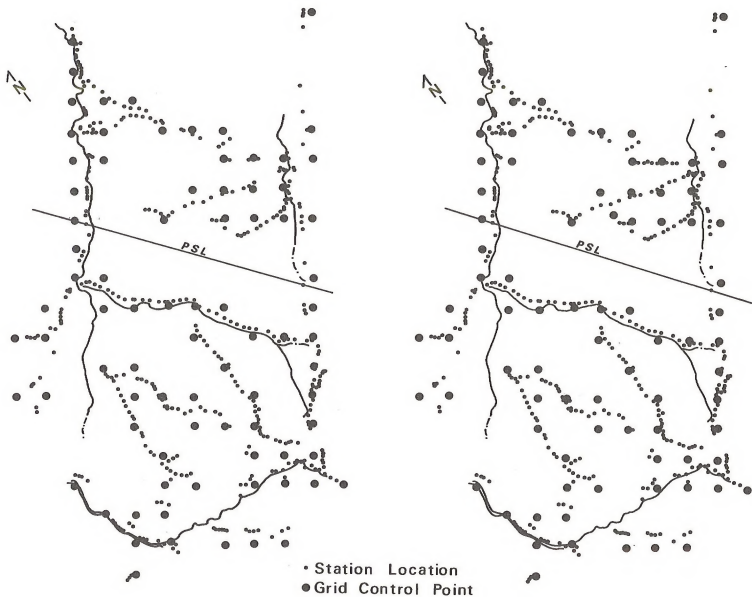
Overlay is registered by North arrow and PSL boundary.

167.

A METHOD TO IDENTIFY ZONES OF INTENSE JOINTING

WITH APPLICATION TO THE PARSONS LINEAMENT, WEST VIRGINIA

by

Jeanette M. Dixon, Research Associate
Devonian Shale Program

West Virginia University
Department of Geology and Geography
Morgantown, West Virginia 26506

INDEX

LIST OF FIGURES

ABSTRACT

A METHOD TO IDENTIFY ZONES OF INTENSE JOINTING
WITH APPLICATION TO THE PARSONS LINEAMENT, WEST VIRGINIA

Studies of water well yields, of three roadcuts, and of field observations indicate that the Parsons lineament in eastern West Virginia is a broad, cross-strike zone of unusually intense jointing. To test this hypothesis, strike, dip, exposed length, exposed depth, and spacing of 1594 joints were measured in interbedded siltstones, mudstones, and shales in the Upper Devonian Chemung facies. Joint sets were determined to strike N 35-55° W, N 25-45° E, and N 80° E - N 80° W. SYMAPS show more intense jointing within the Parsons lineament with the northeast-trending set contributing most to the increase. Identification of zones of intense jointing could be useful in hydrocarbon exploration, mine design, construction, and water-well siting.

INTRODUCTION

Anomalously intense jointing has often been cited as a reason for some gas production from fractured shales, coal mine roof falls, construction problems, and increased water-well yields. Accordingly, a method for measuring joint intensity and locating areas of intense fracturing would be generally useful. As part of the Eastern Gas Shales Project, funded by the Department of Energy, such a method was developed (Wheeler and Dixon, 1979). This paper reports a field test and application of the method. My purpose is to characterize exposed systems of natural fractures that are considered to be analogues of fractured gas reservoirs still buried further west, in central West Virginia (Wheeler, 1978a; 1978b).

SETTING

The Parsons lineament in the Plateau Province in eastern West Virginia was chosen for this study because previous studies (Wheeler and others, 1978; Wheeler and Holland, 1978a; 1978b) indicated that rocks in the lineament are more intensely jointed than rocks juxtaposed to the lineament. The lineament is a northwest trending band, from 7 to 10 km wide, of disruptions in the regular northeast-trending folds and detachments characteristic of the eastern Plateau Province (Gwinn, 1964; Cardwell and others, 1968). The lineament extends at least 55 km, according to terrain corrected gravity, topographic, and LANDSAT data. This paper deals with systematic joints in interbedded siltstones, mudstones, and shales of the Upper Devonian

Chemung facies. Only the Chemung was studied in order to reduce the
effects of differing lithologies. Bed thicknesses range from 0.2 to
200 cm, and typically are 10 to 30 cm. In Tucker County, the Parsons
lineament crosses the outcrop belt of Chemung rocks exposed in the
cores of the northeast-trending Deer Park and Elkins Valley anti-
clines (Cardwell and others, 1968; Gwinn, 1964).

METHOD

A total of 1594 joints were measured at 143 stations in the
Chemung facies (Figure 1). As many as possible of strike, dip, exposed
depth, exposed length, spacing, and bed thickness were measured on each
joint. Exposed depth is the total exposed extent of a joint in the
direction perpendicular to bedding, and exposed length, parallel to
bedding; spacing is the perpendicular distance to the adjacent joint
in the same set (Stubbs and Wheeler, 1975; Wheeler and Stubbs, 1979).
Bed thickness is a measurement of the thickest bed through which the
joint penetrates. Exposure size, regularity or irregularity of spacing,
and number of joint sets exposed determined the number of measurements
taken per station. Fifty-four percent of the joints were measured in
roadcuts; the rest in streamcuts and stream pavements. Statistical
analyses and contour maps of joint intensity and spacing were done with
local modifications of the Statistical Analysis System and of the SYMAP
program.
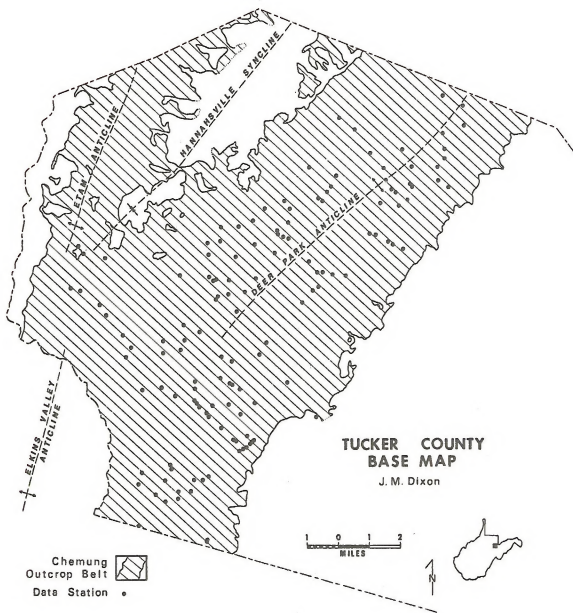
Figure 1. Index map showing the extent of the Chemung Outcrop belt and station locations.

RESULTS

A circular histogram of all measured joints shows three
sets: N 35-55° W (transverse to folds), N 25-45° E (longitudinal),
and N 80° E - N 80° W (diagonal), with the northwest set dominating
(Figure 2). Roadcuts and stream exposures each show all three sets
(Figure 3). All three sets appear north, within, and south of the
lineament, but in different abundances (Figures 2a, b, c). In addi-
tion, a N 05-10° W set appears south of the lineament (Figure 2c).

A measurement of joint intensity, joint surface area per
unit volume of rock (Wheeler and Dixon, 1979; Wheeler, 1979), was
made using inverses of average spacings, summed over all sets in an
exposure (Vailon and others, 1976; Wheeler, 1979; Dixon, 1979).
SYMAP shows areas of more intense jointing within the lineament
(Figure 4). The map was shown to five people: independently, each
chose the boundaries of the lineament where shown in Figure 4.
SYMAPS of average spacing for individual sets indicate that the
northeast-striking set contributes most to the increased intensity
inside the lineament, the northwest-striking set contributes slight-
ly, and the east-striking set contributes little, if at all
(Figures 5, 6, and 7). Mean spacings of each set support that
(Table 1).

A SYMAP of average bed thickness shows a northeast-trending
band of thin beds, reflecting the thinner beds of the lower Chemung
facies exposed along the crest of the Deer Park and Elkins Valley
anticlines (Figure 8). The trends found in the spacing and intensity
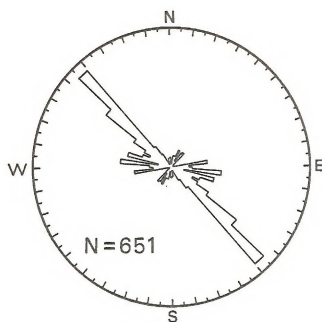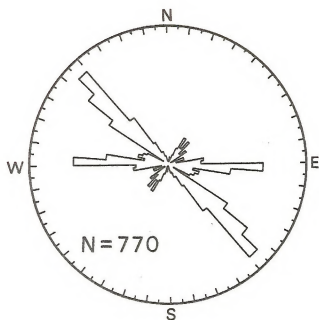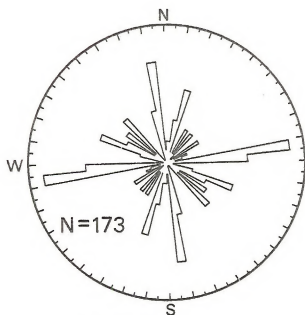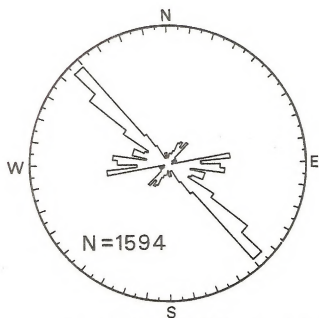
Figure 2. Circular histograms of joints taken north, within, and south of Parsons lineament and a composite of all joints measured.
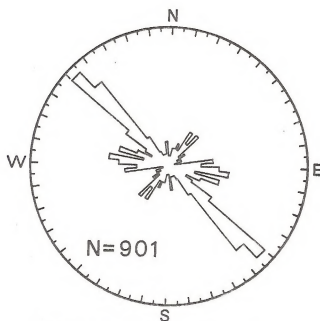
a) ROADCUT JOINTS
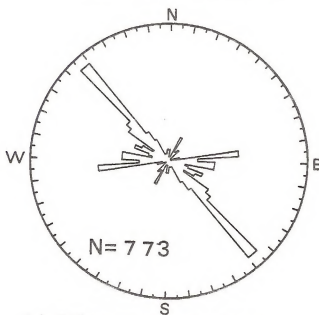
b) STREAM JOINTS

Figure 3. Circular histograms of joints taken (a) along road cuts, (b) along streamcuts and stream pavements.

INTENSITY (Cm²/Cm³)

0.02-0.17

0.17-0.31

0.31-0.46

0.46-0.60

> 0.60

JOINT INTENSITY

J.M.Dixon

1 0 1 2
MILES

N
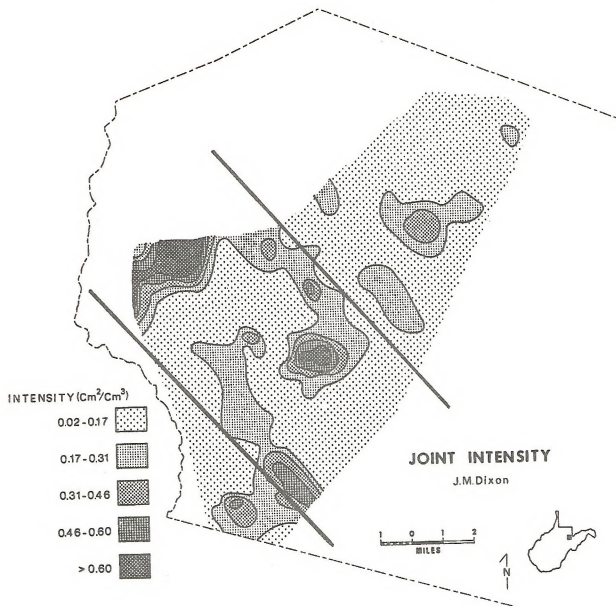
Figure 4. Contour map showing joint intensity, plotted at each station.

SPACING (Cm)

6.0 -14.8

14.8 - 23.6

23.6 - 32.4

32.4 - 41.2

> 41.2

**JOINT SPACING:
N25 - 45E**

J.M.Dixon

1   0   1   2
MILES

N
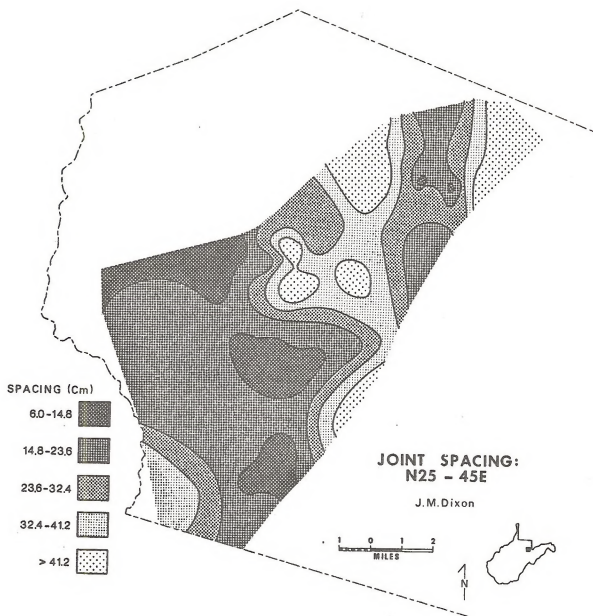
Figure 5. Contour map of the mean spacing, plotted at each station, of the northeast trending joint set.

SPACING (Cm)

- 5.0 - 12.4
- 12.4 - 19.8
- 19.8 - 27.2
- 27.2 - 34.6
- >34.6

**JOINT SPACING:
N35 - 55W**

J.M.Dixon

MILES

N
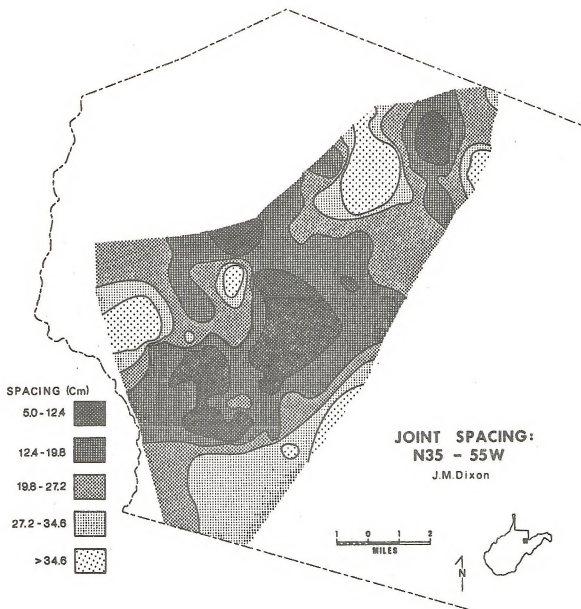
Figure 6. Contour map of mean spacing, plotted at each station, of the northwest-trending joint set.

SPACING (Cm)

0.75-9.00

9.00-17.25

17.25-25.50

25.50-33.75

> 33.75

JOINT SPACING:
N80E – N80W

J.M.Dixon

1   0   1   2
MILES

N
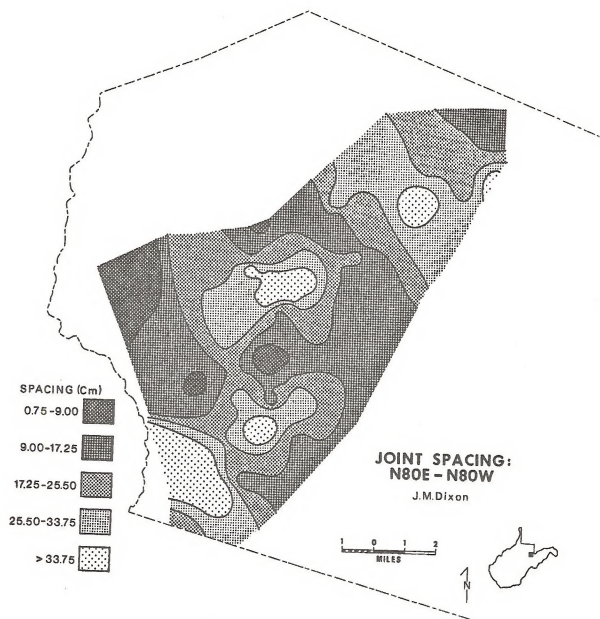
<u>Figure 7</u>. Contour map of mean spacing, plotted at each station,
of the east-trending joint set.

THICKNESS (Cm)

1.0 - 14.4

14.4 - 27.8

27.8 - 41.2

41.2 - 54.6

> 54.6

AVERAGE BED THICKNESS

J. M. Dixon

1 0 1 2
MILES

N
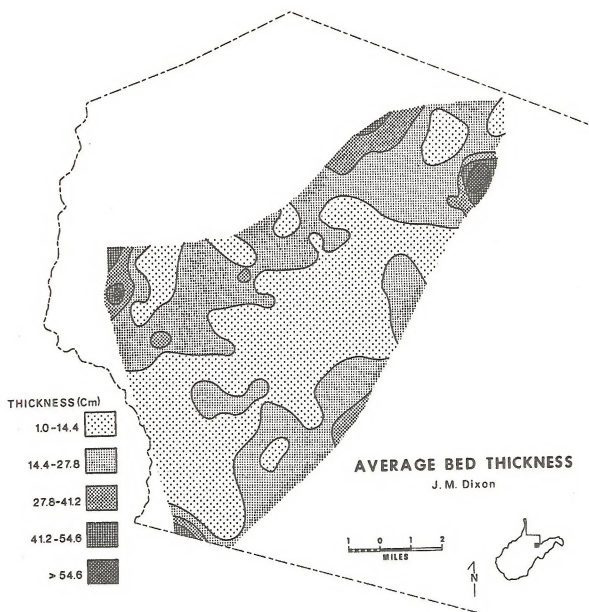
Figure 8. Contour map of the mean bed thickness, plotted at each station.

Location				Joint Set					
	Northeast			Northwest			East-West		
	n	$\overline{s}$	σ_s	n	$\overline{s}$	σ_s	n	$\overline{s}$	σ_s
North	50	31	29.8	232	22	19.8	136	22	14.5
Within	79	17	16.3	270	19	18.9	172	25	23.6
South	15	28	13.2	18	30	27.0	36	42	39.9

Table 1. Mean spacing in cm ($\overline{s}$), number of observations (n), and standard deviations in cm (σ_s) of each joint set north, within, and south of Parsons lineament.

maps are northwest to north, from which I conclude that a factor other than bed thickness controls joint intensity. (Statistical tests show only a minor correlation between bed thickness and joint spacing.) That factor apparently is the Parsons lineament.

Large, northeast-trending anticlines plunge into the Parsons lineament (Figure 1; Cardwell and others, 1968), which may have increased the intensity of the transverse joint set on the anticlinal noses. Smaller, northeast-trending anticlines with wavelengths on the order of half a kilometer are more numerous in the lineament (Trumbo, 1976), and may increase the intensity of the longitudinal set.

CONCLUSIONS

1. The Upper Devonian Chemung facies shows three well-developed, systematic joint sets: N 35-55° W, N 25-45° E, and N 80° E - N 80° W, with the northwest set dominating.

2. Rocks within the Parsons lineament are more intensely jointed than rocks juxtaposed.

3. SYMAPS and statistics show the northeast-trending set contributes most to joint intensity, the northwest-trending set slightly contributes, and the east-trending set contributes little or not at all to increased joint intensity within the Parsons lineament.

4. Joint spacing was found to be the most useful measurement in determining joint intensity.

REFERENCES

Cardwell, D. H., Erwin, R. B., and Woodward, H. P., compilers, 1968, Geologic map of West Virginia: Morgantown, W. Va., West Virginia Geol. and Econ. Survey.

Dixon, J. M., 1979, A method to identify zones of intense jointing with application to the Parsons lineament, West Virginia (abs): Geol. Soc. America Abs. with Programs, v. 11, p. 177.

Gwinn, V. E., 1964, Thin-skinned tectonics in the Plateau and northwestern Valley and Ridge Provinces of the Central Appalachians: Geol. Soc. America Bulletin, v. 75, p. 863-900.

Stubbs, J. L., Jr., and Wheeler, R. L., 1975, Style elements of systematic joints (abs.): Geol. Soc. America Abs. with Programs, v. 7, p. 1286.

Trumbo, D. B., 1976, The Parsons lineament, Tucker County, West Virginia: M. S. thesis, West Virginia University.

Vialon, P., Ruland, M., and Grolier, J., 1976, Elements de tectonique analytique: Paris, Masson, 118 p.

Wheeler, R. L., and Dixon, J. M., 1979, Intensity of systematic joints (in review).

Wheeler, R. L., 1978a, Fracture intensity predictions for eastern gas shales: Morgantown Energy Technology Center Open-File Report, Morgantown, West Virginia.

_____, 1978b, Cross-strike structural discontinuities: possible exploration tool in detached forelands (abs.): Geol. Soc. America Abs. with Programs, v. 10, p. 201.

Wheeler, R. L., Winslow, M., Horne, R. R., Dean, S., Kulander, B., Drahovzal, J. A., Gold, D. P., Gilbert, O. E., Jr., Werner, E., Sites, R., and Perry, W. J., Jr., 1978, Cross-strike structural discontinuities in thrust belts, mostly Appalachian: Southeastern Geology (in press).

Wheeler, R. L., and Holland, S. M., 1978a, Style elements of systematic joints: effects of structural position on an anticline (abs.): in Abs. of the 3rd Internat. Conf. on Basement Tectonics, Durango, Col., Fort Lewis College, p. 51.

_____, 1978b, Style elements of systematic joints: effects of structural position on an anticline (in review).

Wheeler, R. L., and Stubbs, J. L., Jr., 1979, Style elements of systematic joints: in Podwysocki, M., ed., 2nd Internat. Conf. on the Basement Tectonics Proc. (in press).

APPENDIX A

STATION LOCATION OF UTM COORDINATES

STA	LONG	LAT	STA	LONG	LAT
001	4328.28	615.12	076	4336.54	613.30
002	4329.71	613.71	077	4337.21	613.89
003	4330.34	614.08	078	4333.23	616.75
004	4330.80	610.53	079	4333.02	616.46
005	4329.34	612.22	080	4332.42	615.92
006	4325.48	613.10	082	4326.32	616.70
007	4325.20	612.50	083	4332.90	612.91
008	4325.87	611.72	084	4334.70	612.43
009	4327.03	611.25	085	4335.52	611.59
010	4326.43	611.07	086	4335.39	610.92
011	4326.92	610.60	087	4334.81	610.98
012	4323.35	611.10	088	4333.73	609.50
013	4323.17	610.80	089	4330.37	609.76
014	4322.60	610.18	090	4329.88	609.59
015	4329.56	611.70	091	4330.32	608.65
016	4330.60	606.53	092	4329.73	608.64
017	4328.02	603.70	093	4329.95	606.99
018	4325.61	602.99	094	4329.45	606.72
019	4324.87	602.92	095	4331.60	605.67
020	4323.48	602.57	096	4332.16	605.30
021	4319.75	602.58	097	4332.87	604.30
022	4319.98	611.05	098	4332.96	603.77
023	4320.06	611.07	099	4335.13	604.14
024	4322.17	609.52	100	4334.77	604.43
025	4322.02	608.87	101	4334.58	605.56
026	4327.13	610.47	102	4327.19	613.48
027	4327.27	610.34	103	4327.88	612.70
028	4327.50	609.30	104	4328.09	612.32
029	4327.92	608.60	105	4328.47	611.66
030	4327.80	607.57	106	4328.17	612.15
031	4333.67	611.01	107	4327.11	612.15
032	4333.48	611.25	108	4326.60	612.76
033	4332.48	611.38	109	4327.87	610.34
035	4331.16	609.72	110	4328.22	610.35
036	4326.64	610.97	111	4332.66	611.48
037	4325.27	612.38	112	4332.78	612.03
038	4325.21	612.49	113	4333.50	612.08
040	4324.70	612.70	114	4333.54	611.40
041	4324.80	612.88	115	4331.86	612.48
042	4324.88	613.08	116	4338.61	621.52
043	4325.06	613.23	117	4339.48	621.58
044	4325.12	613.30	118	4340.37	621.09
045	4325.18	613.35	119	4338.45	621.62
046	4325.25	613.42	120	4338.15	620.74
047	4334.54	616.24	021	4338.78	620.22
048	4334.00	616.68	123	4337.58	619.92
049	4333.98	616.96	124	4335.95	619.72
050	4333.90	617.47	125	4335.62	620.39
051	4333.79	618.17	126	4335.48	620.62
052	4334.94	614.42	127	4335.23	621.17
054	4333.60	613.45	128	4335.38	613.38
055	4338.43	623.52	129	4335.68	615.17
056	4338.78	622.98	130	4335.77	614.90
057	4338.28	620.51	131	4335.92	614.88
058	4339.40	620.08	132	4336.11	614.55
059	4340.17	619.37	133	4336.51	615.13
060	4341.34	618.56	134	4337.23	615.22
061	4341.94	617.73	135	4323.16	610.33
062	4339.50	622.92	136	4323.69	609.17
063	4339.92	623.30	137	4323.90	609.10
064	4340.42	623.31	138	4320.77	607.69
065	4343.18	623.17	139	4323.12	608.84
066	4342.68	624.21	140	4322.55	609.54
067	4341.22	623.18	141	4322.37	608.36
068	4341.65	624.31	142	4323.48	607.63
069	4337.77	621.36	143	4322.87	607.46
070	4337.48	620.91	144	4323.01	604.68
071	4335.99	619.44	145	4338.96	617.63
072	4337.62	614.91	146	4338.43	617.36
073	4339.38	616.18	147	4338.11	617.15
074	4336.20	611.61	148	4337.66	616.91
075	4336.27	612.53	149	4337.80	616.69

APPENDIX B

TUCKER COUNTY DATA

KEY TO ABBREVIATIONS

STA = station number

STRI = joint strike

DIP = joint dip

LNG = joint length

DPT = joint depth

SPA = joint spacing

BED = bed thickness

EXP = type of exposure: R = roadcut, S = stream pavement,
                           SC = streamcut

SET = indicates into which of the three main joint sets the
        joint falls: NW = northwest, NE = northeast,
                      EW = east-west.

LOC = location with respect to the Parsons lineament:
        IN = within, NT = north, SO = south.

STA	STRI	DIP	LNG	DPT	SPA	BED	EXP	SET	LOC
001	N45W	88SW	106	048	060	020	R	NW	IN
001	N46E	90NW	004	022	013	015	R		IN
001	N45W	88SW	148	020	002	015	R	NW	IN
001	N46E	90NW	007	017	044	017	R		IN
001	N46E	90NW	027	029	060	020	R		IN
001	N45W	88SW	084	021	007	021	R	NW	IN
001	N45W	88SW	074	022	002	022	R	NW	IN
001	N45W	88SW	075	039	005	020	R	NW	IN
001	N46E	90NW	007	015	014	015	R		IN
001	N46E	90NW	009	008	014	008	R		IN
001	N46E	90NW	012	008	022	008	R		IN
002	N84E	81SW	013	002	007	002	R	EW	IN
002	N30E	90NW	026	003	003	003	R	NE	IN
002	N84W	81SW	005	002	005	002	R	EW	IN
002	N45W	90SW	010	125		003	R	NW	IN
002	N20E	90NW	110	070	010	004	R		IN
002	N20E	90NW	087	065	003	004	R		IN
002	N78W	90SW	007	005		005	R		IN
002	N60E	90SW	023	010	007	010	R		IN
002	N60E	90SW	063	011	015	011	R		IN
002	N45W	90SW	027	007		007	R	NW	IN
002	N45W	90SW	035	007	002	007	R	NW	IN
002	N80E	80SE	040	012	045	012	R	EW	IN
002	N30E	90NW	024	001	008	001	R	NE	IN
002	N30E	90NW	020	001	005	001	R	NE	IN
002	N30E	90NW	021	001	008	001	R	NE	IN
002	N30E	90NW	018	001	004	001	R	NE	IN
002	N45W	90SW	100	010	016	010	R	NW	IN
002	N70W	90SW	027	005	016	005	R		IN
002	N30E	90NW	016	001	008	001	R	NE	IN
002	N30E	90NW	005	001	006	001	R	NE	IN
002	N84W	81SW	022	003	016	003	R	EW	IN
002	N84W	81SW	036	002	015	002	R	EW	IN
002	N84W	81SW	020	004	010	004	R	EW	IN
002	N84W	81SW	010	004	004	004	R	EW	IN
002	N84W	81SW	023	004	010	004	R	EW	IN
003	N34E	90NW	028	015	033	015	R	NE	IN
003	N34E	90NW	035	015	017	015	R	NE	IN
003	N34E	90NW	055	015	020	015	R	NE	IN
003	N34E	90NW	045	015	008	015	R	NE	IN
003	N34E	90NW	054	015	024	015	R	NE	IN
003	N87E	80NW	153	015	030	015	R	EW	IN
003	N87E	80NW	055	015	020	015	R	EW	IN
003	N87E	80NW	036	015	022	015	R	EW	IN
003	N87E	80NW	070	015	020	015	R	EW	IN
003	N87E	80NW	033	015	016	015	R	EW	IN
003	N87E	80NW	078	015	016	015	R	EW	IN
003	N34E	90NW	012	003	007	003	R	NE	IN
003	N34E	90NW	010	003	004	003	R	NE	IN
003	N34E	90NW	007	006	008	006	R	NE	IN
003	N87E	80NW	013	006	011	006	R	EW	IN
003	N60E	85SW	105	044	030	006	R		IN
004	N45W	88NE	135	048	050	010	R	NW	IN
004	N45W	88NE	107	020	020	010	R	NW	IN
004	N45W	88NE	175	015	005	010	R	NW	IN
004	N50E	90NW	001	008	036	008	R		IN
004	N50E	90NW	003	026	035	010	R		IN
004	N50E	90NW	020	010	007	010	R		IN
004	N50E	90NW	025	010	012	010	R		IN
005	N55W	73NE	007	005	011	005	R	NW	IN

STA	STRI	DIP	LNG	DPT	SPA	BED	EXP	SET	LOC
005	N40E	15SE	007	007	007	007	R	NE	IN
005	N55W	73NE	015	007	008	007	R	NW	IN
005	N40E	15SE	005	007	003	007	R	NE	IN
005	N40E	15SE	005	005	004	005	R	NE	IN
005	N40E	15SE	001	005	002	005	R	NE	IN
005	N55W	73NE	011	005	005	005	R	NW	IN
005	N55W	73NE	020	006	007	006	R	NW	IN
005	N84E	77SE	022	014	005	014	R	EW	IN
005	N84E	77SE	042	003	003	003	R	EW	IN
005	N84E	77SE	019	008	010	008	R	EW	IN
005	N84E	77SE	024	010	002	010	R	EW	IN
005	N50W	70NE	021	008	011	008	R	NW	IN
005	N50W	70NE	026	015	007	019	R	NW	IN
005	N50W	70NE	045	024	012	024	R	NW	IN
005	N40E	15SE	025	024	033	024	R	NE	IN
005	N40E	15SE	027	030	039	024	R	NE	IN
005	N60W	70NE	032	016	003	010	R		IN
005	N55W	73NE	022	010	008	010	R		IN
005	N40E	15SE	018	020	005	005	R	NE	IN
006	N45W	82NE	007	012	015	012	R	NW	IN
006	N45W	82NE	018	012	020	012	R	NW	IN
006	N45W	82NE	009	020	015	010	R	NW	IN
006	N45W	82NE	009	020	022	010	R	NW	IN
006	N45W	82NE	007	017	012	010	R	NW	IN
006	N45W	82NE	006	021	023	010	R	NW	IN
006	N45W	82NE	035	021	016	011	R	NW	IN
006	N45W	82NE	012	050	009	011	R	NW	IN
006	N45W	82NE	005	020	007	011	R	NW	IN
006	N45W	82NE	050	033	023	033	R	NW	IN
006	N45W	82NE	022	006	010	006	R	NW	IN
006	N45W	82NE	030	006	013	006	R	NW	IN
006	N45W	82NE	031	006	012	006	R	NW	IN
006	N45W	82NE	012	006	011	006	R	NW	IN
006	N40E	56SE	010	006	010	006	R	NE	IN
006	N40E	56SE	011	006	023	006	R	NE	IN
006	N40E	56SE	010	010	011	010	R	NE	IN
006	N40E	56SE	033	014	003	014	R	NE	IN
007	N23W	90SW	104	013	023	019	R		IN
007	N23W	90SW	033	019	022	019	R		IN
007	N23W	90SW	016	019	017	019	R		IN
007	N23W	90SW	001	019	010	019	R		IN
007	N23W	90SW	018	019	011	019	R		IN
007	N23W	90SW	012	019	022	019	R		IN
007	N23W	90SW	022	019	017	019	R		IN
007	N69E	90NW	250	090	048	025	R		IN
007	N69E	90NW	250	048	017	017	R		IN
007	N23W	90SW	010	005	012	005	R		IN
007	N23W	90SW	008	005	014	003	R		IN
007	N23W	90SW	001	008	002	003	R		IN
007	N23W	90SW	001	020	005	005	R		IN
007	N69E	90SE	043	021	011	021	R		IN
007	N69E	90SE	001	034	015	034	R		IN
007	N69E	90NW	015	007	040	007	R		IN
007	N69E	90NW	007	007	041	007	R		IN
007	N69E	90NW	002	007	060	007	R		IN
007	N69E	90NW	002	007	065	007	R		IN
007	N69E	90NW	032	010	010	010	R		IN
007	N69E	90NW	010	010	009	010	R		IN
008	N35E	90NW	010	011	010	011	R	NE	IN
008	N75W	90SW	600	070	055	038	R		IN

STA	STRI	DIP	LNG	DPT	SPA	BED	EXP	SET	LOC
008	N35E	90NW	011	011	028	011	R	NE	IN
008	N35E	90NW	011	011	015	011	R	NE	IN
008	N35E	90NW	012	011	035	011	R	NE	IN
008	N35E	90NW	009	011	021	011	R	NE	IN
008	N85W	56NE	038	020	048	020	R	EW	IN
008	N85W	56NE	165	011	050	011	R	EW	IN
008	N35E	90NW	015	004	013	004	R	NE	IN
008	N35E	90NW	001	004	013	004	R	NE	IN
008	N35E	90NW	001	004	010	004	R	NE	IN
008	N35E	90NW	017	007	014	007	R	NE	IN
008	N35E	90NW	016	007	007	007	R	NE	IN
008	N35E	90NW	014	015	020	015	R	NE	IN
008	N53W	90SW	500	115		060	R	NW	IN
008	N53W	90SW	500	233		085	R	NW	IN
009	N74E	90NW	060	013	008	013	S		IN
009	N74E	90NW	080	013	034	013	S		IN
009	N74E	90NW	080	013	017	013	S		IN
009	N74E	90NW	065	013	020	013	S		IN
009	N74E	90NW	070	013	010	013	S		IN
009	N74E	90NW	051	013	007	013	S		IN
009	N74E	90NW	040	013	020	013	S		IN
009	N74E	90NW	041	013	030	013	S		IN
009	N74E	90NW	007	008	020	008	S		IN
009	N35W	90SW	040	008	030	008	S	NW	IN
009	N35W	90SW	063	013	037	013	S	NW	IN
009	N35W	90SW	042	013	013	013	S	NW	IN
009	N35W	90SW	043	013	021	013	S	NW	IN
009	N35W	90SW	070	013	021	013	S	NW	IN
010	N52W	90SW	105	007	010	007	R	NW	IN
010	N52W	90SW	125	007	002	007	R	NW	IN
010	N52W	90SW	029	007	009	007	R	NW	IN
010	N52W	90SW	040	011	006	011	R	NW	IN
010	N52W	90SW	022	011	010	011	R	NW	IN
010	N52W	90SW	228	070	003	011	R	NW	IN
010	N52E	90NW	001	007	043	007	R		IN
010	N52E	90NW	001	007	011	007	R		IN
010	N52E	90NW	001	007	023	007	R		IN
010	N52E	90NW	010	007	026	007	R		IN
010	N52E	90NW	001	007	043	007	R		IN
010	N52E	90NW	005	007	024	007	R		IN
010	N52E	90NW	009	007	046	007	R		IN
010	N52E	90NW	001	007	038	007	R		IN
010	N52E	90NW	001	007	031	007	R		IN
010	N52E	90NW	001	007	030	007	R		IN
010	N52E	90NW	001	010	021	010	R		IN
010	N52E	90NW	001	010	020	010	R		IN
010	N52E	90NW	001	010	024	010	R		IN
011	N46W	87SW	057	018	030	018	R	NW	IN
011	N46W	87SW	161	030	028	030	R	NW	IN
011	N46W	87SW	022	009	028	009	R	NW	IN
011	N46W	87SW	022	009	018	009	R	NW	IN
011	N46W	87SW	105	030	025	030	R	NW	IN
011	N46W	87SW	098	023	054	023	R	NW	IN
011	N46W	87SW	050	023	020	023	R	NW	IN
012	N48W	90SW	025	105	030	012	R	NW	IN
012	N48W	90SW	020	057	012	012	R	NW	IN
012	N48W	90SW	020	012	030	012	R	NW	IN
012	N48W	90SW	120	130	080	012	R	NW	IN
012	N65E	90NW	075	012	035	012	R		IN
012	N65E	90NW	016	013	014	013	R		IN

STA	STRI	DIP	LNG	DPT	SPA	BED	EXP	SET	LOC
012	N21E	86SE	045	037		012	R		IN
012	N46E	73NW	047	024	009	017	R		IN
012	N46E	73NW	038	017	011	017	R		IN
012	N48W	90SW	160	060	018	030	R	NW	IN
012	N48W	90SW	015	028	022	011	R	NW	IN
012	N48W	90SW	002	030		010	R	NW	IN
012	N30E	90NW	057	020	004	008	R	NE	IN
012	N28E	84NW	023	027	030	012	R	NE	IN
012	N88W	90SW	030	002	005	002	R	EW	IN
012	N88W	90SW	013	007	010	007	R	EW	IN
012	N88W	90SW	014	007	025	007	R	EW	IN
012	N55E	90NW	180	040		040	R		IN
012	N55W	90SW	079	112		040	R	NW	IN
012	N55W	90SW	150	040		040	R	NW	IN
012	N55W	90SW	200	080	060	040	R	NW	IN
013	N68W	90SW	039	058	023	047	R		IN
013	N86W	90SW	038	038	043	038	R	EW	IN
013	N68W	90SW	001	027	003	027	R		IN
013	N68W	90SW	001	047	046	047	R		IN
013	N68W	90SW	003	055	012	055	R		IN
013	N68W	90SW	001	055	023	055	R		IN
013	N68W	90SW	042	018	043	018	R		IN
013	N68W	90SW	027	018	040	018	R		IN
013	N68W	90SW	010	027	037	018	R		IN
013	N68W	90SW	030	018	020	018	R		IN
013	N68W	90SW	005	018	022	018	R		IN
013	N78W	90SW	023	026	028	007	R		IN
013	N78W	90SW	014	005	020	005	R		IN
013	N78W	90SW	010	005	016	005	R		IN
013	N20W	81SW	052	010		010	R		IN
014	N75W	85NE					R		IN
015	N73W	55NE	096	015	029	003	R		IN
015	N73W	55NE	040	006		003	R		IN
015	N73W	55NE	020	007	012	003	R		IN
015	N73W	55NE	012	007	013	003	R		IN
015	N73W	55NE	020	007	022	003	R		IN
015	N73W	55NE	045	007	011	003	R		IN
015	N73W	55NE	045	010	028	003	R		IN
015	N73W	55NE	045	010	038	003	R		IN
015	N73W	55NE	037	010	040	003	R		IN
015	N73W	55NE	035	010	033	003	R		IN
015	N73W	55NE	029	010	025	003	R		IN
016	N49W	76SW	060	050	074	050	R	NW	IN
016	N46W	75SW	138	120	052	065	R	NW	IN
016	N46W	75SW	092	055	049	055	R	NW	IN
016	N46W	75SW	061	040	037	040	R	NW	IN
016	N46W	74SW	064	065	024	060	R	NW	IN
016	N46W	75SW	034	051	026	051	R	NW	IN
016	N46W	75SW	071	035	033	035	R	NW	IN
016	N46W	75SW	045	022	035	022	R	NW	IN
016	N46W	75SW	070	054	078	054	R	NW	IN
016	N46W	75SW	101	075	116	045	R	NW	IN
016	N46W	75SW	083	052	077	052	R	NW	IN
016	N46W	75SW	105	038	045	038	R	NW	IN
016	N46W	75SW	095	038	029	038	R	NW	IN
016	N46W	75SW	010	038	045	045	R	NW	IN
016	N60E	78SE	014	008	021	008	R		IN
016	N60E	72SE	003	008	028	008	R		IN
017	N62E	78SE	006	008	041	008	R		BR
017	N62E	78SE	018	008	057	008	R		BR

STA	STRI	DIP	LNG	DPT	SPA	BED	EXP	SET	LOC
017	N62E	78SE	018	012	039	010	R		BR
017	N62E	78SE	001	012	026	010	R		BR
017	N62E	78SE	014	010	046	010	R		BR
017	N62E	78SE	008	010	030	010	R		BR
017	N62E	78SE	014	006	038	003	R		BR
017	N62E	78SE	002	006	040	006	R		BR
017	N62E	78SE	001	006	035	006	R		BR
018	N42W	75SW	061	004	055	004	R	NW	BR
018	N42W	75SW	024	004	028	004	R	NW	BR
018	N42W	75SW	034	012	045	012	R	NW	BR
018	N42W	75SW	012	010	030	010	R	NW	BR
018	N13E	90NW	043	004	018	004	R		BR
018	N42W	75SW	020	014	014	004	R	NW	BR
018	N42W	75SW	075	004	024	004	R	NW	BR
018	N42W	75SW	028	008	028	008	R	NW	BR
018	N42W	75SW	102	016	044	016	R	NW	BR
018	N13E	90NW	058	016		016	R		BR
018	N87E	90NW	015	001	007	001	R	EW	BR
018	N87E	90NW	012	001		001	R	EW	BR
018	N25E	90NW	087	005	052	005	R	NE	BR
018	N45W	74SW	065	010	060	010	R	NW	BR
018	N45W	75SW	059	049	040	005	R	NW	BR
018	N45W	74SW	030	005	067	005	R	NW	BR
018	N45W	74SW	050	005	059	005	R	NW	BR
019	N33E	73NW	026	005	012	005	R	NE	BR
019	N33E	73NW	013	005	010	005	R	NE	BR
019	N33E	73NW	014	005	010	005	R	NE	BR
019	N33E	73NW	026	005	013	005	R	NE	BR
019	N33E	73NW	019	005	010	005	R	NE	BR
019	N33E	73NW	015	004	005	004	R	NE	BR
019	N33E	73NW	016	004	007	004	R	NE	BR
019	N33E	73NW	016	004	010	004	R	NE	BR
019	N33E	73NW	012	004	007	004	R	NE	BR
019	N33E	73NW	012	003	008	003	R	NE	BR
019	N33E	73NW	001	003	005	003	R	NE	BR
019	N33E	73NW	015	005	012	005	R	NE	BR
019	N33E	73NW	018	005	005	005	R	NE	BR
019	N50W	88SW	005	004	023	004	R	NW	BR
019	N50W	88SW	007	005	015	005	R	NW	BR
019	N50W	88SW	001	005	015	005	R	NW	BR
019	N50W	88SW	001	006	016	006	R	NW	BR
019	N50W	88SW	006	002	015	002	R	NW	BR
019	N50W	88SW	009	003	010	003	R	NW	BR
019	N50W	88SW	006	003	007	003	R	NW	BR
020	N24E	68SE	048	004	007	004	R		BR
020	N35E	67SE	075	009		009	R	NE	BR
020	N35E	66SE	010	007	003	007	R	NE	BR
020	N49W	75SW	007	023	030	004	R	NW	BR
020	N49W	75SW	017	011	065	004	R	NW	BR
020	N49W	75SW	001	013	048	008	R	NW	BR
020	N49W	75SW	001	013	050	008	R	NW	BR
020	N24E	68SE	183	013	003	008	R		BR
020	N24E	68SE	103	008		008	R		BR
020	N05E	58NW	089	026		015	R		BR
020	N05E	58NW	089	014	008	005	R		BR
020	N05E	58NW	035	019	007	008	R		BR
020	N05E	58NW	053	054	019	008	R		BR

STA	STRI	DIP	LNG	DPT	SPA	BED	EXP	SET	LOC
020	N05E	58NW	057	041		005	R			BR
020	N05E	58NW	024	007	005	007	R			BR
021	N37W	85SW	048	024	025	024	R		NW	BR
021	N12E	67NW	066	026	023	026	R			BR
021	N12E	67NW	064	023	004	023	R			BR
021	N12E	67NW	119	023		023	R			BR
021	N12E	67NW	078	023	030	023	R			BR
021	N12E	67NW	045	023	004	023	R			BR
021	N12E	67NW	078	023		023	R			BR
021	N37W	85SW	035	010	024	010	R		NW	BR
021	N37W	85SW	032	012	032	012	R		NW	BR
021	N37W	85SW	006	011	016	001	R		NW	BR
021	N37W	85SW	032	019	031	019	R		NW	BR
021	N37W	85SW	070	023	030	023	R		NW	BR
021	N37W	85SW	037	011	029	011	R		NW	BR
021	N37W	85SW	037	022	026	022	R		NW	BR
021	N37W	85SW	034	022	019	022	R		NW	BR
021	N70W	90SW	007	021	006	021	R			BR
021	N70W	90SW	001	024	004	024	R			BR
021	N70W	90SW	001	024	003	024	R			BR
021	N70W	90SW	001	024	007	024	R			BR
021	N70W	90SW	001	024	008	024	R			BR
021	N70W	90SW	001	024	009	024	R			BR
021	N70W	90SW	001	024	008	024	R			BR
021	N70W	90SW	001	024	026	024	R			BR
022	N57E	78NW	062	039	029	039	R			SO
022	N16E	77SE	040	039	084	039	R			SO
022	N57E	78NW	050	039		039	R			SO
022	N57E	78NW	125	028	025	028	R			SO
022	N57E	78NW	012	037	044	037	R			SO
022	N57E	78NW	027	037	057	037	R			SO
022	N57E	78NW	038	037	018	037	R			SO
022	N16E	77SE	003	007	029	007	R			SO
022	N16E	77SE	030	007	018	007	R			SO
022	N57E	78NW	055	025		025	R			SO
022	N16E	77SE	045	025	075	025	R			SO
022	N16E	77SE	080	025	052	025	R			SO
023	N10E	90NW	025	005	019	005	R			SO
023	N10E	90NW	014	005	028	005	R			SO
023	N10E	90NW	012	005	028	005	R			SO
023	N10E	90NW	009	005	014	005	R			SO
023	N40E	90NW	017	005	023	005	R		NE	SO
023	N40E	90NW	019	005	024	005	R		NE	SO
023	N40E	73SW	014	005	030	005	R		NE	SO
023	N45W	73SW	071	012		012	R		NW	SO
023	N45W	73SW	087	009		009	R		NW	SO
023	N13W	75SW	030	006	013	006	R			SO
023	N13W	75SW	005	006	015	006	R			SO
023	N40E	90NW	017	007	023	007	R		NE	SO
023	N40E	90NW	007	007	005	007	R		NE	SO
023	N40E	90NW	017	007	015	007	R		NE	SO
023	N45W	73SW	010	007	015	007	R		NE	SO
023	N45W	73SW	200	050	025	007	R		NW	SO
024	N08W	70SW	020	007	022	007	R			SO
024	N08W	70SW	021	007	022	007	R			SO
024	N08W	70SW	020	010	022	010	R			SO
024	N08W	70SW	020	002	020	002	R			SO
024	N08W	72SW	044	009	043	009	R			SO
024	N28E	90NW	015	003	025	003	R		NE	SO
024	N28E	90NW	007	005	027	005	R		NE	SO

STA	STRI	DIP	LNG	DPT	SPA	BED	EXP	SET	LOC
024	N08W	72SW	010	006	014	006	R		SO
024	N08W	72SW	017	008		008	R		SO
024	N08W	72SW	049	014	022	014	R		SO
024	N08W	72SW	026	014	018	004	R		SO
024	N10E	65NW	014	005	023	005	R		SO
024	N20E	77NW	007	007	002	007	R		SO
024	N20E	77NW	010	008	008	008	R		SO
025	N10W	69SW	012	017	008	017	R		SO
025	N02E	69SE	006	017	005	017	R		SO
025	N07W	69SW	002	017	008	017	R		SO
025	N07W	69SW	010	017	013	017	R		SO
025	N07W	69SW	010	010	023	010	R		SO
025	N07W	69SW	017	010	014	010	R		SO
025	N07W	69SW	040	025	052	025	R		SO
025	N07W	69SW	057	025	018	025	R		SO
025	N07W	69SW	047	110	026	025	R		SO
025	N07W	69SW	023	004	008	004	R		SO
025	N07W	69SW	009	004	018	004	R		SO
025	N18E	61NW	027	006	006	006	R		SO
025	N18E	61NW	010	006	006	006	R		SO
025	N18E	61NW	017	006	007	006	R		SO
025	N18E	61NW	010	006	004	006	R		SO
025	N18E	61NW	020	008	004	008	R		SO
025	N18E	61NW	007	008	005	008	R		SO
025	N18E	61NW	001	008	008	008	R		SO
025	N18E	61NW	001	008	009	008	R		SO
025	N18E	61NW	001	008	009	008	R		SO
026	N38W	90SW	413	018	010	018	R	NW	IN
026	N80E	60SE	001	018	042	018	R	EW	IN
026	N80E	60SE	001	018	057	018	R	EW	IN
026	N80E	60SE	001	018	029	018	R	EW	IN
026	N80E	60SE	001	018	059	018	R	EW	IN
026	N35W	90SW	057	019	023	029	R	NW	IN
026	N35W	90SW	048	019	013	019	R	NW	IN
026	N35W	90SW	099	019	013	019	R	NW	IN
026	N35W	90SW	099	019	012	019	R	NW	IN
026	N35W	90SW	090	019	014	019	R	NW	IN
026	N35W	90SW	057	019	010	019	R	NW	IN
026	N35W	90SW	056	019	018	019	R	NW	IN
026	N35W	90SW	120	019	024	019	R	NW	IN
026	N80E	60SE	009	009	028	009	R	EW	IN
026	N80E	60SE	003	009	015	009	R	EW	IN
026	N80E	60SE	003	009	012	009	R	EW	IN
026	N80E	60SE	001	009	035	009	R	EW	IN
026	N80E	60SE	016	009	013	009	R	EW	IN
026	N80E	60SE	003	009	032	009	R	EW	IN
026	N80E	60SE	003	009	035	009	R	EW	IN
026	N38W	90SW	014	006	019	006	R	NW	IN
026	N38W	90SW	008	103	015	006	R	NW	IN
026	N38W	90SW	005	006	015	006	R	NW	IN
027	N71W	90SW	114	012		012	R		IN
027	N06W	90SW	127	010		010	R		IN
027	N71W	90SW	022	007		007	R		IN
027	N71W	90SW	032	011		011	R		IN
027	N45E	90NW	038	013		013	R	NE	IN
028	N50W	90SW	075	015	009	015	R	NW	IN
028	N50W	90SW	078	017	014	017	R	NW	IN
028	N50W	90SW	075	013		013	R	NW	IN
028	N50W	90SW	091	008		008	R	NW	IN

STA	STRI	DIP	LNG	DPT	SPA	BED	EXP	SET	LOC
028	N50W	90SW	020	011	015	010	R	NW	IN
028	N50W	90SW	025	008		008	R	NW	IN
028	N50W	90SW	129	006		006	R	NW	IN
028	N77W	74NE	050	013	027	013	R		IN
028	N75W	75NE	072	014	011	014	R		IN
028	N77W	78NE	025	009	011	009	R		IN
028	N77W	78NE	001	009	005	009	R		IN
028	N77W	78NE	030	009	003	009	R		IN
028	N77W	78NE	022	004	011	004	R		IN
028	N77W	78NE	048	004	016	004	R		IN
028	N77W	78NE	020	004	008	004	R		IN
028	N77W	78NE	015	004	006	004	R		IN
028	N77W	78NE	015	003	009	003	R		IN
028	N77W	78NE	028	015	022	004	R		IN
029	N85E	85NW	139	021		021	R	EW	IN
029	N45W	78SW	094	011		011	R	NW	IN
029	N40W	80SW	083	032	008	032	R	NW	IN
029	N40W	80SW	036	032	010	032	R	NW	IN
029	N40W	80SW	042	032	031	032	R	NW	IN
029	N40W	80SW	037	025	005	025	R	NW	IN
029	N40W	80SW	154	025		025	R	NW	IN
029	N40W	80SW	041	012	009	012	R	NW	IN
029	N40W	80SW	047	012	013	012	R	NW	IN
029	N40W	80SW	070	018	020	018	R	NW	IN
029	N40W	80SW	015	012	008	012	R	NW	IN
029	N40W	80SW	074	012		012	R	NW	IN
029	N85E	85NW	052	019	011	0C7	R	EW	IN
029	N85E	85NW	100	018	004	018	R	EW	IN
029	N85E	85NW	195	030		030	R	EW	IN
030	N59W	90SW	017	009	020	003	R		IN
030	N59W	90SW	019	002	012	002	R		IN
030	N59W	90SW	021	002	027	002	R		IN
030	N59W	90SW	020	003	020	003	R		IN
031	N42W	83SW	058	046	103	046	R		IN
031	N87W	85SW	045	069		033	R	EW	IN
031	N65W	89NE	054	028	016	028	R		IN
031	N65W	89NE	012	028		028	R		IN
031	N87W	85SW	030	036	057	036	R	EW	IN
031	N87W	85SW	010	050		050	R	EW	IN
031	N87W	85SW	010	022	045	022	R	EW	IN
031	N87W	85SW	017	024	022	024	R	EW	IN
031	N87W	85SW	005	050		050	R	EW	IN
031	N87W	85SW	017	101	044	050	R	EW	IN
031	N38W	88SW	102	078	058	078	R	NW	IN
031	N42W	83NE	120	078	076	078	R	NW	IN
031	N42W	83NE	078	043	037	043	R	NW	IN
031	N42W	83NE	045	042	044	042	R	NW	IN
031	N42W	83NE	047	026	050	026	R	NW	IN
032	N89E	83NW	024	020	028	020	R	EW	IN
032	N89E	83NW	011	019		019	R	EW	IN
032	N89E	83NW	011	008	017	008	R	EW	IN
032	N89E	83NW	010	002	017	002	R	EW	IN
032	N89E	83NW	005	005	013	005	R	EW	IN
032	N89E	83NW	012	003	0C7	003	R	EW	IN
032	N89E	83NW	022	013	034	013	R	EW	IN
032	N89E	83NW	010	022	075	022	R	EW	IN
032	N89E	83NW	015	022	048	022	R	EW	IN
033	N83W	90SW	037	018	025	018	R	EW	IN
033	N83W	90SW	012	018	020	018	R	EW	IN
033	N83W	90SW	021	014	014	014	R	EW	IN

STA	STRI	DIP	LNG	DPI	SPA	BED	EXP	SET	LOC
033	N83W	90SW	007	006	011	006	R	EW	IN
033	N83W	90SW	021	006	012	006	R	EW	IN
033	N83W	90SW	006	010	008	010	R	EW	IN
033	N83W	90SW	027	016	018	016	R	EW	IN
033	N83W	90SW	087	019	024	019	R	EW	IN
033	N83W	90SW	053	018	024	018	R	EW	IN
033	N83W	90SW	056	025	032	025	R	EW	IN
035	N47W	90SW	300				SC	NW	IN
035	N24E	45SE	200		090		SC		IN
035	N24E	45SE	200		059		SC		IN
035	N24E	45SE	040		029		SC		IN
035	N02E	45SE	040		021		SC		IN
035	N02E	45SE	016		031		SC		IN
035	N02E	45SE	023		011		SC		IN
035	N55W	90SW	048	017	047	010	SC	NW	IN
035	N55W	90SW	017	010	009	010	SC	NW	IN
035	N55W	90SW	030	010	025	010	SC	NW	IN
035	N55W	90SW	039	010	035	010	SC	NW	IN
035	N85W	90SW	020	010	036	010	SC	EW	IN
035	N85W	90SW	047	010	029	010	SC	EW	IN
035	N85W	90SW	036	010	016	010	SC	EW	IN
035	N85W	90SW	036	010	037	010	SC	EW	IN
035	N68W		077				SC		IN
036	N48W	84SW	029	018	010	007	R	NW	IN
036	N81E	82SE	002	007	011	007	R	EW	IN
036	N43E	57NW	012	007	017	007	R	NE	IN
036	N48W	84SW	001	018	020	0C7	R	NW	IN
036	N48W	84SW	029	018	016	007	R	NW	IN
036	N48W	84SW	021	007		007	R	NW	IN
036	N81E	82SE	012	007	010	007	R	EW	IN
036	N81E	82SE	017	007	055	007	R	EW	IN
036	N48W	84SW	086	019	022	0C7	R	NW	IN
036	N48W	84SW	035	007	008	007	R	NW	IN
036	N48W	84SW	001	007	008	007	R	NW	IN
036	N48W	84SW	001	007	008	007	R	NW	IN
036	N81E	82SE	010	007		007	R	EW	IN
036	N43E	57NW	001	007	037	007	R	NE	IN
036	N43E	57NW	001	007	005	0C7	R	NE	IN
036	N43E	57NW	001	007	018	007	R	NE	IN
036	N48W	84SW	015	003	009	003	R	NW	IN
036	N48W	84SW	001	003	010	003	R	NW	IN
036	N48W	84SW	001	003	003	003	R	NW	IN
036	N43E	57NW	019	005	013	005	R	NE	IN
036	N43W	57NW	015	005	014	005	R	NW	IN
036	N81E	82SE	014	005	021	005	R	EW	IN
036	N81E	82SE	018	016	009	005	R	EW	IN
037	N65W	90SW					R		IN
037	N18E	90NW					R		IN
038	N57W	90SW	500	019		019	R		IN
038	N57W	90SW	043	006	012	006	R		IN
038	N57W	90SW	014	006	015	006	R		IN
038	N57W	90SW	007	006	012	006	R		IN
038	N57W	90SW	019	006	010	006	R		IN
038	N57W	90SW	052	006	006	006	R		IN
038	N57W	90SW	250	008	023	008	R		IN
038	N57W	90SW	117	016	020	016	R		IN
039							R		IN
040	N53W	90SW					R	NW	IN
040	N46W	90SW					R	NW	IN

STA	STRI	DIP	LNG	DPT	SPA	BED	EXP	SET	LOC
040	N45W	90SW					R	NW	IN
040	N72W	88NE		150			R		IN
040	N51W	90SW					R	NW	IN
040	N80W	90SW					R	EW	IN
040	N73W	90SW					R		IN
040	N74W	90SW					R		IN
040	N80W	88NE		150	015		R	EW	IN
041	N80W	88NE		150			R	EW	IN
041	N25E	90NW					R	NE	IN
041	N25E	90NW	180	090		090	R	NE	IN
041	N25E	90NW	200				R	NE	IN
042	N53W	90SW	035	006	020	006	R	NW	IN
042	N55W	90SW	010	025	028	012	R	NW	IN
042	N53W	90SW	020	150		012	R	NW	IN
042	N53W	90SW	029	048		012	R	NW	IN
042	N53W	90SW	015	012	020	012	R	NW	IN
042	N53W	90SW	050	120	057	020	R	NW	IN
042	N53W	90SW	020	110	040	020	R	NW	IN
042	N53W	90SW	015	050	040	020	R	NW	IN
043	N46W	90SW	005	064	020	020	R	NW	IN
043	N46W	90SW	005	065	050	020	R	NW	IN
043	N46W	90SW	012	063	027	020	R	NW	IN
043	N46W	90SW	063	051		051	R	NW	IN
043	N46W	90SW	012	006	016	006	R	NW	IN
043	N46W	90SW	009	006	018	006	R	NW	IN
043	N46W	90SW	004	058	029	058	R	NW	IN
043	N46W	90SW	029	019	023	019	R	NW	IN
044	N48W	90SW	210	185		025	R	NW	IN
044	N48W	90SW	104	100		025	R	NW	IN
044	N48W	90SW	200	101		050	R	NW	IN
044	N48W	90SW	500	050		030	R	NW	IN
044	N48W	90SW	001	062	005	026	R	NW	IN
044	N48W	90SW	001	062	075	026	R	NW	IN
045	N65W	90SW	125	092	030	015	R		IN
045	N65W	90SW	025	149		015	R		IN
045	N65W	90SW	003	010	006	003	R		IN
045	N65W	90SW	003	010	005	003	R		IN
045	N65W	90SW	001	010	007	003	R		IN
045	N65W	90SW	001	010	010	003	R		IN
045	N65W	90SW	001	010	006	003	R		IN
046	N85W	90SW	012	182	052	020	R	EW	IN
046	N85W	90SW	007	190	028	020	R	EW	IN
046	N85W	90SW	015	146	007	020	R	EW	IN
046	N85W	90SW	001	097	007	020	R	EW	IN
046	N85W	90SW	002	097	007	020	R	EW	IN
046	N85W	90SW	003	096	002	020	R	EW	IN
046	N85W	90SW	002	092	003	020	R	EW	IN
046	N85W	90SW	002	093	005	020	R	EW	IN
047	N26E	83SE	083	057	065	001	R	NE	NT
047	N26E	83SE	041	059	020	001	R	NE	NT
047	N85W	86SW	014	007	020	007	R	EW	NT
047	N85W	86SW	006	010	013	007	R	EW	NT
047	N85W	86SW	007	006	006	006	R	EW	NT
047	N85W	86SW	010	011	029	011	R	EW	NT
047	N85W	86SW	014	015	017	009	R	EW	NT
047	N85E	86SW	023	009	026	009	R	EW	NT
047	N85E	86SE	009	010	014	010	R	EW	NT
048	N33W	55SW	146	070		003	R		NT
048	N83E	90NW	006	004	007	004	R	EW	NT
048	N83E	90NW	006	004	005	004	R	EW	NT

STA	STRI	DIP	LNG	DPT	SPA	BED	EXP	SET	LOC
048	N83E	90NW	001	004	011	004	R	EW	NT
048	N30W	62SW	012	004		004	R		NT
048	N30W	62SW	009	004		004	R		NT
048	N45W	62SW	010	004	005	004	R	NW	NT
049	N46W	71SW	165	027		027	R	NW	NT
049	N88W	76NE	121	028		028	R	EW	NT
049	N88W	76NE	034	004	008	004	R	EW	NT
049	N46W	71SW	066	016	028	016	R	NW	NT
049	N46W	71SW	050	016	011	016	R	NW	NT
049	N46W	71SW	035	010	011	010	R	NW	NT
049	N88W	76NE	028	018	030	018	R	EW	NT
049	N88W	76NE	036	013	015	013	R	EW	NT
049	N46W	71SW	015	016	014	016	R	NW	NT
049	N12W	28SW	010	022	019	022	R		NT
049	N12W	28SW	012	017		017	R		NT
049	N12W	28SW	005	007	005	007	R		NT
049	N12W	28SW	001	006	006	006	R		NT
049	N12W	28SW	012	027	040	027	R		NT
049	N46W	71SW	028	027	021	027	R	NW	NT
049	N46W	71SW	025	027	013	027	R	NW	NT
049	N46W	71SW	065	027	014	027	R	NW	NT
049	N12W	28SW	010	015	013	015	R		NT
049	N12W	28SW	003	015	020	015	R		NT
049	N88W	76NE	033	017	021	017	R	EW	NT
049	N88W	76NE	023	025	012	025	R	EW	NT
050	N21W	90SW	500		096	001	S		NT
050	N21W	90SW	500		500		S		NT
050	N05W	90SW	386		122	001	S		NT
050	N05W	90SW	238			001	S		NT
050	N05W	90SW	120		025	001	S		NT
050	N05W	90SW	293		036	001	S		NT
050	N05W	90SW	251		037	001	S		NT
050	N03W	90SW	450		150		SC		NT
050	N03W	90SW	223				SC		NT
050	N45W	90SW	048	007	015	007	SC	NW	NT
050	N45W	90SW	061	007	018	007	SC	NW	NT
050	N45W	90SW	081	007	025	007	SC	NW	NT
050	N45W	90SW	105	007	018	007	SC	NW	NT
050	N45W	90SW	014	007	017	007	SC	NW	NT
050	N45W	90SW	015	007	015	007	SC	NW	NT
050	N45W	90SW	028	007	036	007	SC	NW	NT
051	N48W	88SW	081	029	027	029	SC	NW	NT
051	N48W	88SW	081	029	025	029	SC	NW	NT
051	N48W	88SW	078	029	021	029	SC	NW	NT
051	N48W	88SW	066	029	005	029	SC	NW	NT
051	N48W	88SW	048	029	032	029	SC	NW	NT
051	N48W	88SW	049	029	015	029	SC	NW	NT
051	N83W	90SW	130	025	038	025	SC	EW	NT
051	N43W	90SW	072	025	030	025	SC	NW	NT
051	N43W	90SW	086	025	062	025	SC	NW	NT
051	N43W	90SW	090	025	034	025	SC	NW	NT
051	N43W	88SW	035	025		025	SC	NW	NT
051	N48W	88SW	056	005	015	005	SC	NW	NT
051	N48W	88SW	085	005	006	005	SC	NW	NT
051	N48W	88SW	056	005	006	005	SC	NW	NT
051	N48W	88SW	061	005	015	005	SC	NW	NT
051	N48W	88SW	046	005	010	005	SC	NW	NT
051	N48W	88SW	067	005	055	005	SC	NW	NT
052	N58W	75SW	150	080			R		NT
053							R		NT

STA	STRI	DIP	LNG	DPT	SPA	BED	EXP	SET	LOC
054	N66W	90SW			032	013	R		IN
054	N66W	90SW			027	013	R		IN
054	N66W	90SW			021	013	R		IN
054	N66W	90SW			028	013	R		IN
054	N66W	90SW			016	013	R		IN
054	N66W	90SW			015	013	R		IN
054	N66W	90SW			028	013	R		IN
054	N66W	90SW			022	013	R		IN
054	N42E	45NW			059		R	NE	IN
054	N42E	45NW			053		R	NE	IN
054	N42E	45NW			081		R	NE	IN
054	N42E	45NW			068		R	NE	IN
054	N42E	45NW			016		R	NE	IN
054	N42E	45NW			027		R	NE	IN
054	N42E	45NW			038		R	NE	IN
054	N42E	45NW			021		R	NE	IN
054	N88W	90SW			067		R	EW	IN
054	N88W	90SW			030		R	EW	IN
054	N88W	90SW			020		R	EW	IN
054	N88W	90SW			071		R	EW	IN
054	N88W	90SW			027		R	EW	IN
054	N88W	90SW			026		R	EW	IN
054	N88W	90SW			030		R	EW	IN
054	N88W	90SW			009		R	EW	IN
055	N46W	89SW	109	047	019	047	R	NW	NT
055	N87W	89NE	075	034	038	047	R	EW	NT
055	N87W	89NE	138	028	C69	028	R	EW	NT
055	N42E	85NW	010	056		001	R	NE	NT
055	N36E	90NW	050	028	130	028	R	NE	NT
055	N46W	89SW	013	019		028	R	NW	NT
055	N25E	90NW	012	006	009	001	R	NE	NT
055	N25E	90NW	001	006	019	001	R	NE	NT
055	N25E	90NW	001	0C6	020	001	R	NE	NT
055	N36E	90NW	050	027	092	027	R	NE	NT
055	N46W	89SW	048	027		027	R	NW	NT
055	N87W	89NE	030	008	015	008	R	EW	NT
055	N87W	89NE	010	008		008	R	EW	NT
056	N45W	90SW	034	043	036	043	R	NW	NT
056	N45W	90SW	010	043	062	043	R	NW	NT
056	N45W	90SW	120	134		100	R	NW	NT
056	N45W	90SW	038	123	015	100	R	NW	NT
056	N45W	90SW	146	200		200	R	NW	NT
056	N45W	90SW	180	220		200	R	NW	NT
057	N83W	83NE	073	026	018	026	R	EW	NT
057	N83W	84NE	001	026	018	026	R	EW	NT
057	N83W	83NE	020	026	054	026	R	EW	NT
057	N36W	83SW	041	021	016	021	R	NW	NT
057	N36W	83SW	028	021	025	021	R	NW	NT
057	N36W	83SW	033	021	024	021	R	NW	NT
057	N38E	33NW	016	021	046	021	R	NE	NT
057	N38E	33NW	025	021	029	021	R	NE	NT
057	N38E	33NW	024	021	029	021	R	NE	NT
058	N83E	49SE	057	067	006	001	R	EW	NT
058	N73W	75SW	173	049		058	R		NT
058	N83E	49SE	007	075	006	010	R	EW	NT
058	N83E	49SE	008	069	019	010	R	EW	NT
058	N83E	49SE	020	180	063	010	R	EW	NT
058	N83E	49SE	015	250		010	R	EW	NT
058	N83E	49SE	012	053	009	010	R	EW	NT
058	N83E	49SE	006	041	010	010	R	EW	NT

STA	STRI	DIP	LNG	DPT	SPA	BED	EXP	SET	LOC
059	N20E	90NW					R		NT
059	N80W	90SW					R	EW	NT
060	N49W	90SW	042	030	025	030	R	NW	NT
060	N49W	90SW	031	036	030	030	R	NW	NT
060	N49W	90SW	029	030	006	030	R	NW	NT
061	N41W	77SW	019	061	051	061	R	NW	NT
061	N41W	77SW	038	061	041	061	R	NW	NT
061	N41W	77SW	049	058	058	061	R	NW	NT
061	N41W	77SW	033	038	024	038	R	NW	NT
061	N41W	77SW	028	038	023	038	R	NW	NT
061	N41W	77SW	021	038	037	038	R	NW	NT
062	N75W	90SW	300	104		083	R		NT
062	N45E	48NW					R	NE	NT
063	N47W	84NE	091	058	068	058	S	NW	NT
063	N75W	72NE	027	058		058	S		NT
063	N47W	84NE	050	058	064	058	S	NW	NT
063	N47W	84NE	080	047	021	044	S	NW	NT
063	N47W	84NE	087	047	060	044	S	NW	NT
063	N47W	84NE	020	058	037	058	S	NW	NT
063	N47W	34NE	008	058	035	058	S	NW	NT
063	N75W	72NE	001	078	088	058	S		NT
063	N75W	72NE	003	163	100	058	S		NT
063	N75W	72NE	008	080	025	020	S		NT
063	N47W	84NE	031	018	023	018	S	NW	NT
063	N47W	84NE	037	018	019	018	S	NW	NT
063	N75W	72NE	045	018	085	018	S		NT
063	N75W	72NE	060	018	031	018	S		NT
063	N75W	72NE	027	018	051	018	S		NT
064	N75W	80NE	029	005	014	005	R		NT
064	N45W	78SW	025	019	015	012	R	NW	NT
064	N45W	78SW	052	010	012	010	R	NW	NT
064	N75W	80NE	026	005	011	005	R		NT
064	N45W	78SW	022	012	020	012	R	NW	NT
064	N75W	80NE	046	010	007	010	R		NT
064	N45W	78SW	035	019	028	019	R	NW	NT
064	N45W	78SW	007	019	013	019	R	NW	NT
064	N45W	78SW	018	019	014	019	R	NW	NT
064	N45W	78SW	057	012	020	012	R	NW	NT
064	N87E	76NW	021	017	014	017	R	EW	NT
064	N87E	76NW	007	017	015	017	R	EW	NT
064	N87E	76NW	015	017	014	017	R	EW	NT
065	N44W	89SW	058	025	042	025	S	NW	NT
065	N44W	89SW	043	025	010	025	S	NW	NT
065	N44W	89SW	039	025	025	025	S	NW	NT
065	N44W	89SW	037	025	036	025	S	NW	NT
065	N44W	89SW	054	025	027	025	S	NW	NT
065	N44W	89SW	032	012	010	025	S	NW	NT
065	N44W	89SW	028	012	008	025	S	NW	NT
065	N44W	89SW	027	012	013	025	S	NW	NT
065	N44W	89SW	025	012	012	025	S	NW	NT
065	N89W	90SW	053	025	018	025	S	EW	NT
065	N89W	90SW	029	025	009	025	S	EW	NT
066	N72W	66SW	031	007	032	007	R		NT
066	N72W	66SW	011	012	026	012	R		NT
066	N58W	63SW	010	009	011	009	R		NT
066	N58W	63SW	025	009	014	009	R		NT
066	N58W	63SW	029	009	015	009	R		NT
066	N58W	63SW	020	009	012	009	R		NT
066	N49W	76SW	014	010	066	024	R	NW	NT
066	N49W	76SW	031	012	013	012	R	NW	NT

STA	STRI	DIP	LNG	DPT	SPA	BED	EXP	SET	LOC
066	N49W	76SW	026	012	017	012	R	NW	NT
067	N78W	69SW	026	019			R		NT
067	N78W	69SW	035	019			R		NT
068	N40W	90NW	016		065		S		NT
068	N45W	90SW	067	017	020	007	S	NW	NT
068	N45W	90SW	040	027	024	007	S	NW	NT
068	N45W	90SW	058	009	011	009	S	NW	NT
068	N45W	90SW	060	009	026	009	S	NW	NT
068	N45W	90SW	055	009	022	009	S	NW	NT
068	N45W	90SW	072	009	042	009	S	NW	NT
068	N78W	69SW	250				S		NT
068	N78W	69SW	005	006	023	006	S		NT
068	N78W	69SW	008	007	009	006	S		NT
068	N78W	69SW	003	007	020	006	S		NT
068	N78W	69SW	002	009	010	006	S		NT
069	N46W	90SW	121	050	035	050	R	NW	NT
069	N46W	90SW	093	042		042	R	NW	NT
069	N46W	90SW	105	017		020	R	NW	NT
069	N46W	90SW	135	060	021	042	R	NW	NT
069	N46W	90SW	098	043		043	R	NW	NT
069	N46W	90SW	080	035		035	R	NW	NT
069	N34E	90NW	080	035		035	R	NE	NT
069	N64W	90SW	094	046		039	R		NT
069	N46W	90SW	109	053		053	R	NW	NT
069	N46W	90SW	068	025	034	025	R	NW	NT
069	N46W	90SW	055	025		025	R	NW	NT
069	N46W	90SW	025	012	005	012	R	NW	NT
069	N46W	90SW	012	012	007	012	R	NW	NT
069	N46W	90SW	013	012	009	012	R	NW	NT
070	N32E	81NW	461	020	000	032	R	NE	NT
070	N36E	82NW	479	012	000	032	R	NE	NT
070	N41W	90SW	015	006	000	006	R	NW	NT
070	N48E	65NW	025	006	000	006	R		NT
070	N46W	90SW	016	008	009	008	R	NW	NT
070	N41W	90SW	004	008	013	008	R	NW	NT
070	N41W	90SW	022	010	018	010	R	NW	NT
070	N41W	90SW	023	010	000	010	R	NW	NT
070	N43W	90SW	006	013	006	013	R	NW	NT
070	N41W	90SW	005	013	006	013	R	NW	NT
070	N41W	90SW	015	013	009	013	R	NW	NT
070	N41W	90SW	006	010	010	010	R	NW	NT
070	N41W	90SW	007	010	011	010	R	NW	NT
070	N41W	90SW	019	010	007	010	R	NW	NT
070	N41W	90SW	011	017	060	017	R	NW	NT
070	N41W	90SW	011	017	015	017	R	NW	NT
071	N71W	84SW	005	008	011	008	R		NT
071	N71W	84SW	008	008	016	008	R		NT
071	N71W	84SW	001	008	010	008	R		NT
071	N71W	84SW	019	008	013	008	R		NT
071	N71W	84SW	022	008	010	008	R		NT
071	N71W	84SW	004	009	001	009	R		NT
071	N71W	84SW	001	009	012	009	R		NT
071	N71W	84SW	008	009	015	009	R		NT
071	N71W	84SW	003	009	014	009	R		NT
071	N71W	84SW	003	009	002	009	R		NT
071	N11E	59NW	033	006	010	010	R		NT
071	N11E	59NW	028	010	000	010	R		NT
071	N42W	77SW	033	023	017	017	R		NT
071	N42W	77SW	027	027	009	018	R	NW	NT
071	N42W	77SW	010	017	000	022	R	NW	NT

STA	STRI	DIP	LNG	DPT	SPA	BED	EXP	SET	LOC
071	N78W	81SW	007	013	008	013	R		NT
071	N78W	81SW	008	013	010	013	R		NT
071	N78W	81SW	027	013	011	013	R		NT
071	N42W	77SW	025	030	032	030	R	NW	NT
071	N42W	77SW	039	055	032	030	R	NW	NT
072	N60W	90SW	055	018	000	023	R		NT
072	N25E	90NW	039	010	000	010	R	NE	NT
072	N55W	90SW	020	028	000	021	R	NW	NT
072	N60W	90SW	032	032	000	030	R		NT
072	N60W	90SW	027	020	026	020	R		NT
072	N85E	90NW	020	042	000	003	R	EW	NT
072	N70W	83SW	020	083	000	007	R		NT
072	N55W	90SW	038	080	000	015	R	NW	NT
073	N85W	84SW	093	041	000	041	R	EW	NT
073	N31W	79SW	045	036	099	036	R		NT
073	N31W	79SW	039	036	036	036	R		NT
073	N31W	79SW	010	036	036	036	R		NT
073	N85W	84SW	044	020	000	020	R	EW	NT
073	N41W	69SW	036	053	023	029	R	NW	NT
073	N41W	69SW	043	060	000	020	R	NW	NT
074	N87W	76SW	122	134	000	134	R	EW	NT
074	N87W	76SW	070	027	000	023	R	EW	NT
074	N87W	76SW	037	007	018	007	R	EW	NT
074	N87W	76SW	031	007	010	007	R	EW	NT
074	N87W	76SW	053	033	000	007	R	EW	NT
074	N05E	79NW	046	007	000	007	R		NT
075	N70E	60NW	165	010	000	005	R		NT
075	N82E	90NW	135	015	035	015	R	EW	NT
075	N82E	90NW	058	015	000	015	R	EW	NT
076	N15E	90NW	076	012	076	012	S		NT
076	N15E	90NW	050	012	037	012	S		NT
076	N15E	90NW	086	012	047	012	S		NT
076	N15E	90NW	094	012	049	012	S		NT
076	N15E	90NW	080	012	000	012	S		NT
076	N85E	90NW	157	012	000	012	S	EW	NT
077	N22E	90NW	048	019	016	019	S		NT
077	N45E	85NW	071	018	064	018	S	NE	NT
077	N46W	90SW	051	025	019	019	S	NW	NT
077	N87W	90SW	082	000	010	009	S	EW	NT
077	N22E	90NW	037	019	016	019	S		NT
077	N46W	90SW	053	019	014	019	S	NW	NT
077	N45E	85NW	109	034	000	019	S	NE	NT
077	N87W	90SW	110	009	011	009	S	EW	NT
077	N87W	90SW	049	009	011	009	S	EW	NT
078	N63W	90SW	206	034	065	034	R		NT
078	N63W	90SW	101	015	080	015	R		NT
078	N63W	90SW	080	015	000	015	R		NT
078	N63W	90SW	278	034	000	034	R		NT
078	N48W	90SW	050	008	017	008	R	NW	NT
078	N55W	90SW	045	001	008	008	R	NW	NT
078	N55W	90SW	086	001	008	008	R	NW	NT
078	N55W	90SW	088	003	006	008	R	NW	NT
078	N55W	90SW	098	002	005	008	R	NW	NT
078	N55W	90SW	068	001	011	008	R	NW	NT
078	N55W	90SW	062	004	013	008	R	NW	NT
079	N47W	82SW	013	016	014	016	R	NW	NT
079	N47W	82SW	039	019	000	019	R	NW	NT
079	N47W	82SW	008	006	015	006	R	NW	NT
079	N82W	87SW	020	016	038	016	R	EW	NT
079	N82W	87SW	010	014	011	014	R	EW	NT

STA	STRI	DIP	LNG	DPT	SPA	BED	EXP	SET	LOC
079	N82W	87SW	015	014	003	014	R	EW	NT
079	N82W	87SW	018	014	012	014	R	EW	NT
079	N82W	87SW	017	014	024	014	R	EW	NT
079	N47W	82SW	003	017	018	017	R	NW	NT
079	N47W	82SW	018	018	013	018	R	NW	NT
079	N47W	82SW	018	014	015	014	R	NW	NT
079	N82W	87SW	009	014	017	014	R	EW	NT
079	N82W	87SW	032	014	019	014	R	EW	NT
079	N47W	82SW	017	018	012	018	R	NW	NT
079	N47W	82SW	027	020	018	017	R	NW	NT
079	N12W	70SW	043	013	000	013	R		NT
079	N07E	59NW	018	018	001	018	R		NT
079	N12E	48NW	033	013	014	013	R		NT
080	N72W	84SW	033	008	008	008	R		NT
080	N21E	84NW	017	008	018	008	R		NT
080	N72W	84SW	007	008	013	008	R		NT
080	N72W	84SW	024	008	018	008	R		NT
080	N72W	84SW	044	009	015	009	R		NT
080	N72W	84SW	018	009	009	009	R		NT
080	N72W	84SW	018	009	018	009	R		NT
080	N72W	84SW	018	009	011	009	R		NT
080	N21E	84NW	017	008	029	008	R		NT
080	N21E	84NW	001	009	013	009	R		NT
080	N21E	84NW	015	009	012	009	R		NT
080	N21E	84NW	024	009	025	009	R		NT
080	N21E	84NW	010	009	018	009	R		NT
080	N21E	84NW	019	010	017	010	R		NT
082	N23E	74NW	049	026	080	026	R		IN
082	N48W	88SW	064	027	065	026	R	NW	IN
082	N48W	88SW	100	026	000	026	R	NW	IN
082	N48W	88SW	020	036	039	036	R	NW	IN
082	N48W	88SW	060	040	050	040	R	NW	IN
082	N48W	88SW	062	046	067	046	R	NW	IN
082	N84W	87SW	053	040	025	033	R	EW	IN
082	N84W	87SW	005	040	020	033	R	EW	IN
082	N84W	87SW	027	026	000	026	R	EW	IN
082	N23E	74NW	058	030	063	030	R		IN
082	N23E	74NW	072	033	000	033	R		IN
083	N70W	87SW	020	015	000	013	R		IN
083	N46W	88SW	012	004	010	008	R	NW	IN
083	N46W	88SW	003	003	013	008	R	NW	IN
083	N46W	88SW	005	004	010	008	R	NW	IN
083	N70W	87SW	014	009	007	009	R		IN
083	N21E	73NW	129	022	011	007	R		IN
083	N21E	73NW	063	018	012	005	R		IN
084	N85W	88SW	075	142	030	020	R	EW	IN
084	N89W	90SW	034	034	044	034	E	EW	IN
084	N89W	88SW	028	029	021	022	R	EW	IN
084	N89W	88SW	035	056	041	022	R	EW	IN
084	N89W	88SW	015	018	013	006	R	EW	IN
084	N89W	88SW	005	005	008	005	R	EW	IN
084	N35E	84NW	015	019	006	019	R	NE	IN
084	N35E	84NW	024	019	023	019	R	NE	IN
084	N42W	71SW	024	014	000	014	R	NW	IN
084	N89W	88SW	010	014	021	014	R	EW	IN
084	N89W	88SW	010	014	022	014	R	EW	IN
084	N89W	88SW	019	017	016	017	R	EW	IN
084	N45W	84SW	146	018	015	018	R	NW	IN
084	N42W	71SW	105	020	000	020	R	NW	IN

STA	STRI	DIP	LNG	DPT	SPA	BED	EXP	SET	LOC
084	N89W	88SW	216	020	015	012	R	EW	IN
085	N54W	90SW	205	013	000	013	R	NW	IN
085	N30E	51NW	005	036	030	036	R	NE	IN
085	N30E	51NW	047	036	042	036	R	NE	IN
085	N30E	51NW	012	036	023	036	R	NE	IN
085	N30E	51NW	107	048	000	036	R	NE	IN
085	N54W	90SW	102	013	000	013	R	NW	IN
085	N54W	90SW	056	013	000	013	R	NW	IN
086	N33E	90NW	046	005	000	005	S	NE	IN
086	N47E	67NW	034	010	000	010	S		IN
086	N47E	67NW	029	008	000	008	S		IN
086	N33E	90NW	026	006	015	006	S	NE	IN
086	N40W	90SW	030	007	000	007	S	NW	IN
086	N40W	90SW	019	007	016	007	S	NW	IN
086	N40W	90SW	013	007	000	007	S	NW	IN
087	N87W	90SW	008	020	018	010	SC	EW	IN
087	N51W	90SW	034	033	000	013	SC	NW	IN
087	N87W	90SW	022	005	008	005	SC	EW	IN
087	N87W	90SW	015	007	012	007	SC	EW	IN
087	N87W	90SW	015	009	024	009	SC	EW	IN
087	N87W	90SW	005	010	038	011	SC	EW	IN
087	N87W	90SW	014	010	009	010	SC	EW	IN
087	N87W	90SW	007	005	017	007	SC	EW	IN
087	N87W	90SW	010	007	007	017	SC	EW	IN
087	N87W	90SW	015	013	034	007	SC	EW	IN
087	N87W	90SW	018	003	000	007	SC	EW	IN
087	N51W	90SW	010	070	000	010	SC	NW	IN
087	N51W	90SW	010	056	000	010	SC	NW	IN
087	N43W	90SW	070	061	000	010	SC	NW	IN
087	N51W	90SW	197	050	000	015	SC	NW	IN
087	N51W	90SW	040	012	026	012	SC	NW	IN
087	N84E	90NW	182	057	011	007	SC	EW	IN
087	N84E	90NW	085	043	011	007	SC	EW	IN
087	N84E	90NW	063	038	000	007	SC	EW	IN
087	N87W	90SW	047	067	006	007	SC	EW	IN
087	N73W	90SW	124	073	032	006	SC		IN
087	N73W	90SW	117	060	031	006	SC		IN
088	N45W	90SW	050	019	030	019	S	NW	IN
088	N45W	90SW	043	019	033	019	S	NW	IN
088	N45W	90SW	047	019	000	019	S	NW	IN
088	N86W	75SW	142	022	039	022	S	EW	IN
088	N86W	75SW	062	022	031	022	S	EW	IN
088	N86W	75SW	032	020	000	022	S	EW	IN
089	N62W	72SW	060	039	038	039	SC		IN
089	N62W	72SW	077	039	009	039	SC		IN
089	N62W	72SW	045	039	005	039	SC		IN
089	N62W	72SW	035	039	011	039	SC		IN
089	N62W	72SW	064	039	007	039	SC		IN
089	N03E	52SW	060	019	003	019	SC		IN
089	N03E	52NW	043	014	004	007	SC		IN
089	N28E	44NW	025	010	000	007	SC	NE	IN
089	N62W	72SW	040	039	007	039	SC		IN
089	N62W	72SW	038	039	006	039	SC		IN
089	N28E	44NW	015	014	011	014	SC	NE	IN
089	N28E	44NW	010	008	008	008	SC	NE	IN
089	N28E	44NW	020	005	001	005	SC	NE	IN
090	N43W	90SW	020	009	003	009	SC	NW	IN
090	N43W	90SW	016	009	000	009	SC	NW	IN
090	N43W	90SW	011	009	003	009	SC	NW	IN
090	N43W	90SW	012	009	010	009	SC	NW	IN

STA	STPI	DIP	LNG	DPI	SPA	PED	EXP	SET	LOC
090	N43W	90SW	018	017	005	009	SC	NW	IN
090	N43W	90SW	018	013	006	009	SC	NW	IN
090	N43W	90SW	018	017	010	009	SC	NW	IN
090	N43W	90SW	019	013	014	009	SC	NW	IN
090	N43W	90SW	010	017	007	009	SC	NW	IN
090	N43W	90SW	012	017	015	009	SC	NW	IN
090	N43W	90SW	010	017	013	009	SC	NW	IN
090	N43W	90SW	010	017	010	009	SC	NW	IN
091	N36W	87SW	180	025	069	025	S	NW	IN
091	N36W	87SW	130	025	025	025	S	NW	IN
091	N36W	87SW	103	025	012	025	S	NW	IN
091	N36W	87SW	090	025	039	025	S	NW	IN
091	N36W	87SW	087	025	014	025	S	NW	IN
091	N36W	87SW	085	025	040	025	S	NW	IN
091	N36W	87SW	080	025	055	025	S	NW	IN
092	N55W	74SW	017	007	016	007	SC	NW	IN
092	N55W	74SW	020	007	000	007	SC	NW	IN
092	N55W	74SW	005	002	022	002	SC	NW	IN
092	N55W	74SW	005	002	000	002	SC	NW	IN
092	N87E	90NW	051	030	004	004	SC	EW	IN
093	N25E	90NW	206	005	029	005	SC	NE	IN
093	N25E	90NW	174	005	043	005	SC	NE	IN
093	N25E	90NW	089	015	020	005	SC	NE	IN
093	N25E	90NW	355	012	000	005	SC	NE	IN
093	N49W	88SW	039	013	000	013	SC	NW	IN
093	N40W	72SW	043	012	000	012	SC	NW	IN
093	N40W	72SW	031	012	005	012	SC	NW	IN
093	N40W	72SW	011	012	013	012	SC	NW	IN
093	N85W	84SW	021	006	000	006	SC	NW	IN
093	N85W	84SW	043	015	023	015	SC	EW	IN
093	N40W	72SW	010	005	017	005	SC	NW	IN
093	N40W	72SW	014	007	015	008	SC	NW	IN
093	N40W	72SW	011	007	010	008	SC	NW	IN
093	N40W	72SW	008	007	008	009	SC	NW	IN
093	N40W	72SW	004	007	016	010	SC	NW	IN
094	N76W	80SW	020	010	043	010	S		IN
094	N76W	80SW	015	010	050	010	S		IN
094	N76W	80SW	020	010	055	010	S		IN
094	N76W	80SW	022	009	017	009	S		IN
094	N35E	78NW	050	010	015	010	S	NE	IN
095	N36W	84SW	320	014	006	014	R	NW	IN
095	N36W	84SW	340	015	000	015	R	NW	IN
095	N36W	84SW	310	008	000	008	R	NW	IN
095	N36W	84SW	010	010	040	010	R	NW	IN
096	N43W	88SW	073	005	000	005	R	NW	IN
096	N25E	90NW	015	008	026	008	R	NE	IN
096	N25E	90NW	024	008	021	008	R	NE	IN
096	N43W	88SW	050	007	000	007	R	NW	IN
097	N76E	74NW	242	102	008	102	R		IN
097	N76E	74NW	171	102	000	102	R		IN
097	N76E	74NW	190	039	004	039	R		IN
097	N76E	74NW	187	015	000	015	R		IN
098	N84E	75NW	078	026	003	016	R	EW	IN
098	N84E	75NW	196	021	000	011	R	EW	IN
098	N84E	75NW	132	007	000	007	R	EW	IN
098	N84E	75NW	106	007	000	007	R	EW	IN
098	N40E	68NW	053	013	008	013	R	NE	IN
098	N40E	68NW	045	013	007	013	R	NE	IN
099	N10W	69SW	110	046	014	046	R		IN
099	N10W	69SW	040	046	000	046	R		IN

STA	STRI	DIP	LNG	DPT	SPA	BED	EXP	SET	LOC
099	N45W	90SW	055	072	000	072	R		NW	IN
099	N45W	90SW	016	046	048	046	R		NW	IN
100	N72W	76SW	224	011	000	011	R			IN
100	N72W	76SW	133	017	000	017	R			IN
101	N33W	70SW	019	006	012	006	R			IN
101	N33W	70SW	021	006	000	006	R			IN
101	N42E	86NW	031	006	023	006	R		NE	IN
101	N42E	86NW	041	010	000	010	R		NE	IN
101	N77E	90NW	051	008	000	008	R			IN
101	N65W	87SW	094	023	004	023	R			IN
101	N65W	87SW	096	043	000	023	R			IN
102	N41W	85SW	084	014	032	005	S		NW	IN
102	N41W	85SW	109	013	052	005	S		NW	IN
102	N41W	85SW	045	005	008	005	S		NW	IN
102	N41W	85SW	109	005	013	007	S		NW	IN
102	N41W	85SW	034	012	036	007	S		NW	IN
102	N41W	85SW	108	015	000	015	S		NW	IN
102	N87W	84SW	142	023	042	023	S		EW	IN
102	N87W	84SW	035	012	012	012	S		EW	IN
102	N87W	84SW	024	012	019	012	S		EW	IN
102	N87W	84SW	048	014	054	014	S		EW	IN
102	N87W	84SW	092	021	000	021	S		EW	IN
102	N41W	85SW	174	011	025	006	S		NW	IN
102	N41W	85SW	153	013	012	006	S		NW	IN
102	N41W	85SW	085	009	032	006	S		NW	IN
102	N41W	85SW	174	013	038	006	S		NW	IN
102	N87W	84SW	092	010	051	010	S		EW	IN
102	N87W	84SW	095	009	040	009	S		EW	IN
102	N87W	84SW	057	005	034	009	S		EW	IN
103	N38W	84SW	014	008	007	008	S		NW	IN
103	N38W	84SW	013	008	012	008	S		NW	IN
103	N38W	84SW	023	007	009	007	S		NW	IN
103	N38W	84SW	017	007	011	007	S		NW	IN
103	N38W	84SW	013	008	000	008	S		NW	IN
103	N38W	84SW	010	010	009	010	S		NW	IN
103	N38W	84SW	012	010	008	010	S		NW	IN
103	N38W	84SW	016	010	010	010	S		NW	IN
103	N85E	58NW	022	006	008	006	S		EW	IN
103	N85E	58NW	015	014	006	005	S		EW	IN
103	N85E	58NW	011	007	003	003	S		EW	IN
103	N85E	58NW	005	004	009	006	S		EW	IN
104	N42W	86SW	057	012	012	012	S		NW	IN
104	N42W	86SW	030	012	014	012	S		NW	IN
104	N42W	86SW	039	009	007	009	S		NW	IN
104	N42W	86SW	053	009	010	009	S		NW	IN
104	N42W	86SW	058	009	007	009	S		NW	IN
104	N42W	86SW	115	007	032	007	S		NW	IN
104	N42W	86SW	042	008	004	008	S		NW	IN
104	N42W	86SW	021	008	006	008	S		NW	IN
105	N77W	75SW	045	023	015	023	S			IN
105	N77W	75SW	016	023	000	023	S			IN
105	N44W	85SW	023	022	040	022	S		NW	IN
105	N44W	85SW	020	022	040	022	S		NW	IN
105	N44W	85SW	010	014	025	014	S		NW	IN
105	N44W	85SW	023	012	016	012	S		NW	IN
105	N44W	85SW	012	012	012	012	S		NW	IN
105	N44W	85SW	015	022	029	022	S		NW	IN
105	N44W	85SW	016	018	023	018	S		NW	IN
105	N44W	85SW	030	016	009	016	S		NW	IN
105	N44W	85SW	038	023	019	012	S		NW	IN

STA	STRI	DIP	LNG	DPT	SPA	BED	EXP	SET	LOC
105	N44W	85SW	035	023	016	012	S	NW	IN
105	N44W	85SW	015	020	000	012	S	NW	IN
106	N51W	82SW	050	025	011	025	S	NW	IN
106	N51W	82SW	101	025	010	025	S	NW	IN
106	N51W	82SW	240	025	019	025	S	NW	IN
106	N51W	82SW	111	015	014	015	S	NW	IN
106	N51W	82SW	099	007	005	007	S	NW	IN
106	N51W	82SW	097	007	004	007	S	NW	IN
106	N51W	82SW	089	007	015	007	S	NW	IN
106	N51W	82SW	078	007	011	007	S	NW	IN
106	N32E	58NW	130	025	000	025	S	NE	IN
106	N32E	58NW	050	015	000	015	S	NE	IN
106	N01E	58NW	026	007	000	007	S		IN
106	N01E	58NW	019	015	000	015	S		IN
107	N82E	70NW	053	004	006	004	S	EW	IN
107	N82E	70NW	058	015	012	015	S	EW	IN
107	N82E	70NW	030	015	020	015	S	EW	IN
107	N46W	90SW	100	019	034	025	S	NW	IN
107	N46W	90SW	101	007	000	025	S	NW	IN
108	N88W	77SW	055	005	035	005	SC	EW	IN
108	N88W	77SW	047	005	027	005	SC	EW	IN
108	N88W	77SW	055	005	036	005	SC	EW	IN
108	N18W	80SW	033	045	000	045	SC		IN
108	N18W	80SW	073	045	030	045	SC		IN
108	N18W	80SW	065	045	000	045	SC		IN
108	N18W	80SW	075	007	006	007	SC		IN
108	N18W	80SW	052	008	000	008	SC		IN
108	N18W	80SW	062	045	037	045	SC		IN
108	N35E	90NW	044	045	038	045	SC	NE	IN
108	N35E	90NW	010	045	000	045	SC	NE	IN
109	N43W	83SW	044	012	012	012	SC	NW	IN
109	N43W	83SW	058	014	021	014	SC	NW	IN
109	N43W	83SW	055	021	014	021	SC	NW	IN
109	N43W	83SW	042	020	012	020	SC	NW	IN
109	N43W	83SW	020	020	012	020	SC	NW	IN
109	N43W	83SW	023	009	003	009	SC	NW	IN
109	N43W	83SW	023	009	009	009	SC	NW	IN
109	N43W	83SW	023	009	003	009	SC	NW	IN
109	N43W	83SW	025	009	007	009	SC	NW	IN
109	N43W	83SW	054	039	000	067	SC	NW	IN
110	N48W	90SW	020	053	020	007	S	NW	IN
110	N48W	90SW	021	054	029	007	S	NW	IN
110	N48W	90SW	005	008	009	008	S	NW	IN
110	N48W	90SW	006	008	004	008	S	NW	IN
110	N48W	90SW	005	008	004	008	S	NW	IN
110	N48W	90SW	005	008	010	008	S	NW	IN
110	N48W	90SW	002	008	008	008	S	NW	IN
111	N87W	85SW	144	012	025	012	SC	EW	IN
111	N87W	85SW	152	012	019	012	SC	EW	IN
111	N87W	85SW	178	014	024	014	SC	EW	IN
111	N87W	85SW	195	014	016	014	SC	EW	IN
111	N87W	85SW	117	014	013	014	SC	EW	IN
111	N87W	85SW	025	010	019	010	SC	EW	IN
111	N87W	85SW	057	010	020	010	SC	EW	IN
111	N87W	85SW	049	010	020	01	SC	EW	IN
111	N87W	85SW	070	010	010	010	SC		IN
111	N08E	72NW	020	010	030	010	SC		IN
111	N08E	72NW	020	010	047	010	SC		IN
111	N08E	72NW	010	010	027	010	SC		IN

STA	STRI	DIP	LNG	DPT	SPA	BED	EXP	SET	LOC
111	N08E	72NW	022	015	047	015	SC		IN
111	N08E	72NW	013	015	025	015	SC		IN
112	N84W	87SW	728	020	085	020	S	EW	IN
112	N84W	87SW	720	020	123	020	S	EW	IN
112	N84W	87SW	320	022	076	022	S	EW	IN
112	N34W	57SW	085	020	046	020	S		IN
112	N34W	57SW	085	020	053	020	S		IN
112	N34W	57SW	085	020	085	020	S		IN
112	N34W	57SW	123	020	088	020	S		IN
112	N34W	57SW	123	020	164	020	S		IN
112	N84W	87SW	007	022	062	022	S	EW	IN
112	N84W	87SW	340	022	106	022	S	EW	IN
112	N84W	87SW	320	022	052	022	S	EW	IN
112	N84W	87SW	750	022	069	022	S	EW	IN
112	N84W	87SW	720	042	083	042	S	EW	IN
112	N84W	87SW	715	020	177	020	S	EW	IN
113	N50W	90SW	082	010	000	003	S	NW	IN
113	N45W	87SW	180	010	000	010	S	NW	IN
113	N50W	90SW	017	008	007	008	S	NW	IN
113	N50W	90SW	019	008	004	008	S	NW	IN
113	N50W	90SW	034	008	007	008	S	NW	IN
113	N50W	90SW	009	005	008	003	S	NW	IN
113	N50W	90SW	020	005	006	003	S	NW	IN
114	N87W	85SW	130	010	035	010	S	EW	IN
114	N87W	85SW	063	010	016	010	S	EW	IN
114	N87W	85SW	174	010	021	010	S	EW	IN
114	N87W	85SW	040	010	012	010	S	EW	IN
114	N87W	85SW	102	010	031	010	S	EW	IN
115	N83W	89SW	032	012	025	012	S	EW	IN
115	N83W	89SW	015	012	019	012	S	EW	IN
115	N83W	89SW	015	012	020	012	S	EW	IN
115	N83W	89SW	023	012	010	012	S	EW	IN
115	N83W	89SW	019	012	006	012	S	EW	IN
115	N83W	89SW	017	012	013	012	S	EW	IN
116	N44W	88SW	158	061	029	061	SC	NW	NT
116	N44W	88SW	132	030	058	030	SC	NW	NT
116	N44W	88SW	061	030	000	030	SC	NW	NT
116	N38W	85SW	049	031	018	031	SC	NW	NT
116	N38W	85SW	058	005	000	005	SC	NW	NT
116	N38W	85SW	057	026	044	026	SC	NW	NT
116	N38W	85SW	045	026	000	026	SC	NW	NT
117	N55W	87SW	025	040	010	040	R	NW	NT
117	N55W	87SW	024	040	009	040	R	NW	NT
117	N01W	86SW	020	009	000	009	R		NT
117	N01W	86SW	021	016	000	016	R		NT
117	N55W	87SW	015	012	010	012	R	NW	NT
117	N55W	87SW	019	012	009	012	R	NW	NT
117	N55W	87SW	017	012	008	012	R	NW	NT
117	N55W	87SW	023	012	007	012	R	NW	NT
117	N55W	87SW	015	012	010	012	R	NW	NT
117	N55W	87SW	007	014	017	012	R	NW	NT
117	N55W	87SW	015	042	015	025	R	NW	NT
117	N55W	87SW	012	025	019	025	R	NW	NT
118	N41W	77SW	020	006	016	006	SC	NW	NT
118	N41W	77SW	010	006	011	006	SC	NW	NT
118	N41W	77SW	021	006	008	006	SC	NW	NT
118	N41W	77SW	022	006	004	006	SC	NW	NT
118	N41W	77SW	023	006	003	006	SC	NW	NT
118	N41W	77SW	026	006	004	006	SC	NW	NT

STA	STRI	DIP	LNG	DPT	SPA	BED	EXP	SET	LOC
118	N41W	77SW	013	006	009	006	SC	NW	NT
118	N41W	77SW	022	006	007	006	SC	NW	NT
118	N41W	77SW	015	006	008	006	SC	NW	NT
118	N41W	77SW	027	006	004	006	SC	NW	NT
119	N80E	76NW	040	014	006	014	SC	EW	NT
119	N80E	76NW	084	014	018	014	SC	EW	NT
119	N80E	76NW	095	014	018	014	SC	EW	NT
119	N80E	76NW	057	014	024	014	SC	EW	NT
119	N80E	76NW	079	014	017	014	SC	EW	NT
119	N80E	76NW	069	014	030	014	SC	EW	NT
119	N80E	76NW	077	014	011	014	SC	EW	NT
119	N80E	76NW	075	014	021	014	SC	EW	NT
119	N44E	44NW	079	014	016	014	SC	NE	NT
119	N44E	44NW	091	014	009	014	SC	NE	NT
119	N44E	44NW	138	014	014	014	SC	NE	NT
119	N44E	44NW	179	014	008	014	SC	NE	NT
119	N44E	44NW	202	014	005	014	SC	NE	NT
119	N44E	44NW	203	014	030	014	SC	NE	NT
120	N83E	90NW	083	016	026	016	S	EW	NT
120	N83E	90NW	058	016	028	016	S	EW	NT
120	N83E	90NW	053	016	048	016	S	EW	NT
120	N83E	90NW	046	016	015	016	S	EW	NT
120	N83E	90NW	046	025	028	025	S	EW	NT
120	N83E	90NW	062	025	039	025	S	EW	NT
120	N83E	90NW	032	025	003	025	S	EW	NT
120	N83E	90NW	019	025	022	025	S	EW	NT
120	N83E	90NW	044	025	036	025	S	EW	NT
120	N32W	87SW	054	012	030	012	S		NT
120	N32W	87SW	058	012	013	012	S		NT
120	N32W	87SW	065	012	026	012	S		NT
120	N32W	87SW	057	012	018	012	S		NT
120	N32W	87SW	025	012	027	012	S		NT
120	N32W	87SW	030	012	015	012	S		NT
121	N85W	80SW	005	012	036	012	R	EW	NT
121	N85W	80SW	047	012	025	012	R	EW	NT
121	N85W	80SW	003	014	010	014	R	EW	NT
121	N85W	80SW	010	014	024	014	R	EW	NT
121	N85W	80SW	019	014	035	014	R	EW	NT
121	N35E	80NW	015	019	020	019	R	NE	NT
121	N35E	80NW	013	019	008	019	R	NE	NT
121	N35E	80NW	012	015	012	015	R	NE	NT
123	N80E	90NW	035	022	033	022	S	EW	NT
123	N80E	90NW	050	022	038	022	S	EW	NT
123	N80E	90NW	028	022	058	022	S	EW	NT
123	N03E	90NW	033	022	035	022	S		NT
123	N03E	90NW	038	022	050	022	S		NT
123	N03E	90NW	058	022	028	022	S		NT
123	N47W	90SW	070	012	038	012	S		NT
123	N47W	90SW	034	012	041	012	S	NW	NT
123	N47W	90SW	057	012	008	012	S	NW	NT
123	N27E	90NW	021	012	038	012	S	NE	NT
123	N27E	90NW	016	012	017	012	S	NE	NT
123	N27E	90NW	018	012	027	012	S	NE	NT
124	N42W	87SW	115	014	025	014	S	NW	NT
124	N42W	87SW	106	014	036	014	S	NW	NT
124	N4E	90NW	190	020	025	007	S		NT
124	N42W	87SW	075	007	000	007	S	NW	NT
124	N42W	87SW	078	010	015	010	S	NW	NT
124	N42W	87SW	055	010	047	010	S	NW	NT
124	N42W	87SW	038	019	035	019	S		NT

STA	STRI	DIP	LNG	DPT	SPA	BED	EXP	SET	LOC
124	N42W	87SW	042	019	031	019	S	NW	NT
124	N42W	87SW	065	019	042	019	S	NW	NT
124	N42W	87SW	069	019	028	019	S	NW	NT
124	N42W	87SW	070	019	025	019	S	NW	NT
124	N42W	87SW	350	035	018	020	S	NW	NT
125	N87E	90NW	196	007	036	007	S	EW	NT
125	N87E	90NW	134	007	024	007	S	EW	NT
125	N87E	90NW	158	007	020	007	S	EW	NT
125	N87E	90NW	152	007	022	007	S	EW	NT
125	N87E	90NW	152	007	021	007	S	EW	NT
125	N87E	90NW	127	073	047	025	S	EW	NT
125	N87E	90NW	097	077	042	025	S	EW	NT
125	N87E	90NW	180	074	032	025	S	EW	NT
126	N87W	85SW	546	270	030	020	SC	EW	NT
126	N87W	85SW	584	240	029	020	SC	EW	NT
126	N87W	85SW	042	020	023	020	SC	EW	NT
126	N35E	85NW	020	035	025	007	SC	NE	NT
126	N35E	85NW	005	007	027	007	SC	NE	NT
126	N35E	85NW	004	007	009	007	SC	NE	NT
126	N35E	85NW	003	007	016	007	SC	NE	NT
126	N35E	85NW	005	007	010	007	SC	NE	NT
127	N85W	90SW	063	007	033	007	S	EW	NT
127	N85W	90SW	030	007	040	007	S	EW	NT
127	N85W	90SW	033	007	020	007	S	EW	NT
127	N85W	90SW	028	007	026	007	S	EW	NT
128	N05E	90NW	074	024	012	024	SC		NT
128	N05E	90NW	055	024	010	024	SC		NT
128	N05E	90NW	012	024	038	024	SC		NT
128	N63W	90SW	035	024	001	024	SC		NT
128	N63W	90SW	014	024	075	024	SC		NT
128	N63W	90SW	023	024	018	024	SC		NT
128	N63W	90SW	022	024	072	024	SC		NT
128	N63W	90SW	015	011	023	007	SC		NT
128	N63W	90SW	013	011	030	007	SC		NT
128	N63W	90SW	021	011	027	007	SC		NT
128	N69W	90SW	106	033	059	033	SC		NT
128	N69W	90SW	074	033	071	033	SC		NT
128	N69W	90SW	150	036	058	033	SC		NT
128	N69W	90SW	135	036	081	033	SC		NT
128	N69W	90SW	150	033	069	033	SC		NT
128	N69W	90SW	083	033	043	033	SC		NT
128	N37W	85SW	030	035	009	019	SC	NW	NT
128	N37W	85SW	027	035	005	019	SC	NW	NT
128	N37W	85SW	007	016	026	016	SC	NW	NT
128	N37W	85SW	018	016	019	016	SC	NW	NT
128	N37W	85SW	027	020	030	020	SC	NW	NT
128	N37E	79NW	147	093	120	004	SC	NE	NT
128	N37E	79NW	180	112	072	004	SC	NE	NT
128	N37E	79NW	130	110	000	004	SC	NE	NT
128	N37E	79NW					SC	NE	NT
129	N73W	60SW	020	017	016	017	S		NT
129	N73W	60SW	010	017	016	017	S		NT
129	N73W	60SW	010	017	000	017	S		NT
129	N73W	60SW	010	029	005	029	S		NT
129	N73W	60SW	001	029	013	029	S		NT
129	N73W	60SW	006	029	018	029	S		NT
130	N35W	90SW	075	008	020	008	S	NW	NT
130	N35W	90SW	089	008	007	008	S	NW	NT
130	N35W	90SW	120	008	023	008	S	NW	NT
130	N35W	90SW	099	008	012	008	S	NW	NT

STA	STRI	DIP	LNG	DPT	SPA	BED	EXP	SET	LOC
130	N35W	90SW	039	008	016	008	S	NW	NT
130	N35W	90SW	104	008	018	008	S	NW	NT
130	N35W	90SW	109	008	008	008	S	NW	NT
130	N35W	90SW	121	008	023	008	S	NW	NT
130	N35W	90SW	083	008	028	008	S	NW	NT
130	N40E	88NW	182	008	033	008	S	NE	NT
130	N40E	88NW	197	008	034	008	S	NE	NT
130	N40E	88NW	184	008	031	008	S	NE	NT
130	N40E	88NW	098	008	000	008	S	NE	NT
131	N53W	90SW	118	055	032	001	SC	NW	NT
131	N53W	90SW	079	055	000	001	SC	NW	NT
131	N53W	90SW	101	012	024	012	SC	NW	NT
131	N53W	90SW	027	012	032	012	SC	NW	NT
131	N53W	90SW	043	012	016	012	SC	NW	NT
131	N53W	90SW	041	012	044	012	SC	NW	NT
131	N53W	90SW	050	012	029	012	SC	NW	NT
131	N53W	90SW	041	012	025	012	SC	NW	NT
131	N53W	90SW	037	012	036	012	SC	NW	NT
131	N53W	90SW	064	012	034	012	SC	NW	NT
131	N53W	90SW	081	012	032	012	SC	NW	NT
131	N53W	90SW	090	012	028	012	SC	NW	NT
131	N53W	90SW	210	156	021	012	SC	NW	NT
131	N53W	90SW	075	075	054	012	SC	NW	NT
131	N53W	90SW	052	063	019	012	SC	NW	NT
131	N53W	90SW	116	056	090	012	SC	NW	NT
131	N53W	90SW	210	124	019	012	SC	NW	NT
131	N53W	90SW	055	052	018	012	SC	NW	NT
131	N53W	90SW	035	061	008	012	SC	NW	NT
131	N53W	90SW	426	170	000	012	SC		NT
132	N58W	83SW	035	027	073	027	SC		NT
132	N58W	83SW	023	027	070	027	SC		NT
132	N58W	83SW	036	027	060	027	SC		NT
132	N58W	83SW	056	027	014	027	SC		NT
132	N58W	83SW	020	027	065	027	SC		NT
132	N58W	83SW	029	027	020	027	SC		NT
132	N58W	83SW	036	027	062	027	SC		NT
132	N58W	83SW	009	040	033	027	SC		NT
132	N58W	83SW	001	027	024	027	SC		NT
132	N58W	83SW	007	027	026	027	SC		NT
132	N58W	83SW	001	027	021	027	SC		NT
132	N58W	83SW	001	027	032	027	SC		NT
132	N40E	79NW	027	016	017	016	SC	NE	NT
132	N40E	79NW	039	016	037	016	SC	NE	NT
132	N40E	79NW	018	016	016	016	SC	NE	AT
132	N40E	79NW	016	017	025	017	SC	NE	NT
132	N40E	79NW	054	017	027	017	SC	NE	NT
133	N84W	82SW	064	012	004	004	S	EW	NT
133	N84W	82SW	030	004	019	004	S	EW	NT
133	N61W	90SW	194	016	040	016	S		NT
133	N61W	90SW	182	016	007	016	S		NT
133	N61W	90SW	085	020	027	016	S		NT
133	N61W	90SW	084	020	029	016	S		NT
133	N61W	90SW	050	016	033	016	S		NT
133	N61W	90SW	174	016	053	016	S		NT
134	N48W	88SW	065	007	014	007	S	NW	NT
134	N48W	88SW	063	007	055	007	S	NW	NT
134	N48W	88SW	031	007	026	007	S	NW	NT
134	N48W	88SW	053	007	026	007	S	NW	NT
134	N48W	88SW	032	007	029	007	S	NW	NT
134	N48W	88SW	043	007	041	007	S	NW	NT

STA	STRI	DIP	LNG	DPT	SPA	BED	EXP	SET	LOC
135	N80E	86NW	054	109	019	005	SC	EW	NT
135	N80E	86NW	025	095	002	009	SC	EW	NT
135	N80E	86NW	077	234	013	009	SC	EW	NT
135	N80E	86NW	033	126	012	009	SC	EW	NT
135	N80E	86NW	035	049	011	006	SC	EW	NT
135	N80E	86NW	022	073	010	006	SC	EW	NT
135	N80E	86NW	042	104	021	008	SC	EW	NT
135	N80E	86NW	012	041	015	005	SC	EW	NT
135	N04W	79SW	067	010	005	001	SC		NT
135	N45W	88SW	059	016	036	016	SC	NW	NT
135	N45W	88SW	049	016	005	016	SC	NW	NT
135	N45W	88SW	040	015	031	015	SC	NW	NT
135	N45W	88SW	032	014	076	014	SC	NW	NT
135	N45W	88SW	050	011	006	011	SC	NW	NT
135	N45W	88SW	084	013	048	013	SC	NW	NT
135	N25W	87SW	068	006		001	SC		NT
135	N06E	75NW	155	012	020	012	SC		NT
135	N06E	75NW	071	015	023	015	SC		NT
135	N06E	75NW	065	017		017	SC		NT
135	N80E	86NW	110	030	038	001	SC	EW	NT
135	N80E	86NW	104	027	013	001	SC	EW	NT
135	N80E	86NW	057	018	023	001	SC	EW	NT
135	N80E	86NW	074	084	011	001	SC	EW	NT
135	N80E	86NW	213	096	015	001	SC	EW	NT
135	N80E	86NW	179	075	025	001	SC	EW	NT
136	N70W	75NE	146	020	022	009	S		NT
136	N70W	75NE	023	003	017	003	S		NT
136	N70W	75NE	176	013	035	003	S		NT
136	N70W	75NE	123	023	036	007	S		NT
136	N70W	75NE	079	006	029	006	S		NT
136	N70W	75NE	065	009	028	006	S		NT
137	N78W	90SW	103	014	007	014	S		NT
137	N78W	90SW	126	024	021	024	S		NT
137	N78W	90SW	043	032	014	012	S		NT
137	N78W	90SW	103	023	016	013	S		NT
137	N78W	90SW	001	015	016	016	S		NT
137	N78W	90SW	031	043	013	020	S		NT
138	N80E	82NW	087	111	057	111	S	EW	SO
138	N80E	82NW	079	062	012	062	S	EW	SO
138	N80E	82NW	030	025	021	062	S	EW	SO
138	N80E	82NW	128	083		083	S	EW	SO
138	N46W	86NE	052	060		060	S	NW	SO
138	N04W	67SW	056	064	038	112	S		SO
138	N15W	78SW	029	063	020	063	S		SO
138	N15W	78SW	072	053	032	053	S		SO
138	N80E	82NW	020	033	010	001	S	EW	SO
138	N80E	82NW	008	030	003	001	S	EW	SO
138	N80E	82NW	010	025	010	001	S	EW	SO
139	N55W	80SW	294	011	064	001	S	NW	SO
139	N55W	80SW	183	005	032	001	S	NW	SO
139	N55W	80SW	031	002	032	001	S	NW	SO
139	N55W	80SW	037	003	022	001	S	NW	SO
139	N55W	80SW	030	018	029	018	S	NW	SO
139	N55W	80SW	045	008	008	008	S	NW	SO
139	N55W	80SW	063	018	0C8	018	S	NW	SO
139	N55W	80SW	104	008	043	008	S	NW	SO
139	N55W	80SW	091	015	034	015	S	NW	SO
139	N72E	85SE	062	024	030	024	S		SO
139	N72E	85SE	062	021	019	018	S		SO
139	N72E	85SE	082	023	010	005	S		SO

STA	STRI	DIP	LNG	DPT	SPA	BED	EXP	SET	LOC
140	N87E	85NW	540	010	068	001	S	EW	SO
140	N87E	85NW	429	010	012	001	S	EW	SO
140	N87E	85NW	092	012	127	001	S	EW	SO
140	N87E	85NW	364	016	087	001	S	EW	SO
140	N87E	85NW	134	001	007	001	S	EW	SO
140	N87E	85NW	182	003	024	001	S	EW	SO
140	N87E	85NW	163	005		001	S	EW	SO
140	N03E	84SE	084	012	028	001	S		SO
140	N03E	84SE	070	007	050	001	S		SO
140	N03E	84SE	136	006	014	001	S		SO
140	N87E	85NW	268	025	003	001	S	EW	SO
140	N87E	85NW	182	019	008	001	S	EW	SO
140	N87E	85NW	204	022	027	001	S	EW	SO
140	N87E	85NW	255	027	095	001	S	EW	SO
140	N87E	85NW	246	025	083	001	S	EW	SO
140	N87E	85NW	217	024	008	001	S	EW	SO
140	N87E	85NW	229	025	010	001	S	EW	SO
140	N87E	85NW	242	025	114	001	S	EW	SO
141	N67W	90SW	180	009	027	009	S		SO
141	N67W	90SW	214	009	030	009	S		SO
141	N67W	90SW	131	009	043	009	S		SO
141	N67W	90SW	108	009	026	009	S		SO
141	N67W	90SW	224	009	015	009	S		SO
141	N67W	90SW	224	009	027	009	S		SO
141	N67W	90SW	182	009	017	009	S		SO
141	N67W	90SW	156	009	016	009	S		SO
141	N67W	90SW	130	009	014	009	S		SO
141	N67W	90SW	100	009	019	009	S		SO
141	N67W	90SW	077	009	009	009	S		SO
141	N67W	90SW	069	009	011	009	S		SO
141	N67W	90SW	065	009	013	009	S		SO
141	N30E	90NW	071	005	048	005	S	NE	SO
141	N30E	90NW	073	005	044	005	S	NE	SO
141	N30E	90NW	302	012	052	012	S	NE	SO
141	N30E	90NW	352	012	030	012	S	NE	SO
141	N30E	90NW	260	012	021	012	S	NE	SO
141	N30E	90NW	134	012	042	012	S	NE	SO
141	N30E	90NW	093	012		012	S	NE	SO
142	N83E	83SE	073	005	012	005	S	EW	SO
142	N83E	83SE	067	005	062	005	S	EW	SO
142	N83E	83SE	107		072		S	EW	SO
142	N83E	83SE	093		015		S	EW	SO
142	N83E	83SE	134		043		S	EW	SO
142	N83E	83SE	087		049		S	EW	SO
142	N83E	83SE	088		084		S	EW	SO
142	N83E	83SE	102		042		S	EW	SO
142	N83E	83SE	080		051		S	EW	SO
142	N83E	83SE	131		031		S	EW	SO
142	N83E	83SE	112		039		S	EW	SO
142	N83E	83SE	111		039		S	EW	SO
142	N83E	83SE	103		058		S	EW	SO
142	N83E	83SE	094		060		S	EW	SO
142	N83E	83SE	110		045		S	EW	SO
142	N83E	83SE	125		039		S	EW	SO
142	N13W	73SW	063		010		S		SO
142	N13W	73SW	029		013		S		SO
142	N13W	73SW	109		013		S		SO
142	N13W	73SW	141	012	026	012	S		SO
142	N13W	73SW	095		013		S		SO
142	N13W	73SW	064	007	003	007	S		SO

STA	STRI	DIP	LNG	DPT	SPA	BED	EXP	SET	LOC
142	N12E	70NW	072	014	019	014	S		SO
142	N12E	70NW	284	011	014	011	S		SO
142	N12E	70NW	141	012	031	012	S		SO
142	N75W	84NE	013	007	031	007	S		SO
142	N75W	84NE	010	010	072	010	S		SO
142	N75W	84NE	030	009	036	009	S		SO
142	N75W	84NE	017	009	029	009	S		SO
142	N75W	84NE	011	009	036	009	S		SO
143	N45W	64SW	030	007	012	007	S	NW	SO
143	N45W	64SW	027	007	011	007	S	NW	SO
143	N45W	64SW	041	007	016	007	S	NW	SO
143	N45W	64SW	029	007	006	007	S	NW	SO
143	N45W	64SW	057	011	037	011	S	NW	SO
143	N45W	64SW	023	011	013	011	S	NW	SO
143	N45W	64SW	025	011	027	011	S	NW	SO
143	N45W	64SW	056	020	042	020	S	NW	SO
143	N68E	75NW	042	007	028	007	S		SO
143	N68E	75NW	018	007	029	007	S		SO
143	N68E	75NW	052	007	023	007	S		SO
143	N68E	75NW	032	020	011	020	S		SO
143	N65W	84SW	034	011	026	011	S		SO
143	N65W	84SW	016	011	012	011	S		SO
143	N65W	84SW	042	007	017	007	S		SO
143	N65W	84SW	031	005	034	005	S		SO
143	N65W	84SW	057	007	025	007	S		SO
143	N65W	84SW	025	017	023	017	S		SO
143	N65W	84SW	038	017	010	017	S		SO
143	N65W	84SW	036	015	012	015	S		SO
144	N28E	90NW	120		018		S	NE	BR
144	N28E	90NW	134		019		S	NE	BR
144	N28E	90NW	172		024		S	NE	BR
144	N28E	90NW	234		023		S	NE	BR
144	N28E	90NW	186		023		S	NE	BR
144	N28E	90NW	100		016		S	NE	BR
144	N28E	90NW	089		014		S	NE	BR
144	N28E	90NW	115		012		S	NE	BR
144	N28E	90NW	140		013		S	NE	BR
144	N46W	90SW	045		082		S	NW	BR
144	N46W	90SW	130		017		S	NW	BR
144	N46W	90SW	090		017		S	NW	BR
144	N46W	90SW	090		024		S	NE	BR
145	N25E	65SE					S		NT
145	N72W	87NE					S		NT
145	N10E	70SE					S	EW	NT
145	N80E	90NW			070		S	NE	NT
145	N25E	65SE			092		S	NE	NT
145	N25E	65SE			060		S	NE	NT
145	N25E	65SE			035		S	NE	NT
145	N25E	65SE			024		S	NE	NT
145	N25E	65SE			031		S		NT
145	N45W	88SW	058	022	128	022	S	NW	NT
145	N45W	88SW	088	022	103	022	S	NW	NT
145	N45W	88SW	020	020	032	020	S	NW	NT
145	N45W	88SW	030	020	090	020	S	NW	NT
145	N45W	88SW	012	020	071	020	S	NW	NT
146	N70W	86SW	070	048	027	012	S		NT
146	N70W	86SW	016	010	042	010	S		NT
146	N70W	86SW	089	010	010	010	S		NT
146	N70W	86SW	083	010		010	S		NT

FIELD TECHNIQUES

FOR MEASURING JOINT INTENSITY

by

Jeanette M. Dixon, Research Associate
Devonian Shale Program

West Virginia University
Department of Geology and Geography
Morgantown, West Virginia 26506

INDEX

INTRODUCTION

Hydrocarbon production from fractured reservoirs, increased water-well yields, coal mine roof falls, and some construction problems often have been cited as having been caused by an increase in fracture intensity. A relatively fast and easy method to measure fracture intensity and locating areas of intense fracturing would be generally useful, and in particular, in potential drilling areas where little or no subsurface data is available. As part of the Eastern Gas Shales Project, funded by the U. S. Department of Energy, such a method was developed (Wheeler and Dixon, in preparation). This paper reports the summary of methods used, a test of operator variability, and a "handbook" of suggested procedures.

METHODS

Joint intensity measurements of systematic joints have been taken in varying lithologies and bed thicknesses with varying amounts of deformation. Some methods remain constant throughout all studies, others vary somewhat according to exposure, amount of deformation, bed thickness, and lithology.

In the initial study, completed in Tucker County (Dixon, 1979a; 1979b), it was determined that joint strike, dip and spacing are the only necessary measurements. Spacing is the perpendicular distance to the adjacent joint in the same set (Stubbs and Wheeler, 1975; Wheeler and Stubbs, in press).

A measurement of joint intensity or joint surface area per unit volume of rock is made using inverses of average spacings, summed over

all sets in an exposure (Vialon and others, 1976; Dixon, 1979a; 1979b; Wheeler, 1979; Wheeler and Dixon, in preparation). If for example, three joint sets were exposed in an outcrop, then the following formula would be used to obtain an intensity (I) measure:

$$I = \frac{1}{S_1} + \frac{1}{S_2} + \frac{1}{S_3} .$$

Regardless of the number of joints measured or the number of sets in an exposure, only one intensity measurement is calculated.

A question of reproducibility of data from operator variance is important in measuring joint intensity. To test this, four operators, with experience in measuring joint orientation but with extensive to no experience in measuring joint intensity, measured strike, dip, and spacing at three stations. No instructions or assistance were given. The operators worked independently, often taking measurements at different places on the outcrop and at different times. The outcrops varied in size, type, and complexity. Although the number of joints measured varied greatly among operators (Table 1), the intensities did not differ significantly (significance level of 0.05) as calculated by the Least-Squares Means and the Kruskal-Wallis tests (Davis, 1973; Gibbons, 1976). Thus, intensity measurements obtained in this or other studies can be considered generally · valid and reproducible. One should note that even though variations might occur among operators, real and valid differences in intensities can well be detected by a single operator as long as he is consistent in his own methods. Operator consistency is an important factor.

TABLE I   OPERATOR VARIANCE

Operator	Station 33		Station 87		Station 35	
	I	n	I	n	I	n
1	0.24	12	0.21	12	0.09	18
2	0.08	32	0.19	31	0.20	40
3	0.22	25	0.04	17	0.19	42
4	0.10	11	0.15	16	0.14	16

Table 1   Intensities (I) and number of observations (n)
measured at data stations in Tucker County.

HANDBOOK TO MEASURING JOINT INTENSITY

This "handbook" is meant to assist people who are about to engage in a joint intensity study, perhaps for the first time. Certain procedures need to be strictly adhered to, regardless of the study; others will vary. Within a study, consistency is most important.

Ideally, the area to be studied should be previewed. Some rocks lend themselves to this type of study better than others. A preliminary investigation of rock type, number of exposures, and a few sample measurements could save time, trouble, and retracing of steps.

Joint strike, dip, and spacing are the only necessary measurements, however, bed thickness is a useful measurement. If the joints are very regular and consistent, only one strike and dip measurement may be necessary; two or three measurements may be useful where joints are less consistent.

Spacing is the perpendicular distance to the next adjacent joint in the same set. In an exposure, one should measure spacing consistently in one direction so as not to repeat a spacing measurement. If part of the exposure has been washed out, covered by vegetation, covered by talus, or in any way covered, spacing should not be measured across the area; a joint may be covered and the spacing measurement would be erroneous. Wherever possible, at least three spacings per set should be measured. The number of joint spacings one should measure at each exposure will vary according to the number of joint sets and the regularity or irregularity of the spacing. If joint spacing in a set is fairly consistent across the exposure, only three to five measurements are necessary; if spacing is

variable, 10-20 measurements may be necessary. The key to measuring spacings is to choose a representative sample. The exception to the rule is massive sandstone where joint spacing may be many meters. If the outcrop is large, and yet has only one or two joints or one or two spacings, then the intensity value may be considered equal to or less than the calculated value. For example, if an outcrop is 25 meters long and two joints at a high angle to the face of the outcrop are found at one end ten meters apart and the next joint spacing is greater than 15 meters, then no other joint from that set will be found in the remaining 15 meters of the outcrop. The average spacing of that set can be considered equal to or less than 10 meters. It is important to note when an outcrop has no joints, particularly if the outcrop is of fair size.

Field equipment is often a personal choice. However, two measuring instruments are found to be useful: a six-foot folding, metric/English carpenter's ruler and a 30m fiberglass tape. The carpenter's ruler is good when spacings are less than a few meters. It is invaluable when measuring high angle cuts where joints are a few feet above your reach. The ruler can be unfolded into an upside down "L" shape, using the long end for extension and the short end for measuring spacings. The 30m fiberglass tape, used when spacings are large, is flexible and will not rust when used in streams or wet areas.

One should beware of blasting fractures, weathering cracks, or other breaks which are not joints. As a general rule, when in doubt, don't. If you are unsure whether or not a fracture is a systematic joint, do not measure it for spacing. When you have completed the study, any differences in joint intensities will be detected from spacings you are sure are real.

Processing of the data will vary from study to study. In areas where a great number of intensity measurements were taken, a simple contour map may best illustrate areas of high or low intensities. When traverses are taken across an area, a line graph may well illustrate intensity variances. Using mean spacings of individual sets can be used to assist in analyzing causes of joint intensity. However, it is only the joint intensity measurement that estimates the total surface area of fractured rock per unit volume. An individual set may show close spacings in an area (i.e., increased intensity); but when added to all joints in the exposure, no increase may exist.

REFERENCES CITED

Davis, J. C., 1978, Statistics and data analysis in geology: John Wiley and sons, Inc., 550 p.

Dixon, J. M., 1979a, A method to identify zones of intense jointing with applications to the Parsons lineament: Morgantown Energy Technology Center Open-File Report, Morgantown, WV, 46p.

Dixon, J. M., 1979b, A method to identify zones of intense jointing with application to the Parsons lineament, West Virginia (abs): Geol. Soc. Amer. Abs. with Programs, v. 7, p. 1286.

Gibbons, J. D., 1976, Nonparametric methods for quantitative analysis: Holt, Rinehart and Winston, 463 p.

Stubbs, J. L., Jr., and Wheeler, R. L., 1975, Style elements of systematic joints (abs): Geol. Soc. America Abs. with Programs, v. 7, p. 1286.

Vialon, P., Ruland, M., and Grolier, J., 1976, Elements de tectonique analytique: Paris, Masson, 118 p.

Wheeler, R. L., 1979, A numerical estimate of joint intensity, confidence limits on it, and applications to large structural lineaments (abs): Geol. Soc. Amer. Abs. with Programs, Northeastern Section of the Geol. Soc. of Amer. 14th Annual Meeting, v. 11, no. 1, p. 58-59.

Wheeler, R. L., and Dixon, J. M., ms, Intensity of systematic joints (in review).

Wheeler, R. L., and Stubbs, J. L., Jr., ms, Style elements of systematic joints: In Podwysocki, M., and Earle, J., eds., 2nd International Conf. on the Basement Tectonics Proc., (in press).

OPERATOR VARIANCE DATA

OPR	STRI	SP	ST	STA
BRI	N74W	06	EW	33
BRI	N83W	08	EW	33
BRI	N87W	13	EW	33
BRI	N53W	07	NW	33
BRI	N18E	03	NE	33
BRI	N25E	10	NE	33
BRI	N83W	22	EW	33
BRI	N82W	26	EW	33
BRI	N86W	11	EW	33
BRI	N86E	28	EW	33
BRI	N10E	28	NN	33
BRI	N14E	29	NN	33
BRI	N75W	31	7W	87
BRI	N77W	32	7W	87
BRI	N73W	12	7W	87
BRI	N23E	27	NE	87
BRI	N83E	31	EW	87
BRI	N80E	20	EW	87
BRI	N15E	21	NN	87
BRI	N45W		NW	87
BRI	N85E	45	EW	87
BFI	N87W	15	EW	87
BRI	N82W	13	EW	87
BPI	N80E	05	EW	87
BRI	N18E	55	NN	87
BRI	N53W		NW	87
BRI	N58W	32	NW	35
BPI	N64W	13	6W	35
BRI	N60W	07	6W	35
BRI	N61W	06	6W	35
BBI	N57W	08	6W	35
BRI	N71W	10	6W	35
BRI	N26E	04	NE	35
BRI	N25E	03	NE	35
BPI	N12E	19	NE	35
BFI	N62W	12	6W	35
BRT	N63W	09	6W	35
BRI	N58W	39	6W	35
BRI	N60E	23	6E	35
BRI	N62E	28	6E	35
BPI	N89W	16	EW	35
BRI	N28E	45	NE	35
BBI	N32E	99	NE	35
TOM	N86W	29	EW	33
TOM	N87W	24	EW	33
TOM	N84W	35	EW	33
TOM	N86W	34	EW	33

OPR	STRI	SP	ST	STA
TOM	N87W	55	EW	33
TOM	N84W	66	EW	33
TOM	N86W	68	EW	33
TOM	N87W	12	EW	33
TOM	N84W	34	EW	33
TOM	N86W	40	EW	33
TOM	N19E	19	NE	33
TOM	N21E	02	NE	33
TOM	N42E	19	NE	33
TOM	N19E	23	NE	33
TOM	N21E	08	NE	33
TOM	N42E	16	NE	33
TOM	N19E	23	NE	33
TOM	N21E	10	NE	33
TOM	N42E	16	NE	33
TOM	N19E	17	NE	33
TOM	N21E	22	NE	33
TOM	N42E	32	NE	33
TOM	N19E	30	NE	33
TOM	N21E	03	NE	33
TOM	N42E	27	NE	33
TOM	N19E	34	NE	33
TOM	N21E	17	NE	33
TOM	N42E	08	NE	33
TOM	N19E	13	NE	33
TOM	N21E	21	NE	33
TOM	N42E	23	NE	33
TOM	N19E	39	NE	33
TOM	N83E	30	EW	87
TOM	N85E	32	EW	87
TOM	N79W	37	EW	87
TOM	N83E	14	EW	87
TOM	N85E	11	EW	87
TOM	N79W	18	EW	87
TOM	N83E	25	EW	87
TOM	N85E	46	EW	87
TOM	N79W	13	EW	87
TOM	N83E	62	EW	87
TOM	N85E	18	EW	87
TOM	N79W	06	EW	87
TOM	N83E	15	EW	87
TOM	N85E	16	EW	87
TOM	N79W	03	EW	87
TOM	N83E	17	EW	87
TOM	N85E	10	EW	87
TOM	N79W	12	EW	87
TOM	N83E	09	EW	87

OPR	STRI	SP	ST	STA
TOM	N85E	06	EW	87
TOM	N79W	30	EW	87
TOM	N83E	10	EW	87
TOM	N85E	10	EW	87
TOM	N79W	16	EW	87
TOM	N83E	07	EW	87
TOM	N85E	17	EW	87
TOM	N40W		NW	87
TOM	N20E	15	NE	87
TOM	N26E	28	NE	87
TOM	N24E	13	NE	87
TOM	N20E	08	NE	87
TOM	N26E	06	NE	87
TOM	N44E	42	NE	35
TOM	N25E	35	NE	35
TOM	N29E	07	NE	35
TOM	N25E	46	NE	35
TOM	N61W	13	NW	35
TOM	N51W	23	NW	35
TOM	N51W	34	NW	35
TOM	N53W	35	NW	35
TOM	N53W	11	NW	35
TOM	N51W	32	NW	35
TOM	N53W	28	NW	35
TOM	N51W	15	NW	35
TOM	N53W	08	NW	35
TOM	N51W	39	NW	35
TOM	N53W	79	NW	35
TOM	N51W	39	NW	35
TOM	N73E	27	7E	35
TOM	N73E	23	7E	35
TOM	N52W	14	NW	35
TOM	N53W	15	NW	35
TOM	N51W	26	NW	35
TOM	N02E	12	NN	35
TOM	N02E	11	NN	35
TOM	N51W	32	NW	35
TOM	N53W	08	NW	35
TOM	N51W	07	NW	35
TOM	N53W	17	NW	35
TOM	N51W	24	NW	35
TOM	N25E	99	NE	35
TOM	N29E	37	NE	35
TOM	N25E	35	NE	35
TOM	N29E	14	NE	35
RUS	N87W	19	EW	33
RUS	N84W	12	EW	33

OPR	STRI	SP	ST	STA
RUS	N82W	10	EW	33
RUS	N84W	18	EW	33
RUS	N87W	31	EW	33
RUS	N84W	07	EW	33
RUS	N83W	12	EW	33
RUS	N39W	16	NW	33
RUS	N46W	18	NW	33
RUS	N47W	24	NW	33
RUS	N47W	27	NW	33
RUS	N39W	13	NW	33
RUS	N46W	18	NW	33
RUS	N47W	70	NW	33
RUS	N47W	36	NW	33
RUS	N39W	29	NW	33
RUS	N67W	17	6W	33
RUS	N63W	04	6W	33
RUS	N67W	C8	6W	33
RUS	N21E	43	NE	33
RUS	N14E	26	NE	33
RUS	N14E	29	NE	33
RUS	N17E	53	NE	33
RUS	N21E	34	NE	33
RUS	N14E	33	NE	33
RUS	N14E	23	NE	33
RUS	N21E	59	NE	33
RUS	N14E	71	NE	33
RUS	N87E	70	EW	87
RUS	N85E	05	EW	87
RUS	N89E	99	EW	87
RUS	N85E	38	EW	87
RUS	N87E	06	EW	87
RUS	N85E	07	EW	87
RUS	N89E	03	EW	87
RUS	N85E	72	EW	87
RUS	N87E	70	EW	87
RUS	N85E	28	EW	87
RUS	N70W	30	7W	87
RUS	N72W	99	7W	87
RUS	N71W	32	7W	87
RUS	N72W	48	7W	87
RUS	N70W	43	7W	87
RUS	N72W	48	7W	87
RUS	N71W	47	7W	87
RUS	N58W	12	NW	35
RUS	N57W	11	NW	35
RUS	N57W	13	NW	35
RUS	N62W	09	NW	35

OPR	STRI	SP	ST	STA
RUS	N58W	24	NW	35
RUS	N57W	36	NW	35
RUS	N62W	38	NW	35
RUS	N74W	22	7W	35
RUS	N70W	12	7W	35
RUS	N70W	05	7W	35
RUS	N74W	08	7W	35
RUS	N70W	21	7W	35
RUS	N70W	16	7W	35
RUS	N70W	11	7W	35
RUS	N74W	02	7W	35
RUS	N70W	05	7W	35
RUS	N70W	24	7W	35
RUS	N70W	13	7W	35
RUS	N70W	13	7W	35
RUS	N70W	39	7W	35
RUS	N70W	32	7W	35
RUS	N70W	12	7W	35
RUS	N70W	16	7W	35
RUS	N70W	28	7W	35
RUS	N70W	30	7W	35
RUS	N57W	06	NW	35
RUS	N55W	09	NW	35
RUS	N57W	09	NW	35
RUS	N55W	08	NW	35
RUS	N57W	19	NW	35
RUS	N27E	28	NE	35
RUS	N17E	25	NE	35
RUS	N27E	32	NE	35
RUS	N17E	45	NE	35
RUS	N27E	03	NE	35
JAN	N80W	25	EW	33
JAN	N83W	20	EW	33
JAN	N80W	14	EW	33
JAN	N80W	11	EW	33
JAN	N83W	12	EW	33
JAN	N83W	08	EW	33
JAN	N80W	18	EW	33
JAN	N83W	24	EW	33
JAN	N80W	24	EW	33
JAN	N83W	32	EW	33
JAN	N50W	16	NW	33
JAN	N45W	20	NW	33
JAN	N48W	19	NW	33
JAN	N50W	12	NW	33
JAN	N87W	18	EW	87
JAN	N87W	08	EW	87

OPR	STEI	SP	ST	STA
JAN	N87W	12	EW	87
JAN	N87W	24	EW	87
JAN	N87W	38	EW	87
JAN	N87W	09	EW	87
JAN	N87W	17	EW	87
JAN	N87W	17	EW	87
JAN	N87W	34	EW	87
JAN	N51W	07	NW	87
JAN	N51W	26	NW	87
JAN	N84E	11	EW	87
JAN	N84E	11	EW	87
JAN	N73W	32	7W	87
JAN	N73W	31	7W	87
JAN	N24E	90	NE	35
JAN	N24E	59	NE	35
JAN	N24E	29	NE	35
JAN	N02E	21	NN	35
JAN	N02E	31	NN	35
JAN	N02E	11	NN	35
JAN	N55W	47	NW	35
JAN	N55W	09	NW	35
JAN	N55W	25	NW	35
JAN	N54W	35	NW	35
JAN	N85W	36	EW	35
JAN	N85W	29	EW	35
JAN	N85W	12	EW	35
JAN	N85W	16	EW	35
JAN	N85W	37	EW	35

STATION LOCATIONS IN TUCKER COUNTY

APPENDIX A

STATION LOCATIONS IN TUCKER COUNTY
(in UTM Grid Coordinates)

Key to Abbreviations:

STA - station number

STA	LATITUDE	LONGITUDE	STA	LATITUDE	LONGITUDE
001	4328.280	615.120	050	4333.900	617.470
002	4329.710	613.710	051	4333.790	618.170
003	4330.340	614.080	052	4334.940	614.420
004	4330.800	610.530	054	4333.600	613.450
005	4329.340	612.220	055	4338.430	623.520
006	4325.480	613.100	056	4338.780	622.980
007	4325.200	612.500	057	4338.280	620.510
008	4325.870	611.720	058	4339.400	620.080
009	4327.030	611.250	059	4340.170	619.370
010	4326.430	611.070	060	4341.340	618.560
011	4326.920	610.600	061	4341.940	617.730
012	4323.350	611.100	062	4339.500	622.920
013	4323.170	610.800	063	4339.920	623.300
014	4322.600	610.180	064	4340.420	623.310
015	4329.560	611.700	065	4343.180	623.170
016	4330.600	606.530	066	4342.680	624.210
017	4328.020	603.700	067	4341.220	623.180
018	4325.610	602.990	068	4341.650	624.310
019	4324.870	602.920	069	4337.770	621.360
020	4323.480	602.570	070	4337.480	620.910
021	4319.750	602.580	071	4335.990	619.440
022	4319.980	611.050	072	4337.620	614.910
023	4320.060	611.070	073	4339.380	616.180
024	4322.170	609.520	074	4336.200	611.610
025	4322.020	608.870	075	4336.270	612.530
026	4327.130	610.470	076	4336.540	613.300
027	4327.270	610.340	077	4337.210	613.890
028	4327.500	609.300	078	4333.230	616.750
029	4327.920	608.600	079	4333.020	616.460
030	4327.800	607.570	080	4332.420	615.920
031	4333.670	611.010	082	4326.500	616.700
032	4333.480	611.250	083	4332.900	612.910
033	4332.480	611.380	084	4334.700	612.430
035	4331.160	609.720	085	4335.520	611.590
036	4326.640	610.970	086	4335.390	610.920
037	4325.270	612.380	087	4334.810	610.980
038	4325.210	612.490	088	4333.730	609.500
040	4324.700	612.700	089	4330.370	609.760
041	4324.800	612.880	090	4329.880	609.590
042	4324.880	613.080	091	4330.320	608.650
043	4325.060	613.230	092	4329.730	608.640
044	4325.120	613.300	093	4329.950	606.990
045	4325.180	613.350	094	4329.450	606.720
046	4325.250	613.420	095	4331.600	605.670
047	4334.540	616.240	096	4332.160	605.300
048	4334.000	616.680	097	4332.870	604.300
049	4333.980	616.960	098	4332.960	603.770

STA	LATITUDE	LONGITUDE	STA	LATITUDE	LONGITUDE
099	4335.130	604.140	125	4335.620	620.390
100	4334.770	604.430	126	4335.480	620.620
101	4334.580	605.560	127	4335.230	621.170
102	4327.190	613.480	128	4335.380	613.380
103	4327.880	612.700	129	4335.680	615.170
104	4328.090	612.320	130	4335.770	614.900
105	4328.470	611.660	131	4335.920	614.580
106	4328.170	612.150	132	4336.110	614.550
107	4327.110	612.150	133	4336.510	615.130
108	4326.600	612.760	134	4337.230	615.220
109	4327.870	610.340	135	4323.160	610.330
110	4328.220	610.350	136	4323.690	609.170
111	4332.660	611.480	137	4323.900	609.100
112	4332.780	612.030	138	4320.770	607.490
113	4333.500	612.080	139	4323.120	608.840
114	4333.540	611.400	140	4322.550	609.540
115	4331.860	612.480	141	4322.370	608.360
116	4338.610	621.520	142	4323.480	607.630
117	4339.480	621.580	143	4322.870	607.460
118	4340.370	621.090	144	4323.010	604.680
119	4338.450	621.620	145	4338.960	617.630
120	4338.150	620.740	146	4338.430	617.360
121	4338.780	620.220	147	4338.110	617.150
123	4337.580	619.920	148	4337.660	616.910
124	4335.950	619.720	149	4337.900	616.690

APPENDIX B

TUCKER COUNTY DATA

<u>Key to Abbreviations</u>:

STA - station number

STRI- joint strike

DIP - joint dip

LNG - joint length (in cm)

DTH - joint depth (in cm)

SPA - joint spacing (in cm)

BED - bed thickness (in cm)

EX - type of exposure: R = roadcut, S = stream pavement, SC = streamcut

ST - indicates into which of three main joint sets the joint falls: NW = northwest, NE = northeast, EW = east-west

LO - location with respect to the Parsons lineament: IN = within, NO = north, SO = south

GR - group with respect to the Parsons lineament: IN = within, OT = outside

STA	STRI	DIP_	LNG	DTH	SPA	BED	EX	ST	LO	GP
001	N45W	88SW	106	048	060	020	R		IN	IN
001	N46E	90NW	004	022	013	015	R		IN	IN
001	N45W	88SW	148	020	002	015	R	NW	IN	IN
001	N46E	90NW	007	017	044	017	R		IN	IN
001	N46E	90NW	027	029	060	020	R		IM	IN
001	N45W	88SW	084	021	007	021	P	NW	IN	IN
001	N45W	88SW	074	022	002	022	R	NW	IN	IN
001	N45W	88SW	075	039	005	020	R	NW	IN	IN
001	N46E	90NW	007	015	014	015	R		IN	IN
001	N46E	90NW	009	008	014	009	R		IN	IN
001	N46E	90NW	012	008	022	008	R		IN	IN
002	N84W	81SW	013	002	007	002	R	EW	IN	IN
002	N30E	90NW	026	003	003	003	R	NE	IN	IN
002	N84W	81SW	005	002	005	002	R	EW	IN	IN
002	N45W	90SW	010	125		003	R	NW	IN	IN
002	N20E	90NW	110	070	010	004	R		IN	IN
002	N20E	90NW	087	065	003	004	R		IN	IN
002	N78W	90SW	007	005		005	R		IN	IN
002	N60W	90SW	023	010	007	010	R		IN	IN
002	N60W	90SW	063	011	015	011	R		IN	IN
002	N45W	90SW	027	007		007	R	NW	IN	IN
002	N45W	90SW	035	007	002	007	R	NW	IN	IN
002	N80E	80SE	040	012	045	012	R	EW	IN	IN
002	N30E	90NW	024	001	008	001	R	NE	IN	IN
002	N30E	90NW	020	001	005	001	R	NE	IN	IN
002	N30E	90NW	021	001	008	001	R	NE	IN	IN
002	N30E	90NW	018	001	004	001	R	NE	IN	IN
002	N45W	90SW	100	010	016	010	R	NW	IN	IN
002	N70W	90SW	027	005	016	005	R		IN	IN
002	N30E	90NW	016	001	008	001	R	NE	IN	IN
002	N30E	90NW	005	001	006	001	R	NE	IN	IN
002	N84W	81SW	022	003	016	003	R	EW	IN	IN
002	N84W	81SW	036	002	015	002	R	EW	IN	IN
002	N84W	81SW	020	004	010	004	R	EW	IN	IN
002	N84W	81SW	010	004	004	004	R	EW	IN	IN
002	N84W	81SW	023	004	010	004	R	EW	IN	IN
003	N34E	90NW	028	015	033	015	P	NE	IN	IN
003	N34E	90NW	035	015	017	015	P	NE	IN	IN
003	N34E	90NW	055	015	020	015	P	NE	IN	IN
003	N34E	90NW	045	015	008	015	P	NE	IN	IN
003	N34E	90NW	054	015	024	015	P	NE	IN	IN
003	N87E	80NW	153	015	030	015	R	EW	IN	IN
003	N87E	80NW	055	015	020	015	R	EW	IN	IN
003	N87E	80NW	036	015	022	015	R	EW	IN	IN
003	N87E	80NW	070	015	020	015	R	EW	IN	IN
003	N87E	80NW	033	015	016	015	R	EW	IN	IN
003	N87E	80NW	078	015	016	015	R	EW	IN	IN

STA	STRI	DIP	LNG	DTH	SPA	BED	EX	ST	LO	GR
003	N34E	90NW	012	003	007	003	R	NE	IN	IN
003	N34E	90NW	010	003	004	003	P	NE	IN	IN
003	N34E	90NW	007	006	008	006	P	NE	IN	IN
003	N87E	80NW	013	006	011	006	P	NE	IN	IN
003	N60W	85SW	105	044	030	006	P		IN	IN
004	N45W	88NE	135	048	050	010	P	NW	IN	IN
004	N45W	83NE	107	020	020	010	P	NW	IN	IN
004	N45W	88NE	175	015	005	010	P	NW	IN	IN
004	N50E	90NW	001	008	036	008	R		IN	IN
004	N50E	90NW	003	026	035	010	R		IN	IN
004	N50E	90NW	020	010	007	010	P		IN	IN
004	N50E	90NW	025	010	012	010	R		IN	IN
005	N55W	73NE	007	005	011	005	P	NW	IN	IN
005	N40E	15SE	007	007	007	007	R	NE	IN	IN
005	N55W	73NE	015	007	008	007	P	NW	IN	IN
005	N40E	15SE	005	007	003	007	P	NE	IN	IN
005	N40E	15SE	005	005	004	005	R	NE	IN	IN
005	N40E	15SE	001	005	002	005	P	NE	IN	IN
005	N55W	73NE	011	005	005	005	P	NW	IN	IN
005	N55W	73NE	020	006	007	006	R	NW	IN	IN
005	N84E	77SE	022	014	005	014	R	EW	IN	IN
005	N84E	77SE	042	003	005	003	P	EW	IN	IN
005	N84E	77SE	019	008	010	008	P	EW	IN	IN
005	N84E	77SE	024	010	002	010	R	EW	IN	IN
005	N50W	70NE	021	008	011	008	P	NW	IN	IN
005	N50W	70NE	026	015	007	010	R	NW	IN	IN
005	N50W	70NE	045	024	012	024	P	NW	IN	IN
005	N40E	15SE	025	024	033	024	R	NE	IN	IN
005	N40E	15SE	027	030	039	024	P	NE	IN	IN
005	N60W	70NE	032	016	003	010	P		IN	IN
005	N55W	73NE	022	010	008	010	R	NW	IN	IN
005	N40E	15SE	018	020	005	005	R	NE	IN	IN
006	N45W	82NE	007	012	015	012	P	NW	IN	IN
006	N45W	82NE	018	014	020	012	R	NW	IN	IN
006	N45W	82NE	009	020	015	010	R	NW	IN	IN
006	N45W	82NE	009	020	022	010	P	NW	IN	IN
006	N45W	82NE	007	017	012	010	P	NW	IN	IN
006	N45W	82NE	006	021	023	010	R	NW	IN	IN
006	N45W	82NE	035	021	016	011	R	NW	IN	IN
006	N45W	82NE	012	050	009	011	P	NW	IN	IN
006	N45W	82ND	005	020	007	011	P	NW	IN	IN
006	N45W	82NE	050	033	023	033	P	NW	IN	IN
006	N45W	82NE	022	006	010	006	P	NW	IN	IN
006	N45W	82NE	030	006	013	006	P	NW	IN	IN
006	N45W	82NE	031	006	012	006	P	NW	IN	IN
006	N45W	82NE	012	006	011	006	P	NW	IN	IN
006	N40E	56SE	010	006	010	006	R	NE	IN	IN

STA	STRI	DIP	LNG	DTH	SPA	BED	EX	ST	LO	GR
006	N40E	56SE	011	006	023	006	R	NE	IN	IN
006	N40E	56SE	010	010	011	010	R	NE	IN	IN
006	N40E	56SE	033	014	003	014	R	NE	IN	IN
007	N23W	90SW	104	019	023	019	P		IN	IN
007	N23W	90SW	033	019	022	019	R		IN	IN
007	N23W	90SW	016	019	017	019	P		IN	IN
007	N23W	90SW	001	019	010	019	P		IN	IN
007	N23W	90SW	018	019	011	019	R		IN	IN
007	N23W	90SW	012	019	022	019	R		IN	IN
007	N23W	90SW	022	019	017	019	R		IN	IN
007	N69E	90NW	260	090	048	025	R		IN	IN
007	N69E	90NW	250	048	017	017	R		IN	IN
007	N23W	90SW	010	005	012	005	R		IN	IN
007	N23W	90SW	008	005	014	003	R		IN	IN
007	N23W	90SW	001	008	002	003	P		IN	IN
007	N23W	90SW	001	020	005	005	R		IN	IN
007	N69E	90NW	043	021	011	021	R		IN	IN
007	N69E	90SE	001	034	015	034	R		IN	IN
007	N69E	90NW	015	007	040	007	R		IN	IN
007	N69E	90NW	007	007	041	007	P		IN	IN
007	N69E	90NW	002	007	060	007	P		IN	IN
007	N69E	90NW	002	007	065	007	P		IN	IN
007	N69E	90NW	032	010	010	010	R		IN	IN
007	N69E	90NW	010	010	009	010	R		IN	IN
008	N35E	90NW	010	011	010	011	R	NE	IN	IN
008	N75W	90SW	600	070	055	038	R		IN	IN
008	N35E	90NW	011	011	028	011	P	NE	IN	IN
008	N35E	90NW	011	011	015	011	R	NE	IN	IN
008	N35E	90NW	012	011	035	011	R	NE	IN	IN
008	N35E	90NW	009	011	021	011	R	NE	IN	IN
008	N85W	56NE	038	020	048	020	P	EW	IN	IN
008	N85W	56NE	165	011	050	011	R	EW	IN	IN
008	N35E	90NW	015	004	013	004	R	NE	IN	IN
008	N35E	90NW	001	004	013	004	R	NE	IN	IN
008	N35E	90NW	001	004	010	004	R	NE	IN	IN
008	N35E	90NW	017	007	014	007	R	NE	IN	IN
008	N35E	90NW	016	007	007	007	R	NE	IN	IN
008	N35E	90NW	014	015	020	015	P	NE	IN	IN
008	N53W	90SW	500	115		060	R	NW	IN	IN
008	N53W	90SW	500	233		085	R	NW	IN	IN
009	N74E	90NW	060	013	008	013	S		IN	IN
009	N74E	90NW	080	013	034	013	S		IN	IN
009	N74E	90NW	080	013	017	013	S		IN	IN
009	N74E	90NW	065	013	020	013	S		IN	IN
009	N74E	90NW	070	013	010	013	S		IN	IN
009	N74E	90NW	051	013	007	013	S		IN	IN
009	N74E	90NW	040	013	020	013	S		IN	IN

STA	STRI	DIP	LNG	DTH	SPA	BED	EX	ST	LO	GR
009	N74E	90NW	041	013	030	013	S		IN	IN
009	N74E	90NW	007	008	020	008	S		IN	IN
009	N35W	90SW	040	008	030	008	S	NW	IN	IN
009	N35W	90SW	063	013	037	013	S	NW	IN	IN
009	N35W	90SW	042	013	013	013	S	NW	IN	IN
009	N35W	90SW	043	013	021	013	S	NW	IN	IN
009	N35W	90SW	070	013	021	013	S	NW	IN	IN
010	N52W	90SW	105	007	010	007	R	NW	IN	IN
010	N52W	90SW	125	007	002	007	R	NW	IN	IN
010	N52W	90SW	029	007	009	007	R	NW	IN	IN
010	N52W	90SW	040	011	006	011	R	NW	IN	IN
010	N52W	90SW	022	011	010	011	R	NW	IN	IN
010	N52W	90SW	228	070	003	011	R	NW	IN	IN
010	N52E	90NW	001	007	043	007	R		IN	IN
010	N52E	90NW	001	007	011	007	R		IN	IN
010	N52E	90NW	001	007	023	007	R		IN	IN
010	N52E	90NW	010	007	026	007	R		IN	IN
010	N52E	90NW	001	007	043	007	R		IN	IN
010	N52E	90NW	005	007	024	007	R		IN	IN
010	N52E	90NW	009	007	046	007	R		IN	IN
010	N52E	90NW	001	007	038	007	R		IN	IN
010	N52E	90NW	001	007	031	007	R		IN	IN
010	N52E	90NW	001	007	030	007	R		IN	IN
010	N52E	90NW	001	010	021	010	R		IN	IN
010	N52E	90NW	001	010	020	010	R		IN	IN
010	N52E	90NW	001	010	024	010	R		IN	IN
011	N46W	87SW	057	018	030	018	R	NW	IN	IN
011	N46W	87SW	161	030	028	030	R	NW	IN	IN
011	N46W	87SW	022	009	028	009	R	NW	IN	IN
011	N46W	87SW	022	009	018	009	R	NW	IN	IN
011	N46W	87SW	105	030	025	030	R	NW	IN	IN
011	N46W	87SW	098	023	054	023	R	NW	IN	IN
011	N46W	87SW	050	023	020	023	R	NW	IN	IN
012	N48W	90SW	025	105	012	012	R	NW	IN	IN
012	N48W	90SW	020	057	012	012	R	NW	IN	IN
012	N48W	90SW	020	012	030	012	R	NW	IN	IN
012	N48W	90SW	120	130	080	012	R	NW	IN	IN
012	N65E	90NW	075	012	035	012	R		IN	IN
012	N65E	90NW	016	013	014	013	R		IN	IN
012	N21E	86SE	045	037		012	R		IN	IN
012	N46E	73NW	047	024	009	017	R		IN	IN
012	N46E	73NW	088	017	011	017	R		IN	IN
012	N48W	90SW	160	060	018	030	R	NW	IN	IN
012	N48W	90SW	015	028	022	011	R	NW	IN	IN
012	N48W	90SW	002	030		010	R	NW	IN	IN
012	N30E	90NW	057	020	004	008	R	NE	IN	IN
012	N28E	84NW	023	027	030	012	R	NE	IN	IN

STA	STRI	DIP	LNG	DTH	SPA	BED	EX	ST	LO	GR
012	N88W	90SW	030	002	005	002	R	EW	IN	IN
012	N88W	90SW	013	007	010	007	R	EW	IN	IN
012	N88W	90SW	014	007	025	007	R	EW	IN	IN
012	N55E	90NW	180	040		040	R		IN	IN
012	N55W	90SW	079	112		040	R	NW	IN	IN
012	N55W	90SW	150	040		040	R	NW	IN	IN
012	N55W	90SW	200	080	060	040	R	NW	IN	IN
013	N68W	90SW	039	058	023	047	R		IN	IN
013	N86W	90SW	038	038	043	038	R	EW	IN	IN
013	N68W	90SW	001	027	003	027	R		IN	IN
013	N68W	90SW	001	047	046	047	R		IN	IN
013	N68W	90SW	003	055	012	055	R		IN	IN
013	N68W	90SW	001	055	023	055	R		IN	IN
013	N68W	90SW	042	018	043	018	R		IN	IN
013	N68W	90SW	027	018	040	018	R		IN	IN
013	N68W	90SW	010	027	037	018	R		IN	IN
013	N68W	90SW	030	018	020	018	R		IN	IN
013	N68W	90SW	005	018	022	018	R		IN	IN
013	N78W	90SW	023	026	028	007	R		IN	IN
013	N78W	90SW	014	005	020	005	R		IN	IN
013	N78W	90SW	010	005	016	005	R		IN	IN
013	N20W	81SW	052	010		010	R		IN	IN
014	N75W	85NE					R		IN	IN
015	N73W	55NE	096	015	029	003	R		IN	IN
015	N73W	55NE	040	006		003	R		IN	IN
015	N73W	55NE	020	007	012	003	R		IN	IN
015	N73W	55NE	012	007	013	003	R		IN	IN
015	N73W	55NE	020	007	022	003	R		IN	IN
015	N73W	55NE	045	007	011	003	R		IN	IN
015	N73W	55NE	045	010	028	003	R		IN	IN
015	N73W	55NE	045	010	038	003	R		IN	IN
015	N73W	55NE	037	010	040	003	R		IN	IN
015	N73W	55NE	035	010	033	003	R		IN	IN
015	N73W	55NE	029	010	025	003	R		IN	IN
016	N49W	76SW	060	050	074	050	R	NW	IN	IN
016	N46W	75SW	138	120	052	065	R	NW	IN	IN
016	N46W	75SW	092	055	049	055	R	NW	IN	IN
016	N46W	75SW	061	040	037	040	R	NW	IN	IN
016	N46W	74SW	064	065	024	060	R	NW	IN	IN
016	N46W	75SW	034	051	026	051	R	NW	IN	IN
016	N46W	75SW	071	035	033	035	R	NW	IN	IN
016	N46W	75SW	045	022	035	022	R	NW	IN	IN
016	N46W	75SW	070	054	078	054	R	NW	IN	IN
016	N46W	75SW	101	075	116	045	R	NW	IN	IN
016	N46W	75SW	083	052	077	052	R	NW	IN	IN
016	N46W	75SW	105	038	045	038	R	NW	IN	IN
016	N46W	75SW	095	038	029	038	R	NW	IN	IN

STA	STRI	DIP	LNG	DTH	SPA	BED	EX	ST	IO	GE
016	N46W	75SW	010	038	045	045	R	NW	IM	IN
016	N60E	78SE	014	008	021	008	R		IN	IN
016	N60E	72SE	003	008	028	008	R		IN	IN
017	N62E	78SE	006	008	041	008	R		BR	OT
017	N62E	78SE	018	008	057	008	R		BR	OT
017	N62E	78SE	018	012	039	010	R		BR	OT
017	N62E	78SE	001	012	026	010	R		BR	OT
017	N62E	78SE	014	010	046	010	R		BR	OT
017	N62E	78SE	008	010	030	010	R		BR	OT
017	N62E	78SE	014	006	038	003	R		BR	OT
017	N62E	78SE	014	006	035	006	R		BR	OT
017	N62E	78SE	002	006	040	006	R		BR	OT
017	N62E	78SE	001	006	035	006	R		BR	OT
018	N42W	75SW	061	004	055	004	R	NW	BR	OT
018	N42W	75SW	024	004	028	004	R	NW	BR	OT
018	N42W	75SW	034	012	045	012	R	NW	BR	OT
018	N42W	75SW	012	010	030	010	R	NW	BR	OT
018	N13E	90NW	043	004	018	004	R		BR	OT
018	N42W	75SW	020	014	014	004	R	NW	BR	OT
018	N42W	75SW	075	004	024	004	R	NW	BR	CT
018	N42W	75SW	028	008	028	008	R	NW	BR	OT
018	N42W	75SW	102	016	044	016	R	NW	BR	OT
018	N13E	90NW	058	016		016	R		BR	OT
018	N87E	90NW	015	001	007	001	R	EW	BR	OT
018	N87E	90NW	012	001		001	R	FW	BR	OT
018	N25E	90NW	087	005	052	005	R	NE	BR	OT
018	N45W	74SW	065	010	060	010	R	NW	BR	OT
018	N45W	75SW	059	049	040	005	R	NW	BR	OT
018	N45W	74SW	030	005	067	005	R	NW	BR	OT
018	N45W	74SW	050	005	059	005	R	NW	BR	OT
019	N33E	73NW	026	005	012	005	R	NE	BR	OT
019	N33E	73NW	013	005	010	005	R	NE	BR	OT
019	N33E	73NW	014	005	010	005	R	NE	BR	OT
019	N33E	73NW	026	005	013	005	R	NE	BR	OT
019	N33E	73NW	019	005	010	005	R	NE	BR	OT
019	N33E	73NW	015	004	005	004	R	NE	BR	OT
019	N33E	73NW	016	004	007	004	R	NE	BR	OT
019	N33E	73NW	016	004	010	004	R	NE	BR	OT
019	N33E	73NW	012	004	007	004	R	NE	BR	OT
019	N33E	73NW	012	003	008	003	R	NE	BR	OT
019	N33E	73NW	001	003	005	003	R	NE	BR	OT
019	N33E	73NW	015	005	012	005	R	NE	BR	OT
019	N33E	73NW	018	005	005	005	R	NE	BR	OT
019	N50W	88SW	005	004	023	004	R	NW	BR	OT
019	N50W	88SW	007	005	015	005	R	NW	BR	OT
019	N50W	88SW	001	005	015	005	R	NW	BR	OT
019	N50W	88SW	001	006	016	006	R	NW	BR	OT

STA	STRI	DIP	LNG	DTH	SPA	BED	EX	ST	LO	GR
019	N50W	88SW	001	006	014	006	R	NW	BR	OT
019	N50W	88SW	006	002	015	002	R	NW	BR	OT
019	N50W	88SW	007	002	011	002	R	NW	FR	OT
019	N50W	88SW	009	003	010	003	R	NW	BR	OT
019	N50W	88SW	006	003	007	003	R	NW	BR	OT
020	N24E	68SE	048	004	007	004	R		BR	OT
020	N35E	67SE	075	009		009	R	NE	BR	OT
020	N35E	66SE	010	007	003	007	R	NE	BR	OT
020	N49W	75SW	007	023	030	004	R	NW	BR	OT
020	N49W	75SW	017	011	065	004	R	NW	BR	OT
020	N49W	75SW	001	013	048	008	R	NW	PR	OT
020	N49W	75SW	001	013	050	008	R	NW	BR	OT
020	N24E	68SE	183	013	003	008	R		BR	OT
020	N24E	68SE	103	008		008	R		BR	OT
020	N05E	58NW	089	026		015	R		BR	OT
020	N05E	58NW	089	014	008	005	R		BR	OT
020	N05E	58NW	035	019	007	008	R		BR	OT
020	N05E	58NW	053	054	019	008	R		BR	OT
020	N05E	58NW	057	041		005	R		BR	OT
020	N05E	58NW	024	007	005	007	R		BR	OT
021	N37W	85SW	048	024	025	024	R	NW	BR	OT
021	N12E	67NW	066	026	023	026	R		PR	OT
021	N12E	67NW	064	023	004	023	R		BR	OT
021	N12E	67NW	119	023		023	R		BR	OT
021	N12E	67NW	078	023	030	023	R		PR	OT
021	N12E	67NW	045	023	004	023	R		BB	OT
021	N12E	67NW	078	023		023	R		BR	OT
021	N37W	85SW	035	010	024	010	R	NW	BR	OT
021	N37W	85SW	032	012	032	012	P	NW	BR	OT
021	N37W	85SW	006	011	016	001	R	NW	BR	OT
021	N37W	85SW	032	019	031	019	R	NW	BR	OT
021	N37W	85SW	070	023	030	023	R	NW	BF	OT
021	N37W	85SW	037	011	029	011	R	NW	BB	OT
021	N37W	85SW	037	022	026	022	R	NW	BP	OT
021	N37W	85SW	034	022	019	022	R	NW	BR	OT
021	N70W	90SW	007	021	006	021	R		BR	OT
021	N70W	90SW	001	024	004	024	R		BR	OT
021	N70W	90SW	001	024	003	024	R		BR	OT
021	N70W	90SW	001	024	007	024	R		BR	OT
021	N70W	90SW	001	024	008	024	R		BP	OT
021	N70W	90SW	001	024	009	024	R		BP	OT
021	N70W	90SW	001	024	008	024	R		BB	OT
021	N70W	90SW	001	024	026	024	R		BB	OT
022	N57E	78NW	062	039	029	039	R		SO	OT
022	N16E	77SE	040	039	084	039	R		SO	OT
022	N57E	78NW	050	039		039	R		SO	OT
022	N57E	78NW	125	028	025	028	R		SO	OT

STA	STRI	DIP	LNG	DTH	SPA	BED	EX	ST	LO	GR
022	N57E	78NW	012	037	044	037	R		SO	OT
022	N57E	78NW	027	037	057	037	R		SO	OT
022	N57E	78NW	038	037	018	037	R		SO	OT
022	N16E	77SE	003	007	029	007	R		SO	OT
022	N16E	77SE	030	007	018	007	R		SO	OT
022	N57E	78NW	055	025		025	P		SO	OT
022	N16E	77SE	045	025	075	025	R		SO	OT
022	N16E	77SE	080	025	052	025	R		SO	OT
023	N10E	90NW	025	005	018	005	R		SO	OT
023	N10E	90NW	014	005	028	005	R		SO	OT
023	N10E	90NW	012	005	028	005	R		SO	OT
023	N10E	90NW	009	005	014	005	R		SO	OT
023	N40E	90NW	017	005	023	005	R	NE	SO	OT
023	N40E	90NW	019	005	024	005	R	NE	SO	OT
023	N40E	90NW	014	005	030	005	R	NE	SO	OT
023	N45W	73SW	071	012		012	R	NW	SO	OT
023	N45W	73SW	087	009		009	R	NW	SO	OT
023	N13W	75SW	030	006	013	006	R		SO	OT
023	N13W	75SW	005	006	015	006	P		SO	OT
023	N40E	90NW	017	007	023	007	R	NE	SO	OT
023	N40E	90NW	007	007	005	007	R	NE	SO	OT
023	N40E	90NW	017	007	015	007	R	NE	SO	OT
023	N40E	90NW	010	007	015	007	R	NE	SO	OT
023	N45W	73SW	200	050	025	007	R	NW	SO	OT
024	N08W	70SW	020	007	022	007	R		SO	OT
024	N08W	70SW	021	007	022	007	R		SO	OT
024	N08W	70SW	020	010	022	010	R		SO	OT
024	N08W	70SW	020	002	020	002	R		SO	OT
024	N08W	72SW	044	009	043	009	R		SO	OT
024	N28E	90NW	015	003	025	003	P	NE	SO	OT
024	N28E	90NW	007	005	027	005	R	NE	SO	OT
024	N08W	72SW	010	006	014	006	P		SO	OT
024	N08W	72SW	017	008		008	R		SO	OT
024	N08W	72SW	049	014	022	014	R		SO	OT
024	N08W	72SW	026	014	018	004	R		SO	OT
024	N10E	65SW	014	005	023	005	R		SO	OT
024	N20E	77NW	007	007	002	007	R		SO	OT
024	N20E	77NW	010	008	008	008	R		SO	OT
025	N10W	69SW	012	017	009	017	R		SO	OT
025	N02E	69SE	006	017	005	017	R		SO	OT
025	N07W	69SW	002	017	008	017	P		SO	OT
025	N07W	69SW	010	017	013	017	R		SO	OT
025	N07W	69SW	010	010	023	010	P		SO	OT
025	N07W	69SW	017	010	014	010	R		SO	OT
025	N07W	69SW	040	025	052	025	R		SO	OT
025	N07W	69SW	057	025	018	025	R		SO	OT
025	N07W	69SW	047	110	026	025	R		SO	OT

STA	STRI	DIP	LNG	DTH	SPA	BED	EX	ST	LO	GR
025	N07W	69SW	023	004	008	004	R		SO	OT
025	N07W	69SW	009	004	018	004	R		SO	OT
025	N18E	61NW	027	006	006	006	R		SO	OT
025	N18E	61NW	010	006	004	006	R		SO	OT
025	N18E	61NW	017	006	007	006	R		SO	OT
025	N18E	61NW	010	006	004	006	R		SO	OT
025	N18E	61NW	020	008	004	008	R		SO	OT
025	N18E	61NW	007	008	005	008	R		SO	OT
025	N18E	61NW	001	008	008	008	R		SO	OT
025	N18E	61NW	001	008	009	008	R		SO	OT
025	N18E	61NW	001	008	009	008	R		SO	OT
026	N38W	90SW	413	018	010	018	R	NW	IN	IN
026	N80E	60SE	001	018	042	018	R	EW	IN	IN
026	N80E	60SE	001	018	057	018	R	EW	IN	IN
026	N80E	60SE	001	018	029	018	R	EW	IN	IN
026	N80E	60SE	001	018	059	018	R	EW	IN	IN
026	N35W	90SW	057	019	023	029	R	NW	IN	IN
026	N35W	90SW	048	019	013	019	R	NW	IN	IN
026	N35W	90SW	099	019	013	019	R	NW	IN	IN
026	N35W	90SW	099	019	012	019	R	NW	IN	IN
026	N35W	90SW	090	019	014	019	R	NW	IN	IN
026	N35W	90SW	057	019	010	019	R	NW	IN	IN
026	N35W	90SW	056	019	018	019	R	NW	IN	IN
026	N35W	90SW	120	019	024	019	R	NW	IN	IN
026	N80E	60SE	009	009	028	009	R	EW	IN	IN
026	N80E	60SE	003	009	026	009	R	EW	IN	IN
026	N80E	60SE	003	009	015	009	R	EW	IN	IN
026	N80E	60SE	001	009	012	009	R	EW	IN	IN
026	N80E	60SE	003	009	035	009	R	EW	IN	IN
026	N80E	60SE	016	009	013	009	R	EW	IN	IN
026	N80E	60SE	003	009	032	009	R	EW	IN	IN
026	N80E	60SE	003	009	035	009	R	EW	IN	IN
026	N38W	90SW	014	006	019	006	R	NW	IN	IN
026	N38W	90SW	008	103	015	006	R	NW	IN	IN
026	N38W	90SW	005	006	015	006	R	NW	IN	IN
027	N71W	90SW	114	012		012	R		IN	IN
027	N06W	90SW	127	010		010	R		IN	IN
027	N71W	90SW	022	007		007	R		IN	IN
027	N71W	90SW	032	011		011	R		IN	IN
027	N45E	90NW	038	013		013	R	NE	IN	IN
028	N50W	90SW	075	015	009	015	R	NW	IN	IN
028	N50W	90SW	078	017	014	017	R	NW	IN	IN
028	N50W	90SW	075	013		013	R	NW	IN	IN
028	N50W	90SW	091	008		008	R	NW	IN	IN
028	N50W	90SW	020	010	015	010	R	NW	IN	IN
028	N50W	90SW	025	008		008	R	NW	IN	IN
028	N50W	90SW	129	006		006	R	NW	IN	IN

STA	STRI	DIP	LNG	DTH	SPA	BED	EX	ST	LO	GR
028	N77W	74NE	050	013	027	013	R		IN	IN
028	N75W	75NE	072	014	011	014	R		IN	IN
028	N77W	79NE	025	009	011	009	R		IN	IN
028	N77W	79NE	001	009	005	009	R		IN	IN
028	N77W	78NE	030	009	003	003	R		IN	IN
028	N77W	78NE	022	004	011	004	R		IN	IN
028	N77W	78NE	048	004	016	004	R		IN	IN
028	N77W	78NE	020	004	008	004	R		IN	IN
028	N77W	78NE	015	004	006	004	R		IN	IN
028	N77W	78NE	015	003	009	003	R		IN	IN
028	N77W	78NE	028	015	022	004	R		IN	IN
029	N85E	85NW	139	021		021	R	EW	IN	IN
029	N45W	78SW	094	011		011	R	NW	IN	IN
029	N40W	80SW	083	032	008	032	R	NW	IN	IN
029	N40W	80SW	036	032	010	032	R	NW	IN	IN
029	N40W	80SW	042	032	031	032	R	NW	IN	IN
029	N40W	80SW	037	025	005	025	R	NW	IN	IN
029	N40W	80SW	154	025		025	R	NW	IN	IN
029	N40W	80SW	041	012	009	012	R	NW	IN	IN
029	N40W	80SW	047	012	013	012	R	NW	IN	IN
029	N40W	80SW	070	018	020	018	R	NW	IN	IN
029	N40W	80SW	015	012	008	012	R	NW	IN	IN
029	N40W	80SW	074	012		012	R	NW	IN	IN
029	N85E	85NW	052	019	011	007	R	EW	IN	IN
029	N85E	85NW	100	018	004	018	R	EW	IN	IN
029	N85E	85NW	195	030		030	R	EW	IN	IN
030	N59W	90SW	017	003	020	003	R		IN	IN
030	N59W	90SW	019	002	012	002	R		IN	IN
030	N59W	90SW	021	002	027	002	R		IN	IN
030	N59W	90SW	020	003	020	003	R		IN	IN
031	N42W	83SW	058	046	103	046	R	NW	IN	IN
031	N87W	85SW	045	069		033	R	EW	IN	IN
031	N65W	89NE	054	028	016	028	R		IN	IN
031	N65W	89NE	012	028		028	R		IN	IN
031	N87W	85SW	030	036	057	036	R	EW	IN	IN
031	N87W	85SW	010	050		050	R	EW	IN	IN
031	N87W	85SW	010	022	045	022	R	EW	IN	IN
031	N87W	85SW	017	024	022	024	R	EW	IN	IN
031	N87W	85SW	005	050		050	R	EW	IN	IN
031	N87W	85SW	017	101	044	050	R	EW	IN	IN
031	N38W	88SW	102	078	058	078	R	NW	IN	IN
031	N42W	83NE	120	078	076	078	R	NW	IN	IN
031	N42W	83NE	078	043	037	043	R	NW	IN	IN
031	N42W	83NE	045	042	044	042	R	NW	IN	IN
031	N42W	83NE	047	026	050	026	R	NW	IN	IN
032	N89E	83NW	024	020	028	020	R	EW	IN	IN
032	N89E	83NW	011	019		019	R	EW	IN	IN

STA	STRI	DIP	LNG	DTH	SPA	BED	EX	ST	LO	GR
032	N89E	83NW	011	008	017	008	R	EW	IN	IN
032	N89E	83NW	010	002	017	002	R	EW	IN	IN
032	N89E	83NW	005	005	013	005	R	EW	IN	IN
032	N89E	83NW	012	003	007	003	R	EW	IN	IN
032	N89E	83NW	022	013	034	013	R	EW	IN	IN
032	N89E	83NW	010	022	075	022	R	EW	IN	IN
032	N89E	83NW	015	022	048	022	R	EW	IN	IN
033	N83W	90SW	037	018	025	018	P	EW	IN	IN
033	N83W	90SW	012	018	020	018	R	EW	IN	IN
033	N83W	90SW	021	014	014	014	R	EW	IN	IN
033	N83W	90SW	007	006	011	006	R	EW	IN	IN
033	N83W	90SW	021	006	012	006	R	EW	IN	IN
033	N83W	90SW	006	010	008	010	R	EW	IN	IN
033	N83W	90SW	027	016	018	016	R	EW	IN	IN
033	N83W	90SW	087	019	024	019	R	EW	IN	IN
033	N83W	90SW	053	018	024	018	R	EW	IN	IN
033	N83W	90SW	056	025	032	025	R	EW	IN	IN
035	N47W	90SW	300				SC	NW	IN	IN
035	N24E	45SE	200		090		SC		IN	IN
035	N24E	45SE	200		059		SC		IN	IN
035	N24E	45SE	040		029		SC		IN	IN
035	N02E	45SE	040		021		SC		IN	IN
035	N02E	45SE	016		031		SC		IN	IN
035	N02E	45SE	023		011		SC		IN	IN
035	N55W	90SW	048	017	047	010	SC	NW	IN	IN
035	N55W	90SW	017	010	009	010	SC	NW	IN	IN
035	N55W	90SW	030	010	025	010	SC	NW	IN	IN
035	N55W	90SW	039	010	035	010	SC	NW	IN	IN
035	N85W	90SW	020	010	036	010	SC	EW	IN	IN
035	N85W	90SW	047	010	029	010	SC	EW	IN	IN
035	N85W	90SW	036	010	016	010	SC	EW	IN	IN
035	N85W	90SW	036	010	037	010	SC	EW	IN	IN
035	N68W		077				SC		IN	IN
036	N48W	84SW	029	018	010	007	R	NW	IN	IN
036	N81E	82SE	002	007	011	007	R	EW	IN	IN
036	N43E	57NW	012	007	017	007	R	NE	IN	IN
036	N48W	84SW	001	018	020	007	R	NW	IN	IN
036	N48W	84SW	029	018	016	007	R	NW	IN	IN
036	N48W	84SW	021	007		007	R	NW	IN	IN
036	N81E	82SE	012	007	010	007	R	EW	IN	IN
036	N81E	82SE	017	007	055	007	R	EW	IN	IN
036	N48W	84SW	086	019	022	007	R	NW	IN	IN
036	N48W	84SW	031	007	008	007	R	NW	IN	IN
036	N48W	84SW	001	007	008	007	R	NW	IN	IN
036	N48W	84SW	001	007	008	007	R	NW	IN	IN
036	N81E	82SE	010	007		007	R	EW	IN	IN
036	N43E	57NW	001	007	037	007	R	NE	IN	IN

STA	STRI	DIP	LNG	DTH	SPA	RFD	EX	ST	LO	GR
036	N43E	57NW	001	007	005	007	P	NE	IN	IN
036	N43E	57NW	001	007	018	007	R	NE	IN	IN
036	N48W	84SW	015	003	009	003	R	NW	IN	IN
036	N48W	84SW	003	003	005	003	R	NW	IN	IN
036	N48W	84SW	001	003	010	003	R	NW	IN	IN
036	N48W	84SW	001	003	003	003	R	NW	IN	IN
036	N43E	57NW	019	005	013	005	P	NE	IN	IN
036	N43W	57NW	015	005	014	005	P	NW	IN	IN
036	N81E	82SE	014	005	021	005	R	EW	IN	IN
036	N81E	82SE	018	016	009	005	R	EW	IN	IN
037	N65W	90SW					R		IN	IN
037	N18E	90NW					R		IN	IN
038	N57W	90SW	500	019		019	R		IN	IN
038	N57W	90SW	043	006	012	006	R		IN	IN
038	N57W	90SW	014	006	015	006	P		IN	IN
038	N57W	90SW	007	006	012	006	R		IN	IN
038	N57W	90SW	019	006	010	006	R		IN	IN
038	N57W	90SW	052	006	006	006	R		IN	IN
038	N57W	90SW	250	008	023	008	R		IN	IN
038	N57W	90SW	117	016	020	016	R		IN	IN
039							P		IN	IN
040	N53W	90SW					P	NW	IN	IN
040	N46W	90SW					R	NW	IN	IN
040	N45W	90SW					R	NW	IN	IN
040	N72W	88NE		150			R		IN	IN
040	N80W	90SW					R	NW	IN	IN
040	N51W	90SW					R		IN	IN
040	N73W	90SW					R		IN	IN
040	N74W	90SW					R		IN	IN
040	N80W	90SW		150	015		R	EW	IN	IN
041	N80W	88NE		150			R	EW	IN	IN
041	N25E	90NW					R	NE	IN	IN
041	N25E	90NW	180	090		090	R	NE	IN	IN
041	N25E	90NW		200			P	NE	IN	IN
042	N53W	90SW	035	006	020	006	R	NW	IN	IN
042	N55W	90SW	010	025	028	012	R	NW	IN	IN
042	N53W	90SW	020	150		012	R	NW	IN	IN
042	N53W	90SW	029	048		012	R	NW	IN	IN
042	N53W	90SW	015	012	020	012	R	NW	IN	IN
042	N53W	90SW	050	120	057	020	R	NW	IN	IN
042	N53W	90SW	020	110	040	020	R	NW	IN	IN
042	N53W	90SW	015	050	040	020	R	NW	IN	IN
043	N46W	90SW	005	064	020	020	R	NW	IN	IN
043	N46W	90SW	005	065	050	020	R	NW	IN	IN
043	N46W	90SW	012	063	027	020	R	NW	IN	IN
043	N46W	90SW	063	051		051	R	NW	IN	IN
043	N46W	90SW	012	006	016	006	R	NW	IN	IN

STA	STRI	DIP	LNG	DTH	SPA	BED	EX	ST	LO	GR
043	N46W	90SW	009	006	018	006	R	NW	IN	IN
043	N46W	90SW	004	058	029	058	R	NW	IN	IN
043	N46W	90SW	029	019	023	019	R	NW	IN	IN
044	N48W	90SW	210	185		025	R	NW	IN	IN
044	N48W	90SW	104	100		025	R	NW	IN	IN
044	N48W	90SW	200	101		050	R	NW	IN	IN
044	N48W	90SW	500	050		030	R	NW	IN	IN
044	N48W	90SW	001	062	005	026	R	NW	IN	IN
044	N48W	90SW	001	062	075	026	R	NW	IN	IN
045	N65W	90SW	125	092	030	015	R		IN	IN
045	N65W	90SW	025	149		015	R		IN	IN
045	N65W	90SW	003	010	006	003	R		IN	IN
045	N65W	90SW	003	010	005	003	R		IN	IN
045	N65W	90SW	001	010	007	003	R		IN	IN
045	N65W	90SW	001	010	010	003	R		IN	IN
045	N65W	90SW	001	010	006	003	R		IN	IN
046	N85W	90SW	012	182	052	020	R	EW	IN	IN
046	N85W	90SW	007	190	028	020	R	EW	IN	IN
046	N85W	90SW	015	146	007	020	R	EW	IN	IN
046	N85W	90SW	001	097	007	020	R	EW	IN	IN
046	N85W	90SW	002	097	002	020	R	EW	IN	IN
046	N85W	90SW	003	096	002	020	R	EW	IN	IN
046	N85W	90SW	002	092	003	020	R	EW	IN	IN
046	N85W	90SW	002	093	005	020	R	FW	IN	IN
047	N26E	83SF	083	057	065	001	R	NE	NO	OT
047	N26E	83SF	041	059	020	001	R	NE	NO	OT
047	N85W	86SW	014	007	020	007	R	EW	NO	OT
047	N85W	86SW	006	010	013	007	R	EW	NO	OT
047	N85W	86SW	007	006	006	006	R	FW	NO	OT
047	N85W	86SW	010	011	029	011	R	EW	NO	OT
047	N85W	86SW	014	015	017	009	R	EW	NO	OT
047	N85E	86SW	023	009	026	009	P	EW	NO	OT
047	N85E	86SE	009	010	014	010	R	EW	NO	OT
048	N33W	55SW	146	070		003	R		NO	OT
048	N83E	90NW	006	004	007	004	R	EW	NO	OT
048	N83E	90NW	006	004	005	004	R	FW	NO	OT
048	N83E	90NW	001	004	011	004	R	EW	NO	OT
048	N30W	62SW	012	004		004	R		NO	OT
048	N30W	62SW	009	004		004	R		NO	OT
048	N45W	62SW	010	004	005	004	R	NW	NO	OT
049	N46W	71SW	165	027		027	P	NW	NO	OT
049	N88W	76NE	121	028		028	R	EW	NO	OT
049	N88W	76NF	034	004	008	004	R	EW	NO	OT
049	N46W	71SW	066	016	028	016	R	NW	NO	OT
049	N46W	71SW	050	016	011	016	R	NW	NO	OT
049	N46W	71SW	035	010	011	010	R	NW	NO	OT
049	N88W	76NE	028	018	030	018	P	EW	NO	OT

STA	STRI	DIP	LNG	DTH	SPA	BED	EX	ST	LO	GR
049	N88W	76NE	036	013	015	013	R	EW	NO	OT
049	N46W	71SW	015	016	014	016	R	NW	NO	OT
049	N12W	28SW	010	022	019	022	R		NO	OT
049	N12W	28SW	012	017		017	R		NO	OT
049	N12W	28SW	005	007	005	007	R		NO	OT
049	N12W	28SW	001	006	006	006	R		NO	OT
049	N12W	28SW	012	027	040	027	R		NO	OT
049	N46W	71SW	028	027	021	027	R	NW	NO	OT
049	N46W	71SW	025	027	013	027	R	NW	NO	OT
049	N46W	71SW	065	027	014	027	R	NW	NO	OT
049	N12W	28SW	010	015	013	015	R		NO	OT
049	N12W	28SW	003	015	020	015	R		NO	OT
049	N88W	76NE	033	017	021	017	R	EW	NO	OT
049	N88W	76NE	023	025	012	025	R	EW	NO	OT
050	N21W	90SW	500		096	001	S		NO	OT
050	N21W	90SW	500				S		NO	OT
050	N05W	90SW	386		122	001	S		NO	OT
050	N05W	90SW	238			001	S		NO	OT
050	N05W	90SW	120		025	001	S		NO	OT
050	N05W	90SW	293		036	001	S		NO	OT
050	N05W	90SW	251		037	001	S		NO	OT
050	N03W	90SW	450		150		SC		NO	OT
050	N03W	90SW	223				SC		NO	OT
050	N45W	90SW	048	007	015	007	SC	NW	NO	OT
050	N45W	90SW	061	007	018	007	SC	NW	NO	OT
050	N45W	90SW	081	007	025	007	SC	NW	NO	OT
050	N45W	90SW	105	007	018	007	SC	NW	NO	OT
050	N45W	90SW	014	007	017	007	SC	NW	NO	OT
050	N45W	90SW	015	007	015	007	SC	NW	NO	OT
050	N45W	90SW	028	007	036	007	SC	NW	NO	OT
051	N48W	88SW	081	029	027	029	SC	NW	NO	OT
051	N48W	88SW	081	029	025	029	SC	NW	NO	OT
051	N48W	88SW	078	029	021	029	SC	NW	NO	OT
051	N48W	88SW	066	029	005	029	SC	NW	NO	OT
051	N48W	88SW	048	029	032	029	SC	NW	NO	OT
051	N48W	88SW	049	029	015	029	SC	NW	NO	OT
051	N83W	90SW	130	025	038	025	SC	EW	NO	OT
051	N43W	90SW	072	025	030	025	SC	NW	NO	OT
051	N43W	90SW	086	025	062	025	SC	NW	NO	OT
051	N43W	90SW	090	025	034	025	SC	NW	NO	OT
051	N48W	88SW	035	025		025	SC	NW	NO	OT
051	N48W	88SW	056	005	015	005	SC	NW	NO	OT
051	N48W	88SW	085	005	006	005	SC	NW	NO	OT
051	N48W	88SW	056	005	006	005	SC	NW	NO	OT
051	N48W	88SW	061	005	015	005	SC	NW	NO	OT
051	N48W	88SW	046	005	010	005	SC	NW	NO	OT
051	N48W	88SW	067	005	055	005	SC	NW	NO	OT

STA	STRI	DIP	LNG	DTH	SPA	BED	EX	ST	LQ	GR
052	N58W	75SW	150	080			R		NO	OT
053							R		NO	OT
054	N66W	90SW			032	013	R		IN	IN
054	N66W	90SW			027	013	R		IN	IN
054	N66W	90SW			021	013	R		IN	IN
054	N66W	90SW			028	013	R		IN	IN
054	N66W	90SW			016	013	R		IN	IN
054	N66W	90SW			015	013	R		IN	IN
054	N66W	90SW			028	013	R		IN	IN
054	N66W	90SW			022	013	R		IN	IN
054	N42E	45NW			059		R	NE	IN	IN
054	N42E	45NW			053		R	NE	IN	IN
054	N42E	45NW			081		R	NE	IN	IN
054	N42E	45NW			068		R	NE	IN	IN
054	N42E	45NW			016		R	NE	IN	IN
054	N42E	45NW			027		R	NE	IN	IN
054	N42E	45NW			038		R	NE	IN	IN
054	N42E	45NW			021		R	NE	IN	IN
054	N88W	90SW			067		R	EW	IN	IN
054	N88W	90SW			030		R	EW	IN	IN
054	N88W	90SW			020		R	EW	IN	IN
054	N88W	90SW			071		R	EW	IN	IN
054	N88W	90SW			027		R	EW	IN	IN
054	N88W	90SW			026		R	EW	IN	IN
054	N88W	90SW			030		R	EW	IN	IN
054	N88W	90SW			009		R	EW	IN	IN
055	N46W	89SW	109	047	019	047	R	NW	NO	OT
055	N87W	89NE	075	034	038	047	R	EW	NO	OT
055	N87W	89NE	138	028	069	028	R	EW	NO	OT
055	N42E	85NW	010	056		001	R	NE	NO	OT
055	N36E	90NW	050	028	130	028	R	NE	NO	OT
055	N46W	89SW	013	019		028	R	NW	NO	OT
055	N25E	90NW	012	006	009	001	R	NE	NO	OT
055	N25E	90NW	001	006	019	001	R	NE	NO	OT
055	N25E	90NW	001	006	020	001	R	NE	NO	OT
055	N36E	90NW	050	027	092	027	R	NE	NO	OT
055	N46W	89SW	048	027		027	R	NW	NO	OT
055	N87W	89NE	030	008	015	008	R	EW	NO	OT
055	N87W	89NE	010	008		008	R	EW	NO	OT
056	N45W	90SW	034	043	036	043	R	NW	NO	OT
056	N45W	90SW	010	043	062	043	R	NW	NO	OT
056	N45W	90SW	120	134		100	R	NW	NO	OT
056	N45W	90SW	038	123	015	100	R	NW	NO	OT
056	N45W	90SW	146	200		200	R	NW	NO	OT
056	N45W	90SW	180	220		200	R	NW	NO	OT
057	N83W	83NE	073	026	018	026	R	EW	NO	OT
057	N83W	84NE	001	026	018	026	R	EW	NO	OT

STA	STRI	DIP	LNG	DTH	SPA	BED	EX	ST	LO	GR
057	N83W	83NE	020	026	054	026	R	EW	NO	OT
057	N36W	83SW	041	021	016	021	R	NW	NO	OT
057	N36W	83SW	028	021	025	021	R	NW	NO	OT
057	N36W	83SW	033	021	024	021	R	NW	NO	OT
057	N38E	33NW	016	021	046	021	R	NE	NO	OT
057	N38E	33NW	025	021	029	021	R	NE	NO	OT
057	N38E	33NW	024	021	029	021	R	NE	NO	OT
058	N83E	49SE	057	067	006	001	R	EW	NO	OT
058	N73W	75SW	173	049		058	R			OT
058	N83E	49SE	007	075	006	010	R	EW	NO	OT
058	N83E	49SE	008	069	019	010	R	EW	NO	OT
058	N83E	49SE	020	180	063	010	R	EW	NO	OT
058	N83E	49SE	015	250		010	R	EW	NO	OT
058	N83E	49SE	012	053	009	010	R	EW	NO	OT
058	N83E	49SE	006	041	010	010	R	EW	NO	OT
059	N20E	90NW					R		NO	OT
059	N80W	90SW					R	EW	NO	OT
060	N49W	90SW	042	030	025	030	R	NW	NO	OT
060	N49W	90SW	031	030	036	030	R	NW	NO	OT
060	N49W	90SW	029	030	006	030	R	NW	NO	OT
061	N41W	77SW	019	061	051	061	R	NW	NO	OT
061	N41W	77SW	038	061	041	061	R	NW	NO	OT
061	N41W	77SW	049	061	058	061	R	NW	NO	OT
061	N41W	77SW	033	038	024	038	R	NW	NO	OT
061	N41W	77SW	028	038	023	038	R	NW	NO	OT
061	N41W	77SW	021	038	037	038	R	NW	NO	OT
062	N75W	90SW	300	104		083	R		NO	OT
062	N45E	48NW					R	NE	NO	OT
063	N47W	84NE	091	058	068	058	S	NW	NO	OT
063	N75W	72NE	027	058		058	S		NO	OT
063	N47W	84NE	050	058	064	058	S	NW	NO	OT
063	N47W	84NE	080	047	021	044	S	NW	NO	OT
063	N47W	84NE	087	047	060	044	S	NW	NO	OT
063	N47W	84NE	020	058	037	058	S	NW	NO	OT
063	N47W	84NE	008	058	035	058	S	NW	NO	OT
063	N75W	72NE	001	078	088	058	S		NO	OT
063	N75W	72NE	003	163	100	058	S		NO	OT
063	N75W	72NE	008	080	025	020	S		NO	OT
063	N47W	84NE	031	018	023	018	S	NW	NO	OT
063	N47W	84NE	037	018	019	018	S	NW	NO	OT
063	N75W	72NE	045	018	085	018	S		NO	OT
063	N75W	72NE	060	018	031	018	S		NO	OT
063	N75W	72NE	027	018	051	018	S		NO	OT
064	N75W	80NE	029	005	014	005	R		NO	OT
064	N45W	78SW	025	019	015	012	R	NW	NO	OT
064	N45W	78SW	052	010	012	010	R	NW	NO	OT
064	N75W	80NE	026	005	011	005	R		NO	OT

STA	STRI	DIP	LNG	DTH	SPA	BED	EX	ST	LO	GR
064	N45W	78SW	022	012	020	012	R	NW	NO	OT
064	N75W	80NE	046	010	007	010	R		NO	OT
064	N45W	78SW	035	019	028	019	R	NW	NO	OT
064	N45W	78SW	007	019	013	019	R	NW	NO	OT
064	N45W	78SW	018	019	014	019	R	NW	NO	OT
064	N45W	78SW	057	012	020	012	R	NW	NO	OT
064	N87E	76NW	021	017	014	017	R	EW	NO	OT
064	N87E	76NW	007	017	015	017	R	EW	NO	OT
064	N87E	76NW	015	017	014	017	R	EW	NO	OT
065	N44W	89SW	058	025	042	025	S	NW	NO	OT
065	N44W	89SW	043	025	010	025	S	NW	NO	OT
065	N44W	89SW	039	025	025	025	S	NW	NO	OT
065	N44W	89SW	037	025	036	025	S	NW	NO	OT
065	N44W	89SW	054	025	027	025	S	NW	NO	OT
065	N44W	89SW	032	012	010	025	S	NW	NO	OT
065	N44W	89SW	028	012	008	025	S	NW	NO	OT
065	N44W	89SW	027	012	013	025	S	NW	NO	OT
065	N44W	89SW	025	012	012	025	S	NW	NO	OT
065	N89W	90SW	053	025	018	025	S	EW	NO	OT
065	N89W	90SW	029	025	009	025	S	EW	NO	OT
066	N72W	66SW	031	007	032	007	R		NO	OT
066	N72W	66SW	011	012	026	012	R		NO	OT
066	N58W	63SW	010	009	011	009	R		NO	OT
066	N58W	63SW	025	009	014	009	R		NO	OT
066	N58W	63SW	029	009	015	009	R		NO	OT
066	N58W	63SW	020	009	012	009	R		NO	OT
066	N49W	76SW	014	010	066	024	R	NW	NO	OT
066	N49W	76SW	031	012	013	012	R	NW	NO	OT
066	N49W	76SW	026	012	017	012	R	NW	NO	OT
067	N78W	69SW	026	019			R		NO	OT
067	N78W	69SW	035	019			R		NO	OT
068	N40W	90NW	016		065		S	NW	NO	OT
068	N45W	90SW	067	017	020	007	S	NW	NO	OT
068	N45W	90SW	040	027	024	007	S	NW	NO	OT
068	N45W	90SW	058	009	011	009	S	NW	NO	OT
068	N45W	90SW	060	009	026	009	S	NW	NO	OT
068	N45W	90SW	055	009	022	009	S	NW	NO	OT
068	N45W	90SW	072	009	042	009	S	NW	NO	OT
068	N78W	69SW	250				S		NO	OT
068	N78W	69SW	005	006	023	006	S		NO	OT
068	N78W	69SW	008	007	009	006	S		NO	CT
068	N78W	69SW	003	007	020	006	S		NO	OT
068	N78W	69SW	002	009	010	006	S		NO	OT
069	N46W	90SW	121	050	035	050	R	NW	NO	OT
069	N46W	90SW	093	042		042	R	NW	NO	OT
069	N46W	90SW	105	017		020	R	NW	NO	OT
069	N46W	90SW	135	060	021	042	R	NW	NO	OT

STA	STRI	DIP	LNG	DTH	SPA	BED	FX	ST	IO	GE
069	N46W	90SW	098	043		043	R	NW	NO	OT
069	N46W	90SW	080	035		035	R	NW	NO	OT
069	N34E	90NW	080	035		035	R	NE	NO	OT
069	N64W	90SW	094	046		039	R		NO	OT
069	N46W	90SW	109	053		053	R	NW	NO	OT
069	N46W	90SW	068	025	034	025	R	NW	NO	OT
069	N46W	90SW	055	025		025	R	NW	NO	OT
069	N46W	90SW	025	012	005	012	R	NW	NO	OT
069	N46W	90SW	012	012	007	012	R	NW	NO	OT
069	N46W	90SW	013	012	009	012	R	NW	NO	OT
070	N32E	81NW	461	020	000	032	R	NE	NO	OT
070	N36E	82NW	479	012	000	032	R	NE	NO	OT
070	N41W	90SW	015	006	000	006	R	NW	NO	OT
070	N48P	65NW	025	006	000	006	P		NO	OT
070	N46W	90SW	016	008	009	008	R	NW	NO	OT
070	N41W	90SW	004	008	013	008	R	NW	NO	OT
070	N41W	90SW	022	010	018	010	R	NW	NO	OT
070	N41W	90SW	023	010	000	010	R	NW	NO	OT
070	N43W	90SW	006	013	006	013	R	NW	NO	OT
070	N41W	90SW	005	013	006	013	R	NW	NO	OT
070	N41W	90SW	015	013	009	013	R	NW	NO	OT
070	N41W	90SW	006	010	010	010	R	NW	NO	OT
070	N41W	90SW	007	010	011	010	R	NW	NO	OT
070	N41W	90SW	019	010	007	010	R	NW	NO	OT
070	N41W	90SW	011	017	060	017	R	NW	NO	OT
070	N41W	90SW	011	017	015	017	R	NW	NO	OT
071	N71W	84SW	005	008	011	008	P		NO	OT
071	N71W	84SW	008	008	016	008	R		NO	OT
071	N71W	84SW	001	008	010	008	R		NO	OT
071	N71W	84SW	019	008	013	009	R		NO	OT
071	N71W	84SW	022	008	010	008	P		NO	OT
071	N71W	84SW	004	009	001	009	R		NO	OT
071	N71W	84SW	001	009	012	009	R		NO	OT
071	N71W	84SW	008	009	015	009	R		NO	OT
071	N71W	84SW	003	009	014	009	R		NO	OT
071	N71W	84SW	003	009	002	009	R		NO	OT
071	N11E	59NW	033	010	006	010	R		NO	OT
071	N11E	59NW	028	010	000	010	R		NO	OT
071	N42W	77SW	033	023	017	017	R	NW	NO	OT
071	N42W	77SW	027	027	009	018	R	NW	NO	OT
071	N42W	77SW	010	017	000	022	P	NW	NO	OT
071	N78W	81SW	007	013	008	013	R		NO	OT
071	N78W	81SW	008	013	010	013	R		NO	OT
071	N78W	81SW	027	013	011	013	R		NO	OT
071	N42W	77SW	025	030	032	030	R	NW	NO	OT
071	N42W	77SW	039	055	032	030	R	NW	NO	OT
072	N60W	90SW	055	018	000	023	R		NO	OT

STA	STRI	DIP	LNG	DTH	SPA	BED	EX	ST	LO	GR
072	N25E	90NW	039	010	000	010	R	NE	NO	OT
072	N55W	90SW	020	028	000	021	R	NW	NO	OT
072	N60W	90SW	032	032	000	030	R		NO	OT
072	N60W	90SW	027	020	026	020	R		NO	OT
072	N85E	90NW	020	042	000	003	R	EW	NO	OT
072	N70W	83SW	020	083	000	007	R		NO	OT
072	N55W	90SW	038	080	000	015	R	NW	NO	OT
073	N85W	84SW	093	041	000	041	R	EW	NO	OT
073	N31W	79SW	045	036	099	036	R		NO	OT
073	N31W	79SW	039	036	099	036	R		NO	OT
073	N31W	79SW	010	036	000	036	R		NO	OT
073	N85W	84SW	044	020	000	020	R	EW	NO	OT
073	N41W	69SW	036	053	023	029	R	NW	NO	OT
073	N41W	69SW	043	060	000	020	R	NW	NO	OT
074	N87E	76SW	122	134	000	134	R	EW	NO	OT
074	N87W	76SW	070	027	000	023	R	EW	NO	OT
074	N87W	76SW	037	007	018	007	R	EW	NO	OT
074	N87W	76SW	031	007	010	007	R	EW	NO	OT
074	N87W	76SW	053	033	000	007	R	EW	NO	OT
074	N05E	79NW	046	007	000	007	R		NO	OT
075	N70E	60NW	165	010	000	005	R		NO	OT
075	N82E	90NW	135	015	035	015	R	EW	NO	OT
075	N82E	90NW	058	015	000	015	R	EW	NO	OT
076	N15E	90NW	076	012	076	012	S		NO	OT
076	N15E	90NW	050	012	037	012	S		NO	OT
076	N15E	90NW	086	012	047	012	S		NO	OT
076	N15E	90NW	094	012	049	012	S		NO	OT
076	N15E	90NW	080	012	000	012	S		NO	OT
076	N85E	90NW	157	012	000	012	S	EW	NO	OT
077	N22E	90NW	048	019	016	019	S		NO	OT
077	N45E	85NW	071	018	064	018	S	NE	NO	OT
077	N46W	90SW	051	025	019	019	S	NW	NO	OT
077	N87W	90SW	082	000	010	009	S	EW	NO	OT
077	N22E	90NW	037	019	016	019	S		NO	OT
077	N46W	90SW	053	019	014	019	S	NW	NO	OT
077	N45E	85NW	109	034	000	019	S	NE	NO	OT
077	N87W	90SW	110	009	011	009	S	EW	NO	OT
077	N87W	90SW	049	009	011	009	S	EW	NO	OT
078	N63W	90SW	206	034	065	034	R		NO	OT
078	N63W	90SW	101	015	080	015	R		NO	OT
078	N63W	90SW	080	015	000	015	R		NO	OT
078	N63W	90SW	278	034	000	034	R		NO	OT
078	N48W	90SW	050	008	017	008	R	NW	NO	OT
078	N55W	90SW	045	001	008	008	R	NW	NO	OT
078	N55W	90SW	086	001	008	008	R	NW	NO	OT
078	N55W	90SW	088	003	006	008	R	NW	NO	OT
078	N55W	90SW	098	002	005	008	R	NW	NO	OT

STA	STRI	DIP	LNG	DTH	SPA	BED	EX	ST	LO	GR
078	N55W	90SW	068	001	011	008	R	NW	NO	OT
078	N55W	90SW	062	004	013	009	R	NW	NO	OT
079	N47W	82SW	013	016	014	016	R	NW	NO	OT
079	N47W	82SW	039	019	000	019	R	NW	NO	OT
079	N47W	82SW	008	006	015	006	R	NW	NO	OT
079	N82W	87SW	020	016	038	016	R	EW	NO	OT
079	N82W	87SW	010	014	011	014	R	EW	NO	OT
079	N82W	87SW	015	014	003	014	R	EW	NO	OT
079	N82W	87SW	018	014	012	014	R	EW	NO	OT
079	N82W	87SW	017	014	024	014	R	EW	NO	OT
079	N47W	82SW	003	017	018	017	R	NW	FO	OT
079	N47W	82SW	018	018	013	018	R	NW	NO	OT
079	N47W	82SW	018	014	015	014	R	NW	NO	OT
079	N82W	87SW	009	014	017	014	R	EW	NO	OT
079	N82W	87SW	032	014	019	014	R	FW	NO	OT
079	N47W	82SW	017	018	012	018	R	NW	NO	OT
079	N47W	82SW	027	020	018	017	R	NW	NO	OT
079	N12W	70SW	043	013	000	013	R		NO	OT
079	N07E	59NW	018	018	001	018	R		NO	OT
079	N12E	48NW	033	013	014	013	R		NO	OT
080	N72W	84SW	033	008	008	008	R		NO	OT
080	N21E	84NW	017	008	018	008	R		NO	OT
080	N72W	84SW	007	008	013	008	R		NO	OT
080	N72W	84SW	024	008	018	008	R		NO	OT
080	N72W	84SW	044	009	015	009	R		NO	OT
080	N72W	84SW	018	009	009	009	R		NO	OT
080	N72W	84SW	018	009	018	009	R		NO	OT
080	N72W	84SW	018	009	011	009	R		NO	OT
080	N21E	84NW	017	008	029	008	R		NO	OT
080	N21E	84NW	001	009	013	009	R		NO	OT
080	N21E	84NW	015	009	012	009	R		NO	OT
080	N21E	84NW	024	009	025	009	R		NO	OT
080	N21E	84NW	010	009	018	009	R		NO	OT
080	N21E	84NW	019	010	017	010	R		NO	OT
082	N23E	74NW	049	026	080	026	R		IN	IN
082	N48W	88SW	064	027	065	027	R	NW	IN	IN
082	N48W	88SW	100	026	000	026	R	NW	IN	IN
082	N48W	88SW	020	036	039	036	R	NW	IN	IN
082	N48W	88SW	060	040	050	040	R	NW	IN	IN
082	N48W	88SW	062	046	067	046	R	NW	IN	IN
082	N84W	87SW	053	040	025	033	R	EW	IN	IN
082	N84W	87SW	005	040	020	033	R	EW	IN	IN
082	N84W	87SW	027	026	000	026	R	EW	IN	IN
082	N23E	74NW	058	030	063	030	R		IN	IN
082	N23E	74NW	072	033	000	033	R		IN	IN
083	N70W	87SW	020	015	000	013	R		IN	IN
083	N46W	88SW	012	004	010	008	R	NW	IN	IN

STA	STRI	DIP	LNG	DTH	SPA	BED	EX	ST	LO	GR
083	N46W	88SW	003	003	013	008	R	NW	IN	IN
083	N46W	88SW	005	004	010	008	R	NW	IN	IN
083	N70W	87SW	014	009	007	009	R		IN	IN
083	N21E	73NW	129	022	011	007	R		IN	IN
083	N21E	73NW	063	018	012	009	R		IN	IN
084	N85W	88SW	075	142	030	020	R	EW	IN	IN
084	N89W	90SW	034	034	044	034	R	EW	IN	IN
084	N89W	88SW	028	029	021	022	R	EW	IN	IN
084	N89W	88SW	035	056	041	022	R	EW	IN	IN
084	N89W	88SW	015	018	013	006	R	EW	IN	IN
084	N89W	88SW	012	026	014	006	R	EW	IN	IN
084	N89W	88SW	005	005	008	005	R	EW	IN	IN
084	N35E	84NW	015	019	006	019	R	NE	IN	IN
084	N35E	84NW	024	019	023	019	R	NE	IN	IN
084	N42W	71SW	024	014	000	014	R	NW	IN	IN
084	N89W	88SW	010	014	021	014	R	EW	IN	IN
084	N89W	88SW	010	014	022	014	R	EW	IN	IN
084	N89W	88SW	019	017	016	017	R	EW	IN	IN
084	N45W	84SW	146	018	015	018	R	NW	IN	IN
084	N42W	71SW	105	020	000	020	R	NW	IN	IN
084	N89W	88SW	216	020	015	012	R	EW	IN	IN
085	N54W	90SW	205	013	000	013	R	NW	IN	IN
085	N30E	51NW	005	036	030	036	R	NE	IN	IN
085	N30E	51NW	047	036	042	036	R	NE	IN	IN
085	N30E	51NW	012	036	023	036	R	NE	IN	IN
085	N30E	51NW	107	048	000	036	R	NE	IN	IN
085	N54W	90SW	102	013	000	013	R	NW	IN	IN
085	N54W	90SW	056	013	000	013	R	NW	IN	IN
086	N33E	90NW	046	005	000	005	S	NE	IN	IN
086	N47E	67NW	034	010	000	010	S		IN	IN
086	N47E	67NW	029	008	000	008	S		IN	IN
086	N33E	90NW	026	006	015	006	S	NE	IN	IN
086	N40W	90SW	030	007	000	007	S	NW	IN	IN
086	N40W	90SW	019	007	016	007	S	NW	IN	IN
086	N40W	90SW	013	007	000	007	S	NW	IN	IN
087	N87W	90SW	008	020	018	010	SC	EW	IN	IN
087	N51W	90SW	034	033	000	013	SC	NW	IN	IN
087	N87W	90SW	022	005	008	005	SC	EW	IN	IN
087	N87W	90SW	015	007	012	007	SC	EW	IN	IN
087	N87W	90SW	015	009	024	009	SC	EW	IN	IN
087	N87W	90SW	005	010	038	011	SC	EW	IN	IN
087	N87W	90SW	014	010	009	010	SC	EW	IN	IN
087	N87W	90SW	007	005	017	007	SC	EW	IN	IN
087	N87W	90SW	010	007	017	007	SC	EW	IN	IN
087	N87W	90SW	015	013	034	007	SC	EW	IN	IN
087	N87W	90SW	018	003	000	007	SC	EW	IN	IN
087	N51W	90SW	010	070	000	010	SC	NW	IN	IN

STA	STRI	DIP	LNG	DTH	SPA	BED	EX	ST	LO	GR
087	N51W	90SW	010	056	000	010	SC	NW	IN	IN
087	N43W	90SW	070	061	000	010	SC	NW	IN	IN
087	N51W	90SW	197	050	007	015	SC	NW	IN	IN
087	N51W	90SW	040	012	026	012	SC	NW	IN	IN
087	N84E	90NW	182	057	011	007	SC	EW	IN	IN
087	N84E	90NW	085	043	011	007	SC	EW	IN	IN
087	N84E	90NW	063	038	000	007	SC	EW	IN	IN
087	N87W	90SW	047	067	006	007	SC	EW	IN	IN
087	N73W	90SW	124	073	032	006	SC		IN	IN
087	N73W	90SW	117	060	031	006	SC		IN	IN
088	N45W	90SW	050	019	030	019	S	NW	IN	IN
088	N45W	90SW	043	019	033	019	S	NW	IN	IN
088	N45W	90SW	047	019	000	019	S	NW	IN	IN
088	N86W	75SW	142	022	039	022	S	EW	IN	IN
088	N86W	75SW	062	022	031	022	S	EW	IN	IN
088	N86W	75SW	032	020	000	022	S	EW	IN	IN
089	N62W	72SW	060	039	038	039	SC		IN	IN
089	N62W	72SW	077	039	009	039	SC		IN	IN
089	N62W	72SW	045	039	005	039	SC		IN	IN
089	N62W	72SW	035	039	011	039	SC		IN	IN
089	N62W	72SW	064	039	007	039	SC		IN	IN
089	N03E	52NW	060	019	008	019	SC		IN	IN
089	N03E	52NW	043	014	004	007	SC		IN	IN
089	N28E	44NW	025	010	000	007	SC	NE	IN	IN
089	N62W	72SW	040	039	007	039	SC		IN	IN
089	N62W	72SW	038	039	006	039	SC		IN	IN
089	N28E	44NW	015	014	011	014	SC	NE	IN	IN
089	N28E	44NW	010	008	008	008	SC	NE	IN	IN
089	N28E	44NW	020	005	001	005	SC	NE	IN	IN
090	N43W	90SW	020	009	003	009	SC	NW	IN	IN
090	N43W	90SW	016	009	009	009	SC	NW	IN	IN
090	N43W	90SW	011	009	003	009	SC	NW	IN	IN
090	N43W	90SW	012	009	010	009	SC	NW	IN	IN
090	N43W	90SW	018	017	005	009	SC	NW	IN	IN
090	N43W	90SW	018	013	006	009	SC	NW	IN	IN
090	N43W	90SW	018	017	010	009	SC	NW	IN	IN
090	N43W	90SW	018	013	014	009	SC	NW	IN	IN
090	N43W	90SW	010	017	007	009	SC	NW	IN	IN
090	N43W	90SW	012	017	015	009	SC	NW	IN	IN
090	N43W	90SW	010	017	013	009	SC	NW	IN	IN
090	N43W	90SW	010	017	010	009	SC	NW	IN	IN
091	N36W	87SW	180	025	068	025	S	NW	IN	IN
091	N36W	87SW	130	025	025	025	S	NW	IN	IN
091	N36W	87SW	103	025	012	025	S	NW	IN	IN
091	N36W	87SW	090	025	039	025	S	NW	IN	IN
091	N36W	87SW	087	025	014	025	S	NW	IN	IN
091	N36W	87SW	085	025	040	025	S	NW	IN	IN

STA	STRI	DIP	LNG	DTH	SPA	BED	EX	ST	LO	GR
091	N36W	87SW	080	025	055	025	S	NW	IN	IN
092	N55W	74SW	017	007	016	007	SC	NW	IN	IN
092	N55W	74SW	020	007	000	007	SC	NW	IN	IN
092	N55W	74SW	005	002	022	002	SC	NW	IN	IN
092	N55W	74SW	005	002	000	002	SC	NW	IN	IN
092	N87E	90NW	051	030	004	004	SC	EW	IN	IN
093	N25E	90NW	206	005	029	005	SC	NE	IN	IN
093	N25E	90NW	174	005	043	005	SC	NE	IN	IN
093	N25E	90NW	355	012	000	005	SC	NE	IN	IN
093	N25E	90NW	089	015	020	010	SC	NE	IN	IN
093	N49W	88SW	039	013	000	013	SC	NW	IN	IN
093	N40W	72SW	043	012	000	012	SC	NW	IN	IN
093	N40W	72SW	031	012	005	012	SC	NW	IN	IN
093	N40W	72SW	011	012	013	012	SC	NW	IN	IN
093	N85W	84SW	021	006	000	006	SC	EW	IN	IN
093	N85W	84SW	043	015	023	015	SC	EW	IN	IN
093	N40W	72SW	010	005	017	005	SC	NW	IN	IN
093	N40W	72SW	014	007	015	008	SC	NW	IN	IN
093	N40W	72SW	011	007	010	008	SC	NW	IN	IN
093	N40W	72SW	008	007	008	009	SC	NW	IN	IN
093	N40W	72SW	004	007	016	010	SC	NW	IN	IN
094	N76W	80SW	020	010	043	010	S		IN	IN
094	N76W	80SW	015	010	050	010	S		IN	IN
094	N76W	80SW	020	010	055	010	S		IN	IN
094	N76W	80SW	022	009	017	009	S		IN	IN
094	N35E	78NW	050	010	015	010	S	NE	IN	IN
095	N36W	84SW	320	014	006	014	R	NW	IN	IN
095	N36W	84SW	340	015	000	015	R	NW	IN	IN
095	N36W	84SW	310	008	000	008	R	NW	IN	IN
095	N36W	84SW	010	010	040	010	R	NW	IN	IN
096	N43W	88SW	073	005	000	005	R	NW	IN	IN
096	N25E	90NW	015	008	026	008	R	NE	IN	IN
096	N25E	90NW	024	008	021	008	R	NE	IN	IN
096	N43W	88SW	050	007	000	007	R	NW	IN	IN
097	N76E	74NW	242	102	008	102	R		IN	IN
097	N76E	74NW	171	102	000	102	R		IN	IN
097	N76E	74NW	190	039	004	039	R		IN	IN
097	N76E	74NW	187	015	000	015	R		IN	IN
098	N84E	75NW	078	026	003	016	R	EW	IN	IN
098	N84E	75NW	196	021	000	011	R	EW	IN	IN
098	N84E	75NW	132	007	000	007	R	EW	IN	IN
098	N84E	75NW	106	007	000	007	R	EW	IN	IN
098	N40E	68NW	053	013	008	013	R	NE	IN	IN
098	N40E	68NW	045	013	007	013	R	NE	IN	IN
099	N10W	69SW	110	046	014	046	R		IN	IN
099	N10W	69SW	040	046	000	046	R		IN	IN
099	N45W	90SW	055	072	000	072	R	NW	IN	IN

STA	STRI	DIP	LNG	DTH	SPA	BED	EX	ST	LO	GR
099	N45W	90SW	016	046	048	046	R	NW	IN	IN
100	N72W	76SW	224	011	000	011	R		IN	IN
100	N72W	76SW	133	017	000	017	R		IN	IN
101	N33W	70SW	019	006	012	006	R		IN	IN
101	N33W	70SW	021	006	000	006	R		IN	IN
101	N42E	86NW	031	006	023	006	R	NE	IN	IN
101	N42E	86NW	041	010	000	010	R	NE	IN	IN
101	N77E	90NW	051	008	000	008	R		IN	IN
101	N65W	87SW	094	023	004	023	R		IN	IN
101	N65W	87SW	096	043	000	023	R		IN	IN
102	N41W	85SW	084	014	032	005	S	NW	IN	IN
102	N41W	85SW	109	013	052	005	S	NW	IN	IN
102	N41W	85SW	045	005	008	005	S	NW	IN	IN
102	N41W	85SW	109	005	013	007	S	NW	IN	IN
102	N41W	85SW	034	012	036	007	S	NW	IN	IN
102	N41W	85SW	108	015	000	015	S	NW	IN	IN
102	N87W	84SW	142	023	042	023	S	EW	IN	IN
102	N87W	84SW	035	012	012	012	S	EW	IN	IN
102	N87W	84SW	024	012	019	012	S	EW	IN	IN
102	N87W	84SW	048	014	054	014	S	EW	IN	IN
102	N87W	84SW	092	021	000	021	S	EW	IN	IN
102	N41W	85SW	174	011	025	006	S	NW	IN	IN
102	N41W	85SW	153	013	012	006	S	NW	IN	IN
102	N41W	85SW	085	009	032	006	S	NW	IN	IN
102	N41W	85SW	174	013	038	006	S	NW	IN	IN
102	N87W	84SW	092	010	051	010	S	EW	IN	IN
102	N87W	84SW	095	009	040	009	S	EW	IN	IN
102	N87W	84SW	057	005	034	009	S	EW	IN	IN
103	N38W	84SW	014	008	007	008	S	NW	IN	IN
103	N38W	84SW	013	008	012	009	S	NW	IN	IN
103	N38W	84SW	023	007	009	007	S	NW	IN	IN
103	N38W	84SW	017	007	011	007	S	NW	IN	IN
103	N38W	84SW	013	008	000	008	S	NW	IN	IN
103	N38W	84SW	010	010	009	010	S	NW	IN	IN
103	N38W	84SW	012	010	008	010	S	NW	IN	IN
103	N38W	84SW	016	010	010	010	S	NW	IN	IN
103	N85E	58NW	022	006	008	006	S	EW	IN	IN
103	N85E	58NW	015	014	006	006	S	EW	IN	IN
103	N85E	58NW	011	007	003	003	S	EW	IN	IN
103	N85E	58NW	005	004	009	006	S	EW	IN	IN
104	N42W	86SW	057	012	012	012	S	NW	IN	IN
104	N42W	86SW	030	012	014	012	S	NW	IN	IN
104	N42W	86SW	039	009	007	009	S	NW	IN	IN
104	N42W	86SW	053	009	010	009	S	NW	IN	IN
104	N42W	86SW	058	009	007	009	S	NW	IN	IN
104	N42W	86SW	115	007	032	007	S	NW	IN	IN
104	N42W	86SW	042	008	004	008	S	NW	IN	IN

STA	STRI	DIP_	LNG	DTH	SPA	BED	EX	ST	LO	GR
104	N42W	86SW	021	008	006	008	S	NW	IN	IN
105	N77W	75SW	045	023	015	023	S		IN	IN
105	N77W	75SW	016	023	000	023	S		IN	IN
105	N44W	85SW	023	022	040	022	S	NW	IN	IN
105	N44W	85SW	020	022	040	022	S	NW	IN	IN
105	N44W	85SW	010	014	025	014	S	NW	IN	IN
105	N44W	85SW	023	012	016	012	S	NW	IN	IN
105	N44W	85SW	012	012	012	012	S	NW	IN	IN
105	N44W	85SW	015	022	029	022	S	NW	IN	IN
105	N44W	85SW	016	018	023	018	S	NW	IN	IN
105	N44W	85SW	030	016	009	016	S	NW	IN	IN
105	N44W	85SW	038	023	019	012	S	NW	IN	IN
105	N44W	85SW	035	023	016	012	S	NW	IN	IN
105	N44W	85SW	015	020	000	012	S	NW	IN	IN
106	N51W	82SW	050	025	011	025	S	NW	IN	IN
106	N51W	82SW	101	025	010	025	S	NW	IN	IN
106	N51W	82SW	240	025	019	025	S	NW	IN	IN
106	N51W	82SW	111	015	014	015	S	NW	IN	IN
106	N51W	82SW	099	007	005	007	S	NW	IN	IN
106	N51W	82SW	097	007	004	007	S	NW	IN	IN
106	N51W	82SW	089	007	015	007	S	NW	IN	IN
106	N51W	82SW	078	007	011	007	S	NW	IN	IN
106	N32E	58NW	130	025	000	025	S	NE	IN	IN
106	N32E	58NW	050	015	000	015	S	NE	IN	IN
106	N01E	58NW	026	007	000	007	S		IN	IN
106	N01E	58NW	019	015	000	015	S		IN	IN
107	N82E	70NW	053	004	006	004	S	EW	IN	IN
107	N82E	70NW	058	015	012	015	S	EW	IN	IN
107	N82E	70NW	030	015	020	015	S	EW	IN	IN
107	N46W	90SW	100	019	034	025	S	NW	IN	IN
107	N46W	90SW	101	007	000	025	S	NW	IN	IN
108	N88W	77SW	055	005	035	005	SC	EW	IN	IN
108	N88W	77SW	047	005	027	005	SC	EW	IN	IN
108	N88W	77SW	055	005	036	005	SC	EW	IN	IN
108	N18W	80SW	033	045	006	045	SC		IN	IN
108	N18W	80SW	073	045	030	045	SC		IN	IN
108	N18W	80SW	065	045	000	045	SC		IN	IN
108	N18W	80SW	075	007	006	007	SC		IN	IN
108	N18W	80SW	052	008	000	008	SC		IN	IN
108	N18W	80SW	062	045	037	045	SC		IN	IN
108	N35E	90NW	044	045	038	045	SC	NE	IN	IN
108	N35E	90NW	010	045	000	045	SC	NE	IN	IN
109	N43W	83SW	044	012	012	012	SC	NW	IN	IN
109	N43W	83SW	058	014	012	014	SC	NW	IN	IN
109	N43W	83SW	055	021	014	021	SC	NW	IN	IN
109	N43W	83SW	042	020	012	020	SC	NW	IN	IN
109	N43W	83SW	020	020	012	020	SC	NW	IN	IN

STA	STRI	DIP_	LNG	DTH	SPA	BED	EX	ST	LO	GP
109	N43W	83SW	023	009	003	009	SC	NW	IN	IN
109	N43W	83SW	023	009	009	009	SC	NW	IN	IN
109	N43W	83SW	023	009	003	009	SC	NW	IN	IN
109	N43W	83SW	025	009	007	009	SC	NW	IN	IN
109	N43W	83SW	054	039	008	067	SC	NW	IN	IN
110	N48W	90SW	020	053	020	007	S	NW	IN	IN
110	N48W	90SW	021	054	029	007	S	NW	IN	IN
110	N48W	90SW	005	008	009	008	S	NW	IN	IN
110	N48W	90SW	006	008	004	008	S	NW	IN	IN
110	N48W	90SW	005	008	004	008	S	NW	IN	IN
110	N48W	90SW	005	008	010	008	S	NW	IN	IN
110	N48W	90SW	002	008	008	008	S	NW	IN	IN
110	N48W	90SW	002	008	007	009	S	NW	IN	IN
111	N87W	85SW	144	012	025	012	SC	EW	IN	IN
111	N87W	85SW	152	012	019	012	SC	EW	IN	IN
111	N87W	85SW	178	014	024	014	SC	EW	IN	IN
111	N87W	85SW	195	014	016	014	SC	EW	IN	IN
111	N87W	85SW	117	014	013	014	SC	EW	IN	IN
111	N87W	85SW	025	010	019	010	SC	EW	IN	IN
111	N87W	85SW	057	010	020	010	SC	EW	IN	IN
111	N87W	85SW	049	010	020	01	SC	EW	IN	IN
111	N87W	85SW	070	010	010	010	SC	EW	IN	IN
111	N08E	72NW	020	010	030	010	SC		IN	IN
111	N08E	72NW	020	010	047	010	SC		IN	IN
111	N08E	72NW	010	010	027	010	SC		IN	IN
111	N08E	72NW	022	015	047	015	SC		IN	IN
111	N08E	72NW	013	015	025	015	SC		IN	IN
112	N84W	87SW	728	020	085	020	S	EW	IN	IN
112	N84W	87SW	720	020	123	020	S	EW	IN	IN
112	N84W	87SW	320	022	076	022	S	EW	IN	IN
112	N34W	57SW	085	020	046	020	S		IN	IN
112	N34W	57SW	085	020	053	020	S		IN	IN
112	N34W	57SW	085	020	085	020	S		IN	IN
112	N34W	57SW	123	020	088	020	S		IN	IN
112	N34W	57SW	123	020	164	020	S		IN	IN
112	N84W	87SW	007	022	062	022	S	EW	IN	IN
112	N84W	87SW	340	022	106	022	S	EW	IN	IN
112	N84W	87SW	320	022	052	022	S	EW	IN	IN
112	N84W	87SW	750	022	069	022	S	EW	IN	IN
112	N84W	87SW	720	042	083	042	S	EW	IN	IN
112	N84W	87SW	715	020	177	020	S	EW	IN	IN
113	N50W	90SW	082	010	000	003	S	NW	IN	IN
113	N45W	87SW	180	010	000	010	S	NW	IN	IN
113	N50W	90SW	017	008	007	008	S	NW	IN	IN
113	N50W	90SW	019	008	004	008	S	NW	IN	IN
113	N50W	90SW	034	008	007	008	S	NW	IN	IN
113	N50W	90SW	040	008	003	008	S	NW	IN	IN

STA	STRI	DIP	LNG	DTH	SPA	BED	EX	ST	IO	GR
113	N50W	90SW	009	005	008	003	S	NW	IN	IN
113	N50W	90SW	020	005	006	003	S	NW	IN	IN
114	N87W	85SW	130	010	035	010	S	EW	IN	IN
114	N87W	85SW	063	010	016	010	S	EW	IN	IN
114	N87W	85SW	174	010	021	010	S	EW	IN	IN
114	N87W	85SW	040	010	012	010	S	EW	IN	IN
114	N87W	85SW	102	010	031	010	S	EW	IN	IN
115	N83W	89SW	032	012	025	012	S	EW	IN	IN
115	N83W	89SW	015	012	019	012	S	EW	IN	IN
115	N83W	89SW	015	012	020	012	S	EW	IN	IN
115	N83W	89SW	023	012	010	012	S	EW	IN	IN
115	N83W	89SW	019	012	006	012	S	EW	IN	IN
115	N83W	89SW	017	012	013	012	S	EW	IN	IN
116	N44W	88SW	158	061	029	061	SC	NW	NO	OT
116	N44W	88SW	132	030	058	030	SC	NW	NO	OT
116	N44W	88SW	061	030	000	030	SC	NW	NO	OT
116	N38W	85SW	049	031	018	031	SC	NW	NO	OT
116	N38W	85SW	058	005	000	005	SC	NW	NO	OT
116	N38W	85SW	057	026	044	026	SC	NW	NO	OT
116	N38W	85SW	045	026	000	026	SC	NW	NO	OT
117	N55W	87SW	025	040	010	040	R	NW	NO	OT
117	N55W	87SW	024	040	009	040	R	NW	NO	OT
117	N01W	86SW	020	009	000	009	R		NO	OT
117	N01W	86SW	021	016	000	016	R		NO	OT
117	N55W	87SW	015	012	010	012	R	NW	NO	OT
117	N55W	87SW	019	012	009	012	R	NW	NO	OT
117	N55W	87SW	017	012	008	012	R	NW	NO	OT
117	N55W	87SW	023	012	007	012	R	NW	NO	OT
117	N55W	87SW	015	012	010	012	R	NW	NO	OT
117	N55W	87SW	007	014	017	012	R	NW	NO	OT
117	N55W	87SW	015	042	015	025	R	NW	NO	OT
117	N55W	87SW	012	025	019	025	R	NW	NO	OT
118	N41W	77SW	020	006	016	006	SC	NW	NO	OT
118	N41W	77SW	010	006	011	006	SC	NW	NO	OT
118	N41W	77SW	021	006	008	006	SC	NW	NO	OT
118	N41W	77SW	022	006	004	006	SC	NW	NO	OT
118	N41W	77SW	023	006	003	006	SC	NW	NO	OT
118	N41W	77SW	026	006	004	006	SC	NW	NO	OT
118	N41W	77SW	013	006	009	006	SC	NW	NO	OT
118	N41W	77SW	022	006	007	006	SC	NW	NO	OT
118	N41W	77SW	015	006	008	006	SC	NW	NO	OT
118	N41W	77SW	027	006	004	006	SC	NW	NO	OT
119	N80E	76NW	040	014	006	014	SC	EW	NO	OT
119	N80E	76NW	084	014	018	014	SC	EW	NO	OT
119	N80E	76NW	095	014	018	014	SC	EW	NO	OT
119	N80E	76NW	067	014	024	014	SC	EW	NO	OT
119	N80E	76NW	079	014	017	014	SC	EW	NO	OT

STA	STRI	DIP	LNG	DTH	SPA	BED	EX	ST	LO	GP
119	N80E	76NW	069	014	030	014	SC	EW	NO	OT
119	N80E	76NW	077	014	011	014	SC	EW	NO	OT
119	N80E	76NW	075	014	021	014	SC	EW	NO	OT
119	N44E	44NW	079	014	016	014	SC	NE	NO	OT
119	N44E	44NW	091	014	009	014	SC	NE	NO	OT
119	N44E	44NW	138	014	014	014	SC	NE	NO	OT
119	N44E	44NW	179	014	008	014	SC	NE	NO	OT
119	N44E	44NW	202	014	005	014	SC	NE	NO	OT
119	N44E	44NW	203	014	030	014	SC	NE	NO	OT
120	N83E	90NW	083	016	026	016	S	EW	NO	OT
120	N83E	90NW	058	016	028	016	S	EW	NO	OT
120	N83E	90NW	053	016	048	016	S	EW	NO	OT
120	N83E	90NW	046	016	015	016	S	EW	NO	OT
120	N83E	90NW	046	025	028	025	S	EW	NO	OT
120	N83E	90NW	062	025	039	025	S	EW	NO	OT
120	N83E	90NW	032	025	003	025	S	EW	NO	OT
120	N83E	90NW	019	025	022	025	S	EW	NO	OT
120	N83E	90NW	044	025	036	025	S	EW	NO	OT
120	N32W	87SW	054	012	030	012	S		NO	OT
120	N32W	87SW	058	012	013	012	S		NO	OT
120	N32W	87SW	065	012	026	012	S		NO	OT
120	N32W	87SW	057	012	018	012	S		NO	OT
120	N32W	87SW	025	012	027	012	S		NO	OT
120	N32W	87SW	030	012	015	012	S		NO	OT
121	N85W	80SW	005	012	036	012	R	EW	NO	OT
121	N85W	80SW	047	012	025	012	R	EW	NO	OT
121	N85W	80SW	003	014	010	014	R	EW	NO	OT
121	N85W	80SW	010	014	024	014	R	EW	NO	OT
121	N85W	80SW	019	014	035	014	R	EW	NO	OT
121	N35E	80NW	015	019	020	019	R	NE	NO	OT
121	N35E	80NW	013	019	008	019	R	NE	NO	OT
121	N35E	80NW	012	019	015	019	R	NE	NO	OT
123	N80E	90NW	035	022	033	022	S	EW	NO	OT
123	N80E	90NW	050	022	038	022	S	EW	NO	OT
123	N80E	90NW	028	022	058	022	S	EW	NO	OT
123	N03E	90NW	033	022	035	022	S		NO	OT
123	N03E	90NW	038	022	050	022	S		NO	OT
123	N03E	90NW	058	022	028	022	S		NO	OT
123	N47W	90SW	070	012	038	012	S	NW	NO	OT
123	N47W	90SW	034	012	041	012	S	NW	NO	OT
123	N47W	90SW	057	012	008	012	S	NW	NO	OT
123	N27E	90NW	021	012	038	012	S	NE	NO	OT
123	N27E	90NW	016	012	017	012	S	NE	NO	OT
123	N27E	90NW	018	012	027	012	S	NE	NO	OT
124	N42W	87SW	115	014	025	014	S	NW	NO	OT
124	N42W	87SW	106	014	036	014	S	NW	NO	OT
124	N4E	90NW	190	020	025	007	S		NO	OT

STA	STRI	DIP_	LNG	DTH	SPA	BED	EX	ST	LO	GR
124	N42W	87SW	075	007	000	007	S	NW	NO	OT
124	N42W	87SW	078	010	015	010	S	NW	NO	OT
124	N42W	87SW	055	010	047	010	S	NW	NO	OT
124	N42W	87SW	038	019	035	019	S	NW	NO	OT
124	N42W	87SW	042	019	031	019	S	NW	NO	OT
124	N42W	87SW	065	019	042	019	S	NW	NO	OT
124	N42W	87SW	069	019	028	019	S	NW	NO	OT
124	N42W	87SW	070	019	025	019	S	NW	NO	OT
124	N42W	87SW	350	035	018	020	S	NW	NO	OT
125	N87E	90NW	196	007	036	007	S	EW	NO	OT
125	N87E	90NW	134	007	024	007	S	EW	NO	OT
125	N87E	90NW	158	007	020	007	S	EW	NO	OT
125	N87E	90NW	152	007	022	007	S	EW	NO	OT
125	N87E	90NW	152	007	021	007	S	EW	NO	OT
125	N87E	90NW	127	073	047	025	S	EW	NO	OT
125	N87E	90NW	097	077	042	025	S	EW	NO	OT
125	N87E	90NW	180	074	032	025	S	EW	NO	OT
126	N87W	85SW	546	270	030	020	SC	EW	NO	OT
126	N87W	85SW	584	240	029	020	SC	EW	NO	OT
126	N87W	85SW	042	020	023	020	SC	EW	NO	OT
126	N35E	85NW	020	035	025	007	SC	NE	NO	OT
126	N35E	85NW	005	007	027	007	SC	NE	NO	OT
126	N35E	85NW	004	007	009	007	SC	NE	NO	OT
126	N35E	85NW	003	007	016	007	SC	NE	NO	OT
126	N35E	85NW	005	007	010	007	SC	NE	NO	OT
127	N85W	90SW	063	007	033	007	S	EW	NO	OT
127	N85W	90SW	030	007	040	007	S	EW	NO	OT
127	N85W	90SW	033	007	020	007	S	EW	NO	OT
127	N85W	90SW	028	007	026	007	S	EW	NO	OT
128	N05E	90NW	074	024	012	024	SC		NO	OT
128	N05E	90NW	055	024	010	024	SC		NO	OT
128	N05E	90NW	012	024	038	024	SC		NO	OT
128	N63W	90SW	035	024	001	024	SC		NO	OT
128	N63W	90SW	014	024	075	024	SC		NO	OT
128	N63W	90SW	023	024	018	024	SC		NO	OT
128	N63W	90SW	022	024	072	024	SC		NO	OT
128	N63W	90SW	015	011	023	007	SC		NO	OT
128	N63W	90SW	013	011	030	007	SC		NO	OT
128	N63W	90SW	021	011	027	007	SC		NO	OT
128	N69W	90SW	106	033	059	033	SC		NO	OT
128	N69W	90SW	074	033	071	033	SC		NO	OT
128	N69W	90SW	150	036	058	033	SC		NO	OT
128	N69W	90SW	135	036	081	033	SC		NO	OT
128	N69W	90SW	150	033	069	033	SC		NO	OT
128	N69W	90SW	083	033	043	033	SC		NO	OT
128	N37W	85SW	030	035	009	019	SC	NW	NO	OT
128	N37W	85SW	027	035	005	019	SC	NW	NO	OT

STA	STRI	DIP_	LNG	DTH	SPA	BED	EX	ST	LO	GR
128	N37W	85SW	007	016	026	016	SC	NW	NO	OT
128	N37W	85SW	018	016	019	016	SC	NW	NO	OT
128	N37W	85SW	027	020	030	020	SC	NW	NO	OT
128	N37E	79NW	147	093	120	004	SC	NE	NO	OT
128	N37E	79NW	180	112	072	004	SC	NE	NO	OT
128	N37E	79NW	130	110	000	004	SC	NE	NO	OT
128	N37E	79NW					SC	NE	NO	OT
129	N73W	60SW	020	017	016	017	S		NO	OT
129	N73W	60SW	010	017	016	017	S		NO	OT
129	N73W	60SW	010	017	000	017	S		NO	OT
129	N73W	60SW	010	029	005	029	S		NO	OT
129	N73W	60SW	001	029	013	029	S		NO	OT
129	N73W	60SW	006	029	018	029	S		NO	OT
130	N35W	90SW	075	008	020	008	S	NW	NO	OT
130	N35W	90SW	089	008	007	008	S	NW	NO	OT
130	N35W	90SW	120	008	023	008	S	NW	NO	OT
130	N35W	90SW	099	008	012	008	S	NW	NO	OT
130	N35W	90SW	039	008	016	008	S	NW	NO	OT
130	N35W	90SW	104	008	018	008	S	NW	NO	OT
130	N35W	90SW	109	008	008	008	S	NW	NO	OT
130	N35W	90SW	121	008	023	008	S	NW	NO	OT
130	N35W	90SW	083	008	028	008	S	NW	NO	OT
130	N40E	88NW	182	008	033	008	S	NE	NO	OT
130	N40E	88NW	197	008	034	008	S	NE	NO	OT
130	N40E	88NW	184	008	031	008	S	NE	NO	OT
130	N40E	88NW	098	008	000	008	S	NE	NO	OT
131	N53W	90SW	118	055	032	001	SC	NW	NO	OT
131	N53W	90SW	079	055	000	001	SC	NW	NO	OT
131	N53W	90SW	101	012	024	012	SC	NW	NO	OT
131	N53W	90SW	027	012	032	012	SC	NW	NO	OT
131	N53W	90SW	043	012	016	012	SC	NW	NO	OT
131	N53W	90SW	041	012	044	012	SC	NW	NO	OT
131	N53W	90SW	050	012	029	012	SC	NW	NO	OT
131	N53W	90SW	041	012	025	012	SC	NW	NO	OT
131	N53W	90SW	037	012	036	012	SC	NW	NO	OT
131	N53W	90SW	064	012	034	012	SC	NW	NO	OT
131	N53W	90SW	081	012	032	012	SC	NW	NO	OT
131	N53W	90SW	090	012	028	012	SC	NW	NO	OT
131	N53W	90SW	210	156	021	012	SC	NW	NO	OT
131	N53W	90SW	075	075	054	012	SC	NW	NO	OT
131	N53W	90SW	052	063	019	012	SC	NW	NO	OT
131	N53W	90SW	116	056	090	012	SC	NW	NO	OT
131	N53W	90SW	210	124	019	012	SC	NW	NO	OT
131	N53W	90SW	055	052	018	012	SC	NW	NO	OT
131	N53W	90SW	035	061	008	012	SC	NW	NO	OT
131	N53W	90SW	426	170	000	012	SC	NW	NO	OT
132	N58W	83SW	035	027	073	027	SC		NO	OT

STA	STRI	DIP	LNG	DTH	SPA	BED	EX	ST	LO	GR
132	N58W	83SW	023	027	070	027	SC		NO	OT
132	N58W	83SW	036	027	060	027	SC		NO	OT
132	N58W	83SW	056	027	014	027	SC		NO	OT
132	N58W	83SW	020	027	065	027	SC		NO	OT
132	N58W	83SW	029	027	020	027	SC		NO	OT
132	N58W	83SW	036	027	062	027	SC		NO	OT
132	N58W	83SW	009	040	033	027	SC		NO	OT
132	N58W	83SW	001	027	024	027	SC		NO	OT
132	N58W	83SW	007	027	026	027	SC		NO	OT
132	N58W	83SW	001	027	021	027	SC		NO	OT
132	N58W	83SW	001	027	032	027	SC		NO	OT
132	N40E	79NW	027	016	017	016	SC	NE	NO	OT
132	N40E	79NW	039	016	037	016	SC	NE	NO	OT
132	N40E	79NW	018	016	016	016	SC	NE	NO	OT
132	N40E	79NW	016	017	025	017	SC	NE	NO	OT
132	N40E	79NW	054	017	027	017	SC	NE	NO	OT
133	N84W	82SW	064	012	004	004	S	EW	NO	OT
133	N84W	82SW	030	004	019	004	S	EW	NO	OT
133	N61W	90SW	194	016	040	016	S		NO	OT
133	N61W	90SW	182	016	007	016	S		NO	OT
133	N61W	90SW	085	020	027	016	S		NO	OT
133	N61W	90SW	084	020	029	016	S		NO	OT
133	N61W	90SW	050	016	033	016	S		NO	OT
133	N61W	90SW	174	016	053	016	S		NO	OT
134	N48W	88SW	065	007	014	007	S	NW	NO	OT
134	N48W	88SW	063	007	055	007	S	NW	NO	OT
134	N48W	88SW	031	007	026	007	S	NW	NO	OT
134	N48W	88SW	032	007	026	007	S	NW	NO	OT
134	N48W	88SW	022	007	029	007	S	NW	NO	OT
134	N48W	88SW	043	007	041	007	S	NW	NO	OT
135	N80E	86NW	054	109	019	005	SC	EW	NO	OT
135	N80E	86NW	025	095	002	009	SC	EW	NO	OT
135	N80E	86NW	077	234	013	009	SC	EW	NO	OT
135	N80E	86NW	033	126	012	009	SC	EW	NO	OT
135	N80E	86NW	035	049	011	006	SC	EW	PO	OT
135	N80E	86NW	022	073	010	006	SC	EW	NO	OT
135	N80E	86NW	042	104	021	008	SC	EW	NO	OT
135	N80E	86NW	012	041	015	005	SC	EW	NO	OT
135	N04W	79SW	067	010	005	001	SC		NO	OT
135	N45W	88SW	059	016	036	016	SC	NW	NO	OT
135	N45W	88SW	049	016	005	016	SC	NW	NO	OT
135	N45W	88SW	040	015	031	015	SC	NW	NO	OT
135	N45W	88SW	032	014	076	014	SC	NW	NO	OT
135	N45W	88SW	050	011	006	011	SC	NW	NO	OT
135	N45W	88SW	084	013	048	013	SC	NW	NO	OT
135	N25W	87SW	068	006		001	SC		NO	OT
135	N06E	75NW	155	012	020	012	SC		NO	OT

STA	STRI	DIP	LNG	DTH	SPA	BED	EX	ST	LO	GR
135	N06E	75NW	071	015	023	015	SC		NO	OT
135	N06E	75NW	065	017		017	SC		NO	OT
135	N80E	86NW	110	030	038	001	SC	EW	NO	OT
135	N80E	86NW	104	027	013	C01	SC	EW	NO	OT
135	N80E	86NW	057	018	023	001	SC	EW	NO	OT
135	N80E	86NW	074	084	011	001	SC	EW	NO	OT
135	N80E	86NW	213	096	015	001	SC	EW	NO	OT
135	N80E	86NW	179	075	025	001	SC	EW	NO	OT
136	N70W	75NE	146	020	022	009	S		NO	OT
136	N70W	75NE	023	003	017	003	S		NO	OT
136	N70W	75NE	176	013	035	003	S		NO	OT
136	N70W	75NE	123	023	036	007	S		NO	OT
136	N70W	75NE	079	006	029	006	S		NO	OT
136	N70W	75NE	065	009	028	006	S		NO	OT
137	N78W	90SW	103	014	007	014	S		NO	OT
137	N78W	90SW	126	024	021	024	S		NO	OT
137	N78W	90SW	043	032	014	012	S		NO	OT
137	N78W	90SW	103	023	016	013	S		NO	OT
137	N78W	90SW	001	015	016	016	S		NO	OT
137	N78W	90SW	031	043	013	020	S		NO	OT
138	N80E	82NW	087	111	057	111	S	EW	SO	OT
138	N80E	82NW	079	062	012	062	S	EW	SO	OT
138	N80E	82NW	030	025	021	062	S	EW	SO	OT
138	N80E	82NW	128	083		083	S	EW	SO	OT
138	N46W	86NE	052	060		060	S	NW	SO	OT
138	N04W	67SW	056	064	038	112	S		SO	OT
138	N15W	78SW	029	063	020	063	S		SO	OT
138	N15W	78SW	072	053	032	053	S		SO	OT
138	N80E	82NW	020	033	010	001	S	EW	SO	OT
138	N80F	82NW	008	030	003	001	S	EW	SO	OT
138	N80F	82NW	010	025	010	001	S	EW	SO	OT
139	N55W	80SW	294	011	064	001	S	NW	SO	OT
139	N55W	80SW	183	005	032	001	S	NW	SO	OT
139	N55W	80SW	031	002	032	001	S	NW	SO	OT
139	N55W	80SW	037	003	022	001	S	NW	SO	OT
139	N55W	80SW	030	018	029	018	S	NW	SO	OT
139	N55W	80SW	045	008	008	008	S	NW	SO	OT
139	N55W	80SW	063	018	008	018	S	NW	SO	OT
139	N55W	80SW	104	008	043	008	S	NW	SO	OT
139	N55W	80SW	091	015	034	015	S	NW	SO	OT
139	N72E	85SE	062	024	030	024	S		SO	OT
139	N72E	85SE	062	021	019	018	S		SO	OT
139	N72E	85SE	082	023	010	005	S		SO	OT
140	N87E	85NW	540	010	068	001	S	EW	SO	OT
140	N87F	85NW	429	010	012	001	S	FW	SO	OT
140	N87E	85NW	092	012	127	001	S	EW	SO	OT
140	N87E	85NW	364	016	087	001	S	EW	SO	OT

STA	STRI	DIP	LNG	DTH	SPA	BED	EX	ST	LO	GR
140	N87E	85NW	134	001	007	001	S	EW	SO	OT
140	N87E	85NW	182	003	024	001	S	EW	SO	OT
140	N87E	85NW	163	005		001	S	EW	SO	OT
140	N03E	84SE	084	012	028	001	S		SO	OT
140	N03E	84SE	070	007	050	001	S		SO	OT
140	N03E	84SE	136	006	014	001	S		SO	OT
140	N87E	85NW	268	025	003	001	S	EW	SO	OT
140	N87E	85NW	182	019	008	001	S	EW	SO	OT
140	N87E	85NW	204	022	027	001	S	EW	SO	OT
140	N87E	85NW	255	027	095	001	S	EW	SO	OT
140	N87E	85NW	246	025	083	001	S	EW	SO	OT
140	N87E	85NW	217	024	008	001	S	EW	SO	OT
140	N87E	85NW	229	025	010	001	S	EW	SO	OT
140	N87E	85NW	242	025	114	001	S	EW	SO	OT
141	N67W	90SW	180	009	027	009	S		SO	OT
141	N67W	90SW	214	009	030	009	S		SO	OT
141	N67W	90SW	131	009	043	009	S		SO	OT
141	N67W	90SW	108	009	026	009	S		SO	OT
141	N67W	90SW	224	009	015	009	S		SO	OT
141	N67W	90SW	224	009	027	009	S		SO	OT
141	N67W	90SW	182	009	017	009	S		SO	OT
141	N67W	90SW	156	009	016	009	S		SO	OT
141	N67W	90SW	130	009	014	009	S		SO	OT
141	N67W	90SW	100	009	019	009	S		SO	OT
141	N67W	90SW	077	009	009	009	S		SO	OT
141	N67W	90SW	069	009	011	009	S		SO	OT
141	N67W	90SW	065	009	013	009	S		SO	OT
141	N30E	90NW	071	005	048	005	S	NE	SO	OT
141	N30E	90NW	073	005	044	005	S	NE	SO	OT
141	N30E	90NW	302	012	052	012	S	NE	SO	OT
141	N30E	90NW	352	012	030	012	S	NE	SO	OT
141	N30E	90NW	260	012	021	012	S	NE	SO	OT
141	N30E	90NW	134	012	042	012	S	NE	SO	OT
141	N30E	90NW	093	012		012	S	NE	SO	OT
142	N83E	83SE	073	005	012	005	S	EW	SO	OT
142	N83E	83SE	067	005	062	005	S	EW	SO	OT
142	N83E	83SE	107		072		S	EW	SO	OT
142	N83E	83SE	093		015		S	EW	SO	OT
142	N83E	83SE	134		043		S	EW	SO	OT
142	N83E	83SE	087		049		S	EW	SO	OT
142	N83E	83SE	088		084		S	EW	SO	OT
142	N83E	83SE	102		042		S	EW	SO	OT
142	N83E	83SE	080		051		S	EW	SO	OT
142	N83E	83SE	131		031		S	EW	SO	OT
142	N83E	83SE	112		039		S	EW	SO	OT
142	N83E	83SE	111		039		S	EW	SO	OT
142	N83E	83SE	103		058		S	EW	SO	OT

STA	STRI	DIP	LNG	DTH	SPA	BED	EX	ST	LO	GR
142	N83E	83SE	094		060		S	EW	SO	OT
142	N83E	83SE	110		045		S	EW	SO	OT
142	N83E	83SE	125		039		S	EW	SO	OT
142	N13W	73SW	063		010		S		SO	OT
142	N13W	73SW	029		013		S		SO	OT
142	N13W	73SW	109		013		S		SO	OT
142	N13W	73SW	141	012	026	012	S		SO	OT
142	N13W	73SW	095		013		S		SO	OT
142	N13W	73SW	064	007	003	007	S		SO	OT
142	N12E	70NW	072	014	019	014	S		SO	OT
142	N12E	70NW	284	011	014	011	S		SO	OT
142	N12E	70NW	141	012	031	012	S		SO	OT
142	N75W	84NE	013	007	031	007	S		SO	OT
142	N75W	84NE	010	010	072	010	S		SO	OT
142	N75W	84NE	030	009	036	009	S		SO	OT
142	N75W	84NE	017	009	029	009	S		SO	OT
142	N75W	84NE	011	009	036	009	S		SO	OT
143	N45W	64SW	030	007	012	007	S	NW	SO	OT
143	N45W	64SW	027	007	011	007	S	NW	SO	OT
143	N45W	64SW	041	007	016	007	S	NW	SO	OT
143	N45W	64SW	029	007	006	007	S	NW	SO	OT
143	N45W	64SW	057	011	037	011	S	NW	SO	OT
143	N45W	64SW	023	011	013	011	S	NW	SO	OT
143	N45W	64SW	025	011	027	011	S	NW	SO	OT
143	N45W	64SW	056	020	042	020	S	NW	SO	OT
143	N68E	75NW	042	007	028	007	S		SO	OT
143	N68E	75NW	018	007	029	007	S		SO	OT
143	N68E	75NW	052	007	023	007	S		SO	OT
143	N68E	75NW	032	020	011	020	S		SO	OT
143	N65W	84SW	034	011	026	011	S		SO	OT
143	N65W	84SW	016	011	012	011	S		SO	OT
143	N65W	84SW	042	007	017	007	S		SO	OT
143	N65W	84SW	031	005	034	005	S		SO	OT
143	N65W	84SW	057	007	025	007	S		SO	OT
143	N65W	84SW	025	017	023	017	S		SO	OT
143	N65W	84SW	038	017	010	017	S		SO	OT
143	N65W	84SW	036	015	012	015	S		SO	OT
144	N28E	90NW	120		018		S	NE	BR	OT
144	N28E	90NW	134		019		S	NE	BR	OT
144	N28E	90NW	172		024		S	NE	BR	OT
144	N28E	90NW	234		023		S	NE	BR	OT
144	N28E	90NW	186		023		S	NE	BR	OT
144	N28E	90NW	100		016		S	NE	BR	OT
144	N28E	90NW	089		014		S	NE	BR	OT
144	N28E	90NW	115		012		S	NE	BR	OT
144	N28E	90NW	140		013		S	NE	BR	OT
144	N46W	90SW	045		082		S	NW	BR	OT

STA	STRI	DIP	LNG	DTH	SPA	BED	EX	ST	LO	GR
144	N46W	90SW	130		017		S	NW	BR	OT
144	N46W	90SW	090		017		S	NW	BR	OT
144	N46W	90SW	090		024		S	NW	BR	OT
145	N25E	65SE					S	NE	NO	OT
145	N72W	87NE					S		NO	OT
145	N10E	70SE					S		NO	OT
145	N80E	90NW					S	EW	NO	OT
145	N25E	65SE			070		S	NE	NO	OT
145	N25E	65SE			092		S	NE	NO	OT
145	N25E	65SE			060		S	NE	NO	OT
145	N25E	65SE			035		S	NE	NO	OT
145	N25E	65SE			024		S	NE	NO	OT
145	N25E	65SE			031		S	NE	NO	OT
145	N45W	88SW	058	022	128	022	S	NW	NO	OT
145	N45W	88SW	088	022	103	022	S	NW	NO	OT
145	N45W	88SW	020	020	032	020	S	NW	NO	OT
145	N45W	88SW	030	020	090	020	S	NW	NO	OT
145	N45W	88SW	012	020	071	020	S	NW	NO	OT
146	N70W	86SW	070	048	027	012	S		NO	OT
146	N70W	86SW	016	010	042	010	S		NO	OT
146	N70W	86SW	089	010	010	010	S		NO	OT
146	N70W	86SW	083	010		010	S		NO	OT
146	N70W	86SW	045	020	015	005	S		NO	OT
146	N70W	86SW	040	016	067	003	S		NO	OT
146	N70W	86SW	059	014	036	003	S		NO	OT
146	N70W	86SW	065	012	038	003	S		NO	OT
146	N84W	80NE	052	020	068	020	S	EW	NO	OT
146	N84W	80NE	076	041	049	020	S	EW	NO	OT
146	N84W	80NE	063	015	019	015	S	EW	NO	OT
146	N70W	86SW	068	014	035	014	S		NO	OT
146	N70W	86SW	057	014	074	014	S		NO	OT
146	N84W	80NE	080	022	028	022	S	EW	NO	OT
146	N84W	86NE	070	012	014	012	S	EW	NO	OT
146	N84W	80NE	061	012	019	012	S	EW	NO	OT
146	N84W	86NE	073	006	021	006	S	EW	NO	OT
146	N84W	86NE	062	012	048	012	S	EW	NO	OT
146	N70W	86SW	098	022	089	022	S		NO	OT
147	N5W	78NE	070	030	037	030	S	EW	NO	OT
147	N85W	78NE	061	030	043	030	S	EW	NO	OT
147	N85W	78NE	052	030	038	030	S	EW	NO	OT
147	N85W	78NE	032	030	033	030	S	EW	NO	OT
147	N85W	78NE	028	030	031	030	S	EW	NO	OT
147	N85W	78NE	044	030	028	030	S	EW	NO	OT
147	N85W	78NE	056	030	032	030	S	EW	NO	OT
147	N85W	78NE	083	030	043	030	S	EW	NO	OT
147	N85W	78NE	079	030	055	030	S	EW	NO	OT
147	N85W	78NE	075	030	027	030	S	EW	NO	OT

STA	STRI	DIP	LNG	DTH	SPA	BED	EX	ST	LO	GR
147	N85W	78NE	082	030	027	030	S	EW	NO	OT
147	N65W	90SW	013	022	013	022	S		NO	OT
147	N65W	90SW	032	022	013	022	S		NO	OT
148	N80E	90NW	039	025	027	007	S	EW	NO	OT
148	N80E	90NW	079	045	021	009	S	EW	NO	OT
148	N80E	90NW	029	028	016	009	S	EW	NO	OT
148	N80E	90NW	025	015	007	009	S	EW	NO	OT
148	N80E	90NW	039	012	020	009	S	EW	NO	OT
148	N80E	90NW	007	007	020	007	S	EW	NO	OT
148	N80E	90NW	031	007	019	007	S	EW	NO	OT
148	N43W	87SW	024	006	006	006	S	NW	NO	OT
148	N43W	87SW	021	006	009	006	S	NW	NO	OT
148	N43W	87SW	030	006	015	006	S	NW	NO	OT
148	N43W	87SW	069	022	012	022	S	NW	NO	OT
148	N43W	87SW	061	012	013	012	S	NW	NO	OT
148	N43W	87SW	050	012	012	012	S	NW	NO	OT
149	N44W	85NE	025	012	009	012	S	NW	NO	OT
149	N44W	85NE	022	012	018	012	S	NW	NO	OT
149	N44W	85NE	016	012	014	012	S	NW	NO	OT
149	N44W	85NE	032	012	013	012	S	NW	NO	OT
149	N44W	85NE	033	012	011	012	S	NW	NO	OT
149	N44W	85NE	023	012	015	012	S	NW	NO	OT
149	N44W	85NE	029	012	016	012	S	NW	NO	OT
149	N44W	85NE	035	012	007	012	S	NW	NO	OT
149	N44W	85NE	028	012	013	012	S	NW	NO	OT
149	N44W	85NE	025	012		012	S	NW	NO	OT
149	N60W	41SW	027	020	016	007	S		NO	OT
149	N60W	41SW	024	020	010	020	S		NO	OT
149	N60W	41SW	018	007	017	007	S		NO	OT
149	N60W	41SW	035	027	036	007	S		NO	OT
149	N60W	41SW	016	037	017	012	S		NO	OT
149	N60W	41SW	021	040	032	012	S		NO	OT

APPENDIX C

STATION LOCATIONS AT THE ALLEGHENY FRONT
(in UTM Grid Coordinates)

Key to Abbreviations:

STA - station number

STA	LATITUDE	LONGITUDE
001	4317.020	646.880
002	4317.090	647.220
003	4316.590	647.850
004	4316.560	648.050
005	4324.310	648.460
006	4324.360	648.690
007	4324.870	649.130
008	4318.570	646.500
009	4318.720	647.550
010	4318.660	647.870
011	4318.510	648.280
012	4313.750	645.430
013	4313.470	646.070
014	4313.320	646.300
015	4313.120	646.420
016	4314.670	645.500
017	4314.740	645.640
018	4314.610	646.050
019	4314.460	646.420
020	4314.280	646.640
021	4309.770	644.080
022	4309.550	643.560
023	4309.130	644.310
024	4310.800	646.980
025	4307.000	642.710
026	4313.210	647.910
027	4313.760	648.230
028	4318.500	650.010
029	4314.090	645.800

APPENDIX D

ALLEGHENY FRONT DATA

Key to Abbreviations:

STA - station number

STRI- joint strike

DIP - joint dip

SPA - joint spacing (in cm)

LTH - unit: MPO = Pocono, DCK = Catskill,
      DCH = Chemung, DBS = black shales

LO - location with respect to the Petersburg
      lineament: IN = within, NO = north,
      SO = south

GR - group with respect to the Petersburg
      lineament: IN = within, OT = outside

STA	STRI	DIP	SPA	LTH	LO	GP
001	N70W	86SW	170	MPO	IN	IN
001	N65W	90SW	165	MPO	IN	IN
001	N71W	82SW	044	MPO	IN	IN
001	N70W	86SW	105	MPO	IN	IN
001	N69E	90SE	112	MPO	IN	IN
001	N75E	87SE	023	MPO	IN	IN
001	N75E	83SE	053	MPO	IN	IN
001	N69E	90SE	350	MPO	IN	IN
001	N12E	67SE		MPO	IN	IN
001	N30E	72SE	019	MPO	IN	IN
001	N25E	71SE	049	MPO	IN	IN
002	N78E	57SE	103	DCK	IN	IN
002	N68E	67SE	093	DCK	IN	IN
002	N78E	57SE	105	DCK	IN	IN
002	N68E	67SE	320	DCK	IN	IN
003	N63W	88NE	050	DCK	IN	IN
003	N69W	90SW	085	DCK	IN	IN
003	N73W	85SW	130	DCK	IN	IN
003	N63W	88NE	038	DCK	IN	IN
003	N69W	90SW	058	DCK	IN	IN
003	N73W	85SW	056	DCK	IN	IN
003	N88W	78SW	200	DCK	IN	IN
003	N86W	64SW	075	DCK	IN	IN
003	N88W	78SW	090	DCK	IN	IN
003	N27E	37SE	092	DCK	IN	IN
003	N37E	30SE	097	DCK	IN	IN
003	N28E	33SE	060	DCK	IN	IN
003	N27E	37SE	057	DCK	IN	IN
003	N37E	30SE	029	DCK	IN	IN
003	N28E	33SE	021	DCK	IN	IN
003	N27E	37SE	034	DCK	IN	IN
003	N37E	30SE	046	DCK	IN	IN
003	N28E	33SE	031	DCK	IN	IN
003	N27E	37SE	061	DCK	IN	IN
003	N37E	30SE	030	DCK	IN	IN
003	N28E	33SE	070	DCK	IN	IN
003	N27E	37SE	085	DCK	IN	IN
003	N37E	30SE	065	DCK	IN	IN
003	N28E	33SE	031	DCK	IN	IN
003	N27E	37SE	026	DCK	IN	IN
003	N28E	33SE	032	DCK	IN	IN
003	N27E	37SE	095	DCK	IN	IN
003	N37E	30SE	094	DCK	IN	IN
004	N86W	43SW	240	DCH	IN	IN
004	N86W	43SW	190	DCH	IN	IN
004	N86W	43SW	130	DCH	IN	IN
004	N86W	43SW	055	DCH	IN	IN

STA	STRI	DIP	SPA	LTH	LO	GR
004	N86W	43SW	030	DCH	IN	IN
004	N86W	43SW	238	DCH	IN	IN
004	N86W	43SW	157	DCH	IN	IN
004	N86W	43SW	100	DCH	IN	IN
004	N86W	43SW	050	DCH	IN	IN
004	N11W	39NE	028	DCH	IN	IN
004	N11W	39NE	033	DCH	IN	IN
004	N11W	39NE	035	DCH	IN	IN
004	N11W	39NE	056	DCH	IN	IN
004	N70W	69SW	024	DCH	IN	IN
004	N70W	71SW	026	DCH	IN	IN
004	N70W	69SW	015	DCH	IN	IN
004	N70W	71SW	083	DCH	IN	IN
004	N70W	69SW	055	DCH	IN	IN
004	N70W	71SW	067	DCH	IN	IN
004	N70W	69SW	044	DCH	IN	IN
004	N70W	71SW	036	DCH	IN	IN
004	N70W	69SW	045	DCH	IN	IN
004	N70W	71SW	047	DCH	IN	IN
004	N70W	69SW	075	DCH	IN	IN
004	N70W	71SW	066	DCH	IN	IN
005	N15E	87SW	132	MPO	NO	OT
005	N14E	83SE	370	MPO	NO	OT
005	N19E	76SE	022	MPO	NO	OT
005	N15E	87SE	230	MPO	NO	OT
005	N14E	83SE	050	MPO	NO	OT
005	N52W	89SW	066	MPO	NO	OT
005	N58W	89NE	045	MPO	NO	OT
005	N51W	90SW	042	MPO	NO	OT
005	N52W	89SW	113	MPO	NO	OT
005	N58W	89NE	310	MPO	NO	OT
005	N51W	90SW	195	MPO	NO	OT
005	N52W	89SW	110	MPO	NO	OT
005	N58W	89NE	054	MPO	NO	OT
005	N51W	90SW	020	MPO	NO	OT
005	N52W	89SW	092	MPO	NO	OT
005	N58W	89NE	078	MPO	NO	OT
005	N51W	90SW	030	MPO	NO	OT
005	N52W	89SW	115	MPO	NO	OT
005	N85W	84SW	048	MPO	NO	OT
005	N85W	84SW	035	MPO	NO	OT
005	N85W	84SW	030	MPO	NO	OT
005	N85W	84SW	070	MPO	NO	OT
005	N85W	84SW	050	MPO	NO	OT
005	N85W	84SW	085	MPO	NO	OT
006	N12E	58SE	086	DCK	NO	OT
006	N12E	61SE	300	DCK	NO	OT

STA	STRI	DIP	SPA	LTH	LO	GR
006	N19E	54SE	065	DCK	NO	OT
006	N12E	58AQ	380	DCK	NO	OT
006	N44W	90NE	250	DCK	NO	OT
006	N43W	90NE	084	DCK	NO	OT
006	N48W	88NE	068	DCK	NO	OT
006	N40W	90NE	089	DCK	NO	OT
006	N44W	90NE	036	DCK	NO	OT
006	N43W	90NE	178	DCK	NO	OT
006	N48W	88NE	361	DCK	NO	OT
006	N85E	75NW	030	DCK	NO	OT
006	N85W	80NE	028	DCK	NO	OT
006	N85E	75NW	250	DCK	NO	OT
006	N85W	80NE	125	DCK	NO	OT
006	N85E	75NW	222	DCK	NO	OT
006	N85W	80NE	180	DCK	NO	OT
006	N85E	75NW	030	DCK	NO	OT
006	N85W	80NE	221	DCK	NO	OT
007	N84E	87SE	120	DCK	NO	OT
007	N85E	82SE	043	DCK	NO	OT
007	N84E	87SE	148	DCK	NO	OT
007	N85E	82SE	050	DCK	NO	OT
007	N84E	87SE	100	DCK	NO	OT
007	N85E	82SE	150	DCK	NO	OT
007	N84E	82SE	110	DCK	NO	OT
007	N35W	80NE	134	DCK	NO	OT
007	N40W	85NW	110	DCK	NO	OT
007	N35W	80NE	115	DCK	NO	OT
007	N40W	85NE	180	DCK	NO	OT
007	N35W	80NE	114	DCK	NO	OT
007	N40W	85NE	128	DCK	NO	OT
007	N12E	50SE	092	DCK	NO	OT
007	N13E	50SE	150	DCK	NO	OT
007	N09E	60SE	180	DCK	NO	OT
007	N12E	50SE	212	DCK	NO	OT
007	N13E	50SE	250	DCK	NO	OT
008	N52W	90NE	053	MPO	NO	OT
008	N50W	90NE	080	MPO	NO	OT
008	N52W	90NE	075	MPO	NO	OT
008	N50W	90NE	200	MPO	NO	OT
008	N10E	70SE	105	MPO	NO	OT
008	N10E	70SE	180	MPO	NO	OT
008	N10E	70SE	085	MPO	NO	OT
008	N10E	70SE	075	MPO	NO	OT
008	N10E	70SE	040	MPO	NO	OT
008	N83E	90NW	150	MPO	NO	OT
008	N84E	90NW	055	MPO	NO	OT
008	N83E	90NW	064	MPO	NO	OT

STA	STRI	DIP	SPA	LTH	LO	GP
008	N84E	90NW	175	MPO	NO	OT
008	N83E	89NW	150	MPO	NO	OT
008	N35W	90NE	060	MPO	NO	OT
008	N41W	90NE	045	MPO	NO	OT
008	N36W	90NE	070	MPO	NO	OT
008	N41W	90NE	035	MPO	NO	OT
008	N36W	90NE	060	MPO	NO	OT
009	N82E	88NE		DCK	NO	OT
009	N88E	88NW	050	DCK	NO	OT
009	N88E	88NW	600	DCK	NO	OT
009	N88E	88NW	350	DCK	NO	OT
009	N88E	88NW	160	DCK	NO	OT
009	N88E	88NW	150	DCK	NO	OT
009	N05W	88SW	180	DCK	NO	OT
009	N00W	88SW	250	DCK	NO	OT
009	N05W	88SW	180	DCK	NO	OT
009	N00W	88SW	065	DCK	NO	OT
009	N05W	88SW	200	DCK	NO	OT
009	N00W	88SW	025	DCK	NO	OT
009	N05W	88SW	072	DCK	NO	OT
009	N00W	88SW	098	DCK	NO	OT
010	N40E	79SE	073	DCK	NO	OT
010	N32E	80SE	200	DCK	NO	OT
010	N40E	79SE	150	DCK	NO	OT
010	N28E	72NW	180	DCK	NO	OT
010	N25E	56SE	073	DCK	NO	OT
010	N25E	67SE	030	DCK	NO	OT
010	N28E	72NW	078	DCK	NO	OT
010	N25E	56SE	055	DCK	NO	OT
010	N25E	67SE	054	DCK	NO	OT
010	N28E	72NW	044	DCK	NO	OT
010	N78W	80NE	027	DCK	NO	OT
010	N83W	88SW	100	DCK	NO	OT
010	N78W	77NE	079	DCK	NO	OT
010	N80W	88NE	200	DCK	NO	OT
010	N78W	80NE	230	DCK	NO	OT
010	N83W	88SW	100	DCK	NO	OT
010	N78W	77NE	054	DCK	NO	OT
010	N80W	88NE	288	DCK	NO	OT
010	N78W	80NE	070	DCK	NO	OT
010	N50W	72NE	200	DCK	NO	OT
010	N50W	72NE	250	DCK	NO	OT
011	N32E	53SE	100	DCH	NO	OT
011	N32E	53SE	200	DCH	NO	OT
011	N32E	53SE	190	DCH	NO	OT
011	N32E	53SE	060	DCH	NO	OT
011	N32E	53SE	150	DCH	NO	OT

STA	STRI	DIP	SPA	LTH	LO	GR
011	N83W	90SW	050	DCH	NO	OT
011	N77W	90SW	070	DCH	NO	OT
011	N83W	90SW	050	DCH	NO	OT
011	N77W	90SW	095	DCH	NO	OT
011	N83W	90SW	040	DCH	NO	OT
011	N77W	90SW	110	DCH	NO	OT
011	N83W	90SW	150	DCH	NO	OT
011	N77W	90SW	110	DCH	NO	OT
011	N83W	90SW	080	DCH	NO	OT
011	N16E	70SE	170	DCH	NO	OT
011	N16E	70SE	120	DCH	NO	OT
012	N42W	89SW	062	MPO	IN	IN
012	N45W	88SW	055	MPO	IN	IN
012	N39W	90SW	088	MPO	IN	IN
012	N50W	85SW	043	MPO	IN	IN
012	N42W	89SW	110	MPO	IN	IN
012	N45W	88SW	085	MPO	IN	IN
012	N39W	90SW	120	MPO	IN	IN
012	N50W	85SW	075	MPO	IN	IN
012	N42W	89SW	130	MPO	IN	IN
012	N45W	88SW	068	MPO	IN	IN
012	N39W	90SW	049	MPO	IN	IN
012	N28E	90SE	080	MPO	IN	IN
012	N28E	80SE	060	MPO	IN	IN
012	N24E	85SE	110	MPO	IN	IN
012	N28E	90SE	074	MPO	IN	IN
012	N28E	80SE	096	MPO	IN	IN
012	N24E	85SE	060	MPO	IN	IN
012	N10E	75SE	042	MPO	IN	IN
012	N15E	90SE	055	MPO	IN	IN
012	N10E	75SE	040	MPO	IN	IN
012	N15E	90SE	027	MPO	IN	IN
012	N10E	75SE	080	MPO	IN	IN
012	N15E	90SE	060	MPO	IN	IN
013	N75W	86NE	058	DCK	IN	IN
013	N75W	86NE	095	DCK	IN	IN
013	N75W	86NE	105	DCK	IN	IN
013	N74W	86NE	047	DCK	IN	IN
013	N30E	53SE	057	DCK	IN	IN
013	N30E	53SE	052	DCK	IN	IN
013	N30E	53SE	045	DCK	IN	IN
013	N30E	53SE	049	DCK	IN	IN
013	N30E	53SE	059	DCK	IN	IN
013	N30E	53SE	083	DCK	IN	IN
013	N30E	53SE	048	DCK	IN	IN
013	N30E	53SE	045	DCK	IN	IN
014	N65W	86SW	150	DCK	IN	IN

STA	STRI	DIP	SPA	LTH	LO	GR
014	N65W	90SW	240	DCK	IN	IN
014	N65W	86SW	090	DCK	IN	IN
014	N64W	90SW	100	DCK	IN	IN
014	N65W	86SW	030	DCK	IN	IN
014	N65W	86SW	030	DCK	IN	IN
014	N65W	90SW	080	DCK	IN	IN
014	N65W	86SW	120	DCK	IN	IN
014	N08E	78NW	040	DCK	IN	IN
014	N08E	78NW	040	DCK	IN	IN
014	N08E	78NW	100	DCK	IN	IN
014	N08E	78NW	100	DCK	IN	IN
014	N08E	78NW	090	DCK	IN	IN
014	N35E	55SE	039	DCK	IN	IN
014	N35E	55SW	045	DCK	IN	IN
014	N35E	55SW	030	DCK	IN	IN
014	N35E	55SW	050	DCK	IN	IN
014	N35E	55SW	040	DCK	IN	IN
014	N35E	55SW	050	DCK	IN	IN
014	N35E	55SW	063	DCK	IN	IN
014	N35E	55SW	049	DCK	IN	IN
014	N88W	60SW	039	DCK	IN	IN
014	N88W	60SW	022	DCK	IN	IN
014	N88W	60SW	030	DCK	IN	IN
015	N85W	88SW	026	DCH	IN	IN
015	N85W	88SW	034	DCH	IN	IN
015	N85W	88SW	026	DCH	IN	IN
015	N85W	88SW	033	DCH	IN	IN
015	N85W	88SW	080	DCH	IN	IN
015	N02E	27SE	020	DCH	IN	IN
015	N02E	27SE	030	DCH	IN	IN
015	N02E	27SE	038	DCH	IN	IN
015	N02E	27SE	055	DCH	IN	IN
015	N02E	27SE	038	DCH	IN	IN
015	N02E	27SE	024	DCH	IN	IN
015	N02E	27SE	025	DCH	IN	IN
015	N02E	27SE	050	DCH	IN	IN
016	N18E	78SE	081	DCK	IN	IN
016	N20E	70SE	008	DCK	IN	IN
016	N18E	78SE	016	DCK	IN	IN
016	N20E	70SE	040	DCK	IN	IN
016	N18E	78SE	045	DCK	IN	IN
016	N20E	70SE	040	DCK	IN	IN
016	N18E	78SE	035	DCK	IN	IN
016	N20E	70SE	080	DCK	IN	IN
016	N18E	70SE	045	DCK	IN	IN
016	N20E	70SE	110	DCK	IN	IN
016	N26W	74NE	068	DCK	IN	IN

STA	STRI	DIP	SPA	LTH	LO	GE
016	N26W	74NE	074	DCK	IN	IN
016	N26W	74NE	050	DCK	IN	IN
016	N26W	74NE	022	DCK	IN	IN
016	N85W	90SW	025	DCK	IN	IN
016	N85W	90SW	015	DCK	IN	IN
016	N85W	90SW	043	DCK	IN	IN
016	N85E	75SE	030	DCK	IN	IN
016	N85W	90SW	027	DCK	IN	IN
016	N85W	90SW	016	DCK	IN	IN
016	N85W	90SW	012	DCK	IN	IN
016	N85W	90SW	023	DCK	IN	IN
016	N85W	90SW	026	DCK	IN	IN
016	N85W	90SW	038	DCK	IN	IN
016	N85W	90SW	032	DCK	IN	IN
016	N85W	90SW	052	DCK	IN	IN
016	N85W	90SW	033	DCK	IN	IN
016	N85W	90SW	041	DCK	IN	IN
016	N85W	90SW	075	DCK	IN	IN
016	N85W	90SW	053	DCK	IN	IN
016	N85W	90SW	035	DCK	IN	IN
016	N85W	90SW	025	DCK	IN	IN
016	N85W	90SW	030	DCK	IN	IN
016	N85W	90SW	120	DCK	IN	IN
017	N82E	90SE		DCK	IN	IN
017	N10E	75SE	070	DCK	IN	IN
017	N10E	75SE	036	DCK	IN	IN
017	N10E	75SE	073	DCK	IN	IN
017	N10E	75SE	045	DCK	IN	IN
017	N10E	75SE	073	DCK	IN	IN
017	N45W	90SW	090	DCK	IN	IN
017	N45W	90SW	110	DCK	IN	IN
017	N45W	90SW	080	DCK	IN	IN
018	N80W	86NE	020	DCK	IN	IN
018	N80W	86NE	053	DCK	IN	IN
018	N80W	86NE	040	DCK	IN	IN
018	N80W	86NE	045	DCK	IN	IN
018	N80W	86NE	042	DCK	IN	IN
018	N80W	86NE	023	DCK	IN	IN
018	N80W	86NE	080	DCK	IN	IN
018	N50E	62SE	076	DCK	IN	IN
018	N50E	62SE	023	DCK	IN	IN
018	N50E	62SE	029	DCK	IN	IN
018	N50E	62SE	040	DCK	IN	IN
018	N50E	62SE	078	DCK	IN	IN
018	N50E	62SE	058	DCK	IN	IN
018	N50E	62SE	060	DCK	IN	IN
018	N50E	62SE	100	DCK	IN	IN

STA	STRI	DIP	SPA	LTH	LO	GR
019	N85W	83SW	060	DCK	IN	IN
019	N85W	83SW	082	DCK	IN	IN
019	N85W	83SW	060	DCK	IN	IN
019	N85W	83SW	040	DCK	IN	IN
019	N85W	83SW	023	DCK	IN	IN
019	N85W	83SW	040	DCK	IN	IN
019	N85W	83SW	150	DCK	IN	IN
019	N85W	83SW	150	DCK	IN	IN
019	N85W	83SW	040	DCK	IN	IN
019	N85W	83SW	018	DCK	IN	IN
019	N85W	83SW	028	DCK	IN	IN
019	N85W	83SW	032	DCK	IN	IN
020	N80W	90SW	070	DCH	IN	IN
020	N80W	90SW	050	DCH	IN	IN
020	N80W	90SW	040	DCH	IN	IN
020	N80W	90SW	020	DCH	IN	IN
020	N80W	90SW	050	DCH	IN	IN
020	N80W	90SW	040	DCH	IN	IN
020	N80W	90SW	080	DCH	IN	IN
020	N80W	90SW	020	DCH	IN	IN
020	N80W	90SW	040	DCH	IN	IN
020	N10E	50SE	020	DCH	IN	IN
020	N10E	50SE	020	DCH	IN	IN
020	N10E	50SE	020	DCH	IN	IN
020	N10E	50SE	040	DCH	IN	IN
021	N15E	66SE	110	MPO	SO	OT
021	N15E	66SE	175	MPO	SO	OT
021	N15E	66SE	080	MPO	SO	OT
021	N50W	80NE	150	MPO	SO	OT
021	N50W	80NE	120	MPO	SO	OT
021	N50W	80NE	120	MPO	SO	OT
021	N50W	80NE	070	MPO	SO	OT
021	N50W	80NE	050	MPO	SO	OT
021	N50W	80NE	070	MPO	SO	OT
021	N50W	80NE	200	MPO	SO	OT
021	N50W	80NE	175	MPO	SO	OT
021	N50W	80NE	075	MPO	SO	OT
021	N50W	80NE	250	MPO	SO	OT
022	N40E	70SE	300	DCK	SO	OT
022	N40E	70SE	175	DCK	SO	OT
022	N45W	88NE	070	DCK	SO	OT
022	N45W	88NE	300	DCK	SO	OT
022	N45W	88NE	250	DCK	SO	OT
022	N45W	88NE	150	DCK	SO	OT
023	N50E	21NW	070	DCK	SO	OT
023	N50E	21NW	075	DCK	SO	OT
023	N50E	21NW	090	DCK	SO	OT

STA	STRI	DIP	SPA	LTH	LC	GR
023	N50E	21NW	200	DCK	SO	OT
023	N50E	21NW	040	DCK	SO	OT
023	N50E	21NW	060	DCK	SO	OT
023	N51W	90SW	160	DCK	SO	OT
023	N51W	90SW	060	DCK	SO	OT
023	N51W	90SW	075	DCK	SO	OT
023	N51W	90SW	100	DCK	SO	OT
023	N51W	90SW	070	DCK	SO	OT
023	N51W	90SW	080	DCK	SO	OT
023	N51W	90SW	030	DCK	SO	OT
023	N51W	90SW	150	DCK	SO	OT
023	N51W	90SW	300	DCK	SO	OT
023	N34E	53NW		DCK	SO	OT
024	N81W	89NE	057	DCH	SO	OT
024	N81W	89NE	060	DCH	SO	OT
024	N81W	89NE	054	DCH	SO	OT
024	N81W	89NE	035	DCH	SO	OT
024	N81W	89NE	067	DCH	SO	OT
024	N81W	89NE	115	DCH	SO	OT
024	N81W	89NE	100	DCH	SO	OT
024	N81W	89NE	037	DCH	SO	OT
024	N81W	89NE	150	DCH	SO	OT
024	N81W	89NE	115	DCH	SO	OT
024	N81W	89NE	075	DCH	SO	OT
024	N81W	89NE	105	DCH	SO	OT
024	N16E	76NW	160	DCH	SO	OT
024	N16E	76NW	075	DCH	SO	OT
024	N16E	76NW	169	DCH	SO	OT
024	N16E	76NW	065	DCH	SO	OT
024	N16E	76NW	175	DCH	SO	OT
024	N16E	76NW	160	DCH	SO	OT
024	N16E	76NW	120	DCH	SO	OT
024	N16E	76NW	070	DCH	SO	OT
024	N16E	76NW	070	DCH	SO	OT
024	N16E	76NW	100	DCH	SO	OT
025	N50W	54SW	018	DBS	SO	OT
025	N50W	54SW	018	DBS	SO	OT
025	N50W	54SW	016	DBS	SO	OT
025	N50W	54SW	019	DBS	SO	OT
025	N50W	54SW	017	DBS	SO	OT
025	N50W	54SW	017	DBS	SO	OT
025	N50W	54SW	022	DBS	SO	OT
025	N50W	54SW	017	DBS	SO	OT
025	N50W	54SW	015	DBS	SO	OT
025	N50W	54SW	014	DBS	SO	OT
025	N50W	54SW	013	DBS	SO	OT
025	N50W	54SW	009	DBS	SO	OT

STA	STRI	DIP	SPA	LTH	LO	GR
025	N85W	30NE	030	DBS	SO	OT
025	N85W	30NE	017	DBS	SO	OT
025	N85W	30NE	025	DBS	SO	OT
025	N85W	30NE	040	DBS	SO	OT
025	N85W	30NE	030	DBS	SO	OT
025	N85W	30NE	040	DBS	SO	OT
025	N85W	30NE	020	DBS	SO	GT
025	N85W	30NE	052	DBS	SO	OT
025	N85W	30NE	016	DBS	SO	OT
025	N85W	30NE	050	DBS	SO	OT
026	N83E	71NW	045	DBS	IN	IN
026	N83E	71NW	007	DBS	IN	IN
026	N83E	71NW	007	DBS	IN	IN
026	N83E	71NW	013	DBS	IN	IN
026	N83E	71NW	015	DBS	IN	IN
026	N83E	71NW	008	DBS	IN	IN
026	N83E	71NW	009	DBS	IN	IN
026	N83E	71NW	015	DBS	IN	IN
026	N83E	71NW	010	DBS	IN	IN
026	N83E	71NW	028	DBS	IN	IN
026	N83E	71NW	013	DBS	IN	IN
026	N83E	71NW	015	DBS	IN	IN
026	N83E	71NW	018	DBS	IN	IN
026	N83E	71NW	025	DBS	IN	IN
026	N83E	71NW	007	DBS	IN	IN
026	N14E	34SE	028	DBS	IN	IN
026	N14E	34SE	028	DBS	IN	IN
026	N14E	34SE	019	DBS	IN	IN
026	N14E	34SE	011	DBS	IN	IN
027	N50E	45SE	016	DBS	IN	IN
027	N50E	45SE	010	DBS	IN	IN
027	N50E	45SE	020	DBS	IN	IN
027	N50E	45SE	020	DBS	IN	IN
027	N50E	45SE	020	DBS	IN	IN
027	N50E	45SE	009	DBS	IN	IN
027	N50E	45SE	010	DBS	IN	IN
027	N50E	45SE	030	DBS	IN	IN
027	N50E	45SE	019	DBS	IN	IN
027	N55W	86NE	013	DBS	IN	IN
027	N55W	86NE	012	DBS	IN	IN
027	N55W	86NE	007	DBS	IN	IN
027	N55W	86NE	007	DBS	IN	IN
027	N55W	86NE	012	DBS	IN	IN
027	N55W	86NE	030	DBS	IN	IN
028	N35E	55NW	020	DBS	NO	OT
028	N35E	55NW	016	DBS	NO	OT
028	N35E	55NW	009	DBS	NO	OT

STA	STRI	DIP_	SPA	LTH	LO	GP
028	N35E	55NW	023	DBS	NO	OT
028	N35E	55NW	017	DBS	NO	OT
028	N35E	55NW	023	DBS	NO	OT
028	N35E	55NW	034	DBS	NC	OT
028	N35E	55NW	025	DBS	NO	OT
028	N50W	60SW	040	DRS	NO	OT
028	N50W	60SW	026	DBS	NO	OT
028	N50W	60SW	038	DBS	NO	OT
028	N50W	60SW	041	DRS	NO	OT
028	N50W	60SW	033	DBS	NO	OT
029			058	MPO	IN	IN
029			059	MPO	IN	IN
029			090	MPO	IN	IN
029			052	MPO	IN	IN
029			049	MPO	IN	IN
029			042	MPO	IN	IN
029			033	MPO	IN	IN
029			034	MPO	IN	IN
029			076	MPO	IN	IN
029			075	MPO	IN	IN
029			057	MPO	IN	IN
029			082	MPO	IN	IN

APPENDIX E

STATION LOCATIONS OF THE WESTWARD EXTENSIONS
PARSONS AND PETERSBURG LINEAMENTS
(in UTM Grid Coordinates)

Key to Abbreviations:

STA - station number

STA	LATITUDE	LONGITUDE	STA	LATITUDE	LONGITUDE
038	4340.470	592.200	081A	4311.470	580.210
042	4330.820	586.670	082	4313.780	578.540
043	4338.920	585.530	083	4314.000	578.020
044	4340.010	589.220	084	4308.180	576.310
045	4341.180	591.640	085	4307.770	576.620
046	4341.700	591.610	087	4304.660	586.050
047	4341.900	591.450	088	4304.510	586.690
048	4341.960	591.270	089	4305.600	588.780
049	4342.500	591.740	090	4313.450	589.900
050	4353.810	592.840	091	4311.540	589.900
051	4355.000	591.780	092	4306.030	585.600
052	4355.360	591.260	093	4305.130	583.910
053	4354.980	588.700	094	4321.510	581.100
054	4359.300	593.310	095	4303.280	588.650
055	4362.350	595.450	096	4300.260	588.170
056	4363.770	596.120	097	4299.210	587.180
057	4360.580	595.570	098	4296.560	582.920
058	4356.220	592.020	099	4296.800	582.100
059	4349.870	591.830	100	4294.590	578.900
060	4342.910	592.070	101	4302.330	575.710
061	4343.110	592.010	102	4344.770	584.380
062	4367.310	580.420	103	4322.850	589.800
063	4367.070	581.080	104	4331.470	586.340
064	4359.870	578.640	105	4326.170	578.380
065	4349.260	594.170	106	4326.480	578.480
066	4350.070	591.320	107	4302.250	570.990
068	4361.550	577.800	108	4302.720	571.330
069	4361.340	577.910	109	4303.100	571.520
070	4360.840	578.170	110	4332.110	587.660
071	4360.630	578.380	111	4334.280	589.070
072	4370.410	579.710	112	4334.550	590.570
078	4359.160	587.580	113	4337.390	588.710
079	4355.410	586.060	114	4339.020	588.090
080	4354.770	582.400	115	4339.940	587.960
081	4354.320	580.710			

APPENDIX F

WESTWARD EXTENSIONS DATA

Key to Abbreviations:

STA - station number

STRI- joint strike

DIP - joint dip

SPA - joint spacing (in cm)

LTH - unit: PAL = Allegheny, PPV = Pottsville

LOC - location with respect to lineaments.
      See Figure 14 for sub-area locations

GR - group with respect to lineaments: IN =
      within, OT = outside

STA	STRI	DIP	SPA	LTH	LOC	GE
038	N22E		0367	PPV	I-2	I N
038	N22E		0202	PPV	I-2	I N
038	N22E		0220	PPV	I-2	I N
038	N22E		0200	PPV	I-2	I N
038	N22E		0900	PPV	I-2	I N
038	N22E		0760	PPV	I-2	I N
038	N22E		0280	PPV	I-2	I N
038	N22E		0400	PPV	I-2	I N
038	N22E		0260	PPV	I-2	I N
038	N22E		0297	PPV	I-2	I N
038	N80E		0220	PPV	I-2	I N
038	N80E		0360	PPV	I-2	I N
038	N80E		0227	PPV	I-2	I N
042	N85E	77NE	0900	PAL	0-5	0T
042	N85E	77NE	1500	PAL	0-5	0T
042	N14E	82SE	0300	PAL	0-5	0T
042	N14E	82SE	0560	PAL	0-5	0T
042	N14E	82SE	0750	PAL	0-5	0T
042	N14E	82SE	0280	PAL	0-5	0T
042	N49W	86NE	0550	PAL	0-5	0T
042	N49W	86NE	1500	PAL	0-5	0T
042	N49W	86NE	1450	PAL	0-5	0T
043	N34E	85SE	0450	PAL	0-5	0T
043	N34E	85SE	0800	PAL	0-5	0T
043	N34E	85SE	0520	PAL	0-5	0T
043	N34E	85SE	1080	PAL	0-5	0T
043	N34E	85SE	0630	PAL	0-5	0T
043	N76E	88SE	0490	PAL	0-5	0T
043	N76E	88SE	0104	PAL	0-5	0T
043	N76E	88SE	0295	PAL	0-5	0T
043	N76E	88SE	0310	PAL	0-5	0T
043	N76E	88SE	0276	PAL	0-5	0T
043	N76E	88SE	0130	PPV	0-5	0T
043	N75E	88SE	0100	PPV	0-5	0T
044	N70W	90SW	0340	PPV	0-5	0T
044	N70W	90SW	0190	PPV	0-5	0T
044	N70W	90SW	0210	PPV	0-5	0T
044	N70W	90SW	0710	PPV	0-5	0T
044	N70W	90SW	0580	PPV	0-5	0T
044	N70W	90SW	0238	PPV	0-5	0T
044	N70W	90SW	0320	PPV	0-5	0T
044	N10E	90NW	1390	PPV	0-5	0T
044	N10E	90NW	0400	PPV	0-5	0T
044	N10E	90NW	1120	PPV	0-5	0T
044	N10E	90NW	0205	PPV	0-5	0T
044	N10E	90NW	0605	PPV	0-5	0T
044	N10E	90NW	0505	PPV	0-5	0T

STA	STRI	DIP	SPA	LTH	LOC	GR
045	N13E	81NW	0170	PPV	I-2	IN
045	N13E	81NW	0150	PPV	I-2	IN
045	N13E	81NW	0230	PPV	I-2	IN
045	N13E	81NW	0095	PPV	I-2	IN
045	N13E	81NW	0180	PPV	I-2	IN
045	N13E	81NW	0370	PPV	I-2	IN
045	N87E	75SE	0940	PPV	I-2	IN
045	N87E	75SE	0190	PPV	I-2	IN
045	N87E	75SE	0380	PPV	I-2	IN
045	N87E	75SE	0370	PPV	I-2	IN
046	N30W	77SW	0230	PPV	I-2	IN
046	N30W	77SW	0220	PPV	I-2	IN
046	N30W	77SW	0250	PPV	I-2	IN
047	N72E	87SE	0150	PAL	I-2	IN
047	N72E	87SE	0150	PAL	I-2	IN
047	N72E	87SE	0100	PAL	I-2	IN
047	N72E	87SE	0200	PAL	I-2	IN
047	N72E	87SE	0115	PAL	I-2	IN
047	N72E	87SE	0100	PAL	I-2	IN
047	N72E	87SE	0130	PAL	I-2	IN
047	N72E	87SE	0110	PAL	I-2	IN
047	N72E	87SE	0120	PAL	I-2	IN
047	N72E	87SE	0200	PAL	I-2	IN
047	N72E	87SE	0300	PAL	I-2	IN
047	N72E	87SE	0170	PAL	I-2	IN
048	N70E	90NW	0380	PAL	I-2	IN
048	N70E	90NW	0440	PAL	I-2	IN
048	N70E	90SW	0730	PAL	I-2	IN
048	N70E	90NW	0570	PAL	I-2	IN
048	N70E	90NW	0770	PAL	I-2	IN
048	N35E	90NW	0300	PAL	I-2	IN
048	N35E	90NW	0280	PAL	I-2	IN
048	N35E	90NW	0410	PAL	I-2	IN
048	N35E	90NW	0240	PAL	I-2	IN
048	N35E	90NW	0150	PAL	I-2	IN
048	N35E	90NW	0200	PAL	I-2	IN
049	N85W	70NE	0150	PAL	I-2	IN
049	N85W	70NE	0125	PAL	I-2	IN
049	N85W	70NE	0200	PAL	I-2	IN
049	N85W	70NE	0150	PAL	I-2	IN
049	N85W	70NE	0180	PAL	I-2	IN
049	N35E	90NW	0200	PAL	I-2	IN
049	N35E	90NW	0250	PAL	I-2	IN
050	N88E	88NW	0020	PST	I-1	IN
050	N88E	88NW	0055	PST	I-1	IN
050	N88E	88NW	0280	PST	I-1	IN
050	N88E	88NW	0200	PST	I-1	IN

STA	STRI	DIP	SPA	LTH	LOC	GE
050	N22E	90NW	0200	PST	I-1	IN
050	N22E	90NW	0220	PST	I-1	IN
051	N19E	72SE	0300	PAL	I-1	IN
051	N19E	72SE	0180	PAL	I-1	IN
051	N19E	72SE	0150	PAL	I-1	IN
051	N19E	72SE	0150	PAL	I-1	IN
051	N19E	72SE	0180	PAL	I-1	IN
051	N19E	72SE	0275	PAL	I-1	IN
051	N75E	90NW	0300	PAL	I-1	IN
051	N75E	90NW	0300	PAL	I-1	IN
051	N75E	90NW	0180	PAL	I-1	IN
051	N75E	90NW	0250	PAL	I-1	IN
051	N75E	90NW	0270	PAL	I-1	IN
051	N75E	90NW	0200	PAL	I-1	IN
051	N75E	90NW	0200	PAL	I-1	IN
051	N75E	90NW	0350	PAL	I-1	IN
052	N24E	90NW	0270	PAL	I-1	IN
052	N24E	90NW	0690	PAL	I-1	IN
052	N24E	90NW	1020	PAL	I-1	IN
052	N83E	75NW	0140	PAL	I-1	IN
052	N83E	75NW	0040	PAL	I-1	IN
052	N83E	75NW	0940	PAL	I-1	IN
052	N83E	75NW	0100	PAL	I-1	IN
052	N83E	75NW	0400	PAL	I-1	IN
052	N36W	75NW	0350	PAL	I-1	IN
052	N35W	75NW	0150	PAL	I-1	IN
053	N85W	90NE	0200	PAL	I-1	IN
053	N86W	90NE	0300	PAL	I-1	IN
053	N86W	90NE	0220	PAL	I-1	IN
053	N30W	89NE	0220	PAL	I-1	IN
053	N30W	89NE	0350	PAL	I-1	IN
053	N30W	89NE	0180	PAL	I-1	IN
054	N50W		0300	PAL	O-1	OT
054	N50W		0500	PAL	O-1	OT
054	N24E		0210	PAL	O-1	OT
054	N24E		0310	PAL	O-1	OT
054	N24E		0380	PAL	O-1	OT
054	N24E		0300	PAL	O-1	OT
054	N24E		0530	PAL	O-1	OT
055	N25E		0620	PAL	O-1	OT
055	N25E		0530	PAL	O-1	OT
055	N25E		0400	PAL	O-1	OT
055	N25E		0850	PAL	O-1	OT
055	N55W		0425	PAL	O-1	OT
055	N55W		0280	PAL	O-1	OT
055	N55W		0240	PAL	O-1	OT
055	N55W		0590	PAL	O-1	OT

STA	STRI	DIP	SPA	LTH	LOC	GR
055	N55W		0370	PAL	0-1	OT
055	N55W		0340	PAL	0-1	OT
056	N52W		0330	PAL	0-1	OT
056	N52W		1150	PAL	0-1	OT
056	N52W		0800	PAL	0-1	OT
056	N52W		0940	PAL	0-1	OT
057	N15E	88SE	1060	PAL	0-1	OT
057	N15E	88SE	0580	PAL	0-1	OT
057	N15E	88SE	0330	PAL	0-1	OT
057	N54W	80SW	0290	PAL	0-1	OT
057	N54W	80SW	0300	PAL	0-1	OT
057	N54W	80SW	0340	PAL	0-1	OT
057	N15E	88SE	0270	PAL	0-1	OT
058	N54W	90SW	0870	PAL	0-1	OT
058	N54W	90SW	0900	PAL	0-1	OT
058	N54W	90SW	0840	PAL	0-1	OT
058	N54W	90SW	0590	PAL	0-1	OT
058	N54W	90SW	0500	PAL	0-1	OT
058	N54W	90SW	0450	PAL	0-1	OT
058	N54W	90SW	0470	PAL	0-1	OT
058	N54W	90SW	0560	PAL	0-1	OT
058	N33E	75NW	0340	PAL	0-1	OT
058	N33E	75NW	0340	PAL	0-1	OT
058	N33E	75NW	0350	PAL	0-1	OT
058	N33E	75NW	0360	PAL	0-1	OT
059	N02W	75SW	0510	PAL	0-4	OT
059	N02W	75SW	2000	PAL	0-4	OT
059	N02W	75SW	0510	PAL	0-4	OT
059	N02W	75SW	1070	PAL	0-4	OT
059	N20E	75SW	0330	PAL	0-4	OT
060	N80W	80NE	0570	PPV	0-4	OT
060	N80W	80NE	0720	PPV	0-4	OT
060	N80W	80NE	1110	PPV	0-4	OT
060	N80W	80NE	0840	PPV	0-4	OT
060	N80W	80NE	0245	PPV	0-4	OT
060	N80W	80NE	0955	PPV	0-4	OT
060	N80W	80NE	0815	PPV	0-4	OT
060	N80W	80NE	0160	PPV	0-4	OT
060	N80W	80NE	0420	PPV	0-4	OT
060	N80W	80NE	0295	PPV	0-4	OT
060	N80W	80NE	0170	PPV	0-4	OT
060	N80W	80NE	0460	PPV	0-4	OT
060	N80W	80NE	0210	PPV	0-4	OT
060	N80W	80NE	0170	PPV	0-4	OT
060	N80W	80NE	0270	PPV	0-4	OT
061	N25E			PPV	0-4	OT
061	N04W	80SW	0480	PPV	0-4	OT

STA	STRI	DIP	SPA	LTH	LOC	GE
061	N04W	90SW	0400	PPV	0-4	OT
061	N85E		0500	PPV	0-4	OT
061	N85E		0500	PPV	0-4	OT
061	N85E		0800	PPV	0-4	OT
061	N85E		0740	PPV	0-4	OT
062	N11E		0350	PPV	0-2	OT
062	N11E		0200	PPV	0-2	OT
063	N56W	90SW	0380	PAL	0-2	OT
063	N56W	90SW	0360	PAL	0-2	OT
064	N75W	90SW	0184	PAL	0-3	OT
064	N75W	90SW	0227	PAL	0-3	OT
064	N75W	90SW	0250	PAL	0-3	OT
064	N75W	90SW	0530	PAL	0-3	OT
064	N75W	90SW	0445	PAL	0-3	OT
064	N75W	90SW	0320	PAL	0-3	OT
064	N75W	90SW	0100	PAL	0-3	OT
064	N75W	90SW	0180	PAL	0-3	OT
064	N75W	90SW	0100	PAL	0-3	OT
064	N75W	90SW	0200	PAL	0-3	OT
064	N75W	90SW	0210	PAL	0-3	OT
064	N75W	90SW	0240	PAL	0-3	OT
064	N75W	90SW	0310	PAL	0-3	OT
064	N75W		0440	PAL	0-3	OT
064	N75W		0610	PAL	0-3	OT
065	N45E		0250	PAL	I-1	IN
065	N45E		0325	PAL	I-1	IN
065	N45E		0200	PAL	I-1	IN
065	N45E		0225	PAL	I-1	IN
065	N45E		0325	PAL	I-1	IN
065	N38W		0280	PAL	I-1	IN
065	N38W		0350	PAL	I-1	IN
065	N38W		0350	PAL	I-1	IN
065	N38W		0300	PAL	I-1	IN
065	N38W		0150	PAL	I-1	IN
065	N38W		0175	PAL	I-1	IN
065	N38W		0275	PAL	I-1	IN
065	N38W		0275	PAL	I-1	IN
066	N15W		1117	PAL	0-4	OT
066	N15W		0420	PAL	0-4	OT
066	N15W		0640	PAL	0-4	OT
066	N37W		0260	PAL	0-4	OT
066	N37W		0330	PAL	0-4	OT
066	N37W		0220	PAL	0-4	OT
066	N37W		0240	PAL	0-4	OT
066	N37W		0140	PAL	0-4	OT
066	N37W		0310	PAL	0-4	OT

STA	STRI	DIP	SPA	LTH	LOC	GP
068	N75W		0200	PAL	0-3	OT
068	N75W		0190	PAL	0-3	OT
068	N75W		0460	PAL	0-3	OT
068	N75W		0350	PAL	0-3	OT
068	N75W		0260	PAL	0-3	OT
069	N70W		0560	PAL	0-3	OT
069	N70W		0560	PAL	0-3	OT
069	N70W		0700	PAL	0-3	OT
070	N18E	88NW	0675	PAL	0-3	OT
070	N18E	88NW	0475	PAL	0-3	OT
070	N75W	86NE	0775	PAL	0-3	OT
070	N75W	86NE	0690	PAL	0-3	OT
070	N75W	86NE	1090	PAL	0-3	OT
070	N75W	86NE	1030	PAL	0-3	OT
070	N75W	86NE	0530	PAL	0-3	OT
071	N69W	89NE	0330	PAL	0-3	OT
071	N69W	89NE	0520	PAL	0-3	OT
071	N69W	89NE	0230	PAL	0-3	OT
071	N69W	89NE	0450	PAL	0-3	OT
072	N07E		0530	PAL	0-2	OT
072	N07E		0340	PAL	0-2	OT
072	N07E		0280	PAL	0-2	OT
072	N80E		0790	PAL	0-2	OT
078	N01E	89NW		PAL	I-1	IN
078	N45W	79SW	0490	PAL	I-1	IN
078	N45W	79SW	0410	PAL	I-1	IN
078	N80W	85SW	0220	PAL	I-1	IN
079	N87W	90SW	0350	PAL	0-4	OT
080	N25E	90NW	0540	PAL	0-3	OT
080	N25E	90NW	0190	PAL	0-3	OT
080	N25E	90SW	0430	PAL	0-3	OT
081	N15E	90NW	0570	PAL	0-3	OT
081	N15E	90NW	0480	PAL	0-3	OT
081	N15E	90NW	0840	PAL	0-3	OT
081	N15E	90NW	0430	PAL	0-3	OT
081	N85W	74SW	1200	PAL	0-3	OT
81A	N20E	90NW	1810	PPV	0-6	OT
81A	N20E	90NW	1270	PPV	0-6	OT
81A	N20E	90NW	1950	PPV	0-6	OT
81A	N20E	90NW	1410	PPV	0-6	OT
81A	N45W	80NE	0230	PPV	0-6	OT
81A	N45W	80NE	0760	PPV	0-6	OT
81A	N45W	80NE	1730	PPV	0-6	OT
81A	N45W	80NE	1200	PPV	0-6	OT
082	N40E	90NW	1030	PAL	0-6	OT
082	N40E	90NW	0830	PAL	0-6	OT
082	N40E	90NW	0670	PAL	0-6	OT

STA	STRI	DIP	SPA	LTH	LOC	GP
082	N80E	75SE	0070	PAL	0-6	OT
082	N80E	75SE	0220	PAL	0-6	OT
082	N80E	75SE	0400	PAL	0-6	OT
083				PAL	0-6	OT
084	N80W	88SW	1220	PAL	0-6	OT
084	N03E	87SE			0-6	OT
086	N75E	89SE	0130	PPV	0-6	OT
086	N75E	89SE	0110	PPV	0-6	OT
086	N75E	89SE	0230	PPV	0-6	OT
087	N73E	87SE	1000	PAL	I-3	IN
087	N73E	87SE	0460	PAL	I-3	IN
087	N01E	77NW	0740	PAL	I-3	IN
088	N81E	90NW	0330	PPV	I-3	IN
088	N81E	90NW	0330	PPV	I-3	IN
088	N81E	90NW	0340	PPV	I-3	IN
088	N81E	90NW	0380	PPV	I-3	IN
088	N81E	90NW	0440	PPV	I-3	IN
088	N81E	90NW	0490	PPV	I-3	IN
088	N81E	90NW	0240	PPV	I-3	IN
088	N81E	90NW	0190	PPV	I-3	IN
088	N60W	90SW	0270	PPV	I-3	IN
088	N60W	90SW	0260	PPV	I-3	IN
089	N25E	83SE	0450	PPV	I-3	IN
089	N65W	90SW	0275	PPV	I-3	IN
090	N55E	78NW	0620	PAL	0-6	OT
090	N55E	78NW	0710	PAL	0-6	OT
090	N85E	85NW	0800	PAL	0-6	OT
091	N75E	78SE	0810	PAL	0-6	OT
091	N75E	78SE	1900	PAL	0-6	OT
091	N75E	78SE	0650	PAL	0-6	OT
091	N75E	78SE	0260	PAL	0-6	OT
091	N75E	78SE	1130	PAL	0-6	OT
091	N75E	78SE	0520	PAL	0-6	OT
092	N10E	90NW	0160	PAL	I-3	IN
092	N10E	90NW	0110	PAL	I-3	IN
092	N10E	90NW	1320	PAL	I-3	IN
092	N10E	90NW	0840	PAL	I-3	IN
092	N85E	90NW	1140	PAL	I-3	IN
092	N27E	75NW	0160	PAL	I-3	IN
093	N22W	82SW	0120	PPV	I-3	IN
093	N22W	82SW	0100	PPV	I-3	IN
093	N22W	82SW	0080	PPV	I-3	IN
093	N45W	90SW		PPV	I-3	IN
094	N35E	90NW		PAL	0-6	OT
095	N65W	90SW	0150	PPV	I-3	IN
095	N89W	90SW	0480	PPV	I-3	IN
096	N75E	78NW	0180	PPV	I-3	IN

STA	STRI	DIP	SPA	LTH	LOC	GR
096	N75E	78NW	0300	PPV	I-3	IN
096	N75E	78NW	0190	PPV	I-3	IN
096	N75E	78NW	0080	PPV	I-3	IN
096	N75E	78NW	0210	PPV	I-3	IN
096	N75E	78NW	0210	PPV	I-3	IN
096	N75E	78NW	0140	PPV	I-3	IN
096	N75E	78NW	0140	PPV	I-3	IN
096	N75E	78NW	0510	PPV	I-3	IN
096	N75E	78NW	0490	PPV	I-3	IN
096	N05W	77NE	0190	PPV	I-3	IN
096	N05W	77NE	0780	PPV	I-3	IN
096	N05W	77NE	0250	PPV	I-3	IN
096	N05W	77NE	0340	PPV	I-3	IN
097	N72E	83SE	0440	PAL	O-7	OT
097	N72E	83SE	1070	PAL	O-7	OT
097	N10W	90SW	1500	PAL	O-7	OT
097	N10W	90SW	0580	PAL	O-7	OT
097	N10W	90SW	0450	PAL	O-7	OT
098	N75E	78NW	0870	PPV	O-7	OT
098	N75E	78NW	1230	PPV	O-7	OT
098	N75E	78NW	1430	PPV	O-7	OT
099	N55E	90NW		PPV	O-7	OT
100				PPV	O-7	OT
101	N52E	80SE		PAL	O-8	OT
102	N53W	65SW	0950	PAL	O-5	OT
102	N55W	65SW	1910	PAL	O-5	OT
102	N34E	80SE	0510	PAL	O-5	OT
103	N12E	80SE		PAL	O-6	OT
104	N30W	85SW	0640	PAL	O-5	OT
104	N30W	85SW	0700	PAL	O-5	OT
104	N70W	90SW	0850	PAL	O-5	OT
105				PAL	O-5	OT
106	N05W	78NE	1000	PAL	O-5	OT
106	N67E	90NW	1060	PAL	O-5	OT
106	N67E	90NW	0850	PAL	O-5	OT
107	N37E	85SE	0850	PAL	O-8	OT
107	N37E	85SE	0480	PAL	O-8	OT
107	N85E	90SW	0750	PAL	O-8	OT
108	N20W	80SW	0700	PAL	O-8	OT
108	N20W	80SW	0600	PAL	O-8	OT
108	N20W	80SW	0800	PAL	O-8	OT
108	N20W	80SW	0600	PAL	O-8	OT
108	N20W	80SW	0900	PAL	O-8	OT
108	N75E	90NW	0700	PAL	O-8	OT
109	N70W	90SW		PAL	O-8	OT
110	N56E	87NW		PAL	O-5	OT
110	N25W	77NE	0410	PAL	O-5	OT
111	N81E	89NW	0670	PAL	O-5	OT
111	N81E	89NW	2100	PAL	O-5	OT
112	N22E	80SE		PAL	O-5	OT
113	N10W	79NE	0970	PPV	O-5	OT

STA	STRI	DIP	SPA	LTH	LOC	GR
113	N62E	90NW	1700	PPV	0-5	OT
114	N21E	88SE	0400	PPV	0-5	OT
115	N87W	90SW	0800	PPV	0-5	OT
115	N87W	90SW	0600	PPV	0-5	OT
115	N87W	90SW	1000	PPV	0-5	OT
115	N87W	90SW	1000	PPV	0-5	OT

APPENDIX G

OPERATOR VARIANCE DATA

Key to Abbreviations:

OPR - operator

STRI- joint strike

SP - joint spacing (in cm)

ST - joint set: EW = east-west, 7W = N 70-
      79°W, 6W = N 60-69°W, NE = northeast,
      NN = N 05°W to N 05°E, NW = northwest

STA - station number. See Appendix A, Station
      Locations in Tucker County

OPR	STRI	SP	ST	STA
BRI	N74W	06	EW	33
BRI	N83W	08	EW	33
BRI	N87W	13	EW	33
BRI	N53W	07	NW	33
BRI	N18E	03	NE	33
BRI	N25E	10	NE	33
BRI	N83W	22	EW	33
BRI	N82W	26	EW	33
BRI	N86W	11	EW	33
BRI	N86E	29	EW	33
BRI	N10E	28	NN	33
BRI	N14E	29	NN	33
BRI	N75W	31	7W	87
BRI	N77W	32	7W	87
BRI	N73W	12	7W	87
BRI	N23E	27	NE	87
BRI	N83E	31	EW	87
BRI	N80E	20	EW	87
BRI	N15E	21	NN	87
BRI	N45W		NW	87
BRI	N85E	45	EW	87
BRI	N87W	15	EW	87
BRI	N82W	13	EW	87
BRI	N80E	05	EW	87
BRI	N18E	55	NN	87
BRI	N53W		NW	87
BRI	N58W	32	NW	35
BRI	N64W	13	6W	35
BRI	N60W	07	6W	35
BRI	N61W	06	6W	35
BRI	N57W	08	6W	35
BRI	N71W	10	6W	35
BRI	N26E	04	NE	35
BRI	N25E	03	NE	35
BRI	N12E	19	NE	35
BRI	N62W	12	6W	35
BRI	N63W	09	6W	35
BRI	N58W	39	6W	35
BRI	N60E	23	6E	35
BRI	N62E	28	6E	35
BRI	N89W	16	EW	35
BRI	N28E	45	NE	35
BRI	N32E	99	NE	35
TOM	N86W	29	EW	33
TOM	N87W	24	EW	33
TOM	N84W	35	EW	33
TOM	N86W	34	EW	33

OPR	STRI	SP	ST	STA
TOM	N87W	55	EW	33
TOM	N84W	66	EW	33
TOM	N86W	68	EW	33
TOM	N87W	12	EW	33
TOM	N84W	34	EW	33
TOM	N86W	40	EW	33
TOM	N19E	19	NE	33
TOM	N21E	02	NE	33
TOM	N42E	19	NE	33
TOM	N19E	23	NE	33
TOM	N21E	08	NE	33
TOM	N42E	16	NE	33
TOM	N19E	23	NE	33
TOM	N21E	10	NE	33
TOM	N42E	16	NE	33
TOM	N19E	17	NE	33
TOM	N21E	22	NE	33
TOM	N42E	32	NE	33
TOM	N19E	30	NE	33
TOM	N21E	03	NE	33
TOM	N42E	27	NE	33
TOM	N19E	34	NE	33
TOM	N21E	17	NE	33
TOM	N42E	08	NE	33
TOM	N19E	13	NE	33
TOM	N21E	21	NE	33
TOM	N42E	23	NE	33
TOM	N19E	39	NE	33
TOM	N83E	30	EW	87
TOM	N85E	32	EW	87
TOM	N79W	37	EW	87
TOM	N83E	14	EW	87
TOM	N85E	11	EW	87
TOM	N79W	18	EW	87
TOM	N83E	25	EW	87
TOM	N85E	46	EW	87
TOM	N79W	13	EW	87
TOM	N83E	62	EW	87
TOM	N85E	18	EW	87
TOM	N79W	06	EW	87
TOM	N83E	15	EW	87
TOM	N85E	16	EW	87
TOM	N79W	03	EW	87
TOM	N83E	17	EW	87
TOM	N85E	10	EW	87
TOM	N79W	12	EW	87
TOM	N83E	09	EW	87

OPR	STRI	SP	ST	STA
TOM	N85E	06	EW	87
TOM	N79W	30	EW	87
TOM	N83E	10	EW	87
TOM	N85E	10	EW	87
TOM	N79W	16	EW	87
TOM	N83E	07	EW	87
TOM	N85E	17	EW	87
TOM	N40W		NW	87
TOM	N20E	15	NE	87
TOM	N26E	28	NE	87
TOM	N24E	13	NE	87
TOM	N20E	08	NE	87
TOM	N26E	06	NE	87
TOM	N44E	42	NE	35
TOM	N25E	35	NE	35
TOM	N29E	07	NE	35
TOM	N25E	46	NE	35
TOM	N61W	13	NW	35
TOM	N51W	23	NW	35
TOM	N51W	34	NW	35
TOM	N53W	35	NW	35
TOM	N53W	11	NW	35
TOM	N51W	32	NW	35
TOM	N53W	28	NW	35
TOM	N51W	15	NW	35
TOM	N53W	08	NW	35
TOM	N51W	39	NW	35
TOM	N53W	79	NW	35
TOM	N51W	39	NW	35
TOM	N73E	27	7E	35
TOM	N73E	23	7E	35
TOM	N52W	14	NW	35
TOM	N53W	15	NW	35
TOM	N51W	26	NW	35
TOM	N02E	12	NN	35
TOM	N02E	11	NN	35
TOM	N51W	32	NW	35
TOM	N53W	08	NW	35
TOM	N51W	07	NW	35
TOM	N53W	17	NW	35
TOM	N51W	24	NW	35
TOM	N25E	99	NE	35
TOM	N29E	37	NE	35
TOM	N25E	35	NE	35
TOM	N29E	14	NE	35
BUS	N87W	19	EW	33
BUS	N84W	12	EW	33

OPR	STRI	SP	ST	STA
RUS	N82W	10	EW	33
RUS	N84W	18	EW	33
RUS	N87W	31	EW	33
RUS	N84W	07	EW	33
RUS	N83W	12	EW	33
RUS	N39W	16	NW	33
RUS	N46W	18	NW	33
RUS	N47W	24	NW	33
RUS	N47W	27	NW	33
RUS	N39W	13	NW	33
RUS	N46W	18	NW	33
RUS	N47W	70	NW	33
RUS	N47W	36	NW	33
RUS	N39W	29	NW	33
RUS	N67W	17	6W	33
RUS	N63W	04	6W	33
RUS	N67W	08	6W	33
RUS	N21E	43	NE	33
RUS	N14E	26	NE	33
RUS	N14E	29	NE	33
RUS	N17E	53	NE	33
RUS	N21E	34	NE	33
RUS	N14E	33	NE	33
RUS	N14E	23	NE	33
RUS	N21E	59	NE	33
RUS	N14E	71	NE	33
RUS	N87E	70	EW	87
RUS	N85E	05	EW	87
RUS	N89E	09	EW	87
RUS	N85E	38	EW	87
RUS	N87E	06	EW	87
RUS	N85E	07	EW	87
RUS	N89E	03	EW	87
RUS	N85E	72	EW	87
RUS	N87E	70	EW	87
RUS	N85E	28	EW	87
RUS	N70W	30	7W	87
RUS	N72W	09	7W	87
RUS	N71W	32	7W	87
RUS	N72W	48	7W	87
RUS	N70W	43	7W	87
RUS	N72W	48	7W	87
RUS	N71W	47	7W	87
RUS	N58W	12	NW	35
RUS	N57W	11	NW	35
RUS	N57W	13	NW	35
RUS	N62W	09	NW	35

OPR	STRI	SP	ST	STA
RUS	N58W	24	NW	35
RUS	N57W	36	NW	35
RUS	N62W	38	NW	35
RUS	N74W	22	7W	35
RUS	N70W	12	7W	35
RUS	N70W	05	7W	35
RUS	N74W	08	7W	35
RUS	N70W	21	7W	35
RUS	N70W	16	7W	35
RUS	N70W	11	7W	35
RUS	N74W	02	7W	35
RUS	N70W	05	7W	35
RUS	N70W	24	7W	35
RUS	N70W	13	7W	35
RUS	N70W	13	7W	35
RUS	N70W	39	7W	35
RUS	N70W	32	7W	35
RUS	N70W	12	7W	35
RUS	N70W	16	7W	35
RUS	N70W	28	7W	35
RUS	N70W	30	7W	35
RUS	N57W	06	NW	35
RUS	N55W	09	NW	35
RUS	N57W	09	NW	35
RUS	N55W	08	NW	35
RUS	N57W	19	NW	35
RUS	N27E	29	NE	35
RUS	N17E	25	NE	35
RUS	N27E	32	NE	35
RUS	N17E	45	NE	35
RUS	N27E	03	NE	35
JAN	N80W	25	EW	33
JAN	N83W	20	EW	33
JAN	N80W	14	EW	33
JAN	N80W	11	EW	33
JAN	N83W	12	EW	33
JAN	N83W	08	EW	33
JAN	N80W	18	EW	33
JAN	N83W	24	EW	33
JAN	N80W	24	EW	33
JAN	N83W	32	EW	33
JAN	N50W	16	NW	33
JAN	N45W	20	NW	33
JAN	N48W	19	NW	33
JAN	N50W	12	NW	33
JAN	N87W	18	EW	87
JAN	N87W	08	EW	87

OPR	STRI	SP	ST	STA
JAN	N87W	12	EW	87
JAN	N87W	24	EW	87
JAN	N87W	38	EW	87
JAN	N87W	09	EW	87
JAN	N87W	17	EW	87
JAN	N87W	17	EW	87
JAN	N87W	34	EW	87
JAN	N51W	07	NW	87
JAN	N51W	26	NW	87
JAN	N84E	11	EW	87
JAN	N84E	11	EW	87
JAN	N73W	32	7W	87
JAN	N73W	31	7W	87
JAN	N24E	90	NE	35
JAN	N24E	59	NE	35
JAN	N24E	29	NE	35
JAN	N02E	21	NN	35
JAN	N02E	31	NN	35
JAN	N02E	11	NN	35
JAN	N55W	47	NW	35
JAN	N55W	09	NW	35
JAN	N55W	25	NW	35
JAN	N54W	35	NW	35
JAN	N85W	36	EW	35
JAN	N85W	29	EW	35
JAN	N85W	12	EW	35
JAN	N85W	16	EW	35
JAN	N85W	37	EW	35

APPENDIX H

COAL CLEAT INTENSITY DATA

Key to Abbreviations:

STA - station number

STRI - joint strike

DIP - joint dip

CLEAT- type of cleat: FACE, BUTT

SPA - cleat spacing (in cm)

BT   - bed thickness (in cm)

STA	STRI	DIP	CLEAT	SPA	BT
001	N75W	90SW	FACE	02.5	40
001	N75W	90SW	FACE	02.0	40
001	N75W	90SW	FACE	04.5	40
001	N75W	90SW	FACE	03.0	40
001	N75W	90SW	FACE	01.0	40
001	N75W	90SW	FACE	02.5	40
001	N75W	90SW	FACE	03.0	40
001	N75W	90SW	FACE	01.0	40
001	N75W	90SW	FACE	02.5	40
001	N75W	90SW	FACE	02.0	40
001	N11E	75SE	BUTT	03.5	40
001	N11E	75SE	BUTT	05.0	40
001	N11E	75SE	BUTT	03.0	40
001	N11E	75SE	BUTT	07.0	40
001	N11E	75SE	BUTT	04.0	40
001	N11E	75SE	BUTT	08.0	40
001	N11E	75SE	BUTT	04.0	40
001	N11E	75SE	BUTT	10.0	40
001	N11E	75SE	BUTT	04.0	40
001	N11E	75SE	BUTT	05.5	40
002	N70W	90SW	FACE	03.0	38
002	N70W	90SW	FACE	04.0	38
002	N70W	90SW	FACE	06.0	38
002	N70W	90SW	FACE	02.5	38
002	N70W	90SW	FACE	02.5	38
002	N70W	90SW	FACE	03.0	38
002	N70W	90SW	FACE	03.0	38
002	N70W	90SW	FACE	03.0	38
002	N70W	90SW	FACE	03.0	38
002	N70W	90SW	FACE	02.5	38
002	N05E	70SE	BUTT	02.5	38
002	N05E	70SE	BUTT	02.0	38
002	N05E	70SE	BUTT	03.0	38
002	N05E	70SE	BUTT	02.0	38
002	N05E	70SE	BUTT	04.0	38
002	N05E	70SE	BUTT	01.5	38
002	N05E	70SE	BUTT	02.0	38
002	N05E	70SE	BUTT	03.5	38
002	N05E	70SE	BUTT	04.0	38
002	N05E	70SE	BUTT	01.5	38
004	N74W	90SW	FACE	02.0	35
004	N74W	90SW	FACE	02.0	35
004	N74W	90SW	FACE	02.5	35
004	N74W	90SW	FACE	01.0	35
004	N74W	90SW	FACE	02.5	35
004	N74W	90SW	FACE	02.5	35
004	N74W	90SW	FACE	02.0	35

STA	STRI	DIP	CLEAT	SPA	BT
004	N74W	90SW	FACE	01.5	35
004	N74W	90SW	FACE	02.5	35
004	N74W	90SW	FACE	03.0	35
004	N15E	83SE	BUTT	09.0	35
004	N15E	83SE	BUTT	05.0	35
004	N15E	83SE	BUTT	04.0	35
004	N15E	83SE	BUTT	05.0	35
004	N15E	83SE	BUTT	05.0	35
004	N15E	83SE	BUTT	04.0	35
004	N15E	83SE	BUTT	04.0	35
004	N15E	83SE	BUTT	06.0	35
004	N15E	83SE	BUTT	05.0	35
004	N15E	83SE	BUTT	08.5	35
006	N78W	90SW	FACE	03.5	20
006	N78W	90SW	FACE	03.0	20
006	N78W	90SW	FACE	03.0	20
006	N78W	90SW	FACE	02.0	20
006	N78W	90SW	FACE	02.0	20
006	N78W	90SW	FACE	01.5	20
006	N78W	90SW	FACE	02.0	20
006	N78W	90SW	FACE	04.0	20
006	N78W	90SW	FACE	04.0	20
006	N78W	90SW	FACE	02.5	20
006	N22E	87NW	BUTT	03.0	20
006	N22E	87NW	BUTT	02.0	20
006	N22E	87NW	BUTT	03.5	20
006	N22E	87NW	BUTT	02.5	20
006	N22E	87NW	BUTT	04.0	20
006	N22E	87NW	BUTT	04.0	20
006	N22E	87NW	BUTT	07.0	20
006	N22E	87NW	BUTT	03.0	20
006	N22E	87NW	BUTT	03.0	20
006	N22E	87NW	BUTT	03.5	20
007	N75W	90SW	FACE	07.0	35
007	N75W	90SW	FACE	08.5	35
007	N75W	90SW	FACE	07.0	35
007	N75W	90SW	FACE	08.0	35
007	N75W	90SW	FACE	09.5	35
007	N75W	90SW	FACE	06.5	35
007	N75W	90SW	FACE	07.5	35
007	N75W	90SW	FACE	06.5	35
007	N75W	90SW	FACE	09.0	35
007	N75W	90SW	FACE	07.5	35
007	N15E	80NW	BUTT	08.5	35
007	N15E	80NW	BUTT	09.0	35
007	N15E	80NW	BUTT	10.5	35
007	N15E	80NW	BUTT	12.0	35

STA	STRI	DIP	CLEAT	SPA	BT
007	N15E	80NW	BUTT	10.5	35
007	N15E	80NW	BUTT	08.0	35
007	N15E	80NW	BUTT	08.0	35
007	N15E	80NW	BUTT	09.5	35
007	N15E	80NW	BUTT	08.0	35
007	N15E	80NW	BUTT	10.0	35
008	N75W	89SW	FACE	02.0	40
008	N75W	89SW	FACE	03.0	40
008	N75W	89SW	FACE	03.5	40
008	N75W	89SW	FACE	03.0	40
008	N75W	89SW	FACE	05.5	40
008	N75W	89SW	FACE	03.5	40
008	N75W	89SW	FACE	02.5	40
008	N75W	89SW	FACE	02.5	40
008	N75W	89SW	FACE	02.5	40
008	N75W	89SW	FACE	02.0	40
008	N11E	73SE	BUTT	08.0	40
008	N113	73SE	BUTT	10.0	40
008	N11E	73SE	BUTT	06.0	40
008	N11E	73SE	BUTT	05.0	40
008	N11E	73SE	BUTT	11.0	40
008	N11E	73SE	BUTT	13.0	40
008	N11E	73SE	BUTT	06.0	40
008	N113	73SE	BUTT	06.5	40
008	N11E	73SE	BUTT	13.0	40
008	N11E	73SE	BUTT	05.0	40
011	N77W	89NE	FACE	02.0	40
011	N77W	89NE	FACE	02.0	40
011	N77W	89NE	FACE	02.0	40
011	N77W	89NE	FACE	03.0	40
011	N77W	89NE	FACE	02.0	40
011	N77W	89NE	FACE	02.0	40
011	N77W	89NE	FACE	02.0	40
011	N77W	89NE	FACE	01.0	40
011	N77W	89NE	FACE	03.0	40
011	N77W	89NE	FACE	01.0	40
011	N15E	77SE	BUTT	06.0	40
011	N15E	77SE	BUTT	09.0	40
011	N15E	77SE	BUTT	07.0	40
011	N15E	77SE	BUTT	05.0	40
011	N15E	77SE	BUTT	07.0	40
011	N15E	77SE	BUTT	05.0	40
011	N15E	77SE	BUTT	07.0	40
011	N15E	77SE	BUTT	12.0	40
011	N15E	77SE	BUTT	10.0	40
011	N15E	77SE	BUTT	10.0	40
012	N73W	86SW	FACE	04.0	40

STA	STRI	DIP	CLEAT	SPA	BT
012	N73W	86SW	FACE	02.5	40
012	N73W	86SW	FACE	06.0	40
012	N73W	86SW	FACE	04.0	40
012	N73W	86SW	FACE	05.0	40
012	N73W	86SW	FACE	03.0	40
012	N73W	86SW	FACE	06.0	40
012	N73W	86SW	FACE	05.0	40
012	N73W	86SW	FACE	03.0	40
012	N73W	86SW	FACE	02.0	40
012	N18E	90NW	BUTT	08.0	40
012	N18E	90NW	BUTT	04.0	40
012	N18E	90NW	BUTT	04.5	40
012	N18E	90NW	BUTT	03.0	40
012	N18E	90NW	BUTT	04.0	40
012	N18E	90NW	BUTT	05.0	40
012	N18E	90NW	BUTT	06.0	40
012	N18E	90NW	BUTT	06.0	40
012	N18E	90NW	BUTT	07.0	40
012	N18E	90NW	BUTT	06.0	40
013	N76W	90SW	FACE	03.0	40
013	N76W	90SW	FACE	03.0	40
013	N76W	90SW	FACE	03.0	40
013	N76W	90SW	FACE	03.5	40
013	N76W	90SW	FACE	02.5	40
013	N76W	90SW	FACE	03.0	40
013	N76W	90SW	FACE	03.0	40
013	N76W	90SW	FACE	04.0	40
013	N76W	90SW	FACE	03.0	40
013	N76W	90SW	FACE	02.5	40
013	N25E	75SE	BUTT	11.0	40
013	N25E	75SE	BUTT	09.0	40
013	N25E	75SE	BUTT	04.0	40
013	N25E	75SE	BUTT	14.0	40
013	N25E	75SE	BUTT	09.0	40
013	N25E	75SE	BUTT	10.0	40
013	N25E	75SE	BUTT	11.0	40
013	N25E	75SE	BUTT	12.0	40
013	N25E	75SE	BUTT	08.0	40
013	N25E	75SE	BUTT	11.0	40
014	N74W	85SW	FACE	05.0	35
014	N74W	85SW	FACE	03.5	35
014	N74W	85SW	FACE	06.0	35
014	N74W	85SW	FACE	05.0	35
014	N74W	85SW	FACE	05.5	35
014	N74W	85SW	FACE	06.5	35
014	N74W	85SW	FACE	06.0	35
014	N74W	85SW	FACE	05.0	35

STA	STRI	DIP	CLEAT	SPA	BT
014	N74W	85SW	FACE	04.0	35
014	N74W	85SW	FACE	06.0	35
014	N10E	83SE	BUTT	07.5	35
014	N10E	83SE	BUTT	12.0	35
014	N10E	83SE	BUTT	12.5	35
014	N10E	83SE	BUTT	13.0	35
014	N10E	83SE	BUTT	13.0	35
014	N10E	83SE	BUTT	13.0	35
014	N10E	83SE	BUTT	17.0	35
014	N10E	83SE	BUTT	16.0	35
014	N10E	83SE	BUTT	10.0	35
014	N10E	83SE	BUTT	09.0	35
015	N72W	90SW	FACE	08.0	35
015	N72W	90SW	FACE	07.0	35
015	N72W	90SW	FACE	04.0	35
015	N72W	90SW	FACE	05.0	35
015	N72W	90SW	FACE	10.0	35
015	N72W	90SW	FACE	07.0	35
015	N72W	90SW	FACE	10.0	35
015	N72W	90SW	FACE	11.0	35
015	N72W	90SW	FACE	11.0	35
015	N72W	90SW	FACE	11.0	35
015	N12E	80NW	BUTT	14.0	35
015	N12E	80NW	BUTT	18.0	35
015	N12E	80NW	BUTT	16.0	35
015	N12E	80NW	BUTT	05.0	35
015	N12E	80NW	BUTT	07.0	35
015	N12E	80NW	BUTT	18.0	35
015	N12E	80NW	BUTT	11.0	35
015	N12E	80NW	BUTT	17.0	35
015	N12E	80NW	BUTT	14.0	35
015	N12E	80NW	BUTT	13.0	35

STYLE ELEMENTS, INTENSITY, AND RELATIVE AGES OF JOINTS ON A DETACHED ANTICLINE

Wheeler, Russell L., U. S. Geological Survey, Denver, Colorado 80225;
Holland, Sally M., 103 North Rowling Road, Baltimore, Maryland 21228;
Dixon, Jeanette M.,* Department of Geology and Geography, West Virginia
University, Morgantown, West Virginia 26506; and Kulander, Byron R.,
Department of Geology, Alfred University, Alfred, New York 14802.

ABSTRACT

Previous work showed that sets of systematic joints can differ signifi-
cantly in values of joint style elements - aspects of orientation, size,
spacing, shape, and rock character. As part of a project funded by the
Department of Energy to improve exploration for fractured Appalachian gas
reservoirs from New York State to Virginia, we studied effects on joint
types of structural position on an anticline in Upper Devonian siltstones
and mudstones in the eastern Plateau province of northern West Virginia.
In one road cut exposing the anticline, Holland measured as many as feasible
of 32 style elements on each of 100 planar, mostly filled joints in beds of
relatively constant thickness and lithology. Partial repetition by four
others showed operator variability to be insignificant. Joint spacing and
size vary significantly between sets but insignificantly between limbs. On
limbs, nonsystematic longitudinal cross joints are bigger and more abundant
than are systematic diagonals. Joint surface area per unit volume varies
little between and within limbs. Joint intersections and delicate struc-
tures on joint faces show that rare systematic transverse joints formed
first, then the diagonals, and lastly the longitudinals. In 149 nearby
exposures of the same lithologies, transverse joints form the most abundant
set but the sets formed in the same order. In the single road cut, rela-
tive ages of folding and jointing are indeterminate. From fillings and
Secor's model, we infer that the joints formed under increasing effective
stresses and stress difference.

Surface Fracture Data

Mark A. Evans
Kevin D. Lee
Brian R. Long

FRACTURE DENSITY AND ORIENTATION STUDY OF THE MERC #1 CORE

FROM MONONGALIA COUNTY, WEST VIRGINIA

by

Mark A. Evans
West Virginia University
Department of Geology and Geography
Morgantown, West Virginia 26506

INDEX

LIST OF ILLUSTRATIONS

ABSTRACT

Fracture data based on the description of the MERC #1 Core shows the relationships of natural fractures in the Devonian shales of West Virginia to depth and stratigraphy. Core induced fractures, mineralized and unmineralized natural fractures (joints), slickensided surfaces, and slickenlines were differentiated in the MERC #1 oriented Devonian shale core.

Two major subvertical to vertical fracture (joint) sets were found, N80°E and N70°W. Inclined slickensided surfaces (>10° dip) show one major set, N0°-30°E. The major trend of the slickenlines (striations) on the slickensides is N70°W. This is the direction of regional tectonic transport. The highest densities of slickensides occur near the base of the Mahantango Formation and near the base of the Marcellus Shale. These two intervals may represent decollement horizons. Many of the fractures are mineralized, some with fibrous mineral growth which is indicative of high fluid pressure within the shale.

Eventually the results of this study will be combined with those of other cored wells to present an integrated regional analysis of Devonian shale fractures.

PURPOSE

The study of the MERC #1 Core is conducted under DOE Contract number DE-AC21-76MC05194 with West Virginia University. This is the second in a series of reports planned to document the results of our analysis of fractures found in oriented cores taken from several Devonian shale wells. These wells were drilled by private industry in cooperation with ERDA-DOE under the Eastern Gas Shales Program. Each report will serve as a record of all fractures logged from the oriented shale core taken in that particular well. Some preliminary interpretations will be made. However, it is the author's intent to record, summarize, and present a visual comparison of fracture data from each core. Then, in a separate report, written at the end of the investigation, he will integrate and compare the data from the several reports written by the author and other investigators. The final report will interpret the significance of fractures found in all oriented cores, and it will attempt to relate the findings to shale production and to the regional tectonics of the study area.

LOCATION AND DRILLING DATA

The MERC #1 Well is located in Monongalia County, West Virginia, approximately two miles north of the city of Morgantown in the Morgantown North quadrangle at latitude 39°40'14" N and longitude 79°58'44" W (Figure 1). Ground level elevation at the well site is 959' above sea level. The borehole diameter at corepoint was 8-23/32 inches. A plastic sleeve was used inside the inner core barrel, and a 3-1/2 inch core was retrieved.

The core was oriented by the author at the Morgantown Energy Technology Center's Core Lab according to guidelines set forth by Byrer and Komar (1977). Interval '7232'-'7290' of the core could not be oriented because of a malfunction of the camera taking orientation photographs of the core. The interval was not used in this study to obtain fracture orientation data; however, fracture frequency data from this interval was recorded.

MERC #1
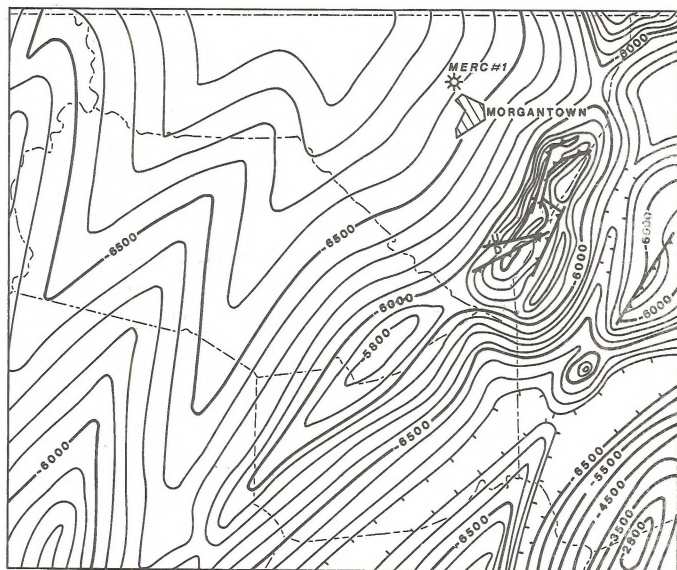
MORGANTOWN

STRUCTURE
Top of the Onondaga Limestone

Modified from Cardwell, 1974

CI= 100 ft, 500 ft in eastern folded areas

M. EVANS   1979

MILES

Figure 1

STRATIGRAPHIC INTERVAL CORED

A total of 341 feet of the Devonian sediment was cored, from 7168' to 7509', plus 11 feet of the Onondaga Limestone to 7520' (Figures 2 and 3). The top of the core includes the Tully(?) Limestone (7168'-6192'), the Mahantango Formation (7192'-7395'), and the highly radioactive Marcellus Shale (7395'-7509'). The bottom of the core includes the top portion of the underlying Onondaga Limestone (7509'-7520') (Schwietering, personal communication).
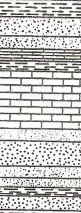
GENERALIZED GEOLOGIC COLUMN

SERIES	GROUP OR FORMATION	IMPORTANT ROCK UNITS	ROCK COLUMN	DRILLERS TERMS
PERMIAN	DUNKARD	Gilmore SS		Gilmore Coal
		Rockport LS		
		Nineveh Coal		Nineveh Sand
		Dunkard Coal		
		Jollytown Coal		Jollytown Sand
				Hundred Sand
		Upper Marietta SS		
				Washingtown Coal
PENNSYLVANIAN	MONONGAHELA	Waynesburg Coal		Uniontown Coal
		Sewickley Coal		Redstone Coal
		Pittsburgh Coal		
	CONEMAUGH	Connellsville SS		Morgantown Sand
		Bakerstown Coal		Saltsburg Sand
		Mahoning SS		
	ALLEGHENGY	Lower Freeport SS		Burning Springs Sand
				Gas Sand
	POTTSVILLE	Salt Sands		1st Salt Sand
				2nd Salt Sand
				3rd Salt Sand
MISSISSIPPIAN	MAUCH CHUNK	Maxton SS		Ravencliff Sand
				Lower Maxon
				Little Lime
	GREENBRIER	Greenbrier Limestone		Big Lime
		Big Injun SS		Keener Sand
	POCONO	Squaw SS		
		Weir Sand		
		Berea SS		Sunbury Shale
DEVONIAN	HAMPSHIRE	Fifty-foot SS		
	CHEMUNG	Gordon SS		
	BRALLIER	Fifth Sand		
	HARRELL	Burkett Mbr		BROWN SHALE
	TULLY (?)			
	MAHANTANGO			
	MARCELLUS			
	ONONDAGA	Onondaga LS		Corniferous LS
	HELDERBERG			Oriskany Sand
		Helderberg LS		
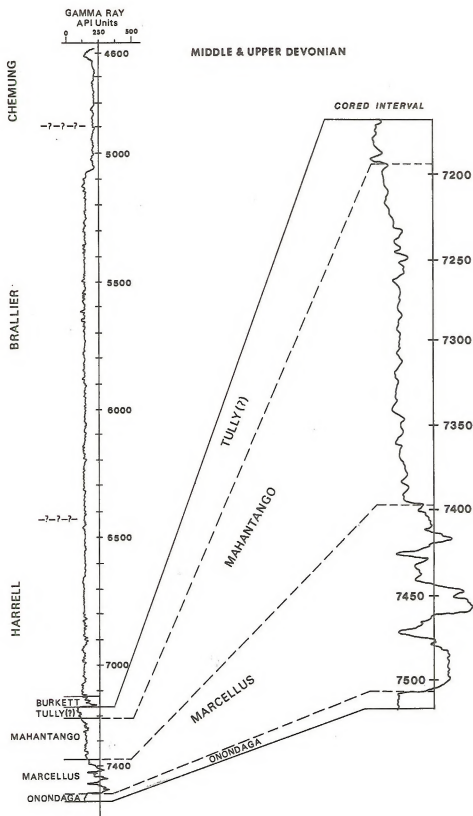
Figure 2

Figure 3

REGIONAL GEOLOGY

Structure

The MERC #1 Well is located on the western flank of the Fayette anticline, which is just west of the large N30°E trending Chestnut Ridge anticline. Regional structure of the Devonian shales shows a monoclinal dip of less than 1° (Figure 1) to the northwest.

Stratigraphy

The surface rocks of the area are Permian, Pennsylvanian, Mississippian, and Devonian in age (Figure 2). The Permian Dunkard Group covers the western portion on Monongalia County and includes the Washington Coal. Rocks of Pennsylvanian age exposed in the area of the well includes the Monongahela and Conemaugh Groups, Allegheny Formation and the Pottsville Group. Rocks of Mississippian age are exposed in the eastern portion of the county on the crest of the Chestnut Ridge anticline and in stream valleys. These rocks include the Mauch Chunk Group, the Greenbrier Group, containing the Productive Big Lime of West Virginia, and the lowest group of the Mississippian, the Pocono, which includes the Big Injun Sandstone and Berea Sandstone at its base. The uppermost portion of the Devonian Catskill Formation is exposed in the channel of the Cheat River which cuts through the Chestnut Ridge anticline. In the subsurface the Devonian is divided into the Catskill Formation, the Chemung Formation, the Brallier Formation, Harrell Formation, Tully(?) Limestone, Mahantango Formation and Marcellus Shale. Lower Devonian sediments include the Onondaga Limestone, Oriskany Sandstone, and Helderberg Formation.

HYDROCARBON PRODUCTION

There is very little current hydrocarbon production from the general area around the MERC #1 Well. The nearest fields in West Virginia include the Cassville-Bowlby Field, which produced gas from the Mississippian Big Injun Sand, and the Westover Field, which produced gas from the Big Injun Sand and the Pennsylvanian Cow Run Sand. Both fields are now inactive. The nearest active field is the South Burns Chapel Field on the crest of the Chestnut Ridge anticline southeast of MERC #1. Production is mainly from the Devonian Huntersville and Oriskany (Cardwell 1977).

The MERC #1 Well had shows of gas from the Big Injun, Squaw, Gordon, 4th, 5th, Baynard, and Riley Sands, all of which are well above the cored interval. The only significant production from the Devonian shales was from the Burkett Member of the Harrell Formation, which produced 25 MCF per day after fracing. This is immediately above the cored interval.

FRACTOGRAPHIC LOGGING

The fracture data was collected by the author at the Morgantown
Energy Technology Center's Core Lab. During the study certain structural
and surface features were used to interpret the type or origin of the
fractures. The terminology used to describe these fractures may be
unfamiliar to most readers, so before proceeding with a discussion of
the fracture analysis it is necessary to discuss this terminology.

Surface Features Observed on Rock Fractures

Most features on the surface of fractures are called transient fea-
tures. According to Kulander, Dean, and Barton (1977), transient fea-
tures are short range perturbations of a fracture surface which can be
attributed to:

1) material inhomogeneties (fossils, pyrite nodules, pore space,
    etc.)
2) sonic wave interference
3) local changes in stress directions and stress gradients in the
    dominant stress field
4) fracture velocity variations

Among the more common transient features are _arrest lines_ or rib
marks (Figure 4a) which are generated through temporary fracture hesita-
tion resulting from a momentarily decreased stress field or a sudden
change in principle stress direction. Essentially, they record an
instantaneous picture of the fracture front configuration at a particu-
lar point in time during fracture propagation (Kulander, Dean and Barton,
1977).

Inclusion hackle (Figure 4a) is most likely generated when a fracture front advances into the vicinity of an inclusion (pore space, weakly cemented area, grain of different composition or size, etc.). The fracture plane may be locally warped by the interference of local stress gradients associated with the inclusion boundary. This planar warping, occurring as the main fracture plan passes around the inclusion, often results in the fracture being at different levels by the time it reaches the far side of the inclusion (side opposite that first encountered by the fracture). This divergence results in a fracture plane that is not interconnected. Therefore, after passing the inclusion, the fracture advances on two closely spaced subparallel levels which soon rejoin to advance as a single front with the trailing fracture stepping (hooking up or down) into the other. This step forms on the far side of the inclusions that points in the direction of fracture propagation.

Twist hackle (Figure 4a) is generated at the fracture fronts when the direction of principle tension rotates in the plane containing the fracture front. The entire fracture front cannot instantaneously rotate to a new planar direction perpendicular to the new principle stress. Therefore, the fracture at the fracture front breaks up into individual en echelon elongate tongues. Each tongue is inclined to the original fracture plant and each tongue is perpendicular to the local resultant principle tension. These tongues continue to spread laterally and eventually curve into one another to complete the fracture, thereby producing the steps seen as hackle markings.

Another common transient feature is hackle plume or "feather feature" (Figure 4a). Hackle plumes are made up of twist hackle and inclusion hackle.

They consist of a central axis that originates at the initial point of fracture propagation and faint ridges which diverge outward from the axis in a plumose fashion toward the edge of the fracture plane. The presence of plumose markings on a fracture surface indicate that there has been no significant lateral movement along the fracture surface (Roberts, 1961).

Besides transient fracture features there are also tendential fracture features. These features arise from long range changes in the stress field and are recorded as undulations in the fracture profile or trace line formed by the intersection of the fracture plane and a previously existing free surface. The bifurcation (forking) or directional change in the fracture trace generally reflects long-range stress alterations rather than the local stress perturbations responsible for transient features.

One tendential feature, hooking (Figure 4b), results when a fracture plane curves due to interaction with a neutral surface of a flexed object, or when a fracture plane curves in an attempt to meet a free surface orthogonally. Another tendential feature, forking (Figure 4b), is applied to fracture bifurcation into two or more diverging fracture planes. Forking is generated when a fracture reaches a limiting velocity in an increasing stress field (Kulander, Dean and Barton, 1977).

Types of Fractures

There are two types of fractures found in cores, core-induced fractures and natural fractures (pre-core fractures of Kulander, et al, 1977). Core induced fractures occur in response to stresses produced by the drilling and/or core extraction process. Pre-core or natural fractures are formed as a result of the failure of the rock under natural tensile and

shear stresses. Natural fractures may be subdivided into mineralized surfaces, unmineralized surfaces, and slickenlined surfaces (slickensides). In this study, slickensides are small faults which are discussed separately. Natural fractures, exclusive of slickensides, are referred to simply as "natural fractures," and they are the joints of surface rocks.

The orientations of the striations or slickenlines on the slickensides are considered separately. These striations appear only when the surfaces of the fracture are forced past one another during slippage. The criteria used by the West Virginia Geological Survey personnel and by the author to distinguish pre-core from core-induced fractures were set forth by Kulander, Dean, and Barton, (1977) and are presented below.

Core induced fractures have the following characteristics:

1) A fracture origin at the core boundary or within the core itself.

2) Hackle marks diverging and attempting to meet the core boundary or pre-existing fracture surface orthogonally.

3) Hackle marks becoming more coarse, the hackle steps increasing in relief in the immediate vicinity of the core boundary or pre-existing fracture surface.

4) Twist hackle originating near the core boundary or pre-existing fracture surface.

5) Hackle plumes on sub-horizontal fractures that diverge from the central core area in a spiral pattern indicating a torque stress.

6) Closely spaced arrest lines on vertical and inclined fractures; arrest lines are convex downcore and symmetrical about the imaginary line down the fracture surface center.

b) Tendential Features
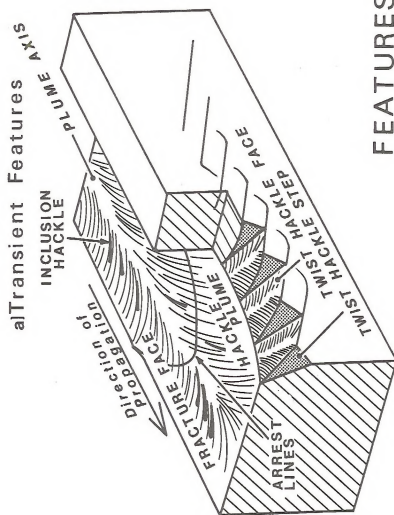
a) Transient Features
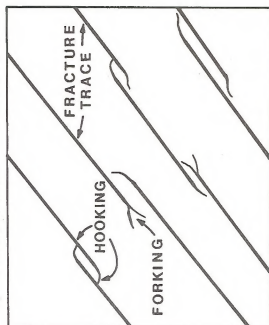
FEATURES OF
NATURAL FRACTURES

Figure 4

7) Hackle marks on vertical or inclined fractures that diverge downcore symmetrically about an imaginary line down the fracture surface center.

8) Fractures that hook abruptly towards the core boundary or a precore fracture surface.

Natural fractures have the following characteristics:

1) Polished and slickensided fracture faces (almost always smooth and planar).

2) Fractures filled by fibrous or non-fibrous mineralization.

3) Smooth fractures extending entirely across the core and against which later fractures usually terminate.

4) Inclined-vertical fracture faces displaying small, often conchoidal chips at the fracture-drilled core boundary intersection. The chips hook to meet the inclined fracture orthogonally.

DISCUSSION OF CORE INDUCED FRACTURES

There were very few well defined core-induced fractures in the MERC #1 Core. Of the four basic types of core-induced fractures - petal, scallop, torsion, and bedding plane fractures - only the last two were identified in this core. This lack of core-induced fractures may be the result of the physical characteristics of the rock and/or stress conditions present in the rock. The lack of petal and scallop fractures also restricts our ability to infer in situ stress directions in the Devonian sediments of this area.

The orientations of horizontal to subhorizontal bedding plane fractures and torsion fractures were not measured; these fractures will not be treated further.

DISCUSSION OF NATURAL FRACTURES

A total of 103 subvertical to vertical natural fractures were measured in the 283 feet of core studied. Certain fractures are up to four feet in length, and in many cases, the fractures cut diagonally across the core. Figure 5 shows an unmineralized fracture from the upper portion of the Mahantango Formation. Some unmineralized fracture faces exhibit the common hackle plume as well as twist hackle and arrest lines. The ends of two calcite mineralized fractures occur in the Upper Mahantango (Figure 6). The Tully (?) Limestone and Marcellus Shales have the greatest proportion of natural fractures, while, the Mahantango Formation has relatively few natural fractures.

Nearly all of the natural fractures are mineralized with either calcite, dolomite (rare), anhydrite, pyrite, barite, or some combination of these. A natural fracture mineralized with calcite and pyrite is shown in Figure 7. A fracture mineralized with calcite, pyrite, and anhydrite is shown in Figure 8. The mineralization is usually crystalline but also occurs as thin massive or fibrous coatings covering the fracture faces. Mineral growth fibers, perpendicular to the fracture, may imply fracture development where mineralization has occurred parallel to the principle tension as the fracture opened (Durney and Ramsay 1973). This situation is most likely to occur under very high fluid pressure conditions. Mineralization may also take place long after fracture development and merely fill void space created by the fracture. Most of the mineralized fractures are found in the Marcellus Shale, many are also found in the Tully (?) Limestone. The Mahantango Formation has few mineralized fractures. The type of mineralization filling a fracture shows no preference for fracture orientation, lithology, or depth (Plate 1).

An equal area net projection of poles to natural fracture surfaces plotted and contoured by the Mellis method and a rose diagram, were plotted for all natural fractures measured (Figures 9A and 9B). Unless otherwise stated, all rose diagrams presented in this paper have a five-degree class interval. Overall, two major fracture sets, having strikes of N80°E and N70°W, are predominant. Since most of the natural fractures are subvertical to vertical, the equal area net projection shows four clusters corresponding to the strike of two main fracture groups.

Equal area net projections and rose diagrams were plotted for 30 feet intervals wherever orientation data could be obtained. These plots are presented next to a gamma-ray log in order that the reader can compare changes in fracture patterns with depth and stratigraphy (Figure 10).

The natural fracture orientations in the core show a great amount of scatter with depth. This may be due to variations in stress conditions with depth and lithology. The low number of fractures present in some of the intervals studied may not be representative of the number and orientation of all fractures in those intervals as the sample area of a core for a particular lithology is very small. Subvertical to vertical fractures are less likely to be sampled than low dipping fractures.

One of the most interesting natural fractures found in the core is illustrated in Figure 11. One end of the vertical calcite mineralized fracture shows twist hackle which died out into the surrounding rock.
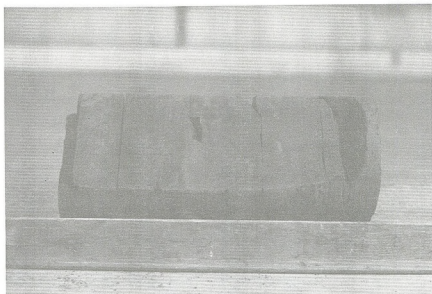
Figure 5
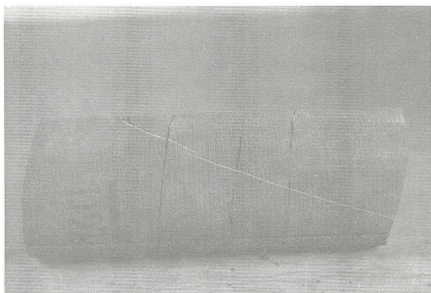
Figure 6

Figure 7

Figure 8

(a)

(b)

NATURAL FRACTURES

N=103

20%

N

S

1-6   7-12   13-18
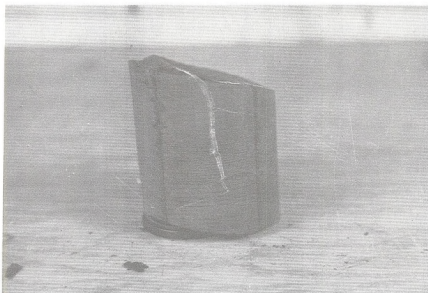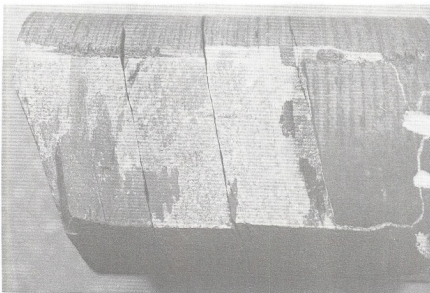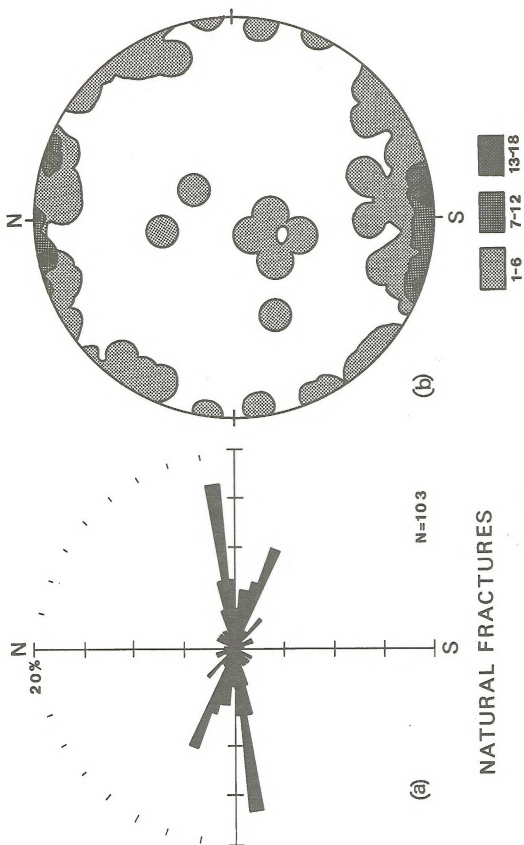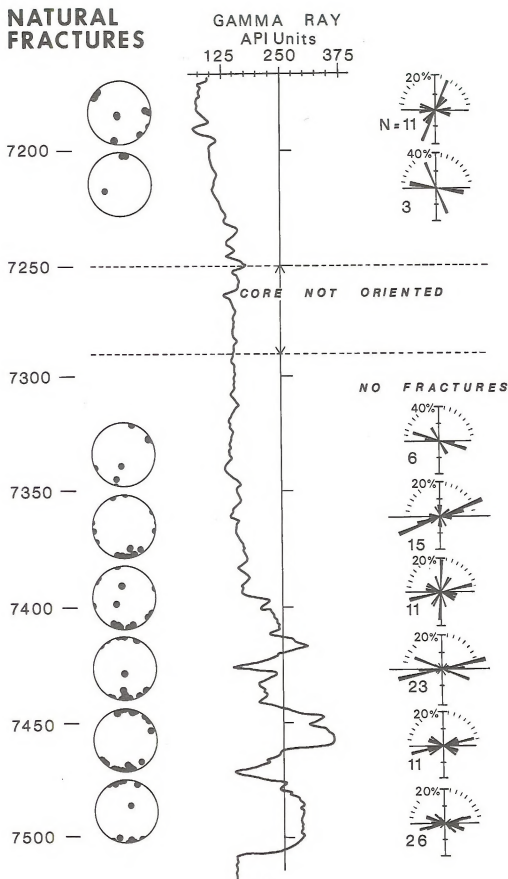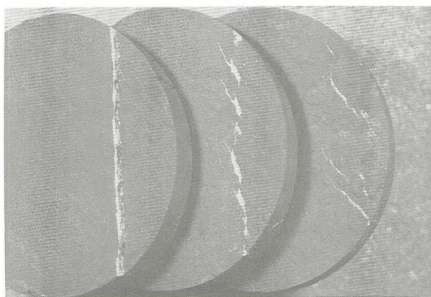
Figure 9

Figure 10

Figure 11

SLICKENSIDES AND SLICKENLINES

Slickensides are created by the movement of one fracture face past the other. The orientation of the slickensides reveals information about the movement subsequent to or synchronous with fracture formation. In this particular case the strong preference of lines to an orientation perpendicular to fold trends suggest that they are tectonic in origin.

Slickensides in the MERC #1 Core were divided into two classes, subhorizontal to horizontal (dip <10°) and inclined (dip >10°). Due to the irregularity of the fracture surfaces the orientations of the subhorizontal to horizontal slickensides were not measured; however, the trends of the slickenlines (striations) on these surfaces were recorded. Figure 12 illustrates an inclined slickenside; Figure 13, a horizontal slickenside; and Figure 14, an inclined slickenside exhibiting twist hackle. Slickensides are most abundant in the Tully (?) Limestone, and in the lower portions of both the Mahantango Formation and Marcellus Shale.

An equal area net projection of poles to inclined slickensided fracture faces and a rose diagram were plotted for all 106 inclined slickensides measured in the MERC #1 Core (Figures 15A and 15B). There is one major inclined slickensided fracture set in the core, N0°-30°E. Dips for the inclined slickensides are generally unimodal to the west and southwest and most are low angle (10°-30°).

Equal area net projections and rose diagrams of inclined slickensides were plotted for each 30' interval of the core. They are presented next to a gamma-ray log of the cored interval (Figure 16) in order that the reader can easily compare changes in both dip and orientation of the inclined slickensides with depth and stratigraphy.

Throughout the core the strikes of inclined slickensides are quite variable. There is no apparent relationship between depth and stratigraphy. The orientations of the strikes of several of the slickensides may not be reliable due to their low dips.

Slickenlines (striations) on a slickenside show the relative movement trend of one fracture face past another. The trends and plunges for 194 slickenlines on both horizontal and inclined slickensides were measured. An equal area net projection of lines and a rose diagram were plotted for all slickenlines (Figures 17A and 17B). One major slickenline trend which averages N70°W is present. This trend transects the maxima of poles to surfaces, and thus it is really at right angles to the general strike of the low dipping slickensides. The equal area net plot illustrates the low dips of the northwest-southeast trending slickenlines. There is very little scatter in trends of the slickenlines.

Equal area net projections and rose diagrams were plotted for each 30' interval of the core. They are presented next to a gamma-ray log of the cored interval (Figure 18) in order that the reader can compare changes in trend and plunge of the slickenlines with depth and stratigraphy.

There is very little variation in the trend (N45°-80°W) or plunge (0°-30°) of the slickenlines throughout the core. The greatest amount of scatter occurs in interval 7351'-7380' which is near the base of the Mahantango Formation.

Many of the slickensides in the core are mineralized with calcite (most common), dolomite, barite, or anhydrite, or some combination of these. The mineralization is usually found on the horizontal (dip <10°) slickensides and is in the form of vertical to curved fibers (Figure 19).

These horizontal fiber-filled fractures are indicative of a very high fluid pressure in bedding planes of the shales, and of the fact that the shales acted as a decollement horizon.

Figure 12

Figure 13

Figure 14

(a)

20% N

Class interval=10°

SLICKENSIDES
(Inclined - ≥10°)

N=104

S

(b)

N

S

1-6   7-12   13-18

Figure 15

Figure 16

31-40

21-30

11-20

1-10

N

S

(b)

N=192

N

20%

S

SLICKENLINES

(a)
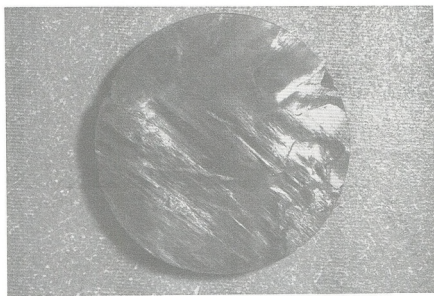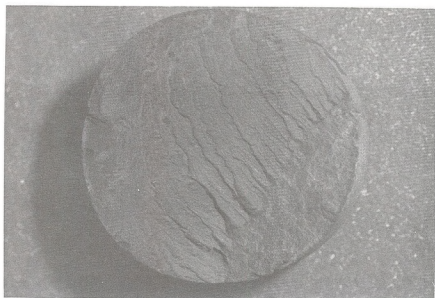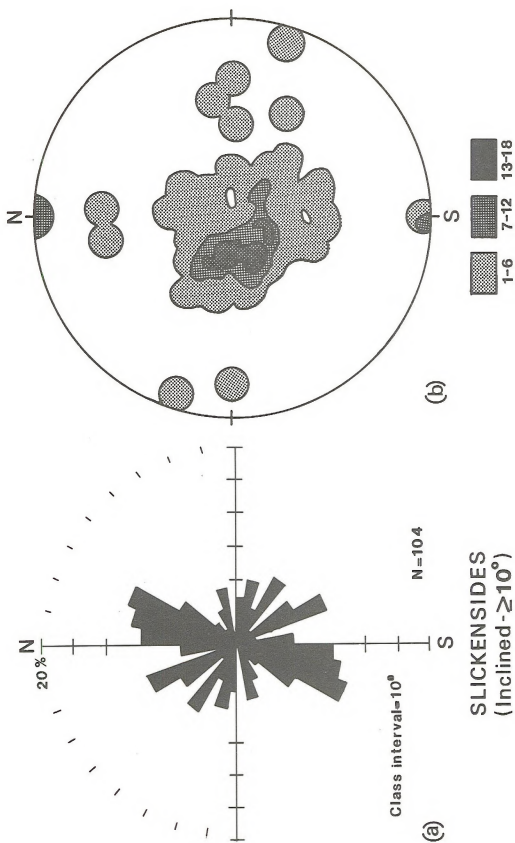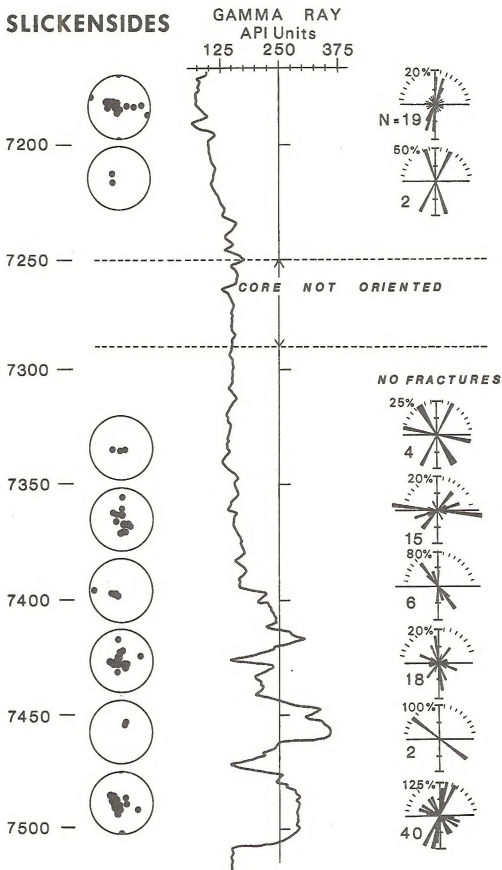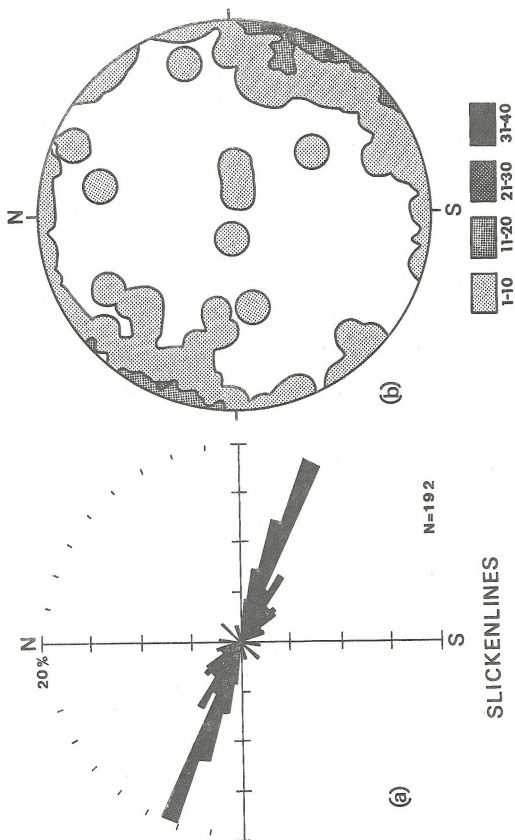
Figure 17

SLICKENLINES

GAMMA RAY
API Units
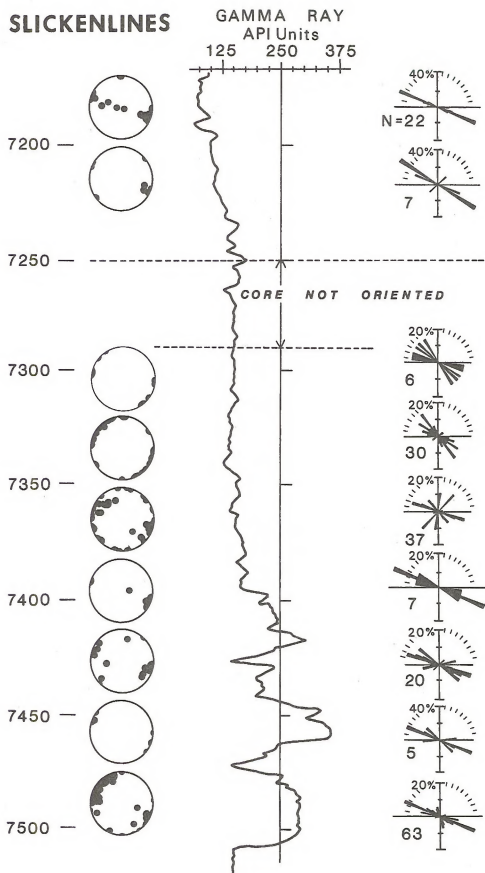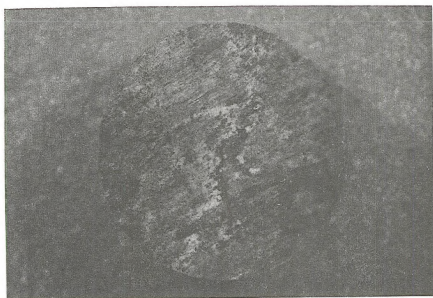
Figure 18

Figure 19

SUMMARY

All fractures found in the MERC #1 Core could be subdivided into four types, core-induced fractures, unmineralized natural fractures, mineralized natural fractures, and slickensided fractures. A visual summary of fracture density and orientations is presented in Plate 1.

Core-induced fractures were the least common and only bedding plane and torsion fractures were identified. The lack in petal and scallop fractures restricts the ability to determine the in situ stress of the area.

The subvertical to vertical natural fractures (joints) can be subdivided by strike into two fracture sets, N70°W and N80°E. The Tully (?) Limestone and Marcellus Shale have the greatest proportion of natural fractures. Most of these fractures are mineralized with calcite, dolomite, anhydrite, pyrite, barite, or some combination of these.

The slickensided fractures in the core are most abundant in the Tully (?) Limestone, and in the lower portion of both the Mahantango Formation and Marcellus Shale. These lower intervals may represent decollement horizons. The strike of the surfaces of these slickensides is quite variable, however, one major set, N0°-30°E, can be distinguished.

Trends of the slickenlines (striations) are generally N70°W and most vary between N45°W to N80°W. Many of the horizontal slickensides are filled with fibrous mineral growth which is indicative of very high fluid pressure in the bedding planes of the shales, and which suggests that the shales acted as a decollement horizon.

From the orientations of the natural fractures and the trends of the slickenlines it can be concluded that the major tectonic stress was directed in a northwest-southeast direction. This is the same stress direction as that forming the Alleghenian folds. It is presumed that the fractures relate to Alleghenian deformation.

REFERENCES

Byrer, C. W. and Komar, C. A., Field and Laboratory Procedures for Oriented Core Analysis of Devonian Shales, August 1977, MERC/SP-77/4, 26 pp.

Cardwell, D. H., Oil and Gas Fields of West Virginia, WVGS Min. Res. Series No. 7, 1977.

Cardwell, D. H., Oriskany and Huntersville Gas Fields of West Virginia, WVGS Min. Res. Series No. 5, 1974.

Frone, K. H., Deep Devonian Shale Gas Test in Northern West Virginia, in Preprints for: Second Eastern Gas Shale Symposium Vol. 2, 1978, pp. 89-99.

Haught, O. L., Oil and Gas Report and Map of Monongalia, Marion, and Taylor Counties, West Virginia, WVGS Bull. No. 13, 1956.

Kulander, B. R., Barton, C. C., and Dean, S. L., ms, The Application of Fractography to Core and Outcrop Fracture Investigations: In review by Morgantown Energy Technology Center, U.S. Department of Energy, 167 pp.

Kulander, B. R., Dean, S. L., and Barton, C. C., Fractographic Logging for Determination of Pre-Core and Core Induced Fractures - Nicholas Combs No. 7239 Well, Hazard, Kentucky, January, 1977, MERC/CR-77/3, 44 pp.

Overbey, W. K., Jr., and Rough, R. L., Surface Studies Predict Orientation of Induced Formation Fractures. Producers Monthly vol. 32, No. 6, 1969, pp. 16-19.

Roberts, J. C., Feather-Fracture, and the Mechanics of Rock-Jointing, Am. Jour. Sci., vol. 259, Summer 1961, pp. 481-492.

Secor, D. T., Jr., Mechanics of Natural Extension Fracturing at Depth in the Earth's Crust, in Research in Tectonics, Canada Geol. Survey Paper 68-52, 1969, pp. 3-48.

Schwietering, J. F., Neal, D. W., and Dowse, M. E., Tully (?) Limestone and Hamilton Group in North-Central and East-Central West Virginia, in Preprints for: Second Eastern Gas Shale Symposium Vol. 1, 1978, pp. 240-250.

Shumaker, R. C., Porous Fracture Facies in the Devonian Shales of Eastern Kentucky and West Virginia.

GAMMA RAY API Units · BULK DENSITY Grams/cc · TOTAL NATURAL FRACTURES · MINERALIZED NATURAL FRACTURES · SLICKENSIDED FRACTURES (Inclined) · SLICKENLINES (Horiz. & Incl.) · MINERALIZED SLICKENSIDES

CORE NOT ORIENTED

Ⓓ—DISTRIBUTION Ⓞ—ORIENTATION

TULLY(?) · MAHANTANGO · MARCELLUS · ONONDAGA
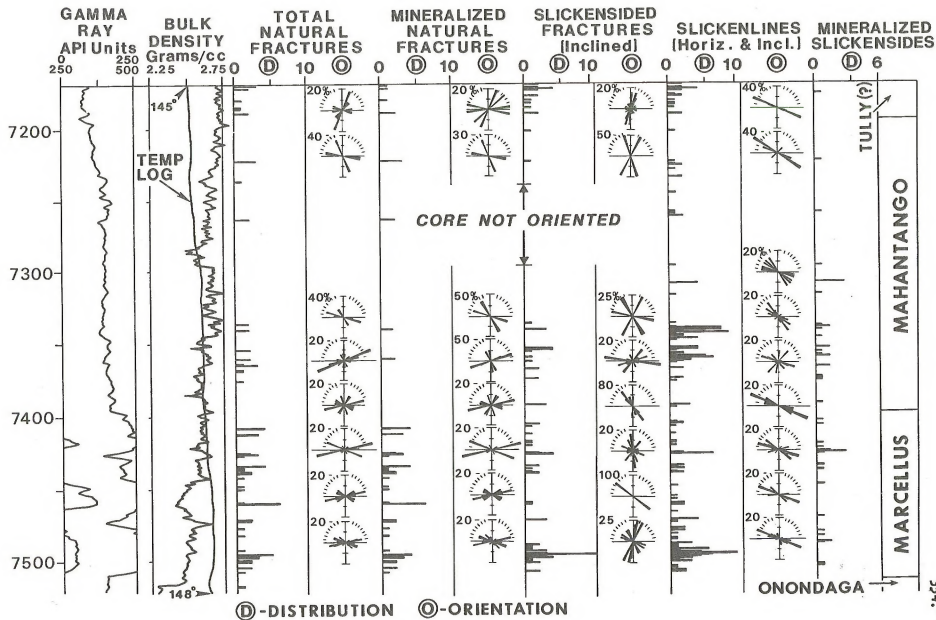
Plate 1

REGIONAL SURVEY OF SURFACE JOINTS IN EASTERN KENTUCKY

by

Brian R. Long
Research Associate, Devonian Shale Program
West Virginia University
Department of Geology and Geography
425 White Hall
Morgantown, West Virginia 26506

ABOUT THE AUTHOR

Mr. Long received his A.B. from Alfred University, Alfred, New York, in 1971. He received his M.S. degree from West Virginia University, Morgantown, West Virginia, in 1979, and is presently employed by the Department of Natural Resources' Reclamation Office, Charleston, West Virginia.

ABSTRACT

A regional survey of eastern Kentucky surface joints was completed. Maps of joint strikes plotted a. rose diagrams show coal has the most consistent regional orientation of joints of all lithologies studied. Coal face cleats and coal structure form lines swing in the foreland of the Pine Mountain thrust fault. The face cleat swing could be due to the thrust, but may instead be a separate system related to basement shape or an edge effect created by the Russell Fork tear fault. The apparent independence of coal cleat strikes from the Pine Mountain thrust may be a result of isolation of coal from fault stress by movement along the fault plane or by the coal having too low a rank for fracturing when faulting occurred.

Outcropping Devonian shales show consistent joint strikes of N25E, N45E and N65W. First-formed and second-formed joints strike northeast and northwest, respectively. The N45E joint strikes occur predominantly along the eastern flanks of the Cincinnati Arch and Nashville Dome. The N25E joint strikes are concentrated in the Cumberland saddle between the Cincinnati Arch and Nashville Dome.

INTRODUCTION-LOCATION

It is generally believed that fractures in the Devonian shale provide the permeability needed for significant commercial gas production. It follows that if the nature, orientation and intensity of jointing in the Devonian shale can be determined, then the extent and location of potentially productive permeable zones can be predicted and better estimates of ultimate gas production realized. Jointing of the Devonian shales in gas producing areas may be reflected in surface joints through regional joint strike, size and spacing trends. A survey of surface joints was completed in order to establish these trends within the largest Devonian shale gas field in the world, the Big Sandy Field.

The study area is located in the unglaciated Appalachian Plateau of eastern Kentucky (Figure 1). Joints from 130 quadrangles east of a north-south line drawn between Maysville and Middlesboro, Kentucky and from quadrangles in the Devonian shale outcrop belt on the east side of the Cincinnati Arch were documented.

Rocks of Pennsylvania, Mississippian and Devonian age are exposed in the study area. Pennsylvanian strata are composed of deltaic sequences of sandstone, shale and coal. The Mississippian contains sandstones with some shales and older massive limestone formations. The Devonian comprises black shales underlain in some areas by a thin limestone.

METHOD

A random sampling system was used by considering the boundaries of 7½ minute quadrangles as a grid and obtaining one or more stations within each quadrangle. At each sampling station the strike and dip of joints, lithology (shales separated by color only), bed thickness, horizontal and vertical joint extent and joint spacing were noted.

The sequence of jointing was determined through abutting relationships. Kulander and others (1977) have shown that tension joints which form first provide a free surface which, unless cemented closed, cannot be crossed by later formed tension joints. Therefore, first-formed joints are abutted by second-formed joints, usually at or near a 90 degree angle. The first- and second-formed joint sets are generally the best formed joints at any given outcrop.

RESULTS

In addition to dewatering and devolatilization, tectonic stress plays an important part in coal cleat formation (Ting, 1977). Cleats generally have a directional relationship relative to coal form line structure and basement structure trends in West Virginia (Kulander and Dean, 1979) and eastern Kentucky. In eastern Kentucky, coal face cleat strikes rotate in the foreland of the Pine Mountain thrust (Figure 2). The thrust appears to have caused the cleat rotation; however, with the limited data available several alternative possibilities are feasible.

If coal fracturing occurred at the same time and as a direct result of the Pine Mountain thrust movement, then the coal cleats should have extension and release orientations relative to thrust movement. The thrust movement is presumed to be northwestward, so the tensional joint trend should be northwestward. These extension-release orientations would be expected to form a second cleat set

with any previously formed sets. These trends are not present. The coals do show one simple face-butt cleat set but it has a regional rotation.

Assuming coal cleats formed prior to the Pine Mountain thrust, a second fracture system related to the thrust should be present on the foreland, but it is not. The simplicity of cleat sets and their rotation in the foreland suggest that the cleat formation may be post thrust in response to basement deformation shape. Basement shape is poorly defined in the Pine Mountain thrust, however, the coal form line map (Figure 3) shows a general contour swing in this area. Coal face cleats show a consistent orthogonal relationship to coal form lines through West Virginia and rotate with them in front of Pine Mountain.

A second explanation for the absence of a fracture system related to the Pine Mountain thrust is linked to the time of coal lithification. Coal lithification may not have progressed far enough by the time of the thrust movement to allow significant fracturing. Lignite will fracture with wide spacing compared to normal coal fracturing; these fractures may have formed, but could have been obscured by later fractures operating under a different stress field.

A third explanation for coal cleat rotation in the foreland may relate to the Russell Fork fault. The junction of the Russell Fork and Pine Mountain faults (Figure 1) appears to be the hub around which coal face cleats rotate (Figure 2). This junction was probably an area of considerable stress between the Pine Mountain thrust sheet and sheets adjacent to it. Coal cleat rotation may be the foreland effect of two sheets moving at different speeds and having a definite point of stress at their extreme edges.

Plotting of joint strikes as rose diagrams by station and lithology on the map reveal consistent coal face cleat orientations over relatively large areas (Figure 2). Shale and sandstone joints are not consistently oriented and their first- and second- formed joint strikes were plotted separately to determine their degree of correlation with coal cleat strikes. Plotting of the angles formed between coal cleats and first- and second-formed joints as histograms found several relationships. Black shales show 46 percent of the angles are within 10 degrees of coal cleats and 37 percent lie between 20-30 degrees of coal cleats. This fairly good correlation may reflect the close proximity of coal and black shale often seen in the stratigraphic sequence. Gray shales show 41 percent of the angles are within 15 degrees of coal cleats and 44 percent are between 25-40 degrees. The lack of close proximity of gray shales to coal and their increased silt content (with resulting change in strength characteristics) may account for these angular relationships. Sandstone showed no significant angular relationship to coal cleats. This indicates sandstone jointing in the deltaic Pennsylvanian sequence is too complex for regional interpretation.

DEVONIAN SHALE

Devonian shales along the eastern flank of the Cincinnati Arch and Nashville Dome (Figure 1) show consistent joint strikes of N25E, N45E and N65W. First-formed and second-formed joints strike northeast and northwest, respectively. The N45E joint strikes occur predominantly along the eastern flanks of the Cincinnati Arch and Nashville Dome. This strike set is roughly parallel to the N40E striking outcrop belt and may have formed as a tension feature related to the regional dip of the Cincinnati Arch and Nashville Dome. The N25E joint strike set is concentrated in the Cumberland saddle area (Figure 1) and is clearly a rotation from the previously discussed strike set. The Cumberland saddle is an area of Cambrian age basement faulting which probably rotated the regional stress fields of the Cincinnati Arch and Nashville Dome.

REFERENCES

Kulander, B. R., and Dean, S. L., 1979, ms, Rome trough relationship to fracture domains, regional stress history and decollement structures: (in review for Proc. of the Southeast Section Geol. Soc. of America Symposium on Western Limits of Detachment and Related Structures in the Appalachian Foreland).

Kulander, B. R., Dean, S. L., and Barton, C. C., 1977, Fractographic logging for determination of pre-core and core induced fractures - Nicholas Combs No. 7239 Well, Hazard, Kentucky: MERC-77/3, Distribution Category VC-02, Energy Research Center, Morgantown, W. Va., p. 20 and 33.

Ting, F. T. C., 1977, Origin and spacing of cleats in coal beds: Journal of Pressure Vessel Technology, v. 99, p. 624-626.

Figure 1
LOCATION MAP
B Long

Figure 2

COAL FACE CLEATS
B. LONG

10   0   10   20
MILES

FACE CLEATS WITH (B.Long)
COAL FORM LINES (Shumaker,1974)

10   0   10   20
MILES

Figure 3
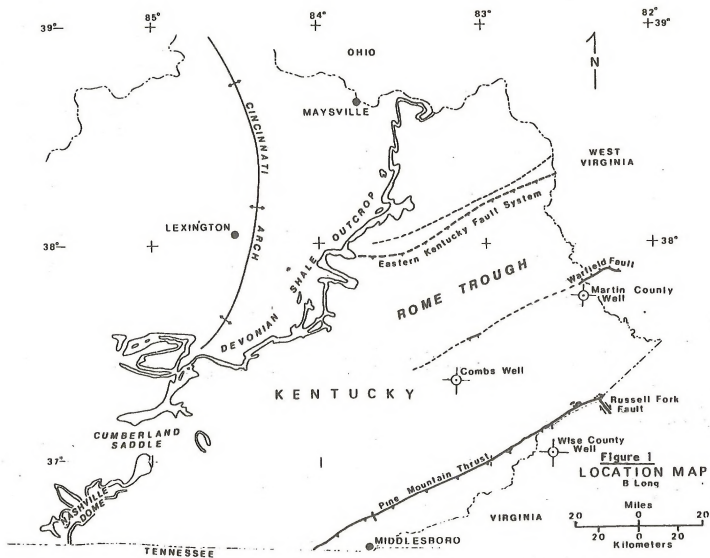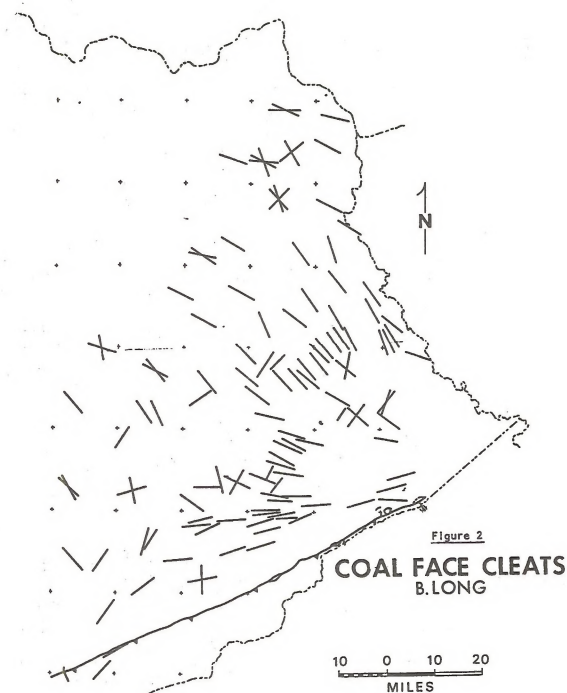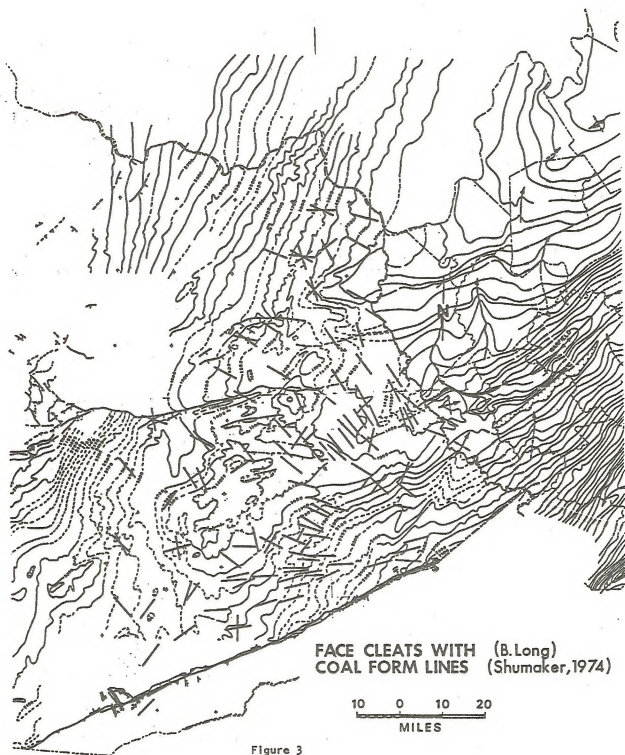
FRACTURES FROM DEVONIAN SHALE OUTCROPS
ALONG THE PINE MOUNTAIN THRUST

by

Kevin D. Lee
West Virginia University
Department of Geology and Geography

May 1979

INDEX

Abstract

Fracture patterns in the Devonian shale exposed along the Pine Mountain Thrust show much greater complexity than the overlying units. However, the trends of fractures in the upper part of the Devonian shale are nearly those of the overlying units. The amount and complexity of fracturing reflects the degree of, and distance from, the basal detachment fault plain.

Two zones of movement were found within the shales. The major fault occurs at the base of the shale, and the shales adjacent to the thrust plain show the most deformation. However, a zone of lesser movement occurred in the upper part of the shale. The two zones of deformation may match the reported productive zones found in the Big Sandy shale gas field to the west.

Joints in the Grainger shales and Berea sandstone have trends similar to that of the upper part of the underlying shale, but they are less variable.

Jointing in the overlying Newman limestone along Pine Mountain is similar but slightly rotated from the underlying Grainger shales. The joint trends consist of a dominant set parallel to the Pine Mountain Fault; and a less dominant set, perpendicular to the thrust front.

Eventually the results of this study will be combined with those of cored wells and other surface studies to present an integrated regional analysis of Devonian shale farctures.

LIST OF FIGURES

Purpose

Natural gas in the Big Sandy field of eastern Kentucky produces from fractures within the Devonian shale. There are only two areas where one can study these shale fractures at the surface near this field. The Devonian shales crop out in central Kentucky along the Cincinnati Arch, and in eastern Kentucky, they crop out just above the Pine Mountain Thrust. A separate study will report on fractures in the shales along the eastern flank of the Arch (Long, in progress). This study reports on the nature and origin of fractures in the Devonian shale that crop out along the Pine Mountain Thrust.

We hope that thru the documentation of fracture patterns in adjacent outcrops, meaningful comparisons can eventually be made with the production of natural gas from the Big Sandy gas field.

FIGURE 1

LOCATION MAP

OHIO

WEST
VIRGINIA

KENTUCKY

"BIG SANDY"
GAS FIELD

RUSSEL FORK
FAULT

PINE MOUNTAIN THRUST

VIRGINIA

0 5 10 15 20 MILES

TENNESSEE

Modified from Ray, 1976

EASTERN KENTUCKY
NW   SYNCLINE   MIDDLESBORO BASIN   SE
+3 MILES   +3

BIG SANDY GAS FIELD   OUTCROP AREA
KY-W.V. COMBS   FIRE CLAY   DEVONIAN SHALE   PINE MOUNTAIN
7239
0   0
            PENNSYLVANIAN
            DEVONIAN SHALE

-3 MILES   PRE-CAMBRIAN   -3
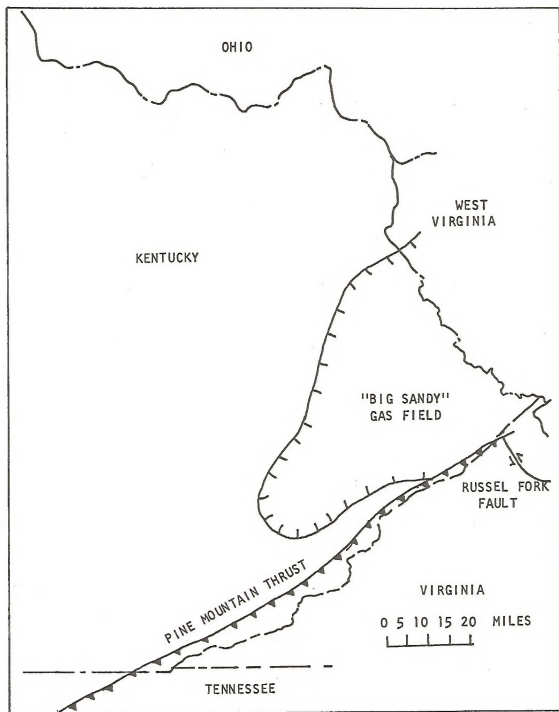
NO EXAGGERATION   SHUMAKER - 76
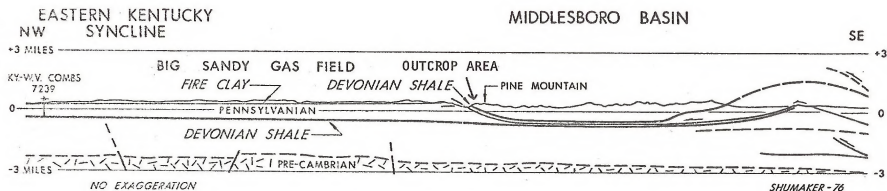
PINE MOUNTAIN THRUST AREA
COMBS-7239 WELL

FIGURE 2
CROSS-SECTION-BIG SANDY GAS FIELD-
PINE MOUNTAIN THRUST

Location and Geologic Setting

Pine Mountain is a linear feature about 125 miles long extending from just northeast of Elkhorn City, Kentucky, where it abuts against the Russel Fork fault, southwestward to near Jacksboro, Tennessee, where it abuts against the Jacksboro fault (see Figure 1). It was interpreted by Rich, 1934, and many others since as the surface expression of a major ramp of a detachment thrust in the Devonian shale, across more competent units, either to extend the surface or to an incompetent horizon in the Pennsylvanian clastics. The upper part of the ramp has since been eroded. The movement of the upper plate along the ramp has brought sediments of Devonian and Mississippian age to the surface. Presumably the stress that created the thrust also extended into the foreland in the area of the Big Sandy shale gas field. However, major movement was diverted by the ramp of the thrust at Pine Mountain so that extensive transpost did not occur under the Big Sandy shale gas field. However, if the stress and some minor movement did extend into the shales under the Big Sandy field, as suggested by Shumaker (1978), then the documentation of joints on the Pine Mountain may lead to insights concerning the fracture patterns and production in the Big Sandy shale gas field. For a more complete analysis and discussion of the geology of the area, readers are referred expecially to Harris (1970) and Harris and Milici (1977).

PENNSYLVANIAN
and MISSISSIPPIAN
SANDSTONE and
SHALE
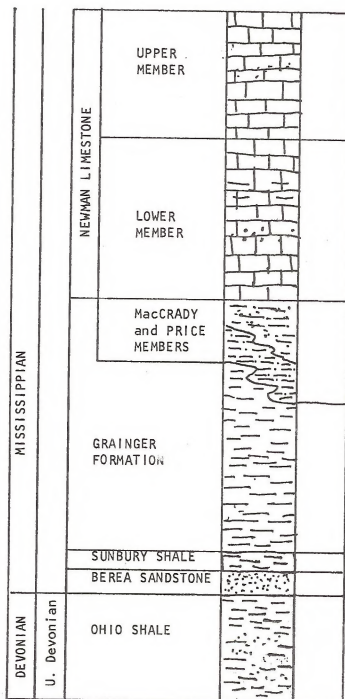
FIGURE 3
GENERAL STRATIGRAPHIC COLUMN

Method of Investigation

Field work was undertaken during July and August, 1978, to study fractures in the Devonian shales exposed along the base of Pine Mountain. Usually the shales are poorly exposed except in a few areas. The most complete exposures of the shale are along roads which cross the mountain or along quarry access roads to limestone which overlies the Devonian shale. Six exposures were found that were adequate to provide sufficient data for analyses of joints and outcrop-scale structures (Figures 4).

Except for the shale outcrop KL6 in the Bledsoe Quad, all exposures were moderately to intensely weathered.

Only joint sets that were consistant and repetitious throughout the outcrop were measured. Those joints judged to be random or unrepresentative of the dominant directions in the outcrop were noted, but not measured.
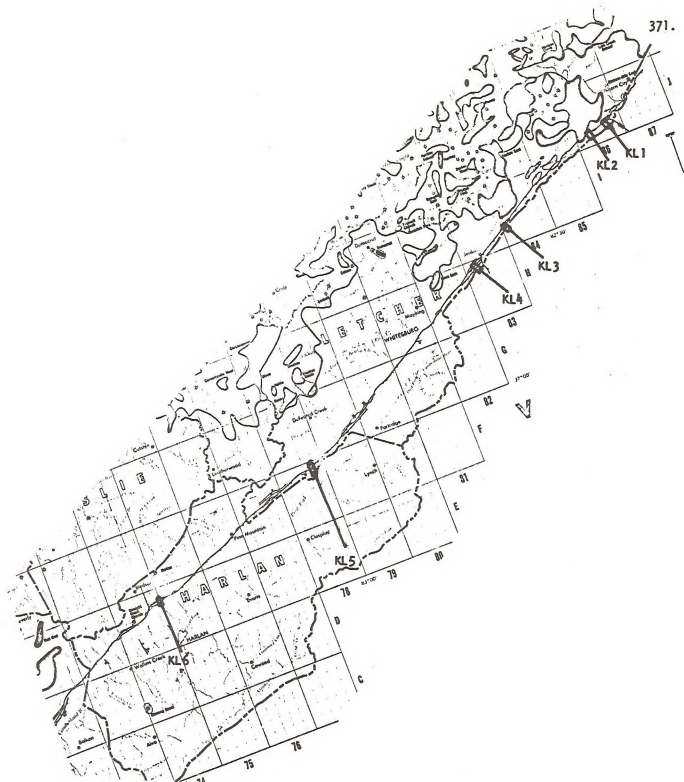
FIGURE 4
OUTCROP LOCATIONS

COLUMN LOCATION,
SHOWN ON FIG. 4

BLEOSOE QUAD
RT. 421 — QUADRANGLE AND LOCATION
KL6   OF COLUMN

PLOT OF STRIKES OF
JOINTS IN OUTCROP
LONGER LINES ARE
MORE DOMINANT SETS

PLOT OF POLES TO PLANES
OF JOINT FACES

A GROUP OF DOTS
REPRESENTS ONE JOINT
FACE

ONE CIRCLE MEANS TWO
OVERLAPPING GROUPS

NEWMAN LS

COVERED

SHALE, LIGHT

SHALE, DARK

FAULT ZONE
1"=40'

180

N35W/65SW

IN THIS EXAMPLE,
THE N75-80E SET
IS THE MOST
DOMINANT SET IN
THE OUTCROP

FIGURE 5
KEY TO COLUMNAR SECTIONS -
GUIDE TO INTERPRETATION

FIGURE 13A
KL6, CUMMULATIVE

LONGEST LINE IS STRIKE
OF THE PINE MOUNTAIN FAULT

DOT REPRESENTS
DIP OF THRUST FAULT
DIP - 65SW

SHORTER LINE IS THRUST FAULT
IN OUTCROP - N35W/65SW

HERE IS A DENSITY
OF TWO

HERE IS A DENSITY
OF FOUR
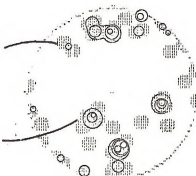
CUMMULATIVE DIPS FOR ENTIRE
OUTCROP
47 READINGS

CUMMULATIVE STRIKES FOR
ENTIRE OUTCROP

NUMBER OF JOINT READINGS
IN COLUMN

OUTCROP LOCATION

SECTION OF GEOLOGIC MAP SHOWING
OUTCROP AREA

FIGURE 6
KEY TO COLUMN CUMULATIVE DATA -
GUIDE TO INTERPRETATION

374.

ELKHORN CITY QUAD
ACCESS ROAD TO ELKHORN
CITY GRAVEL CO.

KL1

NEWMAN LS

380

GRAINGER SH

BEDDING DIP: 30°SE

GRAINGER SH

280

BEREA SS

BEREA SS

230

DEV. SHALE

BEDDING DIP: 30°SE

COVERED

120
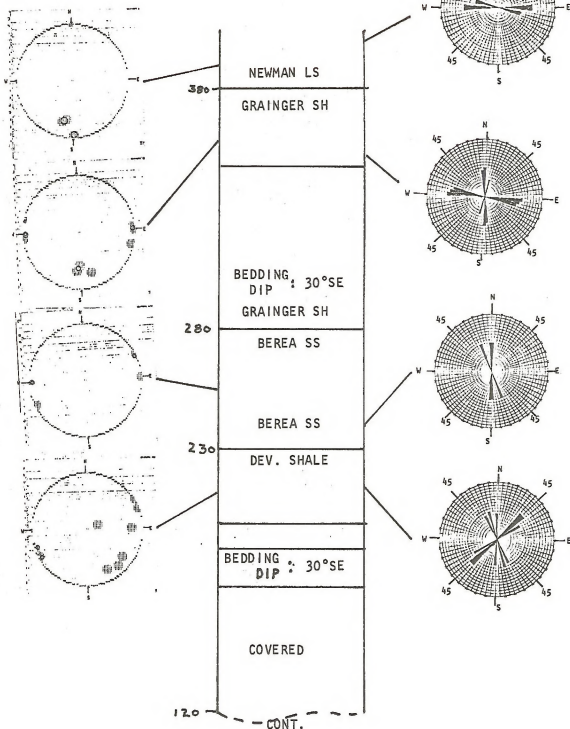
CONT.

FIGURE 7

ELKHORN CITY QUAD
CONT.

KL1
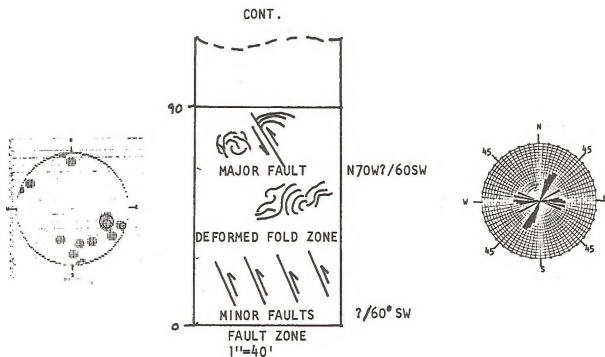
FIGURE 7A

FIGURE 7B
KL1, CUMMULATIVE

34READINGS

OUTCROP LOCATION
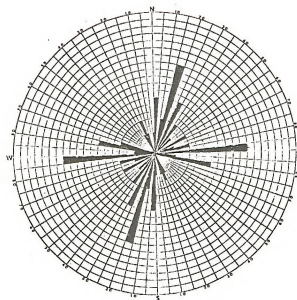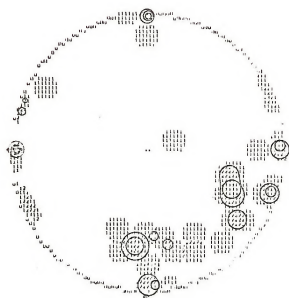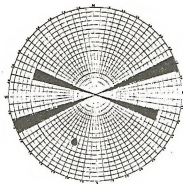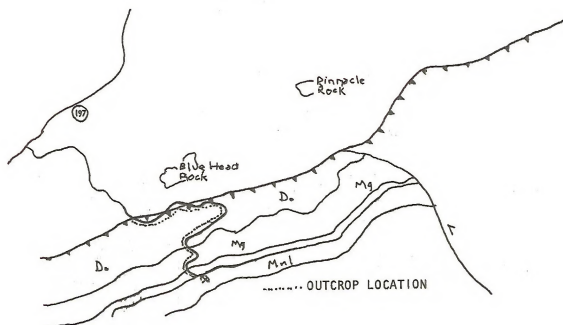
HELLIER QUAD
ACCESS ROAD TO JOHNSON
BROS. LS QUARRY
SECTION 10 IN THREE
LICK BED: GUIDE BOOK

KL2

NEWMAN LS

BEDDING: 30°SE

BASE OF GRAINGER

UNIT 28

BASE OF BEREA

UNIT 26

DISTURBED ZONE

UNIT 24

UNIT 23

COVERED

IRON STAINS ON
BEDDING
VERY FRACTURED

CONT.

IRON COATED
FRACTURES
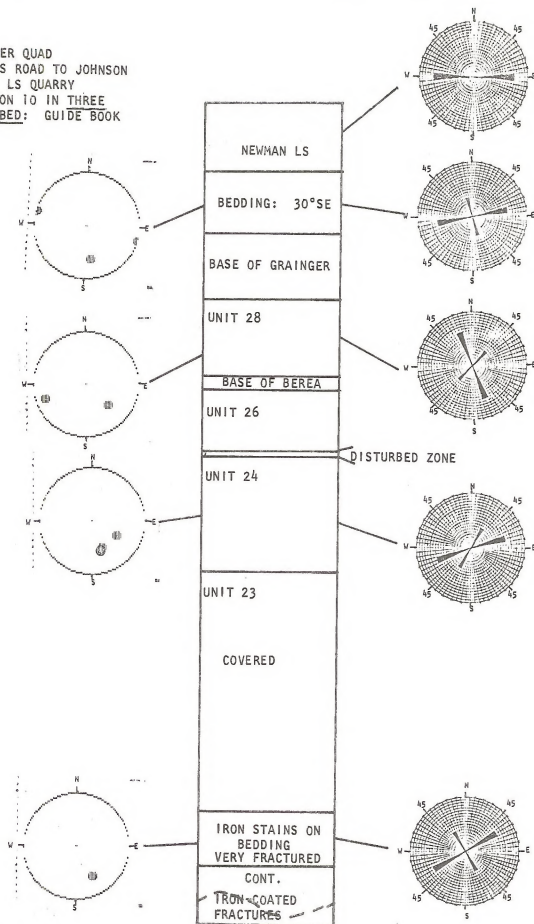
FIGURE 8

HELLIER QUAD
CONT.

KL2

CONT.

IRON-COATED
FRACTURES

UNIT 20

UNIT 19-13

COVERED

BEDDING: 25°SE

UNIT 11-9

COVERED

UNIT 8-6

BEDDING: 45°SW

UNIT 3-1
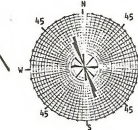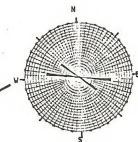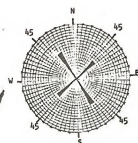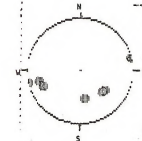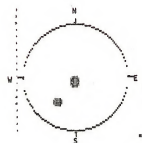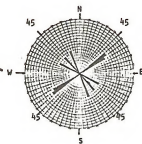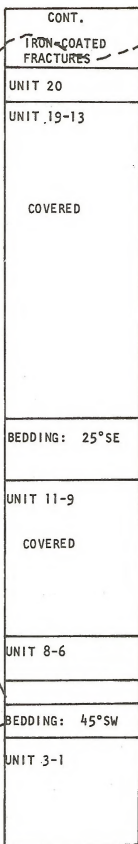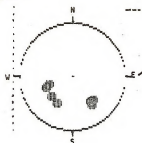
FAULT ZONE
1" = 40'

FIGURE 8A

26 READINGS

.... OUTCROP LOCATION
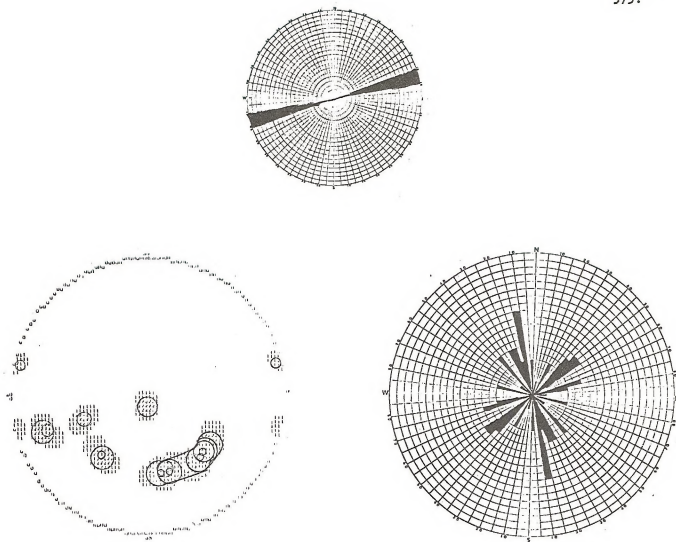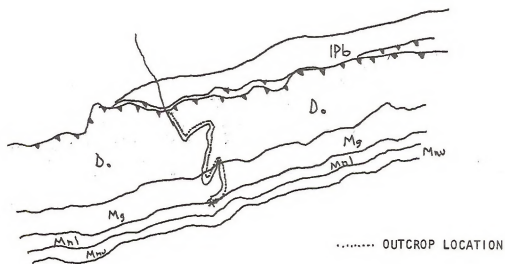
FIGURE 8B
KL2, CUMMULATIVE

JENKINS EAST QUAD
ACCESS ROAD TO ADAMS STONE
CORP. LS QUARRY

KL3

360

NEWMAN LS

GRAINGER SH

GRAINGER SH

230

CONTORTED ZONE
DEV. SH

200

BEDDING: 35°SE

160
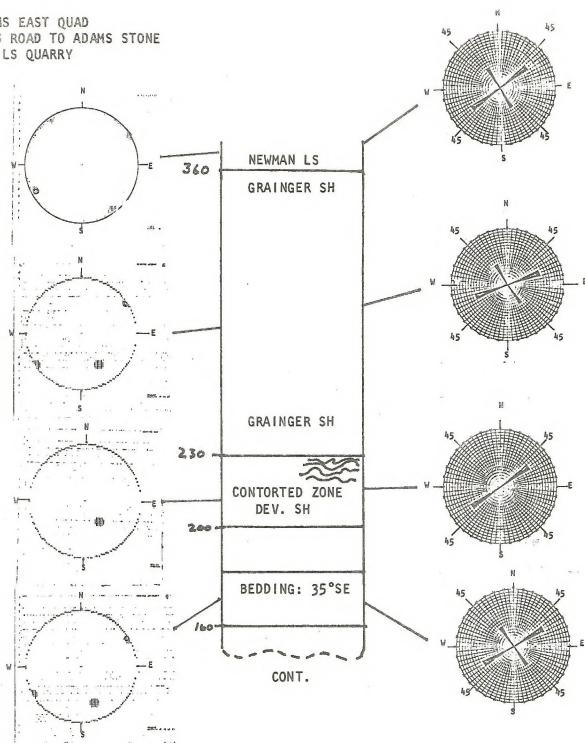
CONT.

FIGURE 9.

JENKINS EAST QUAD
CONT.

KL3

CONT.

JOINT FREQUENCY,
DIRECTIONAL VAR.
INCREASE DOWN

IRON-STAINED
JOINTS

PLASTIC-FLOW
DEFORMATION

FAULT ZONE
1"=40'

60

0
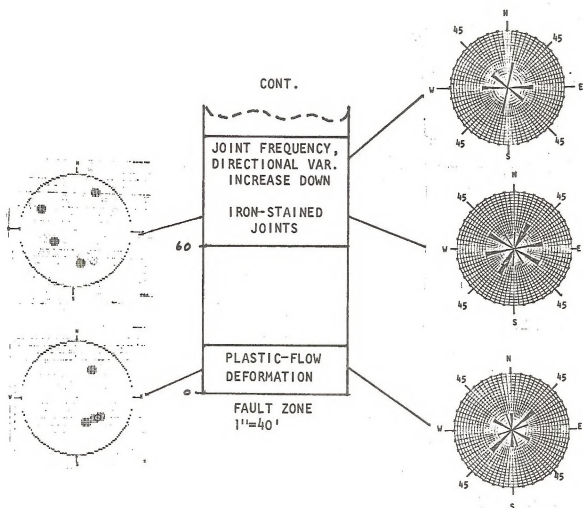
FIGURE 9A

FIGURE 9B.
KL3, CUMMULATIVE

25 READINGS

.... OUTCROP LOCATION
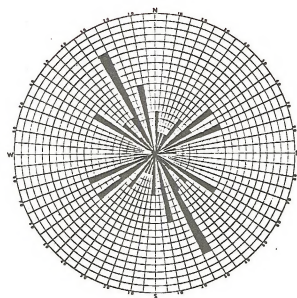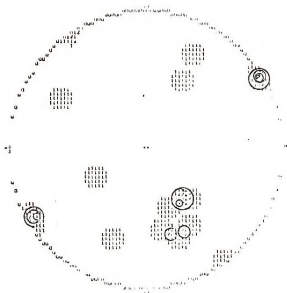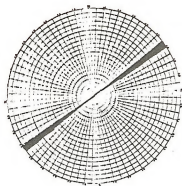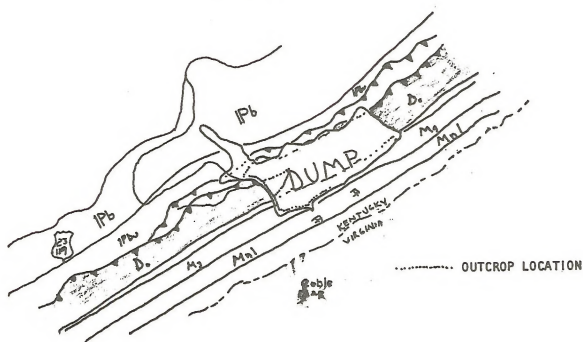
JENKINS WEST QUAD
RTS. 23 and 119, ABOUT
1 MILE SOUTH OF JENKINS

KL4

NEWMAN LS

BEDDING: 30°SE

GRAINGER SHALE

GRAINGER SHALE

DEV. SHALE

SPLAY FAULT?

COVERED

EXTREME
DEFORMATION

FAULT ZONE
1"=40'

FIGURE 10

25 READINGS

······· OUTCROP LOCATION
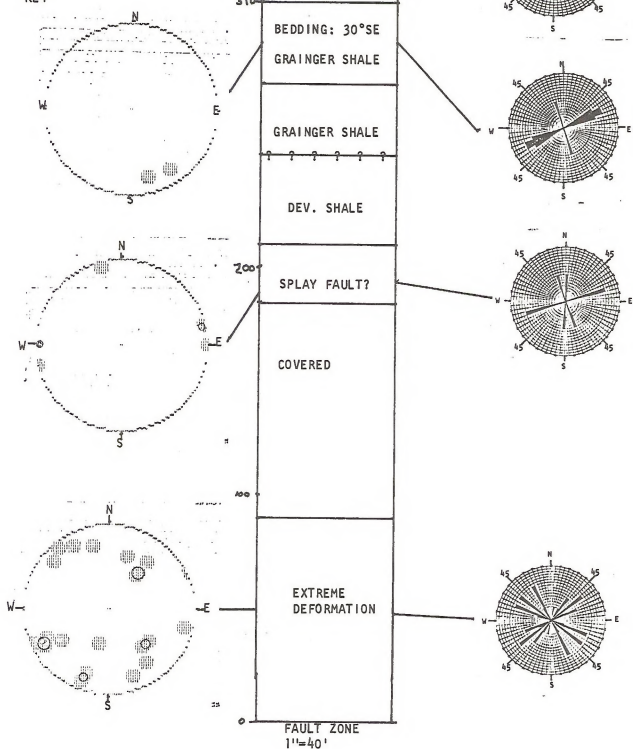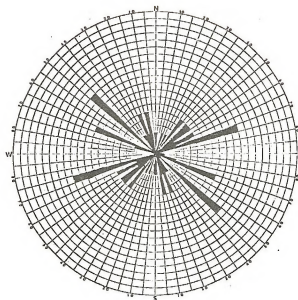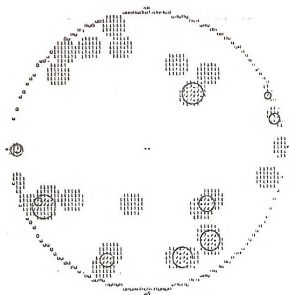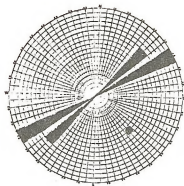
FIGURE 10A
KL 4; CUMULATIVE
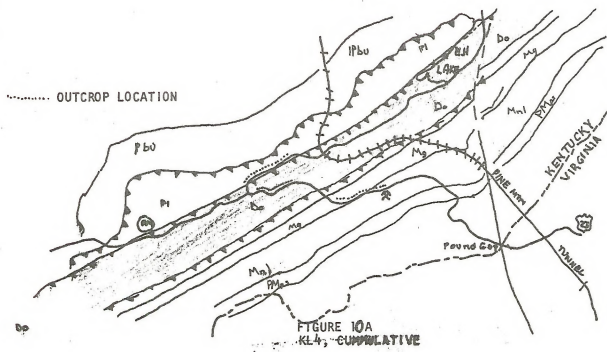
LOUELLEN QUAD
RT. 160, BELOW
HURRICANE PASS

KL5

NEWMAN LS

GRAINGER SHALE

GRAINGER SHALE

COVERED

SPLAY FAULTS
MINERALIZED FRACTURES

JOINTS CHANGE
DIRECTION

DEFORMED ZONE

MINERALIZED FRACTURES

N55W/50SW

COVERED

CLAY ZONE

SLICKENSIDES

FAULT ZONE
1"=40'

FIGURE 11

38 READINGS

.... OUTCROP LOCATION

FIGURE 11A
KL5, CUMMULATIVE

Hurricane Gap

BLEDSOE QUAD
RT. 421

KL6

NEWMAN LS

COVERED

SHALE, LIGHT

SHALE, DARK

N35W/65SW

FAULT ZONE
1"=40'

180
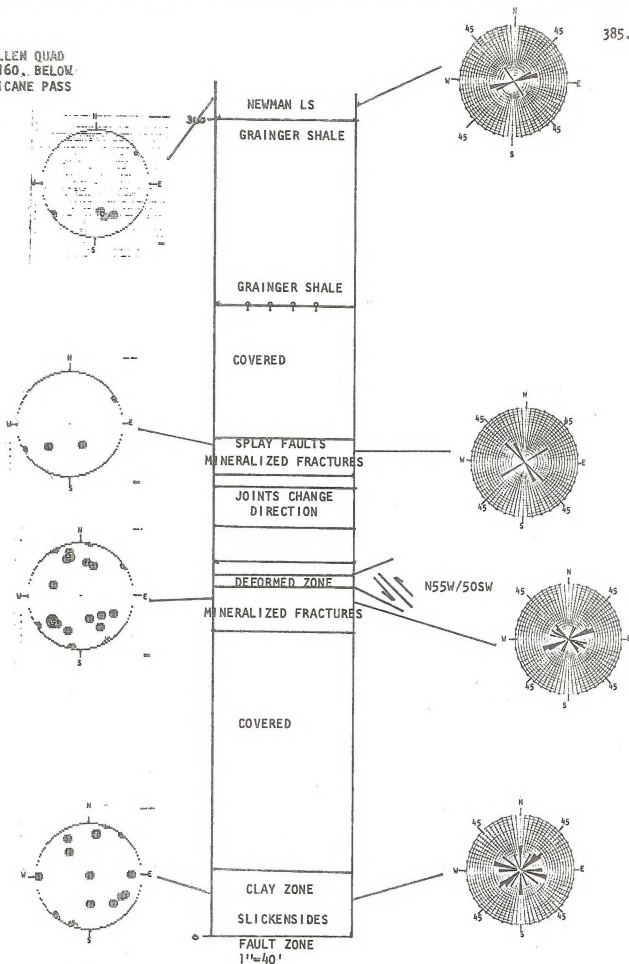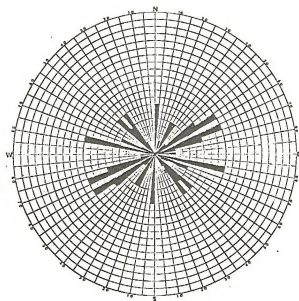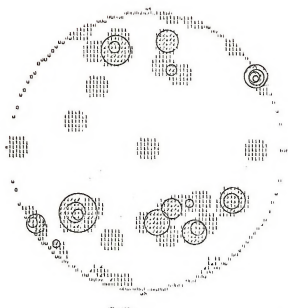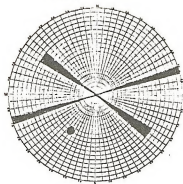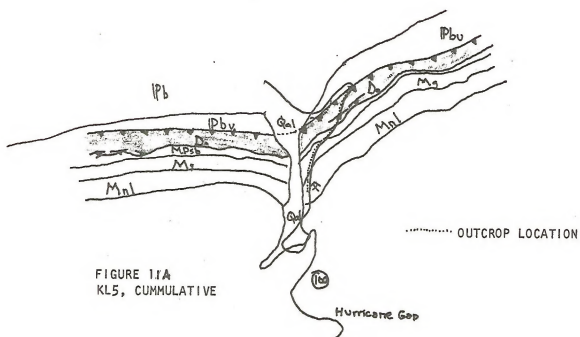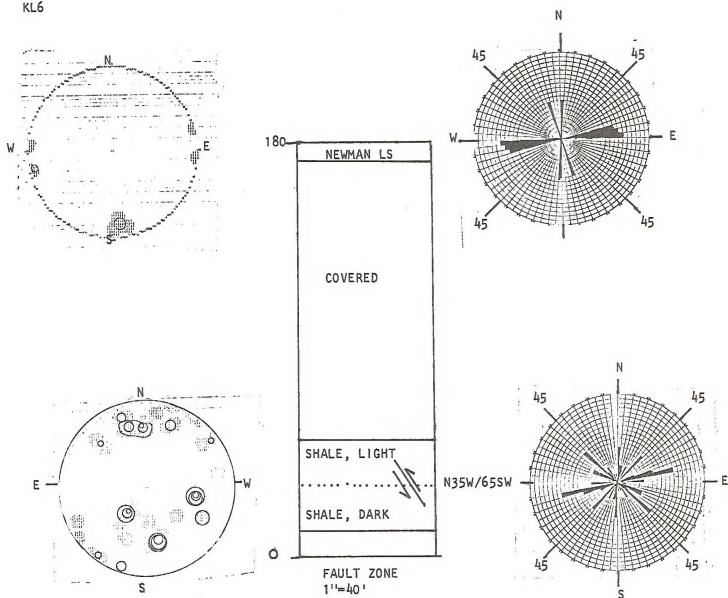
FIGURE 12

FIGURE 12A
KL6, CUMMULATIVE
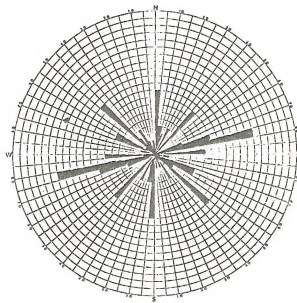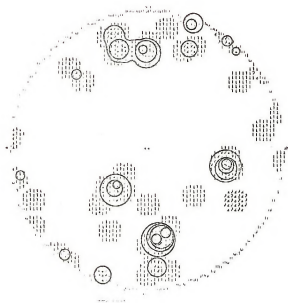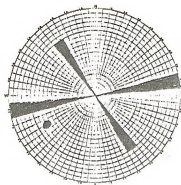
47 READINGS
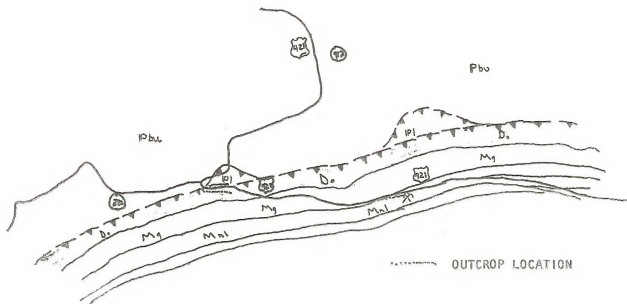
OUTCROP LOCATION

	CLOSE TO PINCHOUT OF SHALE ALONG STRIKE	SPLAY FAULTS ON OUTCROP SCALE	THRUST FAULTS ON OUTCROP SCALE	RANDOM FRACTURES	FLOW CHARACTERISTICS		JOINT DENSITY INCREASES DOWN	JOINTS CHANGE DIRECTION DOWN
					AT TOP OF SHALE	AT BOTTOM OF SHALE		
JOHNSON BROS. QUARRY **KL 2** ROAD	NO	NO	NO	YES	YES	NO	?	YES
JENKINS EAST QUARRY **KL 3** ROAD	NO	?	?	YES	YES	YES	YES	YES
JENKINS WEST **KL 4** ROADCUT	YES	YES	YES	YES	?	YES	?	?
HURRICANE PASS **KL 5**	NO	YES	YES	YES	?	YES	?	YES
BLEDSOE CHURCH **KL 6**	NO	?	YES	YES	?	?	?	?
ELKHORN QUARRY ROAD **KL**	YES	NO	YES	YES	NO	YES	YES	YES

FIGURE 13
CHART OF STRUCTURAL FEATURES

389.

Conclusions

1) Jointing in the Newman Limestone consists of a dominate strike set
   parallel to the Pine Mountain thrust, and a dip set perpendicular
   to the thrust front.

2) Jointing in the underlying Grainger shales and Berea sandstone are
   similar to jointing in the limestone, but can show slight rotation
   of joint strike, and greater variability in the strike of joint
   directions, especially in the second, or dip set.

3) A Narrow zone of deformation may be present near the top of the
   Devonian shales. This zone may reflect flexurial flow as the stiffer
   units above glided over the weaker shales during formation of the main
   Pine Mountain thrust, found at the base of the shale.

4) The number of joint sets throughout an outcrop increase with depth,
   or, the closer to the fault zone, the greater the trend and number
   of joint sets. Shumaker (1976) noted anamolous dip readings in the
   dip meters of the No. 1 Combs well in the Big Sandy field (perhaps
   reflecting mineralized fractures) in organic zones near the base of
   the shale and near the top of the shale. The two zones also contain
   slickensides indicative of movement (Shumaker, 1976). In addition
   Ray (1967) reports two main zones of production from these same organic
   layers. (See Figure 14) It seems possible that the two deformed zones
   at Pine Mountain correlate with those discussed by Shumaker (1978) and
   Ray (1967).

5) The strikes of joint sets at the top of the Devonian shales do not
   match the strikes of joint sets at the bottom of the Devonian shales.
   Somewhere between the top and bottom of the Devonian shales is a zone,
   sometimes narrow, where the joints change strike. This is graphically
   illustrated on KL3 between elev. 80 and 160, and was seen on one outcrop

FRACTURED DEVONIAN SHALE WELLS
PERRY COUNTY, KY.

NOT FRAC'D.
NATURAL-180 M
AFT.-PERF-133 M

BF.-0 M
AF.-307 M

G.R.   B.D.

BF.-0 M
AF.-119 M

G.R   B.D.

BF. - 84 M
AF.-183 M

BF.-0 M
AF.-198 M

G.R.   B.D.

BEREA-L
BEDFORD

DEVONIAN SHALE

BF.-0 M
AF.-47 M

G.R.   B.D.
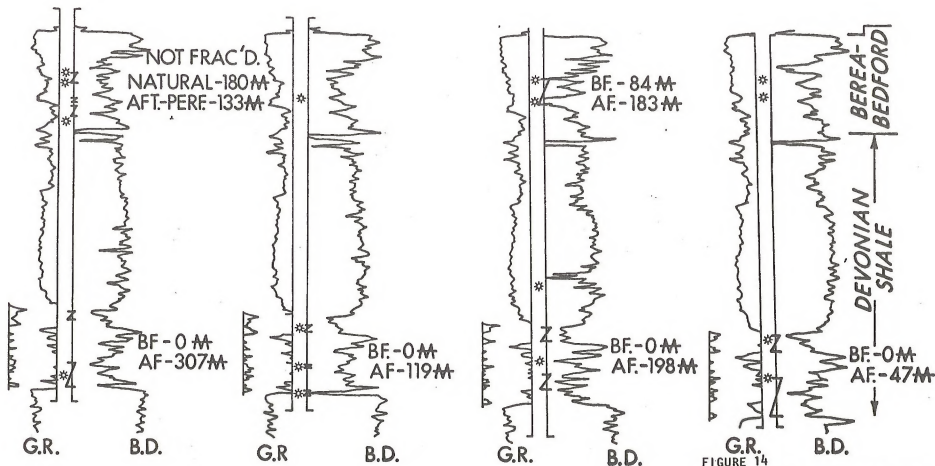
FIGURE 14
PRODUCTIVE ZONES IN DEVONIAN SHALE

RAY-1967

on KL5.

6) The most deformed zones occur in the lower part of the Devonian shales near to the disappearance of the shales along strike of the Pine Mountain thrust, and conversely as the shale thickens above the thrust there is a greater section of undeformed shale.

7) Thrust faults in the Devonian shale, as seen in outcrop, are not parallel to the main Pine Mountain fault. Thrust faults in the shale that are parallel to the main thrust may be obscured on bedding planes. A clay rich zone at the bottom of KL5 may be one such fault.

8) Random fractures, or non-systematic fractures throughout entire outcrops, were noted in some exposures at every column studied. These could be related to blasting, weathering, or tectonic deformation.

9) Each column usually has joint sets sub-parallel and sub-perpendicular to the Pine Mountain thrust.

10) Where thrust faults are detectable in outcrop, the strikes consistently correspond to strikes of a joint pattern. However, the dips of the thrust faults do not consistently correspond to dips of a joint pattern.

Harris, L.D., 1970, Details of thin-skinned tectonics in parts of Valley and Ridge and Cumberland Plateau provinces of the southern Appalachians, in Fisher, G. W., and others, eds., Studies of Appalichian Geology-central and Southern: New York, Interscience Publishers, p. 161-173.

Harris, L. D. and Milici, R.C., 1977, Characteristics of Thin-Skinned Style of Deformation in the Southern Appalachians, and Potential Hydrocarbon Traps: Geol. Surv. Professional Paper 1018, 40p.

Provo. L.J., Kepferle, R. C., and Potter, P.E., 1977, "Three Lick Bed: Useful Stratigraphic Marker in Upper Devonian Shale in Eastern Kentucky and Adjacent Areas of Ohio, West Virginia, and Tennessee." MERC/CR-77/2,.56p.

Ray, Edward O., 1967, Reference Location Unknown

Ray, Edward O., 1976, Devonian Shale Development in Eastern Kentucky in Natural Gas From Unconventional Geologic Sources; National Academy of Sciences, Washington, D. C.

Rich, J.K., 1934, Mechanics of low-angle overthrust faulting as illustrated by Cumberland thrust block, Virginia, Kentucky, and Tennessee: Am. Assoc. Petroleum Geologists Bull., V. 18, No.12, p. 1584-1596.

Shumaker, Robert C., 1976, Kentucky, West Virginia Gas Company Final Report—Well No. 7239, Perry County, Kentucky: Text of U.S. Energy Research and Development Administration Contract No. E (46-1) 8000.

Shumaker, Robert C., 1978, Porous Fracture Facies in the Devonian shales of Eastern Kentucky and West Virginia: Geology Dept., West Virginia University.
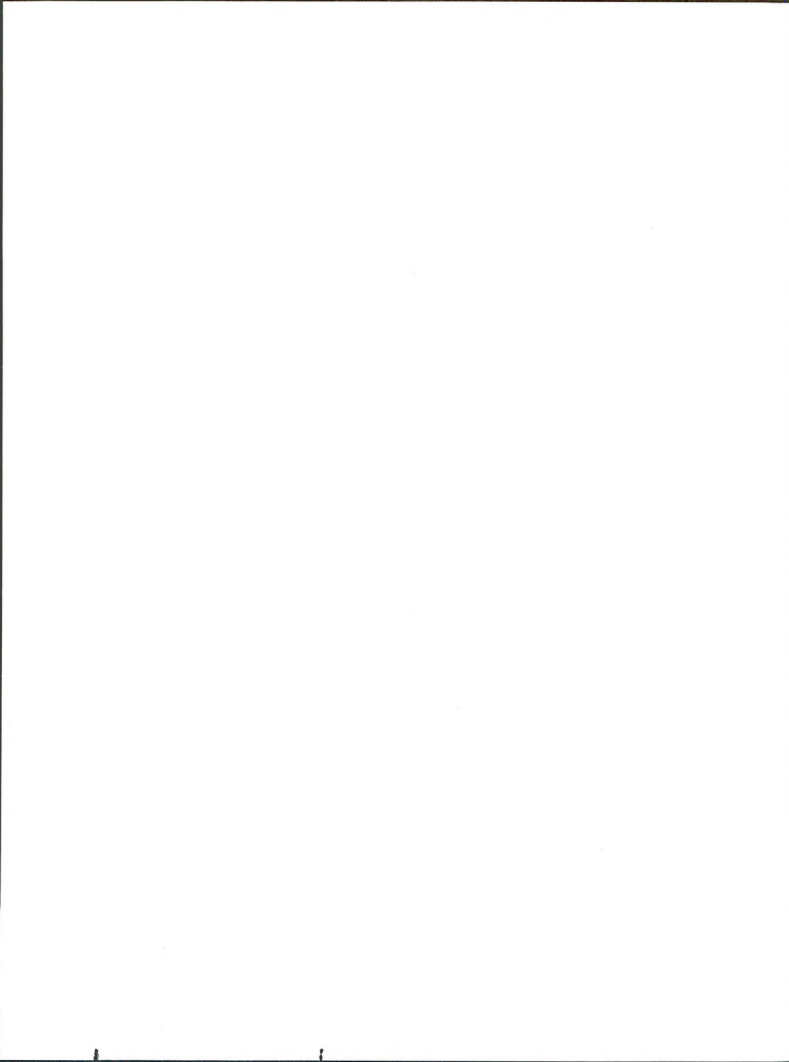
APPENDIX D

Production Data

Jane Negus-de Wys
E. B. Nuckols III

RELATIONSHIPS OF GAS OCCURRENCE TO GEOLOGICAL

PARAMETERS IN THE EASTERN KENTUCKY GAS FIELD(S)

J. Negus de Wys *
R. C. Shumaker
West Virginia University
Department of Geology and Geography
Devonian Shale Program
425 White Hall
Morgantown, West Virginia 26506

ABSTRACT

A study of initial open flow gas data from 4750 wells in the Eastern Kentucky Gas Field(s) relates gas occurrence to geological parameters including structural/stratigraphic sections, lithology, and geochemistry.

Approximately 300 formation density logs are used for stratigraphic correlation, reinforced by data from two cored wells and cuttings from 11 wells in this 3,000 square mile, 10 county study area known historically as the Big Sandy Field. This field has produced for over 50 years.

Trend traces of initial open flow data are interpreted as zones of more intense fracturing and show four preferential directional trends.

The gentle anticlinal structure in the northern part of the field, which may be an extension of the Paint Creek Uplift, broadens to the south and bifurcates. Small faults are identified to the southwest of the main field and the Rome Trough occurs across the northern portion of the field.

The 100' per mile dip to the southeast of the basement rocks is subdued to 30-50' per mile dip in the producing Devonian shale sequence which thickens by an order of magnitude into the basin to the northeast.

Relationships of these parameters and geochemistry from well cuttings are presented.

EASTERN KENTUCKY GAS FIELD:
STRUCTURAL-STRATIGRAPHIC CROSS SECTIONS AND POTENTIAL PRODUCTION PATTERNS

by
J. Negus de Wys
R. C. Shumaker
Department of Geology and Geography
West Virginia University
425 White Hall
Morgantown, West Virginia 26506

ABOUT THE AUTHOR(S)

Mrs. de Wys received her BA with honors in geology from Miami University, Oxford, Ohio. She attended graduate school at the University of Wisconsin, Ohio State University, and U.C.L.A. in Los Angeles, and Law School at Texas Tech University. She is presently studying for her doctorate in Geology at West Virginia University.

Mrs. de Wys taught Geology at Case Western Reserve University; was Curator of the Geology Museum in Madison, Wisconsin; worked with Shell Oil in Midland, Texas, and Mene Grande Corporacion in Venezuela; was Research Associate in the Ohio State Research Foundation Mapping and Charting Laboratories (Radar Interpretation); was Senior Scientist and Surveyor Experimenter at Cal-Tech Jet Propulsion Laboratory (Magnet Experiment); was Assistant to Director of Research at the University of Utah Research Institute. Mrs. de Wys has, in addition, worked in top level business management for six years in Jackson, Wyoming. She is included in 1978 Who's Who in the West.

In August of 1977, Mrs. de Wys joined the staff on the Devonian Shale Program as Research Associate in the Geology Department at West Virginia University. Her Ph.D. dissertation is STUDY OF THE EASTERN KENTUCKY GAS FIELD(S): GEOLOGICAL PARAMETERS AND POSSIBLE RELATIONSHIPS TO GAS OCCURRENCE AND PRODUCTION.

Dr. Shumaker received his A.B. degree in Geology from Brown University and his M.S. and Ph.D. degrees in Geology from Cornell University.

He was employed with Exxon Corporation at their research lab in Houston for six years and in their operations exploration department in Midland, Texas, and New Orleans, Louisiana, for seven years. For the past six years he has been teaching petroleum geology, photo geology, and basin structure courses within the Department of Geology and Geography at West Virginia University.

Preliminary results on a projected three-year study of about 3000 square miles of Eastern Kentucky Gas Field(s) are presented. Initial open flow data are compared with basement structure, dip and strike, and thicknesses of producing units in Devonian Ohio shales.

A series of seven preliminary cross sections are presented for comparison of log signature changes and correlation, stratigraphy and structure. A three-dimensional plexiglas model is presented for spatial relationships of the geological parameters to the initial open flow values and gas occurrence shown on temperature logs.

On-going studies on this field include lithology study of samples from each county, and geochemical analysis of samples for vertical and horizontal variation.

A preliminary computer-produced map of contours on the initial open flow data has been run using the Fortran SYMAP program. Additional refinements are being made prior to running a final map. A hand contoured map is also being prepared.

Comparison of the initial open flow map will then be made with the geological parameters.

INTRODUCTION

Ed Ray of Kentucky-West Virginia Gas has described the historical development of this area which has undergone exploratory drilling for over 150 years, first for brine, then oil and eventually for gas. "The commercial production of gas commenced in the 1920's and now comprises 85% of the gas produced in Kentucky. The most important producing horizon in the Eastern Kentucky Field is the Upper Devonian Ohio 'Brown Shale' which includes the Cleveland Shales, Three Lick of Chagrin, and the Huron Shales. These highly organic units are 200-900 feet thick in this area and have a southeast monoclinal dip of 30-50 feet per mile. Only 5% of completed wells have natural commercial open flows. Shooting with explosives was shown to bring 40% of nonproducers into commercial production. Presently hydrofracturing is the standard procedure, which results in only 43% of drilled wells falling within 0-100Mcf range as against 54% of total completions with shot wells in that range.

These procedures reflect the fact that the Devonian Brown Shale of Eastern Kentucky is a relatively small volume producer in individual wells but the productive life far exceeds any other producing formation in the area. An explanation for this slow but long well life may lie in the concept of production from "fracture facies" of the shales, possibly related to deep basement structural features, coupled with the extremely low average matrix porosity and permeability. This field is the largest gas field in the Appalachian Basin, having produced over 1.7 trillion cubic feet of gas."

PURPOSE OF STUDY

The purpose of this investigation is to identify and describe geological parameters and relate these to gas occurrence and potential production. Geological parameters in this study include stratigraphy, structure, lithology, and geochemistry. Identification of Protosalvinia (also described as Foerstia) in well cuttings and cores is included as a possible time line or restricted habitat zone.

Gas occurrence data is derived from temperature logs. Initial open flow data is used as an indicator of gas occurrence and potential production.

Data

The data to be included in this study consists of:

1) Approximately 300 formation density logs,
2) approximately 75 temperature logs,
3) initial open flow data on approximately 4750 wells,
4) well cuttings from ten counties,
5) core data on two wells and one tunnel,
6) fracture study data from 2 cores and field surface studies,
7) outcrop data to the west,
8) West Virginia University and Geological Survey studies to the east,
9) literature including especially work by the Kentucky Geological Survey, the U. S. Geological Survey, the University of Kentucky, the University of Cincinnati, Ohio, State University, and

especially the dissertations of Linda Provo and J. Schwietering.

Status of investigation

The work presented in this paper includes seven preliminary stratigraphic-structural cross sections and preliminary initial open flow data patterns. Some gas occurrence from temperature logs is included on cross-sections, although this work has not yet been completed.

Structural, isopach maps, lithology, geochemistry, and final analysis are yet to be accomplished.

Stratigraphic-structural maps

The seven cross sections presented in this report are oriented as follows:

1) three in a SW – NE direction, and
2) four in NNW – SSE directions.

See Figure 1.

These sections are shown in a 1/163 ratio of the horizontal to vertical scale in order to emphasize the gentle structure and permit the display of the fine intertonguing gray and black shales in the Cleveland section.

The cross sections show a more sharply defined anticline in the northernmost SW – NE cross section, broadening in the central part of the field and gently bifurcating to the south. The NW – SE cross sections show the regional dip to the SE at about 30-60 feet per mile, with some suggestion of slight interruptions of this dip in the form of small steps. In the central SW – NE cross section two small normal faults are apparent in the extreme SW. These are not apparent in the other two near parallel sections. A fault is suggested in the vicinity of the Warfield fault and possibly to the NE.

The stratigraphic sections thicken by as much as an order of magnitude to the east.

The intertonguing of the gray and black shales in the Cleveland sequence is reflected in the natural radioactivity in the gamma-gamma readings on the formation density logs. Core samples bear out the color changes. However, a simple gray/black designation is actually not truly representative of this section. A more detailed study should show a gradation in grays from very light to extremely dark or black. This study is only showing relative changes and thus the cross sections show only two relative gradations.

Gas occurrence from temperature logs is shown on the cross sections. This work has not yet been completed; the lack of gas occurrence shown on some logs may be due to lack of data at this time.

Initial open flow data from 4750 wells is used to develop pattern maps and run a Fortran SYMAP program. The pattern maps shown show the results in terms of four levels as 1) a color representation with red as highest, orange as second highest, yellow as third, and dots as fourth; and 2) as a black pattern. See Figures 2 and 3. Points were connected where not contra-indicated. In the black pattern in Figure 3 several linear band-like trends may be noted, within which there appear suggestions of arcuate or almost meandering patterns. Sample checks across these bands are planned to investigate lithology changes.

The first completely run SYMAP on twice the scale of the original map is presented. This will be contoured from the printout and reduced for comparison with other parameters.

A three-dimensional plexiglas model of the field with cross sections discussed here and an areal histogram of initial open flow data is presented in the poster session area.

Protosalvinia has been identified and photographed in both cores and has been found in the well samples studied to date. The existence of this brown algae may represent a time line, or, more possibly represent a restricted unique set of environmental habit conditions in which this form could flourish.

This paper represents essentially a status report on the first year of an on-going three-year study. As such, conclusions are not drawn at this time. However, inferences at this point in the investigation suggest both structural and stratigraphic influences on gas occurrence in this field.
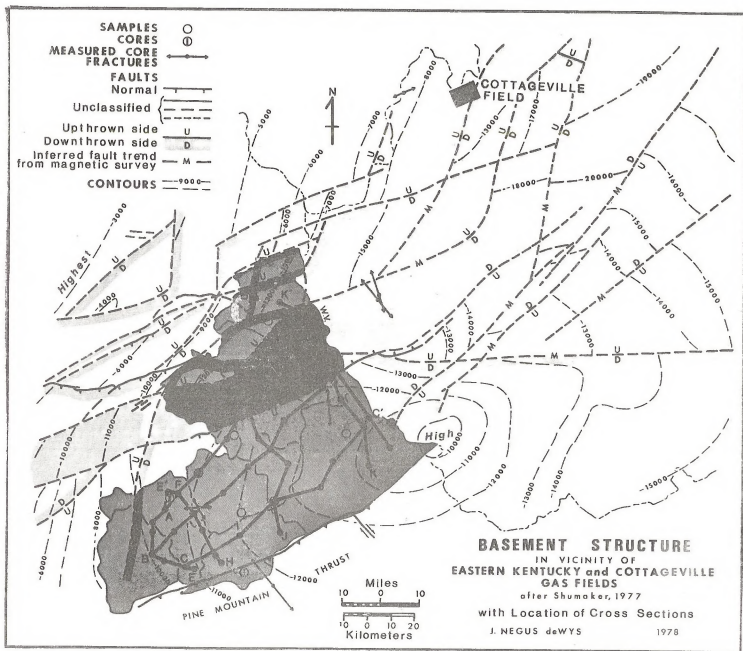
Figure 1: Location of study area showing cross sections under study and structural setting.

KEY
● INITIAL OPEN FLOW
  >2 MM cf/day
● INITIAL OPEN FLOW
  >1 MM cf/day
○ INITIAL OPEN FLOW
  >.5 MM cf/day
  <.5 MM cf/day

EASTERN KENTUCKY GAS FIELD
INITIAL OPEN FLOW DATA
PATTERN OF WELLS IN 4
LEVELS AND CONNECTED
WHERE NOT CONTRAINDICATED

J. Negus deWys   June, 1978
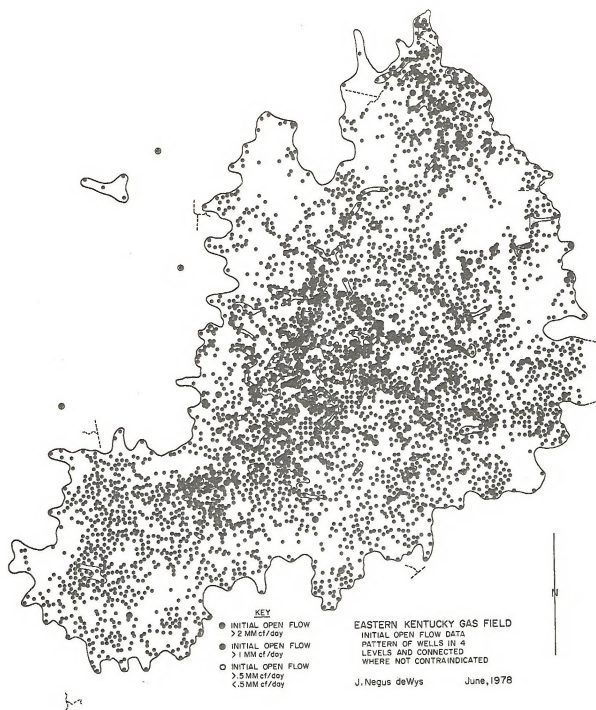
.Figure 2. Location of open flow data points (from Griffiths 1976).

EASTERN KENTUCKY GAS FIELD
INITIAL OPEN FLOW DATA
PATTERN OF ALL WELLS >.5MMcf/day
WELLS ARE CONNECTED WHERE
NOT CONTRAINDICATED ON A
MAP WITH ~5000 WELLS

J.Negus deWys   June,1978
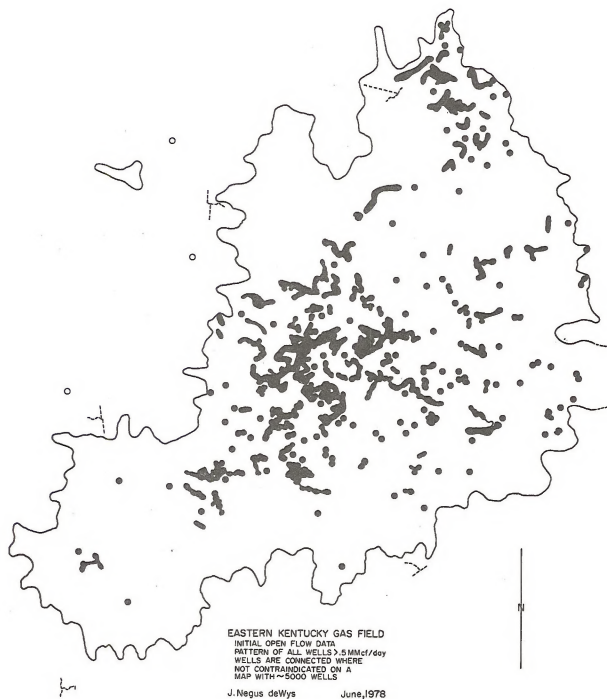
Figure 3. Pattern resulting from connection of all wells with open
flow ≥ 0.5. No wells with lower flow occur within the pattern.

ACKNOWLEDGEMENTS

TREND ANALYSIS OF GAS PRODUCTION IN THE COTTAGEVILLE FIELD

by
J. Negus de Wys
R. C. Shumaker
West Virginia University
Department of Geology and Geography
425 White Hall
Morgantown, West Virginia 26506

ABOUT THE AUTHOR(S)

Mrs. de Wys received her BA with honors in geology from Miami University, Oxford, Ohio. She attended graduate school at the University of Wisconsin, Ohio State University, and U.C.L.A. in Los Angeles, and Law School at Texas Tech University. She is presently studying for her doctorate in Geology at West Virginia University.

Mrs. de Wys taught Geology at Case Western Reserve University; was Curator of the Geology Museum in Madison, Wisconsin; worked with Shell Oil in Midland, Texas, and Mene Grande Corporacion in Venezuela; was Research Associate in the Ohio State Research Foundation Mapping and Charting Laboratories (Radar Interpretation); was Senior Scientist and Surveyor Experimenter at Cal-Tech Jet Propulsion Laboratory (Magnet Experiment); was Assistant to Director of Research at the University of Utah Research Institute. Mrs. de Wys has, in addition, worked in top level business management for six years in Jackson, Wyoming. She is included in 1978 Who's Who in the West.

In August of 1977, Mrs. de Wys joined the staff on the Devonian Shale Program as Research Associate in the Geology Department at West Virginia University. Her Ph.D. dissertation is STUDY OF THE EASTERN KENTUCKY GAS FIELD(S): GEOLOGICAL PARAMETERS AND POSSIBLE RELATIONSHIPS TO GAS OCCURRENCE AND PRODUCTION.

TREND ANALYSIS OF GAS PRODUCTION IN THE COTTAGEVILLE FIELD

by
J. Negus de Wys
R. C. Shumaker
West Virginia University
Department of Geology and Geography
425 White Hall
Morgantown, West Virginia 26506

ROBERT C. SHUMAKER

Dr. Shumaker received his A.B. degree in Geology from Brown University and his M.S. and Ph.D. degrees in Geology from Cornell University.

He was employed with Exxon Corporation at their research lab in Houston for six years and in their operations exploration department in Midland, Texas, and New Orleans, Louisiana, for seven years. For the past six years he has been teaching petroleum geology, photo geology, and basin structure courses within the Department of Geology and Geography at West Virginia University.

ABSTRACT

Results of a trend analysis study of the Cottageville Gas Field are presented. A series of maps are developed from geological factors, gas production data, and production decline calculations. Trends are plotted on each map and then compared on a compass rose.

Relationships of geological trends to production and production decline are shown through a stacked block diagram sequence.

Suggestion of a fault or faults is made by production and production decline map trends which do not relate to other geological factors.

This method of analysis is presently being applied to the Eastern Kentucky Field(s).

INTRODUCTION

The purpose of this study is to apply various methods of gas production data analysis to gas field data in order to objectively evaluate and explore relationships in the production history of the Cottageville gas field in the Devonian shale. An understanding of such relationships may contribute to estimation of recoverable reserves and to conclusions or hypotheses in the study area which may be applied to other potential gas producing shale areas.

The scope of the study is the gas production from 63 wells from Devonian shales in the southwestern Jackson County and eastern Mason County. This paper represents a step further in analysis and conclusions from a paper by the authors in 1977 (de Wys and Shumaker, 1977).

Devonian shales underlie approximately 100,000 square miles in Kentucky, Ohio, West Virginia, Pennsylvania, and New York. It has been estimated that this area contains about 460 trillion tons of shale readily accessible to drilling, and most of this at about 10,000 feet in depth (Columbia Gas System).

The horizon of "brown shales" from which most gas has been produced is a 400' section with finer grain size, darker colors with spores and brown algae (Protosalvinia) reported. Above this zone is 1,200 feet of gray to greenish-gray shales with sandy and silty zones and a dark gray to black interval. Grain size coarsens upward from the producing horizon. Below the producing horizon is 300-400 feet of greenish-gray shale with no silt and below that 200-400 feet of lower black shale, calcareous in the bottom portion (Tully Ls.). Gas has been produced from the Brown Shale horizon for nearly 50 years from low-volume shallow wells in the western one-third of West Virginia.

Up to 4.4% by weight organic content is found in the brown shales.

Porosity in Devonian shales is very low. In two Jackson County wells in West Virginia, porosity ranged from .1 - 4.6% with overburden of 1650 PSI and 3700 PSI (obtained by oil method). By comparison, highly productive sandstone reservoirs show 10-20% of total rock volume. Most pore space found in shales is between the mineral crystals or grains and in micro and macrofractures (Science Applications, Inc., 1977).

Permeability values for the same two Jackson County wells range from .0001 - .001 Md with overburden pressures of 1650 and 3700 PSI. This is very low permeability which limits the rate of gas production by the rate at which gas can diffuse through the matrix and reach a free surface such as a bore hole or a fracture. Compared with sandstones this results in low production rates, but extended production life. Clastic silt-size quartz and feldspar are commonly segregated into lenses parallel to bedding in the very dark, organic-rich shale specimens. Higher permeability in such lenses may permit migration through such silt zones to accumulation fracture facies areas.

Mineral lined vertical fractures were commonly noted in the pay zones of two wells in western and southwestern West Virginia. In one core from western West Virginia filled and unfilled natural fractures resemble parts of nearly vertical systematic joints (Wheeler, et al., 1976). The fractures strike N 40° - 50° E above the pay zone, and show four dominant orientations within the pay zone. As noted earlier a higher percentage of total production appears to be the result of absorbed (matrix) and adsorbed (on fracture surfaces) than from free gas. Wheeler, et al. suggest that fracture density on a larger scale may be influenced by old or reactivated suballochthon faults, by allochthony itself, by erosional release, or by two or more of these factors interacting. They further suggest slickensides can seal fractures and thus decrease permeability.

Rogers (1971) concludes from stratigraphic evidence that after a period of extensional tectonics accompanying the main subsidence, a period of true compression ensued in late Mississippian to early Permian time during which the final group of clastic sediments were deposited and the whole section deformed.

The outline of Brown shale production in West Virginia coincides strikingly with the trend of the Rome Trough. Martin and Nuckols (1976) postulated that fractures in the Devonian shales in the gas-producing areas result from reactivated movement of the basement fault blocks comprising the Rome Trough. Weaver, 1972, noted the relationship of the structure to Devonian gas production. The basement structure and magnetic intensity values in the Cottageville area (Shumaker, 1978) show the magnetic intensity contours are closely correlated with the edge of the Rome Trough which comprises a valley rift system on the Precambrian basement level. It is reasonable to assume that fracture facies developed over fault movements associated with the Rome Trough structure.

The term fracture facies is proposed for use in certain Devonian shales with the following definition of the term: rock facies containing fractures that occur over a wide area within a distinct stratigraphic interval. As applied to Cottageville field, the image conveyed is similar to a stratigraphic trap - but one where the porosity is caused by laterally limited fracture porosity with a distinct stratigraphic interval.

Data

Production data has been used as given. No standardization or altering of the data has been attempted. The complete data analysis includes mapping of production data in various relationships and decline curve analysis by computer programs and historical relationships. The comparison of production data map trends to trends of geological factors is presented here. This study includes trends from the following maps: (Figures and complete study available in MERC Technical Series Publication MERC/CR/78/6 July, 1978.)

Drilling Completion Dates,
Isocontours of Highest Annual Production (1st or 2nd year production),
Isocontours of First Five Years Accumulated Gas Production,
Isocontours of Total Accumulated Production,
Isocontours of Mean Annual Gas Production,
Loss Ratio Isocontours for First Year of Gas Production Decline,
Loss Ratio Isocontours for Second Year of Gas Production Decline,
Loss Ratio Isocontours for Third Year of Gas Production Decline,
Loss Ratio Isocontours for Gas Production Decline from 1st to 5th Year of Production,
Structure Contours on Top of the Onondaga,
Structure Contours on the Bottom of the Huron Shales,
Isopressure Contours of Initial Well Pressures,
Fracture Facies Orientation, and Devonian Shale Dip and Strike.

Gas production data was tabulated by year. From this tabulation the highest annual production, accumulated total production, first five years accumulated production, and mean production are computed. Most of these computations are fairly standard procedure, however, loss ratios may be unfamiliar. Loss ratios (Arps, 1944; Campbell, 1973) are computed in this study as follows:

$$d = \frac{q_1 - q_2}{q_1}$$

where: d = fraction or percent production lost

$q_1 - q_2$ = The gas production for the first year considered less the gas production for the second year considered.

q_1 = The gas production for the first year considered.

The resultant value represents the slant of the gas production decline curve for the period under consideration. Loss ratio values are computed for 1-2 years, 2-3 years, 3-4 years, and 1-5 years.

Structure contour maps are shown for the top of the Onondaga below the Devonian shales and for the structure at the bottom of the Huron shales which overlie the producing Devonian shales. The trend strike of the Devonian shale isopachs (N 6° E) is also used in the map comparison.

Isopressure contours are drawn on the initial pressure data obtained following well completion. No adjustment of pressure data to standardize these data has been attempted.

DISCUSSION AND CONCLUSIONS

Erwin, et al. (1976) described the problem of the Devonian shales as the nature, cause, timing of fractures, relation to regional stress and structural patterns below, within, and above the Devonian shales. This pilot study of gas production analysis methods applied to a portion of the Cottageville Field is an attempt to look at these relationships in terms of axial trends to examine what correlations may exist. Highest annual production could be indicative of porosity, fractures (permeability), gas entrapment, migration, and possibly connection with other wells (when compared with chronology of drilling). First five years total accumulation may represent aspects of permeability, total gas reserves, and gas pressures. Total accumulation should reflect all the factors related to first five year production plus a stronger indication of permeability, and reserves. Mean of Total Accumulation may show a field porosity trend and permeability interrelationship of wells. This may be one of the better indicators of reserves. Loss Ratio maps are related to permeability, pressure, and supply.

The production data, calculated production decline, and geological data computed for each well is contoured on a series of maps. The trends of the contour axes on each map are traced onto a common overlay and these trends are tabled according to correlation of trend angle with other sections of the study area. For a comparison of major map trends of the geology, production, and production decline, the trends are plotted on a compass rose in Figure 12. It can be observed that the angular relationship is very restricted and not a broad interval. The strike of the basement magnetic survey trends relate to the first five years cumulative production and initial pressure. The dip again relates to initial pressure as well as production decline the 1-2 years. These relationships suggest the basement affects collection and availability of free gas as compared with adsorbed or absorbed gas.

The strike of structure on the top of the Onondaga limestone relates to highest annual production, first five years cumulative production, total production and the fracture facies direction (40-50° NE) of 80% of fractures in the Baler well above the gas zone and 21% in the production zone. The dip of the Onondaga relates to total production, mean annual production, and initial gas pressure. The top of this more brittle rock, as compared with shale, may represent the lower control, which reflects the basement, on the formation of fracture facies. Differential compaction of the shales over basement structures and faults may be the causal agent in fracture facies formation.

The strike on the bottom of the Huron shales relates to production decline trends both for the 3-4 years and 1-5 years. The dip relates to total production, mean annual production and initial pressure. The production decline trend for 2-3 years is also very close. The difference is possibly due to structure anomalies. Thus, the structure on the bottom of the Huron appears to affect permeability, as reflected in the slope of production decline curves.

The fracture facies orientations taken from the CGSC #11940 well in Jackson County (Larese and Heald, 1977) show three predominant directions. The main direction is 40-50° NE and relates to five production maps: highest annual production, first five years production, total production, mean annual production, and initial pressure. This strike direction is also related to strike of the top of the Onondaga limestone and to the production decline map 1-2 years. Thus, the major fracture facies direction is strongly correlated with free gas accumulation and availability, and this trend is similar in its lower limits to the top of the Onondaga. This fact as mentioned above may relate to the genesis of the fractures.

Initial gas pressure it may be noted is related to all the geologic maps, suggesting that these different geological parameters may each play a role in accumulation and availability.

The highest degree of production relationships is seen with the top of the Onondaga limestone. Second is the fracture facies main trend, which in turn relates to the Onondaga.

The highest degree of production decline correlation is seen with the bottom of the Huron and close to it, which suggests that the structure at the base of the producing Devonian shales is somehow

influencing permeability. Differential compaction, and variations in silt and organic content could be related factors in paleoenvironment. Also the fact that the permeability, as reflected in decline curves, is related to strike on the bottom of the Huron, suggests that permeability differences may occur along strike onlap of beds onto the craton during the time of deposition. These various suggested relationships point to the importance of studying paleoenvironments of these stratigraphic units in projecting gas resources.

Application of this type of analysis and suggested relationships will be tested on the Eastern Kentucky Gas Field, which is presently under study.

ACKNOWLEDGEMENT

REFERENCES

Arps, J. J., 1944, Analysis of Decline Curves, Petroleum Technology, September, pp. 126-135.

Bagnall, W. D., and Ryan, W. M., 1976, The Geology, Reserves, and Production Characteristics of the Devonian Shale in Southwestern West Virginia, in Devonian Shale Production and Potential, MERC/SP-76/2, ERDA Morgantown Energy Research Center, Morgantown, West Virginia 26505.

Campbell, J. M., 1973, Decline Curve Analysis, Chapter 9 in Petroleum Reservoir Property Evaluation, published by John M. Campbell, 121 Collier Drive, Norman, Oklahoma 73069, pp. 204-233.

de Wys, J. Negus, and R. C. Shumaker, 1977, Pilot Study of Gas Production Analysis Methods Applied to Cottageville Field, West Virginia University, Geology Department, Morgantown Energy Research Center Publication No. MERC/CR/78/6, July 1978.

Erwin, R. B., Woodfork, L. D., Patchen, D. G., Larese, R. E., Renton, J. J., Behling, M. C., Schwietering, J. F., Neal, D. W., Vinopal, R. J., Duffield, S. L., (1976) Characterization of the Devonian Shales.

Foster, John C., 1977, A new gas supply - Devonian shales, the Oil and Gas Journal, January 3, pp. 100-101.

Larese, R. E., and M. T. Heald, 1977, Petrography of selected Devonian shale core samples from the CGTC 20403 and CGSC 11940 wells, Lincoln and Jackson Counties, West Virginia, MERC/CR-77/6.

Marten, P., and Nuckols, E. B., 1976, Geology and oil and gas occurrence in the Devonian shales: northern West Virginia, in Devonian shale production and potential: Proceedings of the 7th Appalachian Petroleum Geology Symposium, MERC/SP-76/2, ERDA, Morgantown, W. Va., pp. 20-40.

Patchen, Douglas G. and Larese, R. E., 1976, Stratigraphy and Petrology of the Devonian "Brown" Shale in West Virginia in Devonian Shale Production and Potential, edited by R. C. Shumaker and W. K. Overbey, Jr., MERC/SP-76/2, ERDA Morgantown Energy Research Center, Morgantown, West Virginia 26505.

Patchen, Douglas G., 1977, Subsurface Stratigraphy and Gas Production of the Devonian Shales in West Virginia, ERDA Morgantown Energy Research Center, Morgantown, West Virginia 26505, MERC/CR-77/5.

Rodgus, John, 1971 Evolution of Thought on Structure of Middle and Southern Appalachians: Second Paper, in Appalachian Structures Origin Evolution, and Possible Potential for New Exploration Frontiers, A Seminar, W. Va. Univ. and W. Va. Geological and Economic Survey, 1972.

Science Applications, Inc., 1977, A Special Publication on Enhanced Gas Recovery from Shales, MERC/SP-77/3.

Selin, M. A., 1976, Methods of Reserve Estimation, presented at Devonian Symposium 1976 in Morgantow
    Morgantown, West Virginia. Author with H. J. Gruy Associates, 2501 Cedar Spring Rd., Dallas,
    Texas 75201.

Weaver, O. D., Calvert, W. L., McQuire, W. H., 1972, Gas and Oil potential of Appalachian basin,
    Oil and Gas Journal, January.

Wheeler, R. L., Shumaker, R. C., Woodfork, L. D. and Overbey, W. K., Jr., 1976. Gas from Devonian
    Shales, _Geotimes_ 21:10, pp. 18-19.

EXPLORATION PARAMETERS DERIVED FROM
HISTORICAL DEVONIAN SHALE PRODUCTION IN WESTERN WEST VIRGINIA

by

E. B. Nuckols III, Research Associate
Devonian Shale Program
Department of Geology and Geography
West Virginia University
305 White Hall
Morgantown, West Virginia 26505

ABOUT THE AUTHOR

Mr. Nuckols received his BS degree in Geology (1970) from Virginia Polytechnic Institute and State
University. From 1970 to 1975 he was a staff geologist with the Virginia Division of Mineral
Resources in Charlottesville, Virginia where he worked in the Piedmont, Blue Ridge and Valley and
Ridge provinces of Virginia. In 1975 he joined the staff of Consolidated Gas Supply Corporation in
Clarksburg, West Virginia as an exploration geologist. In early 1977 he left Consolidated Gas to
pursue graduate studies at West Virginia University where he was a Research Associate under a
Department of Energy Contract. Also in 1977 he joined the staff of TRW Energy Systems as a systems
engineer involved in various Department of Energy contracts.

ABSTRACT

Successful application of exploration parameters to "tight" Devonian organic shales can be formulated from prior development of Devonian shale gas fields. One such field, the Cottageville Gas Field in western West Virginia, has been producing for almost 50 years. A random exploration rationale implemented in this field has produced less than optimal results in maximizing gas production. However, from a detailed analysis of development history and geologic variables, a Devonian shale exploration rationale using critical exploration parameters can be derived. These parameters are as follows:

Stratigraphic Parameters

- To maximize the potential for gas production, the existence of several organic shale zones is required.

- Regional shale gas producing horizons should be evaluated with the goal of obtaining maximum producing shale thickness.

- Geochemical composition and thermal maturity are important factors which must be considered in exploration.

Structural Parameters

- Fracturing resulting from basement movement.

- Folding or faulting causing structural disruption (i.e. fracturing) of rock units.

- Surface fracturing, principal stress directions and subsurface fracturing are direct indicators of potential Devonian shale gas production.

INTRODUCTION

The Cottageville Devonian Shale Gas Field lies in the western portion of the Appalachian Basin near the West Virginia - Ohio border in the West Virginia counties of Jackson and Mason (Figure 1). Hydrocarbon production (mostly natural gas) from this field originates from organic shale zones found within the Middle Devonian Lower Huron Shale Member of the Ohio Shale Formation. Drilling activity within this gas field since the late 1920's has seen the completion of 110 shale wells with production of more than 10 Billion cubic feet of natural gas (Figure 2). Delineation of production parameters that have controlled the accumulation and production of these hydrocarbon follows.

Stratigraphic Parameters

The Devonian age formations that underlie the Cottageville Gas Field are approximately 2,300 feet thick. The middle and upper Devonian shales comprise the upper 2,100 feet of the total section. The upper contact of the Devonian shales is placed at the base of the Mississippian Age Berea Sandstone, and the lower contact is with the Onondaga Limestone. Within this predominantly shale section, are found light grey to brown-black shales, light to medium grey siltstones and very rarely white to light grey sandstones. Of these different lithologies, the dark organic rich shale zones occupy approximately 500 feet or 23 percent of the entire shale section. These highly organic shale zones occur in three stratigraphically distinct portions of the shale section, and they are easily recognizable on gamma-ray and density logs (Figure 3). The upper two organic zones (Zones II and III) are found within the Lower Huron Shale Member of the Ohio Shale Formation. These two zones are mainly composed of dark brown-black organic rich shales, but occasionally they have light to medium grey shale and siltstone interbeds. Separating the lower and upper organic rich shale zones of the Huron are lithologies of shale and siltstone with an occassional thin organic shale bed. Within the Cottageville Gas Field, these two zones have an average combined thickness of 250 feet, and they the main reservoirs of Devonian shale gas production. Below these two organic zones found in the Huron is a third organic zone found in the Westfalls Formation. Like the younger shales found in the Huron Shale, this organic rich shale has interbeds of light to medium grey shale and siltstones. This organic rich shale has an average thickness of 100 feet, but has rarely produced any gas within the Cottageville area.

Regional east-west correlations of the Devonian shale sequence (Figure 4) indicate the absence of deposition of the Huron organic rich shale zones just to the east of the Cottageville field. The gradual facies change of the organic shales to the east seems to coincide with the western edge of
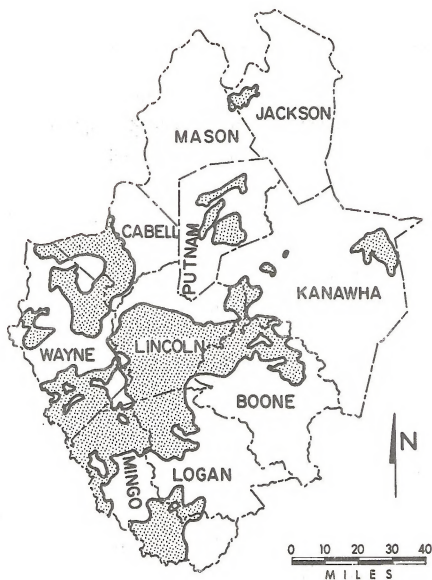
Figure 1 Gas fields with production from the Brown shale in southwestern West Virginia. Production extends northward from Cabell County into Ohio, and southwestward from Wayne and Mingo Counties into the Big Sandy Field, eastern Kentucky.(after Patchen, 1977).

413.
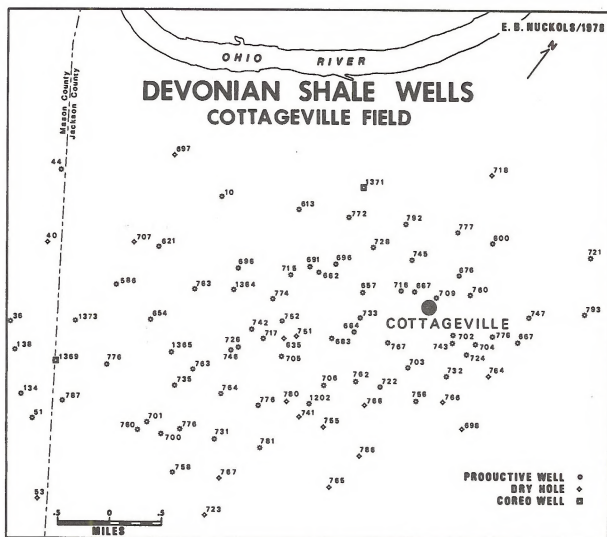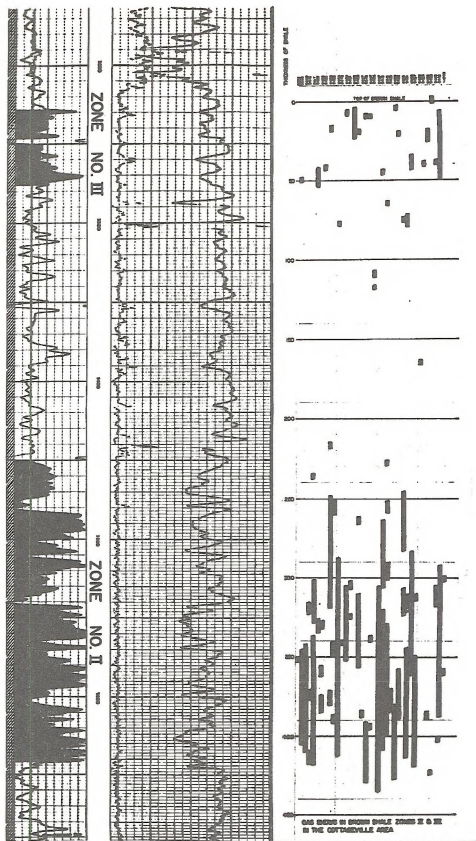
FIGURE 2

Figure 3 – Gamma ray log portraying organic rich shale zones of the Lower Huron Shale Member of the Ohio Shale with gas shows from 37 wells drilled within the Cottageville Field (after Martin and Nuckols, 1976).

CONSOLIDATED GAS SUPPLY CORPORATION

CROSS SECTION A-A'
SHOWING
DEVONIAN BROWN SHALE CORRELATIONS
IN
CENTRAL & WESTERN
WEST VIRGINIA

FIGURE 4
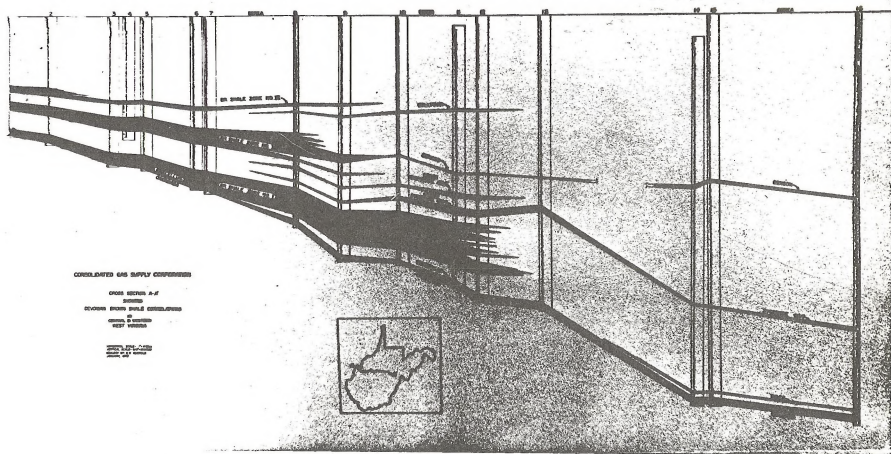
the Rome Trough, thereby indicating a change in the depositional environment.

The following stratigraphic exploration parameters must be satisfied if potential gas production is to be economically realized:

- To maximize the potential for gas production, the existence of several organic rich shale zones is required. The Cottageville Gas Field as seen on Figure 4 is located approximately where logs 3, 4 and 5 occur. Since the organic rich shale zones of the Lower Huron are the primary producer of natural gas in this region, the gas field is located strategically close to where the organic shale lithologies disappear to the east (into the Rome Trough). Therefore it is fortuitous that the gas field is located proximal to the maximum thickness of organic rich shales before they disappear.

- Regional shale gas producing horizons should be evaulated with the goal of obtaining maximum producing shale thickness. Gas production from the Cottageville area has primarily been associated with Zone II organic shales within the Lower Huron Shale Member (Figure 5). In addition gas shows within the field have predominantly been associated with Zone II organic shales (Figure 3).

- Geochemical composition and thermal maturity are also important factors which must be considered in exploration. A statistical zonation analysis of the Jackson - 1369 core (Figure 2) revealed that Zone II of the Lower Huron Shale Member of the Ohio Shale had a lower average porosity (2.93%); higher average residual oil saturation (7.31%); lower average residual water saturation; and lower average grain density (2.64 grams/cc) than either organic Zone III shales or the shale interval between Zone's II and III$_1$.

  An evaulation of the thermal maturity of The Lower Huron Shale Member was performed on cored Wells Jackson 1369 and 1371 (Figure 2). The results of these analysis are$_2$:

  Oil Prone
  - The amorphous-herbaceous kerogen is the predominant type of organic matter.

  Moderately Mature
  - The kerogen coloration ranges from 2 to 2+ and the vitrinite reflectance values range from 0.8 to 1.10% R_o.
  - The thermal history places the organic matter in the early to middle stages of petroleum generation.

  Extremely Variable in Organic Richness
  - The organic carbon content ranges from 0.24% to 3.12%.

Structural Parameters
- Fracturing resulting from basement movement.

  A mega structural feature that is proximal to the Cottageville Field is the Rome Trough (Figure 6), which comprises a valley rift system on the Pre-Cambrian basement. This Cambrian age feature has influenced, in all likelihood, sedimentation and structural regimes from early Cambrian time up to Silurian and possibly through Devonian time. The western boundary of this feature may consist of en echelon faults that may have been reactivated throughout time, thus causing warping and fracturing of overlying sediments. Figure 7 shows the basement structure based on magnetic intensity values for the Cottageville area (Shumaker, 1978). The basement contours are closely correlated with the edge of the Rome Trough and give an appearance of en echelon blocks that step-up to the west. Martin and Nuckols (1976) postulated that fractures in the Devonian shales in the Cottageville gas-producing areas result from reactivation movement of the basement fault blocks comprising the trough.

1. Analysis performed by Lamey, Biabolok and Childers (1978).
2. Analysis performed by Geochem Laboratories, Inc.

ISOPACH
ZONE II - LOWER HURON

E. B. NUCKOLS/1978

CONTOUR INTERVAL: 10 FT
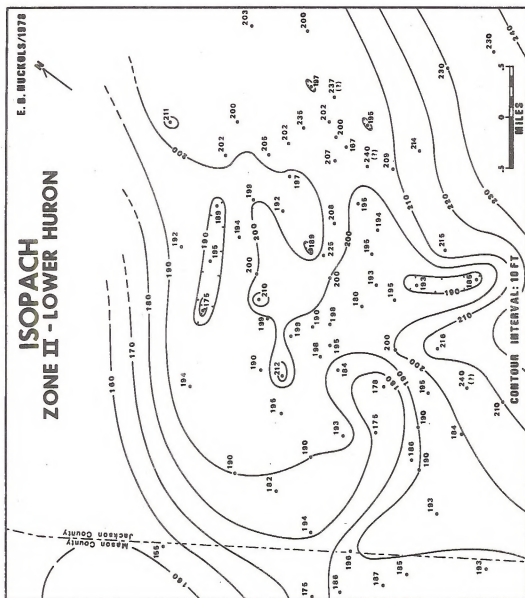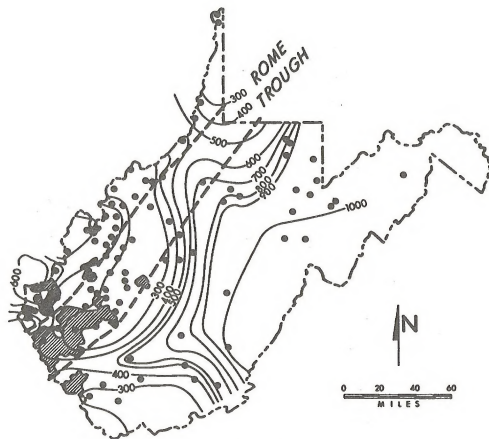
FIGURE 5

Figure 6   Brown shale gas fields, thickness of Brown shales (from deWitt, et al, 1975), and approximate position of the Rome Trough in West Virginia. Thick areas of dark organic-rich shale that overlie this Cambrian fault block may be the area of greatest potential for new exploration (after Patchen, 1977).
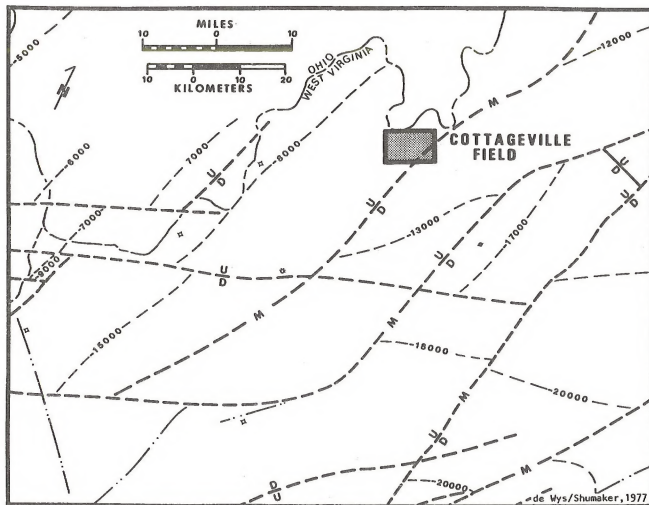
FIGURE 7— Cottageville Field Setting in Relationship to Basement Structures and Magnetic Intensity Contours.

FIGURE 8

STRUCTURE
BOTTOM OF LOWER HURON

E. B. NUCKOLS/1978

CONTOUR INTERVAL: 10 FT

MILES
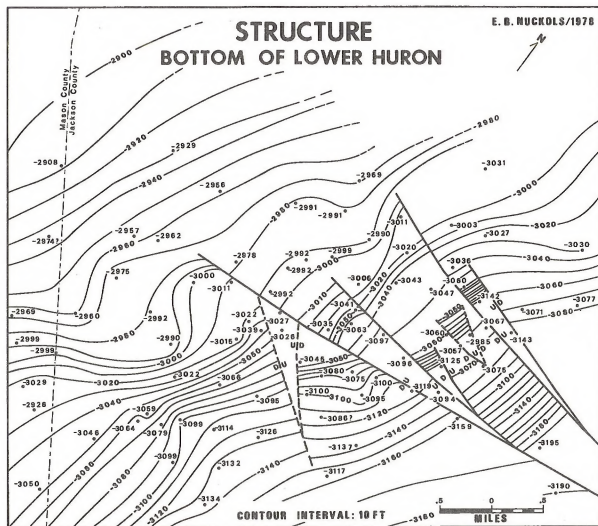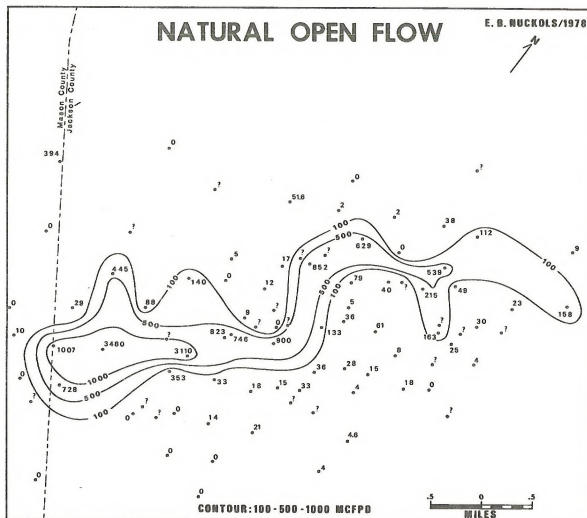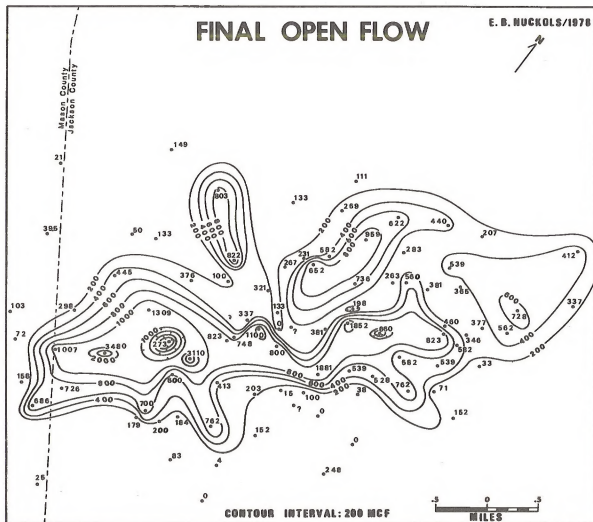
FIGURE 9

FIGURE 10

FIGURE 11

WELL HEAD PRESSURE DECLINE
Cottageville Field
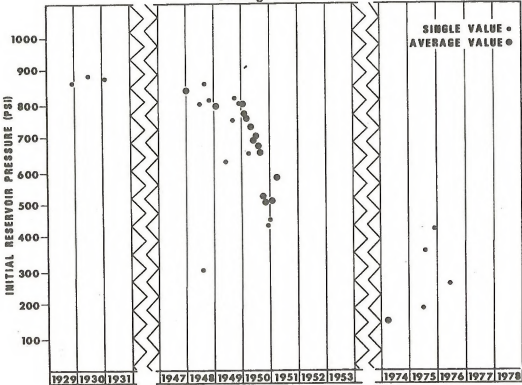
FIGURE 12

● Folding and/or faulting causing structural disruptions (fracturing) of rock units. Structural anomalies and disruptions are the main mechanisms for gas production in the Devonian Shales. Within certain areas of the Gas Field "bench-like" or "hinge-like" structural features can be discerned. These features appear as stair-step like features on structural cross sections and could possibly be the last remnents of basement associated en echelon faults of the west flank of the Rome Trough (Figures 8 and 9). In addition to this structural feature are the multiple cross faults that have created other fracture systems (Figures 8 and 9).

A direct consequence of these fracturing mechanisms can be exhibited in Natural Open Gas Flows (Figure 10) and Final Open Gas Flows (wells that have been stimulated – Figure 11). Another effect of fractures and faults upon the organic shale reservoir rock is the reservoir pressure decline after years of infield drilling. This can easily be illustrated by graphically plotting initial reservoir pressures against the year in which the wells were drilled (Figure 12). As displayed graphically in Cottageville, the shale reservoir appears to be somewhat pressure depleated after 1942 (Figure 12); i.e. fracture systems.

● Surface fracturing, principal stress directions and subsurface fracturing play key roles as direct indicators of potential shale gas production. Surface joint measurements in the Mt. Alto and Cottageville 7½ minute quadrangle, primary stress directions from shallow core sites in the southern portion of the gas field, along with mineral lined fractures found in core well Jackson – 1369 all indicate three primary directions of potential fracturing:

| | DIRECTION | | |
	I	II	III
Surface Joints[3]	East – West	N – N 20° W	*N 50° – 60° W
Primary Stress Direction[4]	N 65° – 90° W(E–W)	N 10° W – N 15° E	N 40° – 60° E
Mineral Lined Fractures[5]	N 80° – 90° W(E–W)	N 10° – 20° W	N 40° – 50° E

From this data it is very apparent that surface fracture data (i.e. joints) can directly be correlated with subsurface fracture data.

REFERENCES

1. Bagnall, W. D., and Ryan, W. M., 1976, The geology, reserves, and production characteristics of the Devonian shale in southwestern West Virginia, in–Devonian shale production and potential: Proceedings of the 7th Appalachian Petroleum Geology Symposium, MERC/Sp–76/2, ERDA, Morgantown, W. Va., p. 41–53.

2. de Wys, J. Negus and Shumaker, R. C., 1978, Pilot Study of Gas Production Analysis Methods Applied to the Cottageville Field (in press).

3. E. D'Appolonia Consulting Engineers, Inc., 1976, Stress State Determinations in West Virginia and Kentucky – Baden Site, Technical report prepared for the Energy Research and Development Administration, Morgantown Energy Research Center, Morgantown, W. Va.

---

* From the original data a N 40° – 50° E set of joint data exists but has fewer data points that the N 50° – 60° W

3, 4 Analysis performed by E. D'Appolonia Consulting Engineers, Inc.

5 Analysis performed by Larese and Heald (1976).

4. Geochem Laboratories, Inc., 1976, Hydrocarbon Evaluation Study of Shales from Wells #R-109, #R041, and #11940, Technical report prepared for the Energy Research and Development Administration, Morgantown Energy Research Center, Morgantown, W. Va.

5. Lamey, Steven C., Bialobok, S. J., and Childers, E. E., 1978, Organic Composition of Devonian Shale Cores from Well #11940 and #12041, Cottageville, Jackson Co., West Virginia, METC/TPR, DOE, Morgantown, W. Va., p. 1-26.

6. Larese, Richard E., and Heald, Milton T., 1976, Petrography of Selected Devonian Shale Core Samples from the CGTC 20403 and CGSC 11940 Wells, Lincoln and Jackson Counties, West Virginia, MERC/CR-77/6, ERDA, Morgantown, W. Va.

7. Marten, P., and Nuckols, E. B., 1976, Geology and oil and gas occurrence in the Devonian Shales: northern West Virginia, in Devonian shale production and potential: Proceedings of the 7th Appalachian Petroleum Geology Symposium, MERC/SP-76/2, ERDA, Morgantown, W. Va., p. 20-40.

8. Nuckols, E. B., III, "Production Characteristics of Devonian Organic Shales in the Cottageville Field Near Ripley, West Virginia," paper presented in the First Eastern Gas Shale Symposium, sponsored by the Morgantown Energy Research Center, October 17-19, 1977, Morgantown, W. Va.

9. Patchen, D. G., and Larese, R. E., 1976, Stratigraphy and petrology of the Devonian "Brown" shale in West Virginia, in Devonian shale production and potential: Proceedings of the 7th Appalachian Petroleum Geology Symposium, MERC/SP-76/2, ERDA, Morgantown, W. Va., p. 4-19.

10. Patchen, Douglas G., 1977, Subsurface Stratigraphy and Gas Production of the Devonian Shales in West Virginia, ERDA Morgantown Energy Research Center, Morgantown, West Virginia, 26505, MERC/CR-77/5.

11. Wallace, Laure G., Roen, J. B., and de Witt, W. Jr., 1977, Preliminary Stratigraphic Cross Section Sharing Radioactive Zones in the Devonian Black Shales in the Western Part of the Appalachian Basin, Department of the Interior, United States Geological Survey, Oil and Gas Investigators.

APPENDIX E

Hydrology Data

Henry W. Rauch
D. Scott Jones
Robert R. Beebe

LINEAMENTS AND GROUND-WATER QUALITY AS EXPLORATION TOOLS FOR GROUND

WATER AND GAS IN THE COTTAGEVILLE AREA OF WESTERN WEST VIRGINIA

by

D. Scott Jones
and
Dr. Henry W. Rauch

ABOUT THE AUTHORS

Mr. Jones received his BA degree in Geology from Susquehanna University in 1976. He has been attending West Virginia University since 1976 and is working toward an MS degree in Geology. He is presently employed by the Pennsylvania Department of Environmental Resources – Division of Strip Mine Reclamation.

Dr. Rauch received his BA degree in Chemistry-Geology from Alfred University in 1965. He also received his Ph.D. degree in Geochemistry from The Pennsylvania State University in 1972. Since 1970 he has been employed by West Virginia University, Department of Geology and Geography, and is an Associate Professor of Geology. He is also a co-investigator on an Eastern Gas Shale Project contract at West Virginia University, which is funded by the U. S. Department of Energy. His primary research interests are in hydrogeology and geochemistry.

ABSTRACT

As part of a hydrogeologic study of west-central Jackson County, lineaments were mapped and water wells were characterized for physical and chemical parameters, especially in the Cottageville area. Short straight photolineaments are significantly associated with water well yields in gallons per minute, with wells closer than 100 feet having higher yields. Such lineaments act as anomalous zones about 200 feet in width with respect to water wells. Short photolineaments are not in general associated with gas well yield, but gas wells located within 0.5 miles of a short photolineament bearing N 60°W-N90°W (WNW) yield at significantly greater rates (as natural initial open flow) than wells near other photolineaments. The density of WNW photolineaments is also significantly and directly associated with gas well yield. Water well yield has no relationship to Landsat or curvilinear lineaments. However, gas wells located within 0.25 miles of one Landsat lineament or within 0.5 miles of a curvilinear lineament over one mile long yield at significantly lower rates. High concentrations of nitrate and sulfate, and especially of bicarbonate and total hardness in shallow ground water are significantly associated with high expected (interpolated) gas well yield. Tentative conclusions from sparce data indicate that gas well yield will be significantly higher when gas wells are located in areas having ground-water concentrations exceeding 500 mg/1, 250 mg/1, 13 mg/1, and 34 mg/1 for bicarbonate, total hardness, nitrate, and sulfate respectively. In summary, short photolineaments make a good exploration tool for locating water wells; both WNW photolineament density and ground water quality may serve new exploration techniques for Devonian shale gas in the Cottageville, but Landsat and curvilinear lineaments should be avoided.

INTRODUCTION

A hydrogeologic investigation in the Cottageville area of Jackson County, West Virginia, was undertaken in part to explore the possibility of relating hydrogeology and aqueous geochemistry to the occurrence of Devonian shale gas. Any relationships established between near-surface hydrogeologic or geochemical parameters and gas yield would be useful in developing additional exploration techniques for Devonian shale gas.

Figure 1 depicts the study areas. The first phase of this study involved the investigation of 86 water wells and one spring in the hydrogeology study area.[1] Physical well parameters such as well depth, depth to water, well yield, and casing depth were obtained from well owners and drillers. The topographic setting and most probable aquifer unit were determined with the aid of topographic maps, a structural contour map of the Pittsburgh Coal, and a general stratigraphic column for the study area.

Short photolineaments were also mapped for the hydrogeologic study area from low altitude black and white photography having scales of 1:20,000 and 1:38,000. The photolineaments represent nearly straight stream channel or valley segments over 0.25 miles in length (but usually less than one mile long). These were identified and plotted on 7 1/2 minute topographic maps for the study area.[1] Also identified and plotted were a few Landsat lineaments defined by straight stream or valley sections or aligned stream meander bends. A third type of lineament is the curvilinear type. These lineaments are generally at least one mile in length and are defined by continuously curved valleys or streams which lack inflection points in their general curvature. They were determined from and plotted on the 7 1/2 minute topographic maps.

Water quality tests were also performed for 86 wells and one spring.[1] Temperature and specific conductance were measured in the field, and two water samples were taken from each well. One sample was treated with acid and later analyzed in the laboratory for iron, calcium, and magnesium concentrations. The second sample was treated with a biocidal agent which also retarded algae growth, and was kept cool until chemical analyses for pH, bicarbonate, nitrate, sulfate, chloride, and sodium could be performed in the laboratory.

PHOTOLINEAMENT ASSOCIATIONS

Mapped lineaments for the gas field study area are shown in Figure 2. Several short photolineaments, five curvilinear lineaments, and one Landsat lineament are evident in this area. Water well yield (in gallons per minute) was tested as a function of well proximity to each of the three types of mapped lineaments for the entire hydrogeology study area (see Figure 1).

Water wells located within 100 feet of a short photolineament yield water at significantly greater rates than more distant wells. This difference is significant with a 0.06 probability of error (probability that there is no significant difference between two groups of tested data), by the

Mann Whitney U (1-tailed) statistical test.[2] Of those wells within 100 feet of a short photolineament, wells within 50 feet yield water at significantly greater water (about 50 percent greater) than wells 50-100 feet from such a lineament. This difference is significant with a 0.05 error probability by the Mann Whitney U test. These trends in well yield were expected and have been well documented by Lattman and Parizek as well as other researchers.[3] Apparently, short photolineaments often represent underlying fracture zones which are associated with significantly increased aquifer permeability. Hence water wells located on photolineaments usually have higher-than-average yields. The probable fracture zones under photolineaments of the study area are roughly 200 feet in width.

Landsat and curvilinear lineaments seem to have no definite relationships with water well yield. No significant associations were found between water well yield and well proximity to either Landsat or curvilinear lineaments, based on the Mann Whitney U test. Landsat lineaments (and other lineaments from high altitude imagery) mapped by Werner were tested in addition to those few Landsat lineaments mapped by the authors.[4] Water wells near the curvilinear lineaments produced at about the same rate as wells in other valleys. Whatever the reason for these non-associations, Landsat and curvilinear lineaments are both distinctly different from short photolineaments in both appearance and effects.

Gas well yield was next tested for possible associations with mapped lineaments in the gas field study area (see Figures 1 and 2). Figure 2 shows the locations of Devonian shale gas wells both within and surrounding the Cottageville gas field. Only depicted are those wells for which natural initial open flows are known (E. B. Nuckols III, personal communication, 1978). Natural initial open flow was judged to be the most reliable gas production variable representing relative gas reservoir and gas well potential. Therefore, only this variable was used in statistical tests of lineament associations. Significant research on gas well production trends and associations is reported by several researchers.[4,5,6,7,8,9]

Considering short photolineaments of Figure 2 first, there is no apparent relationship between natural open flow and the proximity of gas wells to short photolineaments. No significant flow difference exists (by the Mann Whitney U test) between gas wells within 0.5 miles and gas wells greater than 0.5 miles from a short photolineament. Natural open flow likewise does not change significantly for wells between 0.0 and 0.5 miles of a photolineament.

However, when short photolineament orientation is taken into account, it is evident from Figure 3 that natural open flow varies with the orientation of nearby photolineaments. Gas wells within 0.5 miles of short photolinraments bearing N 60°W to N 90°W, or WNW, have a greater proportion of high-yielding gas wells (over 100 MCF/day) than do gas wells within 0.5 miles of other short photolineaments. This difference is significant by the 2X2 Fisher contigency test, with an error probability of 0.03. Furthermore, Figure 3 indicated that gas wells within 0.5 miles of short photolineaments oriented N 75°E to N 90°E are relatively high producers, on average. Combining this class of gas wells with the WNW class produces a combined class within 0.5 miles of photolineaments bearing N 60°W to N 105°W, which has the maximum potential for high-yielding gas wells. A 2X2 chi-square contingency test comparison of this enlarged well class with other wells shows a significant difference at the 0.05 alpha probability.

Although WNW-bearing photolineaments have a significantly great proportion of high-yielding gas wells in their vicinity, a more direct test of such photolineaments was necessary to determine their usefulness as an exploration tool. The density of WNW photolineaments is compared to contoured trends for natural initial open flow in Figure 4. The 100 and 500 MCF/day contours for natural open flow were plotted assuming that the changes in gas flow rate would be linear between adjacent gas wells. These contours are partly a function of the density of gas wells; contours in areas with low gas well densities, such as the northwestern extension of the 100 MCF/day contour, are probably overly optimistic in their prediction of shale gas reserves. These contours therefore represent a liberally depicted version of the Cottageville gas field.

The density of plotted WNW photolineaments was calculated from Figure 2 by use of a moving average technique and an orthogonal grid of lines defining square sections. The grid was oriented parallel to the north-south and east-west directions, and had sections that were 0.5 miles long on each side. The WNW photolineament density was calculated for 1.0 square mile sections by the moving average technique, and was plotted at the center of each square mile section. This density was then contoured. Figure 4 illustrates WNW photolineament density contours of 1.0 mile length per square mile area, and of 50 percent by total length per square mile area. The highest WNW photolineament densities occur inside the depicted contours and within the Cottageville gas field.

Chi-square contingency (2X2) tests were then performed on the moving average data for WNW photo-lineaments. Eighty one sample points were classified in two 2X2 tests for each density variable. One test compared greater-than-100 MCF/day with less-than-100 MCF/day points, and the second test compared greater-than-500 MCF/day with less-than-500 MCF/day points. The statistical test results indicate that WNW photolineament density (both as miles length per square mile area and as percentage of lineament lenght per square mile) is significantly associated with both the greater-than-100 MCF/day and greater-than-500 MCF/day contoured areas of Figure 4, at alpha probability values ranging from 0.02 to 0.001. However, these tests are biased because the 81 tested points are not mutually independent samples, since they were generated by the moving average technique.

Therefore, a second set of contingency tests were performed on the four sets of independent 1.0 mile square sections that define the 81 points tested above. First, the number of tested points was increased from 20 to 80 by multiplying each box of the 2X2 contingency tables by 4. This step had the effect of increasing the sample frequencies to a hypothetical number of independent sample points which were about equal to the 81 non-independent points tested initially. This action was taken to overcome the biasing effect of 2X2 contingency tests against statistical significance for a low number of samples. The net result of these test sets was that at least 3 out of 4 tests of independent sample points were significant at a 0.05 or lower alpha probability, for associations between WNW photolineament density and gas well yield areas from Figure 4. Therefore, the association of high WNW photolineament density and high gas production areas (either greater-than-100 MCF/day or greater-than-500 MCF/day) is considered significant by the authors.

The WNW photolineament density could serve as the basis of a new exploration tool for Devonian shale gas in the Cottageville area. Figure 4 shows that if gas wells are located within areas having densities greater than 1.0 mile per square mile, about 75 percent of these wells would have natural open flows exceeding 100 MCF/day, and about 50 percent of these wells would have flows exceeding 500 MCF/day. When gas wells are located in areas with more than 50 percent of photolineaments bearing WNW per square mile, about 62 percent of the wells would have natural open flows exceeding 100 MCF/day and about 38 percent would exceed 500 MCF/day.

Statistical tests were also performed on gas well yield as a function of WNW photolineament densities of less-than-0.50 versus greater-than-0.50 miles length per square mile. The associations are again significant at the 0.05 alpha probability, but using the area within the 0.50 density contour (not shown in Figure 4) would not prove as successful as the area within the 1.0 density contour for gas exploration. Testing of gas wells within 0.5 miles of short photolineaments bearing N 60°W-N 105°W yielded similar results to those already described for the WNW photolineaments. However, the density of photolineaments in the enlarged orientation class do not associate quite as well with gas production rate as the WNW photolineaments previously described.

An explanation of the associations between WNW photolineaments and gas yield must involve the subsurface geologic structure represented by these photolineaments. It is reported that a major fracture orientation exists in the east-west direction in the Cottageville gas field, based on surface outcrop and core data.[8] Increased gas reservoir permeability, along fractures oriented approximately east-west, is probably a major cause for the high gas yields in the Cottageville field. A more extensive structural analysis of gas trends is given by Nuckols.[8]

Both Landsat and curvilinear lineaments were also tested against gas well yield for the gas field study area. The one Landsat lineament along Mill Creek appears to have a negative effect on gas production, as shown in Figure 4. Natural open flow is lower for gas wells located within 0.25 miles of this lineament than for wells 0.25 to 0.50 miles distant. This relationship is significant at the 0.05 alpha probability level by the Mann Whitney U test, but not by the contingency test. This result supports the conclusion of Werner, that Landsat lineaments appear to be detrimental to gas production in the Cottageville area.[4,5] A test of curvilinear lineaments shows gas yield to be significantly lower for gas wells located within 0.5 miles of such lineaments than for more distant wells. This difference is significant for a 0.01 alpha probability by the Mann Whitney U test. Therefore, Landsat and curvilinear lineaments are to be avoided in exploring for Devonian shale gas, at least in the Cottageville area. Perhaps deeply penetrating fractures have bled off the shale gas under these lineaments, as suggested by Werner.[4,5]

GROUND WATER-GAS YIELD ASSOCIATIONS

Water well yield and well water quality were next compared to the yields of nearby gas wells in the gas field study area, to see if water well data could provide new exploration techniques for Devonian

shale gas. A hypothetical figure for expected gas well yield was generated by linear interpolation between the two gas wells nearest and on opposite sides of a water well or spring, for each of the 20 wells and one spring within the gas field area. Only one water well could not be assigned an expected gas yield value.

Results of plots and tests for water well (and spring) yield indicate that no apparent relationships exist between water yield (in gallons per minute) and expected natural open flow (in MCF/day).

Water quality parameters were next tested for possible associations with expected natural open flow. Figure 5 illustrates plots of concentration versus gas flow rate, for the four most promising parameters of those analyzed. The horizontal dashed lines on these four plots arbitrarily separate the gas yields into high and low classes, for comparison to concentration. Statistical tests, involving 2X2 contingency tables and the Fisher exact probability test, were used to identify any significant gas yield differences between high and low concentrations. Vertical lines were arbitrarily drawn to distinguish high from low concentration values. Although the data are sparce, statistically positive trends are evident from the statistical tests; expected gas yield tends to be higher near wells with high concentrations of bicarbonate, total hardness, nitrate, or sulfate. Test results are significant at the 0.007, 0.031, 0.079, and 0.094 error probabilities respectively, for bicarbonate, total hardness, nitrate, and sulfate. High concentration samples also show significantly higher gas yields then low concentration values, as determined by the Mann Whitney U test at the 0.05 alpha level. Other tested chemical parameters which did not significantly relate to expected gas yield are total iron, temperature, pH, chloride, and sodium.

The chemical parameters of ground water which seem to best relate to expected gas yield are bicarbonate and total hardness concentrations. These parameters show the strongest statistical associations which are least likely to be coincidental. These two ground water parameters may be applied with caution as exploration tools. From the tested data, about 83 percent of the selected well sites with over 500 mg/l bicarbonate have high expected gas open flows (over 100 MCF/day). An even higher percentage of wells with over 250 mg/l hardness would make good gas well sites, as defined above. These data suggest that some relationship exists between gas reservoir production potential and shallow ground water quality. However, the scarcity of data requires that these associations be considered tentative, until more water well information can be collected to further test the observed associations of Figure 5.

No explanations are apparent to the authors for the observed associations of ground water quality and expected natural open flow. Water wells with high concentrations of bicarbonate, total hardness, nitrate, or sulfate have no common factor in their hydrogeologic setting. These wells differ in aquifer type, well elevation, well depth, well bottom elevation, well yield, topographic setting, and lineament proximity.

REFERENCES

1. Jones, D. S., and Rauch, H. W.: "A Hydrologic Study of Water Well Yields and Ground-Water Quality Related to Stratigraphic and Structural Settings in Western Jackson County, West Virginia", a final project report on open file at the Morgantown Energy Technology Center, January, 1978.

2. Siegel, S.: "Nonparametric Statistics for Behavioral Sciences", McGraw-Hill, New York, 1956.

3. Lattman, L. H., and Parizek, R. R.: "Relationship between Fracture Traces and the Occurrence of Ground-Water in Carbonate Rocks", Jour. Hydrology, vol 2, 1964.

4. Werner, E.: "Application of Remote Sensing Studies to the Interpretation of Fracture Systems and Structural Styles in the Plateau Regions of Eastern Kentucky, Southwestern Virginia, and Southwestern West Virginia for Application to Fossil Fuel Extraction Processes" a final project report on open file at the Morgantown Energy Technology Center, December, 1977.

5. Werner, E.: "Interrelationships of Photolineaments, Geologic Structures, and Fracture Production of Natural Gas in the Appalachian Plateau of West Virginia", Proc. of Seventh Appalachian Petroleum Geology Symposium, Morgantown, West Virginia, March 1-4, 1976, Morgantown Energy Research Center.

6. Martin, P., and Nuckols, E. B.: "Geology and Oil and Gas Occurrence in the Devonian Shale of Northern West Virginia", Proc. of Seventh Appalachian Petroleum Geology Symposium, Morgantown, West Virginia, March 1-4. 1976, Morgantown Energy Research Center.

7. Nuckols, E. B.: "Production Characteristics of Devonian Organic Shales in the Cottageville Field near Ripley, West Virginia", Proc. of First Eastern Gas Shale Symposium, Morgantown, West Virginia, October 17-19, 1977, Morgantown Energy Research Center.

8. Nuckols, E. B.: "Exploration Parameters Derived from Historical Devonian Shale Production in Western West Virginia", Proc. of Second Eastern Gas Shale Symposium, Morgantown, West Virginia, October, 1978, Morgantown Energy Technology Center.

9. De Wys, J. N. and Shumaker, R. N.: "Pilot Study of Gas Production Analysis Methods Applied to the Cottageville Field", in press, Morgantown Energy Technology Center.
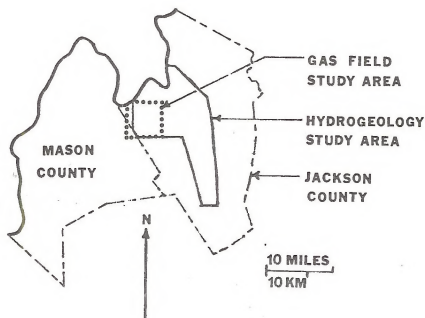
Fig. 1 – Location of study areas in West Virginia.
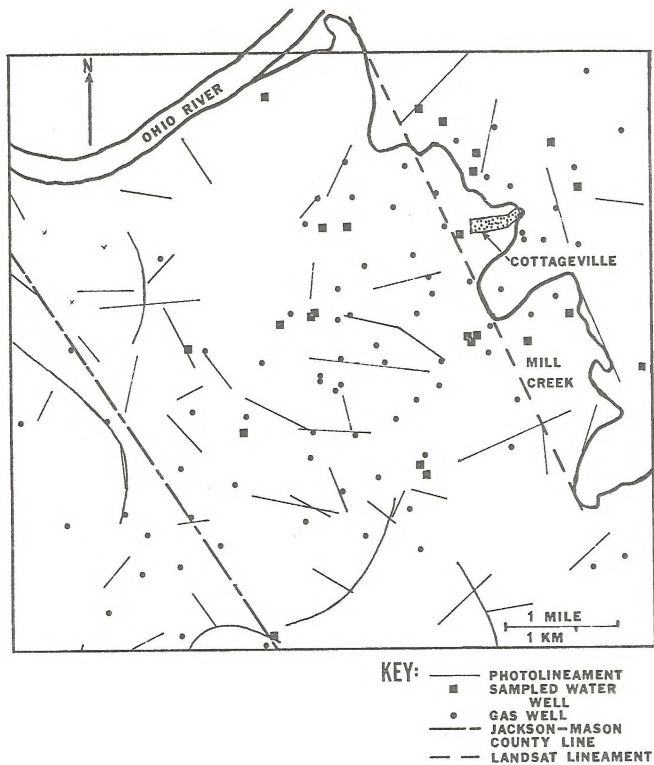
Fig. 2 - Map of gas field study area, near Cottageville.
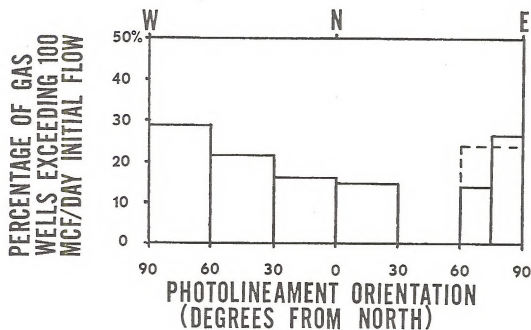
Fig. 3 - Gas well yield versus photolineament orientation.
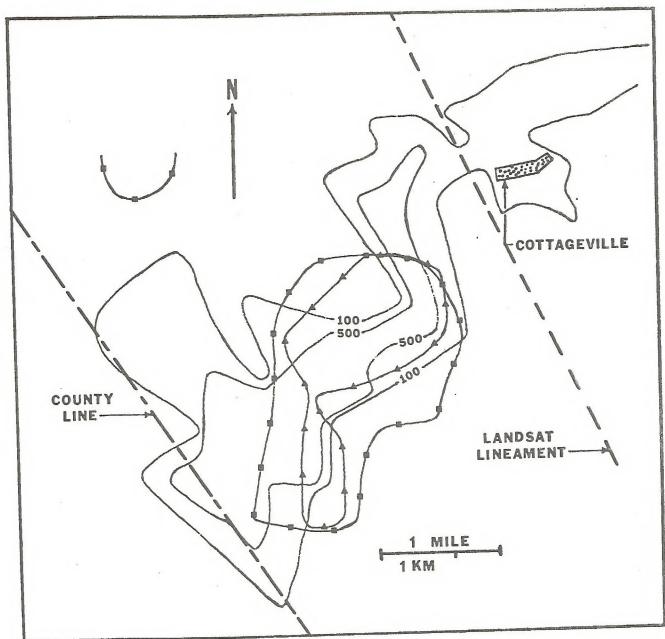
KEY: —₁₀₀–100 MCF/DAY CONTOUR FOR
INITIAL GAS FLOW
—₅₀₀–500 MCF/DAY CONTOUR FOR
INITIAL GAS FLOW
——▲——1 MI/MI² DENSITY CONTOUR
FOR SHORT PHOTOLINEAMENTS
BEARING N 60° W—N 90° W
——■——50% CONTOUR FOR PERCENTAGE
OF SHORT PHOTOLINEAMENTS
PER SQUARE MILE BEARING
N 60° W—N 90° W

Fig. 4 – Gas well yield related to photolineament density.
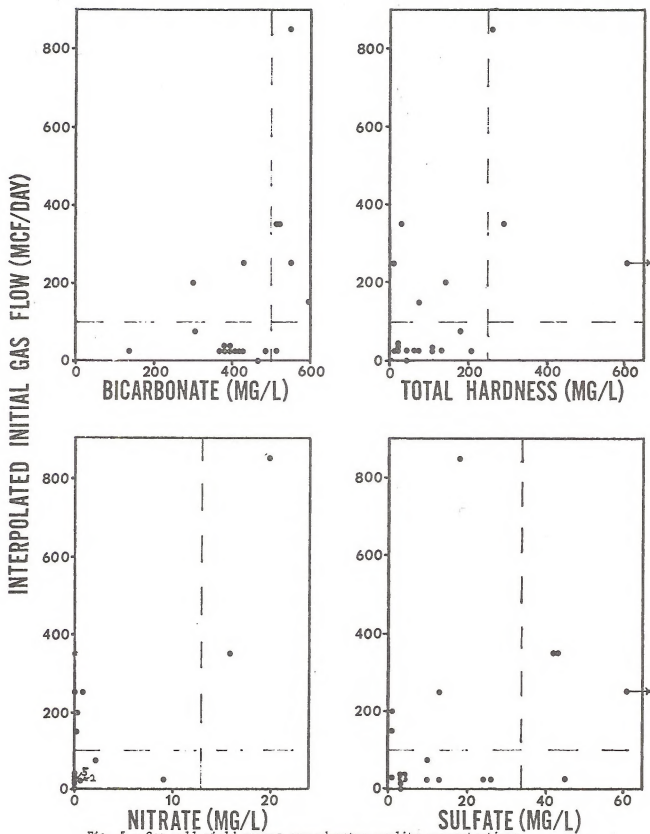
Fig. 5 - Gas well yield versus ground-water quality concentrations.

A STUDY OF HYDROGEOLOGIC TRENDS IN EXPLORATION

FOR DEVONIAN SHALE GAS IN THE MIDWAY-EXTRA GAS FIELD

OF PUTNAM COUNTY, WEST VIRGINIA

by

Robert R. Beebe
West Virginia University
Department of Geology and Geography
Morgantown, West Virginia 26506

1979

TABLE OF CONTENTS

LIST OF FIGURES

LIST OF TABLES

<center>INTRODUCTION</center>

PURPOSE AND SCOPE

There is an increasing demand for natural gas and other fossil fuels today. Locating sites of high-yielding Devonian shale gas wells would help satisfy future demands for natural gas. Developing new and inexpensive exploration techniques for Devonian shale gas based on hydrogeologic criteria would aid in locating such well sites. There is also an increasing demand for fresh ground water today. Developing ground-water exploration methods for high-yielding water wells with good quality water would help satisfy future fresh water needs. Future economic growth and rural quality of life are both dependent on securing increased supplies of adequate water.

The purpose of this study was to investigate for possible associations between near-surface hydrogeologic variables and Devonian shale gas production in the Midway-Extra field of northern Putnam County, West Virginia. The foremost goal of this research was to discover inexpensive exploration techniques for locating high-yielding Devonian shale gas wells. Other objectives were to determine what effect hydrogeologic setting has on water-well yield and ground-water quality. The major hydrogeologic parameters investigated were photo-lineaments, water-well yield, and shallow ground-water chemistry. Photolineament and stream proximity, topographic setting, and aquifer sequence were investigated for their influence on water-well yield

and ground-water quality, as future aids in ground-water exploration.

LOCATION OF STUDY AREA

The study area lies in the northern portion of Putnam County and is covered by six 7 1/2 minute quadrangle maps (Figure 1). The northern boundary is the Mason County line; the western and southwestern boundary is the Kanawha River floodplain; the southeastern boundary is State Route 34; and the eastern boundary is the Jackson County line. Surface rocks of the study area are in the Dunkard and Monongahela groups (Wilmoth, 1966). The area is in the Appalachian Plateau physiographic province, and is characterized by high-relief terrain with elevations ranging from 500 to 1,500 feet. The population is primarily clustered in small communities along the Kanawha River, with scattered settlements occurring on ridge tops and valley floors.

GEOLOGY OF STUDY AREA

Stratigraphic Setting

The study area is underlain by basically horizontal strata, the Permio-Pennsylvanian Dunkard and Monongahela groups. These groups are composed primarily of cyclic sequences of sandstone, siltstone, red and grey shale, limestone and coal (Krebs, 1911). The Dunkard Group overlies the Monongahela Group. Quaternary alluvium that is present along the Kanawha River has been excluded from the study.
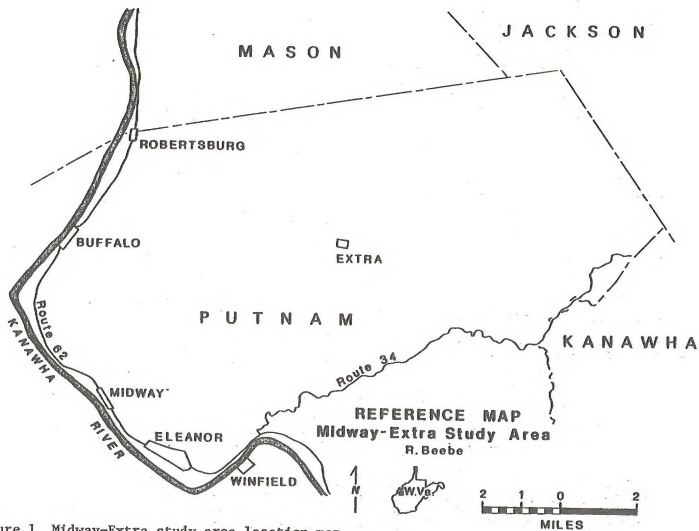
Figure 1 Midway-Extra study area location map.

MASON

JACKSON

ROBERTSBURG

BUFFALO

EXTRA

PUTNAM

KANAWHA

Route 62

Route 34

KANAWHA

RIVER

MIDWAY

ELEANOR

WINFIELD

N

W.Va.

REFERENCE MAP
Midway-Extra Study Area
R.Beebe

2 1 0   2

MILES

The Dunkard Group is the youngest group of consolidated rocks in the area and is exposed in the northwestern portion of Putnam County. Only the lower 570 foot portion of the Dunkard Group is present (Wilmoth, 1966). It consists of interstratified red and varicolored sandy or limy shale, grey, green, and brown sandstone, some calcareous shale, a few thin beds of coal, and nodular fresh-water limestone (Wilmoth, 1966). The Dunkard Group reportedly has more red shale and less coal than the Monongahela Group. Owing to this lithologic feature, and its higher topographic position, the Dunkard Group is in general a poorer water-bearing formation than the Monongahela Group (Wilmoth, 1966).

The Monongahela Group is 230 to 320 feet thick in the study area and it occurs at the land surface throughout most of Putnam County. The Monongahela Group is composed of grey and brown sandstone, red and varicolored shales, minor beds of limestone, coal and fireclay. Several coal units occur in this group, including the Pittsburgh, Redstone, Sewickley, and Waynesburg coals (Wilmoth, 1966).

The rock units of these two groups are largely discontinuous laterally, which makes detailed analysis and construction of a generalized stratigraphic column difficult for Dunkard or Monongahela group strata (Wilmoth, 1966).

Structural Setting

The study area lies within the Plateau Province of the central

Appalachians. The structure of the surface rocks in the area is characterized by very low relief synclinal and anticlinal folds. The rocks generally range in dip from 7 to 145 feet per mile (Wilmoth, 1966).

The major structural features of economic importance in the study area are located at depth, and parallel Devonian brown shale gas production (Figure 2). The dominant structural features are the Midway anticline and adjacent synclines. The anticline can be traced in the subsurface from Kentucky into the study area, striking approximately N60°E and plunging northeastward into the Appalachian basin (Schaefer, 1979).

Separating the Midway and Extra sections of the Midway-Extra gas field is a low-relief anticline which strikes about N15°W. This structure intersects the Midway anticline near the center of the study area, and the structural relief is greatly reduced where the two structures merge (Schaefer, 1979).

Midway-Extra Gas Field

Located in Putnam County, West Virginia, the Midway-Extra gas field is defined for this study by a narrow band of 97 gas wells producing primarily from the Devonian brown shales. This field is approximately 100 square miles in area, with only about one third of the total area producing significant flows (Schaefer, 1979).

The first well in the area was drilled and completed in 1947. Of
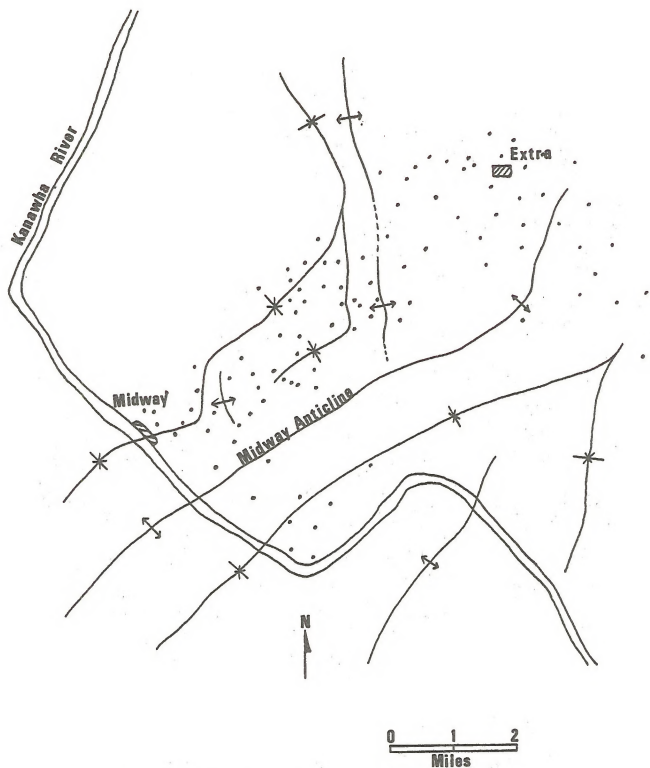
Figure 2 Structure on base of brown shale in Midway-Extra study area
(after Schaefer, 1979).

the 97 wells drilled within the producing margin of this field, slightly
better than 50 percent were drilled during the period 1947 to 1952.
This drilling completed the Midway section of the field. Current drill-
ing in the Midway-Extra field is concentrated in the Extra portion
of the area (Schaefer, 1979).

The Devonian brown shales referred to in this study occupy only
a small part of the total Devonian shale section. These shales are
commonly identified by their high radioactivity and low density, and
are equivalent to the Lower Huron Shale Member of the Ohio Shale
(Schaefer, 1979).

The overall thickness of the Upper and Middle Devonian shales
ranges from less than 1,000 feet in the extreme western counties of
West Virginia, to over 3,200 feet in eastern Kanawha County (Bagnall
and Ryan, 1976). The entire Upper and Middle Devonian section changes
facies eastward, generally becoming coarser in grain size (Schaefer,
1979).

As reported by Schaefer (1979) there appears to be a definite
correlation between production and stratigraphy within the Devonian
shales of the Midway-Extra field. Not only are the brown shales the
more productive, but specific low-density, high-organic zones within
these shales are the most productive. While there is not a precise
one-to-one correlation between stratigraphy and shows from well to
well, there is clearly a tendency for shows to correlate by stratigraphic

position.

PREVIOUS INVESTIGATIONS

With respect to previous investigations, only previous hydro-geologic and lineament studies which may relate directly or indirectly to natural gas production will be discussed. Reported studies are limited to the immediate study area or to similar terrains elsewhere in West Virginia.

Several studies by Werner (1976, 1977a, 1977b), Jones and Rauch (1978a), and Ryan (1976) involved investigations of possible associations of photolineaments with natural open flow gas production. Werner (1976, 1977a, and b) reported on the association of lineaments derived from Landsat imagery (Landsat lineaments) with natural open flow gas production. Werner (1977a) examined Landsat lineaments in Wayne, Mason, and Jackson counties of West Virginia, and concluded that the natural open flow is lower for gas wells located on or near such lineaments. Jones and Rauch (1978a) found that in the Cottageville area of Mason and Jackson counties, gas wells located within 0.25 miles of one Landsat lineament or within 0.50 miles of a curvilinear lineament over one mile long produced at significantly lower rates, and that in general Landsat and curvilinear lineaments should be avoided when locating Devonian brown shale gas wells.

Ryan (1976) found results that conflict with those of Werner

(1977a) with respect to Landsat lineaments and natural open flow gas
production within the Haysi field of western Virginia and southeastern
Kentucky. Geologically, the Haysi area is located at the northeastern
end of the Pine Mountain overthrust, with the Haysi gas field located
within the tear-faulted zone. The main producing formation in that
area is in the Berea Siltstone at an average depth of 4,000 feet (Ryan,
1976). Considering only the hydraulically fractured Berea wells, Ryan
(1976) stated that those gas wells located on or within 1,500 feet of
major lineament zones have an open flow after fracturing greater than
those wells more than 1,500 feet from a lineation. In conclusion, Ryan
(1976) believes that better wells are associated with natural fracture
zones in this type of geologic and topographic terrain. Werner (1977a)
expressed several possible reasons for the discrepancy in findings of
the two studies. First, the lithologies of the producing formations
are different. The producing horizon in the Haysi field is the Berea
Siltstone; the producing horizon in western West Virginia is the Devonian
shale. The two rock types behave differently under stresses which
produce fracturing. Second, the Haysi field is located in an area of
Appalachian thin-skinned tectonics where the area in West Virginia is
probably not. Another point which may have a bearing on this relation-
ship is one indicated by Kulander, Dean, and Barton (1977); if the gas
conduits in the Devonian shales were primarily horizontal fractures
and those in the more competent silts and sands of the Berea (or similar

units) were nearly vertical fractures, the widely different associations observed between Landsat lineaments and gas production might be reasonable. Also, if horizontal fractures are the primary natural conduits of Devonian shale gas to wells, and if the lineaments studied represent major vertical fracture zones, then the vertical fractures may have vented sufficient gas to make rock in their immediate vicinity nonproductive (after Werner, 1977a).

Short photolineaments, defined by low-altitude black-and-white aerial photography, were studied by Jones and Rauch (1978a) in the Cottageville, West Virginia area. These photolineaments were shown to have a positive influence on natural open flow gas production. Their findings indicate that gas wells located within 0.50 miles of a short photolineament bearing N60°W-N90°W (WNW) yield at significantly greater rates than gas wells near other photolineaments, but that short photolineaments are not in general associated with gas well yield (Jones and Rauch, 1978a). The importance of these short WNW-oriented photolineaments may be in their relationship to mineralized fracture orientations dominant within the gas producing horizons at Cottageville. The primary reservoir in the Cottageville field is Brown Shale Zone II. Rock cores taken from a high-producing well in this field show that fracture orientations down through Zone II exhibit considerable dispersion in the orientation of mineral-lined fractures, however three directions predominate: N40°-50°E, N10°-20°W, and N80°-90°W

(Larese and Heald, 1976). Furthermore, the WNW photolineament trend
is oriented about 60°-90° from the regional structural (fracture)
trend of N40°-50°E in the Cottageville area as reported by Martin and
Nuckols (1976). The combination of fracture orientations N40°-50°E
and N60°-90°W might tend to maximize fracture permeabilities within
the gas bearing formations.

Short photolineaments and their relationship to the occurrence
of ground water in clastic rock terrains, within the Appalachian Pla-
teau geologic province of West Virginia, have been investigated by
several workers: Sole (1975), Jones and Rauch (1978a, 1978b), Holland,
Rauch, and Werner (1977), and Steffy (1975). All of these reports agree
on the original relationship cited by Lattman and Parizek (1964), that
increased yields for wells in close proximity to photolineaments pro-
bably indicates a greater degree of weathering and therefore higher
porosity and permeability for nearby rocks. Lattman and Parizek (1964)
originally defined such photolineaments as fracture traces less than
one mile in length, with a zone of influence about 400 feet wide in
the carbonate rock terrain of central Pennsylvania. However, they
also indicated that the distance within which a well must be located
of a photolineament before its yield is greatly influenced is naturally
dependent upon the width of the associated fracture zone, the rock
lithology within the lineament, and the structural characteristics of
this rock. Sole (1975), in studying the hydrogeology of the Pricetown,

West Virginia area, found that the water well productivity and well
proximity to the nearest photolineament are significantly associated
above the 90 percent probability level. Jones and Rauch (1978a, 1978b)
tested water well yield as a function of well proximity to photo-
lineaments. They found that wells located within 100 feet of a photo-
lineament yield water at significantly greater rates than more distant
wells at a 0.05 alpha probability level. Of those wells within 100
feet of a photolineament center line, wells within 50 feet yield water
at significantly greater rates than wells 50–100 feet from the lineament,
at an 0.05 alpha probability level. Holland, Rauch, and Werner (1977),
in their hydrogeologic study of water well yields and ground-water
quality in north-central Tyler County, West Virginia, tested well
proximity to photolineaments against water well yield. Results show
that wells located within 200 feet of a photolineament had signifi-
cantly higher yields than all other wells. Furthermore, median yield
differences indicate that near-lineament wells produce at about 2 1/2
times the rate of wells not near photolineaments. Steffy (1975),
used nonparametric statistics to test for associations of well yield
(gpm) with well proximity to the nearest photolineament in Tucker County,
West Virginia; wells located within 100 feet of a photolineament in this
area had significantly higher yields than more distant wells, at an 0.07
alpha probability level.

Some researchers have investigated the relationships between ground-water chemistry and photolineament proximity. Sole (1975), found no definite relationships between photolineaments and ground-water chemical parameters, except that the variable pH was significantly higher near photolineaments; he concluded that this association had no logical cause for its significance. Steffy (1975) found that iron and total hardness were both significantly greater in wells which are within 100 feet of a photolineament. Jones and Rauch (1978b) found that photolineaments appear not to be related to ground-water chemistry in their study area. Holland, Rauch, and Werner (1977) found that photolineaments appear to be minimally associated with ground-water chemistry; for wells within 200 feet of a photolineament, the iron and calcium concentrations were significantly higher at the 0.05 alpha probability level, magnesium concentrations were significantly higher for wells near photolineaments at the 0.10 alpha probability level. Explanations for these associations are uncertain (Holland, Rauch, and Werner; 1977). Steele et. al. (1976) however, found that wells located off of photolineaments had greater calcium and magnesium concentrations than those located on photolineaments. Steele et. al. (1976) conducted an investigation in carbonate rock terraine, which could explain why they found different associations between hardness and photolineaments than did Steffy and Holland et. al. for West Virginia clastic rock terrains. Steele et. al. (1976) also found that nitrate

and phosphate were present in higher concentrations in wells located on photolineaments, probably because of the greater ease of entry of pollutants, such as fertilizer and animal wastes, into wells near photolineaments.

Jones and Rauch (1978a) also investigated possible relationships between shallow ground-water chemistry and natural open flow gas production from Devonian shales in the Cottageville, West Virginia area. Their findings indicate that certain ground-water chemistry parameters are significantly related to natural open flow gas production. Specifically, they found that concentrations of nitrate and sulfate, and especially of bicarbonate and total hardness are significantly associated with high expected (interpolated) gas well yield, near water well sites (Jones and Rauch, 1978a).

METHODS OF INVESTIGATION

LINEAMENT MAPPING

Landsat Lineaments

Lineaments derived from Landsat satellite imagery, termed Landsat lineaments, were located on images having scales of 1:1,000,000 and plotted on the appropriate 7 1/2 minute topographic quadrangle maps. The Landsat lineaments were defined as natural straight-line features, such as straight stream or valley segments, aligned stream meander bends, or tonal streaks in vegetation or soil cover. The instrument used to locate and identify such lineaments was the 12-Color Datacolor/ Edge Enhancer System. The four mapped Landsat lineaments were then ranked with regard to the certainty of their existence, with a rank of "1" indicating near certainty and a rank of "2" indicating questionable certainty. Furthermore, the Landsat lineaments were classified according to the nature of their appearance on the Landsat image; a classification of "T" indicates a tonal appearance derived during contrast mixing visual enhancement, and a classification of "E" indicates an edge appearance found during edge enhancement observation of the satellite image representing the study area.

Short Photolineaments

Short photolineaments were also mapped for the study area from

low-altitude black-and-white photographs having scales of about 1:20,000 and 1:38,000. The photographs were examined with the aid of a pocket stereoscope which facilitated recognition of rectilinear surface features as defined by Rauch (1979, oral communication), and Lattman (1958). Lattman (1958) defined short photolineaments to be fracture traces, believing that such lineaments usually represent fracture zones. Approximately 270 short photolineaments were plotted on six 7 1/2 minute topographic quadrangles of the study area. The photolineaments represent rectilinear surface features corresponding to nearly straight stream channels, valley segments or tonal differences in soil cover or vegetation. Plotted photolineaments are at least 0.25 miles in length and are not generally more than 1.00 miles long. Each plotted photolineament was recorded and ranked in order of the certainty of its existence. A ranking of "1" indicates a most-certain photolineament location while a ranking of "3" indicates a least certain photolineament location; a ranking of "2" is intermediate, or indicates moderate certainty.

FIELD METHODS

Geophysical Techniques

Electrical resistivity surveying was used as a geophysical technique to test for the possible presence of a near-surface fracture zone under a selected short photolineament located within the study area. A class "1" photolineament, mapped from low-altitude black-and-white aerial

photographs, was tested. A perpendicular survey line was chosen across
the selected photolineament, as shown in Figure 3.

A tri-potential resistivity survey was performed, as described
by Kirk (1976). This type of survey involved four metal electrodes
placed in line in the ground, with a 30 foot electrode spacing. A Soil
Test resistivity meter was used to determine the electrical resistance
of the ground area under the survey line. As a general rule, the pene-
tration depth of the electrical current is about equal to the distance
between adjacent electrodes (Kirk, 1976). Three electrode arrays were
used, the CPPC, CPCP, and the CCPP arrays, where "C" represents a current
electrode and "P" represents a potential electrode. Apparent electrical
resistance was recorded from the resistivity meter for all three arrays
at each survey station. The survey was run on nearly-level ground in
order to minimize the effects of topography on the observed resistivities.

During electrical resistivity surveying, an electrical current
is put into the ground artificially and the potential difference between
the current that returns and the original current is measured. This
enables one to calculate the apparent resistance of the medium in quest-
ion. The apparent resistivity was then calculated from the apparent
resistance values by use of equation (1), after Kirk (1976).

$$\rho = R(A/L) \tag{1}$$
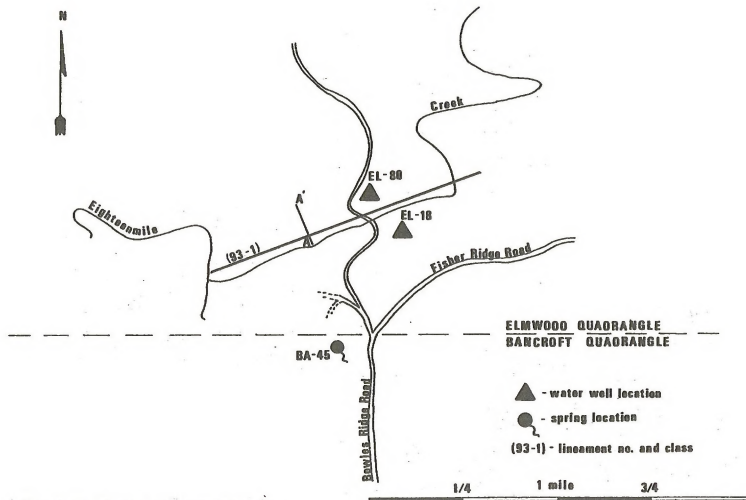
Figure 3 Electrical resistivity
survey location map. Line A–A' is the survey trace.

Map labels: N, Creek, EL-80, EL-18, Eighteenmile, (93-1), A', A, Fisher Ridge Road, Bowles Ridge Road, BA-45

ELMWOOD QUADRANGLE
BANCROFT QUADRANGLE

▲ - water well location

● - spring location

(93-1) - lineament no. and class

1/4   1 mile   3/4

where, ρ = apparent resistivity

R = resistance

A = cross-sectional area of medium in question

L = length of medium in question

The electrical resistivity is defined as the resistance of a given material of a given unit dimension (Kirk, 1976).

Several equations were utilized to correct data collected from the resistivity meter for non-homogenous geologic and geometric considerations. The correction factors from Kirk (1976) are as follows:

$$\rho CPPC = 2\pi a \cdot R \tag{2}$$

$$\rho CPCP = 3\pi a \cdot R \tag{3}$$

$$\rho CCPP = 6\pi a \cdot R \tag{4}$$

where, ρ = apparent resistivity

a = electrode spacing

R = resistance measured by resistivity meter

C = current electrode

P = potential electrode

In general, large differences among the apparent resistivity values for the three electrode arrays indicate anomalous resistivity zones.

Another useful quantity determined from an electrical resistivity survey is $\triangle$ %. This variable is a measure of the asymmetry of resistivity and is determined by the following equation from Kirk (1976):

$$\triangle \% = \frac{\rho CPPC - (\rho CCPP + \rho CPCP)}{\rho CPPC} \times 100 \tag{5}$$

Large absolute values of $\triangle$ % generally indicate a resistivity anomaly zone.

A fracture zone may exhibit no discernible difference in resistivity from that of the surrounding rock, or it may raise or lower measured resistivity values (Kirk, 1976). For example, a clean sandstone with a fracture zone would tend to show a lower resistivity than the surrounding rock; this is due to the introduction of ground water with relatively high dissolved solids into the fracture porosity, replacing the relatively dilute ground water in the surrounding rock. A fracture zone in shales, however, would tend to have a higher resistivity than that of the surrounding rock due to relatively fresh water being introduced in comparison to the water trapped in pore spaces within the shale. This trapped pore water would have a higher dissolved solids concentration than that for the more permeable sandstone. This latter case is similar in effect to that presumed to occur in the area of Figure 3, because of the predominant shale nature of the country rock in the study area.

Water Well Sampling

Seventy-three domestic water wells and 7 springs were inventoried in the study area. The inventoried wells and springs are located primarily along secondary roads. Wells to be inventoried were selected where available, within the heart of the Midway-Extra gas field, and a

spacing of at least one mile between adjacent wells was generally used for the whole study area. Figure 4 shows the locations of springs and water wells inventoried for this study. Wells that were sampled are limited to drilled wells only; dug wells and wells with water conditioners were avoided.

Water well data of this study were primarily obtained by the author. The data collected for each well were: well use; well depth; depth to static water level; well yield (gpm); well diameter; depth of casing; depth of pump placement; pump capacity; and a number or ranking of yield. These physical water well parameters were determined from interviews with well owners and/or well drillers. In addition, the topographic setting of each well (hill, slope, or valley) was obtained from on-sight inspection. Six 7 1/2 minute topographic quadrangles covering parts of the study area were used to determine the well-top elevation of each inventoried well. A complete list of physical water-well data is contained in Appendix A of this report.

Of the 73 water wells and 7 springs inventoried, 32 water samples were collected. Sampling sites were selected so as to permit about 50 percent of these sites to be located within the producing margin of the Midway-Extra gas field; the remaining well sites were located beyond the producing margin of the gas field. Before collecting each water sample, the water pump was allowed to run to empty the holding tank and pipes of standing water present; this allowed direct sampling of ground
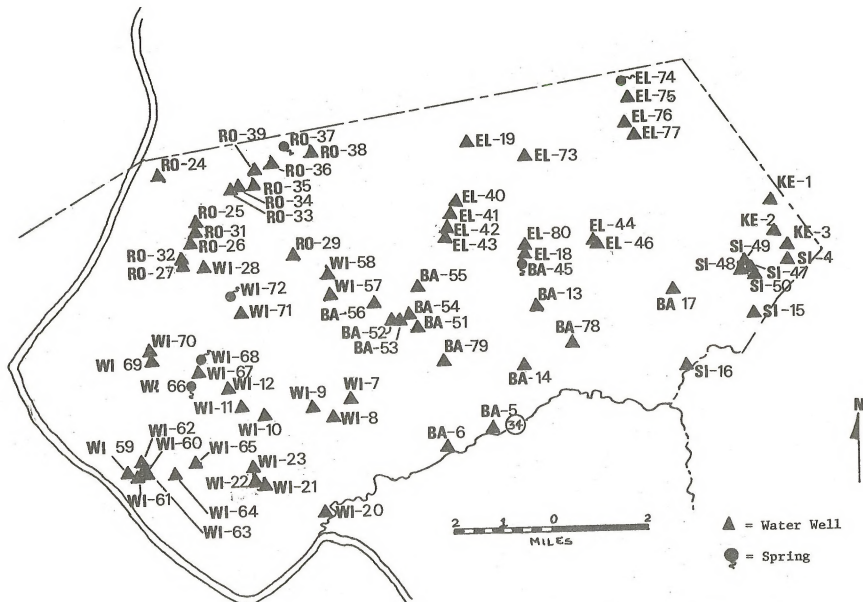
Figure 4 Location map of springs and water wells for Midway-Extra study area.

494.

water from the aquifer. For each well sampled two water samples were collected and stored in quart-sized containers. The water temperature was recorded with a standard Celsius thermometer, and the specific conductance was determined by a Beckman Solu-Bridge conductance meter in the field. Approximately 10 drops of concentrated HCl were added to one sample container to insure that dissolved iron, calcium, and magnesium would remain in solution. The unacidified samples were kept cool in a cooler while in the field, then in a refrigerator until chemical analyses were completed in the laboratory.

Pumping Tests

Pumping tests were performed on two water wells where access to the well top was possible. Pumping tests were performed for the purpose of obtaining more accurate determinations of water well yield and aquifer transmissivity for wells in the study area. Owner permission to conduct the pumping tests was difficult to obtain, since it was a cost and inconvenience to the well owner. Pumping tests were performed on wells EL-80 and RO-29. Data obtained from these pumping tests are contained in Appendix H of this report.

A Soil Test electric well line was used to first determine the depth of the static water level before pumping, and well water was not pumped or used for at least one hour prior to each pumping test. Next, the well was pumped continuously for 20 and 10 minutes time for wells

EL-80 and RO-29 respectively, and the pumping rate was periodically measured in gallons per minute with the aid of a watch and a 3 gallon measuring bucket. The depth to water was recorded and both the drawdown and specific capacity of the well were determined, using the following formulas:

$$\text{Drawdown} = (\text{static water depth}) - (\text{water depth after pumping}) \quad (6)$$

$$\text{Specific Capacity} = \frac{\text{Pumping Rate (gpm)}}{\text{Drawdown (ft)}} \quad (7)$$

Transmissivity is an indication of the permeability of an aquifer. It was determined by the following formula modified after Jacob (1963):

$$T = \frac{264 \, Q}{s} \log_{10} t/t'$$

Where T is transmissivity in gallons per day per foot of aquifer width; Q is the pumping rate in gallons per minute; s is the drawdown in feet; t is the time in minutes since pumping began; and t' is the time in minutes since pumping stopped. This formula assumes that the coefficient of storage (S) remains constant during and after well pumping. In reality this does not necessarily occur. Jacob (1963) discussed the problem and offered an appropriate correction by modified equation (9):

$$T = \frac{264 \, Q}{s} \left[(\log_{10} t/t') - \log_{10} (S/S') \right] \quad (9)$$

Where S is the coefficient of storage during pumping and S' is the coefficient of storage after pumping. The graphic plotting of drawdown (s) versus the common log of ratio t/t' can be expressed by equation (10) after Jacob (1963):

$$\text{Slope} = \triangle s / \triangle \log_{10} (t/t') \qquad (10)$$

After determining the slope of the line, the coefficient of transmissivity can be calculated by equation (11) modified after Jacob (1963):

$$T = 264 \ Q/\text{Slope} \qquad (11)$$

When the coefficient of storage does not remain constant, the plotted slope line of equation (10) does not pass through the origin and the calculated value of T is somewhat inaccurate (Jacob, 1963).

DETERMINING ADEQUACY OF WATER WELL YIELD

Where possible, the author recorded well yield in gallons per minute (gpm). However, where gpm yield data were not available an ordinal measure of water well adequacy was recorded as an estimate of yield. The assigned adequacy rankings are as follows: IA = inadequate for owners' supply of water; BA = barely adequate for the owners' supply of water; A = adequate water supply; TD = more than adequate supply of water or supplies two dwellings; and AA = well driller reported inability to bail the well dry.

The adequacy ranking technique used was a modified version of that used by Friel and Bain (1971). The purpose of the adequacy ranking was to attempt to assign a median water well yield (gpm) to water wells without known or reported gpm yield data. Before assigning an adequacy rank to any well, certain important factors were considered. For instance, each well owner was questioned about his water well use, especially concerning appliances such as washing machines and dish washers which use large amounts of water. Furthermore, the number of residents and wash rooms were considered before an adequacy rank was assigned.

When the water well inventory was completed and adequacy ranks were applied to all wells, a list of known water well yields was constructed for each adequacy group as shown in Table 1. The median water well yield in gpm for each adequacy group was then recorded. These median values were then assigned to other wells of each adequacy group which lacked reported water gpm yield data. In this way every water well could be later used for nonparametric statistical tests of hydrogeologic or gas well variables which might possibly be associated with water well yield.

AQUIFER DETERMINATIONS

Inventoried water wells were located in the stratigraphic column to determine the rock units most likely to supply water to these wells. Because of the scarcity of published stratigraphic descriptions or geo-

TABLE 1

WATER WELL ADEQUACY RANKING

Adequacy rating for water well yield	IA	BA	A	TD	AA
No. of wells in each class	12	7	19	2	9
Median well yield (gpm) when known	0.0	0.58	1.0	12.5	no data

Key:

IA = inadequate supply of water

BA = barely adequate supply of water

A = adequate supply of water

TD = more than adequate supply of water or supplies two dwellings

AA = well driller reported inability to bail well dry

physical logs, and the complexity and extreme lateral variation of
strata, unequivocal aquifer determinations for each water well were
impossible. Indirect methods were therefore employed to determine the
major stratigraphic sequence containing the aquifer for each inven-
toried water well in the study area. Two major sources of stratigraphic
data were provided by Krebs (1911) and Wilmoth (1966), and limited
amounts of stratigraphic data were also supplied by well drillers and
well owners. A generalized stratigraphic column was then prepared from
these data.

The data supplied by Krebs (1911) consisted of three stratigraphic
sections: (1) the Pliney core section located in Pliny of the Buffalo
District in Putnam County, at the mouth of Plantation Creek; (2) the
Bear Branch section taken descending into Bear Branch of the Buffalo
District in Putnam County, and joining the Henderson core drill hole
(P-25); and (3) the Sigman section taken descending into Sycamore Branch,
1 1/2 miles south of Sigman of the Pocatalico District in Putnam County,
and joining the O.P. Honaker core drill hole located on the Sycamore
Branch of the Left Fork of the Poca River. From these data a generalized
stratigraphic cross section was constructed through the study area.
For each core of the stratigraphic cross section the top of the Pittsburgh
Coal was used as datum.

The minimum elevation of the aquifer supplying water to each well
was first determined by subtracting the well depth from the elevation

at the well top. Next, this well bottom elevation was translated on a
perpendicular line to the stratigraphic cross section, and was corrected
for structure by using the elevation of the Pittsburgh Coal at each well
site, as determined from the structural contour map from Krebs (1911).
After having located the well bottom within the stratigraphic cross
section, the entire well depth was then constructed on this section,
from which determinations of the most probable aquifer sequence was
derived for each of the 74 water wells inventoried.

Because of the previously mentioned variability in thickness
and lateral continuity of the individual rock units of northeastern
Putnam County, a stratigraphic section or "aquifer sequence" was
assigned to each well, rather then a single lithologic unit. Aquifer
sequences range from 50 to 165 feet in total thickness, and each aquifer
sequence contains at least one major sandstone unit capable of supplying
water to a well. Relatively thin limestone beds are present in the
study area (Wilmoth, 1966) but they are too discontinuous to be con-
sidered as major aquifers.

A generalized stratigraphic column was constructed from the
stratigraphic cross section and is shown in Figure 5. This generalized
stratigraphic column represents the defined aquifer sequences which were
assigned to water wells of the study area. The Dunkard and Monongahela
rock units considered in this study are commonly highly variable and
largely discontinuous laterally. Caution must therefore be exercised
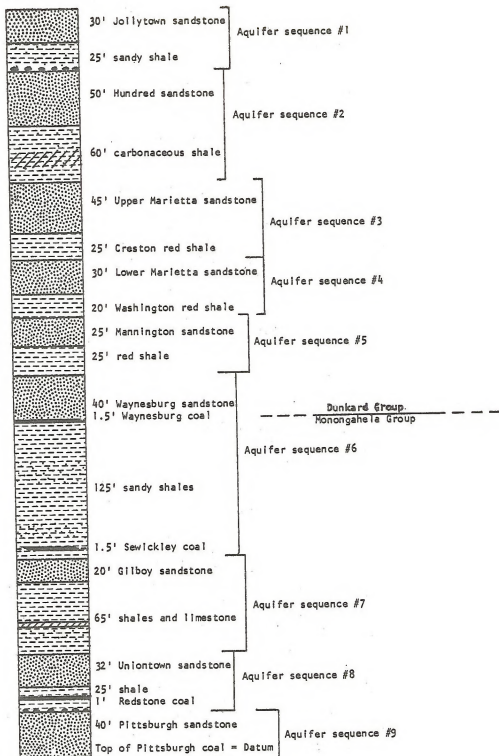
Figure 3 Generalized stratigraphic column, for the study area.

when making interpretations from Figure 5.

CHEMICAL ANALYSIS

Field measurements were made for each sampled water well for temperature and specific conductance. Each set of water samples was then analyzed in the laboratory for concentrations or values of the following aqueous geochemical parameters: pH, bicarbonate, total iron, nitrate, total hardness, calcium hardness, sulfate, chloride, and sodium. All parameters were measured within 48 hours after sampling to reduce the possibility of chemical changes before analysis.

The pH value of each unacidified water sample was determined by a Beckman Electromate pH meter in the laboratory. The probable error involved in determining the pH value is $\pm$ 0.10 considering analytical error and possible changes over time between field collection and laboratory analysis.

Bicarbonate (HCO_3^{-1}) was analyzed on the unacidified water samples, by titration for alkalinity with a standard HCl solution and a Beckman Electromate pH meter (after Brown et. al., 1970). The inflection point of the bicarbonate titration curve was then used to determine the titration endpoint (at approximately 4.5 pH). The bicarbonate concentration was then calculated, assuming bicarbonate is the only component of alkalinity. The probable error involved in determining the bicarbonate concentration is $\pm$ 3 percent, considering analytical error and possible

changes due to time.

Total iron (dissolved and suspended) was determined by colori-
metry analysis with the Hach Chemical Company DR-EL chemical analysis
kit, using the acidified water samples (Brown et. al., 1970). Final
concentration values were determined after the initial values were
adjusted for meter scale, reagent blank, and sample bottle corrections.
The estimated precision error for iron is $\pm$ 3 percent.

Nitrate was analyzed on unacidified water samples using the
Hach Chemical Company DR-EL unit. A cadmium-reduction method described
by Brown et. al. (1970) was followed, according to instructions by
Hach Chemical Company (1977). The initial nitrate values were also
corrected in a similar fashion as those for iron to determine the
final nitrate concentration values. The estimated precision error
for nitrate concentrations is $\pm$ 10 percent.

Sulfate was determined using acidified water samples and the Hach
Chemical Company DR-EL test kit (Hach Chemical Company, 1977). The
turbidimetric method was used in this case, and after the tests were
completed the initial concentrations were corrected in the same manner
as for iron and nitrate. The estimated precision error for sulfate
concentrations is $\pm$ 10 percent.

EDTA titration methods, modified after those described by the
Hach Chemical Company (1973), were followed to determine the calcium
and total hardness values for the acidified water samples. Hardness

was expressed as mg/l equivalents of dissolved calcium carbonate ($CaCO_3$). The estimated precision error for these chemical variables is $\pm$ 2 percent. The calcium concentration was then determined from the calcium hardness titration tests. Magnesium hardness was determined by subtracting the calcium hardness from total hardness values, and magnesium concentration was then calculated. It was assumed that only calcium and magnesium compose total hardness and that other alkali earth cations are negligible.

Chloride was analyzed for using the standard mercuric nitrate titration technique as outlined by the Hach Chemical Company (1973). Unacidified water samples were titrated with a standard $Hg(NO_3)_2$ solution. The estimated precision error for chloride concentrations measured in this study is $\pm$ 3 percent.

Sodium was analyzed for using an Evans Electoselenium Ltd. atomic absorption spectrophotometer (Brown et. al., 1970). NaCl standards were run before and after every five samples for calibration of the analysis technique. Unacidified water samples were used, and the estimated precision error for sodium concentrations is $\pm$ 5 percent.

A complete list of chemical variables for the analyzed waters is contained in Appendix B of this report.

DATA ANALYSIS

An exploratory data analysis, followed by appropriate statistical

tests, was conducted to investigate possible associations among the collected data. The author was specifically interested in determining what measured parameters might relate to water well yield, water well chemistry, and Devonian shale gas well yield. Several methods were used to detect possible association trends in the data. The exploratory analysis methods used involved visual data inspection, scattergrams, graphs, histograms, and 2x2 contingency tables.

Photolineaments were also considered with respect to statistical analysis. After the photolineaments were plotted on the appropriate maps, the proximity of each water well and gas well to the nearest photo- lineament was measured and recorded as was the photolineament class (see Appendicies E, F, and G). Statistical tests were then performed to determine the significance of any relationships of water well and gas well yields with photolineament proximity. Appropriate photo- lineament orientations were also recorded and later tested statistically for any significant associations with gas well yields. In addition to locating the short photolineaments on the appropriate 7 1/2 minute quadrangle maps, two photolineament density maps were constructed. The photolineament density maps depict class "1" photolineament density in miles per square mile, and N60°W-N30°E photolineament density in miles per square mile. The two photolineament density maps were con- structed by placing a square-mile orthogonal grid overlay on the study area with grid lines parallel to the north-south and east-west

directions. The length of each photolineament in question was then measured, and the cumulative lineament length per square-mile section of grid was determined and plotted at the center point of each square-mile grid section. A total of 100 square-mile grid sections were considered. The center points of these grid sections were then hand contoured.

Nonparametric statistical tests were used to test for significant differences between sets of data which would indicate critical associations. These are "distribution free" tests and do not require many observations or samples. Also, few assumptions or criteria must be met by the data tested (Siegel, 1956). Two statistical tests were primarily used to test for differences between two sets of data — the Mann-Whitney U test, and the Yates-corrected chi-square test for two independent samples (Siegel, 1956).

Mann-Whitney U test

When at least ordinal data are involved, the Mann-Whitney U test may be used to test whether two independent groups of observations have been drawn from the same population. This is one of the most powerful of the nonparametric tests, and it is a most useful alternative to the parametric t test when one cannot meet the t test's assumptions, or when interval or ratio scale data are not available (Siegel, 1956).

Given two groups of observations from two populations, population

A and B, the null hypothesis (H_o) is that A and B have the same distribution. The alternative hypothesis (H_a) against which we test H_o is that A is stochastically larger than B, a directional hypothesis (Siegel, 1956). Next, ranks are assigned to each observation for the composite of both groups of observations, for a particular variable. Then H_a is tested to see if the observation ranks for the first group are significantly different from those of the second group. For group sample sizes greater than 20 the equations (from Siegel, 1956) for computing U are:

$$U = n_1 n_2 + \frac{n_1(n_1 + 1)}{2} - R_1 \tag{12}$$

$$U' = n_1 n_2 + \frac{n_2(n_2 + 1)}{2} - R_2 \tag{13}$$

where, R_1 = sum of the ranks assigned to the smaller group whose sample size is n_1; R_2 = sum of the ranks assigned to the larger group whose sample size is n_2.

The statistical significance of U or U', whichever is smaller, is then determined from the appropriate table (Siegel, 1956). Furthermore, as n_1 and n_2 increase in size, the sampling distribution of U rapidly approaches the normal distribution, and one may determine the significance of an observed value of U by calculating z (Siegel, 1956).

$$z = \frac{U - (n_1 n_2 / 2)}{\sqrt{\dfrac{n_1 n_2 (n_1 + n_2 + 1)}{12}}} \tag{14}$$

Tables provided by Siegel (1956) are used to determine the statistical significance of the observed z value. U' is calculated primarily to provide a check for the value of U; only U is used in determining the value of z.

Yates-Corrected Chi-Square Test

The Yates-corrected chi-square test is used for testing trends in observed frequencies of a 2x2 contingency table with respect to an H_0. The form of such a table is given in Table 2. The following formula is used to calculate the Yates-corrected chi-square value:

$$x^2 = \frac{N(AD - BC - N/2)^2}{(A+B)(C+D)(A+C)(B+D)} \tag{15}$$

where, N = the total sample size; A, B, C, and D = observed cell frequencies (see Table 2). This formula has the additional advantage of incorporating a correction for continuity which makes this a conservative test and markedly improves the approximation of the computed x^2 values by the chi-square distribution (Siegel, 1956).

For each of the many tests run using either the Mann-Whitney U or the Yates-corrected chi-square test, the 0.05 alpha probability value was considered the upper limit for statistical significance for calculated error probabilities. However, other less significant probability results were often useful for interperting some data trends. The results of these statistical tests are presented under the RESULTS AND DISCUSSION section.

TABLE 2

2x2 CONTINGENCY TABLE

Variable Tested

	Low	High	
Data Group I	A	B	A + B
Data Group II	C	D	C + D
	A + C	B + D	N

Key:

A, B, C, and D represent cell frequencies or number of observations corresponding to the four data classifications.

RESULTS AND DISCUSSION

LINEAMENTS

Lineaments were mapped and are plotted on Figure 6, both for Landsat and short photolineaments. Landsat lineaments are located primarily in the western and southwestern portion of the study area. Short photolineaments are more abundant and more evenly distributed throughout the area.

The geophysical resistivity survey was performed over a photo-lineament to determine the presence of any underlying fracture zones. Figure 3 shows the location of the short photolineament and perpen-dicular electrical resistivity survey line (A-A'). The overall setting of Figure 3 is also indicated on Figure 6. Figures 7 and 8 show the plotted resistivities and delta percent curves respectively. The most distinct features of the survey plots are the CCPP peaks and trough between stations 3 and 5 of Figure 7, and the delta percent peak centered about stations 3 and 4 of Figure 8. Kirk (1976) defined this type of resistivity display as being typical of the effect of a positive resistivity contrast created by an anomaly associated with a fracture trace, where fracture resistance exceeds rock resistance. This is logical since the photolineament is located within the domi-nantly shale lithologies of the area; the introduction of relatively dilute ground water into fracture porosity in shale would replace more

BASE MAP
MIDWAY-EXTRA STUDY AREA
R. Beebe
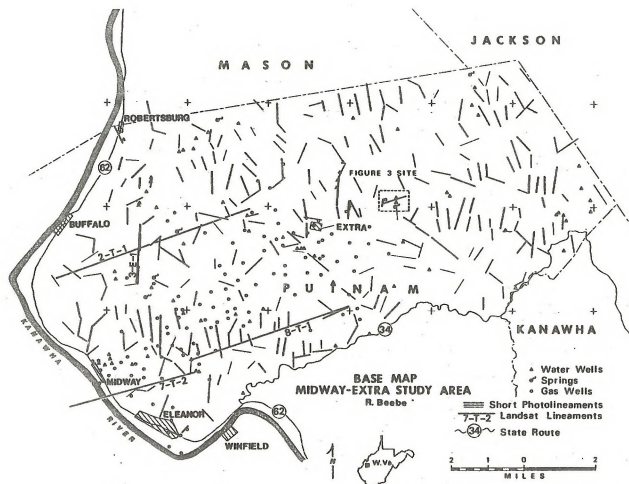
Figure 6 Base map of Midway-Extra study area, showing locations of wells and lineaments.
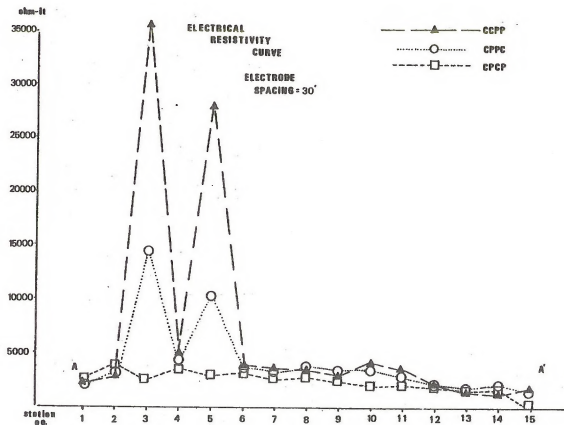
Figure 7   Resistivity plots from electrical resistivity survey of the Midway-Extra study area. The station numbers are spaced 30 feet apart.
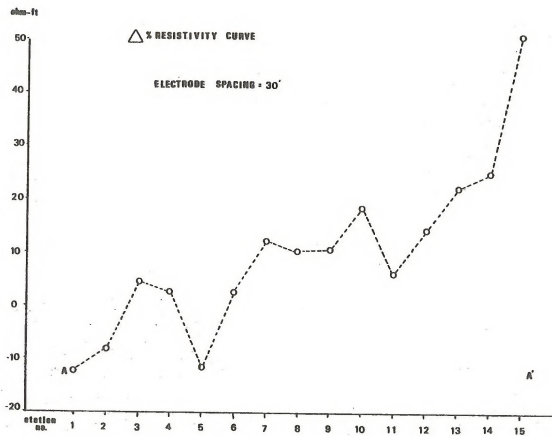
Figure 8 Delta percent plot from electrical resistivity survey for the Midway-Extra study area.

conductive ground water in the surrounding rock, creating a positive resistivity anomaly (Kirk, 1976). The relatively large positive response of the delta percent curve near station 4 of Figure 8 indicates that the probable fracture zone extends to a depth of at least 30 feet. However, no definite determination of the depth can be made since only one electrode spacing survey was run across the fracture zone (Kirk, 1976). The combined plots of Figures 7 and 8 tend to indicate the presence of a fracture zone centered near station 4, with a zone of influence of at least 60 feet in total width (Kirk, oral communication, 1979).

Although electrical resistivity surveys may be useful in locating and confirming surface fracture zones, factors reducing the usefulness of these surveys include topographic, lithologic, and ground-water storage variations as well as improper spacing of the electrodes. One or more of these factors could lead to an incorrect interpretation of the subsurface. For this reason, electrical resistivity surveying alone should not be relied upon to predict subsurface features. However, electrical resistivity surveying was useful in interpretating the subsurface nature of one photolineament in the study area.

WATER WELL YIELD ASSOCIATIONS

Water well yield data and other physical water well data are located in Appendix A of this report. Physical water well data were

collected for 74 domestic water wells and 7 springs in the study area.
Reported depths of sampled water wells range from a minimum of 30 feet
to a maximum of 300 feet, with a median depth of 140 feet. Reported
depths to water varied from 4 feet to 154 feet with a median depth of
35 feet. Approximately 32 percent of the inventoried wells are located
in valleys, with 43 percent located on hills, and the remaining 25 per-
cent located on hill slopes. Generally, water well yields of the area
are considered to be low with a median yield of about 1.0 gallons per
minute (gpm). Inventoried well yields range from a high of 20.0 gpm
to a low of 0.0 gpm. Median gpm yield values, obtained from the pre-
viously mentioned adequacy ranking technique, were assigned to wells
without known gpm yield data. Specific capacity and aquifer trans-
missivity data are available for two wells in the study area and are
contained in Appendix H of this report.

Lineament Proximity

Nonparametric statistical tests were performed to determine if
any associations exist between water well yield (gpm) and water well
proximity to the nearest lineament. Both Landsat lineaments and short
photolineaments were investigated for associations with water well yield.

Landsat Lineaments

Only 6 water wells from the study area are located within a

distance of 2000 feet of a Landsat lineament. Water well yields were
tested statistically for less than versus greater than specific distances
from such lineaments. The distances tested were 500, 1000, and 2000
feet. The statistical tests show that wells located within 2000 feet
of a Landsat lineament do not yield water at significantly different
rates than wells beyond 2000 feet of such lineaments in the study area.
Furthermore, no significant differences exist for yields of water wells
within 500 and 1000 feet of such Landsat lineaments, compared to more
distant wells. Whatever the reason for these non-associations, Landsat
lineaments are distinctly different from short photolineaments in both
appearance and effect.

Short Photolineaments

The Mann-Whitney U test was performed to test the effect of short
photolineament proximity on water well yield. The test was performed
for wells greater than versus less than a specific distance from the
nearest photolineament, as indicated on Figure 6. The specific proximity
distances tested were 100, 150, and 200 feet. Too few wells were
located within 50 feet of a photolineament to warrant statistical
analysis. Results of these tests are given in Table 3. The symbols
H and L are used in these Mann-Whitney U test tables to indicate
high and low median values.

It was found that photolineaments are excellent locations for high-

TABLE 3

WATER WELL PROXIMITY TO PHOTOLINEAMENT
VERSUS
WATER WELL YIELD

well proximity to
nearest photolineament

	≤ 100 feet	>100 feet	Probability of error
No. of wells in each class	6	65	
Median well yield (gpm)	12.5	1.0	
Mann-Whitney U Results (1-tailed)	H	L	0.0102

well proximity to
nearest photolineament

	≤ 150 feet	>150 feet	Probability of error
No. of wells in each class	9	62	
Median well yield (gpm)	12.5	1.0	
Mann-Whitney U Results (1-tailed)	H	L	0.0057

TABLE 3 (continued)

WATER WELL PROXIMITY TO PHOTOLINEAMENT
VERSUS
WATER WELL YIELD

well proximity to
nearest photolineament

	≤200 feet	>200 feet	Probability of error
No. of wells in each class	19	52	
Median well yield (gpm)	4.0	1.0	
Mann-Whitney U Results (1-tailed)	H	L	0.0015

well proximity to
nearest photolineament

	150-200 feet	>200 feet	Probability of error
No. of wells in each class	10	52	
Median well yield (gpm)	2.0-4.0	1.0	
Mann-Whitney U Results (1-tailed)	H	L	0.0329

well proximity to
nearest photolineament

	<150 feet	150-200 feet	Probability of error
No. of wells in each class	9	10	
Median well yield (gpm)	12.5	2.0-4.0	
Mann-Whitney U Results (1-tailed)	H	L	>0.05 (not significant)

yielding water wells. The optimum zone of influence for photo-lineaments is approximately 400 feet wide. Water wells located within 200 feet of a plotted photolineament's center line have significantly higher yields than more distant wells, at a 0.01 alpha probability level. Median yields of wells 150-200 feet of a photolineament center line are less than median yields of wells 0-150 feet from such center lines, but significantly more than wells located greater than 200 feet from these center lines. Within 200 feet of a photolineament center line there are no significant changes in well yield as the center line is approached, at a 0.05 alpha probability level; however, water well yields do tend to increase as the center line of a plotted photolineament is approached. The higher yields for water wells located within 200 feet of a short photolineament are most likely the result of high fracture permeabilities associated with fracture zones.

Other Physical Features

Aspects of hydrogeologic setting, other than lineament proximity, were tested for possible associations with water well yield. The factors tested include topographic setting, stream proximity, and aquifer sequence.

Topographic setting shows a significant effect on water well yields within the 0.05 alpha probability level determined by the Mann-Whitney U test, with test results shown in Table 4. Yields are

TABLE 4

WATER WELL YIELD VERSUS TOPOGRAPHY

	Slope	Hill	Valley	Probability of error
No. of wells in each class	18	31	23	
Median well yield (gpm)	1.0	0.8	5.0	
Mann-Whitney U results (1-tailed)	L		H	0.0329
	H	L		0.0307
		L	H	0.001

WATER WELL YIELD VERSUS STREAM PROXIMITY

well proximity to
nearest stream

	0-200 feet	>200 feet	Probability of error
No.of wells in each class	22	49	
Median well yield (gpm)	1.0-1.7	1.0	
Mann-Whitney U results (1-tailed)	H	L	0.0024

significantly higher for wells in valleys when compared with yields from water wells located on hilltops, at a 0.001 alpha probability level; median water well yields for valley wells are six to seven times greater than those for hilltop wells. Furthermore, hillside-slope yields are significantly greater than hilltop yields at a 0.05 alpha probability level. Valley water well yields are also significantly greater than hillside-slope well yields at a 0.05 alpha probability level. The effect of well proximity to a stream on well yield was also tested, with test results shown in Table 4. Water wells located within 200 feet of a stream have significantly higher yields than more distant wells, according to Mann-Whitney U test results at a 0.01 alpha probability level.

Higher water well yields indicated for valley wells, and especially for wells within 200 feet of a stream, can be explained by the fact that: (1) the recharge area is larger for valley wells than for hilltop or slope wells; (2) the water table is generally closer to the surface in valleys; (3) valleys tend to be more greatly weathered with greater aquifer permeabilities resulting; and (4) recharge from streams may occur for nearby wells (Davis and DeWiest, 1966).

The majority of water wells located within 200 feet of a photo-lineament occupy low topographic positions. Statistical tests were performed to determine if a photolineament's effect on water well yield was strictly a function of topography. The Mann-Whitney U test was

used to determine if any significant relationships exist between in-
creased well yield and short photolineament proximity for valley wells
only. The specific distances tested were 100 and 200 feet, and the
results of these tests are contained in Table 5. Median well yield
differences tend to indicate that valley wells located near photo-
lineaments do yield more on average than other valley wells, but they
do not yield significantly more. These results tend to indicate that
a photolineament's observed effect on water well yield is not strictly
a function of topography.

Of the 69 water wells for which aquifer sequence could be deter-
mined, 28 wells are located in the Dunkard Group and 41 wells are
located in the Monongahela Group. Yields from water wells located
within the aquifer sequences shown in Figure 5 were statistically tested
for possible significant differences in well yield as a function of
aquifer sequence. Table 6 contains the results of these tests. Aquifer
sequences 1 and 4 were excluded from testing because they contain too
few wells for proper tests. No significant differences are apparent
between the six aquifer sequences tested against aquifer sequence
number 6, the highest-yielding sequence, at a 0.05 alpha probability
level. Included in aquifer sequence 6 is the Waynesburg Sandstone;
median well yields tend to indicate that this unit is the best aquifer
for most of the study area. Possible reasons for the importance of
rock sequence 6 as an aquifer unit are: (1) the lateral continuity of

TABLE 5

WATER WELL PROXIMITY TO PHOTOLINEAMENT

VERSUS

VALLEY WATER WELL YIELD

valley well proximity to
nearest photolineament

	0-100 feet	>100 feet	Probability of error
No. of wells in each class	5	18	
Median well yield (gpm)	12.5	1.0-5.0	
Mann-Whitney U results (1-tailed)	H	L	>0.05 (not significant)

valley well proximity to
nearest photolineament

	0-200 feet	>200 feet	Probability of error
No. of wells in each class	11	12	
Median well yield (gpm)	12.5	1.0-5.0	
Mann-Whitney U results (1-tailed)	H	L	>0.10 (not significant)

TABLE 6

WATER WELL YIELD VERSUS AQUIFER SEQUENCE

Aquifer Sequence Number

	2	3	5	6	7	8	9	Probability of error
No. of wells in each class	8	10	4	17	7	8	8	
Median well yield (gpm)	0.0–0.8	0.6	0.8–1.	1.8–17.0	2.0–7.0	1.0	0.8	(all tests non-significant)
Mann–Whitney U results (1-tailed)	L			H				>0.05
		L		H				>0.05
			L	H				>0.05
				H	L			>0.05
				H		L		>0.05
				H			L	>0.05

the Waynesburg Sandstone throughout the study area; (2) a lower strat-
igraphic position for the Waynesburg Sandstone than for the majority
of sandstone lithologies in the stratigraphic column; and (3) a thick
sequence of shales interstratified with thin sandstone beds underlying
the Waynesburg Sandstone in sequence 6, increasing the possibility of
multiple aquifers within this sequence.

GROUND WATER CHEMISTRY

Ten water chemistry variables were measured for 32 tested water
wells and springs to determine if any important chemical trends or
associations are present that might aid in exploration for ground water
or Devonian shale gas in the Midway-Extra study area. The water chemistry
parameters analyzed were concentrations of total iron, chloride, total
hardness, calcium, magnesium, bicarbonate, sulfate, and sodium, as well
as pH and specific conductance; data for these sampled wells are located
in Appendix B. These water chemistry variables were selected because
they represent the major chemical parameters of ground water, and they
are relatively inexpensive and easy to analyze. The following is a
brief report on each water chemistry variable, including its sources
and general nature of occurrence in ground water.

Nitrate

Nitrate was selected for analysis because of its role in indi-

cating pollution from surface contaminants such as sewage or nitrogen fertilizers (Hem, 1970). Also, nitrate was shown to be significantly associated with increased gas well yield in the Cottageville, West Virginia area by Jones and Rauch (1978a).

In this study, nitrate did not exceed the maximum recommended level of 45 mg/l recommended by the United States Public Health Service (1962). The maximum concentration observed occurred in well WI-59 which had 13.6 mg/l nitrate. The data suggest that although high concentrations of nitrate are not common it is a persistent water quality parameter. Nitrate concentrations that are noticeably above background values for this study area (above about 5 mg/l) may well indicate ground-water pollution; this occurs for wells BA-5, WI-9, EL-45, BA-55, and WI-59.

In this study, the highest concentration of nitrate occurred in well WI-59. At the time of sample collection the owner was in the process of relocating his septic tank. His septic system had been located approximately 100 yards directly uphill from the water well. Domestic sewage may have contributed nitrate to the ground-water system. The organic portion of sewage is a source of ammonium ions which is oxidized to form nitrate (Hem, 1970). As nitrate is easily leached from the soil, and readily permeates an aquifer, the high nitrate concentration of well WI-59 may be the result of domestic sewage pollution. The probable sources of high-nitrate values for the remaining wells

could not be determined from field observations, however.

Total Iron

Iron is an abundant and widespread constituent of rocks and soils. Dissolved iron in excess of 0.3 mg/l is objectionable in water for it causes reddish-brown stains on clothing, utensils, and plumbing fixtures (Johnson, 1975).

In the study area, pyritic shales and pyrite in coal seams are probably responsible for significant amounts of iron in sampled ground water. Iron concentrations (for dissolved and colloidal iron combined) vary from 0.04 to 11.20 mg/l for sampled well waters. In this study, the highest concentration of total iron occurred in well WI-8. The owner of this well has reported that a coal seam was encountered during drilling of the well. Seven of the 32 sampled wells have iron contents exceeding 0.3 mg/l. Five of these wells are located in aquifers of the Monongahela Group which reportedly has more coal than the Dunkard Group; this possibly accounts for the high total iron values of these wells.

Sodium and Chloride

Chloride occurs as Cl^- in solution and is present in all natural waters. Sodium is generally in the form of the Na^+ ion (Hem, 1970). The most likely sources for Cl^- and Na^+ in well waters are: (1) connate brines trapped during marine sedimentation; and (2) road salts infil-

trating into the ground-water system from the surface (Davis and DeWiest, 1966).

Three study area wells (RO-24, RO-26, and WI-58) have excessive chloride concentrations (over 250 mg/1), according to U.S.P.H.S. (1962) standards. These same wells have the highest sodium concentrations of those studied, and are in general located in lower Monogahela Group rocks, and in low-elevation areas (with elevations not exceeding 610 feet). Upconing of connate marine brines that were trapped during marine sedimentation is the single most probable source of the high chloride and sodium concentrations for these three wells.

Total Hardness, Calcium and Magnesium

Hardness is a qualitative term representing the soap-consuming capacity of water. The greater the amount of alkaline earth metals dissolved in water, of which calcium and magnesium are the most important, the greater is the amount of soap required to overcome the complexing action of hardness ions. Hardness is expressed in terms of an equivalent concentration of calcium carbonate (Hem, 1970). In the tabulated data "Total Hardness" represents the sum of calcium and magnesium hardness. Calcium and magnesium occur as Ca^{++} and Mg^{++} cations in water (Hem, 1970).

Most dissolved calcium and magnesium are probably derived from the dissolution of carbonate-bearing cement or thin limestone

units in rock strata of the study area. Calcareous shales also consti-
tute a major source of calcium and especially magnesium to ground
water(Hem, 1970). The two highest total hardness wells (greater than
400 mg/1 as $CaCO_3$) are located in aquifer sequences 2 and 3. This
seems logical since sequence 2 is largely composed of calcareous shale.
The well located in sequence 3 may quite possibly be obtaining high
total hardness concentrations from sequence 2.

Bicarbonate

There are two important sources of bicarbonate in natural ground
waters. Dissolved bicarbonate (HCO_3^-) may originate directly or in-
directly from the dissolution of carbonate bearing rocks or minerals
(especially in carbonic acid), and from the decay of organic matter
(hence H_2CO_3). These sources are shown by equation (16):

$$CaCO_3 + H_2CO_3 \rightleftharpoons Ca^{++} + 2HCO_3^- \qquad (16)$$
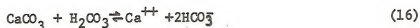
Ten of 14 wells with bicarbonate concentrations exceeding 400 mg/1
are located in aquifers of the Monongahela Group. Wilmoth (1966)
described both the Dunkard and Monongahela group waters as being of the
sodium and calcium bicarbonate type. A third probable source of
bicarbonate relating to methane gas will be discussed later.

Sulfate

The most common form of sulfate under normal Eh conditions is the $SO_4^=$ ion (Hem, 1970). Pyrite (FeS_2), a major source of sulfate in ground water, can occur in all lithologies present in the study area but is primarily associated with coal (Hem, 1970). When pyrite weathers as a result of contact with aerated ground water, the sulfide mineral is oxidized to yield sulfate ions. This is probably the reason for the high sulfate (and total iron) concentration of well WI-8, mentioned earlier with respect to "total iron".

Excessive sulfate concentrations greater than the recommended value of 250 mg/1 (U.S.P.H.S., 1962) can corrode plumbing fixtures and act as a laxative (Hem, 1970). However, sulfate does not usually create any serious health problems. The maximum sulfate content for sampled well waters was 145 mg/1. No adverse effects should be present due to sulfate in ground waters of the study area.

Specific Conductance

Specific conductance represents the total effect of all dissolved ions in ground water, and it is proportional to total dissolved solids. Specific conductance values greater than 750 micro-mhos/cm indicate excessive dissolved solids according to the U.S.P.H.S. (1962) standards, and Hem (1970). Specific conductance ranged from 85 to 6025 micro-mhos/cm in ground waters of the study area. High specific conductance values

are associated with high dissolved NaCl contents, or with high total hardness or bicarbonate concentrations. Most wells with very high conductances (over about 1000 micro-mhos/cm) are located in valleys and are characterized by excessive dissolved NaCl, especially well WI-58. The most likely source of the poor water quality for these wells is upconing of connate marine brines in response to water well pumping.

<div align="center">pH</div>

Values of pH for ground water in the study area range from 5.80 to 8.13. These values are all of acceptable quality. Differences in pH reflect variations in the lithology and mineralogy of rocks located near the well and aquifer. Pyrite and carbonate minerals probably have the greatest potential to affect pH values in the study area. Pyrite reacts to give off H^+ ions into solution when in contact with aerated water, effectively lowering the pH value of water; carbonate-bearing rocks in contact with ground water react to release bicarbonate, effectively raising pH values. The values of pH were determined in the laboratory only, and may differ slightly from the original field pH values because of a 24 hour delay in laboratory measurement.

TRENDS IN GAS YIELD

Initial open flow refers to gas production prior to fracturing of the gas producing horizon. Final open flow refers to gas production after fracturing of the producing horizon. No standard procedure for measuring these flows is believed to have been followed; although somewhat suspect, these flow values are the best that are available. Both initial and final open flows were used in the statistical analysis of possible associations between Devonian shale gas well yield and hydrogeologic setting. When this study began, it was intended that only initial open flow data be used. The assumption was that initial open flow would more nearly represent the geologic environment of the gas producing portion of the study area. However, Schaefer (oral communication, 1979), who has done extensive work on the producing characteristics of the Midway-Extra gas field, asserts that final open flow is a more dependable and representative measure of gas production rate with respect to geologic controls. Furthermore, he suggests that final open flow is more representative of the commercial success for gas wells and of productivity from gas reservoirs. For this reason final open flow gas production was considered with respect to possible associations with lineaments and hydrogeologic parameters. Initial and final open flow for gas wells are in Appendix C of this report and are from Schaefer (1979).

Figure 9 shows the locations of Devonian shale gas wells in the

Figure 9 Location map of Devonian shale gas wells
with permit numbers for the Midway-Extra
gas field, after Schaefer (1979).

Midway-Extra gas field. Figure 6 shows the location of Devonian shale gas wells, domestic water wells, Landsat lineaments, and short photo-lineaments in the study area. Figure 10 shows a polygonal area defining the Midway-Extra gas field portion of the study area. The polygonal area was constructed for the purpose of delineating the area to be tested in the statistical analyses for possible lineament-hydrogeologic trends with gas well yield. The polygonal boundaries were constructed by connecting the outermost gas well locations in the study area as shown. The 8 gas wells shown outside the polygonal area of Figure 10 were not considered because they are outside the defined limits of the Midway-Extra gas field (Schaefer, 1979). Other wells of Figure 9 were excluded from the polygonal area of Figure 10 because they either lacked production data or lay outside the limits of the study area.

Figure 11 shows contoured initial open flow for the study area, and Figure 12 shows final open flow contoured for the study area. Both initial and final open flow contour trends are expressed in terms of thousands of cubic feet of gas per day (MCF/day). The contours were drawn assuming that the changes in gas flow rate would be linear between adjacent wells. The position and trend of the contours are therefore partly a function of gas well density; contours in areas of low gas well density are probably optimistic in their prediction of shale gas reserves.
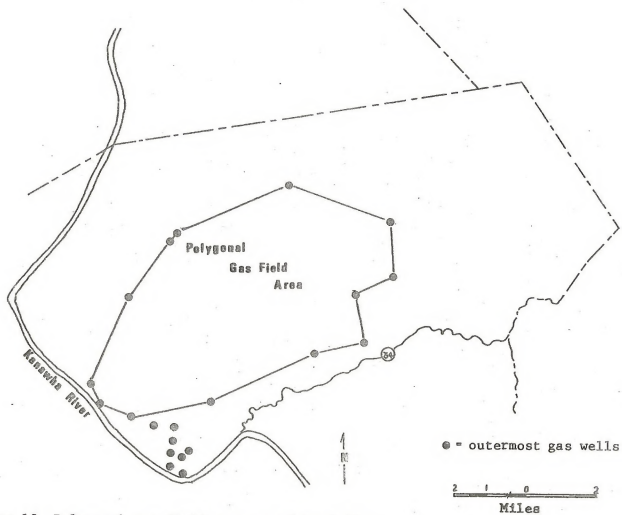
Figure 10   Polygonal gas field area, used to define
the Midway-Extra gas field within the study area.

INITIAL OPEN FLOW
Devonian Brown Shale Gas Production
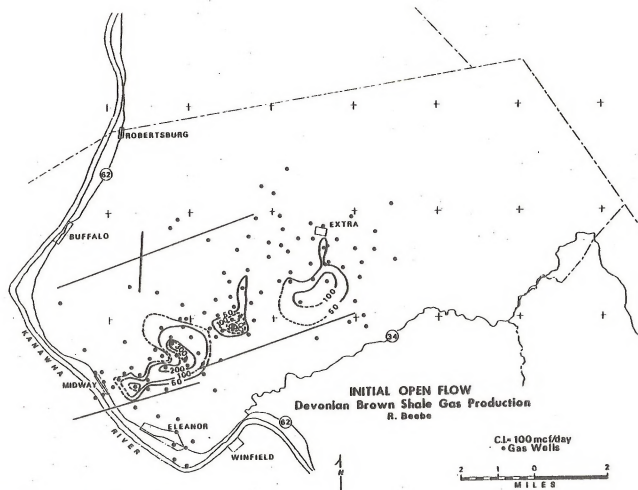R. Beebe

C.I.= 100 mcf/day
• Gas Wells

Figure 11 Initial open flow gas production for
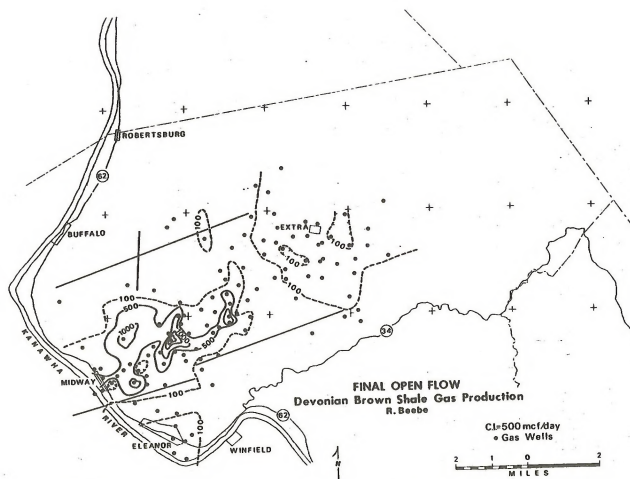Devonian shale wells in the study area.

Figure 12 Final open flow gas production for Devonian shale wells in the study area.

LINEAMENT ASSOCIATIONS WITH GAS WELL YIELD

Landsat Lineaments

The effect of Landsat lineaments was considered with respect to
initial and final open flow gas production for the Midway-Extra study
area. In addition to contoured production trends, Figures 11 and 12
show locations of Landsat lineaments. These figures show that Landsat
lineaments do not intersect high-producing areas of the gas field, but
rather appear to bound these areas to the north and south, and are
generally parallel to the general gas-producing trend. As suggested
by Werner (1977a), perhaps these lineaments represent deeply-penetrat-
ing fractures that have bled off Devonian shale gas to the surface.
In the Midway-Extra area Landsat lineaments are poor locations for
Devonian shale gas wells, and are to be avoided. Werner (1977a), and
Jones and Rauch (1978a) have indicated in these studies that Landsat
lineaments are associated with poor-yielding gas wells in the Cottage-
ville area.

Photolineaments by Orientation

Short photolineaments were next tested for possible associ-
ations with initial and final open flow gas production data within
the study area. Appendices F and G contain initial and final
open flow gas well yields, as well as the orientation, proximity,

and class of the nearest short photolineament for each gas well with production data.

Initial open flow gas well yield is higher for wells near a photolineament, but the association is not a strong one. It was therefore decided to test gas well yield against photolineament orientation. Figure 13 shows plots of initial open flow gas well yield versus photolineament orientation. Median trends for 30° classes, shown in Figure 13, indicate that photolineaments oriented N60°W-N30°E are associated with higher average gas well yields than are photolineaments of other orientations. Statistical test results of Table 7 indicate that gas wells located near photolineaments oriented N60°W-N30°E are relatively high producers when compared to wells located near photolineaments of other orientations. This association is statistically significant at a 0.05 alpha probability level. Short photolineaments bearing N60°W-N0°W show a somewhat less certain association with initial open flow gas well yield, while N0°E-N30°E oriented photolineaments are not significantly associated with open flow at the 0.10 alpha probability level. These results indicate that N60°W-N30°E oriented photolineaments, representing approximately 61 percent of the photolineaments within the gas field, are significantly associated with increased initial open flow gas well yield. However, subdivisions of this optimum 90° photolineament class do not show strong associations with initial open flow, and are not useful.
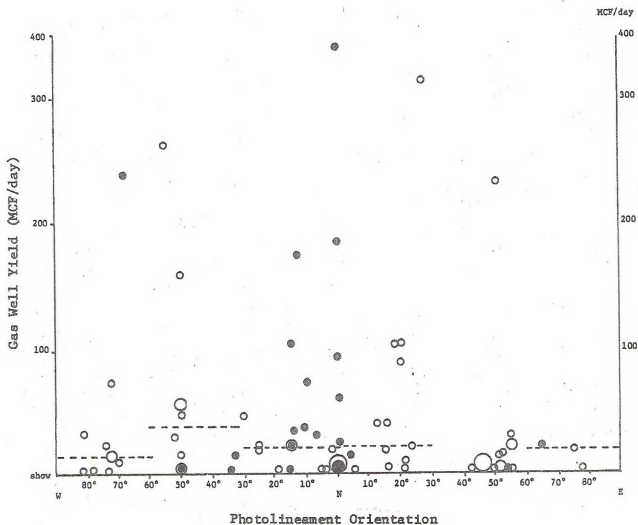
Figure 13 Plots of initial open flow gas well yield (in MCF/day) versus
orientation of the nearest photolineament to a gas well.
Solid dots indicate class "1" photolineaments, larger dots
indicate more than one well.

TABLE 7

INITIAL OPEN FLOW GAS WELL YIELD VERSUS PHOTOLINEAMENT ORIENTATION

(Measured to nearest photolineament)

Photolineament Orientation

	N60°W-N30°E	Others	Probability of error
No. of wells in each class	46	30	
Median well yield (MCF/day)	21-24	14-15	
Mann-Whitney U results (1-tailed)	H	L	0.026

	N60°W-N0°W	Others	Probability of error
No. of wells in each class	35	41	
Median well yield (MCF/day)	24	15	
Mann-Whitney U results (1-tailed)	H	L	0.078

	N0°E-N30°E	Others	Probability of error
No. of wells in each class	21	55	
Median well yield (MCF/day)	21	18	
Mann-Whitney U results (1-tailed)	H	L	0.179 (not significant)

Final open flow is higher on the average for wells near a photo-lineament, but the relationship appears not to be strong. Photolineament orientation was also investigated for stronger associations with final open flow. Figure 14 shows plots of final open flow gas well yield versus photolineament orientation. Again, median yields are greatest for the three photolineament orientation classes between N60°W-N30°E. Short photolineaments bearing N60°W-N30°E and N60°W-N0°W were tested to see if the same associations for initial open flow also show up for final open flow data. Table 8 shows the Mann-Whitney U tests for photo-lineament orientation by final open flow; gas wells located nearest photolineaments oriented N60°W-N0°W are on the average relatively high producers. This is a statistically significant association, at the 0.05 alpha probability level. Short photolineaments oriented N60°W-N30°E show a somewhat less certain relationship to increased final open flow, that would be significant at a 0.10 alpha probability level. The tests of Table 8 indirectly indicate that N0°E-N30°E oriented photo-lineaments are not so important with respect to increased final open flow as are N60°W-N0°W oriented photolineaments. Approximately 42 per-cent of the photolineaments in the gas field area are oriented N60°W-N0°W.

Photolineament Proximity

Initial open flow gas well yield was compared with the proximity
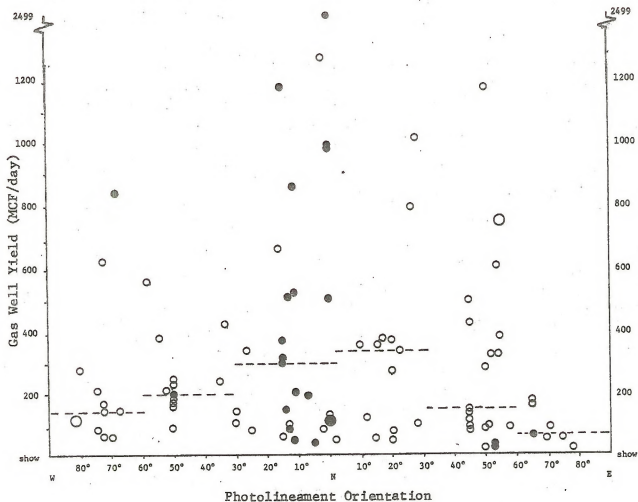
Figure 14 Plots of final open flow gas well yield (in MCF/day) versus orientation of the nearest photolineament to a gas well. Solid dots indicate class "1" photolineaments; larger dots indicate more than one well.

TABLE 8

FINAL OPEN FLOW GAS WELL YIELD VERSUS PHOTOLINEAMENT ORIENTATION

(Measured to nearest photolineament)

Photolineament Orientation

	N60°W–N0°W	Others	Probability of error
No. of wells in each class	40	56	
Median well yield (MCF/day)	202–207	146	
Mann–Whitney U results (1–tailed)	H	L	0.048

Photolineament Orientation

	N60°W–N30°E	Others	Probability of error
No. of wells in each class	55	41	
Median well yield (MCF/day)	207	146	
Mann–Whitney U results (1–tailed)	H	L	0.071

of photolineaments oriented N60°W-N30°E as shown in Figure 15. Statistical tests were performed that compared yields for gas wells within 0.4 kilometers of such photolineaments, with yields for wells located greater than 0.4 kilometers from the nearest photolineament. A critical distance of 0.4 kilometers was chosen because this distance appears to represent a natural break in the plotted yields. Only class "1" and "2" photolineaments were plotted in Figure 15 because they represent better than 95 percent of these photolineaments, and the most certain photolineament locations. It appears from the statistical results of Table 9 that Devonian shale gas wells located within 0.4 kilometers of photolineaments oriented N60°W-N30°E yield at significantly higher rates than do wells located greater than 0.4 kilometers distance of these photolineaments, in the gas field study area.

A direct test of final open flow gas well yield versus photolineament proximity by orientation was not conducted. However, results of other tests concerning final open flow and photolineament proximity by class indicate the importance of photolineament proximity to final open flow gas well yields. These associations are discussed later in this report with respect to 'Photolineaments by Class'.

Photolineament Density

Although photolineaments oriented N60°W-N30°E have a greater proportion of high-yielding gas wells in their vicinity, a more direct
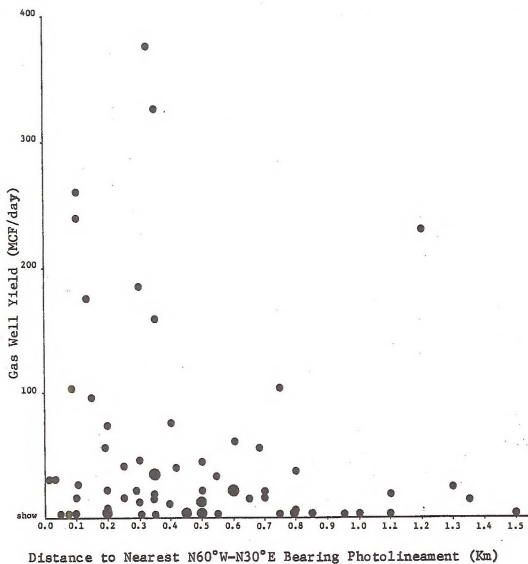
Figure 15 Plot of initial open flow gas well yield (in MCF/day) versus the well proximity to the nearest photolineament oriented N60°W-N30°E. Larger dots indicate more than one well.

TABLE 9

INITIAL OPEN FLOW GAS WELL YIELD VERSUS PHOTOLINEAMENT PROXIMITY

	Distance to nearest class "1" photolineament oriented N60°W–N30°E		
	≤0.4 Km.	>0.4 Km.	Probability of error
No. of wells in each class	17	13	
Median well yield (MCF/day)	30	15	
Mann-Whitney U results (1-tailed)	H	L	0.05

test of such photolineament associations was necessary to determine
their usefulness as an exploration tool. In order to test the use-
fulness of N60°W-N30°E bearing photolineaments in exploration for
Devonian shale gas, a density map was prepared for these lineaments
and compared to the gas yield trends of Figures 11 and 12. The density
map of Figure 16 was prepared as previously indicated in 'Data Analysis'
of this report. Figure 16 represents hand-contoured density in miles
per square mile, based on 100 square-mile sections. The photolineament
density map of Figure 16 was superimposed on the gas yield maps of
Figures 11 and 12, to determine if significant overlaps occur between
high photolineament density and high gas yield areas. A second orth-
ogonal grid defining square sections 2000 feet long on a side was super-
imposed on the overlays of Figure 16 on Figures 11 and 12; grid line
intersections were then counted as points occurring in one of four type
areas - high photolineament density and high gas yield; high photo-
lineament density and low gas yield; low photolineament density and
high gas yield; and low photolineament density and low gas yield.
The 221 grid points were categorized, totaled for each area type, and
plotted in 2x2 contingency tables. Chi-square contingency tests with
the Yates correction were then performed to determine if any significant
associations exist between N60°W-N30°E photolineament density and gas
yield, for both initial and final open flows and for various definitions
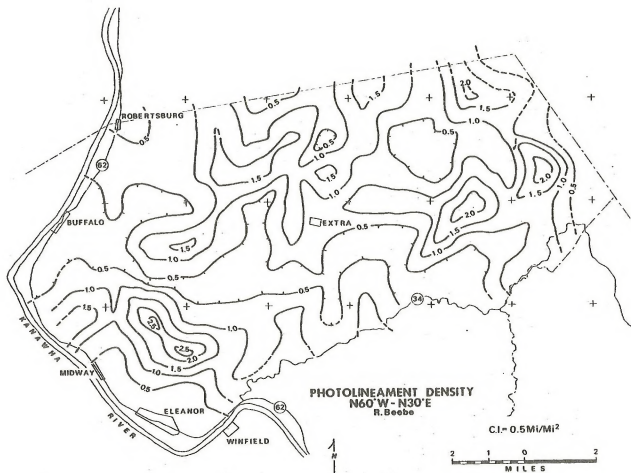of high versus low density and gas yield. The only data tested were for

Figure 16 Contoured density of photolineaments bearing N60 –N30 E of the Midway-Extra study area.
Density is in miles of photolineament length per square mile area.

grid points located within the polygonal area of Figure 10.

A second point counting technique was also used to test for associations between photolineament density and open flow gas production. This technique consisted of classifying individual Devonian shale gas wells within the polygonal area into 2x2 contingency tables for testing. However, statistical tests based on this technique are considered to be more biased than those based on the orthogonal-grid method of point counting, since gas wells are not randomly located; a greater number of gas wells have been drilled close to other successful gas wells. For this reason results from tests performed by this technique are not reported for all cases.

The Yates-corrected chi-square contingency tests (Siegel, 1956) were first performed on initial open flow production data for N60°W-N30°E photolineament density within the polygonal area. The 221 sample points were classified in two 2x2 contingency tests, comparing initial open flow gas yield greater than versus less than 100 MCF/day, with photolineament densities greater than versus less than 1.50 and 2.00 miles per square mile. Both statistical tests of Table 10 indicate that initial open flow gas well yield is significantly associated with N60°W-N30°E photolineament density at a 0.001 alpha probability level. A second set of 2x2 contingency tests were performed similar to those of Table 10, but considering 97 sample points represented by the individual gas well locations instead

TABLE 10

INITIAL OPEN FLOW GAS WELL YIELD
VERSUS
DENSITY OF N60°W-N30°E BEARING PHOTOLINEAMENTS

(Based on orthogonal grid point-counting method)

Photolineament Density

Gas Well Yield	Low	1.50 mi/mi^2	High	
Low	190		11	201
100 MCF/day				
High	11		9	20
	201		20	N=221

Probability of error $\leqslant 0.001$

chi-square = 29.9

Success rate= 45%

Photolineament Density

Gas Well Yield	Low	2.00 mi/mi^2	High	
Low	199		2	201
100 MCF/day				
High	15		5	20
	214		7	N = 221

Probability of error $\leqslant 0.001$

chi-square = 26.8

Success rate = 71%

of the orthogonal grid of points. Statistical test results of Table 11 indicate that initial open flow gas well yield is significantly associated with photolineament density with regard to the 1.50 and 2.00 miles per square mile density contours at the 0.001 and 0.01 alpha probability levels respectively. Although this last technique is considered biased with respect to its test results, it does tend to confirm observed trends found using the orthogonal grid method of point counting.

Tests were also performed for determination of possible associations between N60°W-N30°E photolineament density and final open flow gas production. A total of 221 orthogonal grid points, within the polygonal area, were classified into 2x2 contingency tables and the Yates-corrected chi-square tests were then performed. The test results of Table 12 indicate that N60°W-N30°E photolineament density is significantly associated with final open flow gas production for a critical density of 1.50 miles per square mile and critical production rates of 100, 500, and 1,000 MCF/day, at alpha probability values of 0.01, 0.001, and 0.05 respectively. Furthermore, N60°W-N30°E photolineament density is significantly associated with final open flow gas well yield for a critical density of 2.00 miles per square mile and critical production rates of 100 and 500 MCF/day, at alpha probabilities of 0.05 and 0.01 respectively. Another chi-square contingency test indicated that N60°W-N30°E photolineament

TABLE 11

INITIAL OPEN FLOW GAS WELL YIELD
VERSUS
DENSITY OF N60°W-N30°E BEARING PHOTOLINEAMENTS

(Based on gas well locations as points)

Photolineament Density

Gas Well Yield	Low 1.50 mi/mi^2	High	
Low	75	5	80
100 MCF/day			
High	9	8	17
	84	13	N = 97

Probability of error < 0.001

chi-square = 16.8

Success rate = 62%

Photolineament Density

Gas Well Yield	Low 2.00 mi/mi^2	High	
Low	79	1	80
100 MCF/day			
High	13	4	17
	92	5	N = 97

Probability of error < 0.01

chi-square = 10.0

Success rate = 80%

TABLE 12

FINAL OPEN FLOW GAS WELL YIELD
VERSUS
DENSITY OF N60°W–N30°E BEARING PHOTOLINEAMENTS
(Based on orthogonal grid point–counting method)

Photolineament Density

Gas Well Yield	Low 1.50 mi/mi^2	High		
Low	96	2	98	Probability of error < 0.01
100 MCF/day				chi-square = 9.0
High	106	17	123	Success rate = 89%
	202	19		N = 221

Photolineament Density

Gas Well Yield	Low 1.50 mi/mi^2	High		
Low	186	8	194	Probability of error < 0.001
500 MCF/day				chi-square = 35.9
High	16	11	27	Success rate = 58%
	202	19		N = 221

Photolineament Density

Gas Well Yield	Low 1.50 mi/mi^2	High		
Low	200	17	217	Probability of error < 0.05
1,000 MCF/day				chi-square = 4.3
High	2	2	4	Success rate = 11%
	202	19		N = 221

TABLE 12 (continued)

<u>Photolineament Density</u>

	Low	High		
<u>Gas Well Yield</u>	2.00 mi/mi^2			Probability of
Low	96	0	96	error < 0.05
100 MCF/day				chi-square = 3.9
High	118	7	125	Success rate = 100%
	214	7	N = 221	

<u>Photolineament Density</u>

	Low	High		
<u>Gas Well Yield</u>	2.00 mi/mi^2			Probability of
Low	186	3	189	error < 0.01
500 MCF/day				chi-square = 7.4
High	28	4	32	Success rate = 57%
	214	7	N = 221	

density is not significantly associated with gas well yield when critical values of 2.00 miles per square mile and 1,000 MCF/day final open flow gas production are considered, at the 0.10 alpha probability level.

Results of statistical tests indicate that N60°W-N30°E photolineament density could serve as the basis for a new exploration tool for Devonian shale gas, especially in the Midway-Extra area. The success rate of each 2x2 contingency test was determined by the percentage of gas wells in high photolineament density areas that have high yields. Success rate is in this way a measure of the probability of successfully locating 'high' yielding gas wells as a function of a specific photolineament density contour. Table 10 indicates that if gas wells are located within areas having N60°W-N30°E photolineament densities greater than 2.00 miles per square mile, about 71 percent of these wells would have initial open flows exceeding 100 MCF/day. If gas wells were located in areas having N60°W-N30°E photolineament densities greater than 1.50 miles per square mile, about 45 percent of these wells would have initial open flows exceeding 100 MCF/day. Table 12 indicates that if gas wells were located within areas having N60°W-N30°E photolineament densities greater than 1.50 miles per square mile, about 89 percent of these wells would have final open flows exceeding 100 MCF/day; about 58 percent of these wells would have final open flows exceeding 500 MCF/day; and about

11 percent of these wells would have final open flows exceeding 1,000 MCF/day. If gas wells were located in areas having N60°W-N30°E photolineament densities greater than 2.00 miles per square mile, about 100 percent of these wells would have final open flows exceeding 100 MCF/day, and about 57 percent of these wells would have final open flows exceeding 500 MCF/day. These test results indicate that the 2.00 miles per square mile photolineament density contour is the more successful for gas exploration of the two N60°W-N30°E photolineament density contours tested. However, photolineament density areas exceeding 2.00 miles per square mile are smaller than those exceeding 1.50 miles per square mile, which would place greater restrictions on gas exploration.

Photolineaments by Class

The possible effects of photolineament class on photolineament-gas well yield associations were next tested for initial and final open flow gas well yields. These tests were conducted by comparing the yield of each gas well within the polygonal area to the class of the nearest photolineament to each well. Appendix F contains a list of initial open flow data tested, and Appendix G contains a list of final open flow data tested. These data consist of gas well yield in MCF/day, the distance in kilometers from each of these wells to the nearest photolineament, and the photolineament orientation

and classification.

The effect of photolineament class was determined by the Mann-Whitney U test, with test results shown in Table 13 for initial open flow data. Although initial open flow is usually higher for wells located nearest a class "1" (most certain) photolineament, it is not significantly higher, at the 0.05 alpha probability level, when considering photolineaments of any orientation. However, when N60°W-N30°E photolineament orientation alone is considered, Table 13 indicates that class "1" photolineaments are significantly associated with increased initial open flow gas well yield at a 0.05 alpha probability level, when compared to class "2" and "3" photolineaments.

Final open flow data were next tested for possible associations of gas well yield with photolineaments based on class. The Mann-Whitney U test results of Table 14 indicate that final open flow is not significantly higher for gas wells near class "1" photolineaments at a 0.05 alpha probability level, when photolineament orientation is ignored. However, when just photolineaments oriented N60°W-N0°W are considered, class "1" photolineaments are significantly associated with high final open flows for nearby gas wells at a 0.10 alpha probability level, when compared to yields of wells near class "2" and "3" photolineaments. These combined test results tend to indicate that the class or certainty of expression of photolineaments may be important in associations with gas well yield, but that photolineament class should be used in con-

TABLE 13

INITIAL OPEN FLOW GAS WELL YIELD VERSUS PHOTOLINEAMENT CLASSIFICATION

(Measured to nearest photolineament)

Photolineaments of any orientation

	Class "1"	Class "2" & "3"	Probability of error
No. of wells in each class	23	53	
Median well yield (MCF/day)	24	17	
Mann-Whitney U results (1-tailed)	H	L	> 0.05 (not significant)

Photolineaments oriented N60°W-N30°E

	Class "1"	Class "2" & "3"	Probability of error
No. of wells in each class	21	28	
Median well yield (MCF/day)	24	21	
Mann-Whitney U results (1-tailed)	H	L	0.048

TABLE 14

FINAL OPEN FLOW GAS WELL YIELD VERSUS PHOTOLINEAMENT CLASSIFICATION
(measured to the nearest photolineament)

Photolineaments of any Orientation

	Class "1"	Class "2" & "3"	Probability of error
No. of wells in each class	29	67	
Median well yield (MCF/day)	298	163	
Mann-Whitney U results (1-tailed)	H	L	> 0.10 (not significant)

Photolineaments Oriented N60°W–N0°W

	Class "1"	Class "2" & "3"	Probability of error
No. of wells in each class	23	17	
Median well yield (MCF/day)	315	189	
Mann-Whitney U results (1-tailed)	H	L	0.064

junction with other more important geologic criteria, such as photo-
lineament orientation, for gas exploration in Devonian shales.

Photolineament Proximity

Initial and final open flow gas well yields were next tested
for possible associations with the proximity of gas wells to the near-
est photolineament of a certain class. Figure 17 shows plots of initial
open flow gas well yield versus gas well proximity to the nearest class
"1" or "2" photolineament. A natural break in this plot may occur at
0.4 kilometers, with most high-yielding wells located within 0.4 kilo-
meters of a class "1" or class "2" photolineament. However, Mann-
Whitney U test results of Table 15 indicate that gas wells located
within 0.4 kilometers distance of class "1" or "2" photolineaments are
not significantly associated with higher initial open flow, at the 0.05
alpha probability level. The same test results occurred for wells near
class "1" photolineaments, as shown in Table 15. However, Table 9 also
indicates that gas wells located within 0.4 kilometers of class "1"
photolineaments oriented N60°W-N30°E yield significantly greater amounts
of natural gas than do wells located further than 0.4 kilometers from
such photolineaments, at a 0.05 alpha probability level.

Figure 18 illustrates plots of final open flow gas well yield
versus class "1" photolineament proximity. Again, it appears that high
yields are associated with wells located within 0.4 kilometers of a
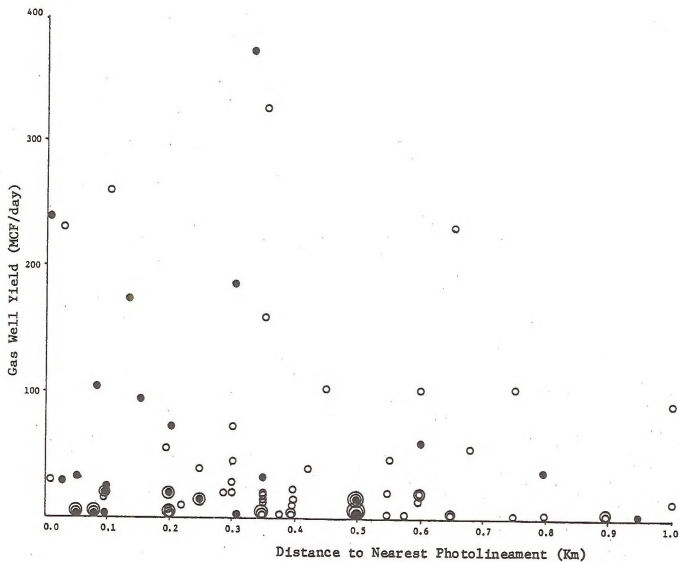
Figure 17 Plot of initial open flow versus gas well proximity to
the nearest class "1" or "2" photolineament. Larger dots
represent more than one well. Black dots represent wells
near class "1" photolineaments.

TABLE 15

INITIAL OPEN FLOW GAS WELL YIELD
VERSUS
PROXIMITY OF PHOTOLINEAMENTS BY CLASS
(measured to the nearest photolineament)

class "1" or "2" photolineaments

	≤0.4 Km.	>0.4 Km.	Probability of error
No. of wells in each class	44	21	
Median well yield (MCF/day)	21	15	
Mann-Whitney U results (1-tailed)	H	L	>0.05 (not significant)

class "1" photolineaments

	≤0.4 Km.	>0.4 Km.	Probability of error
No. of wells in each class	17	6	
Median well yield (MCF/day)	30	show-15	
Mann-Whitney U results (1-tailed)	H	L	>0.05 (not significant)
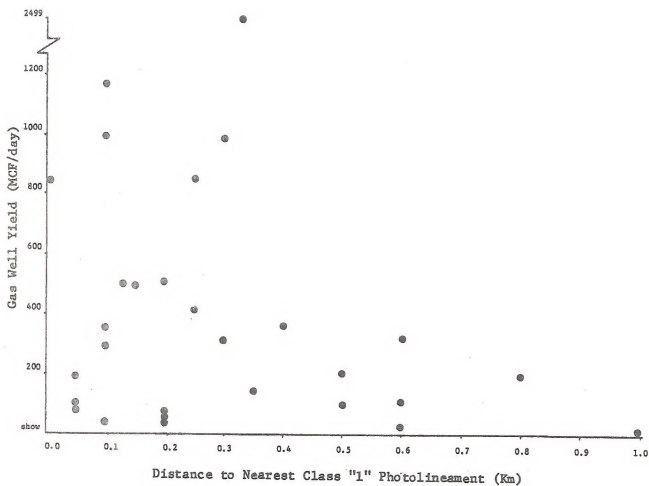
Figure 18 Plots of final open flow versus gas well proximity to
the nearest class "1" photolineament.

class "1" photolineament. The Mann-Whitney U test was used to determine if any significant associations exist between final open flow gas well yield and photolineament proximity. The statistical test results of Table 17 indicate that class "1" photolineaments do relate to final open flow for nearby gas wells, whereas class "2" and "3" photolineaments do not. Table 17 indicates that only gas wells located within 0.4 kilometers of a class "1" photolineament yield at significantly higher rates (at a 0.05 alpha) than do gas wells located greater than 0.4 kilometers from class "1" photolineaments. However, it should be noted that approximately 86 percent of these class "1" photolineaments have N60°W-N0°W orientations. The significant test result for class "1" photolineaments may therefore be a function of photolineament orientation more than photolineament class.

Photolineament Density

Although class "1" photolineaments appear to have a greater proportion of high-yielding gas wells in their vicinity, a more direct test of such photolineament associations was necessary to determine their usefulness as an exploration tool. In order to test the usefulness of class "1" photolineaments in exploration for Devonian shale gas, a density map was prepared for these lineaments and compared to the gas yield trends of Figures 11 and 12. The density map of Figure 19 was prepared as previously indicated in "Data Analysis" of this re-

TABLE 16

FINAL OPEN FLOW GAS WELL YIELD VERSUS PROXIMITY OF
PHOTOLINEAMENTS BY CLASS
(Measured to nearest photolineament)

Class "1" Photolineaments

	≤0.4 Km.	>0.4 Km.	Probability of error
No. of wells in each class	22	7	
Median well yield (MCF/day)	367-377	103	
Mann-Whitney U results (1-tailed)	H	L	0.018

Class "1" & "2" Photolineaments

	≤0.4 Km.	>0.4 Km.	Probability of error
No. of wells in each class	52	28	
Median well yield (MCF/day)	211-207	169-189	
Mann-Whitney U results (1-tailed)	H	L	>0.10 (not significant)

Class "1", "2", & "3" Photolineaments

	≤0.4 Km.	>0.4 Km.	Probability of error
No. of wells in each class	63	33	
Median well yield (MCF/day)	169	163	
Mann-Whitney U results (1-tailed)	H	L	>0.10 (not significant)
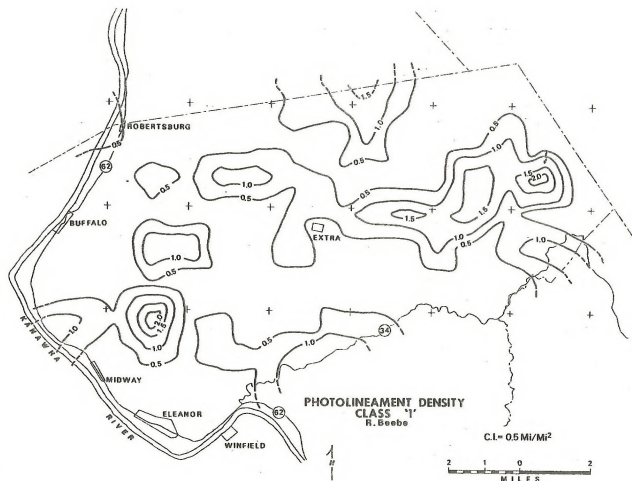
Figure 19 Contoured density map of class "1" photolineaments for the
Midway-Extra study area.

port. Figure 19 represents hand-contoured density in miles per square mile, based on 100 square-mile sections. The class "1" photolineament density map of Figure 19 was superimposed on the gas yield maps of Figures 11 and 12, to determine if significant overlaps occur between high photolineament density and high gas yield areas. A second ortho- gonal grid defining sections 2000 feet square was superimposed on the overlays of Figure 19 on Figures 11 and 12; grid line intersections were then counted as points occurring in one of four type areas - high photolineament density and high gas yield; high photolineament density and low gas yield; low photolineament density and high gas yield; and low photolineament density and low gas yield. The 221 grid points were categorized, totaled for each area type, and plotted in 2x2 con- tingency tables. Chi-square contingency tests with the Yates correction were then performed to determine if any significant associations exist between class "1" photolineament density and gas yield, for both initial and final open flows and for various definitions of high versus low density and gas yield. The only data tested were for grid points located within the polygonal area of Figure 10.

A second point counting technique was also used to test for as- sociations between photolineament density and open flow gas production. This technique consisted of classifying individual Devonian shale gas wells within the polygonal area into 2x2 contingency tables for testing. However, statistical tests based on this technique are considered to be

more biased than those based on the orthogonal-grid method of point counting. For this reason results from tests performed by this technique are not reported for all cases.

Yates-corrected chi-square (2x2) contingency tests were performed with respect to initial open flow gas well yield and the density of class "1" photolineaments shown in Figure 19. Density contours of 0.50 and 1.00 miles per square mile were used and test results are shown in Table 17. These test results indicate that class "1" photolineament density is not significantly associated with high initial open flow gas well yield at a 0.10 alpha probability level. Furthermore, the calculated rate of success is less than 10 percent for each case.

Chi-square (2x2) contingency tests were also performed to determine the existence of possible associations between class "1" photolineament density and final open flow gas well yield by comparing Figure 19 with Figure 12. A total of 221 sample points, obtained from the orthogonal grid within the polygonal area, were classified into four 2x2 contingency tables for the Yates-corrected chi-square tests. The results of Table 18 indicate that class "1" photolineament densities greater than 0.50 miles per square mile are significantly associated with final open flow gas well yield exceeding 100 and 500 MCF/day, with alpha probabilities of 0.10 and 0.01 respectively. Table 18 indicates that class "1" photolineament densities greater than 1.00 miles per

TABLE 17

INITIAL OPEN FLOW GAS WELL YIELD
VERSUS
DENSITY OF CLASS "1" PHOTOLINEAMENTS

(Based on orthogonal grid point-counting method)

Photolineament Density

Gas Well Yield	Low 0.50 mi/mi^2	High		
Low 100 MCF/day	128	72	200	Probability of error >0.10 (not significant) chi-square = 0.0
High	14	7	21	Success rate = 9%
	142	79	N = 221	

Photolineament Density

Gas Well Yield	Low 1.00 mi/mi^2	High		
Low 100 MCF/day	180	20	200	Probability of error >0.10 (not significant)
High	19	2	21	chi-square = 0.2 Success rate = 9%
	199	22	N = 221	

TABLE 18

FINAL OPEN FLOW GAS WELL YIELD
VERSUS
DENSITY OF CLASS "1" PHOTOLINEAMENTS

(Based on orthogonal grid point-counting method)

Photolineament Density

Gas Well Yield	Low 0.50 mi/mi^2	High		
Low	63	32	95	Probability of error ⩽ 0.10
100 MCF/day				chi-square = 3.3
High	67	59	126	Success rate = 65%
	130	91	N = 221	

Photolineament Density

Gas Well Yield	Low 0.50 mi/mi^2	High		
Low	121	72	193	Probability of error ⩽ 0.01
500 MCF/day				chi-square = 8.2
High	9	19	28	Success rate = 21%
	130	91	N = 221	

TABLE 18 (continued)

Photolineament Density

	Low	High	
Gas Well Yield	1.00 mi/mi^2		
Low	124	8	132
100 MCF/day			
High	74	15	89
	198	23	N = 221

Probability of error ≤ 0.05

chi-square = 5.5

Success rate = 65%

Photolineament Density

	Low	High	
Gas Well Yield	1.00 mi/mi^2		
Low	180	14	194
500 MCF/day			
High	18	9	27
	198	23	N = 221

Probability of error ≤ 0.001

chi-square = 14.7

Success rate = 39%

square mile are significantly associated with final open flow gas
well yields exceeding 100 and 500 MCF/day, with alpha probability
levels of 0.05 and 0.001 respectively. A similar set of tests were
performed with the 104 individual gas wells having final open flow
production data as points. The test results of Table 19 indicate
that class "1" photolineament densities greater than 0.50 miles per
square mile are significantly associated with final open flow gas
well yield exceeding 500 MCF/day, at a 0.10 alpha probability level.
Also, class "1" photolineament density areas of greater than 1.00
miles per square mile are significantly associated with final open
flow gas well yields exceeding 500 MCF/day, at a 0.01 alpha proba-
bility level. The statistical test results of Table 18 are consid-
ered to be more trustworthy than those of Table 19. As mentioned
earlier in this report, the technique of point counting individual
gas wells is biased because the points represented by these wells
are not mutually independent observations in the statistical sense.

Results of these statistical tests indicate that class "1" photo-
lineament density could serve as the basis for a moderately success-
ful exploration tool for locating Devonian shale gas wells in the
Midway-Extra area. Table 18 indicates that if gas wells are located
within areas having class "1" photolineament densities exceeding 0.50
miles per square mile, about 65 percent of these wells would have
final open flows exceeding 100 MCF/day, and only about 20 percent of

TABLE 19

FINAL OPEN FLOW GAS WELL YIELD
VERSUS
DENSITY OF CLASS "1" PHOTOLINEAMENTS

(Based on gas well locations as points)

Photolineament Density

Gas Well Yield	Low 0.50 mi/mi^2	High	
Low -500 MCF/day	60	25	85
High	9	10	19
	69	35	N = 104

Probability of error < 0.10

chi-square = 2.8

Success rate = 29%

Photolineament Density

Gas Well Yield	Low 1.00 mi/mi^2	High	
Low 500 MCF/day	81	4	85
High	13	6	19
	94	10	N = 104

Probability of error < 0.01

chi-square = 10.0

Success rate = 60%

these wells would have flows exceeding 500 MCF/day. Table 18 indicates that if gas wells are located in areas with class "1" photolineament densities exceeding 1.00 miles per square mile, approximately 64 percent of these wells would have flows exceeding 100 MCF/day, and about 39 percent of these wells would have final open flows exceeding 500 MCF/day. Table 19 indicates that gas wells located in areas with class "1" photolineament densities exceeding 0.50 miles per square mile, about 29 percent of these wells would have final open flows exceeding 100 MCF/day. In areas with class "1" photolineament densities exceeding 1.00 miles per square mile, about 60 percent of these wells would have flows exceeding 500 MCF/day. Analysis of Table 19 indicates that the proportion of wells yielding over 500 MCF/day exceed the proportion of random grid points in these categories (from Table 18). This fact supports the argument for biased statistical tests involving gas wells as points, since gas wells are not independently located.

A comparison of test results indicate that N60°W-N30°E photolineament density is a better and more accurate exploration tool for locating successful Devonian shale gas wells than is class "1" photolineament density. This might be explained by the fact that classifications of certainty is subjective in nature, while photolineament orientation is not. Also, most class "1" (most certain) photolineaments have the critical N60°W-N30°E orientation.

Summary and Interpretation of Lineament Associations

Test results from both the Mann-Whitney U and the Yates-corrected chi-square (2x2) contingency tests indicate that N60°W-N30°E (and N60°W-N0°W) oriented photolineaments would be important exploration tools for locating successful Devonian shale gas wells in the Midway-Extra area. Locating wells near one or more photolineaments of the right orientation should aid in gas exploration, but all photolineaments (of any orientation or class) are not in general useful. Locating wells near one or more class "1" (most certain) photolineaments, would also appear to be less useful for locating successful Devonian shale gas wells than locating wells near photolineaments oriented N60°W-N30°E and especially N60°W-N0°W. Furthermore, Landsat lineaments appear to have adverse effects on production rates from Devonian gas shale reservoirs.

Test results concerning photolineament orientation and increased Devonian shale gas production, are consistent with the results of Jones and Rauch (1978a) in the Cottageville field of Jackson County, West Virginia. Their findings indicate that gas wells located nearby short photolineaments bearing N60°W-N90°W (WNW) yield at significantly greater rates than do gas wells located near other photolineaments. Martin and Nuckols (1976), found the fracture orientations to be primarily N40°E-N50°E in geologic cores taken from the gas producing horizons (Zones II and III) within the cottageville field. More importantly Larese and Heald (1977) noted that in part of Zone II (the primary reservoir in the

Cottageville field), the primary mineralized fracture trend is about N80°–90°W. The N60°–90°W bearing photolineaments studied by Jones and Rauch (1978a) may therefore represent permeable fractures of the same orientation within Zone II of the Devonian shales. Seismic evidence indicates the presence of Basement faulting, associated with the west side of the Rome trough, dissipating upward into the Devonian shales; this may be the source of fracturing in these shales (Shumaker, et. al., 1979).

The optimum WNW photolineament trend in the Cottageville area is oriented at about a 60° angle to the regional structural trend of N40°–50°E. The regional structural trend in the Midway-Extra area is approximately N60°–70°E, and the optimum photolineament orientation of N60°W–N30°E (or N60°W–N0°W) is about 60°–90° different from this regional structural trend. It appears that the northerly change in regional trend from Midway-Extra to the Cottageville gas field may be consistent with the westerly change in optimum photolineament orientation between Midway-Extra and Cottageville gas fields. This suggests that fractures oriented 60°–90° off strike are critical in defining the cross-strike extent of these shale gas fields.

GROUND-WATER ASSOCIATIONS WITH GAS WELL YIELD

Water-Well Yield

Water well yield was compared to initial and final open flow gas well yields to determine if any associations exist that would suggest a new gas exploration tool based on water well yield. Yields in gallons per minute were obtained and tested for a total of 29 water wells in the polygonal gas field area. The Mann-Whitney U test was used to statistically test these possible associations. In constructing data for the Mann-Whitney U tests of Table 20, yields of the nearest gas well to each of the 29 water wells were considered, and water well yield was treated as the independent variable in classifying water well-gas well pairs into one of two groups for testing. Two groups of well pairs were compared for gas well yield, pairs with water well yield exceeding 1.0 gpm (the median yield) versus pairs with water well yield equal to or less than 1.0 gpm. Statistical test results of Table 20 indicate that water well yield is not significantly associated with gas well yield at a 0.05 alpha probability level. Likewise, no definite trends between water well yield and gas well yield were discovered for the Cottageville gas field (Jones and Rauch, 1978a).

Ground-Water Chemistry

The ground-water chemical parameters of Appendix B were next tested

TABLE 20

INITIAL OPEN FLOW GAS WELL YIELD VERSUS WATER WELL YIELD

	≤ 1.0 gpm	> 1.0 gpm	Probability of error
No. of wells in each class	12	17	
Median well yield (MCF/day)	17	show-15	
Mann-Whitney U results (1-tailed)	H	L	> 0.10 (not significant)

FINAL OPEN FLOW GAS WELL YIELD VERSUS WATER WELL YIELD

	≤ 1.0 gpm	> 1.0 gpm	Probability of error
No. of wells in each class	12	17	
Median well yield (MCF/day)	47	145=280	
Mann-Whitney U results (1-tailed)	L	H	> 0.10 (not significant)

against expected (contoured) initial and final open flow gas well
yield, to determine if any associations are present. These chemical
parameters were tested for 19 water wells sampled within the Midway-
Extra gas field. Of all the chemical parameters tested, none show
statistically significant associations with initial open flow and
just two exhibit significant associations with final open flow.
Figure 20 shows plots of chemical concentrations for bicarbonate and
nitrate versus final open flow gas well yield. These are the only
two chemical parameters displaying strong associations with final
open flow. The two horizontal lines of the scattergram in Figure
20 separate the gas well yields into high and low classes, for com-
parison with chemical concentrations of bicarbonate and nitrate.
Table 21 contains the Mann—Whitney U test results for the data plotted
in Figure 20. The test results indicate that bicarbonate and nitrate
are significantly higher for water wells located in gas field areas
exceeding 100 MCF/day final open flow. These associations are statis-
tically significant at alpha probabilities of 0.05 and 0.025 for
bicarbonate and nitrate respectively. Other chemical parameters of
Appendix B do not significantly relate to expected gas well yield in
the study area. Chemical concentrations were not tested with respect
to 500 MCF/day contoured areas because too few water wells are located
in such areas.

The plotted data of Figure 20 indicate that optimum sites for
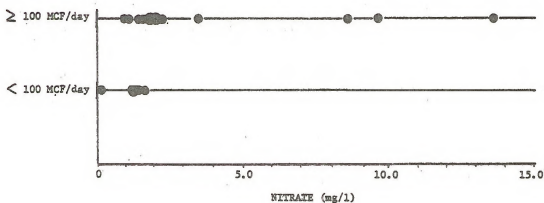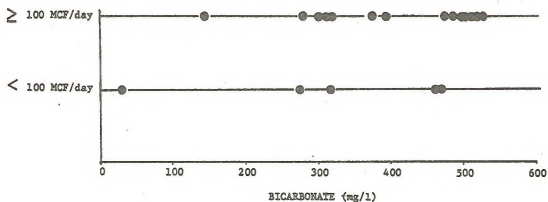
Figure 20 Plots of chemical concentrations of bicarbonate and
nitrate versus final open flow gas well yield, within
the polygonal area of the Midway-Extra gas field.
Larger dots indicate more than one well.

TABLE 21

FINAL OPEN FLOW GAS WELL YIELD VERSUS BICARBONATE CONCENTRATION

	≧100 MCF/day	<100 MCF/day	Probability of error
No. of wells in each class	14	5	
Median Bicarbonate Concentration (mg/l)	397-474	319	
Mann-Whitney U results (1-tailed)	H	L	< 0.05

FINAL OPEN FLOW GAS WELL YIELD VERSUS NITRATE CONCENTRATION

	≧100 MCF/day	<100 MCF/day	Probability of error
No. of wells in each class	14	5	
Median Nitrate Concentrations (mg/l)	1.87-1.98	1.32	
Mann-Whitney U results (1-tailed)	H	L	< 0.025

high-yielding Devonian shale gas wells would be near water wells
having at least 470 mg/1 bicarbonate or at least 1.75 mg/1 nitrate.
From the data tested, about 43 percent of the tested water well sites
in high-yielding gas areas (with over 100 MCF/day final open flow)
exceed 470 mg/1 bicarbonate. Likewise, approximately 70 percent of
the water wells in high-yielding gas areas exceed 1.75 mg/1 nitrate.
On the other hand, no tested wells in low yielding gas areas (with
less than 100 MCF/day final open flow) have chemical concentrations
over 470 mg/1 bicarbonate or over 1.75 mg/1 nitrate.

Jones and Rauch (1978a), in their study of water quality para-
meters and expected natural open flow for gas wells in the Cottageville
area, found that expected gas yield tends to be higher near water wells
with high concentrations of bicarbonate, total hardness, nitrate, and
sulfate. The chemical parameters of ground water which seem to best
relate to expected gas yield in the Cottageville area are bicarbonate
and total hardness concentrations (Jones and Rauch, 1978a). These
parameters show the strongest statistical associations which are least
likely to be coincidental, according to Jones and Rauch (1978a). From
their tested data, they found that about 83 percent of the selected well
sites with over 500 mg/1 bicarbonate have high expected initial open
flows (over 100 MCF/day). The similarities in research findings between
this study and that of Jones and Rauch (1978a) strongly suggest that
some relationship exists between gas production potential and shallow

ground-water chemistry, for at least bicarbonate and nitrate.

A possible explanation may be offered for the extraordinarily high concentrations of bicarbonate in shallow ground waters of the high-producing gas areas; some bicarbonate in these cases may be generated by the oxidization of methane gas by bacteria to form bicarbonate (Rauch, oral communication, 1979). It is possible that trace amounts of methane gas could be migrating upward from the Devonian shales along fracture zones. Once in shallow ground water, such gas would be unstable and oxidize with the help of bacteria, creating high concentrations of bicarbonate over a prolonged time period. No explanations are readily apparent for the observed association between high ground-water nitrate concentration and high final open flow gas well yield. It is possible that this relationship is coincidental, and nitrate may be concentrating in shallow ground water from surface contamination sources, such as septic tanks. However, it is also possible that high nitrate concentrations are tied up in some way with Devonian shale gas production, since Jones and Rauch (1978a) also found nitrate to be associated with high expected gas well yield (over 100 MCF/day). From results obtained so far, ground water chemistry may well prove to be useful in the future as a new exploration tool for locating successful Devonian shale gas wells.

SUMMARY OF CONCLUSIONS

Based on the data collected for this report and statistical analyses performed on that data, the following conclusions concerning hydrogeologic criteria and Devonian shale gas production can be drawn.

1] Landsat lineaments have no apparent effect on water well yields, and are associated with low natural gas production in the Midway-Extra gas field.

2] Water well yields are greater for wells within 200 feet of a short photolineament than for wells located greater than 200 feet from such photolineaments.

3] Topographic position significantly affects water well yields in the study area. Valley wells yield at significantly greater rates than do hillside, slope, or hilltop water wells.

4] In general, ground-water quality in northeastern Putnam County is good, with only a few cases where the maximum recommended concentrations were exceeded.

5] Gas wells located nearest short photolineaments oriented N60°W-N30°E and especially N60°W-N0°W are relatively high producers on the average, with respect to initial and final open flow gas well yields. Short photolineament orientation is therefore useful to con-

sider for locating high-yielding Devonian shale gas wells.

6] Gas well proximity to short photolineaments is not significantly associated with gas well yield in general. However, when photolineaments oriented N60°W-N30°E are considered, there is a significant association between gas well yield and photolineament proximity. Specifically, when gas wells are located within 0.4 kilometers of such a photolineament, they tend to yield significantly greater amounts of natural gas in the Midway-Extra area.

7] High N60°W-N30°E photolineament density areas, when compared to contoured trends for initial and final open flow gas well yields, show a significant association with high Devonian shale gas production. Photolineament density could therefore serve as the basis for a new exploration tool for locating successful Devonian shale gas wells in the Midway-Extra area.

8] Initial and final open flows are not significantly greater for gas wells near class "1" (most certain) photolineaments compared to wells near less certain photolineaments. However, class "1" photolineaments oriented N60°W-N30°E are especially well associated with high producing gas wells.

9] High density areas for class "1" photolineaments are significantly associated with high initial and final open flow gas well yield, but these results are less significant and less useful than associations for N60°W-N30°E photolineament density.

10] Water well yield shows no significant relationship with initial or final open flows for nearby gas wells.

11] Statistical tests indicate that final open flow gas well yield tends to be higher near water wells with high concentrations of bicarbonate and nitrate. Sites where ground-water concentrations exceed 470 mg/l for bicarbonate or 1.75 mg/l for nitrate are especially well associated with high-yielding gas wells. These two ground-water parameters might be applicable in exploration for Devonian shale gas in other areas. Other chemical parameters did not significantly relate to increased expected gas well yield.

REFERENCES

Bagnall, W.D., and Ryan, W.M., 1976, The Geology, Reserves and Production Characteristics of the Devonian Shale in Southwestern West Virginia: Proceedings of the 7th Appalachian Petroleum Geology Symposium, MERC/SP-76/2, ERDA, Morgantown, West Virginia, pp 41-53.

Brown and Others, 1970, Methods for Collection and Analysis of Water Samples for Dissolved Minerals and Gases: Techniques of Water-Resources Investigations of the United States Geol. Survey, Book 5, Chpt. A1, 160 p.

Davis, S.N., and DeWiest, R., 1966, Hydrogeology: John Wiley and Sons Inc., New York, pp 364-374.

Friel, E.L., and Bain, G.L., 1971, Records of Wells, Springs and Test Borings, Chemical Analysis of Water, Sediment Analysis, Standard Stream Flow Data Summaries, and Selected Drillers Logs from the Little Kanawha River Basin in West Virginia: Water Resources Division, U.S. Geol. Survey, Basic Data Report No. 2, 76 p.

Hach Chemical Company, 1973, Methods Manual for Use with Hach DR-EL Direct Reading Engineers Laboratory Series, 9th edition; 119 p.

Hach Chemical Company, 1977, Methods Manual for Use with Hach DR-EL Direct Reading Engineers Laboratory Series, 13th edition; 173 p.

Hem, J.D., 1970, Study and Interpretation of Chemical Characteristics of Natural Water (2nd edition) U.S. Geol. Survey Water Supply Paper No. 1473, 363 p.

Hunt, J., 1978, How Much is Enough? A Minimum Well Formula: Water
    Well Jour., Vol. 1, pp 53-56.

Jacob, C.E., 1963, The Recovery Method for Determining the Coefficient
    of Transmissibility: U.S. Geol. Survey, Water Supply Paper
    1536-I, pp 283-292.

Johnson, E.E., 1975, Ground Water and Wells: Johnson Division
    Universal Oil Products Co., 4_{th} edition, Minneapolis Minnesota,
    440 p.

Jones, S.D., and Rauch, H.W., 1978a, Lineaments and Ground-Water
    Quality as Exploration Tools for Ground-Water and Gas in the
    Cottageville Area of Western West Virginia: Preprints of the
    2_{nd} Eastern Gas Shale Symposium, MERC, Morgantown, West Virginia,
    pp 196-205.

Jones, S.D., and Rauch, H.W., 1978b, A Hydrogeologic Study of Water
    Well Yields and Ground-Water Quality Related to Stratigraphic
    and Structural Settings in Western Jackson County, West Virginia:
    final research report for the Mid-Ohio Valley Regional Council,
    and on open file at the Morgantown Energy Technology Center,
    Morgantown, West Virginia, 19 p.

Kirk, K.G., 1976, Evaluation of the Tri-Potential Resistivity Technique
    in Locating Cavities, Fracture Zones, and Aquifers: research
    report on open file at the Morgantown Energy Technology
    Center, Morgantown, West Virginia, 81 p.

Krauskopf, D.B., 1967, Introduction to Geochemistry: McGraw-Hill, New York, pp 28-116.

Krebs, C.E., 1911, Jackson, Mason, and Putnam Counties: a geological report of the West Virginia Geological and Economic Survey, Morgantown, West Virginia, 387 p.

Larese, R.E., and Heald, M.T., 1977, Petrography of Selected Devonian Shale Core Samples from the CGTC 11940 Wells, Lincoln and Jackson Counties, West Virginia: U.S. ERDA MERC/CR-77/6, 26 p.

LaRiccia, M.P., and Rauch, H.W., 1977, Water Well Productivity Related to Photo-Lineaments in Carbonates of Frederick Valley, Maryland: Proceedings of the 12th International Symposium on Hydrologic Problems in Karst Regions (held at Western Kentucky University, 1976).

Lattman, L.H., 1958, Technique of Mapping Geologic Fracture Traces and Lineaments on Aerial Photographs: Photogrammetric Engineering, Vol. 24, pp 568-576.

Lattman, L.H., and Parizek, R.R., 1964, Relationship between Fracture Traces and the Occurrence of Ground Water in Carbonate Rocks: Jour. of Hydrology, Vol. 2, pp 73-91.

Martin, P., and Nuckols, E.B., 1976, Geology and Oil and Gas in the Devonian Shales: Northern West Virginia: Proceedings of the 7th Appalachian Petroleum Geology Symposium; Morgantown, West Virginia, MERC/SP-76/2, pp 20-40.

Ryan, W.M., 1976, Remote Sensing Fracture Study, Western Virginia and Southeastern Kentucky: U.S. ERDA MERC/SP-76/2, pp 4-19.

Schaefer, W.W., 1979, Geology and Producing Characteristics of Certain Brown Shales in the Midway-Extra Field, Putnam County, West Virginia: Unpublished Masters Thesis, West Virginia University, Morgantown, West Virginia, 61 p.

Shumaker, R.C., et. al., 1979, Parameters of Geologic Structure Which Affect Devonian Shale Gas Production in West Virginia and Eastern Kentucky - A Progress Report - 1978-79, in press.

Siddiqui, S.H., and Parizek, R.R., 1971, Hydrogeologic Factors Influencing Well Yields in Folded and Faulted Carbonate Rocks in Central Pennsylvania: Water Resources Research, Vol. 7, pp 1259-1312.

Siegel, S.M., 1956, Nonparametric Statistics for Behavioral Sciences: McGraw-Hill, New York, pp 95-127.

Sole, T.L., 1975, The Hydrology and Ground Water Chemistry of Pricetown, Wetzel County, West Virginia: Unpublished Masters Thesis, West Virginia University, Morgantown, West Virginia, 79 p.

Steele, K.F., et. al., 1976, Relationship between Linears and Water Quality in a Carbonate Terrane: G.S.A. Abstracts with Programs, Vol. 8, No. 1, pp 66-67.

Steffy, D.A., 1976, Effect of the Parsons Lineament on Water Well Yields and Ground Water Quality in Tucker County, West Virginia: Unpublished Masters Thesis, West Virginia University, Morgantown, West Virginia, 106 p.

U.S. Department of Health, Education, and Welfare, 1962, Public Health
    Service Drinking Water Standards: U.S. Public Health Service
    Publication No. 956, 61 p.

Werner, E., 1976, Interrelationships of Photolineaments, Geologic
    Structures, and Fracture Production of Natural Gas in the
    Appalachian Plateau of West Virginia: Proceedings of the 7th
    Appalachian Petroleum Geology Symposium, Morgantown, West Virginia,
    pp 403-417.

Werner, E., 1977a, Application of Remote Sensing Studies to the Inter-
    pretation of Fracture Systems and Structural Styles in the Plateau
    Regions of Eastern Kentucky, Southwestern Virginia, and Southwestern
    West Virginia for Applications to Fossil Fuel Extraction Processes:
    a final project report on open file at the METC, Morgantown, West
    Virginia, 98 p.

Werner, E., 1977b, Remote Sensing Methods for Application to Natural
    Gas Production from Fractured Devonian Shale.Reservoirs of Western
    West Virginia: Proceedings of the 3rd ERDA Symposium on Enhanced
    Oil and Gas Recovery and Improved Drilling Methods, Vol. 2, Gas
    and Drilling, 7 p.

APPENDIX A

PHYSICAL WATER WELL DATA

PHYSICAL WATER WELL DATA

Data Code:

* – v = valley location, h = hilltop location, s = slope or hillside location.

** – Specific capacity measured as gallons per minute per foot of water drawdown.

*** – Aquifer sequence numbers refer to stratigraphic units described in Figure 4.

**** – Adequacy; IA = inadequate water supply; BA = barely adequate water supply; A = adequate water supply; TD = more than adequate water supply or supplies two dwellings; AA = driller reported inability to bail well dry.

Well Code:

       (BA–) = Bancroft 7-1/2 minute topographic quadrangle
       (EL–) = Elmwood 7-1/2 minute topographic quadrangle
       (RO–) = Robertsburg 7-1/2 minute topographic quadrangle
       (KE–) = Kenna 7-1/2 minute topographic quadrangle
       (SI–) = Sissonville 7-1/2 minute topographic quadrangle
       (WI–) = Winfield 7-1/2 minute topographic quadrangle

WELL NUMBER	OWNER	TOPOGRAPHIC SETTING*	SURFACE ELEVATION (FT.)	WELL DEPTH (FT.)	WELL DIAMETER (IN.)	DEPTH TO WATER (FT.)	DEPTH OF CASING (FT.)	WELL YIELD (GPM)	SPECIFIC CAPACITY**	AQUIFER SEQUENCE***	ADEQUACY****
KE-1	H.R.Bailey	h	1080	220	6			0.0		2	IA
KE-3	D.Jones	h	980	90	6		20	3.3		2	A
SI-4	E.Monday	h	960	150	6	20		0.5		3	BA
BA-5	T.Gibson	h	939	103	6	27		3.0		4	A
BA-6	J.Casto	h	960	200	6			0.0		6	IA
WI-7	R.Hill	h	920	250	6					6	IA
WI-8	C.King	h	920	200	6	30	12			6	A
WI-9	M.Levins	h	930	100	6		12	0.8		5	A
WI-10	M.Hopkins	h	890	150	6					6	A
WI-11	G.Parsons	s	840	152	6	20	20	1.0		7	A
WI-12	S.Workman	h	920	230	6		12	0.0		6	IA
BA-13	D.Starcher	h	960	86	6					2	TD
BA-14	D.Lukiert	h	910	125	6	65	11	0.7		4	BA
SI-15	F.Arthur	v	860	30	6	4	10	0.5		3	BA
SI-16	E.Hanna	s	840	125	6	40	11	0.7		5	BA
BA-17	F.Clendenin	v	700	35	6	5	18			6	AA
EL-18	D.Smalley	s	660	85	6	20	15	17.0		6	TD
EL-19	J.Withrow	h	1000	150	6		11			2	BA
WI-20	V.Casto	h	900	240	6	100	11	0.0		7	IA
WI-21	B.Lukiert	v	600	100	6	30	30			9	A
WI-22	T.Noffsinger	v	620	100	6	20	25	0.8		9	A
WI-23	R.Goddard	v	610	85	6			0.8		9	A
RO-24	J.Grimes	s	600	80	10	10		0.8		8	A
RO-25	G.Martin	v	590	86	6		32			8	AA
RO-26	A.Stover	v	600	157	6					7	AA
RO-27	H.Martin	v	610	75	6	30				7	A
WI-28	D.Wears Sr.	v	620	50	6	20				7	A
RO-29	L.Pennington	s	580	80	6	37	44	2.0	0.74	7	A
RO-30	M.Gates	v	620	70	6	35				6	A
RO-31	W.Boese	v	590		6					8	A
RO-32	G.Stanley	v	600	90	6		30	5.0		8	A
RO-33	H.Blackshire	h	930	175	6			0.0		4	IA
RO-34	C.Bailes	h	900	112	6	60				3	TD
RO-35	J.Bailes	h	830	150	6		30	1.0		3	A
RO-36	T.Bailes	h	920	145	6	60	13	0.8		3	A
RO-38	W.Jividen	h	950	102	6		20	0.8		2	A
RO-39	D.Lukiert	h	900	235	6			0.1		6	IA
EL-40	J.Frye	v	680	42	6	15				5	TD
EL-41	A.Null	v	640		6						A

WELL NUMBER	OWNER	TOPOGRAPHIC SETTING*	SURFACE ELEVATION (FT.)	WELL DEPTH (FT.)	WELL DIAMETER (IN.)	DEPTH TO WATER (FT.)	DEPTH OF CASING (FT.)	WELL YIELD (GPM)	SPECIFIC CAPACITY**	AQUIFER SEQUENCE***	ADEQUACY****
EL-42	M.Frye	v	655								TD
EL-43	E.Null	v	660	40	6					6	AA
EL-44	D.Smalley	h	1000	210	6	110	25	0.5		3	BA
EL-46	D.Arsten	h	980	180	6	120		1.0		3	A
SI-47	A.Smith	h	1050	267	6	37	25			3	IA
SI-48	J.King	h	1020	132	6	60		0.8		2	BA
SI-49	W.Green	h	1030	300	6			0.0		4	IA
SI-50	G.Goldizen	s	950	140	6		20	0.6		3	BA
BA-51	M.Milam	h	840								TD
BA-52	C.French	s	820	175	6	142	25	1.7		6	A
BA-53	R.French	s	820	136	6	120	15	4.0		5	A
BA-54	D.French	s	820	175	6	154	15	1.6		6	A
BA-55	L.Null	s	720	150	6					6	A
BA-56	P.Parsons	h	690	110	6	45	21	1.8		6	A
WI-57	T.Richardson	v	610	79	6	15				6	AA
WI-58	C.Blackenship	v	610	105	6					7	AA
WI-59	T.Cobb	s	670	144	6	17	19	1.0		8	A
WI-60	R.Blackshire	v	600	65	6	18	30			9	AA
WI-61	D.Johnson	v	630	75	6	18	32			9	A
WI-62	R.Blackshire	s	690	125				0.0		8	IA
WI-63	D.Blackshire	v	590	86						9	TD
WI-64	M.Jeromes	v	650	70	6					8	A
WI-65	M.Cobb	v	840	150	6					7	TD
WI-67	H.Gritt	h	840	155	6		21			6	A
WI-69	J.Morton	s	760	250	6			0.0		9	IA
WI-70	B.Morton	h	670	165	6	35	35			8	TD
WI-71	L.Priddy	v	590	200	6					9	AA
EL-73	L.Bush	h	960	102	6	52		0.0		2	IA
EL-75	O.Stone	h	1040	150	6			1.0		1	A
EL-76	S.Arbough	h	1050	125	6		8	0.1		1	IA
EL-77	W.Thompson	h	970	90	6			0.0		2	IA
BA-78	V.Smith	h	1000	200						3	A
BA-79	K.Casto	h	850	130	6		13			6	BA
EL-80	O.Stone	v	640	78	6	25	12	20.0	3.13	6	A

SPRINGS

WELL NUMBER	OWNER	TOPOGRAPHIC SETTING*	SURFACE ELEVATION (FT.)	WELL DEPTH (FT.)	WELL DIAMETER (IN.)	DEPTH TO WATER (FT.)	DEPTH OF CASING (FT.)	WELL YIELD (GPM)	SPECIFIC CAPACITY**	AQUIFER SEQUENCE***	ADEQUACY****
KE-2	D.Jones	s	1000								A
RO-37	D.Johnson	s	940								A
EL-45	R.Willard	s	680								A
WI-66	R.Reedy	s	740								A
WI-68	L.Gritt	s	800								A
WI-72	C.Harmon	s	760								A
EL-74	W.May	s	1000								A

APPENDIX B

CHEMICAL WATER WELL DATA

Well No.	Temperature (Celsius)	Specific Conductance (uMHO/cm)	pH (pH units)	Bicarbonate (mg/l)	Total Iron (mg/l)	Nitrate (mg/l)	Total Hardness (mg/l) *	Calcium (mg/l)	Magnesium (mg/l)	Sulfate (mg/l)	Chloride (mg/l)	Sodium (mg/l)
KE-3	15	1080	7.00	425	0.07	1.32	488	120.0	45.7	7	157	48
SI-4	13	1400	7.20	432	0.13	1.76	548	136.0	51.0	13	186	55
BA-5	13	680	6.78	282	0.05	5.94	282	73.0	24.0	13	64	30
WI-8	18	315	7.05	32	11.20	1.32	130	26.0	16.0	81	9	9
WI-9	17	710	7.71	376	0.07	8.65	220	47.0	25.0	6	52	59
WI-10	16	460	7.99	280	0.12	1.87	280	50.0	22.0	34	5	50
WI-11	18	715	8.13	479	0.04	1.69	198	50.0	18.0	10	5	92
EL-18	13	600	7.30	334	0.15	1.76	119	35.0	8.0	22	17	94
WI-21	20	535	7.99	319	0.10	1.69	158	42.0	13.0	8	9	52
WI-23	14	480	7.90	305	0.52	0.99	120	39.0	5.0	8	28	71
RO-24	14	2100	8.04	587	0.43	1.10	22	6.0	2.0	5	367	546
RO-25	10	1200	7.92	449	0.04	1.54	64	18.0	5.0	5	156	254
RO-26	13	4025	7.90	408	0.08	1.10	58	18.0	4.0	6	974	801
RO-29	11	990	7.10	460	0.92	0.05	149	39.0	13.0	9	133	185
RO-32	12	560	5.80	55	1.68	1.32	206	64.0	11.0	3	167	45
RO-34	9	1100	7.50	596	0.04	0.88	78	22.0	6.0	17	67	234
RO-37	7	340	6.73	156	0.31	0.80	100	26.0	9.0	28	13	30
BA-45	14	85	5.98	13	0.16	5.28	32	8.0	3.0	14	4	4
SI-48	8	240	6.39	109	0.21	1.76	98	29.0	6.0	12	10	8
BA-51	13	300	7.18	144	0.12	1.10	124	31.0	11.0	16	14	11
BA-52	15	860	7.96	508	0.30	3.41	22	5.0	2.0	8	35	234
BA-55	16	650	7.36	313	0.08	9.68	242	66.0	19.0	16	37	22
BA-56	16	560	7.65	311	0.08	2.20	201	54.0	16.0	7	23	34
WI-57	15	520	7.18	278	0.85	1.32	215	71.0	9.0	11	24	19
WI-58	16	6025	7.89	469	0.11	1.54	83	22.0	7.0	7	2032	1722
WI-59	22	1060	7.55	521	0.06	13.60	238	74.0	31.0	145	20	115
WI-60	15	1000	7.89	474	0.21	1.76	68	20.0	4.0	6	90	193
WI-61	19	895	8.13	529	0.05	1.98	86	25.0	6.0	25	34	167
WI-63	17	1275	7.91	495	0.09	1.45	52	15.0	3.0	5	139	234
WI-64	20	800	8.03	499	0.10	1.76	29	8.0	2.0	12	23	162
WI-65	9	650	7.61	397	0.05	1.98	75	21.0	6.0	10	13	113
WI-66	9	195	6.50	68	0.29	1.98	78	20.0	7.0	0	18	26

Well Code ~ BA = Bancroft 7.5-minute topographic quadrangle, EL = Elmwood 7.5-minute topographic quadrangle,
RO = Robertsburg 7.5-minute topographic quadrangle, KE = Kenna 7.5-minute topographic quadrangle
SI = Sissonville 7.5-minute topographic quadrangle, WI = Winfield 7.5-minute topographic quadrangle.

* - Total Hardness is expressed as mg/l CaCO$_3$.

APPENDIX C

MIDWAY-EXTRA GAS PRODUCTION DATA

(FROM SCHAEFER, 1979)

KEY:

Elevations are in feet with respect to sealevel.

IOF = initial open flow gas production,

FOF = final open flow gas production,

BR. SH. = Brown shale.

All data after Schaefer, 1979.

WELL PERMIT NUMBER	WELL TOP ELEV.	SUB-SRA ELEVATION TOP BEREA	TOP BR. SH.	BASE BR. SH.	IOF	FOF/HR	PRESS/HR
300	882	-1495	-2683	-3137	58	246/13	820/18
304	566	-1532	-2726	-3169	24	60/16	NA
307	926	-1524	-2734	-3135	NA	NA	NA
310	589	---	---	---	---	---	---
320	572	-1474	---	---	---	---	---
372	584	-1539	-2696	-3066	NA	150/NA	NA
383	834	-1527	---	---	---	---	---
389	584	-1608	-2801	-3186	26	327/27	880/24
391	593	-1615	-2735	-3134	150	251/NA	850/96
398	658	-1550	-2738	-3122	84	111/NA	NA
400	573	-1620	-2728	-3099	NA	313/NA	NA
408	602	-1533	-2768	-3246	54	133/1	885/72
413	594	-1629	-2739	-3137	NA	1007/3	NA
424	579	-1645	-2771	-2966	Show	329/3	NA
425	618	-1637	-2782	-3132	Show	329/8	900/48
434	613	-1659	-2767	-3162	NA	553/6	NA
437	604	-1632	-2771	-3086	NA	520/1	NA
442	592	-1641	-2773	-3148	Show	103/NA	NA
443	952	-1679	-2798	-3218	94	495/NA	900/24
444	857	-1659	-2823	-3188	NA	800/1	NA
445	798	-1648	-2767	-3156	15	24/19	NA
450	601	-1582	---	-3149	NA	500/4	NA
455	889	-1696	-2931	-3431	12	12/NA	NA
457	888	-1680	-2804	-3231	184	987/NA	900/72
460	839	-1641	-2801	-3168	Show	989/NA	950/24
461	622	-1688	-2758	-3193	18	1265/1	NA
462	729	-1626	-2761	-3126	15	325/NA	650/NA
463	627	-1599	-2797	-3193	18	377/2	NA
465	939	-1610	-2888	-3336	7	152/1	780/96
472	750	-1675	-2805	-3234	103	298/30	900/46
473	706	-1679	-2807	-3209	30	750/2	NA
474	707	-1703	-2852	-3249	21	750/NA	NA
475	661	-1599	-2759	-3147	231	1164/NA	180/1
476	591	-1691	-2784	-3227	Show	603/NA	NA
477	928	-1647	-2837	-3212	377	2499/NA	NA
479	755	-1592	-2753	-3125	NA	152/NA	NA
481	898	-1662	-2809	-3167	45	140/NA	200/2
482	655	-1600	-2760	-3157	238	848/2	175/1
483	591	-1584	-2769	-3189	NA	NA	NA
486	835	-1717	-2725	-3065	21	1175/1	NA
490	700	-1663	-2831	-3195	30	193/11	200/3
491	893	-1670	-2837	-3237	Show	315/NA	300/2
495	572	-1630	-2743	-3124	60	NA	NA
496	901	-1657	-2829	-3209	NA	367/NA	738/21
497	662	-1642	-2773	-3198	30	60/NA	NA
498	603	-1657	-2767	-3077	21	200/NA	NA
499	787	-1624	-2797	-3165	NA	377/NA	200/1
500	876	-1657	-2819	-3239	15	820/NA	120/2
501	835	-1597	-2770	-3151	327	827/NA	125/1
502	870	-1662	-2820	-3230	NA	1009/NA	800/24
503	621	-1691	-2899	-3311	15	412/NA	130/2
504	920	-1641	-2815	-3221	NA	852/NA	750/24
505	811	-1599	-2729	-3139	260	NA	NA
506	678	-1628	-2776	-3181	NA	499/NA	245/1

WELL PERMIT NUMBER	WELL TOP ELEV.	TOP BEREA	TOP BR. SH.	BASE BR. SH.	IOF	FOF/HR	PRESS/HR
			SUB-SEA ELEVATION				
507	886	-1654	-2838	-3252	37	202/18	787/92
508	864	-1658	-2836	-3226	73	511/NA	NA
510	811	-1618	-2779	-3209	21	660/NA	95/1
511	838	-1592	-2746	-3117	103	379/NA	NA
512	914	-1636	-2815	-3222	158	1961/NA	NA
513	923	-1652	-2882	-3218	326	781/NA	800/NA
515	865	-1647	-2822	-3235	73	169/10	405/13
517	654	-1578	-2746	-3158	NA	48/51	865/240
518	637	-1596	-2729	-3153	NA	84/NA	NA
519	880	-1641	-2830	-3248	20	78/30	850/168
520	820	-1645	-2820	-3180	NA	21/NA	NA
521	712	-1547	-2613	-2 78	NA	NA	NA
522	873	-1645	-2762	-3232	15	145/NA	810/72
523	901	-1619	-2796	-3109	NA	100/NA	710/24
524	834	-1549	---	-3076	5	358/NA	NA
525	932	-1594	-2801	-3208	Show	NA	NA
526	910	-1566	-2735	-3124	Show	NA	NA
527	925	-1622	-2740	-3185	Show	23/15	NA
530	620	-1655	-2825	-3203	21	336/1	960/26
535	715	-1649	-2803	-3209	Show	14/23	NA
536	897	-1577	-2695	-3112	21	381/NA	70/1
537	920	-1623	-2794	-3196	174	500/NA	NA
538	955	-1671	-2853	-3339	24	211/1	930/96
539	621	-1604	-2724	-3199	15	327/NA	420/16
543	540	-1644	-2740	-3130	24	250/1	NA
550	823	-1566	-2752	-3147	39	79/15	NA
552	581	-1614	-2740	-3109	NA	876/1	NA
553	662	-1543	-2728	-3144	NA	152/NA	700/NA
558	897	-1661	-2828	-3209	33	146/NA	41/1
566	916	-1597	-2778	-3185	NA	70/24	NA
586	854	-1716	-2926	-3336	60	103/NA	825/48
596	684	-1704	-2941	-3346	33	119/NA	850/62
599	601	-1612	-2766	-3194	7	158/25	800/96
603	598	-1610	-2782	-3188	28	424/8	NA
604	596	-1715	-2927	-3335	18	60/NA	855/72
607	813	-1702	-2909	-3347	15	198/29	880/72
613	608	-1508	-2742	-3237	Show	158/NA	710/NA
618	634	-1694	-2920	-3344	24	73/29	870/72
621	628	-1677	-2893	-3305	47	189/24	890/48
624	933	-1557	-2769	-3247	Show	NA	NA
627	638	-1475	-2622	-2959	Show	15/48	NA
629	840	-1663	-2865	-3308	56	246/NA	920/42
630	848	-1694	-2892	-3304	Show	84/NA	790/72
632	668	-1627	-2849	-3295	29	207/NA	840/24
633	604	-1507	-2708	-3126	NA	43/NA	400/44
634	913	-1622	-2845	-3272	11	61/NA	760/72
635	830	-1685	-2873	-3295	158	231/NA	875/48
637	923	-1620	-2828	-3282	21	60/28	820/72
638	575	-1583	-2719	-3171	8	158/30	790/96
639	647	-1604	-2788	-3172	Show	103/NA	NA
641	907	-1638	-2856	-3320	Show	57/29	680/72
642	992	-1604	-2806	-3247	NA	43/21	NA
646	660	-1635	-2784	-3170	Show	85/NA	480/168
647	905	-1685	-2879	-3315	89	273/NA	800/96
649	777	-1626	-2748	-3159	14	94/32	NA

WELL PERMIT NUMBER	WELL TOP ELEV.	SUB-SEA ELEVATION			IOP	FOP/HR	PRESS/HR
		TOP BEREA	TOP BR. SH.	BASE BR. SH.			
653	918	-1678	-2877	-3320	56	169/NA	765/96
654	921	-1536	-2736	-3119	Show	163/NA	NA
657	909	-1710	-2901	-3336	Show	103/32	750/96
661	915	-1679	-2790	-3225	10	60/NA	780/144
662	841	-1504	-2691	-3069	NA	110/NA	NA
663	833	-1688	-2887	-3292	Show	84/23	640/72
666	646	-1609	-2749	-3198	Show	146/24	745/Max
667	956	-1609	-2814	-3214	24	NA	NA
669	737	-1673	-2813	-3208	NA	55/NA	NA
672	924	-1557	-2724	-3096	133	231/NA	NA
674	917	-1600	-2993	-3208	NA	56/NA	NA
675	656	-1589	---	---	NA	NA	NA
680	672	-1675	-2845	-3228	39	112/29	540/120
685	864	-1544	-2706	-3077	Show	39/3	NA
686	584	-1565	-2758	-3164	NA	NA	NA
691	862	-1661	-2818	-3238	Show	66/NA	585/192
697	970	-1705	-2915	NA	NA	NA	NA
701	601	-1686	-2874	-3305	Show	119/NA	740/264
704	604	-1544	-2696	-3066	Show	25/19	NA
747	896	-1706	---	---	NA	NA	NA
750	828	-1490	---	---	NA	NA	NA
755	592	-1478	-2680	-3098	NA	NA	NA
765	584	-1543	-2716	-3141	NA	NA	NA
770	844	-1665	---	---	Show	NA	NA
778	849	-1662	---	---	NA	NA	NA
781	608	-1698	-2892	-3327	Show	60/24	660/168
783	809	-1713	-2907	-3339	Show	202/24	855/168
785	629	-1706	-2905	-3347	Show	119/19	775/168
788	914	-1672	-2836	-3232	Show	84/24	675/168
789	911	-1625	-2804	-3226	Show	127/24	595/168
790	912	-1645	-2866	-3344	Show	119/24	715/72
792	842	-1650	---	---	17	47/NA	NA
794	838	-1646	-2828	-3258	Show	73/11	565/192
795	609	-1589	---	---	NA	NA	NA
796	629	-1486	---	---	NA	NA	NA
797	799	-1510	-2718	-3153	NA	26/NA	NA
798	595	-1658	-2836	-3257	NA	94/18	950/Max
799	782	-1677	-2849	-3276	NA	94/13	900/168
800	879	-1719	-2911	-3344	NA	239/NA	950/168
801	612	-1680	-2876	-3294	NA	119/17	785/168
802	628	-1676	-2862	-3292	NA	283/16	950/NA
807	634	-1644	-2822	-3244	NA	84/NA	925/NA
808	644	-1644	-2846	-3306	NA	179/NA	760/NA
809	635	-1566	-2782	-3237	NA	315/NA	785/NA
810	696	-1690	-2886	-3304	Show	36/24	NA
811	666	-1590	-2804	-3268	Show	492/NA	650/NA
812	739	-1611	-2829	-3293	Show	103/NA	750/NA
813	732	-1546	-2764	-3220	NA	73/NA	700/NA
814	928	-1572	-2782	-3250	Show	73/NA	720/NA
815	958	-1662	-2862	-3322	NA	163/NA	710/NA
816	583	-1536	-2743	-3192	NA	60/18	560/NA
822	975	-1695	-2899	-3335	NA	386/4	890/NA
823	660	-1680	-2887	-3366	NA	160/4	770/NA
824	852	-1693	-2898	-3368	NA	329/5	830/NA

WELL PERMIT NUMBER	WELL TOP ELEV.	SUB-SEA ELEVATION			IOF	FOF/HR	PRESS/HR
		TOP BEREA	TOP BR. SH.	BASE BR. SH.			
828	942	-1684	-2888	-3346	NA	82/NA	725/NA
829	625	-1720	-2935	-3405	NA	350/4	865/NA
830	711	-1661	---	---	NA	280/4	860/NA
832	852	-1648	-2816	-3235	40	NA	530/NA
833	910	-1695	-2905	-3380	NA	270/5	840/NA
834	897	-1669	-2871	-3313	103	NA	649/NA
835	---	---	---	---	NA	NA	NA
838	---	---	---	---	NA	NA	NA
840	---	---	---	---	NA	NA	NA
845	---	---	---	---	NA	NA	NA
847	650	-1688	-2906	-3395	Show	332/24	925/NA
848	927	-1665	-2851	-3282	NA	NA	NA
849	---	---	---	---	NA	NA	NA
850	---	---	---	---	NA	NA	NA
855	980	-1638	-2820	-3250	NA	NA	NA
857	949	-1695	-2906	-3388	42	322/5½	850/NA
858	662	-1695	-2904	-3383	25	385/4½	800/NA
859	833	-1695	-2906	-3378	27	582/3½	850/NA
862	920	-1655	-2860	-3328	NA	200/4	895/NA
863	800	-1688	-2890	-3350	NA	NA	NA
865	850	-1663	-2870	-3333	NA	120/4	705/NA
867	926	-1708	-2913	---	NA	NA	NA
868	990	-1694	-2910	---	18	120/4	810/NA
870	925	-1707	-2927	---	13	395/4	860/NA
871	863	-1615	-2815	-3262	NA	NA	NA
873	918	-1660	-2844	-3282	NA	NA	NA
874	666	-1684	-2896	-3372	8	170/4	780/NA
875	980	-1709	-2918	-3392	16	280/4	920/NA
876	673	-1685	-2905	-3403	15	280/4	920/NA
904	---	---	---	---	NA	NA	NA
D609	612	-1708	-2794	-3293	NA	146/24	900/Max
D828	618	-1700	-2898	-3343	Show	103/24	525/15
F2657	---	-1626	---	---	NA	NA	NA
F2794	590	-1578	---	---	NA	NA	NA
F2795	573	-1591	---	---	NA	NA	NA
F2796	590	-1599	---	---	NA	NA	NA
F3055	---	---	---	---	NA	NA	NA

APPENDIX D

ELECTRICAL RESISTIVITY FIELD DATA

ELECTRICAL RESISTIVITY FIELD DATA

Station number	CPPC Resistance	CCPP Resistance	CPCP Resistance	Delta percent
1	12.7	4.3	10.0	−12.6
2	17.0	5.0	13.4	−8.24
3	77.0	64.1	9.5	+4.54
4	21.4	8.8	12.0	+2.80
5	55.3	50.2	11.4	−11.4
6	19.7	6.7	12.5	+2.54
7	18.0	6.2	9.6	+12.2
8	18.7	6.0	10.7	+10.7
9	17.5	5.5	10.1	+10.8
10	18.6	7.6	7.6	+18.3
11	15.1	6.4	7.8	+6.00
12	13.3	3.9	7.5	+14.3
13	11.2	2.7	6.0	+22.3
14	10.8	2.4	5.7	+25.0
15	9.2	3.2	1.3	+51.5

Resistance units are in ohm/feet.

APPENDIX E

WATER WELL—PHOTOLINEAMENT PROXIMITY DATA

Proximity of Water Wells to Nearest Photolineament

0-100 feet	101-150 feet	151-200 feet	Greater than 200 feet
BA-17	WI-60	WI-58	RO-26
EL-43	EL-41	EL-18	RO-27
EL-42	RO-25	EL-40	WI-51
WI-63		BA-51	WI-71
RO-30		BA-53	BA-13
RO-31		RO-29	RO-34
		WI-23	WI-70
		RO-24	WI-65
		RO-36	RO-32
		SI-16	KE-3
			BA-5
			BA-56
			BA-52
			BA-54
			WI-8
			WI-10
			WI-11
			WI-21
			WI-28
			RO-35
			EL-46
			BA-55
			WI-59
			WI-61
			WI-64
			WI-67
			EL-75
			BA-78
			RO-38
			SI-48
			WI-9
			WI-22
			BA-14
			EL-19
			SI-50
			SI-4
			SI-15
			EL-44
			EL-76
			RO-39
			BA-6
			KE-1
			WI-7
			WI-12
			WI-20
			RO-33
			SI-47
			SI-49
			WI-62
			WI-69
			EL-73
			EL-77

APPENDIX F

INITIAL OPEN FLOW—PHOTOLINEAMENT DATA

PHOTOLINEAMENT DATA AND INITIAL OPEN FLOW
FOR GAS WELLS

Gas Well Yield (MCF/day)	Distance to Nearest Photolineament (Km)	Photolineament Class	Photolineament Orientation
377	0.33	1	N
326	0.35	2	N27°E
260	0.10	2	N55°W
238	0.00	1	N68°W
231	0.65	3	N51°E
184	0.30	1	N
174	0.13	1	N13°W
158	0.35	2	N50°W
103	0.60	3	N20°E
103	0.10	1	N15°W
103	0.75	2	N18°E
94	0.15	1	N
89	1.00	3	N20°E
73	0.30	2	N72°E
73	0.20	1	N11°W
60	0.60	1	N
56	0.68	2	N50°W
56	0.19	2	N50°W
47	0.55	2	N50°W
45	0.30	2	N30°W
40	0.42	2	N15°E
39	0.25	2	N12°E
37	0.80	1	N11°W
33	0.05	2	N81°W
33	0.35	1	N14°W
30	0.03	1	N7°W
30	0.30	2	N55°W
29	0.00	2	N52°W
24	0.40	2	N74°W
24	0.10	1	N
21	0.20	1	N65°E
21	0.60	2	N15°W
21	0.30	2	N23°E
21	0.10	1	N15°W
21	0.55	2	N55°E
21	0.60	2	N55°E
20	0.20	2	N25°W
18	0.35	3	N75°E
18	0.10	2	N2°W
17	0.35	3	N15°E
15	0.35	2	N50°W
15	0.25	1	N33°W
15	0.50	1	N4°E
15	0.25	2	N72°W
15	0.60	2	N72°W
15	0.50	2	N52°E

Gas Well Yield (MCF/day)	Distance to Nearest Photolineament (Km)	Photolineament Class	Photolineament Orientation
14	1.25	3	N51°E
11	0.22	3	N70°W
10	0.40	2	N21°E
5	0.20	2	N16°E
show	0.40	2	N52°E
show	0.90	2	N52°E
show	0.75	2	N55°E
show	0.10	3	N50°E
show	0.50	2	N21°E
show	0.05	3	N43°E
show	0.10	1	N
show	0.31	1	N15°W
show	0.35	3	N5°E
show	0.40	3	N46°E
show	0.20	2	N5°W
show	0.55	2	N
show	0.65	2	N46°E
show	0.38	2	N73°W
show	0.20	3	N
show	0.35	2	N46°E
show	0.95	1	N54°E
show	0.50	1	N50°W
show	0.10	2	N78°E
show	0.05	2	N81°W
show	0.05	1	N
show	0.20	2	N50°W
show	0.18	2	N19°W
show	0.08	1	N4°W
show	0.50	1	N34°W
show	0.90	2	N46°E

APPENDIX G

FINAL OPEN FLOW—PHOTOLINEAMENT DATA

PHOTOLINEAMENT DATA AND FINAL OPEN FLOW
FOR GAS WELLS

Gas Well Yield (MCF/day)	Distance to Nearest Photolineament (Km)	Photolineament Class	Photolineament Orientation
2499	0.33	1	N
1265	0.10	2	N2°W
1175	0.10	1	N15°W
1164	8.65	3	N51°W
1009	0.50	2	N28°E
989	0.10	1	N
987	0.30	1	N
852	0.25	1	N11°W
848	0.00	1	N68°W
781	0.35	2	N27°E
750	0.55	2	N55°E
750	0.30	2	N55°E
660	0.60	2	N15°W
620	0.25	2	N72°W
603	0.90	2	N54°E
553	0.90	2	N58°E
511	0.20	1	N11°W
500	0.13	1	N13°W
499	0.00	3	N43°E
495	0.15	1	N
424	0.65	3	N45°E
412	0.25	1	N33°W
381	0.60	2	N55°E
379	0.75	2	N18°E
377	0.10	2	N54°W
372	0.50	2	N20°E
367	0.40	1	N15°W
358	0.20	2	N16°E
350	0.10	1	N10°E
336	0.29	2	N23°E
329	0.40	2	N54°E
329	0.60	1	N26°W
325	0.50	2	N52°E
315	0.30	1	N15°W
298	0.10	1	N15°W
283	0.10	2	N50°E
273	1.00	3	N20°E
270	0.10	3	N80°W
246	0.20	2	N50°W
239	0.80	2	N35°W
231	0.35	2	N50°W
211	0.40	2	N74°W
207	0.00	2	N52°W
202	0.50	1	N50°W

Gas Well Yeild (MCF/day)	Distance to Nearest Photolineament (Km)	Photolineament Class	Photolineament Orientation
202	0.80	1	N11°W
198	0.35	2	N50°W
193	0.05	1	N7°W
189	0.55	2	N50°W
179	0.25	3	N65°E
169	0.30	2	N72°W
169	0.70	2	N50°W
163	0.75	3	N65°E
158	0.20	3	N45°E
146	0.05	3	N45°E
146	0.35	1	N14°W
146	0.10	2	N67°W
145	0.60	2	N72°W
140	0.30	2	N30°W
127	0.55	2	N
119	0.50	2	N81°W
119	0.40	2	N45°E
119	0.05	2	N81°W
112	0.25	2	N12°E
103	0.50	1	N30°W
103	0.05	1	N
103	0.60	1	N
100	0.40	2	N28°E
94	1.25	3	N51°E
94	0.15	2	N13°W
94	0.10	2	N71°E
85	0.75	2	N58°E
84	0.05	1	N13°W
84	0.40	3	N50°E
84	0.90	2	N45°E
84	0.20	2	N50°W
84	0.10	2	N3°W
82	1.20	2	N74°W
78	0.20	2	N25°W
73	0.10	3	N20°E
73	0.60	2	N45°E
66	0.40	2	N72°W
61	0.22	3	N70°W
60	0.10	2	N70°E
60	0.20	1	N65°E
60	0.35	3	N75°E
57	0.20	2	N15°W
48	0.20	1	N11°W
47	0.35	2	N15°E
43	0.60	2	N2°E
39	0.50	2	N20°E
36	0.10	1	N5°W
25	0.10	3	N50°E
24	0.30	3	N78°E
21	0.60	1	N53°E
14	1.00	1	N53°E
60	0.40	2	N20°E

APPENDIX H

PUMPING TEST DATA

Pumping Test Data

Well Number and Owner	Probable Aquifer	Static Water Level (feet below surface)	s	Q	C	T	Pumping Time
RO-29 (L. Pennington)	Gilboy (ss)	44.0	8.83'	6.51	0.74	311.68	10 min.
EL-80 (O. Stone)	Waynesburg (ss)	19.25	2.58'	8.09	3.13	1615.55	20 min.

s = drawdown in feet after maximum duration of pumping,

Q = pumping rate in gallons per minute,

C = specific capacity in gallons per minute per foot of drawdown,

T = transmissivity in gallons per day per foot of aquifer width.

ABSTRACT

A hydrogeologic study was conducted in the Midway-Extra gas field where gas wells tap Devonian shales in northern Putnam County, West Virginia. Lineaments were mapped and shallow ground water was surveyed for physical and chemical parameters, to determine if lineaments or ground water may be useful for shale gas exploration. Landsat lineaments, defined from satellite imagery, have no apparent effect on water well yield and are associated with low gas well yields. Short photolineaments, defined from low-altitude stereo photography, are excellent sites for high-yielding water wells and good sites for high-yielding gas wells in general. These lineaments appear to represent permeable zones about 400 feet wide at shallow depth. The density of photolineaments orientated N60°W-N30°E is especially well associated with high-yielding gas well trends. Final open flow is especially great for gas wells near water wells or springs having high bicarbonate or nitrate concentrations. High bicarbonate content is in part likely to be caused by oxidation of methane gas in shallow ground water. Photolineaments and ground water chemistry may well prove to be valuable exploration tools for Devonian shale gas in other areas.

APPENDIX F

Geophysical Data

Richard T. Williams
James E. Ruotsala

A Review of the report by K. G. Kirk which appeared in the 1977-1978 Devonian Shales Project Annual Report under the title "A Petite High Resolution Seismic System for Coal Investigation"

by

Richard T. Williams
James E. Ruotsala

West Virginia University
Department of Geology and Geography
Morgantown, West Virginia 26506

October 1979

A seismic reflection survey was conducted at the Pricetown, West Virginia, in-situ coal gasification site during the 1977-1978 fiscal year. The data and an interpretation were presented in a paper by K. G. Kirk appended to the 1977-1978 annual report. One part of that paper is re-examined here. While similar comments apply to the remainder of the paper, the present discussion is limited to the Pricetown II data.

The Pricetown data were recorded using the Bison 1580 seismograph in a slightly different configuration from its present one. However, the modifications to the system, made since the Pricetown data were recorded, are of a technical nature and do not affect the discussion presented.

Serious problems are readily identifiable in the Pricetown II interpretation, on the basis of fundamental considerations from the theory of reflection profiling. Each of these is treated in a separate paragraph below.

The horizontal scale is incorrect. In the simple case of horizontal subsurface reflectors and lateral homogeneity, reflection depth-points are located midway between the shot-point and geophone. Thus, the horizontal interval at which the subsurface is mapped is one-half the geophone spacing. In this survey the geophone spacing was 40 feet; so the distance between traces on the seismic section should be 20 feet. Because of this error, subsurface features will be incorrectly located, and their horizontal dimension will be distorted. In addition, it is possible that incomplete subsurface coverage was obtained, with gaps between adjacent six-trace records.

Apparent acoustic energy arrives at zero-time. In a seismic reflection survey the first event to arrive on the field record will be either the direct ray, or a critically refracted ray, depending on the local geology and shooting geometry. At the Pricetown II site there is a sandstone that has velocity (V_p) near 7400 ft/sec essentially at the surface, and the first arrival will be the direct ray moving across the geophone spread at that velocity. Prior to this event, the seismic trace will be quiescent. On the Pricetown data, there is apparent acoustic energy from the start of the trace, indicating a severe noise problem at an amplitude as great as any of the events identified as reflections. If this noise persisted throughout the recording interval, it would mask any seismic signals. An alternative explanation of the event at time-zero is that the seismograph was starting late, and that zero-time is incorrectly located on the seismic time section.

Events having opposite polarity on the seismic section are identified as coals. Coal has a very low acoustic impedance compared to most other rocks. For that reason, it will consistently exhibit a negative reflection polarity, as defined by the direction of the first excursion of the reflection wave form. On the Bison system, polarity from trace to trace for a single shot may not be consistent, but on a particular trace the polarity should not change. On the Pricetown II section, reflection events having opposite polarities are both identified as coals, which is impossible.

There are several seismic events missing from the section. Each of the reflection events identified in the previous report coincides with a change in the seismic velocity on a nearby continuous velocity log (CVL). However, a comparison of the section with a synthetic trace, formed by the convolution of a simple wavelet with a reflectivity function derived from the CVL, shows primary events that are not present on the seismic data. The data and synthetic trace are shown for side-by-side comparison in Figure 1. Also missing from the data are the various first-order surface multiples and peg-leg multiples that should be associated with good reflectors, like coals. Multiples are not included in the synthetic trace.

The seismic expression of the interpreted fracture zone is inappropriate. If there were a fracture zone open to near the depth of the Pittsburgh coal, it is quite unlikely that it would completely mask reflections from coals above the Pittsburgh. The expected effect of the fracture zone is to decrease the seismic velocity, and in terms of the reflection travel times it could be manifested in one of two ways:

1. If the subsurface coverage is greater than 36%, ray paths that lie only partially within the fracture zone must exist. On these traces, the normal-move-out (NMO) will not have the usual hyperbolic form, and the NMO correction would be unsuccessful. However, it would be possible to estimate the extent of the fracture zone by modeling the observed move-out.

2. If the subsurface coverage is less than 36%, it would be possible (but unlikely) that ray paths from one shot could lie entirely within the fracture zone, while no other traces were affected. In that case, the NMO correction would be successful and subsurface reflectors would be correctly positioned on the time section, and the resulting anomaly could be interpreted either as an anomaly in vertical velocity or a subsurface structure.

While these two cases illustrate the problem with the previous interpretation of the data as a velocity anomaly, it is the opinion of the authors that neither of the above cases are likely to apply to the Pricetown II data for reasons outlined in the following paragraphs.

The most reasonable explanation of the anomaly previously interpreted as a fracture zone is that it is the result of an inadvertent halving of the sampling interval in the upper 200 milliseconds (ms) of data, either by operator error or instrument malfunction. Close examination of the six anomalous traces on the Pricetown II section shows that the apparent frequency above 200 ms is about 300 Hz. Below 200 ms, and on all other traces on the section, the apparent frequency is exactly double, about 600 Hz. Postponing questions about how it could happen, if the first 205 ms of the six traces is compressed to half that, 102 ms, and the event at 209 ms is moved up unchanged, that event, identified as the Pittsburgh, aligns perfectly with the Waynesburg. Consideration of the character of the anomalous event (polarity and number of cycles in the wave form) supports this alignment. The event has the wrong polarity and perhaps one cycle too many to be the "Pittsburgh" but is consistent with the "Waynesburg," and no other. To understand how 102 ms of data could be represented as 205 ms, some understanding of the operation of the Bison seismograph is required. The seismograph uses an analog-to-digital converter (A/D) to store 256 values of the seismic trace in solid-state memory. The values

are samples of the trace, taken at equal time intervals, for a total record length which is switch-selectable. The switch that controls the record length has seven positions: 10.24 ms, 20.48 ms, 51.2 ms, 102.4 ms, 204.8 ms, 512 ms, and battery check. The last position activates a voltmeter to check the batteries, and must be used frequently. It would be quite easy to accidentally set the record length to 51.2 ms rather than 102.4 ms (labeled 100 ms) after checking the battery, and then to correct the error after checking the battery later, and never notice that the switch had been in the wrong position. At Pricetown the six-trace record was played onto a strip-chart recorder one trace at a time, from the digital memory through a digital-to-analog converter (D/A). The digital record itself was not preserved. The physical length of the analog record from the chart recorder remains constant, regardless of the time length of the record. Thus the sampling interval can be halved on one or more records, and the error can be detected only by a critical examination of the data. Although the problem has been described in terms of operator error, it could also result from an electrical/mechanical malfunction of the record length switch.

In summary, it is clear that no fracture zone was detected on the Pricetown II seismic profile. No statement concerning the existence or nonexistence of a fracture zone can be based on that data. Further, it is unlikely that the events on the data, identified as reflections, have seismic origin. More likely, in the opinion of the authors, the events are fortuitous and optimistic correlations of noise bursts with velocity lows on a nearby CVL. It is possible that this opinion would have to be modified after an examination of the original strip-chart records, but these appear to be lost. It is certain that actual seismic data could not be "cleaner" than the synthetic trace in Figure 1.

In addition to the presentation of the Pricetown data, the report last year also contains unsupportable, optimistic statements concerning the capabilities and value of the seismic system currently under development at West Virginia University. The authors feel that it is necessary to correct any misconceptions resulting from those statements at this time.

It is emphasized that the fundamental concept of a high resolution reflection seismic tool is considered to be very valuable, and attainable. It is only in the technical aspects that the authors consider the earlier report to be unrealistic. This subject has been partially treated in the Executive Summary of the Annual Report containing this paper, and those remarks will not be repeated.

In his report Kirk expresses the opinion that a high resolution seismic system that is inexpensive was demonstrated to work well, and that the data from the system required substantially no processing prior to interpretation. Both of these ideas are wrong. The system has been very expensive, in terms of cost per mile of seismic line. Although the system now appears to be ready for field tests (scheduled for October 16) no usable seismic reflection data has been obtained with it during the past two years. (Its present state

Figure 1. A synthetic seismic trace generated using the sonic log of a well on the seismic line (USBM #2 Dallison) is compared to the data recorded at the Pricetown II site by K. Kirk. The synthetic trace differs from real data in that it does not exhibit the exponential amplitude decrease with two-way time caused by spherical divergence of the wave front, and multiples are not included.

of readiness can be directly attributed to an electronics technician, who has worked with it on a full time basis for the past month.) Further, the capabilities of the present system are limited, as discussed in the Executive Summary. A full-featured seismic field system capable of recording the highest quality data would require a larger initial expenditure, about $250,000 based on a Texas Instruments DFS-V, plus the cost of the shot-hole drill. It would not involve larger personnel costs since it can be operated by the same four-man crew required by the Bison-based system. Since the TI system is delivered tested, and with training for the operators, there need be no delay between the hardware purchase and the start of data collection. The TI system, and similar ones by other manufacturers, are petite in petroleum industry terms, and are as portable as the present WVU system. Their true cost, in terms of their ability to produce geologic information, is less than the cost of the system under development.

The opinion expressed in the previous report, that high resolution seismic data can be processed by microcomputers, is also unrealistic. High resolution processing is more demanding than conventional applications. However, it is not necessarily true that a full size computer is needed, or even that a large computing system will be capable of even modest reflection-seismic processing tasks. (See the discussion of WVNET in the Executive Summary.) In recent years the cost of computing hardware has decreased dramatically (witness calculators and digital watches), and minicomputer-based seismic data processing systems have appeared on the market. In such systems the actual processing is done by specialized peripheral devices (array processors) while the minicomputer itself merely moves the data from tape or disk to the array processor, and finally to the plotter. The cost of such systems can be much less than processing charges on a nonspecialized large system. The low-cost TIMAP by Texas Instruments, for example, costs approximately $160,000 which includes a complete package of processing software and user training.

In reflection seismology, as elsewhere, one gets what one pays for. The method is expensive in absolute terms, but it is the least expensive tool for mapping in detail potential oil and gas reservoirs. It is the method by which virtually all new discoveries are made, and its cost must be balanced against its capabilities. The idea that the resolution can be increased so that the method can be applied to the exploration problems of potential eastern gas shale production seems quite promising. Within the limits of available resources, work towards this goal is continuing at WVU.

SEISMIC MODELING

Ruotsala, James E., Department of Geology and Geography, West Virginia University, Morgantown, WV 26506.

Seismic modeling is a scheme for geologic interpretation of reflection seismic data. The procedure can be summarized in the following steps:

1. A geologic model is postulated;

2. The expected seismic response is computed (this is called the synthetic seismic data);

3. The synthetic data is compared to the real data; and

4. The validity of the geologic model is judged.

Two different modeling efforts will be discussed: structural modeling and stratigraphic modeling.

Structural modeling is an attempt to interpret seismic responses in areas of complex structure or steeply dipping beds. A ray tracing scheme is used for this.

Stratigraphic modeling is the interpretation of seismic responses in terms of lithologies and bed geometry. This approach requires detailed examination of waveforms and amplitudes of events.

Seismic modeling may be divided differently into two types: forward modeling and inverse modeling.

Forward modeling is the computation of the synthetic seismic response from known or postulated geology. One example would be the construction of a synthetic seismogram from well log data to tie to a seismic line. Another example is the computation of the synthetic seismic response of a probable or possible or wished for exploration target. The synthetic data is used as a reconnaissance guide.

Inverse modeling is the computation of a geologic model responsible for an observed seismic response. This approach would be used to explain an unknown feature in the observed seismic data or compute the size of a prospect.

For this discussion minimal time will be spent on the details of the methods. The emphasis, by way of examples, will be on applications to exploration problems.